Chair of Metal Forming

Doctoral Thesis

Systematic Digitalization of a Value Chain from Raw Material to Recycling

Dipl.-Ing. Marcel Sorger, BSc

May 2023

EIDESSTATTLICHE ERKLÄRUNG

Ich erkläre an Eides statt, dass ich diese Arbeit selbständig verfasst, andere als die angegebenen Quellen und Hilfsmittel nicht benutzt, und mich auch sonst keiner unerlaubten Hilfsmittel bedient habe.

Ich erkläre, dass ich die Richtlinien des Senats der Montanuniversität Leoben zu "Gute wissenschaftliche Praxis" gelesen, verstanden und befolgt habe.

Weiters erkläre ich, dass die elektronische und gedruckte Version der eingereichten wissenschaftlichen Abschlussarbeit formal und inhaltlich identisch sind.

Datum 02.05.2023

Unterschrift Verfasser/in
Marcel Sorger

Acknowledgement

Hereby, I would like to express my sincerest gratitude to all the people that supported me during the course of this thesis.

First, I would like to thank Benjamin James Ralph for his guidance, support and contributions during this thesis. The conversations and discussions about all the issues concerning this thesis and especially about those that did not, helped me broaden my horizons and contributed significantly to setting my future goals.

Second, my gratitude goes to Karin Hartl for her support and expertise in the field of material science, which helped to further expand the scope of this thesis.

Also, my thanks go to Benjamin Schödinger, who in his time as a student worker became an integral part of this team, contributing with his knowledge and self-sufficiency.

Additionally, I would like to thank Martin Schoiswohl, whose expertise in metallurgy and simulations significantly contributed to the improvement of the results of this doctoral thesis.

Furthermore, I would like to thank our technicians Christian Stöckl and Ralph Ambrosch for their flexibility, ideas and invaluable craftsmanship.

Also, I would especially thank to Manuel Woschank, whose academic expertise and support showed me the transdisciplinary context of this doctoral thesis.

Furthermore, I would like to thank my supervisor Martin Stockinger and mentor Thomas Antretter for trusting me and giving me the necessary space to move in the different directions I took interest in.

This thesis made me understand the importance of interdisciplinary work, incorporating all the different aspects into the projects, creating results that are more substantial. Furthermore, the different disciplinary and personal backgrounds enabled me to brighten my horizon in many different ways, contributing to an intellectual as well as personal growth, for which I am incredibly thankful. Without my high-performance team, this thesis would not have been possible – thank you.

Especially, I would like to express my heartfelt gratitude to my parents, Karin and Christian, who have made this life journey possible for me and supported me in every matter of life.

In addition, special thanks go to my grandparents, Helga and Karl, as well as to my entire family that stood with me.

I also want to thank my girlfriend Selina Flechsenhar for giving me the support I needed during these sometimes-rough times.

In closing, I would like to thank everybody once again that stood by me during these peculiar and eventful times, going through a pandemic, a resurrected cold war and everything else that happened.

Abstract

The introduction of Industry 4.0 in 2011 resulted in a paradigm shift in the industry that continues to this day. In the course of this digital transformation, established or newly developed technologies have been implemented in the industry and corresponding concepts have been discussed scientifically, yet specific digitalization approaches for the metal forming industry are not sufficiently addressed.

As an initial step, a literature review on the state of the art was conducted to evaluate the current state of digitalization and digital transformation in the manufacturing industry in relation to the value chain and individual companies. The lower level of digitalization in Small and Medium Sized Enterprises (SMEs) compared to other industries is due to machinery that is often no longer up to date, the digitalization of which nevertheless is economically sensible. To also be able to integrate SMEs into a digitalized value chain, standardized yet individual digitalization concepts must be developed, which is why the MUL 4.0 project was initiated - an interdisciplinary cooperation to depict the digitalization of an industry-related value chain. In order to best design the digitalization solutions for SMEs, the machines and aggregates were equipped with suitable low-cost sensors, data acquisition systems and software for process simulation and prediction, transforming them into Cyber Physical Production Systems. Due to the high complexity and high diversity of forming operations, different process modeling approaches were applied, which were realized by specially developed real-physics numerical simulations and data-driven Machine Learning models. Furthermore, Graphical User Interfaces were developed to enable Human Machine Interaction, visualizing relevant information and thus supporting the decision-making process. In order to be able to map the digitalized value chain and to ensure the data governance and interoperability of the cooperating entities, a superordinate production network incorporating a Data Base Management System was implemented. For all solution approaches, open-source programming language were used to the highest possible extent due to the high interoperability and connectivity to other software solutions, avoiding interface problems and the resulting proprietary solutions. As a result of this work, a standardized framework was developed, applicable for the digitalization of SMEs in the metal forming industry. This framework was developed with a special focus on open-source programming languages, cost-effectiveness, standardization and resilience to support SMEs in this industry with the implementation of Industry 4.0, to increase the sustainability of products and processes, and to ensure economic competitiveness in the future.

Kurzfassung

Die Konzeptvorstellung der Industrie 4.0 im Jahre 2011 hatte einen bis heute anhaltenden Paradigmenwechsel in der Industrie zur Folge. Im Zuge dieser digitalen Transformation wurden etablierte oder neue entwickelte Technologien in der Industrie implementiert und entsprechende Konzepte wissenschaftlich diskutiert, dennoch wird nicht ausreichend auf spezielle Digitalisierungsansätze für die umformtechnische Industrie eingegangen.

Als initialer Schritt wurde eine Literaturrecherche zum Stand der Technik durchgeführt, um den aktuellen Stand der Digitalisierung und digitalen Transformation in der Fertigungsindustrie in Bezug auf die Wertschöpfungskette und Einzelunternehmen zu evaluieren. Der geringere Digitalisierungsgrad in kleinen und mittleren Unternehmen (KMUs) ist im Vergleich zu anderen Branchen auf einen oft nicht mehr zeitgemäßen Maschinenpark zurückzuführen, deren Digitalisierung dennoch wirtschaftlich sinnvoll ist. Um auch KMUs in eine digitalisierte Wertschöpfungskette integrieren zu können, müssen standardisierte aber dennoch individuelle Digitalisierungskonzepte entwickelt werden, weshalb das Projekt MUL 4.0 initiiert wurde - eine interdisziplinäre Kooperation, um die Digitalisierung einer industrienahen Wertschöpfungskette abzubilden. Um die Digitalisierungslösungen bestmöglich auf KMUs auszulegen, wurden die Maschinen und Aggregate mit geeigneten kostengünstigen Sensoren, Datenerfassungssystemen und Software zur Prozesssimulation und -vorhersage ausgestattet und diese in Cyber Physical Production Systems transformiert. Aufgrund der hohen Komplexität und hohen Vielfalt von Umformoperationen wurden verschiedene Ansätze zur Prozessmodellierung verfolgt, welche durch speziell entwickelte realphysikalische numerische Simulationen und datengetriebene Machine Learning-Modelle realisiert wurden. Weiterführend wurden grafische Benutzeroberflächen entwickelt, um die Mensch-Maschine-Interaktion zu ermöglichen, prozessrelevante Informationen zu visualisieren und damit den Entscheidungsfindungsprozess zu unterstützen. Um die digitalisierte Wertschöpfungskette übergreifend abbilden zu können und die Datenverwaltung sowie Interoperabilität der kooperierenden Entitäten zu gewährleisten, wurde ein übergeordnetes Produktionsnetzwerk mit eigenem Datenbankmanagementsystem implementiert. Für alle Lösungsansätze wurde im höchstmöglichen Ausmaß Open-Source-Programmiersprachen verwendet, um durch die hohe Interoperabilität und Konnektivität zu anderen Softwarelösungen eine Schnittstellenproblematik und die daraus resultierenden proprietären Lösungen vermeiden zu können. Als Resultat dieser Arbeit wurde ein standardisiertes Framework entwickelt, welches für die Digitalisierung von KMUs in der Umformtechnikindustrie anwendbar ist. Dieses Framework wurde unter speziellem Fokus auf Open-Source-Programmiersprachen, Wirtschaftlichkeit, Standardisierung und Resilienz entwickelt, um KMUs in dieser Industrie bei der Industrie 4.0-Implementierung zu unterstützen, die Nachhaltigkeit von Produkten und Prozessen zu erhöhen, sowie die wirtschaftliche Wettbewerbsfähigkeit auch in Zukunft zu gewährleisten.

Table of Contents

Abbreviations

AI	Artificial Intelligence
AMQP	Advanced Message Queuing Protocol
AR	Augmented Reality
BBM	Black Box Model
CC	Cloud Computing
CoAP	Constrained Application Protocol
CPPS	Cyber Physical Production System
CPS	Cyber Physical System
DAQ	Data Acquisition System
DBMS	Data Bank Management System
DDS	Data Distribution Service
DG CLIMA	European Union's Directorate-General for Climate Action
DM	Digital Model
DS	Digital Shadow
DT	Digital Twin
EBITDA	Earnings Before Interest, Taxes, Depreciation, and Amortization
ERP	Enterprise Resource Planning
FEA	Finite Element Analysis
FVA	Finite Volume Analysis
GBM	Grey Box Model
GDP	Gross Domestic Product
GUI	Graphical User Interface
GVA	Gross Value Added
GVC	Global Value Chain
HMI	Human Machine Interaction
I 4.0	Industry 4.0
ICT	Information and Communication Technology
IIoT	Industrial Internet of Things
IL	Chair of Industrial Logistics
IoT	Internet of Things
JC	Johnson Cook
KPI	Key Performance Indicator
LUS	Laser Ultra Sonics
M	Institute of Mechanics

Abbreviations

MES	Manufacturing Execution System
MF	Chair of Metal Forming
ML	Machine Learning
MQTT	Message Queuing Telemetry Transport
MUL	Montanuniversität Leoben
NFM	Chair of Nonferrous Metallurgy
NIST	National Institute of Standard and Technology
OEE	Overall Operational Effectiveness
OEMs	Original Equipment Manufacturers
OPC UA	Open Platform Communications Unified Architecture
PHP	Hypertext Preprocessor
PLC	Programmable Logic Controllers
PLM	Product Lifecycle Management
PM	Project Management
QC	Quality Control
QMS	Quality Management Systems
R&D	Research and Development
RAMI 4.0	Reference Architecture Model Industry 4.0
RFID	Radio-Frequency Identification
SCADA	Supervisory Control and Data Acquisition
SME	Small and Medium Sized Enterprise
SQL	Structured Query Language
UDP	User Datagram Protocol
VR	Virtual Reality
WBM	White Box Model

List of Publications

This thesis is built upon the following peer reviewed manuscripts and conference proceedings. All listed publications were written in the course of this doctoral thesis at the Chair of Metal Forming at the Montanuniversität Leoben and are attached in A (Associated Publications).

(A 1) Publication 1   M. Sorger, B.J. Ralph, K. Hartl, M. Woschank, M. Stockinger: 'Big Data in the Metal Processing Value Chain: A Systematic Digitalization Approach under Special Consideration of Standardization and SMEs', in: *Applied Sciences* 2021, 11, 9021, doi: 10.3390/app11199021.

(A 2) Publication 2   M. Sorger: 'Quality 5.0 - A data-driven path towards zero waste', in: *XL. Colloquium on Metal Forming*, pp. 06-12, 03.2022, ISBN: 978-3-902078-27-8.

(A 3) Publication 3   B.J. Ralph, M. Woschank, P. Miklautsch, A. Kaiblinger, C. Pacher, M. Sorger, H. Zsifkovits, M. Stockinger: 'MUL 4.0: Systematic Digitalization of a Value Chain from Raw Material to Recycling', in: *Procedia Manufacturing*, Volume 55, pp. 335-342 04.2021, doi: 10.1016/j.promfg.2021.10.047.

(A 4) Publication 4   B. J. Ralph, M. Sorger, B. Schödinger, H.-J. Schmölzer, K. Hartl, M. Stockinger: 'Implementation of a Six-Layer Smart Factory Architecture with Special Focus on Transdisciplinary Engineering Education', in: *Sensors*, 21(9), 2944, 04.2021, doi: 10.3390/s21092944.

(A 5) Publication 5   B.J. Ralph, M. Sorger, K. Hartl, A. Schwarz-Gsaxner, F. Messner, M. Stockinger: 'Transformation of a rolling mill aggregate to a cyber physical production system: from sensor retrofitting to machine learning', in: *Journal of Intelligent Manufacturing* 2022, 33, 493–518, doi: 10.1007/s10845-021-01856-2.

(A 6) Publication 6   M. Sorger, B.J. Ralph, K. Hartl, C. Waiguny, B. Schödinger, M. Schoiswohl, M. Stockinger: 'Transformation of a hydraulic press and furnaces into a Cyber Physical Production System: a brownfield approach from sensor retrofitting to Digital Shadow under special

consideration of predictive maintenance and sustainability', in: *Journal of Intelligent Manufacturing*, under review

(A 7) Publication 7	B.J. Ralph, K. Hartl, M. Sorger, A. Schwarz-Gsaxner, M. Stockinger: 'Machine Learning Driven Prediction of Residual Stresses for the Shot Peening Process Using a Finite Element Based Grey-Box Model Approach', in: *Journal of Manufacturing and Materials Processing,* 5(2), 39, 04.2021, doi: 10.3390/jmmp5020039.
(A 8) Publication 8	K. Hartl, M. Sorger, H. Weiß, M. Stockinger: 'Machine learning driven prediction of mechanical properties of rolled aluminium and development of an in-situ quality control method based on electrical resistivity measurement', in: *Journal of Manufacturing Processes*, under review
(A 9) Publication 9	K. Hartl, M. Sorger, M. Stockinger: 'The Key Role of Laser Ultrasonics in the Context of Sustainable Production in an I 4.0 Value Chain', in: *Applied Sciences* 2023, 13(2), 733, doi: 10.3390/app13020733.

In addition, further manuscripts distantly related to this thesis were published in cooperation with other researchers from other technical fields, emphasizing the interdisciplinary nature of digitalization and I 4.0.

Additional Publication 1	M. Woschank, B.J. Ralph, A. Kaiblinger, P. Miklautsch, C. Pacher, M. Sorger, H. Zsifkovits, M. Stockinger, S. Pogatscher, T. Antretter, H. Antrekowitsch: 'MUL 4.0 – Digitalisierung der Wertschöpfungskette vom Rohmaterial bis hin zum Recycling', *Berg Huettenmaennische Monatshefte* 166, 309–313 (2021), doi: 10.1007/s00501-021-01119-w.
Additional Publication 2	I. Hartl, M. Sorger, B.J. Ralph, K. Hartl: 'Passive seismic monitoring in conventional tunnelling – an innovative approach for automatic process recognition using support vector machines' in: *Tunnelling and Underground Space Technology incorporating Trenchless Technology Research*, doi: 10.1016/j.tust.2023.105149.

Additional Publication 3	A. Janda, B.J. Ralph, Y. Demarty, M. Sorger, S. Ebenbauer, A. Prestl, I. Siller, M. Stockinger, H. Clemenes: 'Ballistic tests on hot-rolled Ti-6Al-4V plates: Experiments and numerical approaches', in: *Defence Technology* 2022, doi: 10.1016/j.dt.2022.11.012.

Furthermore, six bachelor theses and seven master theses were supervised during this doctoral thesis.

Bachelor theses:

1. M. Pfeiffer: 'Linearzuführung zur Verbesserung der Wiederholgenauigkeit der Einzugspositionierung von Walzgut', 03.2021.

2. A. Begovic: 'FE-Parameterstudie eines thermomechanisch gekoppelten Stauchversuches in Abaqus', 04.2021.

3. S. Fichtenbauer: 'Konzipierung, Entwicklung und Implementierung einer Softwarelösung für die automatische Datenverwaltung mittels SQL-Datenbank in einer Industrie 4.0-Umgebung', 11.2021.

4. K. Singnurkar: 'Evaluation of a method for toolless deburring of closed-die forgings', 02.2022.

5. G. Schlemmer: 'Experimentelle Untersuchung eines skalierten Kaltrückwärtsfließpressversuchs mit EN AW-6082-F', 05.2022.

6. O. Lamik: 'Design and experimental validation of a Finite Element Analyses based Digital Model of a Rolling Mill', Work in progress.

Master theses:

1. F. Messner: 'Implementierung eines Low-Cost Human-Machine Interfaces in ein Cyber Physical Production System', 05.2021.

2. D. Roth: 'Konzipierung und Auslegung einer Druckautoklavenanlage für Hochdruckanwendungen in der additiven Fertigung', 06.2022.

3. C. Waiguny: 'Implementation of automated, interconnective Finite Element Analyses for the development of Cyber Physical Production Systems', 10.2022.

4. T. Höfer: 'Konzipierung und Entwicklung eines standardisierten Tiefkühlbehälters für Logistikanwendungen', 11.2022.

5. S.T. Özdemir: 'Entwicklung einer Support Vector Machine zur Eventklassifizierung und -detektion im Bergbau', 11.2022.

6. D. Müller: 'Implementierung eines zentralen Data Acquisition Systems und Softwarelösung zur Datensynchronisation einer Induktionsprüfanlage', 02.2023.

7. M. Schoiswohl: 'Prozessportfolioerweiterung von fließgepressten Aluminium-Abrollkolben für PKW-Luftfedersysteme in einem KMU', Work in progress.

1. Introduction

The fourth industrial revolution has unleashed a fundamental digital paradigm shift, implying and accelerating several drastic changes in the manufacturing industry [1]. The premises of the third industrial revolution automation persist and undergo further refinement supported by new data-driven approaches and technologies. Thus, the Industry 4.0 (I 4.0) implies the increased integration of established and innovative Information and Communication Technology (ICT), such as Machine Learning (ML), Artificial Intelligence (AI), Industrial Internet of Things (IIoT) and Cloud Computing (CC) [2,3]. As a result, the holistic implementation and application of these I 4.0 enabler technologies boost higher productivity, efficiency, competitiveness and sustainability, and the overcoming of various long-standing obstacles to realize a highly automated industry [4,5].

In order to unlock the full potential of the digital transformation, the highly scalable and networked nature of these new technologies makes it imperative to broaden the focus from locally isolated to more global networked solutions [3,4]. For this reason, all value creating production steps of a product of a value chain must be interconnected and networked, allowing transparent data sharing to improve the overall operational effectiveness (OEE) and sustainability of the corresponding value chain [2]. Additionally, more frequent disruptions of global value chains (GVCs) due to shocks, such as COVID-19 or dynamic political changes, accelerate the digital transformation.

Nevertheless, many industries, such as the heavy industry, are still facing obstacles to implement I 4.0 technologies and the necessary ICT infrastructure. In the case of the manufacturing industry, a significant share of value-adding enterprises are Small and Medium Sized Enterprises (SMEs), that have to be incorporated in the digital value chain, enabling a holistic digital transformation by avoiding disruptions along the value chain. Although these SMEs receive the smallest benefit when displayed as a single entity, they have to adapt to the digital transformation to be able to meet future requirements and not be forced out of the market. Furthermore, manufacturing SMEs are obligated to use norms and standards, as they are considered a necessity by customers to be eligible as a supplier. For example the ISO 9001, specifying the requirements of a quality management system. In the context of ICT security, the ISO/IEC 27001 serves as rulebook for establishing, implementing, maintaining and continuously improving an information security management system, and the ISO/IEC 27017 provides guidelines for information security controls for CC. Regarding sustainability, the ISO 14001 provides requirements for an Environmental Management System. The reason for the application of these norms and standards is important for various aspects, such as the quality assurance, risk management, legal compliance, and can therefore also be seen as a competitive advantage. Conversely, key questions regarding data governance have to be clarified. Thus, to fully leverage I 4.0 in GVCs, special but standardized approaches to ensure effective interconnection have to be made as SMEs often face financial and technical obstacles implementing these technologies. Obstacles faced are the transparency and standardization of a digital value chain, concerning data governance between the different entities of a

value chain. Thus, cyber security plays an increasingly important role in order to protect the value chain from cyber attacks and the resulting damage. In essence, value chains in general have to become more resilient in order to be able to withstand and recover from shocks. Besides the technical aspects, the digital transformation also affects the organization and business model of the respective enterprises, changing the way of working. The sustainable implementation and application of I 4.0 requires skilled workers, having several practical socioeconomic implications that have to be taken into account [1]. First, the increasing degree of digitalization reduces the need for manual labor, favoring the reshoring of production to high-wage countries. Furthermore, the increasing need for knowledge-intensive work urges enterprises to invest in tech talent and enrich a positive corporate culture. As a result, a shift from material to intangible assets has been evident. As a further premise, the digital transformation enables more sustainable production and a circular economy, reducing waste along the value chain as a result of the data-driven product and process optimization enabled by I 4.0.

Concluding, to fully leverage I 4.0, which can only be done by a transparent and interconnected value and supply chain, standardization and frameworks for the effective interconnection are imperative. For this reason, this thesis aims to present a holistic and applicable framework for the digitalization of a value chain with special focus on the metal forming industry, being a significant part of the heavy and manufacturing industry, accounting for a significant 18.8 % of the Austrian Gross Domestic Product (GDP) in 2021 [6], and thus ensure the future economic competitiveness of this industry. In order to accomplish this goal, a literature study was conducted, identifying the key enablers of I 4.0 necessary for a holistic digital transformation of a value chain. Building on the findings of the literature study presented in section two, the research questions were derived. Consequently, section three presents how each respective research question was approached, specifying the individual contributions of the published manuscripts to answer the research question. In section four, the scientific contributions and the resulting contribution to the reduction of the research gap is outlined and discussed. In section five, a conclusion and an outlook is presented.

2. State of the art, identified research gaps and resulting research questions

The advancement of I 4.0 has led to the establishment of new technical terms, which have been elaborated ever since. Nevertheless, the definition of key enablers and technologies still shows inconsistency, which furthermore depend on the field of application and industry. Serving as the initial step, a literature study was conducted, identifying I 4.0 key enablers and technologies in the manufacturing industry and presenting the respective state of the art definitions of current literature [3,7–12]. As a result, the analysis of current literature concluded that the following key technologies are crucial for a successful and holistic digitalization and digital transformation [3]:

- Industrial Internet of Things (IIoT)
- Cyber Physical Production Systems (CPPS)
- Visualization Technologies
- Cloud Computing (CC)
- Digital Model (DM), Digital Shadow (DS), Digital Twin (DT)
- Artificial Intelligence (AI) and Machine Learning (ML)
- Big Data

Generically, the IIoT refers to the connection of physical objects through the internet [13]. In the course of this thesis, the refined definition according to Boyes et al. [14] was used: *'A system comprising networked smart objects, cyber-physical assets, associated generic information technologies and optional cloud or edge computing platforms, which enable real-time, intelligent, and autonomous access, collection, analysis, communications, and exchange of process, product and/or service information, within the industrial environment, so as to optimise overall production value. This value may include; improving product or service delivery, boosting productivity, reducing labour costs, reducing energy consumption, and reducing the build-to-order cycle.'*

The CPPS is defined as an interconnected physical and virtual system, capable of controlling and coordinating processes through the means of real-time data gathering, analyzing and sharing through the IIoT [3,14]. The definition of CPPS is further concretized by Cardin et al. and Wu et al. [15,16] with three characteristics and extended by Ralph et al. [17] by two more characteristics, specially tailored to SMEs in the metal processing industry.

1. CPPS are superordinate systems within systems. Thereby, the data exchange across process steps and further process adaptations in the value chain are enabled.
2. CPPS are composed of connected and cooperative elements, capable of adjusting the data transfer situationally appropriate on and between different layers of a production environment.

3. CPPS enhance real-time decision-making and act state dependent. This can be supported by various modeling approaches, enabling real-time predictions based on process parameters and provide recommendations for adaptation.

4. CPPS incorporate user-centered and tailored to the application Human Machine Interfaces (HMIs), also supporting the decision-making process.

5. CPPS exhibit low cost and resilient design. Therefore, exhibiting a suitable combination of low-cost and high-quality hardware and software components under simultaneous consideration of environmental conditions

Complimentary, Visualization Technologies support the reintegration of specific information in the physical world, thus supporting real-time decision-making across all hierarchy layers. Hereby, the visualization can be realized with Graphical User Interfaces (GUIs), Augmented Reality (AR) and Virtual Reality (VR) [13].

According to the National Institute of Standard and Technology (NIST), CC can be defined as [18]: *'A model for enabling convenient, on-demand network access to a shared pool configurable computing resources (e.g., networks, servers, storage, application, and services) that can be rapidly provisioned and released with minimal management effort or service provider interaction'.*

The technology of DM, DS and DT refers to a virtual representation of a physical entity, whereas a differentiation depending on the degree of automated connectivity and thus data transfer between the physical and digital entity has to be made. The DM has no automated connectivity between both entities. Continuing, the DS features a unilateral automated data transfer from one entity to another. Conclusively, the DT exhibits a bilateral automated communication between both entities [3]. Further differentiations have to be made depending on the field of application. Compared to logistics, where a DT for supply and value chains can be considered as more advanced [19–21], the heavy industry is dealing with complex and strongly varying process simulations, e.g. using Finite Element Analysis (FEA) [22]. For this reason, different modeling approaches can be applied, depending on a variety of aspects. Data-driven black box models (BBM) in combination with AI and ML have the potential to substitute complex and time-consuming simulations, but have the disadvantage of requiring a huge amount of data and may be less reliable with highly heterogeneous manufacturing process steps, as compared to real-physics based white box models (WBM). Thus, the combination of both models into a grey box model (GBM) can be seen as a favorable modeling approach, benefitting from the advantages of both models [3].

AI emulates the human intelligence with the superordinate goal of situationally appropriate autonomous decision-making and acting. In addition, ML is a sub-discipline of AI using computational algorithms with the goal to enhance the AI with training data, making it more adaptable, precise and accurate without human interference [13,23–25]. Per definition, AI can be integrated into DM, DS and DT, thus acting as a technology enabler, to substantially enhance the benefit of these technologies.

According to Mills et al. [26], Big Data can be defined as '*large volumes of high velocity, complex and variable data that require advanced techniques and technologies to enable the capture, storage, distribution, management, and analysis of the information*'. As concluded by Sorger et al. [3] in Publication 1 (A 1), a characterization using the 5Vs of Big Data – Volume, Velocity, Variety, Veracity and Value - can be made. In summary, a volume of a least one Petabyte [27] must be processed and continuously or discretely transferred at high speeds. Furthermore, the variety arises from structured, semi-structured and unstructured data, which has to have a certain veracity in order to gain value from the analysis of the data [28–30].

Owing to the impact of I 4.0 and the global situation in recent years, the progressing digital transformation has not only produced locally isolated solutions, but also caused a rethinking of the global interplay and connectivity of value chains. Hereby, a value chain is defined by all material and intangible activities, inputs and steps which are required to produce and deliver a final product or service [31,32]. In order to produce a final product, various steps spanning various enterprises and countries are required, embossing the term of the GVC. Thereby, 70% of today's global trade includes GVCs [32]. Thus, the result of a digital value chain is a network of all value creating steps and enterprises involved in the creation of a product along a value chain, enabling the omnipresent monitoring of processes and products and thus prediction and adjustment of value chains to changing conditions [33,34]. Therefore, a holistic digitalization and digital transformation of entire value chains enables huge benefits in terms of flexibility, circularity and sustainability [1,35].

Logically, the enablers of a digital value chain are congruent with I 4.0 enablers, but face additional value chain specific obstacles. As current literature shows, the main barriers to overcome and enablers include [12,21,36–39]:

- Information and Communication Technology (ICT) infrastructure
- Cyber security
- Transparency
- Real-time monitoring
- Simulations (DT, DS, DT)
- AI and ML
- Quality Control (QC)
- Automation, Advanced Robotics and collaboration

The ICT infrastructure is a key factor for the holistic digital transformation of a value chain, as it is for I 4.0 itself. In order to be able to gather, analyze, share and utilize data, a suitable ICT infrastructure is imperative, e.g. enabling the communication of CPPS and DT through the IIoT, and analyzing Big Data with CC resources. The NIST defines the term of cyber infrastructure as follows [40]: '*Includes electronic information and communications systems and services and the information contained in these systems and services. Information and communications systems and services are composed of all hardware and software that process, store, and communicate information, or any combination of all of*

these elements. Processing includes the creation, access, modification, and destruction of information. Storage includes paper, magnetic, electronic, and all other media types. Communications include sharing and distribution of information. For example: computer systems; control systems (e.g., supervisory control and data acquisition–SCADA); networks, such as the Internet; and cyber services (e.g., managed security services) are part of cyber infrastructure'. Therefore, this thesis defines the ICT infrastructure as everything tangible and intangible, e.g. hardware and software, which enables information distribution in and between systems.

Acting as the integral connective link of ICT, protocols enable communication and interoperability between different systems. The selection of a protocol depends on several factors, including standardization, compatibility, bandwidth, efficiency, scalability and security. Regarding standardization, protocols ensure that all systems are subject to the same rules and standards, thus enabling a uniform and transparent communication. Depending on the different hardware and software of the system, the compatibility with the respective protocol must also be determined, ensuring the communication with other systems. Furthermore, the protocol must depict high efficiency to transfer data quickly and securely. Additionally, protocols also must be able to be compatible with different amounts and types of data, concerning the factor of scalability. Established protocols used in I 4.0 are [41–48]:

- Open Platform Communications Unified Architecture (OPC UA) is a platform-independent protocol, enabling communication between systems in a manufacturing environment. OPC UA offers secure and reliable data exchange between systems, compatible with a wide range of operating systems and programming languages.

- Message Queuing Telemetry Transport (MQTT) is referred to as a lightweight protocol created for the machine-to-machine communication in Internet of Things (IoT) environments, using a publish-subscribe model to enable systems to send and receive messages, supporting reliable and efficient data transfer even with low-bandwidth or unreliable network conditions.

- Advanced Message Queuing Protocol (AMQP) is designed for message-oriented middleware environments, where applications must send and receive messages asynchronously. AMQP supports reliable message delivery, transactions, as well as other features, and is compatible with a wide range of messaging platforms and programming languages.

- Constrained Application Protocol (CoAP) is a lightweight protocol specifically designed for IoT environments, incorporating systems with limited processing power or memory. For this task, the User Datagram Protocol (UDP) is utilized for data transfer, and other operations.

- Data Distribution Service (DDS) is made for real-time, distributed systems, requiring high performance and reliability, using a publish-subscribe model to enable data sharing across systems, also supporting control over data delivery and quality of service.

To provide a structured way to store, manage, and retrieve data generated by various sources, Data Bank Management System (DBMS) are imperative. Due to I 4.0, requirements for DBMSs have increased,

making efficient data management, real-time processing, advanced analytics, and high degree of connectivity and compatibility. Similar to protocols, the selection of a DBMS is highly dependent on the set requirements. Established DBMS and their respective capabilities in I 4.0 include [49–60]:

- Relational DBMSs are the most commonly used type of DBMS in I 4.0, using a relational model to arrange data into tables, supporting Structured Query Language (SQL) for data querying and manipulation. Examples include MySQL, Oracle, SAP HANA, Microsoft SQL Server, PostgreSQL, and MariaDB.

- Time Series DBMSs are designed to store and manage time-series data, e.g. data generated by sensors. Time Series DBMS is optimized for fast data processing and real-time processing. Time Series DBMSs examples are InfluxDB, TimescaleDB, and OpenTSDB.

- Graph DBMSs are used to store and manage graph data, such as network and supply chain data, allowing complex data relationships to be easily queried and modeled. Examples are Neo4j, OrientDB, and ArangoDB.

- Document DBMSs are utilized to store and manage unstructured or semi-structured data, such as JSON and XML data, enabling fast and flexible data modeling and querying. Examples of Document DBMSs are MongoDB, CouchDB, and RavenDB.

- Object-Oriented DBMSs are designed to store and manage object-oriented data, such as object-oriented programming language data structures, enabling efficient object storage and retrieval. Examples of Object-Oriented DBMSs include db4o and ObjectStore.

Due to the interconnected and data-driven nature of the I 4.0 enabler technologies, cyber security plays and increasingly important role [61]. According to the NIST, cyber security can be defined as *'the ability to protect or defend the use of cyberspace from cyber attacks'*, whereas cyber attacks are *'an attack, via cyberspace, targeting an enterprise's use of cyberspace for the purpose of disrupting, disabling, destroying, or maliciously controlling a computing environment/infrastructure; or destroying the integrity of the data or stealing controlled information'* [40]. Concluding, cyber security is applied to protect information, software and hardware from misuse and unauthorized access. As concluded by Lezzi et al. [62], successful cyber attacks and the resulting unauthorized access can lead to the disclosure, disruption, modification or destruction of data or denial of service of networks and computers. As in case of a value chain, this could result in downtime or malfunctions and thus in delays in the entire value chain [33]. The volatility of the resilience of the entire value chain is higher as the resilience of the interconnection within all value chain entities, and thus just as strong as the weakest IT-secured entity within. In further consequence, this vulnerability could lead to trust issues of the individual participants of the value chain and thus also endanger transparency, being one of the major enablers in order to fully depict a digital value chain. As it is often the case, data resides in silos without being managed or analyzed for insights, e.g. in Enterprise Resource Planning (ERP) systems [63]. Therefore, relevant data has to identified and transparently shared throughout the entire product lifecycle, starting with the mining and production of the raw material to the end of the life cycle of the product [64]. As a

consequence, enterprises need to critically scrutinize key questions in terms of data governance in order to provide relevant data to the value chain and conversely reintegrate value chain inputs into the enterprise's processes [65]. Consequently, the aspect of standardization of I 4.0 technologies and communication are a key aspect to support a holistic digital transformation. Therefore, a framework like Reference Architecture Model Industry 4.0 (RAMI 4.0) provides a structured approach for the implementation of I 4.0 technologies, specifying utilized assets along the product life cycle and value stream, hierarchy levels and layers (Figure 4) [3].

Therefore, the transparency and collaboration between the participants of a value chain to some extent requires (near) real-time monitoring [66]. A comprehensive and detailed view of the value chain has to be mapped, identifying all steps and interrelationships along the value chain [64]. As a result, a seamless and transparent data flow can be enabled, allowing an omnipresent real-time monitoring and a simultaneous data gathering of both processes and product, resulting in several practical beneficial implications for the application of AI, ML and QC [25,33,64,66].

In combination with a control tower system, referring to a centralized platform that provides real-time visibility and control over a wide range of business operations, the enterprise-wide real-time monitoring enables end-to-end planning of processes, identification of disruptions, bottlenecks and potential threats to the supply chain, thus increasing the flexibility, efficiency and sustainability [64,66]. As stated by Lund et al. [64], General motors uses a real-time monitoring system to map the flow of products and processes, in order to take action in the case of disruptions, tracking affected products and preventing potential bottlenecks. For this purpose, Product Lifecycle Management (PLM) is an essential process, managing the entire lifecycle of a product, and improving product quality [67]. Despite the benefits PLM software offers, it may not always be applicable for manufacturing SMEs, concerning high costs and complexity in interplay with limited product range and quantity produced, resulting from the low-volume high-complexity tasks. Nevertheless, manufacturing SMEs can adopt alternative software approaches such as Quality Management Systems (QMS), lean manufacturing, or agile manufacturing [68]. Despite PLM and QMS being different systems, QMS and the integrated QC processes can help to manage and improve the quality of products and processes, and serve as a cost-effective alternative software solution for SMEs. Since many manufacturing SMEs perform low-volume high-complexity tasks, the open-source approach enables high modularity and customization to the respective products and processes, resulting in higher flexibility and comparatively low costs, compared to commonly used PLM software.

To support the monitoring, control and optimization of value and supply chains, simulations and other modeling approaches can be utilized. As aforementioned, simulations can be realized using a BBM, WBM and GBM approach. Furthermore, a differentiation depending on the automation of connectivity and thus data transfer between the physical and digital entity can be made, therefore referring to it as either a DM, DS or DT. In the field of manufacturing, simulations are utilized to validate and optimize products and processes, enabling cost reduction, quality improvements and thus waste reduction [1,13],

also incorporating real-time product data for value chain planning and optimization purposes [69,70]. Thus, simulations and analyses provide insights of potential static or dynamic choke points, bottlenecks and its root causes. Additionally, insights about correlations, dependencies and strategic decisions across the entire value chain can be incorporated to better manage and optimize the value chain [66].

Further technologies with value creating capabilities are AI and ML. In essence, AI can help increase the resilience and efficiency of a value chain with analytics-based forecasting, DT value chain simulations and optimization [66]. By utilizing sophisticated AI in a value chain, production planning can be optimized with AI-based transparent end-to-end planning, thus increasing the overall efficiency [66]. Furthermore, the evaluation of risks and uncertainties can be significantly increased, supporting real-time decision-making [66]. As a result of a holistic digital transformation and value chain transparency, the appropriate acting to unplanned events and changing circumstances can lead to the prevention of disruptions [66,71]. As stated by Bosche et al. [25], a technology company developed a QC system, using computer-vision technology, AI, robotics powered by CC, boosting the detection of defective products from 20% to over 99%. Henceforth, this advancement does not only improve the overall process and product quality, but also reduces downtimes and delays in the value chain [25].

Enabled by the omnipresent real-time monitoring, the QC of the product undergoes a disruptive change. As classical QC approaches project the quality of an inspected sample onto the entire population of products, the real-time data enabled QC can evaluate the quality of every individual product [33]. The data of the simultaneous monitoring of product and process can be linked and evaluated for correlations and conclusions about quality can be derived [39,72]. For this purpose, machine vision in combination with AI and ML can be utilized to classify the quality of products, additionally implementing tracking technologies like bar codes or RFID [73]. By implication, root causes for non-compliance of the product quality can be identified. In conjunction with a high level of transparency, the entire value chain can be optimized by analyzing and reintegrating data from the entire life cycle of the product. The optimization also reduces waste, thus increasing the overall sustainability [1,33,39,73–75]. Fueled by the global impact of COVID-19 and the occurrence of further market volatilities, the improvement of the resilience of value chains as well as focusing on environmental footprint reduction has become increasingly important [64,76]. A holistic digital transformation has the potential to fulfill both of these goals. In the case of the heavy industry, it takes many processing steps of globally acting enterprises to produce a finished product [64]. As past years have shown, these GVCs, initially designed on overall cost effectiveness, impose increasing financial risk due to the current VUCA (Volatility, Uncertainty, Complexity, and Ambiguity) environment, for example the impact of the value chain problems in the semiconductor industry on the European automotive industry [77]. As evaluated by Lund et al. [64], disruptions due to cyber attacks lasting over a month are expected to occur every 3.7 years on average, whereby enterprises are estimated to lose 40% of a year's profit every decade on average. Due to the highly connected nature of GVCs, changes regarding locations are often complex, as they can spawn thousands of enterprises under multifaceted geographical and economic circumstances e.g., access to

customer markets, customer relationships and specialization. In summary, the closest thought of relocation is associated with a number of complex factors and thus leads to the alternative of improving the resilience of GVCs. As stated by Camonita et al. [78], recent global developments, such as the Ukraine war, and business closures as a consequence of the pandemic can be seen as a strategic opportunity. Nevertheless, the associated considerable investments are a significant obstacle, compounded by high inflation and the European energy transition trough RED III. Necessary steps for building more resilient GVCs include improving transparency and risk management, including establishing redundancy in supplier networks, increasing stock inventory, creating backup production locations, improving the abilities to deal with shocks and recover from them, as well as other activities [64]. Another development in recent years was outlined by Lund et al. [31], revealing that output and trade increase in absolute terms, but the trade intensity in good-producing value chains decreases as data and service flow play an increasing role in today's global economy. Additionally, GVCs become more knowledge-intensive, whereas low-skill labor is in decline. In fact, global goods trade is not dominated by labor [31]. As stated by Lund et al. [31], this can be attributed to three factors. First, the growing demand of the developing world increases the consumption of the domestic production. Second and third being the trend of reshoring results in more domestic value chains reducing imports [31], being a consequence of the digital paradigm change and utilization of new technologies as result of I 4.0. Due to recurring disruptions in 2020, 76% of enterprises reinforced the application of digital network technologies [63].

The enterprises participating in GVCs can be divided into small, medium and large enterprises. As defined by the European Commission [79,80], these enterprises can be defined by their number of employees, and annual revenue or balance sheet total (Table 1). In Europe, SMEs make up a portion of 99% of all enterprises contributing to over 50% of the added gross value in Europe [13,81]. Focusing on Austria, enterprises specialized on manufacturing represent 18.8% of the industry [82], whereby 99.7% of these enterprises are SMEs [83].

Table 1. Definition of SMEs according to the European Commission [79,80].

Category	Number of employees [-]	Annual revenue [€]	Balance sheet total [€]
Medium enterprise	< 250	≤ 50 M	≤ 43 M
Small enterprise	< 50	≤ 10 M	≤ 10 M

Historically, new technologies open up new opportunities, impose new challenges and promise benefits and advantages but also imply new threats, also applying to the heavy industry. According to Behrendt et al. [2], over 70% of enterprises struggle with implementing and scaling digitalization technologies and thus sustainable improvements. The digital transformation of enterprises and value chains is a multifaceted challenge, implying not only technical but also socio-economic changes. Research by Forth et al. [84] of 70 leading enterprises has shown, that 70% of all digital transformation did not fulfil their

individual set objectives, pointing out the importance of technology but also of the socioeconomic aspects. Thereof, 26% of enterprises fulfilled less than 50% of their objectives. Doing a little better, 44% of these enterprises did not fulfil their objectives, not creating long-term changes. In contrast, the successful 30% of enterprises either met or exceeded the objectives, creating sustainable and lasting changes (Figure 1). These successful digital transformations resulted in an average of 66% more value and an improvement of corporate capabilities by 82%. Furthermore, objectives were met 120% more frequently. Nevertheless, 80% of enterprises are planning to accelerate their digital transformation, pointing out the evidence of improvement of performance and competitive advantage [84]. Hereby, the short term benefits of a digital transformation include improvement of productivity and customer experiences, the medium term benefits open up business model innovation and thus growth opportunities, whereas the long term benefits is the mastering continuous innovation [84].
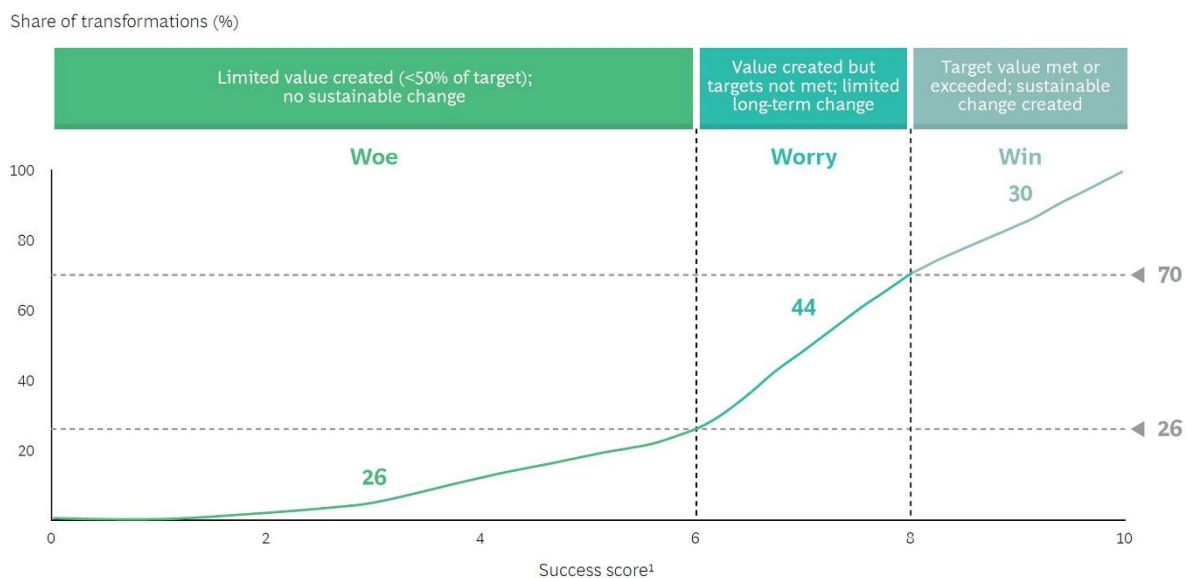
Fig. 1. Share of digital transformations creating no sustainable change (Woe), only limited long-term change (Worry) or sustainable change (Win) [84,85]

To successfully implement and operationalize these new technologies and support a successful digital transformation, a resilient and appropriate foundation has to be built to meet the new requirements. Serving as the foundation of I 4.0, the necessary ICT infrastructure has to be implemented in order to be able to participate in digital value chains and remain economically competitive [84]. ICT has already shown lasting effects in the past decades, but the impact of I 4.0 is estimated to be more complex [31]. As stated by Lund et al. [31], one major impact will be the reduction of transaction costs, supporting logistics, transportation and financing, thus increasing trade in services and goods. The second and third impact will concern production processes and products, due to utilization of the I 4.0 enabler technologies in combination with automation technology [31]. Leading enterprises have already at least partially started to upgrade existing infrastructure allowing the implementation of these new

technologies such as IIoT, CC and CPPS [76,84,86]. Through the utilization of I 4.0 technologies, a general improvement of the flexibility, agility, efficiency, optimization, modularity and sustainability of the respective enterprise and value chain is expected [38,87,88]. Although the term I 4.0 was already established in 2011, especially SMEs struggle with the implementation and application of I 4.0 technologies but steadily increase digitalization efforts [13,38,73,89]. According to Matt et al. and Müller et al. [13,90], this struggle is a result of a limited availability of resources, unclear strategies and insufficient access to external knowledge. Despite these difficulties a global study by McKinsey [91] surveyed 36 manufacturing companies about the impact of I 4.0 on their business. Highlight impacts include a reduction in resource consumption by more than a third while tripling throughput. Others increasing efficiency by more than 10%, reducing CO_2 emissions by 50%, and increasing quality by 300% while reducing costs by 20%.

Serving as nerve center of the networked digital industry, the IIoT is a highly scalable value-creating technology that is imperative for every digital transformation. By implementing resilient IIoT objects, all connected entities, such as CPPSs but also customers, are enabled to communicate near real-time, making a sufficient broadband network imperative [2]. This kind of networking is expected to deliver improvements in performance, flexibility, customer experience and to the reaction of shocks originating from GVCs [2]. Through the application of the 5G or 6G broadband network, data can be transferred at high speeds with low latency, enabling the further utilization of CC, Big Data, AI, ML and sophisticated simulations [2,36,92,93]. The access and computing resources to CC has been significantly improved in recent years, whereby the processing costs have decreased, facilitating the application for SMEs [2]. This is particularly favorable for SMEs with lower financial resources, as many CC companies offer different payment models and services. For instance, utilized computing resources can be paid on demand and thus, surplus financial resources can be used in other projects [94]. A global study conducted by Brinda et al. [94], revealed that enterprises that successfully adopted CC approached for things differently than their peers. First, successful adopters managed and analyzed data for insights, thus driving improvements. Second and third, the reduction of assets and the outsourcing through partnerships serves as a scaler, moving the scalability from production to connection. In essence, the outsourcing of capabilities to collaborates enables faster scaling and is financial more beneficial than internal development. Fourth, the investment in tech talent helped them to develop the further potential of CC [94].

In order to gather and analyze data using CC, entities like shop floor CPPSs have to be connected through the IIoT. Depending on the field of application and enterprise, these CPPSs can be state of the art machines with integrated Programmable Logic Controllers (PLCs) or Data Acquisition Systems (DAQs) or old machines without any sensors or DAQ. Especially in SMEs in the manufacturing industry, old machines are common and due to the great substance of these old machines, a retrofitting following a brownfield approach can be highly applicable. Furthermore, the investment in new state of the art machines can pose as a major financial obstacle for SMEs because of high investment costs. In order to

enable a holistic connection of CPPSs through the IIoT, the following aspects should be specified beforehand implementing them in the IIoT. First, the identification and specification of required value-creating data of the respective CPPS. Hereby, the necessary data has to be specified and documented in terms of data type, format, unit, range and frequency and use, keeping the machine's physics, expected outcome and added value in mind [2,17]. Second, the data of CPPSs, especially of those with integrated PLCs, often are not public available because of proprietary systems. As a result of the previously specified required data from the CPPS, suitable technology such as sensors can selected and retrofitted, thus providing the required data [2]. Third, attention should be paid to the resilience of the system with respect to the retrofitted components, considering the environmental conditions, ease of implementation, reliability and sustainability of the solution [2,17]. According to Lerch et al. [89], Cyber Physical System (CPS) technologies achieved the lowest growth rates in recent years, thus posing as one of the major obstacles of a holistic digital transformation.

Following the automation paradigm of the third industrial revolution in combination with new data-driven solutions, more process automation is enabled. Moving away from the static programming of PLCs to a more agile data-driven and rule-based approach, improvements in labor and quality are expected, additionally reducing conversion costs by up to 25% [4]. In the manufacturing industry, 64% of all work activities could be automated, having 33% more automation potential in comparison to other sectors [5,31]. According to a study by Berruti et al [5], more enterprises are making process automation a strategic priority, whereby 61% have met their automation targets. Hereby, 72% of these defined process automation as one the highest strategic priorities [5]. Furthermore, a study by Doddapaneni et al. [95] concluded that 86% of employees welcome the automation process, including smart robotics, whereby only 14% of employees had the opportunity to engage with it. Furthermore, the incorporation of user-friendly cognitive automation tools, AI and ML promise further potential in automating manual labor and improving efficiency [95].

The implementation of these technologies provides considerable amounts of data ready to be analyzed and drawn insights from. By outsourcing the computing resources to CC providers, AI and ML can provide further advantages. A study conducted by Brinda et al. [94] revealed the increasing use of CC for AI purposes, stating that 15% of today's CC resources are used for AI computing, increasing to 30% by 2025. It is estimated that by 2025, CC based AI will be distributed into 20% vision, 18% natural-language processing, 16% recommendation, 12% intelligent search, 8% cognitive decision and security, 7% optimization engines, 6% automated generators and 14% other applications [94].

A study by Berruti et al. [5] surveyed 793 enterprises regarding the deployment of orchestration and task automation, analytics and decision automation, digitization and process insights. Concerning orchestration and task automation, 57% deployed business-process and/or case-management platforms and 44% utilized assisted or unassisted robotic process automation. Regarding analytics and decision-making, 36% already used ML algorithms. Belonging to digitization, 37% utilized image-recognition tools. Furthermore, 32% applied process mining and documentation tools for process insights [5].

Another important step towards a holistic digital transformation is transparent design of value chains. Here, the hurdles lie in transparency and standardization. As aforementioned, transparency and standardization is required in order to conduct a holistic digital transformation of a value chain, including the deconstruction of data silos, data governance and multinational legal aspects. Thus, the cross-border data flow enables, enhances and simplifies the cooperation between value chain participants. In fact, the globally used cross-border bandwidth has increased by about 1480% from 2005 to 2017, partially reflecting the cross-border interaction of enterprises [31].

Due to the high degree of networking, the vulnerability to cyber attacks increases, making cyber security imperative in order to build a resilient value chain. The awareness of the importance of strong cyber security is reflected in a study of Buehler et al. [61], showing that the number one priority for acquiring IoT products is cyber security, closely followed by reliability.

In order to withstand cyber attacks, accommodate dynamically changing conditions and thus prevent disruptions, resilience is imperative for a well working digital value chain [66]. Hereby, the challenges of building resilience in a value chain are the identification of static and time-variable constraints, the specification of the optimal value chain setup and capacity scheduling, and thus the evaluation of the ideal production strategy [66]. Furthermore, the identification of vulnerabilities to cyber attacks and shocks poses as a cyclical challenge [66]. As stated by Dilda et al. [66], the successful and resilient digital transformation is estimated to result in an increase of two to five percent of earnings before interest, taxes, depreciation, and amortization (EBITDA).

In addition to technological changes and corresponding restructuring, the same applies to the organization and business side of the enterprises. Focusing on the business side, use cases of the application have to be identified, mapped out, prioritized and implemented across all locations [76]. Furthermore, the necessary values and Key Performance Indicators (KPIs) are defined, also considering the monitoring of such for continuous improvement [2]. On the other hand, the organization side has to define the target value of the digital transformation with respective KPIs. Additionally, the way of working has to be rebuild in an interdisciplinary and skill orientated way [2,76]. According to Lerch et al. [96], 59% of survey enterprises reorganizations of production during the lockdown, whereby additional 18% plan to rebuild their supply chain. A survey conducted by Schatteman et al. [63] revealed that the second biggest obstacle in the way of a digital transformation is legacy supply chain architecture, which also concerns the Manufacturing Execution System (MES) and ERP systems, urging the harmonization of proprietary systems [63]. Moreover, providers of such systems like Oracle and SAP will discontinue support for outdated systems [63]. As a result, data management and reconstruction of outdated MES and ERP system and its respective legacy suboptimizations pose as a major obstacle for many enterprises, preventing the beneficial aspect of dynamically responding to changing conditions. More than one-third of enterprises are not able to provide real-time data of their supply chain, imperative for the digital value chain. As aforementioned, the redefinition of the way of working as a result of the

new technologies like CPPS, AI and automation enhances efficiency and quality while reducing the contribution of labor to the overall costs [31].

Other reasons for the reshoring of production beside COVID-19 include the decreasing importance of labor costs due to the advancement of I 4.0 and the shift from material to intangible assets [31,97]. Hindering aspects concern the highly specialized nature of specific value chains that have developed in specific locations with its own ecosystems, making relocation complicated and costly [64]. As stated by Lund et al. [31], the reshoring favors nations with advanced economics, innovation ecosystems, lucrative consumer markets and skilled workforces. Given the premises of lean and just-in-time production, the regionalization enables better interaction between value chains participants and accelerates the speed to market of production [31]. Another benefit lies in the export of good, whereby Lerch et al. [98] concluded the higher export of complex products without correlation to production volume, thus favoring specialized manufacturing enterprises with skilled workforces. Further concluded by Lerch et al. [98], the resulting profits from higher exports allow higher investments in innovations. Thus, the combination of focused domestic production and digitalization strengthens the domestic production and creates the capabilities for new products for export [98]. On the other hand, the reshoring and the greater reliance on domestic production makes value chains more vulnerable to shocks of domestic origin, thus highlighting the importance of resilience [97]. Therefore, the building of redundancy in the form of backup locations poses as another aspect to consider, as done by Henkel [76]. A study by Lerch et al. [98] revealed that 12% of all industrial enterprises in Germany have at least one non-domestic production site, whereby 6% of all industrial enterprises in Germany even have non-domestic Research and Development (R&D) locations. In conclusion, the reshoring and digital transformation implies the need in the heavy industry for high skilled and knowledge-intensive labor, why it is necessary to focus on people, especially on tech talent, and thus on intangible assets.

Besides the technologies, tech talent is high on the agenda in order to implement new systems and keep them running [76,84]. In fact, 90% of enterprises plan to invest in tech talent [73]. A study conducted by Brinda et al. [94] reflects the demand of specific knowledge-intensive skills and tech talent. Thereby, job posting in the USA with the demand of specific skills from 2015 to 2019 increased by 69% for software engineering, 167% for data science, 417% for ML and 443% for DevOps [94]. Recognizing this, the approach of Henkel for a sustainable digital change sees the people as one of three enablers, besides flexibility of production and redundancy [76]. As stated by Sänger et al. [76], enterprises have to invest in their employees, building the right mindset and skills to sense disruptions and how to react and adjust accordingly [76]. Henceforth, commitment from the management is imperative, empowering local teams and tech talents [76]. Factors that inhibit progress are the fear of job loss as a result of automation and new technologies as well as a lack of confidence in employees [95]. As aforementioned, 86% of employees welcome the automation process, but struggle to identify automation potential in their daily work [95]. Therefore, enterprises are obligated to frequently educate and train employees in order to familiarize them with new technologies and create mutual benefits [5,95]. An estimation by

Behrendt et al. [2] concluded, that employees in the manufacturing industry need 15-20% hiring, 10-15% reskilling, 50-65% training and only 10-25% none of the previously stated actions, although the current tech layoff challenges this estimation.

Furthermore, global trade through GVCs is increasingly shifting towards intangible assets [32]. These intangibles include intellectual property such as patents, software, databases and product design [32,99]. As forecasted by Berruti et al. [5], the need for low skill manual labor will decline by about 30% in Europe and the USA over the next decade. On the other hand, technological skills like programming will be increasingly demanded by over 50% and complex cognitive skills by over 33% [5]. Furthermore, skills regarding high emotional intelligence including leadership and entrepreneurship are expected to increase by over 30% [5]. Additional developments are the trade intensity of good-producing value chains and the increasing importance of services, outgrowing goods from 60-300% depending on the sector [31]. A study conducted by Hasan et al. [100] revealed a correlation between the investment in intangibles and Gross Value Added (GVA), an economical metric measuring the contribution of an enterprise or municipality to sector or economy. Based on their main competitive advantages, four sectors were classified: *"(1) innovation-driven services such as ICT, (2) knowledge-intensive services, such as finance and insurance, and professional services; (3) labor-intensive services, such as wholesale trade, transportation and warehousing, accommodation and food services, construction, and healthcare; and (4) resource-intensive goods such as mining, manufacturing and utilities"* [100]. The study revealed a general correlation between investment in intangibles and GVA growth, whereby the manufacturing sector with an average investment of 15.3% of its GVA only achieved 0.4-1.4% GVA growth per year, which is comparably low to other sectors given the relatively high investment [100]. The reason behind this are the high investment costs in R&D for product development, posing as sunken costs [100]. Nevertheless, top growers in the comparably slow growing manufacturing industry outperform the sector by investing 3.2 times more in intangibles, also diversifying their business and focusing in improvements of productivity [100]. This claim is also supported by Roth et al. and Thum-Thysen et al. [101,102], concluding a significant positive relationship between the investment in intangibles and labor productivity growth, being a key component of GVA. This correlation is also observed by Gumbau-Albert et al. [103], however it is suggest that this relationship may be stronger or weaker depending on the type of intangible investment. Concluding, future competitive advantages for manufacturers are likely to result from the incorporation of software and automation of the product, customizable or tailor-made customer solutions and monetization [1]. This correlation between investment in intangible assets and GVA could be positively influenced by the successful implementation of I 4.0 in several ways. First, the enabled data collection from various sources can be used to gain insights about the impact of intangible assets on GVA, enabling the optimization of intangibles investment strategies, consequently increasing GVA. By utilizing technologies as AI and predictive maintenance, efficiency and productivity increases while simultaneously increasing output and reducing resource consumption, resulting in a higher GVA. Similarly, R&D also benefits from the

utilization of these technologies, leading to a reduction of development times, and a decrease of R&D costs, which are very high especially in the manufacturing industry [100]. Consequently, the necessary investment costs in intangible assets are reduced while at the same time GVA increases.

GVA growth and investment in intangibles, US and 10 European countries, 1995–2019, % share of GVA by sector[1]

Size based on adjusted GVA, 2019

GVA compound annual growth rate, 1995–2019, %

Average intangibles investment = 10.0

Mining

Healthcare

Accommodation and food services

Entertain-ment and recreation

Professional services

Education

Finance and insurance

ICT

Average GVA growth = 2.2

Govern-ment

Retail trade

Construction

Transportation and warehousing

Utilities

Manufacturing

Average investment in intangibles, 1995–2019, % share of GVA

Fig. 2. Comparison of the GVA growth of different sectors in dependency of their percentage GVA investment in intangibles [100,104].

Visualized in Figure 2, Cayler et al. [105] identified eight value driving levers and their quantitative benefits. By leveraging I 4.0, optimized resource utilization and improved processes can lead to increased efficiency, increased productivity, and reduced costs. This is possible through the digital value chain and omnipresent monitoring, which enables situational appropriate behavior and adaptation, all under the supervision of superordinate MES and ERP systems. Furthermore, real-time monitoring and predictive maintenance, are a key factor to maximize asset utilization, leading to reduced downtime and increased productivity by taking advantage of the benefits of a digital value chain and interconnected CPPSs, enabling situationally appropriate action-taking and thus increasing the overall flexibility. By supporting HMI with CPPSs by incorporating GUIs, AI, ML and other cooperative elements, the decision-making process on the store floor can be significantly enhanced, increasing labor productivity

and higher job satisfaction. Furthermore, repetitive labor can be automated, resulting in the elimination of isolated data silos and the digitalization of knowledge. Henceforth, the digital value chain enables the inventory optimization, due to omnipresent real-time monitoring and analysis, resulting in reduced shipping costs and improved cash flow. The same implications apply to quality, reducing costs by detecting product defects and additionally increasing customer satisfaction. Furthermore, real-time tracking, analytics, and demand forecasting can enhance supply chain efficiency by aligning supply and demand, leading to faster delivery times, lower expenses, and higher levels of customer contentment. As a consequence of the enhanced collaboration, the time to market can be reduced, driving innovation and competitiveness. Considering the customer, service and after-sales support can be optimized, building stronger relationships with their customers and differentiate their business from competitors. Through the application of predictive maintenance and condition monitoring, data from the entire lifecycle of the product can be gathered and analyzed for optimization purposes, in further consequence increasing the effectiveness of resource utilization and sustainability.

In essence, I 4.0 can help SMEs to become more efficient, competitive, sustainable and customer-focused. Real-time monitoring and predictive maintenance can help SMEs to maximize the utilization of their assets and reduce downtime, consequently leading to increased productivity and profitability. Similarly, data analytics and automation can help SMEs to optimize their processes and reduce costs, while improving product quality and customer service. However, SMEs are facing several obstacles and potential risks associated with the digital transformation. One of the biggest challenges is the cost and complexity of implementing I 4.0 technologies, particularly for businesses with limited resources. Further obstacles arise in terms of data security and privacy, as well as the need to upskill their workforce to effectively use and manage these technologies. Additionally, big enterprises with more resources could take more advantage of the benefits of I 4.0, intensifying existing inequalities in the market. Regardless of enterprise size and industry, and the potential benefits and risks associated with I 4.0, the digital transformation of businesses and industry will continue. SMEs that are able to effectively leverage I 4.0 will be able to compete in the increasingly digital and connected global economy. However, it is imperative to carefully consider associated risks and costs, to invest in the necessary infrastructure, skills, and capabilities to fully realize and leverage the I 4.0 potential.
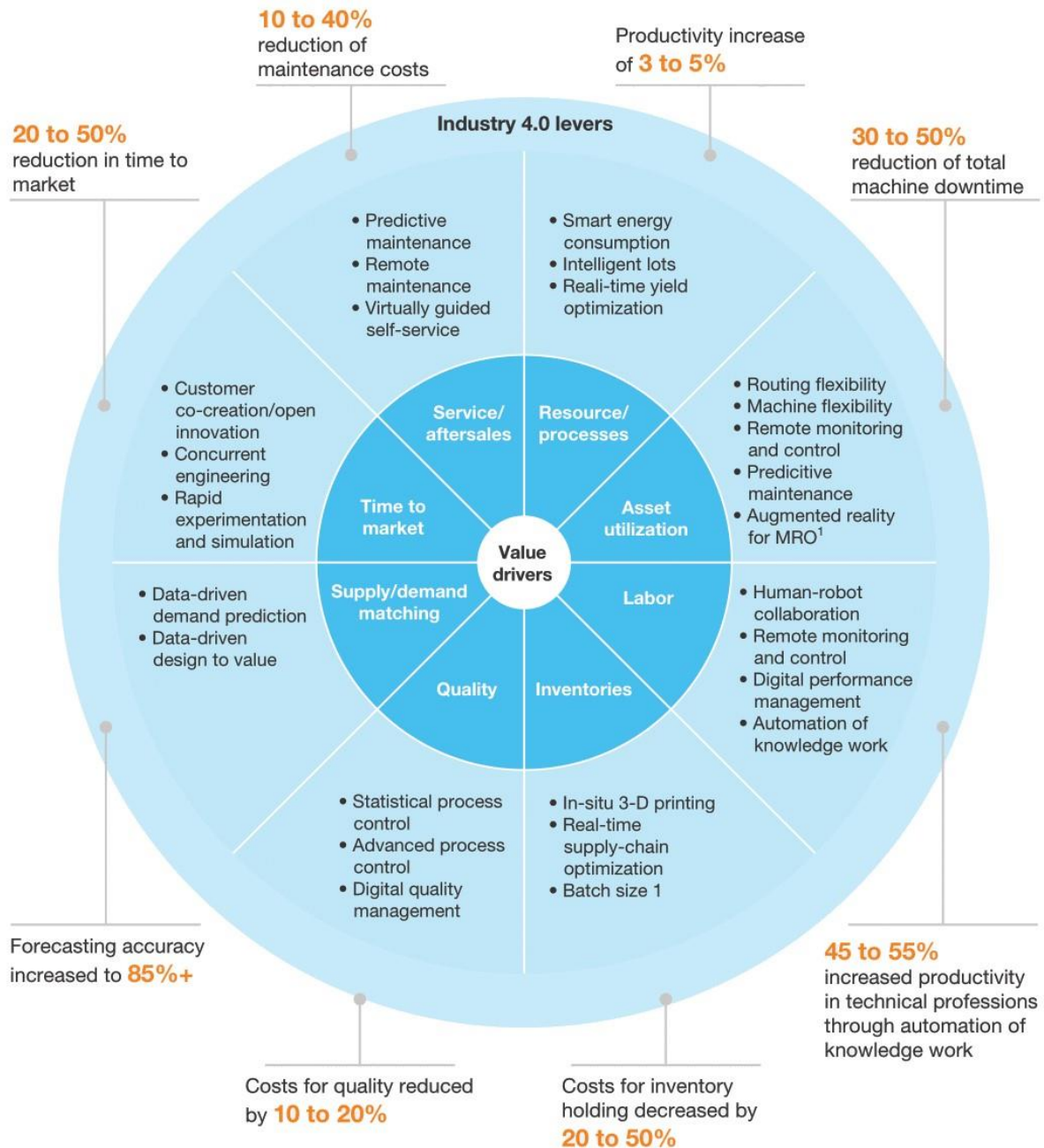
Fig. 3. The eight main value drivers of Industry 4.0 and their benefits according to [105,106].

Following the global disruptions and climate change, GVCs and thus the entire industry are undergoing an additional paradigm shift towards sustainability, as customers also demand sustainable products [1,107]. As a result, enterprises are rebuilding their supply chains and footprints and develop environmental sustainable capabilities in order to stay competitive [1,76,107]. Therefore, a holistic sustainable transformation is imperative to ensure both effectiveness and sustainability [108]. As proposed by Jawahir et al. [109], the sustainable impact on value creation can be observed on the product, process and system level. Therefore, all value-creating manufacturing processes and lifecycle steps of the product have to be considered, following the 6R concept of Reduce, Reuse, Recycle, Redesign, Recover and Remanufacture [110,111]. As concluded in [33], the utilization of I 4.0

technologies and the resulting omnipresent real-time QC helps optimizing processes and products and thus in a reduction of costs, waste, emissions and use of resources [8,75,112–116]. As another result of the sustainable paradigm change, enterprises have to reevaluate their business models, considering a more sustainable and customer-driven rather than purely product-oriented approach [1,81]. Furthermore, the rethinking of the business model and strategy enables the entry in a faster growing market with higher margins [1]. In terms of a green footprint, most enterprises pursue the goal of reducing their Scope 1 and Scope 2 emissions and meeting their net-zero goals, rebuilding production and supply chain [1,117]. Hereby, the term Scope 1 refers to direct emissions due to production, whereas Scope 2 refers to indirect emissions due to energy consumption. Additionally, Scope 3 describes the all remaining indirect emissions originating along the value chain [1]. From this, the idea of a circular economy and zero waste manufacturing manifested [1]. For example, the elevator manufacturer Kone recycles 94% of the production waste and uses 90% recycled metals and other materials for its products. Furthermore, the product and processes optimization using I 4.0 technologies and green energy resulted in 70% energy savings in elevator system and the enterprise estimates to produce zero waste by 2023 [1].

As shown in Figure 3, one of the main I 4.0 value drivers is resources and process, incorporating smart energy consumption. Since the manufacturing industry is very resource intensive, thus also concerning energy consumption, the entire industry is heavily affected by increasing energy prices. Additionally, the green energy transformation has become a significant cost driver for the heavy industry since 2022, requiring significant investments in renewable energy infrastructure, and also increasing the cost of electricity. Driven by global efforts to reduce carbon emissions, the European Union's Directorate-General for Climate Action (DG CLIMA) requires EU states to increase their use of renewable energy sources to at least 32%, an energy efficiency improvement of at least 32.5%, and a reduction of greenhouse gas emission of at least 40% by 2030 [118]. Consequently, the heavy industry has to drastically adapt, shifting from traditional fossil energy sources to renewable energy sources, facing significant costs associated with the implementation of renewable energy infrastructure and purchase of green electricity. Especially for companies with high energy demands, such as automotive Original Equipment Manufacturers (OEMs), the costs for the green energy transformation are particularly high. Additionally, customers of OEMs increasingly demand sustainable operations, making it imperative to shift towards renewable energy and green electricity to remain economically competitive. As a personal hypothesis, I 4.0 will play a significant role in helping the heavy industry transition to green energy sources and reduce their energy costs. By successfully utilizing I 4.0, for instance by adapting production plans depending on the current cost of electricity, reducing the electricity consumption while also increasing flexibility, will be a key factor to achieve sustainability goals and at the same time remain economically competitive.

The state-of-the-art literature review in this thesis and Publication 1 (A 1) led to the identification of I 4.0 and digital value chain enabler technologies and has factually demonstrated its possibilities, opportunities and threats. Based on the fact, that SMEs contribute to 99.7% of all Austrian manufacturing enterprises [83], it is highly likely that at least one SME is incorporated in a domestic or global value chain. Therefore, the incorporation of SMEs in value chains as a result of a holistic standardized digital transformation is imperative for a digital value chain to fully leverage I 4.0. Outlined in Publication 3 (A 3), the project MUL 4.0 maps a value chain composed of multiple geographically separated SMEs, aiming to depict the current situation and conditions in the heavy industry. Given the subject and location of this project, a study conducted by Ralph et al. [119] evaluated the degree of digitalization in the Austrian metal forming industry, coming to following conclusion:

- Big Data and IIoT are hardly applied
- CC is not heavily utilized
- Simulations like FEA are utilized, but rarely integrated in superordinate layers
- Management and technicians welcome and support the digital transformation

Consequently, the following research question and corresponding subquestions can be derived from the literature study in order to support the holistic implementation of I 4.0 technology and thus enable the digital transformation of a value chain:

I. How can a holistic digitalization be executed under special consideration of SMEs?
   a) What is the state of the art in SMEs regarding digital maturity?
   b) What are the limitations of open-source software in the context of an industrial application?
   c) How can real-physical interrelationships and data-driven correlations be used in an Industry 4.0 environment (e.g. FEA, especially within SMEs)?
   d) How must SME specific digitalization solutions build up to ensure compatibility within a value chain?

(I) is a conclusion due to the high share of SMEs in the manufacturing industry and the author's practical experience in this industry and its digitalization issues. The initial step to answer (I), is to evaluate the state of the art of I 4.0, the respective enabler technologies, and consequently the obstacles that complicate the implementation in subquestion (a). Concerning the previously outlined limitations of SMEs, subquestion (b) aims to point out the possibilities and limitations of open-source software, focusing on low-cost but resilient design, simple modification and training in order to prevent proprietary solutions. Subsequently, (c) points out the applications of different modeling approaches in the manufacturing industry, focusing on the practical application and implementation of the models. As a result of the subquestion (a), (b) and (c), (d) concludes insights gained to answer the question of how to holistically implement I 4.0 enabler technologies in the context of manufacturing SMEs.

3. Methodological approach

For this thesis, a multiple methods approach was deemed suitable, considering the interdisciplinarity of the subject [120]. Serving as the initial step, a quantitative and qualitative literature study was conducted. Based on the findings of the literature study and the respective state of the art, case studies were designed and concretized, resulting in the identified research gaps, which were eventually essentialized and transformed into the research questions.

The research question "How can a holistic digitalization be executed under special consideration of SMEs?" can be divided into the corresponding subquestions, presented in the following subsections:

3.1. Answering research question (a): Methodology and contribution

To answer research question (a) regarding the state of the art of I 4.0 technologies in SMEs, a literature study was conducted, identifying the I 4.0 enabler technologies and resulting implications in the first case study and further practical implications on QC in the second case study. Consequently, the gained insights can be applied within the framework of the MUL 4.0 project, enabling further concretization of the project scope, which is the digitalization of various aggregates and machines along the defined value chain. The investigated aspects are addressed in Table 2.

Table 2. Contributions to answer (a).

No.	Case study	Adressed issues	Corresponding publications
3.1.1	Identification and evaluation of Industry 4.0 enabler technologies	Identification, definition and evaluation of I 4.0 enabler technologies; Introduction of a framework for standardized implementation of a digitalized value chain with focus on SMEs; Elaboration of MUL 4.0 in the context of the framework	A 1
3.1.2	Practical implications of Industry 4.0 enabler technologies on Quality Control	Differentiation of traditional QC and QC in the context of I 4.0; Identification of potential applications, opportunities, and challenges for QC for the	A 2

		application of I 4.0 enabler technologies and digitalized value chains	
3.1.3	MUL 4.0: Systematic digitalization of a value chain – from raw material to recycling	Design of a value chain; Concretization of project scope, machines and aggregates; Specification of interconnections of several value chain participants	A 3

3.1.1. *Identification and evaluation of Industry 4.0 enabler technologies*

In this literature study, the enabler technologies of I 4.0 were identified and further concretized, coming to the result presented in section 2. In summary, suitable ICT infrastructure, IIoT, CPPS, CC, DM, DS, DT, AI, ML, Big Data, and Cyber Security were identified as enabler technologies, allowing the implementation of Smart Factories and a digital value chain. As a result of the networked nature of I 4.0, a suitable framework for the structured integration of all entities along the entire value chain must be implemented to ensure uniform and standardized technical communication. For this purpose, the Reference Architecture Model Industry 4.0 (RAMI 4.0) was highlighted and further elaborated in the context of MUL 4.0, concretizing the RAMI 4.0 layer fragments along the Life Cycle & Value Stream, Hierarchy Levels and Layers (Figure 4). Furthermore, a case study and a correlating framework for the digitalization and development of a metal processing value chain for SMEs was introduced. [3]
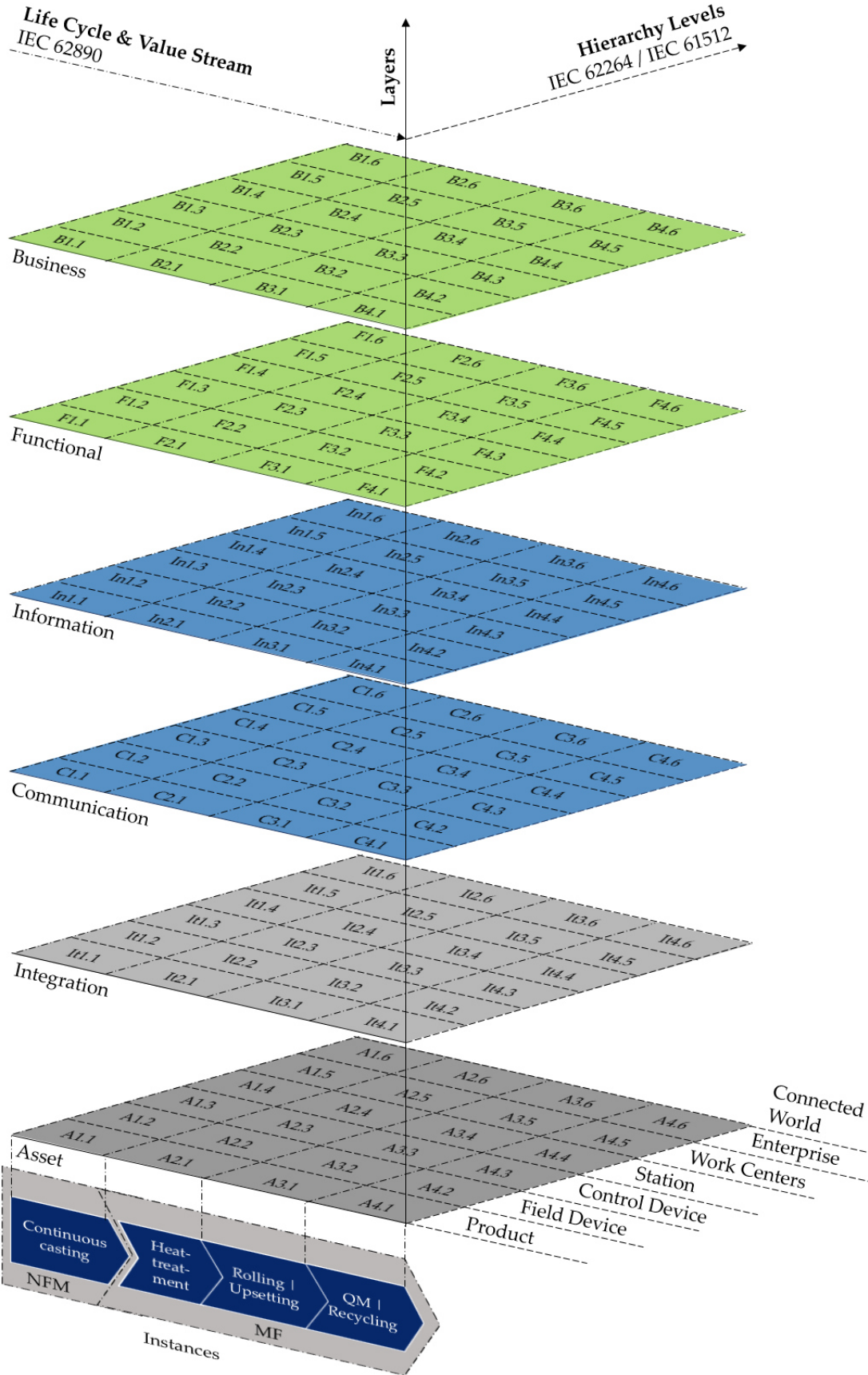
Fig. 4. RAMI 4.0 as a framework for the structured integration and standardized communication between entities of a value chain [3].

For the practical application and networking of value chain participants of MUL 4.0, the Layer 2 production network was designed, developed and implemented, as shown in Figure 5.
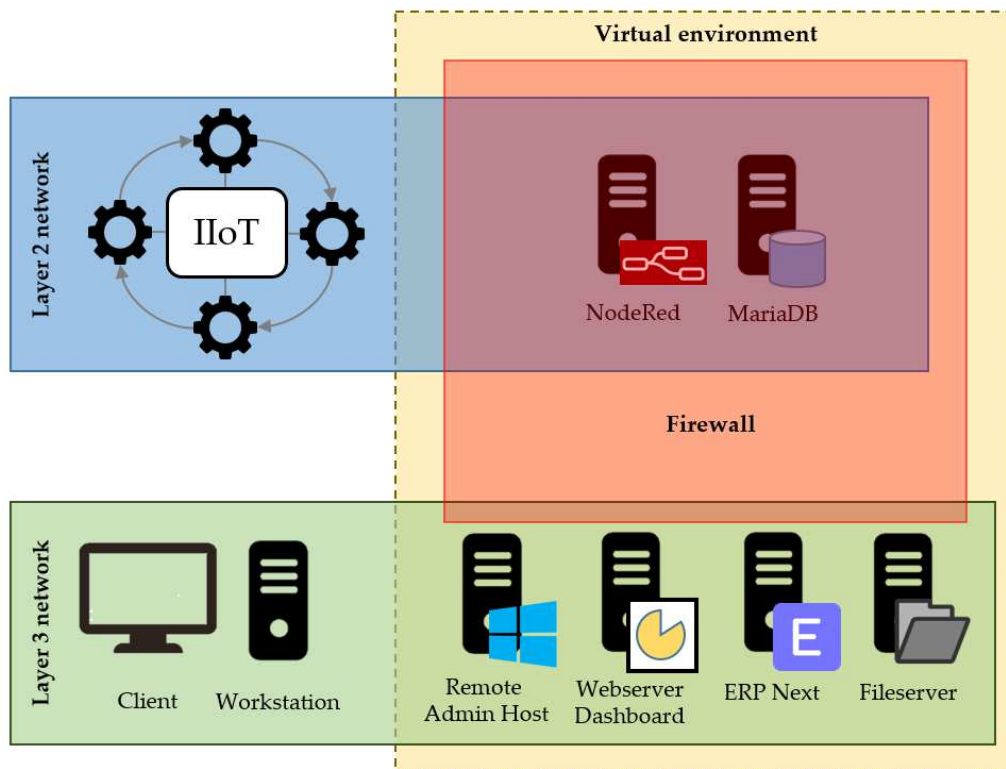

Fig. 5. Schematic of the MUL 4.0 production network [3]

3.1.2. *Practical implications of Industry 4.0 enabler technologies on Quality Control*

In this literature study, the practical implications of I 4.0 on QC were highlighted. In comparison to traditional QC approaches, the high degree of digital data transfer between the individual entities and process steps, and the superordinate data integration in a digitalized value chain, an omnipresent monitoring of product and process is enabled, establishing the term Quality 4.0. In addition to the goals of increasing efficiency and productivity, the interaction between humans and product is also taken into consideration, to collect data of the product along the entire life cycle and value stream, enabling a more holistic data gathering and optimization. This holistic approach of process and product optimization can be used to identify sources of error and optimize the value chain, ultimately leading to waste reduction and higher sustainability in the manufacturing industry [33]. In conclusion, the importance and potentials of new QC approaches for the manufacturing industry were outlined, leading to two newly developed approaches, presented in the publications A 8 and A 9.

3.1.3. *MUL 4.0: Systematic digitalization of a value chain – from raw material to recycling*

The MUL 4.0 project was initialized as an interdisciplinary digitalization project, incorporating different academic chairs at the Montanuniversität Leoben (MUL). In this cooperation, the Chair of Metal

Forming (MF), Chair of Non-Ferrous Metallurgy (NFM), Chair of Industrial Logistics (IL), and the Institute of Mechanics (M) are involved, depicting a value chain representative for the manufacturing industry. Hereby, each chair can be considered as an SME (Table 1) in geographically separated locations and technically different fields, showcasing a low digital maturity, representative for the situation in the manufacturing industry [3,121,122]. The circular value chain is initiated at the NFM with the casting of aluminum alloy using a Finite Volume Analysis (FVA) supported continuous caster, as shown in Figure 6. Subsequently, the cast is cut into specimens, which are subsequently transported to the MF for metal forming processes and QC. At the MF, the specimens can undergo different cold or hot forming processing steps, including rolling with a rolling mill, and upsetting with a hydraulic press, as well as QC. For the process simulation, different modeling approaches were implemented at the MF with the support of M, as elaborated in the respective publications. To conclude the circular value chain, the specimens are remelted at the NFM. For the logistics, the IL was tasked to implement a specimen tracking system as well as implementing a logistics DT. For the proof of practical applicability, the machines and aggregates to be digitalized at the MF show close resemblance to the situation of SMEs in the manufacturing industry, lacking I 4.0 compatible technologies. For the brownfield digitalization approach, the initial setup was analyzed and relevant parameters determined, in order to choose suitable sensors and DAQs, allowing the integration of resulting the CPPSs into a superordinate production network (Figure 5). Consequently, the integration of the CPPSs into the production network enables the data storage in a database, data sharing, and visualization using GUIs. [121]
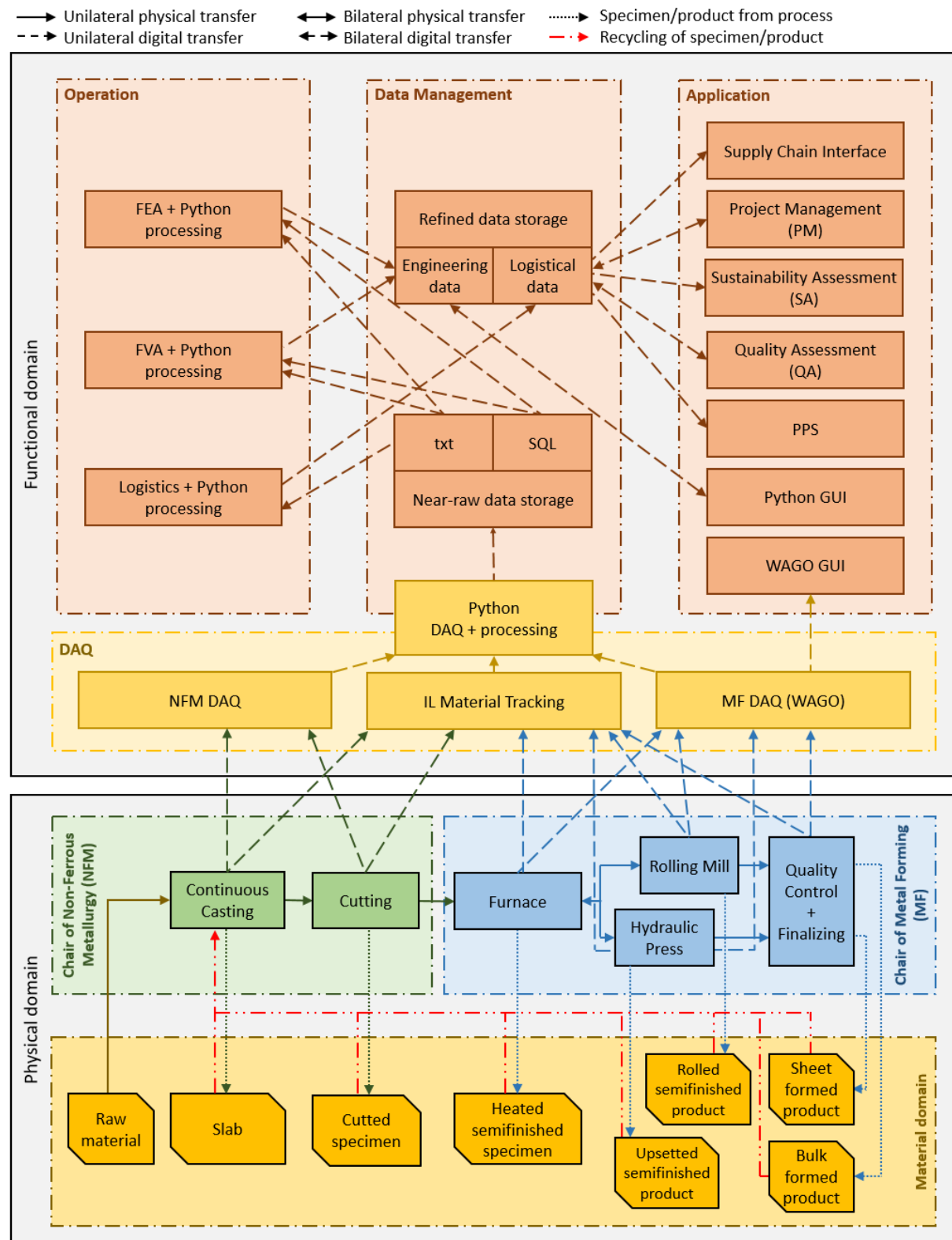
Fig. 6. Schematic value chain and interconnectivity of physical and functional domains of the MUL 4.0 project [121].

3.2. Answering research question (b): Methodology and contribution

To answer research question (b) concerning the limitations of open-source software in the context of an industrial application, five practical case studies were conducted. Hereby, the case studies used open-source software for applications gaining more importance in a digital manufacturing environment, including data analysis, data integration, algorithms, condition monitoring, ML, and the interaction with proprietary software. The contributions made to answer (b) are summarized in Table 3.

Table 3. Contributions to answer (b).

No.	Case study	Adressed issues	Corresponding publications
3.2.1	Implementation of a Six-Layer Smart Factory Architecture	Implementation of a low-cost layer architecture approach for a metal forming smart factory; Integration of a condition monitoring system and interactive project management tool; Integration of different DAQ systems into a superordinate low-cost main processing layer; Implementation of open-source MySQL database	A 4
3.2.2	Transformation of a rolling mill into a CPPS with special focus on the application of open-source software	Implementation of resilient low-cost WAGO DAQ; Development of an open-source data analysis algorithm using supervised ML; Integration into layer architecture; Development of user-centered front-end GUI to support decision-making process	A 5
3.2.3	Transformation of a hydraulic press and furnaces into a CPPS with special focus on the application of open-source software	Implementation of resilient low-cost RevPi DAQ; Development and implementation of a modifiable automated process simulation and data analysis	A 6

	algorithm simulation using Python and Abaqus; Integration of an open-source condition monitoring system; Integration into production network; Development of user-centered front-end GUI to support decision-making process	
3.2.4	Development of an open-source machine learning algorithm for the prediction of stresses for the shot peening process	Development of a modifiable automated process simulation using Python and Abaqus; Development of an open-source data analysis algorithm using supervised ML; Development of user-centered front-end GUI to support decision-making process	A 7
3.2.5	Development of an open-source approach for the synchronization of two proprietary systems to correlate anisotropy and electrical resistivity of rolled aluminum	Development of an open-source data analysis algorithm synchronizing time series data of two proprietary systems	A 8

3.2.1. Implementation of a Six-Layer Smart Factory Architecture

As a predecessor of MUL 4.0, a six-layer architecture was implemented at the MF, serving as the base of a metal forming smart factory (Figure 7). On the machine layer, three machines were digitalized using a brownfield approach, implementing resilient low-cost sensors and DAQs. First, a proprietary CNC lathe was equipped with a three-phase current transducer and a Structured Text (ST) based WAGO DAQ system, publishing data in-situ into a GUI, visualizing data and system related information for the front-end user (Figure 8). Furthermore, the data is published on the preprocessing layer, from which the open-source software Python analyzes available data and publishes obtained information in another Python GUI and on the main processing layer (Figure 7). Second, the rolling mill at the MF was implemented into the layer architecture, which will be elaborated in section 3.2.2. Additionally, a Gleeble 3800 thermal mechanical simulator at the MF was implemented into the layer architecture, using iba hardware and software, following a similar principle as the brownfield approach applied at the CNC lathe, elaborated in section 3.4.2. Consequently, the processed data is stored in an open-source MySQL DBMS

and integrated into the superordinate project management (PM) layers for the implemented open-source Hypertext Preprocessor (PHP) PM tool. This PM tool was deployed at the MF, requiring a user login in order to restrict unauthorized access and enhance data security. Within this case study, the possibilities of the integration of resilient low-cost hardware and software was highlighted, proofing the applicability of non-proprietary open-source software in a metal forming smart factory, showcasing the scalability of such solutions.
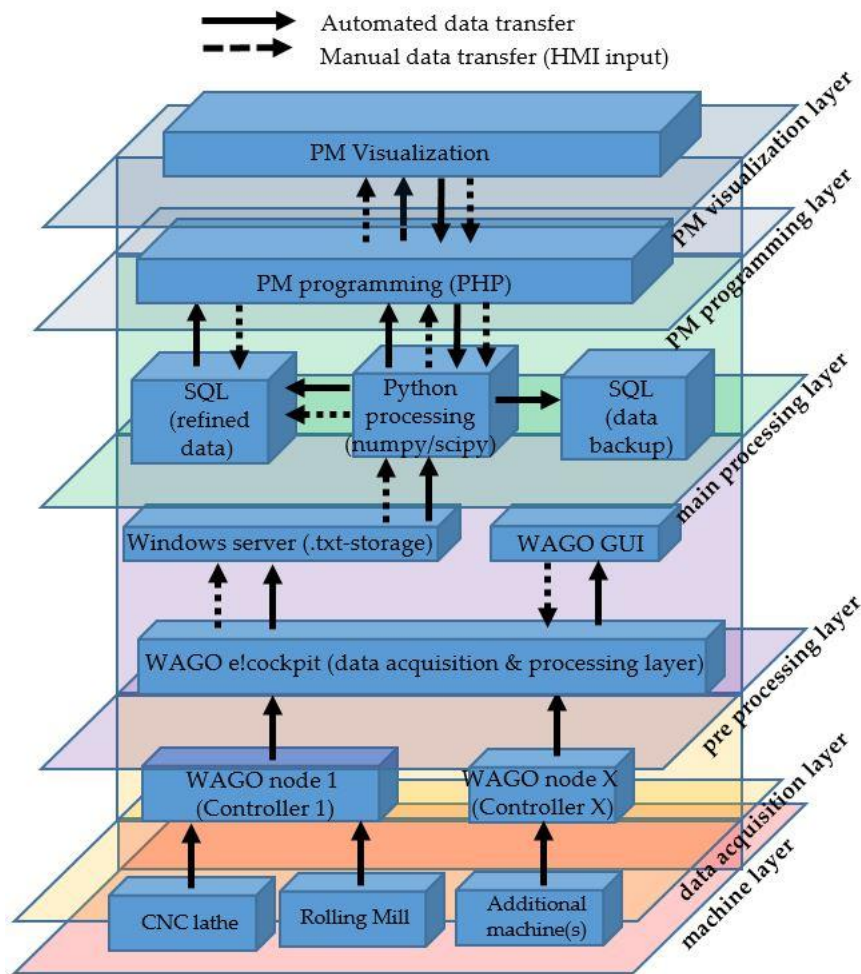
Fig. 7. Six Layer Architecture with respective layers and nodes [123].
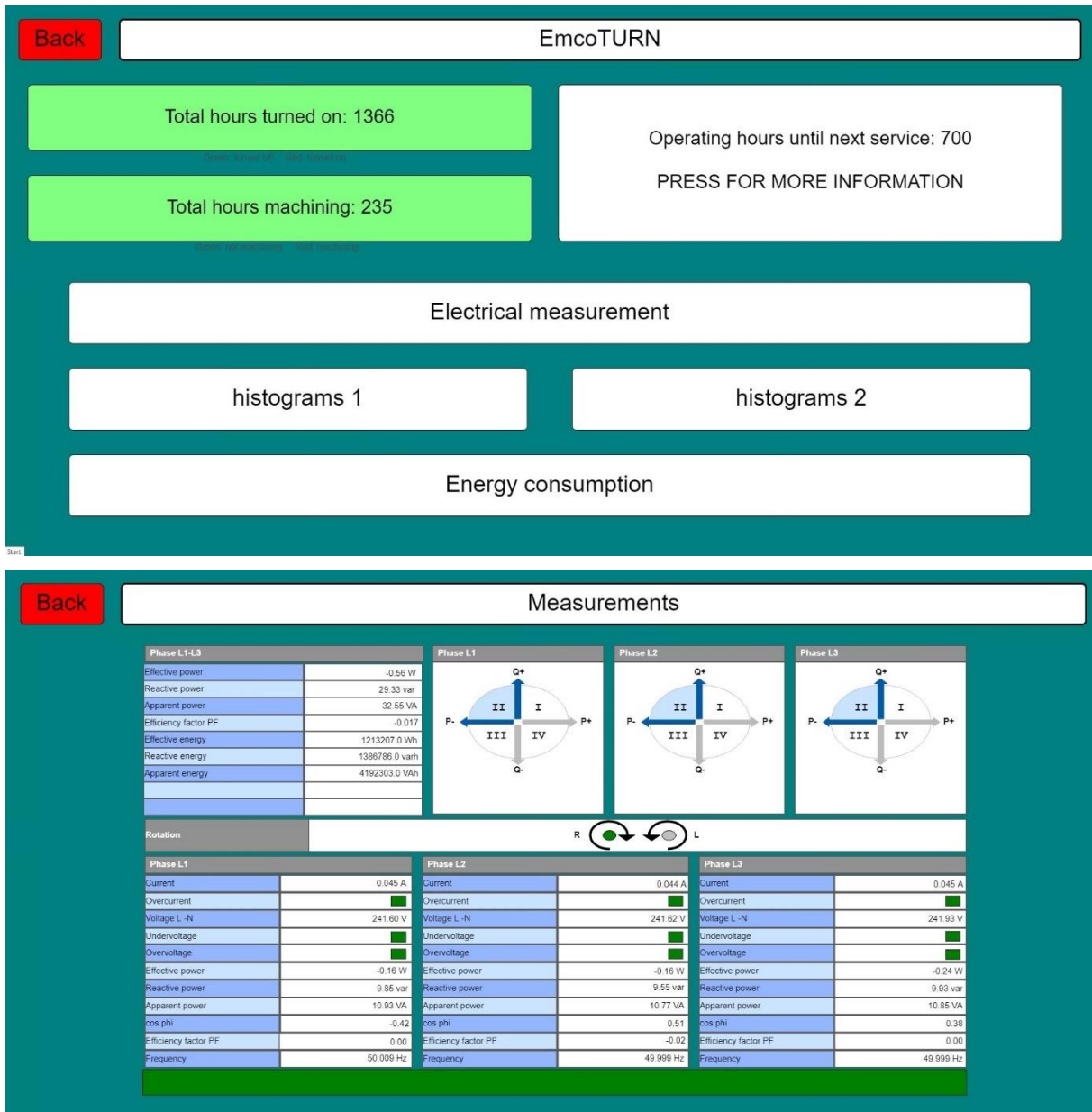
Fig. 8. WAGO GUI of the CNC-lathe, visualizing machining hours (top) and the subordinate electrical measurement GUI (bottom).

3.2.2. *Transformation of a rolling mill into a Cyber Physical Production System with special focus on the application of open-source software*

To proof the scalability of the layer architecture presented in section 3.2.1., the rolling mill at the MF was retrofitted with state of the art resilient low-cost sensors and DAQ, enabling the gathering of processes related data at a sampling rate of 500 Hz. Hereby, the WAGO DAQ system used for the CNC lathe was modified with additional Input/Output (I/O) modules to implement the rolling mill into the smart factory layer architecture, publishing data on the preprocessing layer (Figure 7). To proof the applicability of open-source software in this context, Python was used to analyze data from a statistical experimental setup of over 1900 process steps. As a result, a supervised ML algorithm was developed

(section 3.3.1.), allowing the data-driven prediction of a rolling schedule. To enhance the decision-making process, a rolling schedule predictor was developed, in which the front-end user can input various process and material related parameters into a user-friendly Python GUI, automatically executing the back-end ML algorithm, and thus generating the rolling schedule (Figure 10). Furthermore, additional data sets or data points of the end height of the rolling material can be input into GUI by the user, adding them to the database further improving the prediction accuracy of the algorithm. In addition to the Python GUI, a WAGO GUI (Figure 9) was developed, visualizing process parameters and enabling the manual execution of measurements, which are subsequently published in the layer architecture. In the course of this thesis, the rolling mill CPPS was also implemented in the MUL 4.0 production network. [17]
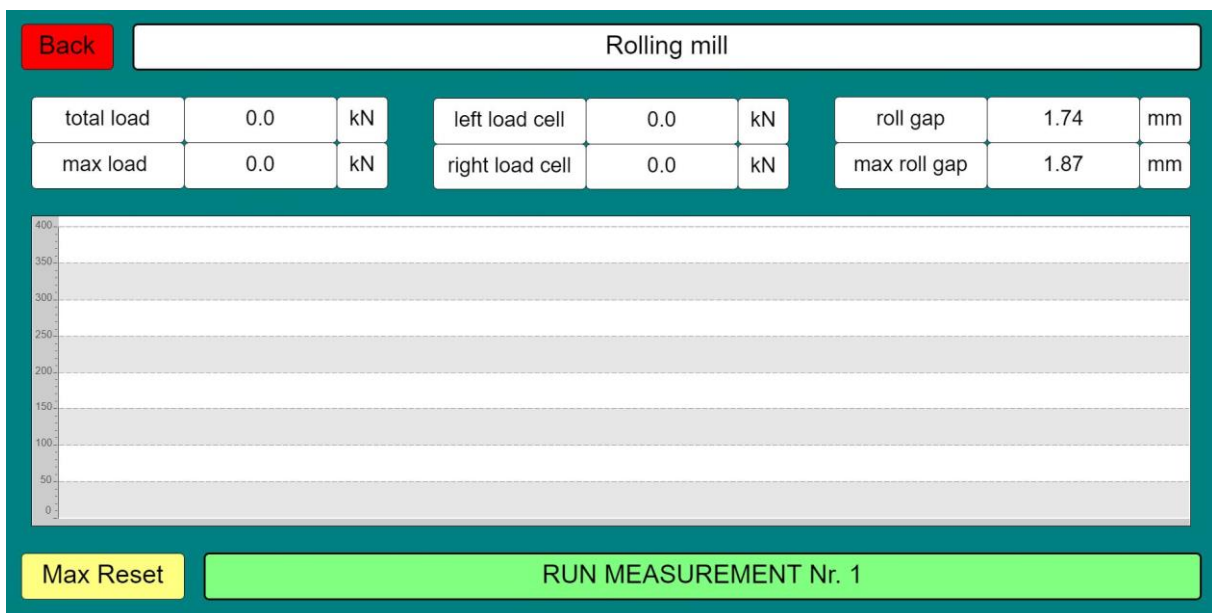

Fig. 9. WAGO GUI of the rolling mill, visualizing relevant process parameters and enabling the recording individual measurements.
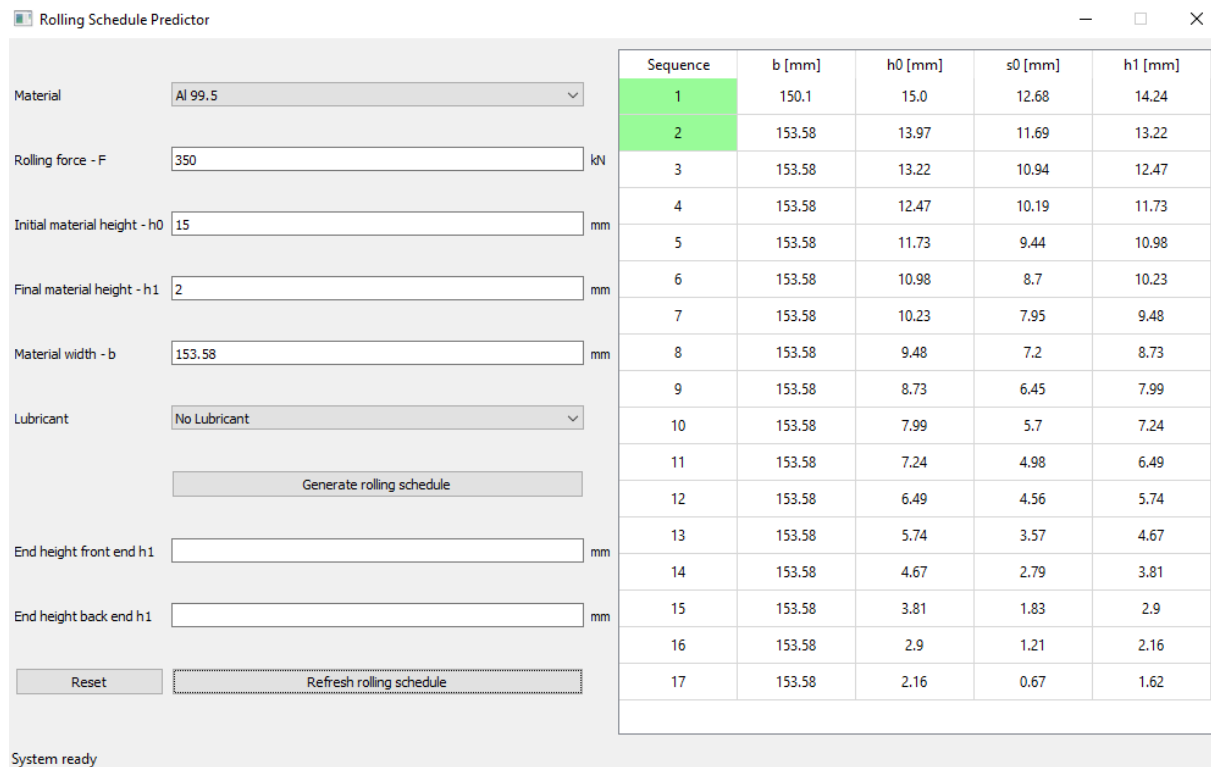
Sequence	b [mm]	h0 [mm]	s0 [mm]	h1 [mm]
1	150.1	15.0	12.68	14.24
2	153.58	13.97	11.69	13.22
3	153.58	13.22	10.94	12.47
4	153.58	12.47	10.19	11.73
5	153.58	11.73	9.44	10.98
6	153.58	10.98	8.7	10.23
7	153.58	10.23	7.95	9.48
8	153.58	9.48	7.2	8.73
9	153.58	8.73	6.45	7.99
10	153.58	7.99	5.7	7.24
11	153.58	7.24	4.98	6.49
12	153.58	6.49	4.56	5.74
13	153.58	5.74	3.57	4.67
14	153.58	4.67	2.79	3.81
15	153.58	3.81	1.83	2.9
16	153.58	2.9	1.21	2.16
17	153.58	2.16	0.67	1.62

Fig. 10. Python GUI for the support of the decision-making process and prediction of a user input-specific rolling schedule [17]

3.2.3. Transformation of a hydraulic press and furnaces into an interconnected Cyber Physical Production System with special focus on the application of open-source software

As part of MUL 4.0, the hydraulic press and two furnaces of the MF were transformed into an interconnected CPPS, which was implemented into the production network, as well as into the six layer architecture. Congruent to the resilient low-cost approach of the rolling mill digitalization (section 3.2.2.), sensors and a RevPi DAQ system were retrofitted to the aggregates, described in more detail in section 3.4.2. (Figure 21). For digital process mapping, a DS was developed, running a modular modifiable multistep Python-scripted FEA, elaborated in section 3.3.2.. Supporting the decision-making process, a user-friendly Python GUI (Figure 12) was developed, allowing the user input of process and material related parameters, which are automatically imported into the respective back-end FEAs. For the visualization of process parameters of the hydraulic press and the furnaces, two individual GUIs were developed and implemented into a superordinate GUI system, using the WAGO DAQ system's software of the rolling mill and CNC lathe (Figure 11). For this purpose, a MODBUS TCP/IP interface was implemented between the RevPi and the WAGO system, enabling the communication of process data. Consequently, a uniform GUI system incorporating all machines' and aggregates' GUIs allows the user to visualize the respective process parameters and take separate measurements. Furthermore, Python was used to implement an in-situ condition monitoring system, aligning in-situ sensor data and data extracted from the respective FEAs, comparing data and giving recommendations for process

adaptation. In addition, an in-situ sanity check system was implemented, which controls the plausibility of sensor data and alerts the machine user in the event of a sensor malfunction to ensure process validity. [124]

Fig. 11. Superordinate WAGO GUI (top), GUI of both furnaces (middle), and GUI of the hydraulic press (bottom) [124]
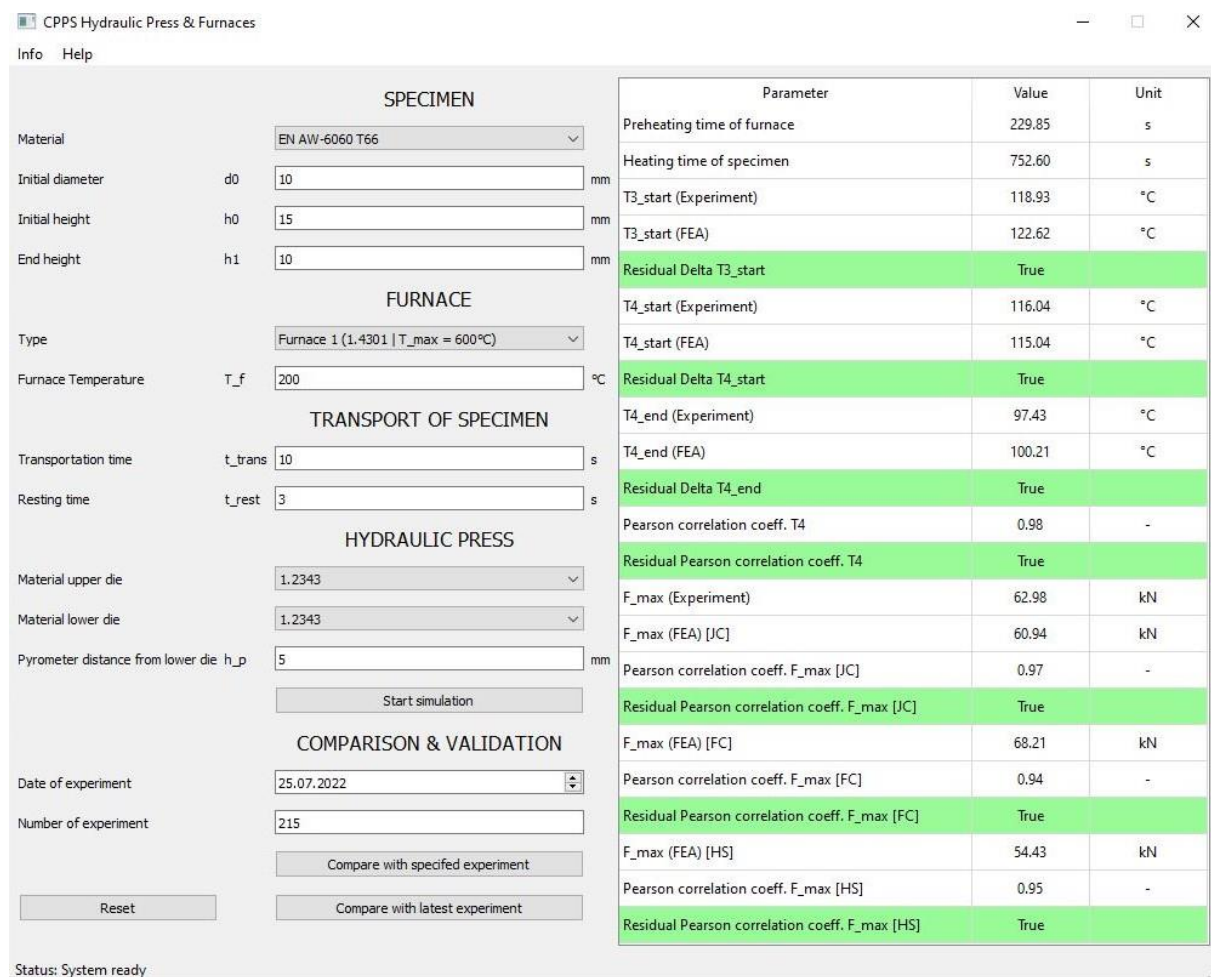
Fig. 12. Python GUI for the support of the decision-making process and validation of experiments with the simulation based on the user input [124].

3.2.4. *Development of an open-source machine learning algorithm for the prediction of stresses for the shot peening process*

Similar to the approach in section 3.2.3., Python was used to generate Abaqus based FEAs of a shot peening process, predicting the material's residual stresses over the depth in dependence of the shot material, radius and velocity. This automated process simulation generates the respective FEA input files, passes them to the FE solver, extracts the results, and stores them in a database. As a result, a front-end GUI (Figure 13) allows the user input of data, executing the back-end algorithm (Figure 14), recommending the shot speed to achieve the desired residual stresses. To further improve the prediction accuracy of this white box modeling algorithm, the possibility of adding experimental data to the database was implemented, transforming it into a supervised grey box ML approach, elaborated in section 3.3.3. [125].

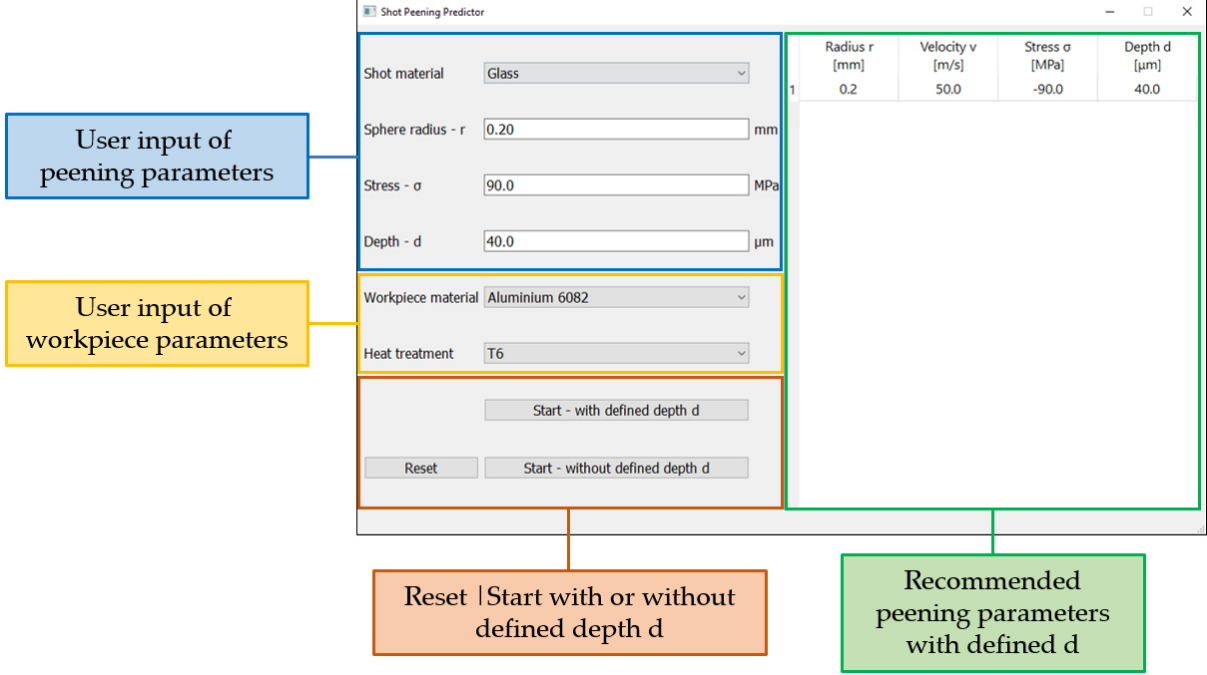**Fig. 13.** Python GUI for the support of the decision-making process of the shot peening process with user input parameters and respective output results [125]
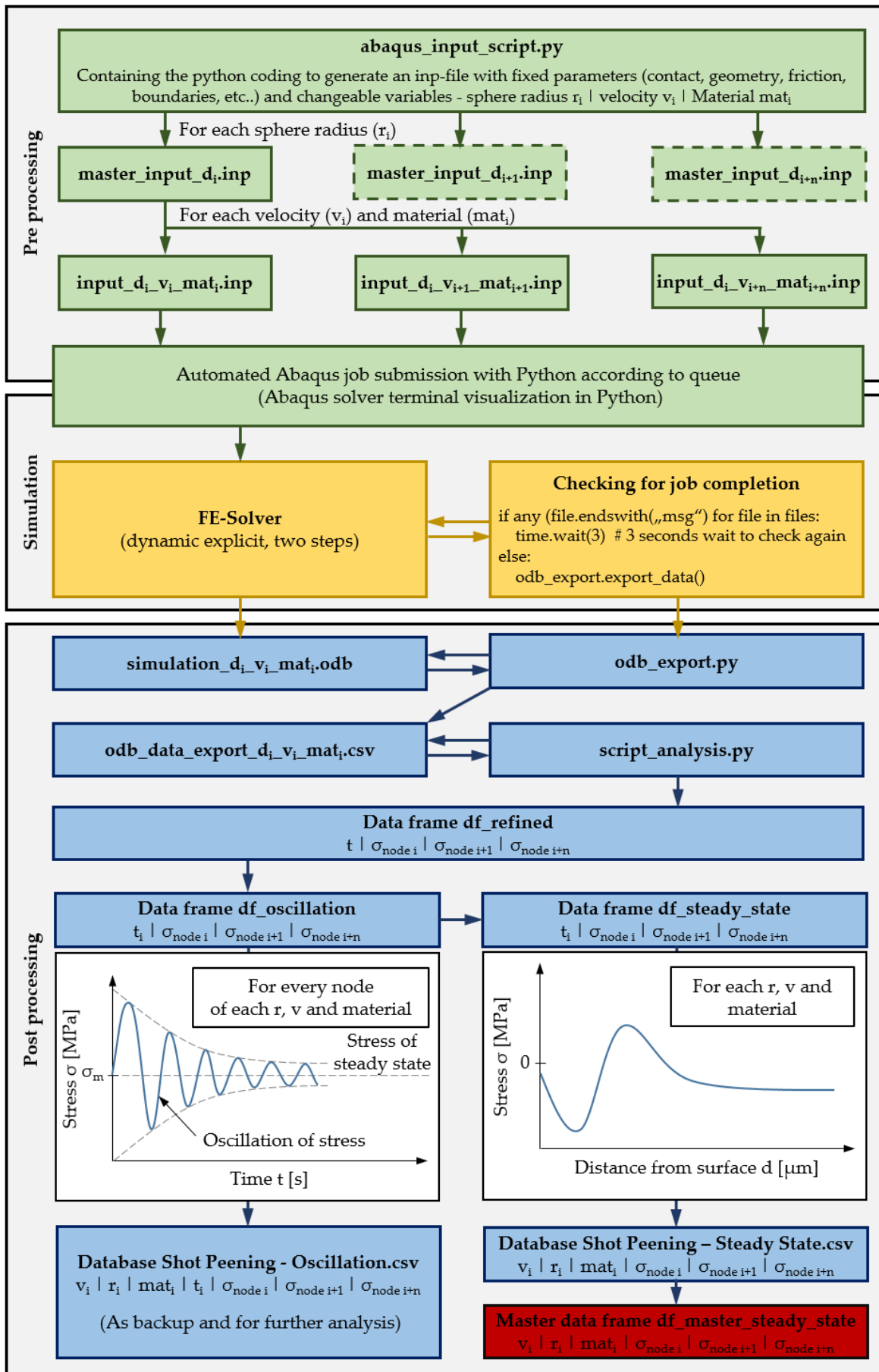
Fig. 14. Algorithm for the automated simulation execution and data extraction of the shot peening process [125]

3.2.5. *Development of an open-source approach for the synchronization of two proprietary systems to correlate anisotropy and electrical resistivity of rolled aluminum*

Within this case study, a method to merge two separate proprietary systems and their respective datasets with Python was developed. Since it was not possible to directly intervene in the proprietary software and no further hardware was implemented to support the low-cost premise, the merging and synchronization was developed as a post-processing step. Here, the time series data of a tensile test machine and an electrical resistivity measurement system showcasing different formats and sampling rates were synchronized, enabling the analyzation and correlation of data sets. For time synchronization, both processes and their datasets were analyzed separately, and their interactions were investigated to evaluate a characteristic value for the automated determination of the synchronization timestamp. By automatically determining the synchronization point in time, an automated open-source QC approach could be developed that, replacing manual data set merging, increasing the quality and reliability of the associated data analysis. Based on this open-source approach, the corresponding black box model described in section 3.3.4 was developed. [126]

3.3. Answering research question (c): Methodology and contribution

The contributions to answer question (c) on how real-physical interrelationships and data-driven correlations can be used in an I 4.0 environment with regard to FEA within SMEs, are shown in Table 4. Therefore, four case studies were designed, showcasing the applicability of black, grey and white box modeling approaches in the context of the metal forming industry.

Table 4. Contributions to answer (c).

No.	Case study	Adressed issues	Corresponding publications
3.3.1	Data-driven black box modeling of the rolling process with a supervised machine learning algorithm	Development and implementation of a data-driven black box model with a supervised ML algorithm for the rolling process based on data of a statistical experimental setup to predict the end height of the material; Data-driven generation of a rolling schedule	A 5
3.3.2	Real-physical white box modeling of a combined heating and upsetting process using FEA	Development and implementation of a real-physical white box model using a modifiable Python scripted Abaqus FEA for the heating and upsetting process; Determination of material parameters based on experimental evaluated material data; Evaluation and comparison of different material models	A 6
3.3.3	Grey box modeling of the shot peening process including a supervised machine learning algorithm	Development and implementation of a real-physical and data-driven grey box model including a supervised ML algorithm for the shot peening process based on data of a FEAs and practical experiments; Prediction of the	A 7

	residual stresses in dependence of the material depth, shot material, velocity and radius	
3.3.4 Data-driven black box modeling of the correlation between anisotropy and electrical resistivity of rolled aluminum using the four-point method	Development and implementation of a data-driven black box model for rolled material to characterize the effect of anisotropic material on the electrical characteristic values	A 8

3.3.1. Data-driven black box modeling of the rolling process with a supervised machine learning algorithm

In this case study, data from statistical experiments conducted at the rolling mill CPPS were used to model a supervised ML algorithm in order to predict the end height of a specimen in dependence of the rolled material, rolling force, initial height, initial width, and lubricant. As described in section 3.2.2., the back-end of the GUI shown in Figure 10, generates a rolling schedule based on experimental data. Within this algorithm, linear interpolation and extrapolation based on given experimental data points is performed, resulting in an iterative evaluation of the end height after each rolling step, consequently leading to the prediction of a rolling schedule. Furthermore, the experimental database can be extended with more data of the respective material, enabling supervised ML, and thus improving the prediction accuracy. This approach can be applied for a wide variety of materials, requiring a statistically experimental setup in order to generate a material specific data set, guaranteeing a high prediction accuracy. [17]
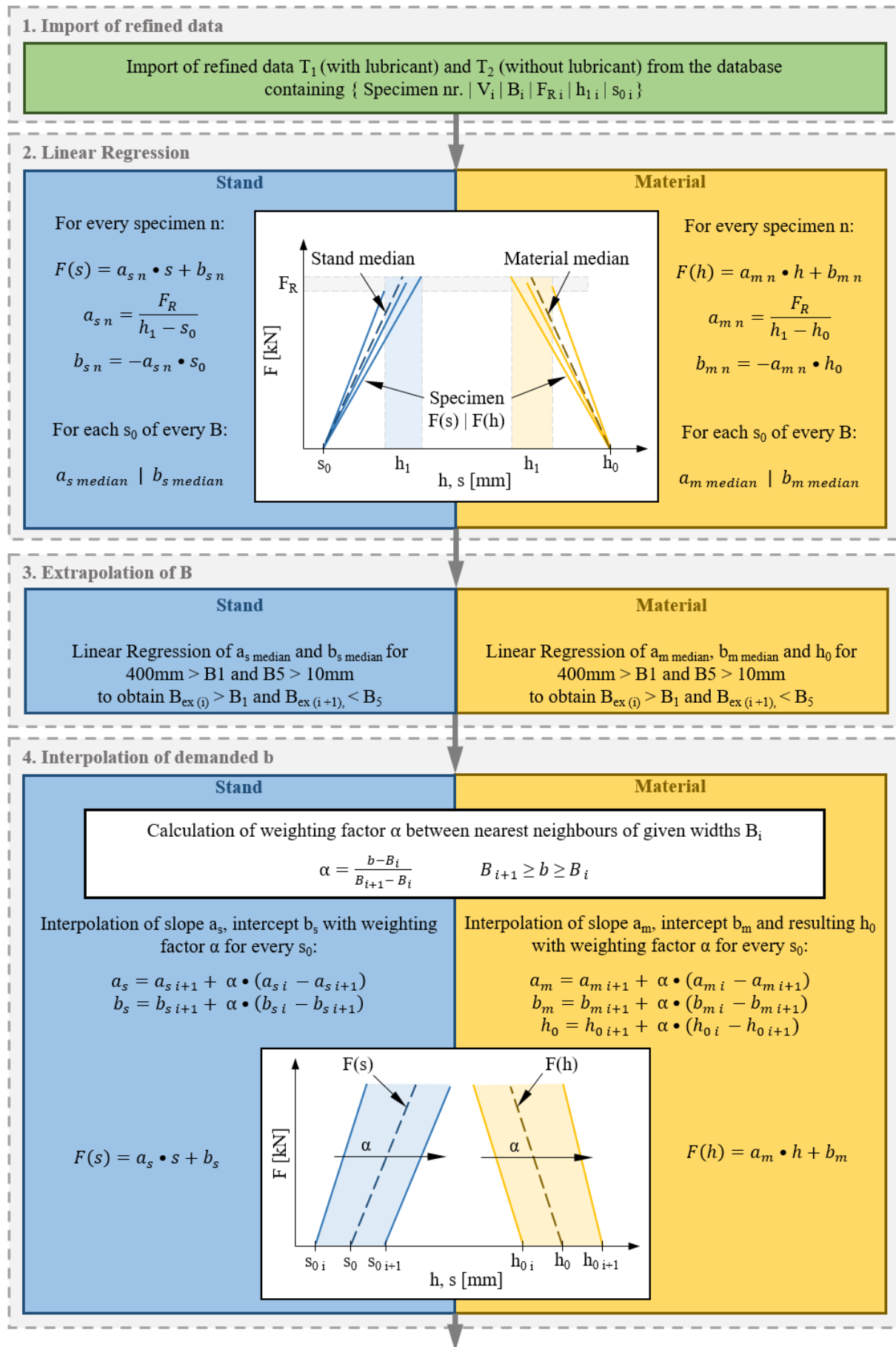
Fig. 15. Logic of the data-driven rolling schedule predictor [17]

5. Extrapolation of s_0

Stand

Extrapolation of $a_{s\,max}$ for $20.0mm > s_{0\,ex} > s_{0\,max}$
Extrapolation of $a_{s\,min}$ for $s_{0\,min} > s_{0\,ex} < 0.1mm$

$s_{0\,max}$ = maximum s_0 obtained from data (5.0mm)
$s_{0\,min}$ = minimum s_0 obtained from data (0.5mm)

For $s_{0\,min} > s_{0\,ex} < 0.1mm$: $a_{s\,ex} = a_{s\,min}$
For $20.0mm > s_{0\,ex} > s_{0\,max}$: $a_{s\,ex} = a_{s\,max}$

Calculation of $b_{s\,ex}$ for corresponding $a_{s\,ex}$:
$$b_{s\,ex} = -a_{s\,ex} \bullet s_{0\,ex}$$

6. Extrapolation of h_0

Material

Extrapolation of $h_0(s_{0\,ex})$ with linear regression for
$s > s_{0\,max}$ and $s < s_{0\,min}$

Calculation of $b_{m\,ex}$ for corresponding $a_{m\,ex}$:
$$b_{m\,ex} = -a_{m\,ex} \bullet h_{0\,ex}$$

7. Interpolation of h_0 and rolling schedule iterator

Stand

Auxiliary variable γ
($0 \leq \gamma \leq 1; stepsize\ 5E-4$)

$$a_{s\,j} = a_{s\,i+1} + \gamma \bullet (a_{s\,i} - a_{s\,i+1})$$
$$b_{s\,j} = b_{s\,i+1} + \gamma \bullet (b_{s\,i} - b_{s\,i+1})$$

Calculation of roll gap height $s_{0\,j}$ height for rolling
schedule step j:

$$s_{0\,j} = \frac{a_{s\,j} \bullet h_{1\,j} - F_R}{b_{s\,j}}$$

Material

Calculation of weighting factor β between nearest
neighbours of h_0

$$\beta = \frac{h_0 - h_{0\,i}}{h_{0\,i+1} - h_{0\,i}} \qquad h_{0\,i+1} \geq h_0 \geq h_{0\,i}$$

$$a_{m\,j} = a_{m\,i+1} + \beta \bullet (a_{m\,i} - a_{m\,i+1})$$
$$b_{m\,j} = b_{m\,i+1} + \beta \bullet (b_{m\,i} - b_{m\,i+1})$$

Calculation of exit height $h_{1\,j}$ for rolling schedule
step j:

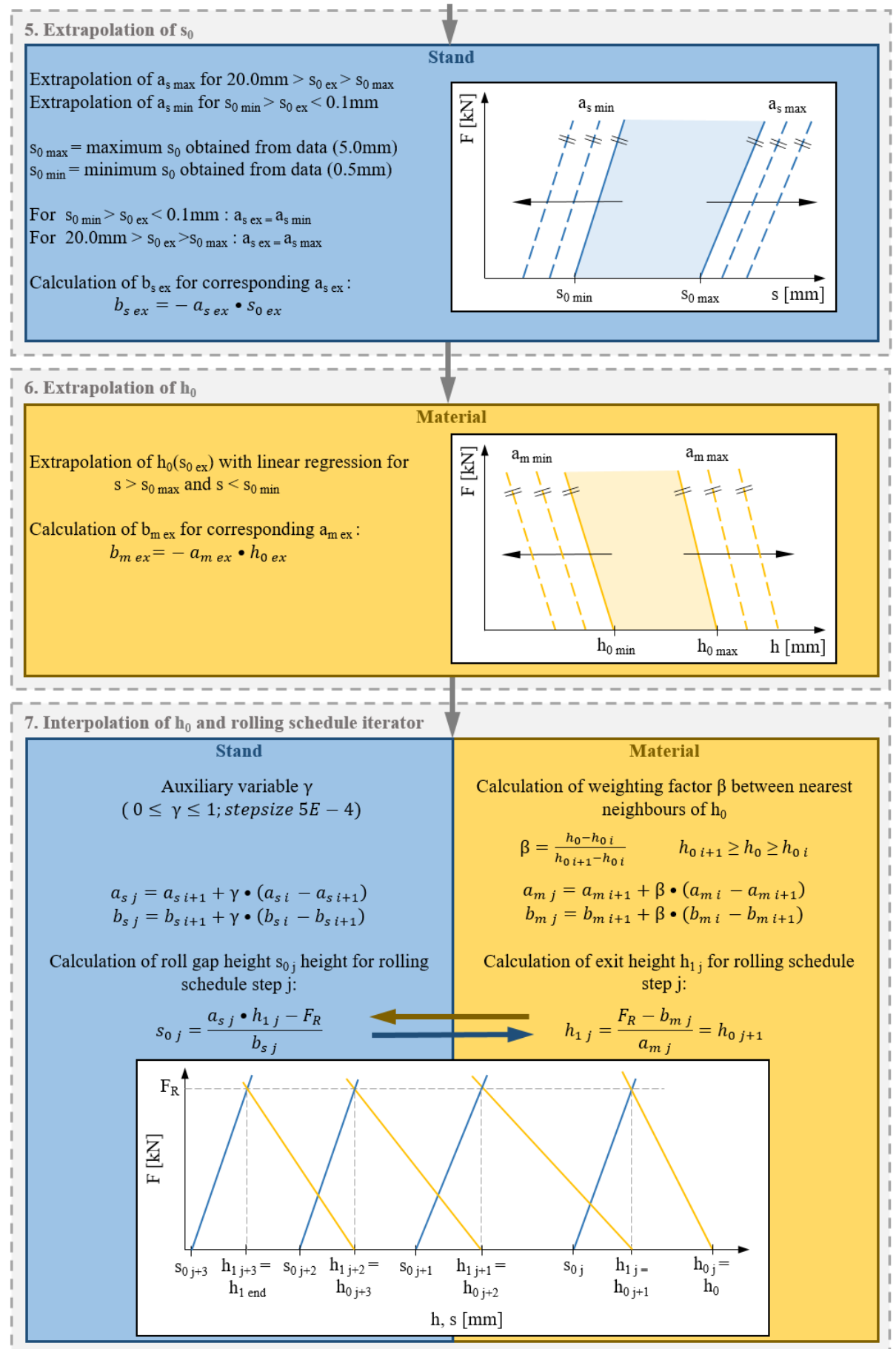$$h_{1\,j} = \frac{F_R - b_{m\,j}}{a_{m\,j}} = h_{0\,j+1}$$

Fig. 15. continued

42

3.3.2. *Real-physical white box modeling of a combined heating and upsetting process using FEA*

Similar to the framework introduced in the case study regarding the rolling mill CPPS, the hydraulic press and two furnaces were transformed into a CPPS implementing resilient low-cost sensor and DAQ, and a real-physical white box modeling approach. For this modeling approach, a modular modifiable multistep WBM approach using a Python-scripted FEA was utilized, enabling an easy modification of the individual simulations and also of the process step sequence. To obtain valid results, experimental investigations had to be conducted for the selected aluminum alloy EN AW-6060, deriving material data for the numerical material models. For the material models, a flow curve, Johnson Cook (JC), and Hensel-Spittel material model were implemented and their results and suitability in relation to different material effects of this process setting were compared. Within this case study, the four-step process sequence was numerically depicted (Figure 16). The first FEA represents the heating process of a specified specimen in one of the two furnaces, followed by the second cooling simulation of the specimen abstracted with Python as a result of the transport from the furnace to the hydraulic press. In the third FEA, the cooling of the specimen when resting on the lower die of the hydraulic press is simulated, followed by the fourth and last FEA, depicting the upsetting process including all heat transfers between specimen and the process environment. Consequently, the results of the simulations are compared with sensor data, serving as a validation. [124]
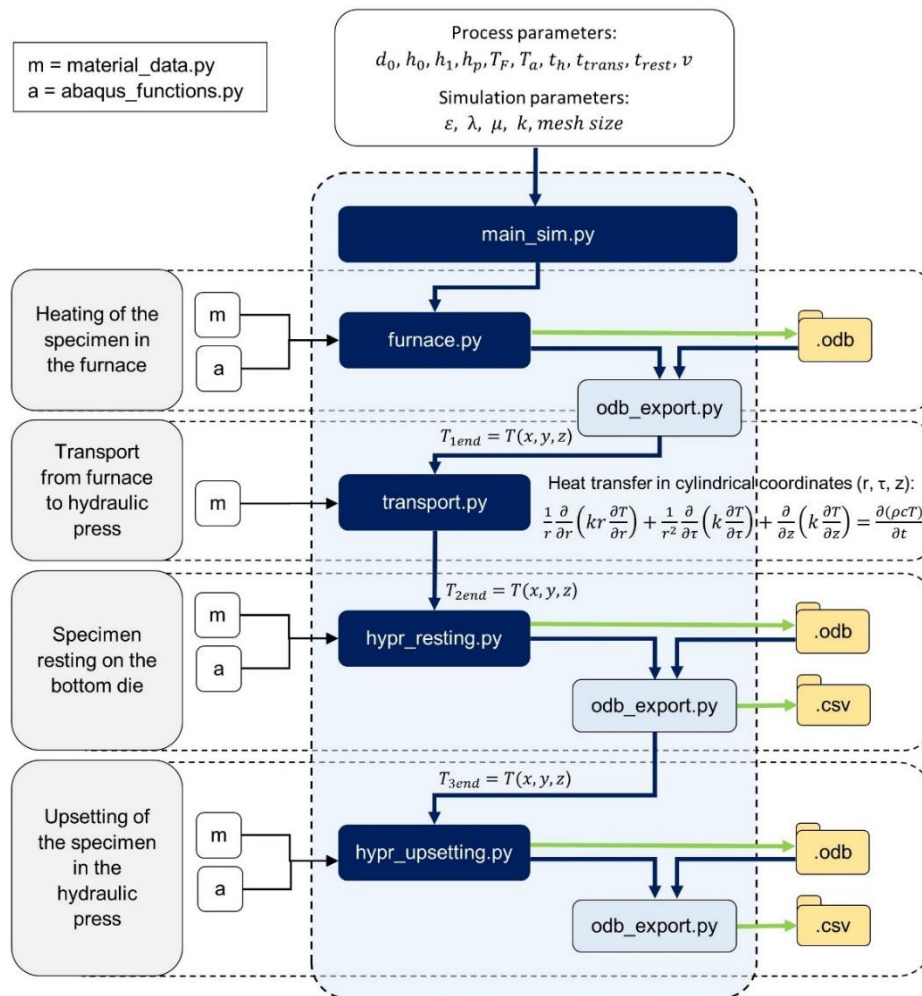
Fig. 16. Digital Shadow of the CPPS incorporating the hydraulic press and furnaces [124].

3.3.3. *Grey box modeling of the shot peening process including a supervised machine learning algorithm*

Combining a data-driven BBM approach and a real-physical WBM approach, a case study was conducted, implementing a mixture of both approaches, resulting in a GBM for a shot peening process, which is commonly used in the metal forming industry as a mechanical surface treatment. As described in section 3.2.5., desired residual stresses and other process parameters are input into a GUI (Figure 13), consequently triggering the FEA algorithm, resulting in the numerical simulation of the process with the specified parameters, as shown in Figure 14. To transform this initial WBM into a GBM, additional experimental data can be implemented into the model, increasing the prediction accuracy of residual stresses (Figure 17). To include experimental data into the database, a second order interpolation is performed, enabling the calculation of residual stresses in dependence of the depth. Consequently, the initial FEA data can be extended by integrating the derived functions into the model. In summary, this framework can be applied for initial WBMs, which can be improved with experimental data by including it in the database. [125]
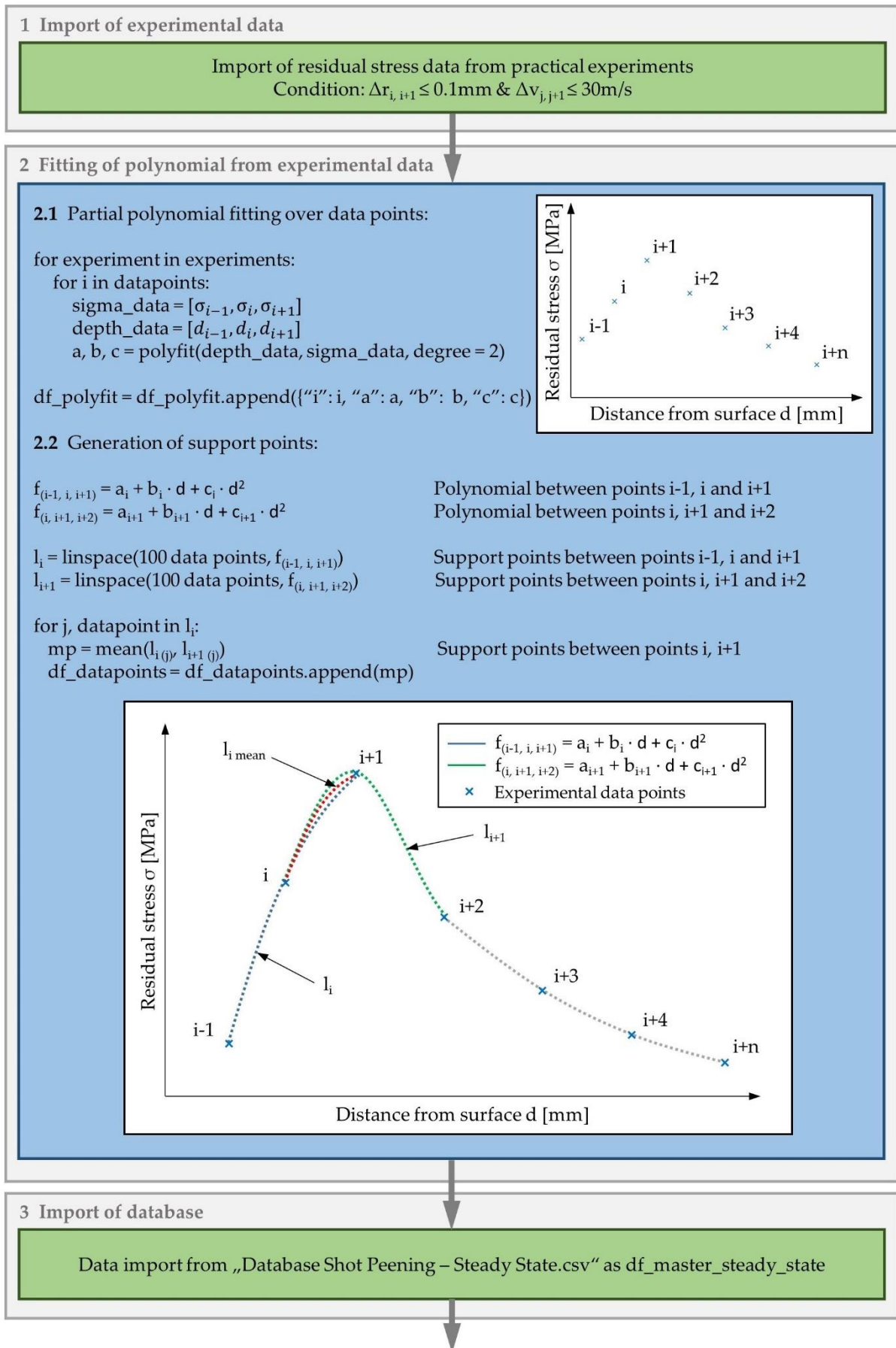
1 Import of experimental data

Import of residual stress data from practical experiments
Condition: $\Delta r_{i,\,i+1} \le 0.1\,mm$ & $\Delta v_{j,\,j+1} \le 30\,m/s$

2 Fitting of polynomial from experimental data

2.1 Partial polynomial fitting over data points:

```
for experiment in experiments:
    for i in datapoints:
        sigma_data = [σ_{i-1}, σ_i, σ_{i+1}]
        depth_data = [d_{i-1}, d_i, d_{i+1}]
        a, b, c = polyfit(depth_data, sigma_data, degree = 2)

df_polyfit = df_polyfit.append({"i": i, "a": a, "b": b, "c": c})
```

2.2 Generation of support points:

$f_{(i-1,\,i,\,i+1)} = a_i + b_i \cdot d + c_i \cdot d^2$ Polynomial between points i-1, i and i+1
$f_{(i,\,i+1,\,i+2)} = a_{i+1} + b_{i+1} \cdot d + c_{i+1} \cdot d^2$ Polynomial between points i, i+1 and i+2

l_i = linspace(100 data points, $f_{(i-1,\,i,\,i+1)}$)   Support points between points i-1, i and i+1
l_{i+1} = linspace(100 data points, $f_{(i,\,i+1,\,i+2)}$)   Support points between points i, i+1 and i+2

```
for j, datapoint in l_i:
    mp = mean(l_{i (j)}, l_{i+1 (j)})          Support points between points i, i+1
    df_datapoints = df_datapoints.append(mp)
```

3 Import of database

Data import from „Database Shot Peening – Steady State.csv" as df_master_steady_state

Fig. 17. Logic of the shot peening residual stress predictor [125]

4 Modification of real and physical data

4.1 Implementation of experimental data (df_datapoints) into df_master_steady_state:

4.2 Exclusion of initial FEA based datasets (FEA plane$_{k+1}$) within interpolation volume:

5 Export of data to database

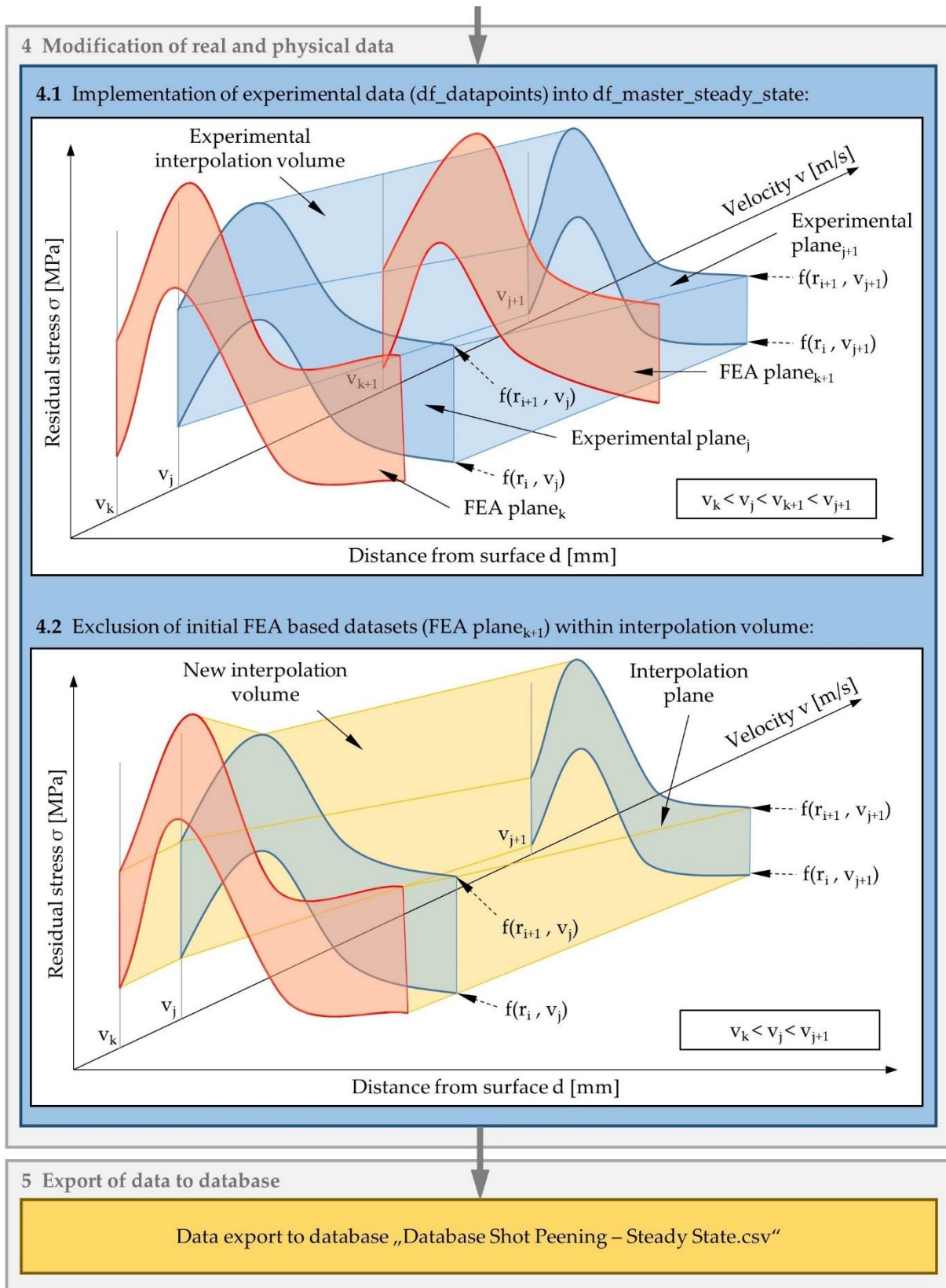Data export to database „Database Shot Peening – Steady State.csv"

Fig. 17. continued

3.3.4. *Data-driven black box modeling of the correlation between electrical resistivity and mechanical properties of rolled aluminum using an electrical resistivity measurement system*

Based on the approach in section 3.3.1., the existing algorithm and data-driven BBM for rolled material was extended by a QC step (Figure 18). By investigating correlations between electrical properties and mechanical properties, it was possible to draw conclusions about certain mechanical properties by measuring the electrical resistance. The additional testing of specimen could expand the data sets of already rolled specimen, whose data were already stored in the algorithm. The mechanical properties were determined by a tensile test and the electrical properties by an electrical resistivity measurement system, whose datasets have been unified and synchronized through a non-proprietary open-source digitalization approach, therefore building upon the initial data-driven BBM approach. [126]
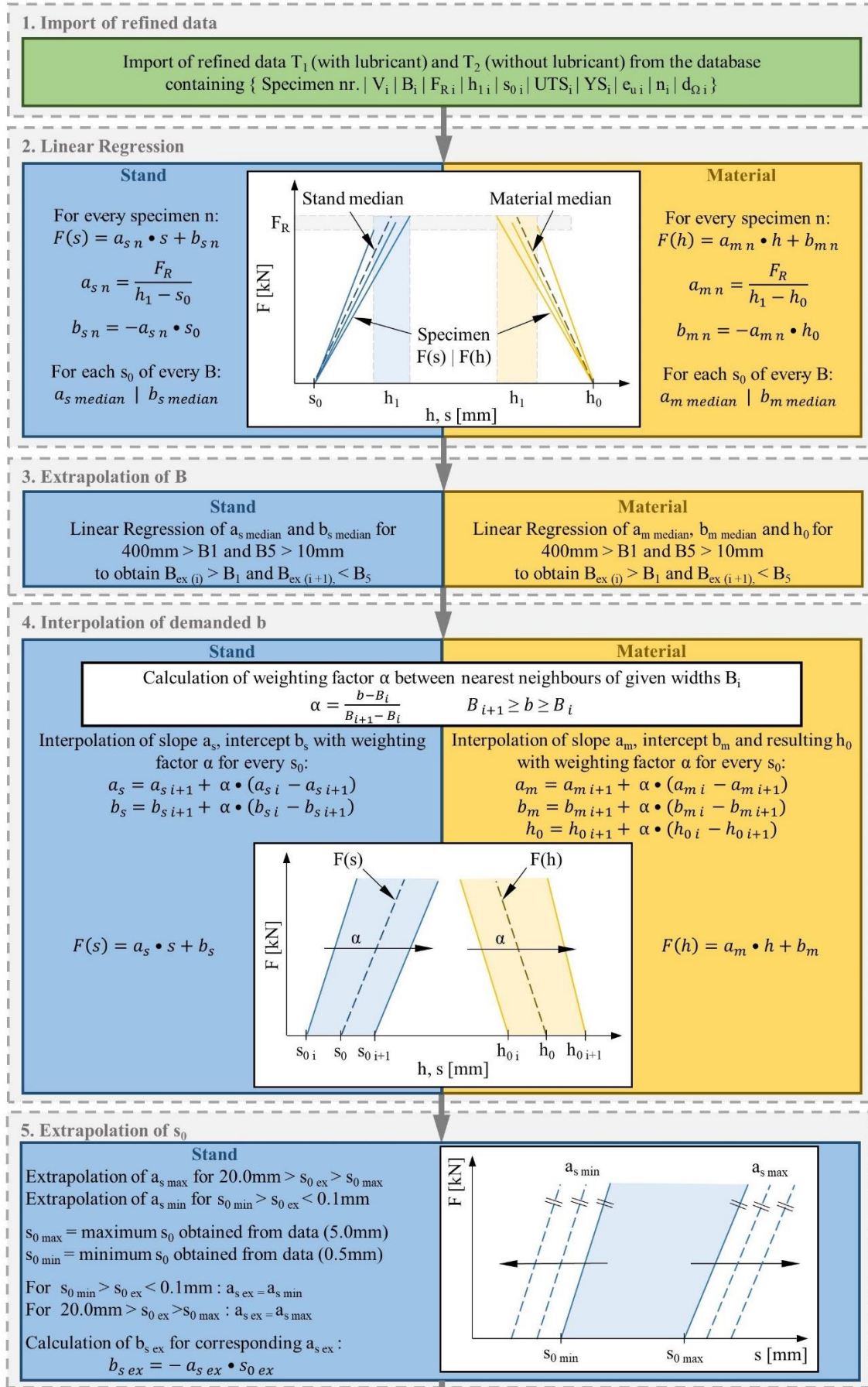
1. Import of refined data

Import of refined data T_1 (with lubricant) and T_2 (without lubricant) from the database containing { Specimen nr. | V_i | B_i | $F_{R\,i}$ | $h_{1\,i}$ | $s_{0\,i}$ | UTS_i | YS_i | $e_{u\,i}$ | n_i | $d_{\Omega\,i}$ }

2. Linear Regression

Stand

For every specimen n:
$$F(s) = a_{s\,n} \bullet s + b_{s\,n}$$

$$a_{s\,n} = \frac{F_R}{h_1 - s_0}$$

$$b_{s\,n} = -a_{s\,n} \bullet s_0$$

For each s_0 of every B:
$$a_{s\,median} \mid b_{s\,median}$$

(graph: F [kN] vs h, s [mm]; Stand median, Material median, Specimen F(s) | F(h); axis labels s_0, h_1, h_1, h_0; F_R)

Material

For every specimen n:
$$F(h) = a_{m\,n} \bullet h + b_{m\,n}$$

$$a_{m\,n} = \frac{F_R}{h_1 - h_0}$$

$$b_{m\,n} = -a_{m\,n} \bullet h_0$$

For each s_0 of every B:
$$a_{m\,median} \mid b_{m\,median}$$

3. Extrapolation of B

Stand
Linear Regression of $a_{s\,median}$ and $b_{s\,median}$ for $400mm > B1$ and $B5 > 10mm$ to obtain $B_{ex\,(i)} > B_1$ and $B_{ex\,(i+1)} < B_5$

Material
Linear Regression of $a_{m\,median}$, $b_{m\,median}$ and h_0 for $400mm > B1$ and $B5 > 10mm$ to obtain $B_{ex\,(i)} > B_1$ and $B_{ex\,(i+1)} < B_5$

4. Interpolation of demanded b

Stand **Material**

Calculation of weighting factor α between nearest neighbours of given widths B_i
$$\alpha = \frac{b - B_i}{B_{i+1} - B_i} \qquad B_{i+1} \geq b \geq B_i$$

Interpolation of slope a_s, intercept b_s with weighting factor α for every s_0:
$$a_s = a_{s\,i+1} + \alpha \bullet (a_{s\,i} - a_{s\,i+1})$$
$$b_s = b_{s\,i+1} + \alpha \bullet (b_{s\,i} - b_{s\,i+1})$$

Interpolation of slope a_m, intercept b_m and resulting h_0 with weighting factor α for every s_0:
$$a_m = a_{m\,i+1} + \alpha \bullet (a_{m\,i} - a_{m\,i+1})$$
$$b_m = b_{m\,i+1} + \alpha \bullet (b_{m\,i} - b_{m\,i+1})$$
$$h_0 = h_{0\,i+1} + \alpha \bullet (h_{0\,i} - h_{0\,i+1})$$

$$F(s) = a_s \bullet s + b_s$$

(graph: F [kN] vs h, s [mm]; F(s), F(h), α; axis labels $s_{0\,i}$, s_0, $s_{0\,i+1}$, $h_{0\,i}$, h_0, $h_{0\,i+1}$)

$$F(h) = a_m \bullet h + b_m$$

5. Extrapolation of s_0

Stand

Extrapolation of $a_{s\,max}$ for $20.0mm > s_{0\,ex} > s_{0\,max}$
Extrapolation of $a_{s\,min}$ for $s_{0\,min} > s_{0\,ex} < 0.1mm$

$s_{0\,max}$ = maximum s_0 obtained from data (5.0mm)
$s_{0\,min}$ = minimum s_0 obtained from data (0.5mm)

For $s_{0\,min} > s_{0\,ex} < 0.1mm$: $a_{s\,ex} = a_{s\,min}$
For $20.0mm > s_{0\,ex} > s_{0\,max}$: $a_{s\,ex} = a_{s\,max}$

Calculation of $b_{s\,ex}$ for corresponding $a_{s\,ex}$:
$$b_{s\,ex} = -a_{s\,ex} \bullet s_{0\,ex}$$

(graph: F [kN] vs s [mm]; $a_{s\,min}$, $a_{s\,max}$; axis labels $s_{0\,min}$, $s_{0\,max}$)

Fig. 18. Logic of the data-driven rolling schedule predictor with extended QC step [126]

6. Extrapolation of h_0

Material

Extrapolation of $h_0(s_{0\,ex})$ with linear regression for
$s > s_{0\,max}$ and $s < s_{0\,min}$

Calculation of $b_{m\,ex}$ for corresponding $a_{m\,ex}$:
$$b_{m\,ex} = -\,a_{m\,ex} \bullet h_{0\,ex}$$

7. Interpolation of h_0 and rolling schedule iterator

Stand

Auxiliary variable γ ($0 \leq \gamma \leq 1; stepsize\ 5E - 4$)
$$a_{s\,j} = a_{s\,i+1} + \gamma \bullet (a_{s\,i} - a_{s\,i+1})$$
$$b_{s\,j} = b_{s\,i+1} + \gamma \bullet (b_{s\,i} - b_{s\,i+1})$$

Calculation of roll gap height $s_{0\,j}$ height for step j:
$$s_{0\,j} = \frac{a_{s\,j} \bullet h_{1\,j} - F_R}{b_{s\,j}}$$

Material

Calculation of weighting factor β between nearest neighbours of h_0
$$\beta = \frac{h_0 - h_{0\,i}}{h_{0\,i+1} - h_{0\,i}} \qquad h_{0\,i+1} \geq h_0 \geq h_{0\,i}$$
$$a_{m\,j} = a_{m\,i+1} + \beta \bullet (a_{m\,i} - a_{m\,i+1})$$
$$b_{m\,j} = b_{m\,i+1} + \beta \bullet (b_{m\,i} - b_{m\,i+1})$$

Calculation of exit height $h_{1\,j}$ for step j:
$$h_{1\,j} = \frac{F_R - b_{m\,j}}{a_{m\,j}} = h_{0\,j+1}$$

8. Checking of target values

$d_\Omega \geq d_{\Omega\,target} + d_{\Omega\,residual}$

d_Ω

$d_\Omega \leq d_{\Omega\,target} - d_{\Omega\,residual}$

Interval bisection method applied to rolling force for iteration k

$$d_{\Omega\,target} - d_{\Omega\,residual}$$
$$\leq d_\Omega \leq$$
$$d_{\Omega\,target} + d_{\Omega\,residual}$$

Rolling schedule valid for defined mechanical properties
UTS | YS | e_u | n

Interval bisection method applied to rolling force for iteration k

$F_R = F_{R\,new}$

Restart at step
2. Linear Regression

$F_R = F_{R\,new}$

Fig. 18. continued

3.4. Answering research question (d): Methodology and contribution

In order to answer (d) on how SME specific digitalization solutions must be build up to ensure compatibility within a value chain, the case studies and correlation contributions are summarized in Table 5.

Table 5. Contributions to answer (d).

No.	Case study	Adressed issues	Corresponding publications
3.4.1	Elaboration of a framework to ensure a standardized technical communication in the context of I 4.0	Elaboration of the RAMI 4.0 in the context of MUL 4.0; Design of a production network to include all value chain participants and ensure IT security	A 1
3.4.2	Framework for the implementation of a smart factory layer architecture in the context of manufacturing SMEs	Proposal of a framework for the design and implementation of a resilient low-cost layer architecture for metal forming smart factories with special focus on SMEs; Framework for the digitalization of a CNC lathe and Gleeble 3800 using a retrofitting approach applicable in the metal forming industry	A 4
3.4.3	Framework for the implementation of a CPPS of a rolling mill	Framework for the implementation of a resilient low-cost CPPS with a retrofitting approach applicable in the metal forming industry; Identification process and product parameters to ensure accurate modeling approach; Integration into a production network to improve IT security and transparency along the value chain	A 5

3.4.4	Framework for the implementation of a CPPS of a hydraulic press and two furnaces	Framework for the implementation of a resilient low-cost CPPS with a retrofitting approach applicable in the metal forming industry; Identification process and product parameters to ensure accurate modeling approach; Integration into a production network to improve IT security and transparency along the value chain	A 6
3.4.5	Development of a machine learning supported quality control approach for the shot peening process	Design of a of digitalized and scalable QC process with focus on the expandability of the database with data from practical experiments and results from numerical simulations	A 7
3.4.6	Development of an analysis algorithm for the correlation between anisotropy and electrical resistivity of rolled aluminum using the four-point method to enhance quality control	Design and integration of digitalized QC processes incorporating two proprietary systems with different data formats and DAQ sampling rates	A 8
3.4.7	Integration of LUS into an Industry 4.0 value chain in the context of sustainable production	Proposal for the integration of an in-situ micro structure characterization QC process into MUL 4.0 value chain and production network	A 9

3.4.1. *Elaboration of a framework to ensure a standardized technical communication in the context of I 4.0*

Within this case study, the RAMI 4.0 was concretized in the context of MUL 4.0, detailing the individual layer fragments. In essence, the importance of an initial alignment to ensure a uniform and standardized

technical communication was highlighted. Furthermore, the application of such standardized frameworks supports the holistic digitalization and digital transformation, ensuring a detailed documentation of all entities and its respective interconnections. Consequently, the design of the MUL 4.0 Layer 2 production network was introduced, ensuring the incorporation of all value chain participants into the network, allowing transparent and secure data storage and sharing, specimen tracking, and communication between value chain participants (Figure 5). Additionally, the design of the Layer 2 networks increases cyber security, by restricting access from unauthorized entities, and thus reduces the likelihood of data security and privacy issues. [3]

3.4.2. *Framework for the implementation of a smart factory layer architecture in the context of manufacturing SMEs*

As illustrated in Figure 7, a potential framework for the design and implementation of a layer architecture was elaborated, focusing on the utilization of resilient low-cost components and open-source software, applicable for SMEs in the manufacturing industry. Through a uniform design and the definition of the individual layers and dataflows, the scalability of this solution was demonstrated through the integration of several CPPSs. Therefore, a CNC lathe (Figure 19) and a Gleeble (Figure 20) were equipped with resilient low-cost software and hardware in order to transform these machines into CPPSs and integrate them into the digital environment, applicable in the context of a manufacturing SME. The developed standardized digitalization approach, which was also applied in section 3.4.3. and 3.4.4., separates the CPPS structure into analog and digital domains. The analog domain contains all physical elements of the machine or aggregate, such as sensors, actuators and DAQs. In the case of the Gleeble, existing sensors were implemented in the iba DAQ, whereas the current transformers of the CNC lathe were mounted on existing phases before being implemented in WAGO DAQ. In any case, the conversion of analog signals takes place in the DAQ, resulting in digital and thus computer-processable signals. Consequently, the data is preprocessed and distributed in the desired format to various systems such as DBMS, GUIs and other processing layers, using applicable protocols. The applied open-source approach combined with non-proprietary DAQs, enables the flexible control and modification of dataflows, facilitating the creation of new interfaces with other entities. In addition, this approach results in an academic learning factory, allowing interested parties to gain knowledge and experience in this environment in order to recruit and teach new tech talent. [123]
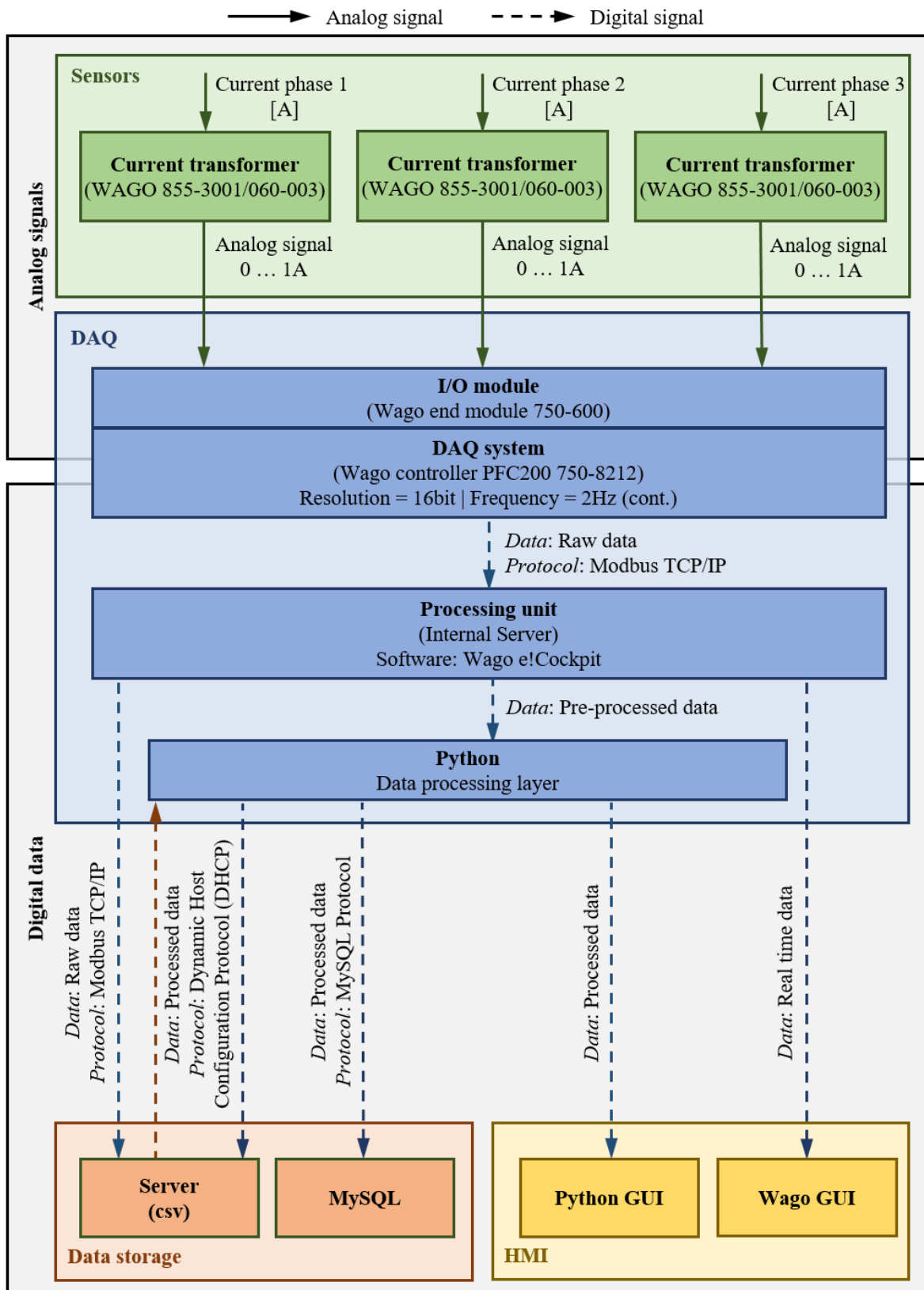
Fig. 19. Digitalization framework of the CNC lathe [123].
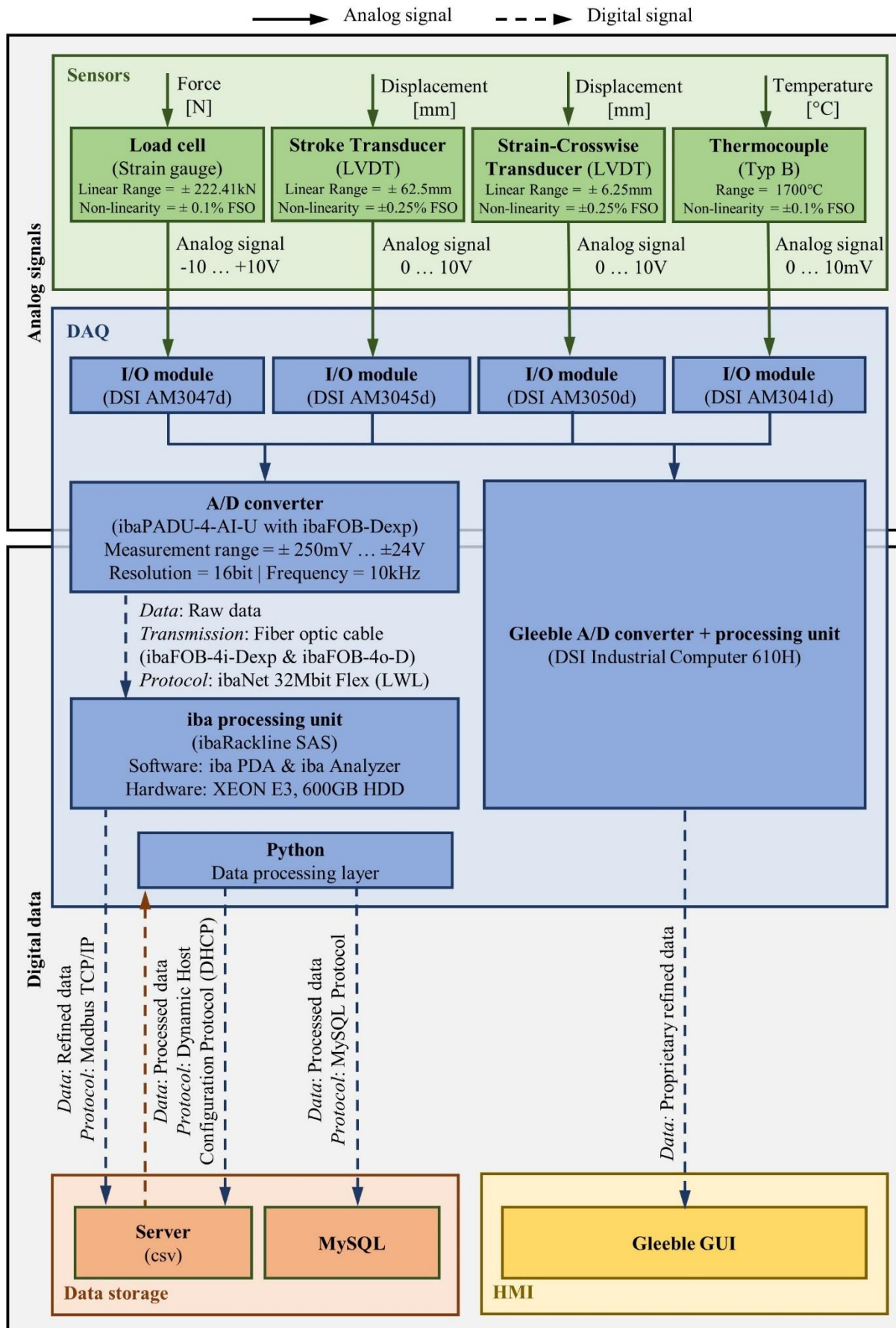
Fig. 20. Digitalization framework of the Gleeble [123].

3.4.3. Framework for the implementation of a CPPS of a rolling mill

Within this case study, a framework for the holistic transformation of a rolling mill into a CPPS was introduced (Figure 21). As highlighted in the previous sections, many SMEs operate machines and aggregates that cannot be implemented into an I 4.0 environment or digital value chain. Nevertheless, this case study demonstrates as standardized approach, implementing suitable sensors and DAQ systems, and thus transforming it into a CPPS. Following the applied brownfield approach, the rolling mill from 1954 at the MF was successfully equipped with resilient low-cost sensor technology and DAQ, following an analysis of the relevant process variables. Accompanying, a guideline for the process-independent definition and determination of process parameters was established, on the basis of which suitable sensors and DAQ technologies can be selected together with fundamental metrological characteristics. Based on the case study of the rolling mill, this guideline was practically applied and the sensors were chosen, adjusted to the respective process parameters to measure. Furthermore, external electronics were selected to transform different analog signal into a uniform analog signal, so that only one I/O module has to be acquired for the WAGO DAQ, supporting a transparent and low-cost approach. As proposed in section 3.4.2., the respective analog sensors signals are transferred into digital signals by the DAQ, and consequently distributed processing units, DBMS and GUIs. As a result of the conducted practical experiments, the developed supervised ML algorithm (Figure 15) was able to accurately predict the end height of the material in dependence of the input parameters, inserted in the GUI (Figure 10). Like the other CPPS, the rolling mill was implemented into the layer architecture and later into the MUL 4.0 production network, ensuring the cyber security and transparency along the entire MUL 4.0 value chain. Furthermore, the successful implementation of open-source based programming, data analysis, black-box modeling, ML and visualization, this case study serves as a proof of the applicability of open-source software in the manufacturing industry. Additionally, the importance of bypassing proprietary hardware or software solutions was highlighted, by implementing a highly connective software and hardware approach. [17]
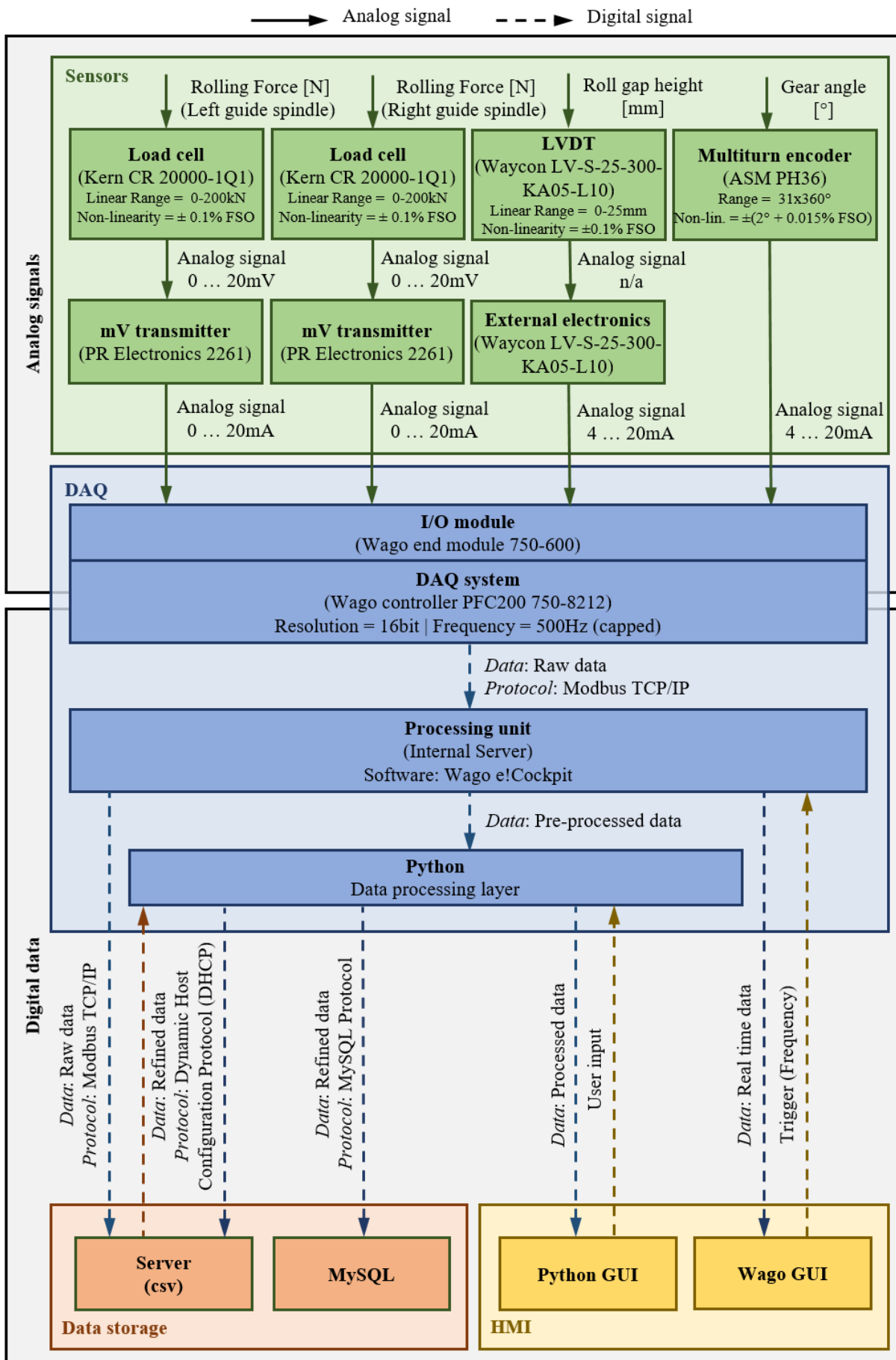
Fig. 21. Digitalization framework of the rolling mill CPPS [17].

3.4.4. *Framework for the implementation of a interconnected CPPS of a hydraulic press and two furnaces*

Similar to the framework of the rolling mill CPPS (section 3.4.3), the hydraulic press from 1952 and two industrial furnaces at the MF were initially not suitable for the I 4.0 application. For this reason, a resilient low-cost retrofitting approach was reapplied, serving as a validation of the practicality of this framework (Figure 22). Based on the established guideline for the process parameter definition, suitable software and hardware was chosen and successfully implemented. Unlike the rolling mill CPPS, a RevPi DAQ was implemented, running the ST based software CODESYS and also being cheaper than the WAGO DAQ. In comparison to the rolling mill CPPS, a modular modifiable multistep WBM using a Python-scripted FEA was developed, depicting an interconnected process sequence between the furnaces and the hydraulic press. The resulting DS (Figure 23) enables automated simulation and sensor data-driven process validation, available to the front-end user through a Python GUI, and thus supporting the decision-making process and situationally appropriate acting. Furthermore, a condition monitoring system performing sanity checks to identity faulty sensors was implemented, further increasing process stability and quality. Once again, the standardization of this framework enables flexible control of data flows and distribution to processing units, GUIs and DBMSs. To emphasize the advantages of highly communicative software and hardware, a superordinate GUI system was implemented, also based on the WAGO e!Cockpit. For this, the CODESYS software running on the RevPi communicates via MODBUS with WAGO e!Cockpit and publishes selected process parameters on the individual GUI of the hydraulic press and furnaces. As a further consequence, a standardized and uniform approach for the integration of different systems from different manufacturers was applied and successfully implemented, bypassing a proprietary solution. In order to further expand the production network and point out the scalability, the resulting CPPS was integrated into the MUL 4.0 production network. [124]
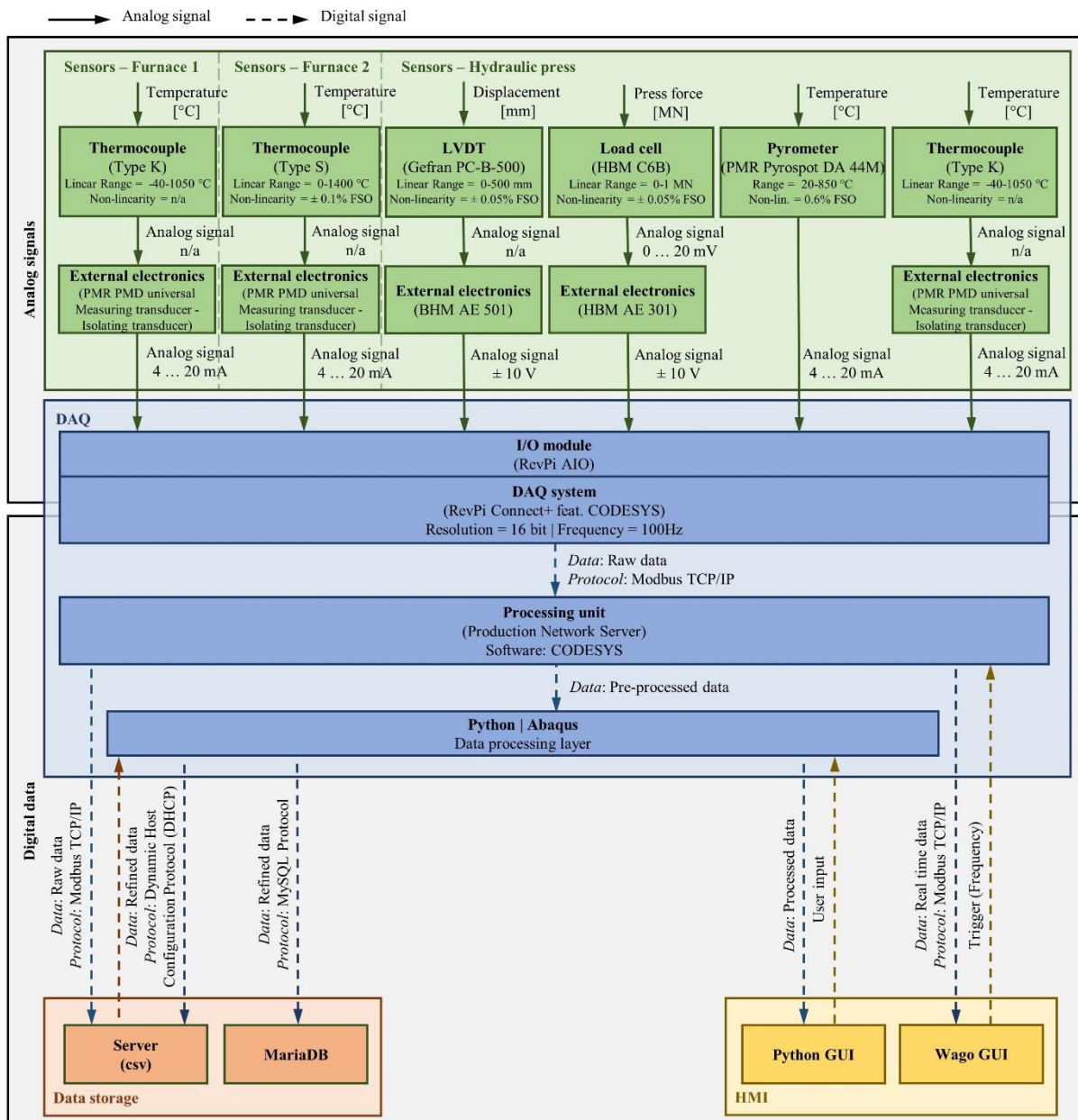
Fig. 22. Digitalization framework of the CPPS, incorporating two furnaces and a hydraulic press [124]
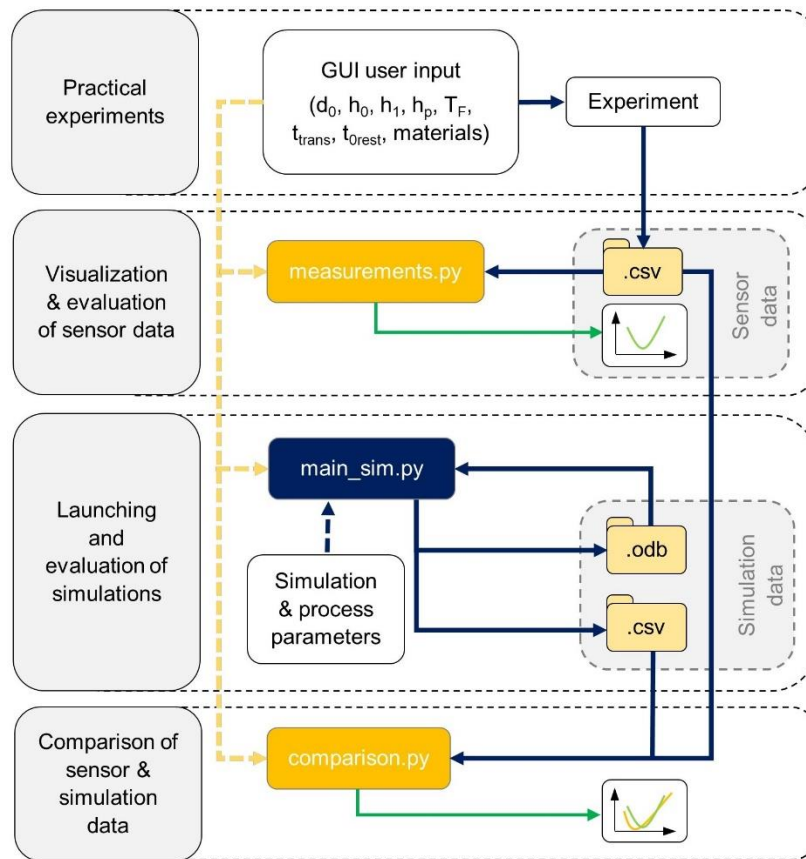
Fig. 23. Digital Shadow of the hydraulic press and furnaces CPPS [124]

3.4.5. Development of a machine learning supported quality control approach for the shot peening process

In this case study, a FEA based GBM incorporating Python was developed, elaborated in section 3.3.3. Serving as the initial step of the design of a digitalization solution or model, the process and the underlying mechanics were analyzed in depth and understood, being a key requirement for the successful implementation. Furthermore, the required inputs, parameter evaluation procedure and desired outputs were defined, as well as their requirements and the benefits, contributing to their respective roles in the QC and decision-making process. Consequently, suitable technology was chosen to digitally depict the process. For this purpose, Abaqus was chosen for the FEA, as it is being widely applied in the industry and academia. To support the interoperability and non-proprietary character of this solution, Python was used to interact with Abaqus, executing FEAs with the user input from a GUI, and eventually visualizing the extracted simulation results for the front-end user to support the decision-making process. Additional focus was set on the expandability of the database with data from practical experiments and results from numerical simulations, designing a digitalized and scalable supervised ML QC process. In other words, these actionable insights of this solution are presented to the user, supporting process optimization, and improving the overall efficiency, quality and sustainability. [125]

3.4.6. Development of an analysis algorithm for the correlation between anisotropy and electrical resistivity of rolled aluminum using the four-point method to enhance quality control

As described in section 3.2.5., the initial step of the digitalization process, was the analysis of both datasets and their interactions, in order to evaluate a characteristic value for the synchronization timestamp, enabling the automated data synchronization and analysis. Based on the data analysis of the interactions, quality parameters were derived that could be used for the digitized QC approach, serving as a validation. In order to actively integrate the resulting BBM (section 3.3.4.) into the decision-making process, user input and output parameters were defined and a corresponding GUI was developed, providing the user with actionable insights. [126]

3.4.7. Integration of LUS into an Industry 4.0 value chain in the context of sustainable production

Based on the developed standardized digitalization framework, a concept for the Laser Ultra Sonics (LUS) was developed, which will be implemented at the MF in the future. This concept builds on the existing Gleeble, complemented by the LUS to observe material responses and microstructural change under different strains, strain rates and temperatures. In order to be able to carry out the high-frequency measurement, an optical fiber-based iba DAQ was chosen (Figure 24). The resulting microstructure model in combination with the LUS can be utilized to operate in-line QC even under very harsh conditions, e.g. hot rolling. For the future expansion of the MUL 4.0 scope, the LUS CPPS will also be integrated into the production network. [127]
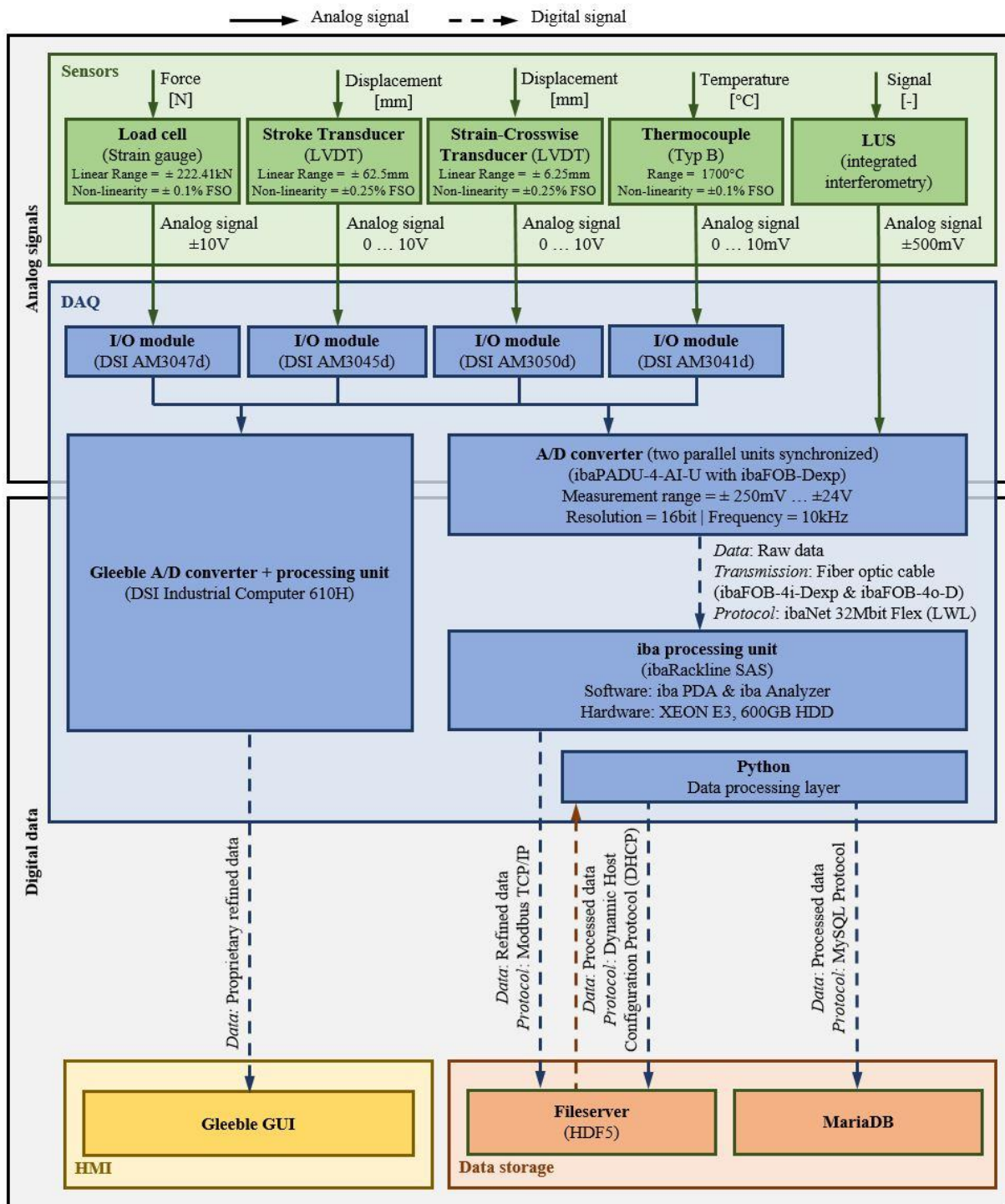
Fig. 24. Digitalization framework of the LUS [127]

4. Results and discussion

To support the digitalization and digital transformation of the manufacturing industry with special focus on SMEs, this thesis aims to answer research question (I) and its respective subquestions (a-d) from current literature and practical case studies. Therefore, nine case studies were conducted, identifying the state of the art regarding I 4.0 and elaborating several frameworks to ensure a successful interdisciplinary digitalization of manufacturing and quality control process, and the integration in a connected value chain. To answer research question (a), the state of the art of I 4.0 in the context of manufacturing was researched and the project MUL 4.0 was established, which was found to be representative of the situation in manufacturing SMEs, concluding a low digital maturity.

To support a holistic digitalization and answer research question (b), the applicability of open-source software was evaluated to avoid interface problems and proprietary systems, furthermore lowering financial obstacles many SMEs face. For this reason, five case studies were conducted, based on a resilient low-cost and open-source software approach. Consequently, several proprietary machines and aggregates were transformed into I 4.0 applicable CPPSs. In the elaborated frameworks, an open-source and low-cost software with high connectivity was enforced, avoiding proprietary solutions. In all case studies, open-source software could be successfully applied for the implementation of data analysis, modeling approaches, algorithms, ML, GUIs and networking of systems, proving the suitability of such approaches.

Due to the high heterogeneity of products and processes in the manufacturing industry, question (c) focused on the suitability of different modeling approaches. Consequently, four case studies were conducted, implementing real-physical WBM approaches with FEA, data-driven BBM, and a combination of both, so-called GBM. The black box approach of the rolling mill CPPS achieved very good results with the supervised ML algorithm in generating a rolling schedule, but requires a sufficiently large amount of statistically representative data, which can only be determined by practical experiments, which can represent a financial obstacle for SMEs. The same applies to the BBM approach of the correlation between anisotropy and electrical resistivity of rolled aluminum using the four-point method. The FEA-based WBM approach used for modeling the hot upsetting process requires material data instead of practical experiments to simulate the process on the basis of real physical interrelationships. On the one hand, a meaningful FEA requires high-quality material data, which, depending on the software and literature, can be evaluated with varying degrees of difficulty and result in a higher computational effort than the implemented BBMs. Nevertheless, the FEA has established itself as an important tool for the simulation of complex geometries and processes, enabling the accurate examination of the product and process behavior. To combine the advantages of both approaches, a GBM was implemented for the shot peening process to predict the process behavior from FEA generated and experimentally determined data, providing good results at lower computation time. With all approaches, very good results could be achieved for the respective processes, which are, however, highly

individual and tailored to the process. The applicability of all modeling tests for the I 4.0 application in SMEs was hereby demonstrated, however, the modeling approach and the respective advantages and disadvantages must be carefully examined initially in order to decide which approach is applicable for the circumstances.

To answer research question (d), seven case studies were conducted to answer how SME specific digitalization solutions build up to ensure compatibility within a value chain. For this purpose, RAMI 4.0 was elaborated and detailed in the context of the MUL 4.0 value chain in order to define interconnections and ensure standardized communication. Consequently, a framework for a six-layer architecture of a smart factory was developed, allowing the integration of CPPSs. For the implementation of these CPPSs, machine and process specific frameworks have also been developed, demonstrating the applicability of resilient low-cost software and hardware. Generally, the use of suitable frameworks is recommended, but individual adaptation to the circumstances must follow. However, what unites these SME specific solutions is the application of resilient low-cost but high-quality components that can withstand the environmental conditions in the manufacturing environment, preventing downtime and value chain disruptions. In additionmode, cyber security and transparency must be ensured through the implementation of an appropriate production network to ensure the resilient and holistic functionality of the digitalized value chain.

By essentializing these four subquestions (a-d), research question (I) can be answered. On the shop floor or field level, machines and aggregates must be examined for relevant process variables and environmental conditions, on the basis of which sensors, actuators and DAQ can be selected. Simultaneously, the type of process modeling approach must be evaluated for the relevant process variables and outcomes in order to enable representative process mapping. Consequently, the resulting data must be analyzed and distributed, in the form of visualization with GUIs or through integration with ERP or MES systems. In the context of the value chain, a standardized framework for standardized integration must therefore be defined for all participants and a production network implemented. The shared production network must be implemented in accordance with the state of the art in cyber security, ensuring the resilience of the entire value chain. In each of these points, standardization, resilience, avoidance of proprietary solutions, and cyber security are the top priorities.

5. Conclusion and Outlook

This thesis presents the development of a framework for the implementation of a digital value chain with special focus on manufacturing SMEs. To accomplish this, a superordinate Layer 2 production network was implemented, to connect all participants of the MUL 4.0 value chain, enabling transparent data storage and distribution in the future. Furthermore, a six layer architecture was implemented to incorporate digitalized machines and aggregates at the MF, which subsequently led to the establishment of a SFL for academic learning. Considering the current degree of digitalization and the arising challenges in manufacturing SMEs, a special focus was set upon the transformation of not I 4.0 suitable machines and aggregates into CPPSs, capable of being integrated in the respective layer architecture and production network. To support the CPPS transformation process, the machines and aggregates were equipped with resilient low-cost sensor technology, DAQ systems and open-source programming, implementing different modeling approaches by using data-driven BBMs, real-physical WBMs or a GBM by combining both. In addition, ML algorithms were developed, supporting the integration of these models into the production process. In order to highlight the new possibilities in the context of QC, several I 4.0-compliant models and frameworks were developed, following the same open-source approach.

To further expand the potential of this digital value chain, additional chairs and institutes within the university as well as industrial partners should be integrated, allowing both academic and industrial development. The implemented production network, the layer architecture and the various practical case studies enable the testing of new digital ideas and concepts without the disadvantage of production downtimes and thus far-reaching financial costs. This opportunity is particularly important in the context of manufacturing SMEs, as such practical use cases for learning and testing new methods are difficult to achieve in a competitive industry and require high financial resources. By utilizing resilient low-cost industrial standard hardware and open-source software, this approach can be applied in the industrial field without having to rely on cost-intensive proprietary solutions, inhibiting a holistic digital transformation and the scalability of digitalized solutions. Another advantage of this approach is the modifiability of such solutions, which can be tailored to product and process, which is essential due to the high heterogeneity of products and processes in the manufacturing industry.

With the future expansion of the MUL 4.0 value chain, a specimen tracking system is also being considered, making it possible to collect specimen data from the production cycle and thus also to better link data in the shared database. In addition, the value chain can be extended with a supply chain DT in order to include the activities of external suppliers. By cooperating with other potential value chain participants, further digitalized machines and aggregates can be integrated into the value chain, whose digitalization can be based on the frameworks presented. Furthermore, existing CPPSs can also be modified with additional sensor technology, actuator technology and alternative or improved modeling approaches. With the inclusion of more value chain participants and thus CPPSs, an expansion of the

production network should also be addressed in order to ensure an efficient digital production environment, due to increased amount of data and need for bandwidth. Consequently, the increasing amount of data can be used to improve existing modeling approaches and algorithms, drawing conclusions about complex interactions through the use of sophisticated analysis methods and ML. For this reason, the cooperation of academic and industrial interests offers an ideal environment to drive holistic digitalization and digital transformation in order to teach and train tech talent in academia in the future.

The concepts and frameworks presented in this doctoral thesis serve as a resilient fundament for the further digitalization of value chains and the implementation of smart factories and digitalized machine systems with special focus on SMEs to support the domestic manufacturing industry in a digital and competitive future.

List of Figures

List of Tables

References

1. Staebe, M.; Lustgaten, T. *Thinking Outside the Machine*: *Global Machinery & Equipment Report 2022*. Available online: https://www.bain.com/globalassets/noindex/2022/bain_report_machinery-and-equipment-report-2022.pdf (accessed on 10 March 2023).

2. Behrendt, A.; Boer, E. de; Kasah, T.; Koerber, B.; Mohr, N.; Richter, G. *Leveraging Industrial IoT and advanced technologies for digital transformation*: *How to align business, organization, and technology to capture value at scale*. Available online: https://www.mckinsey.com/~/media/mckinsey/business%20functions/mckinsey%20digital/our%20insights/a%20manufacturers%20guide%20to%20generating%20value%20at%20scale%20with%20iiot/leveraging-industrial-iot-and-advanced-technologies-for-digital-transformation.pdf (accessed on 10 March 2023).

3. Sorger, M.; Ralph, B.J.; Hartl, K.; Woschank, M.; Stockinger, M. Big Data in the Metal Processing Value Chain: A Systematic Digitalization Approach under Special Consideration of Standardization and SMEs. *Applied Sciences* **2021**, *11*, 9021, doi:10.3390/app11199021.

4. Küpper, D.; Sieben, C.; Boyne, J.; Li, A.; Buchner, T. *The Automation Revolution in Manufacturing*. Available online: https://web-assets.bcg.com/dd/72/f463a37441d3aeb7a9dd5f8e024a/bcg-the-automation-revolution-in-manufacturing-mar-2022.pdf (accessed on 10 March 2023).

5. Berruti, F.; Chesnais, T.; Daub, M.; Hu, A.; Moreno, J.; Phalin, G.; Rosendahl, M.; Schenk, T.; Sood, R.; Wan, X.; et al. *Digital service excellence: Scaling the next-generation operating model*. Available online: https://www.mckinsey.com/~/media/mckinsey/business%20functions/operations/our%20insights/digital%20service%20excellence/digital-service-excellence--scaling-the-next-generation-operating-model.pdf (accessed on 10 March 2023).

6. Dr. Ulrike Oschischnig. *Statistical Yearbook 2022*, Vienna, 2022. Available online: https://wko.at/statistik/jahrbuch/YEARBOOK_2022.pdf (accessed on 3 March 2023).

7. Guo, D.; Li, M.; Lyu, Z.; Kang, K.; Wu, W.; Zhong, R.Y.; Huang, G.Q. Synchroperation in industry 4.0 manufacturing. *International Journal of Production Economics* **2021**, *238*, 108171, doi:10.1016/j.ijpe.2021.108171.

8. Nascimento, D.L.M.; Alencastro, V.; Quelhas, O.L.G.; Caiado, R.G.G.; Garza-Reyes, J.A.; Rocha-Lona, L.; Tortorella, G. Exploring Industry 4.0 technologies to enable circular economy practices in a manufacturing context. *JMTM* **2019**, *30*, 607–627, doi:10.1108/JMTM-03-2018-0071.

9. Ralph, B.J.; Stockinger, M. *Digitalization and Digital Transformation in Metal Forming: Key Technologies, Challenges and Current Developments of Industry 4.0 Applications*, 2020.

References

10. Oztemel, E.; Gursev, S. Literature review of Industry 4.0 and related technologies. *J Intell Manuf* **2020**, *31*, 127–182, doi:10.1007/s10845-018-1433-8.

11. Pereira, A.C.; Romero, F. A review of the meanings and the implications of the Industry 4.0 concept. *Procedia Manufacturing* **2017**, *13*, 1206–1214, doi:10.1016/j.promfg.2017.09.032.

12. Kamble, S.S.; Gunasekaran, A.; Gawankar, S.A. Sustainable Industry 4.0 framework: A systematic literature review identifying the current trends and future perspectives. *Process Safety and Environmental Protection* **2018**, *117*, 408–425, doi:10.1016/j.psep.2018.05.009.

13. Matt, D.T.; Modrák, V.; Zsifkovits, H. *Industry 4.0 for SMEs;* Springer International Publishing: Cham, 2020, ISBN 978-3-030-25424-7.

14. Boyes, H.; Hallaq, B.; Cunningham, J.; Watson, T. The industrial internet of things (IIoT): An analysis framework. *Computers in Industry* **2018**, *101*, 1–12, doi:10.1016/j.compind.2018.04.015.

15. Cardin, O. Classification of cyber-physical production systems applications: Proposition of an analysis framework. *Computers in Industry* **2019**, *104*, 11–21, doi:10.1016/j.compind.2018.10.002.

16. Wu, X.; Goepp, V.; Siadat, A. Concept and engineering development of cyber physical production systems: a systematic literature review. *Int J Adv Manuf Technol* **2020**, *111*, 243–261, doi:10.1007/s00170-020-06110-2.

17. Ralph, B.J.; Sorger, M.; Hartl, K.; Schwarz-Gsaxner, A.; Messner, F.; Stockinger, M. Transformation of a rolling mill aggregate to a cyber physical production system: from sensor retrofitting to machine learning. *J Intell Manuf* **2022**, *33*, 493–518, doi:10.1007/s10845-021-01856-2.

18. Mell, P.M.; Grance, T. *The NIST definition of cloud computing*, Gaithersburg, MD, 2011.

19. Kaiblinger, A.; Woschank, M. State of the Art and Future Directions of Digital Twins for Production Logistics: A Systematic Literature Review. *Applied Sciences* **2022**, *12*, 669, doi:10.3390/app12020669.

20. Zsifkovits, H.; Woschank, M. Smart Logistics – Technologiekonzepte und Potentiale. *Berg Huettenmaenn Monatsh* **2019**, *164*, 42–45, doi:10.1007/s00501-018-0806-9.

21. Strandhagen, J.O.; Vallandingham, L.R.; Fragapane, G.; Strandhagen, J.W.; Stangeland, A.B.H.; Sharma, N. Logistics 4.0 and emerging sustainable business models. *Adv. Manuf.* **2017**, *5*, 359–369, doi:10.1007/s40436-017-0198-1.

22. Shao, G.; Helu, M. Framework for a Digital Twin in Manufacturing: Scope and Requirements. *Manuf. Lett.* **2020**, *24*, doi:10.1016/j.mfglet.2020.04.004.

23. El Naqa, I.; Murphy, M.J. What Is Machine Learning? In *Machine Learning in Radiation Oncology*; El Naqa, I., Li, R., Murphy, M.J., Eds.; Springer International Publishing: Cham, 2015; pp 3–11, ISBN 978-3-319-18304-6.

References

24. Murdoch, W.J.; Singh, C.; Kumbier, K.; Abbasi-Asl, R.; Yu, B. Definitions, methods, and applications in interpretable machine learning. *Proc. Natl. Acad. Sci. U. S. A.* **2019**, *116*, 22071–22080, doi:10.1073/pnas.1900654116.

25. Bosche, A.; Brinda, M.; Crawford, D.; Crupi, M.; Guarraia, M.; Haller, A.; Habury, P.; Heric, M.; Hoecker, A. *Technology Report 2020*: *Taming the Flux*. Available online: https://www.bain.com/globalassets/noindex/2020/bain_report_technology-report-2020.pdf (accessed on 10 March 2023).

26. Mills, S.; Lucas, S.; Irakliotis, L.; Rappa, M.; Carlson, T.; Perlowitz, B. Demystifying big data: A practical guide to transforming the business of government. Available online: https://breakinggov.sites.breakingmedia.com/wp-content/uploads/sites/4/2012/10/TechAmericaBigDataReport.pdf (accessed on 10 March 2023).

27. Zikopoulos P.; Eaton C. *Understanding big data: Analytics for enterprise class Hadoop and streaming data;* McGraw-Hill Osborne Media: New York, 2011, ISBN 978-0-07-179053-6.

28. Ishwarappa; Anuradha, J. A Brief Introduction on Big Data 5Vs Characteristics and Hadoop Technology. *Procedia Computer Science* **2015**, *48*, 319–324, doi:10.1016/j.procs.2015.04.188.

29. Younas, M. Research challenges of big data. *SOCA* **2019**, *13*, 105–107, doi:10.1007/s11761-019-00265-x.

30. Khan, N.; Yaqoob, I.; Hashem, I.A.T.; Inayat, Z.; Ali, W.K.M.; Alam, M.; Shiraz, M.; Gani, A. Big data: survey, technologies, opportunities, and challenges. *ScientificWorldJournal.* **2014**, *2014*, 712826, doi:10.1155/2014/712826.

31. Lund, S.; Manyika, J.; Woetzel, J.; Bughin, J.; Krishnan, M.; Seong, J.; Muir, M. *Globalization in transition: The future of trade and value chains*. Available online: https://www.mckinsey.com/~/media/mckinsey/featured%20insights/innovation/globalization%20in%20transition%20the%20future%20of%20trade%20and%20value%20chains/mgi-globalization%20in%20transition-the-future-of-trade-and-value-chains-full-report.pdf (accessed on 10 March 2023).

32. *Global Value Chain Development Report 2021*: *Beyond Production*, Manila, Philippines, 2021.

33. Sorger, M. Quality 5.0 - A data-driven path towards zero waste. *XL. Colloquium on Metal Forming, Zauchensee*; pp 6–12.

34. Schrauf, S.; Berttram, P. *Industry 4.0*: *How digitization makes the supply chain more efficient, agile, and customer-focused*. Available online: https://www.strategyand.pwc.com/gx/en/insights/2016/industry-4-digitization/industry40.pdf (accessed on 10 March 2023).

35. Yadav, G.; Kumar, A.; Luthra, S.; Garza-Reyes, J.A.; Kumar, V.; Batista, L. A framework to achieve sustainability in manufacturing organisations of developing economies using industry 4.0 technologies' enablers. *Computers in Industry* **2020**, *122*, 103280, doi:10.1016/j.compind.2020.103280.

References

36. Gustavsson, U.; Frenger, P.; Fager, C.; Eriksson, T.; Zirath, H.; Dielacher, F.; Studer, C.; Parssinen, A.; Correia, R.; Matos, J.N.; et al. Implementation Challenges and Opportunities in Beyond-5G and 6G Communication. *IEEE J. Microw.* **2021**, *1*, 86–100, doi:10.1109/JMW.2020.3034648.

37. Luthra, S.; Mangla, S.K. Evaluating challenges to Industry 4.0 initiatives for supply chain sustainability in emerging economies. *Process Safety and Environmental Protection* **2018**, *117*, 168–179, doi:10.1016/j.psep.2018.04.018.

38. Rajput, S.; Singh, S.P. Industry 4.0 − challenges to implement circular economy. *BIJ* **2021**, *28*, 1717–1739, doi:10.1108/BIJ-12-2018-0430.

39. Sader, S.; Husti, I.; Daroczi, M. A review of quality 4.0: definitions, features, technologies, applications, and challenges. *Total Quality Management & Business Excellence* **2021**, 1–19, doi:10.1080/14783363.2021.1944082.

40. Paulsen, C.; Byers, R. Glossary of key information security terms, doi:10.6028/NIST.IR.7298r3.

41. Kathiriya, H.; Pandya, A.; Dubay, V.; Bavarva, A. State of Art: Energy Efficient Protocols for Self-Powered Wireless Sensor Network in IIoT to Support Industry 4.0. In *2020 8th International Conference on Reliability, Infocom Technologies and Optimization (Trends and Future Directions) (ICRITO).* 2020 8th International Conference on Reliability, Infocom Technologies and Optimization (Trends and Future Directions) (ICRITO), Noida, India, 04–05 Jun. 2020; IEEE, 62020; pp 1311–1314, ISBN 978-1-7281-7016-9.

42. Profanter, S.; Tekat, A.; Dorofeev, K.; Rickert, M.; Knoll, A. OPC UA versus ROS, DDS, and MQTT: Performance Evaluation of Industry 4.0 Protocols. In *2019 IEEE International Conference on Industrial Technology (ICIT).* 2019 IEEE International Conference on Industrial Technology (ICIT), Melbourne, Australia, 13–15 Feb. 2019; IEEE, 22019; pp 955–962, ISBN 978-1-5386-6376-9.

43. Silva, D.R.C.; Oliveira, G.M.B.; Silva, I.; Ferrari, P.; Sisinni, E. Latency evaluation for MQTT and WebSocket Protocols: an Industry 4.0 perspective. In *2018 IEEE Symposium on Computers and Communications (ISCC).* 2018 IEEE Symposium on Computers and Communications (ISCC), Natal, 25–28 Jun. 2018; IEEE, 62018; pp 1233–1238, ISBN 978-1-5386-6950-1.

44. Uy, N.Q.; Nam, V.H. A comparison of AMQP and MQTT protocols for Internet of Things. In *2019 6th NAFOSTED Conference on Information and Computer Science (NICS).* 2019 6th NAFOSTED Conference on Information and Computer Science (NICS), Hanoi, Vietnam, 12–13 Dec. 2019; IEEE, 122019; pp 292–297, ISBN 978-1-7281-5163-2.

45. Caiza, G.; Llamuca, E.S.; Garcia, C.A.; Gallardo-Cardenas, F.; Lanas, D.; Garcia, M.V. Industrial Shop-Floor Integration Based on AMQP protocol in an IoT Environment. In *2019 IEEE Fourth Ecuador Technical Chapters Meeting (ETCM).* 2019 IEEE Fourth Ecuador Technical Chapters Meeting (ETCM), Guayaquil, Ecuador, 11–15 Nov. 2019; IEEE, 112019; pp 1–6, ISBN 978-1-7281-3764-3.

46. Alshrif, A.M.; Gouda, A.A.; Razek, M.A. Comparative study among constrained application protocol extensible messaging and presence protocol of IoT. *IJEECS* **2022**, *27*, 546, doi:10.11591/ijeecs.v27.i1.pp546-554.

47. Jenzeri, D.; Chehri, A. Data Analysis for IoT System Using 6LoWPAN and Constrained Application Protocol for Environmental Monitoring. *Procedia Computer Science* **2022**, *207*, 1472–1481, doi:10.1016/j.procs.2022.09.204.

48. Tekinerdogan, B.; Çelik, T.; Köksal, Ö. Architecture Modeling of Industrial IoT Systems Using Data Distribution Service UML Profile. In *The Internet of Things in the Industrial Sector*; Mahmood, Z., Ed.; Springer International Publishing: Cham, 2019; pp 103–119, ISBN 978-3-030-24891-8.

49. Gkamas, T.; Karaiskos, V.; Kontogiannis, S. Performance Evaluation of Distributed Database Strategies Using Docker as a Service for Industrial IoT Data: Application to Industry 4.0. *Information* **2022**, *13*, 190, doi:10.3390/info13040190.

50. Graves, M.; Bergeman, E.R.; Lawrence, C.B. Graph database systems. *IEEE Eng. Med. Biol. Mag.* **1995**, *14*, 737–745, doi:10.1109/51.473268.

51. Duan, L.; Da Xu, L. Data Analytics in Industry 4.0: A Survey. *Inf. Syst. Front.* **2021**, 1–17, doi:10.1007/s10796-021-10190-0.

52. Zymbler, M.; Ivanova, E. Matrix Profile-Based Approach to Industrial Sensor Data Analysis Inside RDBMS. *Mathematics* **2021**, *9*, 2146, doi:10.3390/math9172146.

53. Di Martino, S.; Fiadone, L.; Peron, A.; Riccabone, A.; Vitale, V.N. Industrial Internet of Things: Persistence for Time Series with NoSQL Databases. In *2019 IEEE 28th International Conference on Enabling Technologies: Infrastructure for Collaborative Enterprises (WETICE).* 2019 IEEE 28th International Conference on Enabling Technologies: Infrastructure for Collaborative Enterprises (WETICE), Napoli, Italy, 12–14 Jun. 2019; IEEE, 62019; pp 340–345, ISBN 978-1-7281-0676-2.

54. Villalobos, K.; Ramírez-Durán, V.J.; Diez, B.; Blanco, J.M.; Goñi, A.; Illarramendi, A. A three level hierarchical architecture for an efficient storage of industry 4.0 data. *Computers in Industry* **2020**, *121*, 103257, doi:10.1016/j.compind.2020.103257.

55. Sahal, R.; Breslin, J.G.; Ali, M.I. Big data and stream processing platforms for Industry 4.0 requirements mapping for a predictive maintenance use case. *Journal of Manufacturing Systems* **2020**, *54*, 138–151, doi:10.1016/j.jmsy.2019.11.004.

56. Oliveira, V.F. de; Pessoa, M.A.d.O.; Junqueira, F.; Miyagi, P.E. SQL and NoSQL Databases in the Context of Industry 4.0. *Machines* **2022**, *10*, 20, doi:10.3390/machines10010020.

57. Openko, P.V.; Hohoniants, S.Y.; Starkova, O.V.; Herasymenko, K.V.; Yastrebov, M.I.; Prudchenko, A.O. Problem of Choosing a DBMS in Modern Information System. In *2019 IEEE International Conference on Advanced Trends in Information Theory (ATIT).* 2019 IEEE

International Conference on Advanced Trends in Information Theory (ATIT), Kyiv, Ukraine, 18–20 Dec. 2019; IEEE, 122019; pp 171–174, ISBN 978-1-7281-6144-0.

58. kumar Kaliyar, R. Graph databases: A survey. In *International Conference on Computing, Communication & Automation.* 2015 International Conference on Computing, Communication & Automation (ICCCA), Greater Noida, India, 15–16 May 2015; IEEE, 52015; pp 785–790, ISBN 978-1-4799-8890-7.

59. Zekhnini, K.; Cherrafi, A.; Bouhaddou, I.; Benghabrit, Y.; Garza-Reyes, J.A. Supply chain management 4.0: a literature review and research framework. *BIJ* **2021**, *28*, 465–501, doi:10.1108/BIJ-04-2020-0156.

60. Cui, Y.; Kara, S.; Chan, K.C. Manufacturing big data ecosystem: A systematic literature review. *Robotics and Computer-Integrated Manufacturing* **2020**, *62*, 101861, doi:10.1016/j.rcim.2019.101861.

61. Buehler, K.; Anant, V.; Bailey, T.; Kaplan, J.; Nayfeh, M.; Richter, W. *Cybersecurity in a Digital Era*. Available online: https://www.mckinsey.com/~/media/McKinsey/Business%20Functions/Risk/Our%20Insights/Cybersecurity%20in%20a%20digital%20era/Cybersecurity%20in%20a%20Digital%20Era.pdf (accessed on 23 February 2023).

62. Lezzi, M.; Lazoi, M.; Corallo, A. Cybersecurity for Industry 4.0 in the current literature: A reference framework. *Computers in Industry* **2018**, *103*, 97–110, doi:10.1016/j.compind.2018.09.004.

63. Schatteman, O.; Stephan, J. *Supply Chains Are Looking Up, Literally*. Available online: https://www.bain.com/globalassets/noindex/2021/bain_brief_supply_chains_are_looking_up_literally.pdf (accessed on 10 March 2023).

64. Lund, S.; Manyika, J.; Woetzel, J.; Barriball, E.; Krishnan, M.; Alicke, K.; Birshan, M.; George, K.; Smit, S.; Swan, D.; et al. *Risk, resilience, and rebalancing in global value chains*. Available online: https://www.mckinsey.com/business-functions/operations/our-insights/risk-resilience-and-rebalancing-in-global-value-chains (accessed on 30 May 2022).

65. Biondo, M.; Heid, A.; Henke, N.; Mohr, N.; Ostojic, I.; Pautasso, L.; Wester, L.; Zemmel, R. *Quantum computing: An emerging ecosystem and industry use cases*. Available online: https://www.mckinsey.com/~/media/mckinsey/business%20functions/mckinsey%20digital/our%20insights/quantum%20computing%20use%20cases%20are%20getting%20real%20what%20you%20need%20to%20know/quantum-computing-an-emerging-ecosystem.pdf (accessed on 10 March 2023).

66. Dilda, V.; Gupta, R.; Karlsson, A.; Mori, L.; Reiter, S.; Vasilev, S. *Building value-chain resilience with AI*. Available online: https://www.mckinsey.com/industries/metals-and-mining/our-insights/building-value-chain-resilience-with-ai#/ (accessed on 10 March 2023).

References

67. Stark, J. *Product Lifecycle Management (Volume 1)*: *21st Century Paradigm for Product Realisation*, 5th ed. 2022; Springer International Publishing; Imprint Springer: Cham, 2022, ISBN 978-3-030-98578-3.

68. Kafetzopoulos, D.P.; Psomas, E.L.; Gotzamani, K.D. The impact of quality management systems on the performance of manufacturing firms. *International Journal of Quality & Reliability Management* **2015**, *32*, 381–399, doi:10.1108/IJQRM-11-2013-0186.

69. Alcácer, V.; Cruz-Machado, V. Scanning the Industry 4.0: A Literature Review on Technologies for Manufacturing Systems. *Engineering Science and Technology, an International Journal* **2019**, *22*, 899–919, doi:10.1016/j.jestch.2019.01.006.

70. Rodič, B. Industry 4.0 and the New Simulation Modelling Paradigm. *Organizacija* **2017**, *50*, 193–207, doi:10.1515/orga-2017-0017.

71. Boston Consulting Group; Microsoft. *Ten Guidelines for Product Leaders to Implement AI Responsibly*. Available online: https://web-assets.bcg.com/4f/f1/70a99de3414caafd96145291678a/ten-guidelines-for-product-leaders-to-implement-ai-responsibly.pdf (accessed on 10 March 2023).

72. Sariyer, G.; Mangla, S.K.; Kazancoglu, Y.; Ocal Tasar, C.; Luthra, S. Data analytics for quality management in Industry 4.0 from a MSME perspective. *Ann Oper Res* **2021**, doi:10.1007/s10479-021-04215-9.

73. Agrawal, M.; Eloot, K.; Mancini, M.; Patel, A. *Industry 4.0: Reimagining manufacturing operations after COVID-19*, 2020. Available online: https://www.mckinsey.com/~/media/McKinsey/Business%20Functions/Operations/Our%20Insights/Industry%204%200%20Reimagining%20manufacturing%20operations/industry-4-0-reimagining-manuacturing-ops-after-covid-19.pdf (accessed on 10 March 2023).

74. Sony, M.; Antony, J.; Douglas, J.A. Essential ingredients for the implementation of Quality 4.0. *TQM* **2020**, *32*, 779–793, doi:10.1108/TQM-12-2019-0275.

75. Tao, F.; Cheng, J.; Qi, Q.; Zhang, M.; Zhang, H.; Sui, F. Digital twin-driven product design, manufacturing and service with big data. *Int J Adv Manuf Technol* **2018**, *94*, 3563–3576, doi:10.1007/s00170-017-0233-1.

76. Sänger F. *Achieving supply-chain resiliency in consumer goods amid disruption*. Available online: https://www.mckinsey.com/industries/consumer-packaged-goods/our-insights/achieving-supply-chain-resiliency-in-consumer-goods-amid-disruption (accessed on 10 March 2023).

77. Frieske, B.; Stieler, S. The "Semiconductor Crisis" as a Result of the COVID-19 Pandemic and Impacts on the Automotive Industry and Its Supply Chains. *WEVJ* **2022**, *13*, 189, doi:10.3390/wevj13100189.

78. Camonita, F.; Dantas, C.; Tageo, V.; Moreira, A.; Corsello, A.; Louceiro, J. *Crisis costs for European SMEs*: *How COVID-19 changed the playing field for European SMEs : final report;* EESC: Brussels, 2022, ISBN 978-92-830-5780-2.

79. European Commission. What is an SME? Available online: https://ec.europa.eu/growth/smes/sme-definition_en (accessed on 10 March 2023).

80. European Commission. *User guide to the SME Definition*, Luxembourg.

81. Müller, J.M.; Buliga, O.; Voigt, K.-I. Fortune favors the prepared: How SMEs approach business model innovations in Industry 4.0. *Technological Forecasting and Social Change* **2018**, *132*, 2–17, doi:10.1016/j.techfore.2017.12.019.

82. Statistik Austria. *Anteil der Branche Bergbau und Herstellung von Waren an der gesamten Bruttowertschöpfung in Österreich von 2010 bis 2020*. Available online: https://de.statista.com/statistik/daten/studie/1177726/umfrage/wertschoepfungsanteil-des-verarbeitenden-gewerbes-in-oesterreich/ (accessed on 20 June 2022).

83. Statistik Austria. *Anteil der kleinen und mittleren Unternehmen (KMU) an allen Unternehmen in Österreich von 2015 bis 2019*. Available online: https://de.statista.com/statistik/daten/studie/1172003/umfrage/unternehmensanteil-von-kleinen-und-mittleren-unternehmen-kmu-in-oesterreich/ (accessed on 20 June 2022).

84. Forth, P.; Laubier, R. de; Reichert, T.; Chakraborty, S. *Flipping the Odds of Digital Transformation Success*. Available online: https://web-assets.bcg.com/c7/20/907821344bbb8ade98cbe10fc2b8/bcg-flipping-the-odds-of-digital-transformation-success-oct-2020.pdf (accessed on 10 March 2023).

85. *Exhibit 1 from "Flipping the Odds of Digital Transformation Success", October 2020, Boston Consulting Group, www.bcg.com. Copyright (c) 2023 Boston Consulting Group. All rights reserved. Reprinted by permission.*

86. Ghobakhloo, M. Industry 4.0, digitization, and opportunities for sustainability. *Journal of Cleaner Production* **2020**, *252*, 119869, doi:10.1016/j.jclepro.2019.119869.

87. Faheem, M.; Shah, S.; Butt, R.A.; Raza, B.; Anwar, M.; Ashraf, M.W.; Ngadi, M.; Gungor, V.C. Smart grid communication and information technologies in the perspective of Industry 4.0: Opportunities and challenges. *Computer Science Review* **2018**, *30*, 1–30, doi:10.1016/j.cosrev.2018.08.001.

88. Ardito, L.; Petruzzelli, A.M.; Panniello, U.; Garavelli, A.C. Towards Industry 4.0. *BPMJ* **2019**, *25*, 323–346, doi:10.1108/BPMJ-04-2017-0088.

89. Lerch, C.; Jäger, A. *Industrie 4.0 quo vadis?*: *Neuere Entwicklungen der vierten industriellen Revolution im Verarbeitenden Gewerbe*; MODERNISIERUNG DER PRODUKTION No. 76, 2022. Available online: https://www.isi.fraunhofer.de/content/dam/isi/dokumente/modernisierung-produktion/erhebung2018/PI_76_Industrie_4-0_quo_vadis.pdf (accessed on 10 March 2023).

90. Müller, J.M.; Däschle, S. Business Model Innovation of Industry 4.0 Solution Providers Towards Customer Process Innovation. *Processes* **2018**, *6*, 260, doi:10.3390/pr6120260.

91. Francisco, B.; Boer, E. de; Giraud, Y.; Desnos, V. *The scaling imperative for industry 4.0*, 2022. Available online: https://www.mckinsey.com/capabilities/operations/our-insights/the-scaling-imperative-for-industry-4-point-0#/ (accessed on 4 March 2023).

92. Mecklenbräuker, C. 5G als Basis der Digitalisierung. Anwendungen, Chancen und Ausblick auf 6G. *Elektrotech. Inftech.* **2022**, *139*, 587–588, doi:10.1007/s00502-022-01071-8.

93. Rao, S.K.; Prasad, R. Impact of 5G Technologies on Industry 4.0. *Wireless Pers Commun* **2018**, *100*, 145–159, doi:10.1007/s11277-018-5615-7.

94. Brinda, M.; Buecker, C.; Chabrelié, T.; Coffman, J.; Crawford, D.; Crupi, M.; Dixon, J.; Fiore, G.; Frick, J. *Technology Report 2021*: *The '20s Roar*. Available online: https://www.bain.com/globalassets/noindex/2021/bain_report_technology-report-2021.pdf (accessed on 10 March 2023).

95. Doddapaneni, P.; Heric, M.; Nott, B.; Sheth, A.; Ericson, G. *Overcoming the Automation Paradox*. Available online: https://www.bain.com/globalassets/noindex/2021/bain_brief_overcoming_the_automation-paradox.pdf (accessed on 10 March 2023).

96. Lerch, C.; Jäger, A.; Heimberger, H. *Produktion in Zeiten der Corona-Krise*: *Welche Auswirkungen hat die Pandemie heute und zukünftig auf die Industrie?*; MODERNISIERUNG DER PRODUKTION No. 78, 2020. Available online: https://www.isi.fraunhofer.de/content/dam/isi/dokumente/modernisierung-produktion/erhebung2018/PI_78_Produktion_in_Corona_Web.pdf (accessed on 10.30.2023).

97. *OECD Economics Department Working Papers*, 2022.

98. Lerch, C.; Jäger, A. *Export und Globalisierung in Zeiten des digitalen Wandels*: *Wie Produkthersteller beim Exportgeschäft von der Digitalisierung profitieren können*; MODERNISIERUNG DER PRODUKTION No. 79, 2021. Available online: https://publica-rest.fraunhofer.de/server/api/core/bitstreams/ae417a50-8956-478a-aa92-ec202347aea1/content (accessed on 10 March 2023).

99. *Measuring capital in the new economy ; [papers presented at a conference at the Federal Reserve Board in Washington, DC, held in April 2002 by the Conference on Research in Income and Wealth of the National Bureau of Economic Research]*: *A New Approach to the Valuation of Intangible Capital;* Cummins, J., Ed.; Univ. of Chicago Press: Chicago, Ill., 2005, ISBN 0-226-11612-3.

100. Hazan, E.; Smit, S.; Woetzel, J.; Cvetanovski, B.; Krishnan, M.; Gregg, B.; Perrey, J.; Hjartar, K. *Getting tangible about intangibles*, https://www.mckinsey.com/~/media/mckinsey/business%20functions/marketing%20and%20sales/our%20insights/getting%20tangible%20about%20intangibles%20the%20future%20of%20growth%20and%20productivity/getting-tangible-about-intangibles-the-future-of-growth-and-productivity.pdf (accessed on 10 March 2023).

References

101. Roth, F.; Thum, A.-E. Intangible Capital and Labor Productivity Growth: Panel Evidence for the EU from 1998-2005. *Review of Income and Wealth* **2013**, *59*, 486–508, doi:10.1111/roiw.12009.

102. Thum-Thysen, A.; Voigt, P.; Weiss, C. *Reflections on complementarities in capital formation & production*: *Tangible & intangible assets across Europe;* Publications Office of the European Union: Luxembourg, 2021, ISBN 978-92-76-38753-4.

103. Gumbau-Albert, M.; Maudos, J. The importance of intangible assets in regional economic growth: a growth accounting approach. *Ann. Reg. Sci.* **2022**, *69*, 361–390, doi:10.1007/s00168-022-01138-6.

104. *Exhibit 6 from " Getting tangible about intangibles ", June 2021, McKinsey & Company, www.mckinsey.com. Copyright (c) 2023 McKinsey & Company. All rights reserved. Reprinted by permission.*

105. Cayler, P.-L.; Noterdaeme, O.; Naik, K. *Digital in industry: From buzzword to value creation*. Available online: https://www.mckinsey.com/~/media/McKinsey/Business%20Functions/McKinsey%20Digital/Our%20Insights/Digital%20in%20industry%20From%20buzzword%20to%20value%20creation/Digital-in-industry-From-buzzword-to-value-creation.pdf (accessed on 10 March 2023).

106. *Exhibit 1 from "Digital in industry: From buzzword to value creation", June 2021, McKinsey & Company, www.mckinsey.com. Copyright (c) 2023 McKinsey & Company. All rights reserved. Reprinted by permission.*

107. Betti, F.; Küpper, D.; Bezamat, F.; Fendri, M.; Behaeghe, R. *The Data-Driven Journey Towards Manufacturing Excellence*. Available online: https://www3.weforum.org/docs/WEF_The_Data-Driven_Journey_Towards_Manufacturing_Excellence_2022.pdf (accessed on 16 March 2023).

108. Agrawal, A.; Carmody, K.; Laczkowski, K.; Seth, I.; Nowski, T.; O'Flanagan, M.; Taliento, L.; Childress, T.; Spencer, A.; Wintner, T.; et al. *The Next Normal*: *Transformation with a capital T*. Delivering sustainable change. Available online: https://www.mckinsey.com/~/media/mckinsey/business%20functions/transformation/our%20insights/the%20path%20to%20true%20transformation/transformation-with-a-capital-t.pdf (accessed on 10 March 2023).

109. Jawahir, I.S.; Badurdeen, F.; Rouch, K.E. *Innovation in sustainable manufacturing education*, 2013.

110. Enyoghasi, C.; Badurdeen, F. Industry 4.0 for sustainable manufacturing: Opportunities at the product, process, and system levels. *Resources, Conservation and Recycling* **2021**, *166*, 105362, doi:10.1016/j.resconrec.2020.105362.

111. Jawahir, I.S.; Dillon Jr, O.W. Sustainable manufacturing processes: new challenges for developing predictive models and optimization techniques. *Proceedings of the first international conference on sustainable manufacturing* **2007**, 1–19.

References

112. Song, Z.; Moon, Y. Assessing sustainability benefits of cybermanufacturing systems. *Int J Adv Manuf Technol* **2017**, *90*, 1365–1382, doi:10.1007/s00170-016-9428-0.

113. Rajput, S.; Singh, S.P. Connecting circular economy and industry 4.0. *International Journal of Information Management* **2019**, *49*, 98–113, doi:10.1016/j.ijinfomgt.2019.03.002.

114. Hamilton Ortiz, J. *Industry 4.0 - Current Status and Future Trends;* IntechOpen, 2020, ISBN 978-1-83880-093-2.

115. Frank, A.G.; Dalenogare, L.S.; Ayala, N.F. Industry 4.0 technologies: Implementation patterns in manufacturing companies. *International Journal of Production Economics* **2019**, *210*, 15–26, doi:10.1016/j.ijpe.2019.01.004.

116. Rumsey, A.; Le Dantec, C.A. Manufacturing Change: The Impact of Virtual Environments on Real Organizations. In *Proceedings of the 2020 CHI Conference on Human Factors in Computing Systems.* CHI '20: CHI Conference on Human Factors in Computing Systems, Honolulu HI USA, 25 04 2020 30 04 2020; Bernhaupt, R., Mueller, F.'., Verweij, D., Andres, J., McGrenere, J., Cockburn, A., Avellino, I., Goguey, A., Bjørn, P., Zhao, S., Samson, B.P., Kocielnik, R., Eds.; ACM: New York, NY, USA, 04212020; pp 1–12, ISBN 9781450367080.

117. Billing, F.; Smet, A. de; Reich, A.; Schaninger, B.; Bodem-Schrötgens, J.; Sharma, K.; Gao, W.; Henderson, K.; Hundertmark, T.; Blackburn, S.; et al. *McKinsey Global Surveys, 2021: A year in review*. Available online: https://www.mckinsey.com/~/media/mckinsey/featured%20insights/mckinsey%20global%20surv eys/mckinsey-global-surveys-2021-a-year-in-review.pdf (accessed on 10 March 2023).

118. European Commission. *2030 climate & energy framework*. Available online: https://climate.ec.europa.eu/eu-action/climate-strategies-targets/2030-climate-energy-framework_en (accessed on 10 March 2023).

119. Ralph, B.J.; Woschank, M.; Pacher, C.; Murphy, M. Evidence-based redesign of engineering education lectures: theoretical framework and preliminary empirical evidence. *European Journal of Engineering Education* **2022**, *47*, 636–663, doi:10.1080/03043797.2021.2025341.

120. Chamberlain, K.; Cain, T.; Sheridan, J.; Dupuis, A. Pluralisms in Qualitative Research: From Multiple Methods to Integrated Methods. *Qualitative Research in Psychology* **2011**, *8*, 151–169, doi:10.1080/14780887.2011.572730.

121. Ralph, B.J.; Woschank, M.; Miklautsch, P.; Kaiblinger, A.; Pacher, C.; Sorger, M.; Zsifkovits, H.; Stockinger, M. MUL 4.0: Systematic Digitalization of a Value Chain from Raw Material to Recycling. *Procedia Manufacturing* **2021**, *55*, 335–342, doi:10.1016/j.promfg.2021.10.047.

122. Woschank, M.; Ralph, B.J.; Kaiblinger, A.; Miklautsch, P.; Pacher, C.; Sorger, M.; Zsifkovits, H.; Stockinger, M.; Pogatscher, S.; Antretter, T.; et al. MUL 4.0 – Digitalisierung der Wertschöpfungskette vom Rohmaterial bis hin zum Recycling. *Berg Huettenmaenn Monatsh* **2021**, *166*, 309–313, doi:10.1007/s00501-021-01119-w.

References

123. Ralph, B.J.; Sorger, M.; Schödinger, B.; Schmölzer, H.-J.; Hartl, K.; Stockinger, M. Implementation of a Six-Layer Smart Factory Architecture with Special Focus on Transdisciplinary Engineering Education. *Sensors (Basel)* **2021**, *21*, doi:10.3390/s21092944.

124. Sorger, M.; Ralph, B.J.; Waiguny, C.; Schödinger, B.; Schoiswohl, M.; Stockinger, M. Transformation of a hydraulic press and furnaces into a Cyber Physical Production System: a brownfield approach from sensor retrofitting to Digital Shadow under special consideration of predictive maintenance and sustainability. *J Intell Manuf (Journal of Intelligent Manufacturing) (Under review)* **2023**.

125. Ralph, B.J.; Hartl, K.; Sorger, M.; Schwarz-Gsaxner, A.; Stockinger, M. Machine Learning Driven Prediction of Residual Stresses for the Shot Peening Process Using a Finite Element Based Grey-Box Model Approach. *JMMP* **2021**, *5*, 39, doi:10.3390/jmmp5020039.

126. Hartl, K.; Sorger, M.; Weiß, H.; Stockinger, M. Machine learning driven prediction of mechanical properties of rolled aluminium and development of an in-situ quality control method based on electrical resistivity measurement. *Journal of Materials and Research (Under review)* **2023**.

127. Hartl, K.; Sorger, M.; Stockinger, M. The Key Role of Laser Ultrasonics in the Context of Sustainable Production in an I 4.0 Value Chain. *Applied Sciences* **2023**, *13*, 733, doi:10.3390/app13020733.

A - Associated Publications

This chapter includes the associated publications A 1 to A 9, as described in the chapters 1 to 5. Hereby, each subsection provides information about the author contributions to the respective publication.

A 1   Publication 1

M. Sorger, B.J. Ralph, K. Hartl, M. Woschank, M. Stockinger: 'Big Data in the Metal Processing Value Chain: A Systematic Digitalization Approach under Special Consideration of Standardization and SMEs', in: *Applied Sciences* 2021, 11, 9021, doi: 10.3390/app11199021.

Author contributions:

1. M. Sorger: Conceptualization, Methodology, Software, Validation, Investigation, Data Curation, Writing - Original Draft, Writing - Review & Editing, Project Administration
2. B.J. Ralph: Conceptualization, Methodology, Software, Validation, Investigation, Data Curation, Writing - Original Draft, Writing - Review & Editing, Project Administration
3. K. Hartl: Conceptualization, Methodology, Validation, Investigation, Writing - Original Draft, Writing - Review & Editing, Project Administration
4. M. Woschank: Supervision
5. M. Stockinger: Resources, Supervision

Article

Big Data in the Metal Processing Value Chain: A Systematic Digitalization Approach under Special Consideration of Standardization and SMEs

Marcel Sorger [1] , Benjamin James Ralph [1,]*, Karin Hartl [1] , Manuel Woschank [2] and Martin Stockinger [1]

[1] Metal Forming, Montanuniversität Leoben, Franz Josef Strasse 18, 8700 Leoben, Austria; marcel.sorger@unileoben.ac.at (M.S.); karin.hartl@unileoben.ac.at (K.H.); martin.stockinger@unileoben.ac.at (M.S.)
[2] Industrial Logistics, Montanuniversität Leoben, Erzherzog Johann-Strassße 3/1, 8700 Leoben, Austria; manuel.woschank@unileoben.ac.at
[*] Correspondence: benjamin.ralph@unileoben.ac.at; Tel.: +43-384-240-25611

Abstract: Within the rise of the fourth industrial revolution, the role of Big Data became increasingly important for a successful digital transformation in the manufacturing environment. The acquisition, analysis, and utilization of this key technology can be defined as a driver for decision-making support, process and operation optimization, and therefore increase the efficiency and effectiveness of a complete manufacturing site. Furthermore, if corresponding interfaces within the supply chain can be connected within a reasonable effort, this technology can boost the competitive advantage of all stakeholders involved. These developments face some barriers: especially SMEs have to be able to be connected to typically more evolved IT systems of their bigger counterparts. To support SMEs with the development of such a system, this paper provides an innovative approach for the digitalization of the value chain of an aluminum component, from casting to the end-of-life recycling, by especially taking into account the RAMI 4.0 model as fundament for a standardized development to ensure compatibility within the complete production value chain. Furthermore, the key role of Big Data within digitalized value chains consisting of SMEs is analytically highlighted, demonstrating the importance of associated technologies in the future of metal processing and in general, manufacturing.

Keywords: Big Data; Industry 4.0; Cyber-Physical Production System; Industrial Internet of Things; digitalization; RAMI 4.0; digital manufacturing

1. Introduction

Since the fourth industrial revolution, the majority of industry sectors are compelled to undergo a digital transformation. Besides industries that have the ability to accommodate more rapidly, especially the heavy industry, and within this sector, metal processing facilities have additional obstacles to overcome. This applies especially to small and medium-sized enterprises (SMEs) in this specific industry segment. The required skills, as well as the necessary budget for the implementation of a state-of the-art digitalization solution are conditions that these companies often cannot fulfill, resulting in a reduction of the velocity of the digital transformation [1–4]. Additionally, in-use machine systems within this environment tend to have significantly longer life spans than other industry segments, resulting in a higher amount of mostly more complex brownfield digitization and digitalization approaches [4–6].

To utilize the full potential of the fourth industrial revolution, all enterprises within a supply chain must be able to communicate with other involved entities. Therefore, a common basis for communication is imperative, as this results in a holistic compatibility and extensibility of such. For this purpose, the Reference Architecture Model Industry 4.0 (RAMI 4.0) supports a standardized technical communication within and between different

layers which is necessary for a successful digital transformation [7–9]. Although the utilization of such a methodological approach should result in a reduction of complexity, the integration of relevant data into the value chain results in a significant increase of required data processing technologies and database management systems (DBMS). Additionally, the ongoing approaches to make internal data available to other stakeholders within a value chain, Big Data and correlating technologies gain significant importance in the manufacturing environment, as state-of-the-art research implies [10–14].

This paper aims to concretize the role of Big Data within this increasingly connected environment by utilizing the RAMI 4.0 framework for the digitalization of a small-scale value chain at the Montanuniversität Leoben, which emulates the integration of SMEs within such a connected supply chain.

The paper is structured as follows: A state of the art literature research of the key enablers of the fourth industrial revolution, namely, Smart Factories, Big Data, Cyber-Physical Production Systems (CPPS), Industrial Internet of Things (IIoT), Digital Twins (DT), and Cloud Computing is presented in Section 2. In Section 3, the integration of SMEs within such an environment is discussed in more detail. Furthermore, as part of the MUL 4.0 project at the Montanuniversität Leoben, a small-scale digitalized value chain that serves as a practical demonstration for the theoretical implications resulting from Section 2, is discussed. In addition, machine learning modeling approaches for SMEs and big enterprises with special emphasis on the process level and therefore CPPS are addressed. The resulting value chain consists of several enterprises of different sizes and with different equipment and processes. Based on these chapters, Section 4 demonstrates and critically discusses the concretization of the RAMI 4.0 framework and the role of Big Data for the MUL 4.0 value chain. Based on this analysis, generalizations for the metal processing manufacturing environment are drawn. In the closing section, a brief conclusion and outlook regarding this topic are given.

2. Theoretical Fundamentals and State of the Art

To successfully support a digital transformation and to achieve a better comprehension of the production processes, the first step is to assemble a large amount of data from the production sites to understand the operational sequences and to initiate the digital transformation within a company [15]. One of the key factors in this context promoting this transformation is the utilization of the Big Data concept [16]. According to [17–23], Big Data technologies have to fulfill the three criteria of Volume, Variety, and Velocity. These three requirements can be extended by two further criteria, presented by [24,25] to five characteristics, which are referred to as the 5Vs: volume, velocity, variety, veracity, and value. As new technologies become established, new opportunities, challenges, and threats arise. The opportunities originated up by Big Data initially lie in operational efficiency, leading to a variety of advantages for businesses, and therefore, manufacturing operations [26]. At the production level, this might lead to an improvement in production planning. At the executive level, targeted data integration can support decision-making, strategy development and execution as well as supply chain management [27,28]. All these improvements can subsequently be used to augment customer service [26]. Difficulties occur in the acquisition, transmission, storage, management, analysis, visualization, integration, privacy, and security of data as well as risk management [26,29,30]. These difficulties can be traced back to the 5Vs. The first V, volume, presents a major obstacle in two respects. According to Zikopoulos [21], on the one hand, a large amount of data of at least one petabyte must be processed. On the other hand, the corresponding infrastructure has to be available for the intention to be able to process these data volumes in a reasonable amount of time, leading to the next characteristic, velocity. Velocity is defined as the ability to generate, process, analyze, and store data at high speeds continuously or discretely. The velocity of this refers to the time it takes to get from source to destination including all necessary operations. Variety arises from the different file structures that can be distinguished in structured, semi-structured, and unstructured data sets. In more than 70% of cases, data

is present in the unstructured form [26]. Veracity arises from the failure to provide data of sufficient quality that cannot be used due to a lack of meaningfulness or uncertainty. Since data analysis inevitably depends on the quality of data, low-quality data can lead to an unintentional distortion of the result. Value describes the added value generated by analyzing and linking data [24,25]. An additional threat is the privacy of data that could be leaked through cyberattacks due to a lack of security. Other concerns arise from the data itself, should one criterion of the 5Vs not be met [26,31–35].

One of the major challenges of Big Data analysis in the metal processing environment is the high variety of processes regarding the geometry as well as material and the processing steps concerning the application of the respective workpiece, especially for specialized SMEs and in the metal forming sector. Considering the supply chain of a metal-based product from casting to forming of semi-finished products up to component manufacturing, this variety increases even further. A typical supply chain for high-quality metal components, e.g., the aerospace industry includes multiple specialized SMEs, resulting in a processing chain consisting of a large number of different companies involved [2]. In this case, digitalization solutions are often planned and implemented as stand-alone solutions, especially taking into account the internal restrictions of these companies concerning their confidentiality regulations. Taking a globalized and interconnected supply chain approach into account, the role of standardized interfaces is therefore crucial for further superordinate supply chain optimization.

To make use of new technologies and support the premises of Industry 4.0, individualization, flexibility, decentralization, and resource efficiency, various technologies have to be combined. When operating within the production site scale, this digitalization development within such a facility are combined and defined as Smart Factory [36–40]. According to [40], a Smart Factory can be described as a compound of Cyber-Physical Systems (CPS) connected by the Internet of Things (IoT), to support humans and machines in their activities [34]. As stated by [2,35,41–44], key technologies, especially for the metal forming industry, include a generic infrastructure, consisting of CPPSs, IIoT, DTs, Big Data, and Cloud Computing. Considering the already existing infrastructure within the heavy industry segment focused in this work, the integration of already existing technology by using a brownfield approach results in a mixed form of this theoretical construct: expensive layer 0–4 solutions already implemented but not fulfilling these new requirements cannot be exchanged without unreasonable investments. This statement is especially important for SMEs, which tend to have a generally lower budget for innovation that usually amortize in a medium to long-term period.

To be able to unite already existing structures with these Industry 4.0 (I 4.0) related technologies, a generic infrastructure, serving as a standard for internal and external technological communication must be implemented. To create a uniform understanding of I 4.0 technologies and their standards, the RAMI 4.0 framework, based on the Smart Grid Architecture Model (SGAM) [2,45–47], was developed. RAMI 4.0 can therefore be understood as a structured approach to I 4.0 in order to enable uniform communication between its users. The most important interrelationships between key aspects of I 4.0 are visualized by three axes. For the success of a digitalized process chain, there must be a holistic, corresponding vertical and horizontal integration along the life cycle and value stream. As shown in Figure 1, the "Life Cycle and Value Stream" represents the life cycle of physical entities, including the product, along the process chain over which the horizontal and vertical integration takes place [2,45,46]. Horizontal integration, represented by the hierarchy levels ensures cross-border communication with other entities, representing one of the fundamental premises of I 4.0 [2,45,46]. Vertical integration takes place across the layers and is used for data integration and communication between those [2,45,46]. The RAMI 4.0 model consists of the following layers (Figure 1):

- The Asset layer describes the lowest layer in RAMI 4.0 and contains all physical objects;

- The Integration layer is representative for the connection of physical objects with the digital domain and contains the required hardware and software;
- The Communication layer executes the digital connection and thus can be seen as an IIot equivalent;
- The Information layer contains all process-relevant data and information in different formats;
- The Functional layer contains all functions of a value chain. Depending on their determination, these functions can be of a logistical or data processing character;
- The Business layer houses the business logic and deals with the optimization of products and processes.
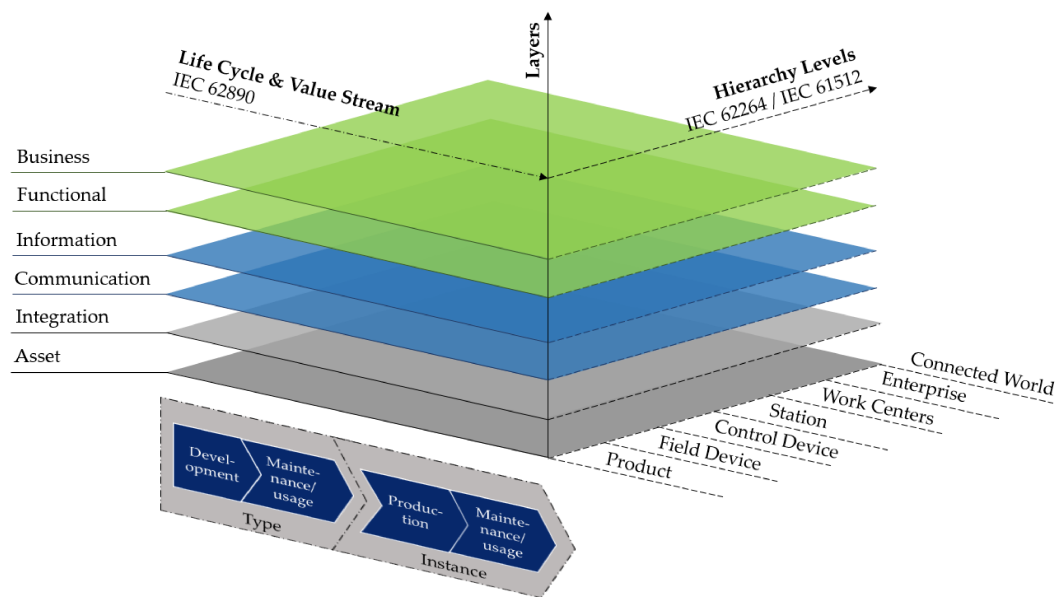
Figure 1. RAMI 4.0 serving as a structured approach for implementing I 4.0 by visualizing the horizontal and vertical integration along the Life Cycle & Value Stream [46].

The hierarchy level is distinguished as follows (Figure 1):

- Product describes the product to be manufactured;
- Field Device includes entities for collecting data, such as sensors and data acquisition (DAQ);
- Control Device describes those operating elements that are used to control the system;
- Station describes the machine or station used for the production step;
- Work Center is to be understood as the production environment;
- Enterprise describes the host enterprise itself.

As a digitalized supply chain in the metal processing industry usually consists of multiple smart factories, often owned by different companies and in general delocalized, smart factories include several CPPSs. A CPPS serves as an extension of a CPS, referring to a system capable of acquiring, storing, analyzing data in real-time using Internet technologies, and reintegrating information from the virtual to the physical world [48], partly dismantling the classical automation pyramid [49]. The reintegration of information involves human–machine interaction, which can be realized with Human Machine Interfaces (HMIs) as shown in, e.g., [2,35]. Building upon the concept of the CPS, a CPPS is using automation technology to a greater extend [2,48]. According to [48,50,51], the following characteristics must be fulfilled: a CPPS: (i) consists of superordinate systems within systems; (ii) consists of connected and cooperative elements acting situationally appropriate between all layers of a production environment; (iii) enhances real-time decision making.

A further extension of these criteria is proposed by [52], adding two additional conditions to be met, especially considering SMEs: (iv) a user-centered CPPS consists of HMIs that are tailored to the application and the respective end-user; (v) a user-centered CPPS for SMEs is resilient and has a short amortization time.

Apparent assistance for the establishment of a CPPS of this kind can be the implementation of DTs, serving as a decision-making support system for the further optimization of the respective production process.

According to [53], a common definition of a DT is a virtual representation of a physical product. This definition can be further refined according to [2,53], depending on the field of application. In the metal industry, a DT can be seen as a partial or complete representation of a production chain, shifting the focus more onto production planning and optimization, or as a representation of one or more process steps in the production chain for the manufacturing of a semi-finished or finished product, whereby the focus shifts on the simulation [2]. To generate advantage of a DT, data from physical space and the information derived from it must be reintegrated from the digital back into physical space. This data transfer between a physical and virtual entity leads to three differentiations depending on its degree of automation [53]. The Digital Model (DM) includes data transfer between the physical and digital space without automated data transfer from the digital to the physical domain or vice versa [53]. A Digital Shadow (DS) consists of a unilateral automated data transfer, in the sense that data is automatically transferred from one domain to the other, while the reverse has to be executed manually [53]. The DT, on the other hand, includes an automated bilateral data transfer, resulting in an algorithm-based process adaption and can adapt the digital domain by utilizing near real-time process data [53]. The fundament of a DM, DS or DT can be a White Box Model (WBM), Black Box Model (BBM) or a mixture of both, defined as Grey Box Model (GBM) [2].

WBMs are based on real physical relationships build up upon known parameters and mathematical correlations. Therefore, the output and how output-related results are obtained are comprehensible [2,54–56]. BBM are often used where a mathematical description based on real physical relationships is too complex [54,55,57] or not available in the required depth and time. As a result, its logic and working methods are not transparent in comparison to a WBM [54]. The output of a BBM has no real physical mechanisms compared to the WBM and is based on stochastic approaches and the correlation of data [2]. The GBM represents the combination of a WBM and a BBM, aiming to merge the benefits of both [2,54]. However, the results may vary depending on the modeling method used and so the use of either a WB, GB or BB model has to be answered individually depending on the given circumstances and resources [56,58]. Taking Machine Learning (ML) into account, the models can be developed into White Box Machine Learning Models (WBMLMs), Grey Box Machine Learning Models (GBMLMs), and Black Box Machine Learning Models (BBMLMs), as demonstrated in [52,56]. In the case of SMEs, initial WBMs are especially important to consider, as there may not be enough experimental investigations nor resources to generate data from tests to meet the 5Vs of Big Data, leading to an unsatisfactory result. In the further production process, data can be collected and fed into the initial WBM, which transforms it into a GBMLM, as shown in [56]. Large enterprises, on the other hand, may have already collected enough data to meet the 5Vs of Big Data and can implement a BBM that is also fed with data collected in the process, transforming it into a BBMLM [52]. Nevertheless, in the event of limited access to sufficient data, a similar approach to SMEs can be adopted. Data that can be used by the models has to be classified and, in the case of an ML approach, supervised learning is recommended [23,54]. To obtain the necessary data in the required quality, time and structure, IIoT solutions, despite classical level 2 automation schemes, are required to realize a true BBM or GBM as well as their further advanced ML-based extensions.

IIot is a derivative of the IoT, which describes the attempt to network smart devices across the board, whereby this term is strongly consumer-related [59,60]. The architecture associated with IoT has to be adopted when implemented in the context of an industrial

environment, especially considering higher IT security and resilience requirements [60]. As concluded by [60], IIoT can be described as a superordinate system including connected cyber-physical entities that enable in-situ data acquisition, analysis, and exchange in an industrial environment leading to process and production optimization and thus serving as a major enabler for a leaner production [60,61]. The resulting benefits are improved productivity and efficiency, reduced cost and energy consumption as well as a strengthened customer relationship [59,60,62]. A major challenge arises from the heterogeneous application of protocols [2,60]. The general term protocols can be divided into data protocols (e.g., XMPP, MQTT), discovery protocols (e.g., mDNS) and infrastructure protocols (e.g., IPv4, IPv6), enabling communication, whereby each of them exhibits their individual advantages as well as disadvantages [60]. As stated by [2,60], Message Queue Telemetry Transport (MQTT) offers itself for industrial use due to efficient data storage. Furthermore, [2] pointed out the suitability of Extensible Messaging and Presence Protocol (XMPP) for HMIs, which serve as a key component in a smart factory. The integration of a large number of smart devices into the IIoT also poses several risks in terms of IT-security and makes production sites particularly vulnerable to cyberattacks [63,64]. A smart factory, consisting of a multitude of cyber-physical entities, offers attack points in the areas of software (viruses, trojans), protocols (man-in-the-middle, denial-of-service), and hardware [63,64]. This can not only paralyze production but also lead to data theft or targeted manipulation of processes [32,59]. As stated by [32], WB(ML)Ms, GB(ML)Ms, and BB(ML)Ms, when connected, e.g., as a DS or DT, can also be impacted by cyberattacks due to manipulation of the general model, underlying ML algorithm or related data sets. To be able to reduce or at best completely avert cyberattacks and the associated potential intellectual and physical damage, the involvement of security experts should be considered in any case when implementing a smart factory. As stated by [65–67], the IIoT furthermore serves as a major enabler for Industry 5.0 focusing on a higher degree of Human-Machine Interaction enabling a virtualized, costumer-driven manufacturing environment [68].

Considering the limited human and architectural IT resources within most SMEs, cloud computing solutions can add significant economic benefits and therefore additionally serve as an accelerator for the digital transformation of these entities [69]. The basic definition of cloud computing is given by the National Institute of Standard and Technology (NIST): "*a model for enabling convenient, on-demand network access to a shared pool configurable computing resources (e.g., networks, servers, storage, application, and services) that can be rapidly provisioned and released with minimal management effort or service provider interaction*" [70]. A Service Level Agreement (SLA) regulates the services to be provided between the consumer and the provider and the services to be provided [71]. Through the combination of IIot and cloud computing it is possible to implement decentralized, on-demand data computation [59,72,73]. As stated by [59], with centralized cloud computation, the probability of potential delays in high-priority data in the event of high data traffic cannot be neglected. However, there is a possibility that highly specialized SMEs, which already have such an infrastructure and know-how, are not willing to outsource computing activities to cloud services due to legal uncertainties regarding data protection and privacy due to different jurisdictions. Despite this uncertainties, decentralized computing resources, in combination with big data, make it possible to monitor and optimize entire process chains in real-time [63].

As already mentioned, through the interaction of networked smart devices subordinate to a CPPS and linked by an IIoT, collected data can be processed through suitable computing resources, such as cloud computing services. To enable regulated access, availability and storage to data, suitable databases and corresponding DBMS must be implemented [3,26]. When selecting a suitable DBMS, it is important to pay particular attention to the system limits, as data to be processed can be too large for specific DBMSs and thus impair performance [74]. Corresponding database models include relational, object-orientated and document-based databases [75,76]. Two programming languages capable of structuring and accessing the data of a database are Structured Query Language

(SQL) and not-only Structured Query Language (noSQL) [76]. Relational databases store the data in structured tables linked together by keys and can be accessed by SQL [75]. Due to the high amount of links between the tables, performance problems occur with large amounts of data, as the relationship models become increasingly complicated [75]. The less commonly used object-oriented databases manage data in an object which internally takes over the data management [76,77]. Depending on the database model, data can be accessed with suitable object-orientated languages. Document-oriented databases follow a non-relational approach where data is stored in documents of different formats by an identifier [76,78]. Data in a document can be accessed with key-value pairs using noSQL [76–79]. As stated by [78], DBMS based on noSQL are suitable for a big amount of data if the data does not demand a relational model, thus gaining popularity, especially when dealing with unstructured data sets [79]. As stated by [79,80], which DBMS to use is highly dependent on the use case, software, and requirements.

I 4.0 is also changing the security requirements for included systems [81,82]. With the increased utilization of HMIs in the manufacturing environment, it is essential to verify the validity of the input and trustworthiness of the operator to ensure operational safety [81]. This risk is further increased by principles such as Bring Your Own Device (BYOD) or Choose Your Own Device (CYOD), which exposes networks to a higher risk of infiltration, e.g., due to a lower level of standardization by a higher degree om heterogeneity of used devices [82]. Therefore, data should be classified according to their confidentiality, integrity and availability (CIA) to prevent unauthorized access and data manipulation [60,81,83–85]. Manipulation or corruption of data could lead to malfunctions, miscalculations, misinterpretation and thus to wrong decisions in the upper two layers of the automation pyramid, the Manufacturing Execution System (MES), and the superordinate Enterprise Resource Planning (ERP) system. As stated by [81], another security risk is the age of the infrastructure, as there is a frequent replacement of equipment over time, making constant planning and updating of security measures necessary. Therefore, a multi-layer architecture approach with multiple safety layers should be implemented, dividing and analyzing the signal flow of each CPPS and cross-validating the signals with those of corresponding CPPS [81]. Other security measures as stated by [81], such as Side-Channel Analysis [86,87] or Post-Production Analysis, can further enhance operational security despite the challenges they pose. A further approach, as mentioned by [88], would be a standardized certification into embedded systems themselves letting those systems check for their security by themselves. Furthermore, [89] proposes that RAMI 4.0 should take greater account of safety and human factors. Another weakness in security planning was pointed out by [90], as stated that a lack of recovery planning in the case of disaster is persistent in I 4.0. Other security measures, as noted by [88,91], include the implementation of a firewall and a private network (VPN) that can only be accessed by devices with authorized IP addresses.

Table 1 summarizes the most important key factors for the implementation of a digitalized metal processing value chain.

Based on the theory elaborated, the authors propose the following hypothesis:

Hypothesis 1 (H1). *When developing a digitalized supply chain within the metal processing environment which is horizontally interconnectable, the 5V condition and therefore the existence of Big Data is automatically fulfilled.*

Table 1. Key factors and corresponding key focus according to literature.

Key Technologies	Key Focus	Literature
Smart Factory	individualization; flexibility; decentralization; resource efficiency	[2,40–43,61]
CPPS	connection and cooperation of layers; acquisition and analysis of data in real-time using Internet technologies; human-machine interaction; enhance real-time decision making	[48–50]
DT	decision making support; partial or complete representation of a production chain/process steps; simulation	[53]
ML/Artificial Intelligence (AI)	supervised learning to enhance decision making within the production environment	[92–96]
IIoT	enables in-situ data acquisition, analysis and exchange for process and production optimization	[59,60,62,63,65]
Cloud computing	on-demand data computation in combination with IIoT	[71–73]
DBMS	store data in structured tables linked together by keys	[41,74–80,97]
IT-security	prevention of unauthorized access and data manipulation; prevention of misinterpretation and corresponding inaccurate decisions of upper layers	[81,82,84–86,89–91,98]

3. Digitalization and Development of a Metal Processing Value Chain: Framework and Corresponding Case Study for SMEs

The presence of SMEs in a value chain varies among the considered industry segment and country. In the case of Austria, 99.7% of the industry consist of SMEs [99], whereas 18.1% of Austria's industry concern the field of manufacturing [100]. Consequently, it is most likely that SMEs are involved within a metal processing value chain. This is particularly evident in the manufacturing sector of the automotive and aerospace industry, where many specialized SMEs supply big enterprises with components that have to fulfill high quality standards and require specific production related expertise [101–104].

To be able to support SMEs within this environment, this section describes the further concretization of the RAMI 4.0 framework for the development of a simplified digitalized value chain for the metal processing industry, that especially considers the additional restrictions SMEs face. The resulting concretized framework is put into operation by a smaller-scale use case at the Montanuniversität Leoben. This use case, which is part of the MUL 4.0 project, does not only serves as a practical testing of the stated hypothesis but pursues to contribute to as a fundament for the state-of-the-art engineering education for future experts in the manufacturing field [105,106].

According to [105], the two main cooperating instances of MUL 4.0 can be characterized as follows: the Chair of Metal Forming (MF) with 15 employees represents a small enterprise, whereas the Chair of Non-Ferrous Metallurgy (NFM) with 72 employees can be seen as a medium enterprise. These chairs are able to provide the required infrastructure for the development of an integrated I 4.0 standard value chain. As a result, by digitalizing and connecting these entities under consideration of providing interfaces for state-of-the-art software used in large enterprises, the steps undertaking to realize these objectives can be utilized by other SMEs within the metal processing environment.

Depending on the product to be manufactured, the respective part has to pass various steps according to RAMI 4.0 [89]. These process steps are carried out in production facilities of various sizes, which, for the sake of simplicity, will be distinguished into SMEs and large enterprises within this work, as visualized in Figure 2.
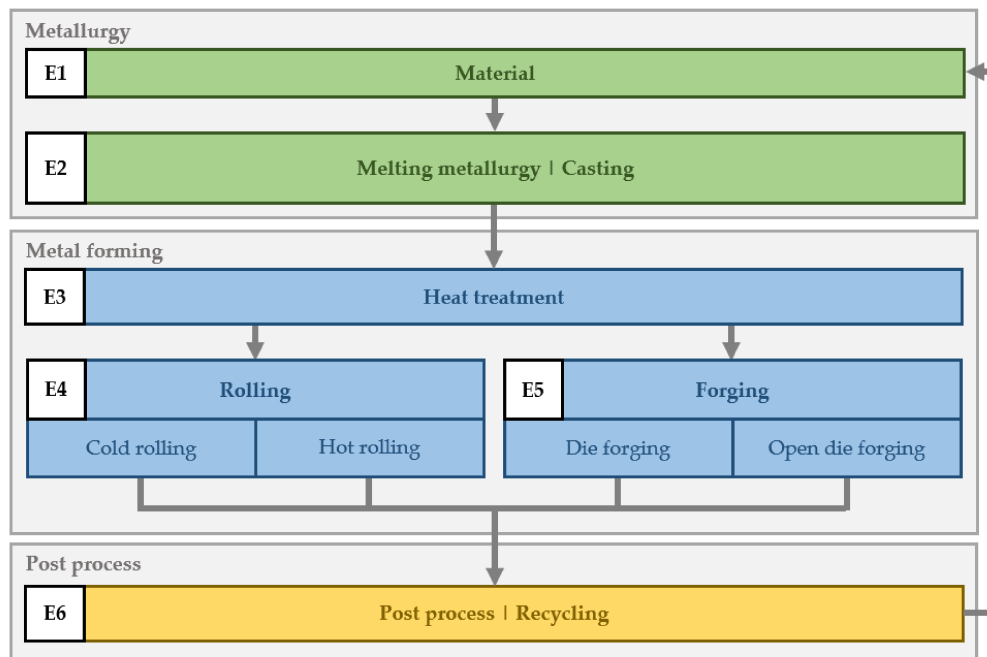
Figure 2. Scheme of a simplified metal forming value chain with different enterprises (E).

To ensure the complete digital transformation of a value chain, both SMEs and large enterprises have to meet the requirements of I 4.0. Disruptions caused by a failure to meet this requirement, e.g., a lack of data to be integrated into the value chain, would lead to an interruption in the processing route. SMEs in particular, often lacking the financial resources and expertise to carry out a successful digital transformation process, pose a risk of such a disruption. Appropriate software and hardware is often expensive and can be a major financial barrier for some SMEs. To overcome this obstacle in terms of hardware and the associated computing resources, an approach with cloud computing is a preferable option. Another advantage would be that respective expertise does not have to be acquired by SMEs themselves, but is already available from the provider of the cloud computing service. Furthermore, providers offer additional solutions such as data processing and can thus be outsourced. Software solutions, serving as another barricade, can be managed with open or closed source products. The choice of whether to use open-source products or closed source products has to be considered from several points of view. Once again, internal know-how is a key factor for the application of open or closed source solutions. If internal human resources with IT expertise are available to implement a customized solution and the requirements and tasks are very specific, an open-source approach may be appropriate. If the requirements are non-specific as they are common in the industry, it would be preferable to use closed source products, pay license fees and thus have access to support and updates. By closing gaps in the value chain, data from other stations or companies can be accessed, depending on authorization, to enable more flexible supply chain management and process planning in the downstream and upstream steps.

Figure 3 shows an exemplary supply chain network for the parallel operation of an SME and larger enterprise.
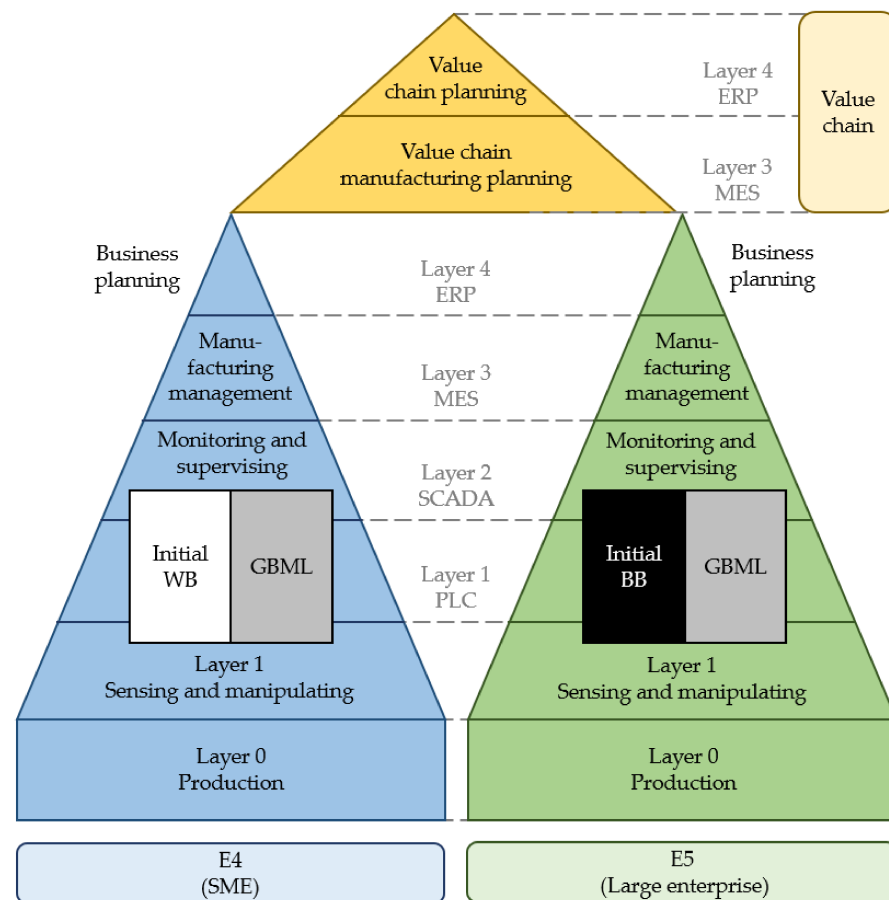
Figure 3. Schematic of a sub-step in a metal processing value chain with two enterprises of different sizes according to the principle of the automation pyramid and its layers.

Digitization and digitalization of both enterprises were based on the model of the automation pyramid. Layer 0 covers all physical production processes. Layer 1 is the DAQ level and contains sensors, actuators and programmable logic controllers (PLCs). Layer 2 acts as the Supervisory Control and Data Acquisition (SCADA) level including HMIs. Layer 3 contains the MES and layer 4 includes the ERP. The data of the respective enterprises can be integrated into the higher-level system from layer 3 and thus act as a lower layer in the higher-level layer system of the value chain. The network includes several servers, which execute several services. If possible, the option of executing only one service per server should be checked according to the "One server, one service" principle. In the event of a server failure, instead of several services, only individual services would be affected, which can be taken over by backup servers. Depending on the available resources, different approaches regarding WBM, GBM, and BBM can be followed. In the case of enterprise 4 (Figure 3, E4), an SME, an initial WBM was chosen using data acquired from a Finite Element Analysis (FEA). Using the external computing resources of a cloud computing service, the data obtained from FEA can be integrated into a WBM, which in turn can be assimilated with further FEA data for refinement, resulting in a WBMLM approach. Another possibility would be to continuously feed process data into the initial WBM, resulting in a GBMLM, as shown in [56]. Enterprise 5 (Figure 3, E5), a large enterprise that already has data that meets the 5Vs criteria, has a similar structure as E4 (Figure 2). Due to the existing amount and value of data, an initial BBM approach is applied within this example. The BBM can be fed and refined with further process data recorded during production and thus establish BBMLM, as shown in [52]. If required data cannot be obtained from the DAQ of the process and would require a WBM based simulation, e.g., FEA for material models or microstructure models, a GBMLM approach

would be followed. In any case, supervised ML should be pursued at the beginning of the implementation to support a successful establishment of the system.

For this exemplary framework, the 5V criterium of Big Data is fulfilled, as demonstrated in Table 2.

Table 2. Overview of the most important data sources and corresponding qualitative estimation for a digitalized metal processing value chain.

Type of Data	Volume	Velocity	Value	Veracity	Variety
Sensor/PLC (e.g., time series data, videos)	low	high	high	high	high (unstructured)
Process-related modeling data (e.g., FEA)	high	low	high	medium-high	high (unstructured)
Inter & intra logistical related data (e.g., smart factory DT)	high	high	high	high	high (unstructured)
WBML	high	Low	high	medium-high	high (unstructured)
GBML	medium	medium	high	medium-high	high (unstructured)
BBML	low	high	high	high	high (unstructured)
IIoT	low	high	high	high	high (unstructured)
MES	medium	medium	high	high	medium (structured/semi-structured)
ERP	high	low	high	high	high (unstructured)

4. Results and Discussion

As part of the MUL 4.0 project, four machines were integrated into a value chain [107]. These are positioned at two different localizations. The continuous caster is located at the NFM and is equipped as standard with sensors and DAQ by the manufacturer. The MF houses the furnace, hydraulic press, and rolling mill, posing as the second production site in the process. The rolling mill from 1954 was transformed into a CPPS utilizing low-cost retrofitting and suitable sensors such as Linear Variable Differential Transformer (LVDT) and load cells to be able to integrate required data into the process [52]. In cooperation with the Chair of Industrial Logistics (IL), a cross-process database was set up to make data available between the cooperating parties. Table 3 shows the technical specifications of the sensors associated with the corresponding machines and their location.

As visualized in Figure 4, the process chain consists of continuous casting of the aluminum specimens, followed by a variable operation of forming processes. At the MF, the specimen can be cold-formed or rolled. In the hot forming process, the specimen is preheated in the furnace before rolling or upsetting. Subsequently, the samples are subjected to quality control and recycled in the final stage.

Table 3. Machines and sensors with technical specifications [107].

Machine	Sensor	Measure	Range	Linearity
Furnace (MF)	Thermocouple (Type K)	Temperature	0–1200 °C	According to DIN EN 60584-2
Rolling mill (MF)	Load cell (Kern CR 20000-1Q1 + PR Electronics 2261)	Rolling force (left guide spindle)	0–200 kN	0.1% FSO
	Load cell (Kern CR 20000-1Q1 + PR Electronics 2261)	Rolling force (right guide spindle)	0–200 kN	0.1% FSO
	LVDT (Waycon LV-S-25-300-KA05-L10 + Waycon LV-S-25-300-KA05-L10)	Roll gap height	0–25 mm	0.1% FSO
	Magnetic multiturn encoder (ASM PH36)	Gear angle	$31 \times 360°$	$\pm(2° + 0.015\%)$ FSO
Hydraulic press (MF)	Load cell	Die force	0–1 MN	0.1% FSO
	LVDT	Die position	0–600 mm	0.1% FSO
	Pyrometer	Temperature	0–1200 °C	According to DIN EN 60584-2
Continuous caster (NFM)	Thermocouple (Type K | Type S)	Crucible temperature	0–1200 °C 0–1500 °C	According to DIN EN 60584-2
	Thermocouple (Type K | Type S)	Die temperature	0–1200 °C 0–1500 °C	According to DIN EN 60584-2
	LVDT	Draw path	0.1–9.9 [mm]	0.1% FSO
	LVDT	Reversing draw path	0.0–9.8 [mm]	0.1% FSO
	Load cell	Draw force	N/A [N]	0.1% FSO
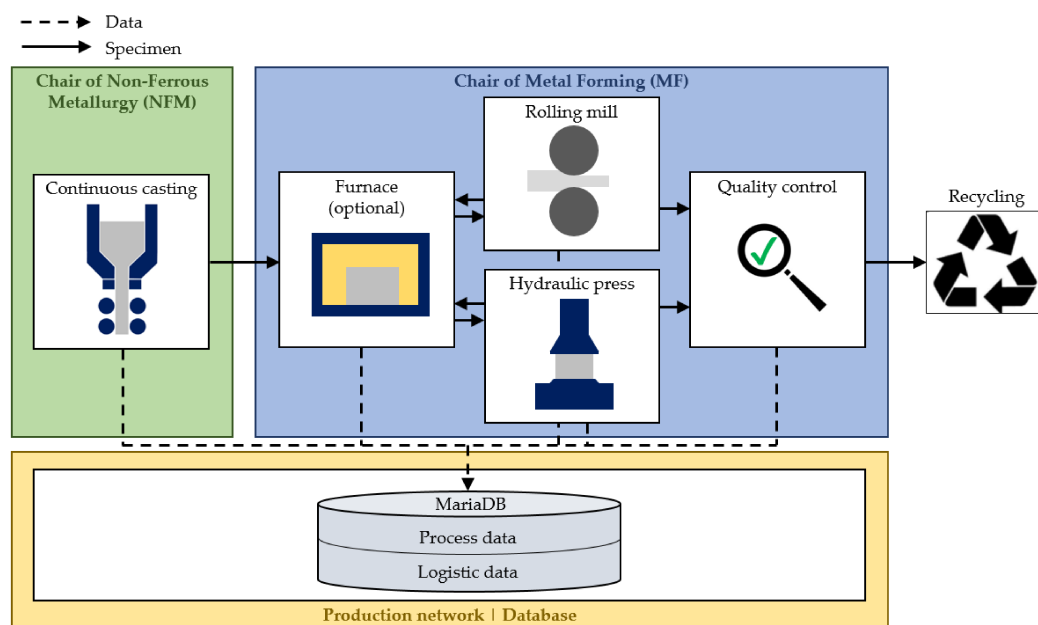
Figure 4. Process chain within the MUL 4.0 project, consisting of the furnace, rolling mill and hydraulic press.

To transfer the data recorded by the sensors into the production network, DAQs were implemented (Table 4). At the MF, a low-cost approach was pursued with DAQ systems from Wago GmbH (Brunn am Gebirge, Austria) and the Wago e!Cockpit software. In addition, data processing, creation and execution of GUIs used with the open-source programming language Python [52].

Table 4. Utilized machines and DAQ with technical specifications within the MUL 4.0 project.

Machine	DAQ	Protocol	Resolution	Frequency
Rolling mill (MF)	Wago PFC200 750-8212 (+I/O modules)	Modbus TCP/IP	15 bit	500 Hz
Furnace (MF)	Wago PFC200 750-8212 (+I/O modules)	Modbus TCP/IP	15 bit	500 Hz
Hydraulic press (MF)	Wago PFC200 750-8212 (+I/O modules)	Modbus TCP/IP	15 bit	500 Hz
Continuous caster (NFM)	Internal DAQ	Modbus TCP/IP	15 bit	>100 Hz

To pursue the low-cost and open-source approach, MariaDB was chosen as SQL-based database, as deemed suitable for the amount of data generated. In the processing chain of MUL 4.0, a distinction can be made between process-related time series data and logistical data. Process-related time series data, e.g., sensor data, data obtained from a FEA or finite volume analysis (FVA), photos and videos need to be accessed and computed in near real-time to create appropriate process DTs. Not all raw data is stored in the database, but selected, filtered data to keep the performance of the database optimal. Data stored in the database can be accessed by authorized users for further data processing or investigation. Furthermore, the MariaDB is linked to an MES and ERP to enable dynamic process chain monitoring, planning and control.

As mentioned in Section 2, cyber security plays a key role in the context of I 4.0. For this reason, an IT-layer architecture was designed and implemented as shown qualitatively in Figure 5. The IIoT in layer 2 can be considered as a closed system, from which data from a NodeRed server and the Maria DB are transferred to layer 3. Layer 3 contains the remote admin host, webserver dashboard, the chosen low-cost ERP system ERP Next and the file server in a virtual environment, which can be accessed by the client by authorized workstations. To prevent unauthorized access and cyber-attacks, a firewall was installed between layers 2 and 3, which only allows layer 3 to query layer 2.
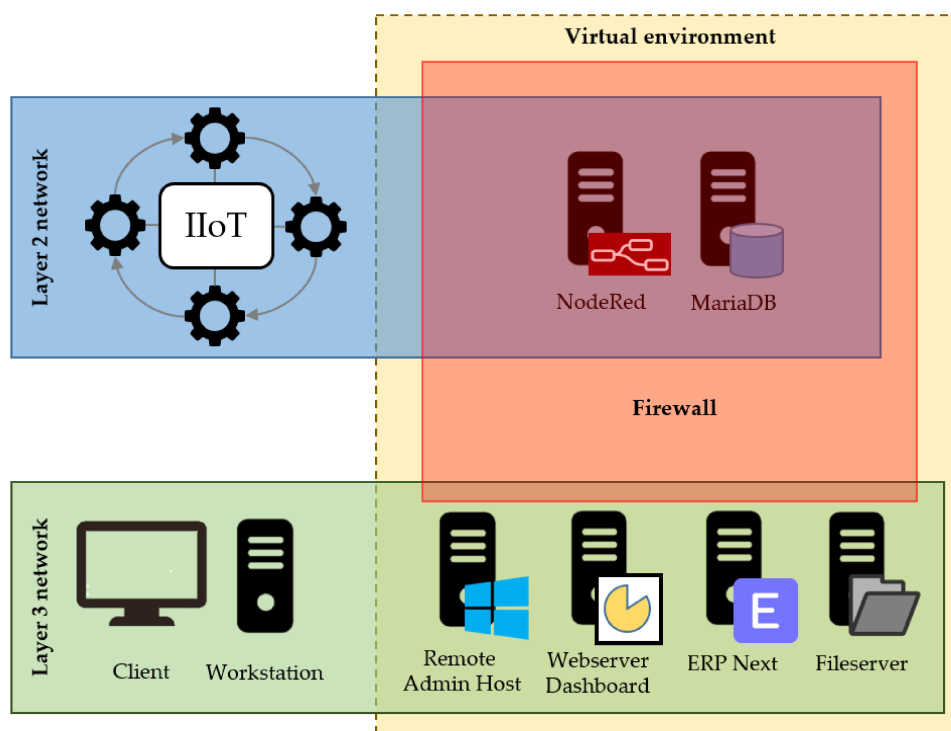
Figure 5. Qualitative illustration of the implemented IT layer system of the MUL 4.0 project.

Figure 6 visualizes the resulting adapted architecture, based on the RAMI 4.0 concept. Tables 5–10 concretizes the corresponding areas within this adapted model.
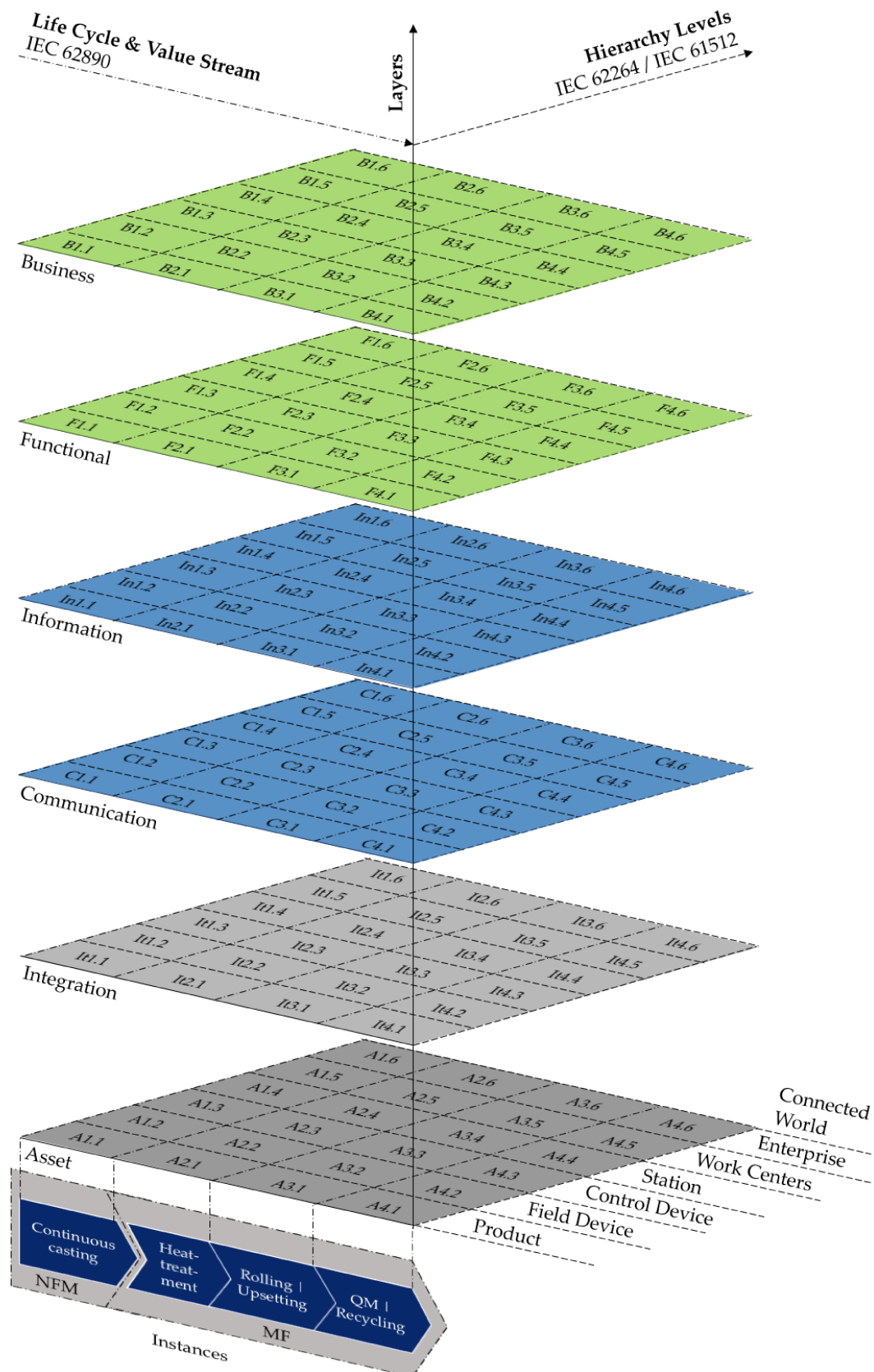

Figure 6. RAMI 4.0 framework adapted to the case of the MUL 4.0 project.

Table 5. Asset layer fragments from Figure 6 and corresponding specifications.

Layer Fragment	Specification
A1.1	Continuous casted specimen
A1.2	Sensors of continuous caster according to Table 3
A1.3	Tablet/PC
A1.4	Continuous Caster
A1.5	Center for Non-Ferrous Metallurgy
A1.6	NFM
A2.1	Heat treated specimen
A2.2	Sensors of furnace according to Table 3
A2.3	Tablet/PC
A2.4	Furnace
A2.5	Center for Metal Forming
A2.6	MF
A3.1	Formed specimen
A3.2	Sensors of rolling mill | hydraulic press according to Table 3
A3.3	Tablet/PC
A3.4	Rolling mill | Hydraulic press
A3.5	Center for Metal Forming
A3.6	MF
A4.1	Quality checked specimen | Recycled specimen
A4.2	Sensor of tensile test machine | recycling aggregate
A4.3	Tablet/PC
A4.4	Tensile test machine | Recycling aggregate
A4.5	Center for Metal Forming
A4.6	MF

Table 6. Integration layer fragments from Figure 6 and corresponding specifications.

Layer Fragment	Specification
It1.1	RFID chip
It1.2	Continuous caster DAQ according to Table 4 + Internal Software
It1.3	GUI + Webserver Dashboard Server (DHCP)
It1.4	CPPS + IIoT
It1.5	MES Server + DHCP protocol
It1.6	ERP Next Server + DHCP protocol
It2.1	RFID chip
It2.2	Furnace DAQ according to Table 4 + Wago e!Cockpit Sofware
It2.3	GUI + Webserver Dashboard Server (DHCP)
It2.4	CPPS + IIoT
It2.5	MES Server + DHCP protocol
It2.6	ERP Next Server + DHCP protocol
It3.1	RFID chip
It3.2	Rolling mill | hydraulic press DAQ according to Table 4 + Wago e!Cockpit Sofware
It3.3	GUI + Webserver Dashboard Server (DHCP)
It3.4	CPPS + IIoT
It3.5	MES Server + DHCP protocol
It3.6	ERP Next Server + DHCP protocol
It4.1	RFID chip
It4.2	Tensile test machine | Recycling aggregate DAQ + Software
It4.3	GUI + Webserver Dashboard Server (DHCP)
It4.4	CPPS + IIoT
It4.5	MES Server + DHCP protocol
It4.6	ERP Next Server + DHCP protocol

Table 7. Communication layer fragments from Figure 6 and corresponding specifications.

Layer Fragment	Specification
C1.1	RFID protocol
C1.2	Modbus TCP/IP
C1.3	DHCP
C1.4	DHCP
C1.5	DHCP
C1.6	DHCP
C2.1	RFID protocol
C2.2	Modbus TCP/IP
C2.3	DHCP
C2.4	DHCP
C2.5	DHCP
C2.6	DHCP
C3.1	RFID protocol
C3.2	Modbus TCP/IP
C3.3	DHCP
C3.4	DHCP
C3.5	DHCP
C3.6	DHCP
C4.1	RFID protocol
C4.2	Modbus TCP/IP
C4.3	DHCP
C4.4	DHCP
C4.5	DHCP
C4.6	DHCP

Table 8. Information layer fragments from Figure 6 and corresponding specifications.

Layer Fragment	Specification
In1.1	Location of specimen
In1.2	Sensor data of continuous caster according to Table 3
In1.3	User input from continuous caster GUI
In1.4	Status of continuous caster
In1.5	Process data acquired by data processing (e.g., utilization factor)
In1.6	Economic data acquired by data processing (e.g., price per unit)
In2.1	Location of specimen
In2.2	Sensor data of furnace according to Table 3
In2.3	User input from furnace GUI
In2.4	Status of furnace
In2.5	Process data acquired by data processing (e.g., utilization factor)
In2.6	Economic data acquired by data processing (e.g., price per unit)
In3.1	Location of specimen
In3.2	Sensor data of rolling mill | hydraulic press according to Table 3
In3.3	User input from rolling mill | hydraulic press GUI
In3.4	Status of rolling mill | hydraulic press
In3.5	Process data acquired by data processing (e.g., utilization factor)
In3.6	Economic data acquired by data processing (e.g., price per unit)
In4.1	Location of specimen
In4.2	Sensor data of tensile test machine | recycling aggregate
In4.3	User input from tensile test machine | recycling aggregate GUI
In4.4	Status of tensile test machine | recycling aggregate
In4.5	Process data acquired by data processing (e.g., utilization factor)
In4.6	Economic data acquired by data processing (e.g., price per unit)

Table 9. Functional layer fragments from Figure 6 and specifications.

Layer Fragment	Specification
F1.1	Statistical data by data processing
F1.2	Statistical data by data processing
F1.3	Statistical data by data processing
F1.4	Machine status
F1.5	MES data processing
F1.6	ERP data processing
F2.1	Statistical data by data processing
F2.2	Statistical data by data processing
F2.3	Statistical data by data processing
F2.4	Machine status
F2.5	MES data processing
F2.6	ERP data processing
F3.1	Statistical data by data processing
F3.2	Statistical data by data processing
F3.3	Statistical data by data processing
F3.4	Machine status
F3.5	MES data processing
F3.6	ERP data processing
F4.1	Statistical data by data processing
F4.2	Statistical data by data processing
F4.3	Statistical data by data processing
F4.4	Machine status
F4.5	MES data processing
F4.6	ERP data processing

Table 10. Business layer fragments from Figure 6 and corresponding specifications.

Layer Fragment	Specification
B1.1	Product optimization
B1.2	Process optimization
B1.3	Human resources optimization
B1.4	Downtime risk minimization
B1.5	Process chain optimization
B1.6	Cost optimization
B2.1	Product optimization
B2.2	Process optimization
B2.3	Human resources optimization
B2.4	Downtime risk minimization
B2.5	Process chain optimization
B2.6	Cost optimization
B3.1	Product optimization
B3.2	Process optimization
B3.3	Human resources optimization
B3.4	Downtime risk minimization
B3.5	Process chain optimization
B3.6	Cost optimization
B4.1	Product optimization
B4.2	Process optimization
B4.3	Human resources optimization
B4.4	Downtime risk minimization
B4.5	Process chain optimization
B4.6	Cost optimization

According to state-of-the-art literature, Big Data analytics is an integral part of the fourth industrial revolution. For the integration of SMEs within the metal processing value chain, this technology can also be seen as an essential component of this process, as this work demonstrates. Furthermore, by including the characteristics of Big Data within the

initial planning phase of an interconnected metal processing supply chain project, the risk of misplanning can be minimized. The combination of structured and standardized planning, relying on the RAMI 4.0 model and the 5V definition of Big Data can thus support SMEs and their stakeholders within the value chain for an accelerated integration approach. The additional consideration of IT security, as well as cloud computing solutions, further increase the resilience of a planned mixed enterprise size value chain integration. Due to the financial and resource challenges especially SMEs have to overcome, the utilization of low-cost but industry-standard solutions, as demonstrated in Section 3 can lead to a significant boost within the digitalization, digital transformation, and finally value chain integration of these company types. The fulfillment of the 5Vs of Big Data analytics, however, is not mandatory for all types of SMEs. By focusing on the metal processing environment, the required volume can easily be reached, as this industry segment heavily relies on FEA-based WBM. For SMEs or even larger companies, operating in industry fields where the process variety is low and/or the process parameters are stable and not complex, volume, as well as variety is not necessarily high. Based on the results of the theory and case study shown in this paper, it can be stated that a fully digitalized metal processing value chain must always include the Big Data concept, therefore H1 cannot be neglected. Despite this conclusion, using the RAMI 4.0 model as a fundament for further concretization for the digital transformation of an SME can add value within all manufacturing-related industry segments. Considering the broader perspective of international supply and value chains, the authors argue that an additional focus on the legal aspect of international collaborations and networks should be additionally focused within the RAMI 4.0 framework, especially when considering legal differences in terms of responsibilities and liabilities in the event of ML-involved accidents at the shopfloor level.

5. Conclusions and Outlook

In this paper, an approach for a systematic standardized digitalization of a value chain is presented. For this purpose, key enablers for a digital transformation were identified according to state-of-the-art literature. The utilization of these key technologies and systems is then elaborated in more depth by applying possible configurations on the theoretical integration of SMEs into a digitalized metal processing value chain, especially considering the requirements of these enterprises operating with heterogeneous and complex processes. Based on this further concretization, the resulting concept is further applied on a small-scale value chain developed at the Montanuniversität Leoben for further analysis and validation. By doing so, the authors state that Big Data is a core element of a fully digitalized value chain within the metal processing environment. With increasing digitalization among all involved stakeholders within the metal processing sector, digital transformation and therefore, digitalized value chains will subsequently increase, leading to further utilization of Big Data and corresponding technologies. As demonstrated within this work, the use of a suitable digital transformation framework can furthermore contribute to a more resilient digital transformation process and decrease the implementation and optimization time required to fulfill the requirements of an I 4.0 compatible supply chain. As already observable in other industry segments, technologies like blockchain can boost this development even more, e.g., by increasing data security [108–110]. Furthermore, the rise of quantum computing and expected utilization in the manufacturing context can further boost the demand for Big Data technologies and required know-how, which increases the importance of corresponding technologies and frameworks in the future even more.

References

1. Reiman, A.; Kaivo-oja, J.; Parviainen, E.; Takala, E.-P.; Lauraeus, T. Human factors and ergonomics in manufacturing in the industry 4.0 context—A scoping review. *Technol. Soc.* **2021**, *65*, 101572. [CrossRef]
2. Ralph, B.J.; Stockinger, M. Digitalization and Digital Transformation in Metal Forming: Key Technologies, Challenges and Current Developments of Industry 4.0 Applications. In *XXXIX Colloquium on Metal Forming 2020*; Montanuniversität: Leoben, Austria, 2020; pp. 13–23, ISBN 978-3-902078-26-1.
3. Ralph, B.J.; Sorger, M.; Schödinger, B.; Schmölzer, H.-J.; Hartl, K.; Stockinger, M. Implementation of a Six-Layer Smart Factory Architecture with Special Focus on Transdisciplinary Engineering Education. *Sensors* **2021**, *21*, 2944. [CrossRef]
4. Zhong, R.Y.; Xu, X.; Klotz, E.; Newman, S.T. Intelligent Manufacturing in the Context of Industry 4.0: A Review. *Engineering* **2017**, *3*, 616–630. [CrossRef]
5. Sorensen, D.G.; Brunoe, T.D.; Nielsen, K. Brownfield Development of Platforms for Changeable Manufacturing. *Procedia CIRP* **2019**, *81*, 986–991. [CrossRef]
6. Enyoghasi, C.; Badurdeen, F. Industry 4.0 for sustainable manufacturing: Opportunities at the product, process, and system levels. *Resour. Conserv. Recycl.* **2021**, *166*, 105362. [CrossRef]
7. Suri, K.; Cadavid, J.; Alferez, M.; Dhouib, S.; Tucci-Piergiovanni, S. Modeling business motivation and underlying processes for RAMI 4.0-aligned cyber-physical production systems. In Proceedings of the 2017 22nd IEEE International Conference on Emerging Technologies and Factory Automation (ETFA), Limassol, Cyprus, 12–15 September 2017; pp. 1–6, ISBN 978-1-5090-6505-9.
8. De Melo, P.F.S.; Godoy, E.P. Controller Interface for Industry 4.0 based on RAMI 4.0 and OPC UA. In *2019 II Workshop on Metrology for Industry 4.0 and IoT (MetroInd4.0&IoT)*; IEEE: Piscataway, NJ, USA, 2019.
9. Flatt, H.; Schriegel, S.; Jasperneite, J.; Trsek, H.; Adamczyk, H. Analysis of the Cyber-Security of industry 4.0 technologies based on RAMI 4.0 and identification of requirements. In Proceedings of the 2016 IEEE 21st International Conference on Emerging Technologies and Factory Automation (ETFA), Berlin, Germany, 6–9 September 2016; pp. 1–4, ISBN 978-1-5090-1314-2.
10. Lee, J.; Lapira, E.; Bagheri, B.; Kao, H. Recent advances and trends in predictive manufacturing systems in big data environment. *Manuf. Lett.* **2013**, *1*, 38–41. [CrossRef]
11. O'Donovan, P.; Leahy, K.; Bruton, K.; O'Sullivan, D.T.J. Big data in manufacturing: A systematic mapping study. *J. Big Data* **2015**, *2*, 20. [CrossRef]
12. Mourtzis, D.; Vlachou, E.; Milas, N. Industrial Big Data as a Result of IoT Adoption in Manufacturing. *Procedia CIRP* **2016**, *55*, 290–295. [CrossRef]
13. Kusiak, A. Smart manufacturing must embrace big data. *Nature* **2017**, *544*, 23–25. [CrossRef]
14. Zhang, Y.; Ren, S.; Liu, Y.; Si, S. A big data analytics architecture for cleaner manufacturing and maintenance processes of complex products. *J. Clean. Prod.* **2017**, *142*, 626–641. [CrossRef]
15. Bordeleau, F.-È.; Felden, C. Digitally Transforming Organisations: A Review of Change Models of Industry 4.0. In Proceedings of the 27th European Conference on Information Systems (ECIS), Stockholm & Uppsala, Sweden, 8–14 June 2019; pp. 1–14, ISBN 978-1-7336325-0-8.
16. Hilbert, M. Big Data for Development: A Review of Promises and Challenges. *Dev. Policy Rev.* **2016**, *34*, 135–174. [CrossRef]
17. Chen, J.; Chen, Y.; Du, X.; Li, C.; Lu, J.; Zhao, S.; Zhou, X. Big data challenge: A data management perspective. *Front. Comput. Sci.* **2013**, *7*, 157–164. [CrossRef]
18. Demchenko, Y.; de Laat, C.; Membrey, P. Defining architecture components of the Big Data Ecosystem. In Proceedings of the 2014 International Conference on Collaboration Technologies and Systems (CTS), Minneapolis, MN, USA, 19–23 May 2014; pp. 104–112, ISBN 978-1-4799-5158-1.
19. Sagiroglu, S.; Sinanc, D. Big data: A review. In Proceedings of the 2013 International Conference on Collaboration Technologies and Systems (CTS), San Diego, CA, USA, 20–24 May 2013; pp. 42–47, ISBN 978-1-4673-6404-1.
20. Ghasemaghaei, M. Understanding the impact of big data on firm performance: The necessity of conceptually differentiating among big data characteristics. *Int. J. Inf. Manag.* **2021**, *57*, 102055. [CrossRef]
21. Zikopoulos, P.; Eaton, C. *Understanding Big Data: Analytics for Enterprise Class Hadoop and Streaming Data*; McGraw-Hill Osborne Media: New York, NY, USA, 2011; ISBN 978-0-07-179053-6.

22. Klein, D.; Tran-Gia, P.; Hartmann, M. Big Data. *Inform. Spektrum* **2013**, *36*, 319–323. [CrossRef]
23. Matt, D.T.; Modrák, V.; Zsifkovits, H. *Industry 4.0 for SMEs*; Springer International Publishing: Cham, Switzerland, 2020; ISBN 978-3-030-25424-7.
24. Ishwarappa; Anuradha, J. A Brief Introduction on Big Data 5Vs Characteristics and Hadoop Technology. *Procedia Comput. Sci.* **2015**, *48*, 319–324. [CrossRef]
25. Younas, M. Research challenges of big data. *Serv. Oriented Comput. Appl.* **2019**, *13*, 105–107. [CrossRef]
26. Khan, N.; Yaqoob, I.; Hashem, I.A.T.; Inayat, Z.; Ali, W.K.M.; Alam, M.; Shiraz, M.; Gani, A. Big data: Survey, technologies, opportunities, and challenges. *Sci. World J.* **2014**, *2014*, 712826. [CrossRef]
27. Bertoncel, T.; Erenda, I.; Bach, M.P.; Roblek, V.; Meško, M. A Managerial Early Warning System at a Smart Factory: An Intuitive Decision-making Perspective. *Syst. Res* **2018**, *35*, 406–416. [CrossRef]
28. Tjahjono, B.; Esplugues, C.; Ares, E.; Pelaez, G. What does Industry 4.0 mean to Supply Chain? *Procedia Manuf.* **2017**, *13*, 1175–1182. [CrossRef]
29. Tupa, J.; Simota, J.; Steiner, F. Aspects of Risk Management Implementation for Industry 4.0. *Procedia Manuf.* **2017**, *11*, 1223–1230. [CrossRef]
30. Yang, C.; Huang, Q.; Li, Z.; Liu, K.; Hu, F. Big Data and cloud computing: Innovation opportunities and challenges. *Int. J. Digit. Earth* **2017**, *10*, 13–53. [CrossRef]
31. Marjani, M.; Nasaruddin, F.; Gani, A.; Karim, A.; Hashem, I.A.T.; Siddiqa, A.; Yaqoob, I. Big IoT Data Analytics: Architecture, Opportunities, and Open Research Challenges. *IEEE Access* **2017**, *5*, 5247–5261. [CrossRef]
32. Hongsong, C.; Yongpeng, Z.; Yongrui, C.; Bhargava, B. Security Threats and Defensive Approaches in Machine Learning System Under Big Data Environment. *Wirel. Pers. Commun.* **2021**, *117*, 3505–3525. [CrossRef]
33. Mills, K.A. What are the threats and potentials of big data for qualitative research? *Qual. Res.* **2018**, *18*, 591–603. [CrossRef]
34. Häckel, B.; Hänsch, F.; Hertel, M.; Übelhör, J. Assessing IT availability risks in smart factory networks. *Bus. Res.* **2019**, *12*, 523–558. [CrossRef]
35. Herrmann, F. The Smart Factory and Its Risks. *Systems* **2018**, *6*, 38. [CrossRef]
36. Lasi, H.; Fettke, P.; Kemper, H.-G.; Feld, T.; Hoffmann, M. Industry 4.0. *Bus. Inf. Syst. Eng.* **2014**, *6*, 239–242. [CrossRef]
37. Strozzi, F.; Colicchia, C.; Creazza, A.; Noè, C. Literature review on the 'Smart Factory' concept using bibliometric tools. *Int. J. Prod. Res.* **2017**, *55*, 6572–6591. [CrossRef]
38. Osterrieder, P.; Budde, L.; Friedli, T. The smart factory as a key construct of industry 4.0: A systematic literature review. *Int. J. Prod. Econ.* **2020**, *221*, 107476. [CrossRef]
39. Forcina, A.; Introna, V.; Silvestri, A. Enabling technology for maintenance in a smart factory: A literature review. *Procedia Comput. Sci.* **2021**, *180*, 430–435. [CrossRef]
40. Hermann, M.; Pentek, T.; Otto, B. Design Principles for Industrie 4.0 Scenarios. In Proceedings of the 2016 49th Hawaii International Conference on System Sciences (HICSS), Koloa, HI, USA, 5–8 January 2016; pp. 3928–3937, ISBN 978-0-7695-5670-3.
41. Wang, S.; Wan, J.; Li, D.; Zhang, C. Implementing Smart Factory of Industrie 4.0: An Outlook. *Int. J. Distrib. Sens. Netw.* **2016**, *12*, 3159805. [CrossRef]
42. Chen, Y. Integrated and Intelligent Manufacturing: Perspectives and Enablers. *Engineering* **2017**, *3*, 588–595. [CrossRef]
43. Mabkhot, M.; Al-Ahmari, A.; Salah, B.; Alkhalefah, H. Requirements of the Smart Factory System: A Survey and Perspective. *Machines* **2018**, *6*, 23. [CrossRef]
44. Beliatis, M.J.; Jensen, K.; Ellegaard, L.; Aagaard, A.; Presser, M. Next Generation Industrial IoT Digitalization for Traceability in Metal Manufacturing Industry: A Case Study of Industry 4.0. *Electronics* **2021**, *10*, 628. [CrossRef]
45. Resman, M.; Pipan, M.; Simic, M.; Herakovic, N. A new architecture model for smart manufacturing: A performance analysis and comparison with the RAMI 4.0 reference model. *Adv Prod. Eng. Manag* **2019**, *14*, 153–165. [CrossRef]
46. Pisching, M.A.; Pessoa, M.A.; Junqueira, F.; dos Santos Filho, D.J.; Miyagi, P.E. An architecture based on RAMI 4.0 to discover equipment to process operations required by products. *Comput. Ind. Eng.* **2018**, *125*, 574–591. [CrossRef]
47. Weber, C.; Königsberger, J.; Kassner, L.; Mitschang, B. M2DDM—A Maturity Model for Data-Driven Manufacturing. *Procedia CIRP* **2017**, *63*, 173–178. [CrossRef]
48. Cardin, O. Classification of cyber-physical production systems applications: Proposition of an analysis framework. *Comput. Ind.* **2019**, *104*, 11–21. [CrossRef]
49. Monostori, L. Cyber-physical Production Systems: Roots, Expectations and R&D Challenges. *Procedia CIRP* **2014**, *17*, 9–13. [CrossRef]
50. Wu, X.; Goepp, V.; Siadat, A. Concept and engineering development of cyber physical production systems: A systematic literature review. *Int. J. Adv. Manuf. Technol.* **2020**, *111*, 243–261. [CrossRef]
51. Alur, R. *Principles of Cyber-Physical Systems*; The MIT Press: Philadelphia, PA, USA, 2015; ISBN 978-0-262-02911-7.
52. Ralph, B.J.; Sorger, M.; Hartl, K.; Schwarz, A.; Messner, F.; Stockinger, M. Transformation of a Rolling Mill Aggregate to a Cyber Physical Production System: From Sensor Retrofitting to Machine Learning. *J Intell. Manuf.* **2021**, in press.
53. Kritzinger, W.; Karner, M.; Traar, G.; Henjes, J.; Sihn, W. Digital Twin in manufacturing: A categorical literature review and classification. *IFAC-Pap.* **2018**, *51*, 1016–1022. [CrossRef]
54. Pintelas, E.; Livieris, I.E.; Pintelas, P. A Grey-Box Ensemble Model Exploiting Black-Box Accuracy and White-Box Intrinsic Interpretability. *Algorithms* **2020**, *13*, 17. [CrossRef]

55. Loyola-Gonzalez, O. Black-Box vs. White-Box: Understanding Their Advantages and Weaknesses from a Practical Point of View. *IEEE Access* **2019**, *7*, 154096–154113. [CrossRef]

56. Ralph, B.J.; Hartl, K.; Sorger, M.; Schwarz-Gsaxner, A.; Stockinger, M. Machine Learning Driven Prediction of Residual Stresses for the Shot Peening Process Using a Finite Element Based Grey-Box Model Approach. *J. Manuf. Mater. Process.* **2021**, *5*, 39. [CrossRef]

57. Rudin, C. Stop explaining black box machine learning models for high stakes decisions and use interpretable models instead. *Nat. Mach. Intell.* **2019**, *1*, 206–215. [CrossRef]

58. Henard, C.; Papadakis, M.; Harman, M.; Jia, Y.; Le Traon, Y. Comparing white-box and black-box test prioritization. In Proceedings of the ICSE '16: 38th International Conference on Software Engineering, Austin, TX, USA, 14–22 May 2016; Dillon, L., Visser, W., Williams, L., Eds.; ACM: New York, NY, USA, 2016; pp. 523–534, ISBN 9781450339001.

59. Xu, H.; Yu, W.; Griffith, D.; Golmie, N. A Survey on Industrial Internet of Things: A Cyber-Physical Systems Perspective. *IEEE Access* **2018**, *6*, 78238–78259. [CrossRef]

60. Boyes, H.; Hallaq, B.; Cunningham, J.; Watson, T. The industrial internet of things (IIoT): An analysis framework. *Comput. Ind.* **2018**, *101*, 1–12. [CrossRef]

61. Sanders, A.; Elangeswaran, C.; Wulfsberg, J. Industry 4.0 implies lean manufacturing: Research activities in industry 4.0 function as enablers for lean manufacturing. *JIEM* **2016**, *9*, 811. [CrossRef]

62. ur Rehman, M.H.; Yaqoob, I.; Salah, K.; Imran, M.; Jayaraman, P.P.; Perera, C. The role of big data analytics in industrial Internet of Things. *Future Gener. Comput. Syst.* **2019**, *99*, 247–259. [CrossRef]

63. Sadeghi, A.-R.; Wachsmann, C.; Waidner, M. Security and privacy challenges in industrial internet of things. In Proceedings of the DAC '15: The 52nd Annual Design Automation Conference 2015, San Francisco, CA, USA, 7–11 June 2015; ACM: New York, NY, USA, 2015; pp. 1–6, ISBN 9781450335201.

64. Hajjaji, Y.; Boulila, W.; Farah, I.R.; Romdhani, I.; Hussain, A. Big data and IoT-based applications in smart environments: A systematic review. *Comput. Sci. Rev.* **2021**, *39*, 100318. [CrossRef]

65. Khan, W.Z.; Rehman, M.H.; Zangoti, H.M.; Afzal, M.K.; Armi, N.; Salah, K. Industrial internet of things: Recent advances, enabling technologies and open challenges. *Comput. Electr. Eng.* **2020**, *81*, 106522. [CrossRef]

66. Nahavandi, S. Industry 5.0—A Human-Centric Solution. *Sustainability* **2019**, *11*, 4371. [CrossRef]

67. Özdemir, V.; Hekim, N. Birth of Industry 5.0: Making Sense of Big Data with Artificial Intelligence, "The Internet of Things" and Next-Generation Technology Policy. *Omics* **2018**, *22*, 65–76. [CrossRef]

68. Javaid, M.; Haleem, A.; Singh, R.P.; Haq, M.I.U.; Raina, A.; Suman, R. Industry 5.0: Potential Applications in COVID-19. *J. Ind. Integr. Manag.* **2020**, *5*, 507–530. [CrossRef]

69. Eller, R.; Alford, P.; Kallmünzer, A.; Peters, M. Antecedents, consequences, and challenges of small and medium-sized enterprise digitalization. *J. Bus. Res.* **2020**, *112*, 119–127. [CrossRef]

70. Mell, P.; Grance, T. *The NIST Definition of Cloud Computing*; NIST: Gaithersburg, MD, USA, 2011.

71. Sheikh, A.; Munro, M.; Budgen, D. Systematic Literature Review (SLR) of Resource Scheduling and Security in Cloud Computing. *IJACSA* **2019**, *10*. [CrossRef]

72. Xu, X. From cloud computing to cloud manufacturing. *Robot. Comput.-Integr. Manuf.* **2012**, *28*, 75–86. [CrossRef]

73. Repschläger, J.; Pannicke, D.; Zarnekow, R. Cloud Computing: Definitionen, Geschäftsmodelle und Entwicklungspotenziale. *HMD* **2010**, *47*, 6–15. [CrossRef]

74. Madden, S. From Databases to Big Data. *IEEE Internet Comput.* **2012**, *16*, 4–6. [CrossRef]

75. Kunda, D.; Phiri, H. A Comparative Study of NoSQL and Relational Database. *Zictjournal* **2017**, *1*, 1–4. [CrossRef]

76. Cattell, R. Scalable SQL and NoSQL data stores. *Sigmod Rec.* **2011**, *39*, 12–27. [CrossRef]

77. Bertino, E.; Martino, L. Object-oriented database management systems: Concepts and issues. *Computer* **1991**, *24*, 33–47. [CrossRef]

78. Moniruzzaman, A.B.M.; Hossain, S.A. NoSQL Database: New Era of Databases for Big data Analytics—Classification, Characteristics and Comparison. *Int. J. Database Theory Appl.* **2013**, *6*, 1–14. Available online: http://arxiv.org/pdf/1307.0191v1 (accessed on 15 June 2021).

79. Li, Y.; Manoharan, S. A performance comparison of SQL and NoSQL databases. In Proceedings of the 2013 IEEE Pacific Rim Conference on Communications, Computers and Signal Processing (PACRIM), Victoria, BC, Canada, 27–29 August 2013; pp. 15–19, ISBN 978-1-4799-1501-9.

80. van der Veen, J.S.; van der Waaij, B.; Meijer, R.J. Sensor Data Storage Performance: SQL or NoSQL, Physical or Virtual. In Proceedings of the 2012 IEEE 5th International Conference on Cloud Computing (CLOUD), Honolulu, HI, USA, 24–29 June 2012; pp. 431–438, ISBN 978-1-4673-2892-0.

81. Prinsloo, J.; Sinha, S.; von Solms, B. A Review of Industry 4.0 Manufacturing Process Security Risks. *Appl. Sci.* **2019**, *9*, 5105. [CrossRef]

82. Pereira, T.; Barreto, L.; Amaral, A. Network and information security challenges within Industry 4.0 paradigm. *Procedia Manuf.* **2017**, *13*, 1253–1260. [CrossRef]

83. Qadir, S.; Quadri, S.M.K. Information Availability: An Insight into the Most Important Attribute of Information Security. *J. Inf. Secur.* **2016**, *7*, 185–194. [CrossRef]

84. Chhetri, S.R.; Faezi, S.; Rashid, N.; Al Faruque, M.A. Manufacturing Supply Chain and Product Lifecycle Security in the Era of Industry 4.0. *J. Hardw. Syst. Secur.* **2018**, *2*, 51–68. [CrossRef]

85. Kiss, M.; Breda, G.; Muha, L. Information security aspects of Industry 4.0. *Procedia Manuf.* **2019**, *32*, 848–855. [CrossRef]
86. Bayens, C.; Le, T.; Garcia, L.; Beyah, T.; Javanmard, M.; Zonouz, S. See No Evil, Hear No Evil, Feel No Evil, Print No Evil? Malicious Fill Patterns Detection in Additive Manufacturing. In Proceedings of the 26th USENIX Security Symposium, Vancouver, BC, Canada, 16–18 August 2017; pp. 1181–1198, ISBN 978-1-931971-40-9.
87. Chhetri, S.R.; Canedo, A.; Faruque, M.A.A. KCAD. In Proceedings of the ICCAD '16: IEEE/ACM International Conference On Computer-Aided Design, Austin, TX, USA, 7–10 November 2016; Liu, F., Ed.; ACM: New York, NY, USA, 2016; pp. 1–8, ISBN 9781450344661.
88. Ervural, B.C.; Ervural, B. Overview of Cyber Security in the Industry 4.0 Era. In *Industry 4.0: Managing the Digital Transformation*; Ustundag, A., Cevikcan, E., Eds.; Springer International Publishing: Cham, Switzerland, 2018; pp. 267–284, ISBN 978-3-319-57869-9.
89. Sharpe, R.; van Lopik, K.; Neal, A.; Goodall, P.; Conway, P.P.; West, A.A. An industrial evaluation of an Industry 4.0 reference architecture demonstrating the need for the inclusion of security and human components. *Comput. Ind.* **2019**, *108*, 37–44. [CrossRef]
90. Radanliev, P.; Mantilla Montalvo, R.; Cannady, S.; Nicolescu, R.; de Roure, D.; Nurse, J.R.; Huth, M. Cyber Security Framework for the Internet-of-Things in Industry 4.0. *Preprints* **2019**, 2019030111. [CrossRef]
91. Khondoker, R.; Larbig, P.; Scheuermann, D.; Weber, F.; Bayarou, K. Addressing Industry 4.0 Security by Software-Defined Networking. In *Guide to Security in SDN and NFV*; Zhu, S.Y., Scott-Hayward, S., Jacquin, L., Hill, R., Eds.; Springer International Publishing: Cham, Switzerland, 2017; pp. 229–251, ISBN 978-3-319-64652-7.
92. Ayvaz, S.; Alpay, K. Predictive maintenance system for production lines in manufacturing: A machine learning approach using IoT data in real-time. *Expert Syst. Appl.* **2021**, *173*, 114598. [CrossRef]
93. Wu, D.; Jennings, C.; Terpenny, J.; Gao, R.X.; Kumara, S. A Comparative Study on Machine Learning Algorithms for Smart Manufacturing: Tool Wear Prediction Using Random Forests. *J. Manuf. Sci. Eng.* **2017**, *139*, 237. [CrossRef]
94. Sharp, M.; Ak, R.; Hedberg, T. A Survey of the Advancing Use and Development of Machine Learning in Smart Manufacturing. *J. Manuf. Syst.* **2018**, *48 Pt C*, 170–179. [CrossRef]
95. Cavalcante, I.M.; Frazzon, E.M.; Forcellini, F.A.; Ivanov, D. A supervised machine learning approach to data-driven simulation of resilient supplier selection in digital manufacturing. *Int. J. Inf. Manag.* **2019**, *49*, 86–97. [CrossRef]
96. Monostori, L.; Markus, A.; van Brussel, H.; Westkämpfer, E. Machine Learning Approaches to Manufacturing. *CIRP Ann.* **1996**, *45*, 675–712. [CrossRef]
97. Cui, Y.; Kara, S.; Chan, K.C. Manufacturing big data ecosystem: A systematic literature review. *Robot. Comput.-Integr. Manuf.* **2020**, *62*, 101861. [CrossRef]
98. Dawson, M. Cyber Security in Industry 4.0: The Pitfalls of Having Hyperconnected Systems. *J. Strateg. Manag. Stud.* **2018**, *10*, 19–28.
99. Statistik Austria. Anteil der Kleinen und Mittleren Unternehmen (KMU) an Allen Unternehmen in Österreich von 2015 bis 2019. Available online: https://de.statista.com/statistik/daten/studie/1172003/umfrage/unternehmensanteil-von-kleinen-und-mittleren-unternehmen-kmu-in-oesterreich/ (accessed on 10 September 2021).
100. Statistik Austria. Anteil der Branche Bergbau und Herstellung von Waren an der Gesamten Bruttowertschöpfung in Österreich von 2010 bis 2020. Available online: https://de.statista.com/statistik/daten/studie/1177726/umfrage/wertschoepfungsanteil-des-verarbeitenden-gewerbes-in-oesterreich/ (accessed on 10 September 2021).
101. Brodeur, J.; Pellerin, R.; Deschamps, I. Collaborative approach to digital transformation (CADT) model for manufacturing SMEs. *JMTM* **2021**. ahead-of-print. [CrossRef]
102. Garzoni, A.; de Turi, I.; Secundo, G.; Del Vecchio, P. Fostering digital transformation of SMEs: A four levels approach. *Manag. Decis.* **2020**, *58*, 1543–1562. [CrossRef]
103. Philippi, C.; Bobek, V.; Horvat, T.; Maček, A.; Justinek, G. Internationalisation of an Austrian SME with a sales agent to Mexico and the USA in the automotive sector. *Int. J. Glob. Small Bus.* **2020**, *11*, 39–64. [CrossRef]
104. Wagner, J.; Burggräf, P.; Dannapfel, M.; Fölling, C. Assembly Disruptions—Empirical Evidence in the Manufacturing Industry of Germany, Austria and Switzerland. *Int. Refereed J. Eng. Sci. (IRJES)* **2017**, *6*, 15–25.
105. Loecher, U. Small and medium-sized enterprises—delimitation and the European definition in the area of industrial business. *Eur. Bus. Rev.* **2000**, *12*, 261–264. [CrossRef]
106. Ralph, B.J.; Pacher, C.; Woschank, M. Conceptualization of the Lecture 'Digitalization and Digital Transformation in Metal Forming' based on Implications from Contemporary Teaching and Learning Theories. In Proceedings of the 2nd African International Conference on Industrial Engineering and Operations Management, Harare, Zimbabwe, 7–10 December 2020; pp. 703–712.
107. Woschank, M.; Ralph, B.J.; Kaiblinger, A.; Miklautsch, P.; Pacher, C.; Sorger, M.; Zsifkovits, H.; Stockinger, M.; Pogatscher, S.; Antretter, T.; et al. MUL 4.0—Digitalisierung der Wertschöpfungskette vom Rohmaterial bis hin zum Recycling. *Berg. Huettenmaenn Mon.* **2021**, *166*, 309–313. [CrossRef]
108. Prinz, W.; Rose, T.; Osterland, T.; Putschli, C. Blockchain. In *Digitalisierung*; Neugebauer, R., Ed.; Springer: Berlin/Heidelberg, Germany, 2018; pp. 311–319, ISBN 978-3-662-55889-8.
109. Kaulartz, M.; Heckmann, J. Smart Contracts—Anwendungen der Blockchain-Technologie. *Comput. Und Recht* **2016**, *32*. [CrossRef]
110. Nofer, M.; Gomber, P.; Hinz, O.; Schiereck, D. Blockchain. *Bus. Inf. Syst. Eng.* **2017**, *59*, 183–187. [CrossRef]

A 2   Publication 2

M. Sorger: 'Quality 5.0 - A data-driven path towards zero waste', in: *XL. Colloquium on Metal Forming*, pp. 06-12, 03.2022, ISBN: 978-3-902078-27-8

Author contributions:

1. M. Sorger: Conceptualization, Literature Study, Methodology, Writing - Original Draft, Writing - Review & Editing

QUALITY 5.0 – A DATA-DRIVEN PATH TOWARDS ZERO WASTE

Marcel Sorger[1*]

[1]Chair of Metal Forming, Montanuniversität Leoben, Franz Josef Straße 18, 8700 Leoben

ABSTRACT: The fourth industrial revolution, commonly referred to as Industry 4.0, has made a permanent impact in the modern production industry. The establishment of technologies like Big Data, Cloud Computing and Smart Factories has driven the persistent trend for more accurate and precise data-driven predictions. Progressing into Industry 5.0 territory, further focus is put on enhanced Human Machine Interaction, giving arise to new opportunities in the field quality management, thus incorporating data from every human involved. Using these new technologies enables an omnipresent quality management including all aspects of the product and process environment from start to end of the lifecycle, characterizing the term Quality 5.0. The benefits include a continuous improvement of product and process, as well as supporting the premises of a sustainable, digitalized value chain by obtaining a greener footprint along the entire value stream, eventually leading to highest goal of zero waste. This paper describes the fundamentals of the term Quality 5.0, highlighting the respective enabler technologies, applications, challenges and opportunities.

1 INTRODUCTION

The ongoing digital revolution, also known as Industry 4.0 (I 4.0), brings a variety of new challenges and opportunities waiting to be mastered and put to use. In order to utilize the full potential of this digital transformation every enterprise along a value chain has to be implemented into such [1]. Depending on the individual enterprise, the machines, processes, conditions, products and therefore requirements scatter heavily. Nevertheless, the common point of interest is consistent and reliable data-driven quality management to ensure and further improve processes and products. Furthermore, with the application of Big Data technologies, the ecological impact can be decreased substantially, thus reducing waste not only at the enterprise level itself but also along the entire value stream. This also includes the incorporation of new digital technologies such as Machine Learning (ML). Going a step further, Industry 4.0 can be further developed by putting more focus on the Human Machine Interaction, giving arise to the term Industry 5.0 (I 5.0) [2]. Therefore, the user-centered approach of I 5.0 supports data-driven decision-making processes across all hierarchy layers, as defined by the RAMI 4.0, and therefore acts as a major contributor to a sustainable, zero-waste circular economy [3–7].

In order to give an overview about these topics and corresponding opportunities and challenges, this paper is structured as follows: Section 2 concludes the key enablers of Quality 5.0, as well as it's applications and evaluation of quality aspects. In section 3, the corresponding challenges arising are discussed. Based on the previous chapters, Section 4 summarizes the most important statements and concludes with an outlook and further implications regarding this topic.

2 FUNDAMENTALS

The key enablers of I 4.0, Smart Factories, Big Data, Cyber Physical Production Systems (CPPS), Industrial Internet of Things (IIoT), Digital Twins (DT) and Cloud Computing can be extended by the Human Machine Interaction (HMI), thus evolving into I 5.0 [1,2,8–13]. Smart Factories, defined as a compound of CPPS connected by the IIoT, on a production site scale, can be seen as one of many steps along the value chain [1]. The data provided by these smart factories is gathered by CPPS and their corresponding sensor and data acquisition (DAQ) technologies, also incorporating different modelling approaches, such as white, grey and black box modelling, in order to extract important information from given data [14–16]. Furthermore, ML can be incorporated to further extract information from the gathered process and product data [1,14,16]. The structured approach for implementing such technologies and infrastructure is the RAMI 4.0, visualizing and connecting the value chain via three axes. As shown in Figure 1, these axes show the Lift Cycle & Value Stream, the Hierarchy Levels and Layers [1,6,17,18]. Hereby, the respective instances created by the three axes conclude the utilized technologies, specifying all physical and digital assets along the entire value chain [1]. As proposed by [3,4,9,11,19–22] the term Quality 4.0 (Q 4.0) can be summarized as the blending of traditional quality management approaches with I 4.0 enablers, but with a shift from manual to fully automated approaches, using real-time data analysis, enabling the quality management data integration along the entire value chain. These I 5.0 enablers lay the groundwork for Quality Management 5.0 (Q 5.0), through backing automation and data gathering in a Big Data approach [2–4].
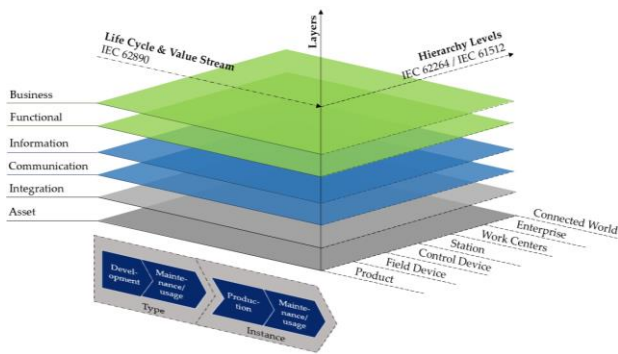
Figure 1: RAMI 4.0 [1,18]

As in the case with traditional statistical quality management approaches, where the quality of an inspected sample is projected on the entire production population, the I 5.0 supported Q 5.0 enables the quality evaluation of each individual product, by processing real-time sensor data of each individual product. By monitoring product and process simultaneously, the corresponding data can be linked to each other and information about the quality of both product and process and therefore, the compliance with the desired quality characteristics can be evaluated [3]. In the case of non-compliance, the gathered data can be analyzed in order to find the root causes of the underlying failure to meet the defined quality requirements [3,4,23,24]. Furthermore, the information gained from analyzing the causes of non-compliance can be reintegrated, thus improving the overall system [3,4]. Therefore, Q 5.0 is not only about monitoring and data processing, but also about finding interrelationships between process, product and previous as well as future processing steps in the value chain [3,4,9]. Additionally, this results not only in the quality improvement on the enterprise level itself, but also along the entire value chain [3,9,11,21]. This can be accomplished by implementing Total Quality Management (TQM), practicing quality management for every enterprise activity or moreover along the entire value chain and product life cycle, driving continuous quality improvements and further improving customer satisfaction as well as corporate sustainability [3,4,25–29]. The incorporation of customer satisfaction, as a part of quality management further undermines the user-centered premises of I 5.0 and Q 5.0, by incorporating not only the enterprise-set quality goals, but also those of the customer, e.g. by social media data [2,3,11].

2.1 ENABLER TECHNOLOGIES

As proposed by [3,28], the enabling technologies besides the beforementioned I 5.0 enablers are Big Data, connectivity, collaboration and data presentation. Per definition, Big Data has to fulfil the 5Vs of big data, namely Volume, Velocity, Variety, Veracity and Value, also incorporating ML in order to enable real-time data analysis and therefore pattern recognition, enabling quality predictions [1,3,4,6,11,30]. Therefore, the connectivity of all products and processes along the entire value chain has to be given to enable data reintegration, further improving quality [9]. Additionally, with the collaboration of all people involved within corresponding processes and resulting products, e.g. machine operators, programmers, costumers, and enhanced HMI, the data presentation is enabled, further advancing into I 5.0 territory [3,20,31].

2.2 APPLICATIONS

As proposed by [3,5,23] the main fields of the application of Q 5.0 are manufacturing, research and development (R&D), service and after-sales, procurement, logistics and sales, further adding data-based decision-making competence. Hereby, the application of Q 5.0 is heavily dependent on the field of application [23]. As in the field of manufacturing, approaches like predictive quality, machine vision quality control, automatic root cause analysis, self-adjustment of machines and process parameters and real-time process simulations contribute significantly to the improvement of decision-making processes on the shop floor level using enhanced HMI [2,23,30,32,33]. Focusing on R&D, the applications range from overall process and product quality improvement and prediction using Artificial Intelligence (AI) and especially ML to a more agile product development, thus leading to a leaner production, reducing time and costs [4,10,23,31,34–36]. Incorporating service and after-sales, field devices transmit data via the Internet of Things (IoT) and IIoT, enabling an improved predictive maintenance of soft- and hardware [23]. This also includes customers and consumers, thus supporting the premises of Big Data leading to steady improvements of predictive maintenance systems, service quality and costumer experience [3,11,23]. Applications in the field of procurement lay in providing data about the suppliers performance and furthermore evaluating quality risks in the supply chain [12,23]. As in logistics and sale, the predictive and agile production planning with a focus on reducing human errors plays a major role [23]. Additionally, the decision-making process is greatly supported by integrating real-time data across all layers, as visualized by RAMI 4.0 (Figure 1) [1,3], allowing for early intervention in case of non-compliance, thus leading to significant reduction of time, cost and waste [3,7,10].
In essence, a holistic, networked value chain with a complete interaction of all digitization measures across all instances is imperative, in order to develop the full potential of Q 5.0, thus avoiding sub optimizations.

2.3 EVALUATION OF QUALITY ASPECTS

In order to support the improvement and success of Q 5.0, a continuous performance evaluation is imperative. As proposed by [37,38] the Quality Scorecard (QSC) performance measurement serves as a suitable framework to evaluate the qualitative performance, allowing the reflection of strategic objects of the enterprise, converting objectives into communicable actions, thus supporting improvements and a successful implementation. Serving as an initial step, a process-requirement analysis has to be carried out [37]. Hereby, Cost of Quality (COQ) is introduced, classifying activities into COQ items of qualitative prevention, appraisal and failure

measures [37,39]. Here, appraisal costs arise from evaluating and measuring the conformity of services and products to quality standards [37]. Furthermore, prevention costs define costs arising from activities preventing non-compliance of quality [37]. Ultimately, failure costs are seen as the costs resulting from non-compliance of quality standards and therefore poor quality [37]. Expanding the COQ, the Cost of Quality Framework (COQF) further breaks the COQ items down, classifying as internal, external, visible and invisible costs as shown in Table 1 [37].

Table 1: Specification of COQF costs [37]

Costs	Internal	External	Total
Visible	(1) Scrap, repair, waste, prevention, appraisal	(3) Warranty	1+3
Invisible	(2) Internal inefficiencies, prevention, appraisal	(4) Bad management, loss of goodwill	2+4
Total	1+2	3+4	1+2+3+4

Based on this framework, the qualitative measures are defined using the Quality Function Deployment (QFD) approach, representing the viewpoints of Supplier, Input, Process, Output and Customer (SIPOC) [37]. As a result, the QSC defines environment dependent simple (S-QSC), general (G-QSC) and detailed (D-QSC) performance measures for prevention, appraisal and final result measures [37]. Here, the prevention measures list the supplier quality assurance, product/service development, operation quality assurance, risk assurance and customer/market demand analysis on the S-QSC level, further specifying them on the G-QSC and D-QSC level [37]. The appraisal measures contain the supplier and product evaluation, operational system evaluation, product and field evaluation and customer/market analysis on the S-QSC level [37]. The D-QSC level of the final result measure lists leadership, human recourses, operations, products/services, customer services, financial and market results [37]. Per definition of the QSC, this leads to 15 S-QSC units, 30 G-QSC units and 60 D-QSC units [37]. As exemplary shown in Table 2, the S-QSC serves as the basis for the G-QSC, further serving as the basis for D-SQC, leading to a specification of the previous measure.

Table 2: Schematic QSC for prevention measures [37]

	S-QSC	G-QSC	D-QSC
Prevention Measures	Supplier Quality Assurance	Supplier's Quality Plan	Purchase Oder Review Supplier's Quality Plan
		Supplier Evaluation	Supplier Evaluation

Furthermore, the G-QSC can be interlinked to the enterprises' 19 Key Performance Indicators (KPIs), categorized into Profitability, Activity, Growth, Stability and Productivity [37].

As shown in Figure 2, the visualization of the QSC is done by the means of a QSC wheel, containing the previously mentioned S-QSC, G-QSC and D-QSC units [37]. Hereby, every unit represented in the QSC wheel is categorized into units of strong, medium, weak or no relevance, thus posing as the enterprises' performance indicators [37].
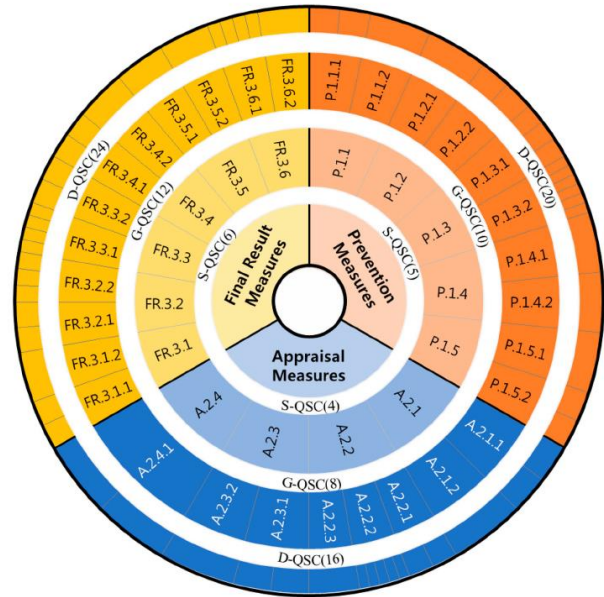

Figure 2: QSC wheel with respective S-QSC, g-QSC and D-QSC units [37]

As concluded by [37], the QSC is a capable tool to identify the enterprises' performance, but should undergo further customization depending on the respective industry and the paradigm change regarding I 4.0 and I 5.0.

Expanding on the QSC taking Big Data into account, the data quality poses as a KPI itself, thus leading to the term Data Quality Scorecard (DQSC) [40]. Hereby, the data is continuously checked for the compliance with enterprise specific rules, making a statement about how well the data supports analytical and operative processes and data-driven projects [40].

3 CHALLENGES

According to [3,4,11,32,41–43] the main challenges are technology, organization, management and human resources. Furthermore, Q 5.0 not only contributes to a greener and more sustainable production, but also improving the overall organizational performance reducing inspection costs once successfully implemented [3,7,24,27]. As concluded by [7], current quality management practices correlate negatively with the increasing importance of green and sustainable production, thus limiting enterprises in their

competitiveness. As addressed previously, the data-driven premises of Q 5.0 include sophisticated data analysis and therefore requires high potential personnel, capable of dealing with these new technologies in order to utilize the potentials of a digitalized quality management [2–4,11,19,44,45]. In order to be able to implement resilient Q 5.0 technologies, the management has to be aware of new technologies as well as traditional quality management techniques, building upon them and further refining them with IT [3,22,36,41]. Therefore, the management, quality and IT teams must be able to communicate the individual needs and goals, thus supporting a successful organizational and digital transformation [3,19,45]. Thus, these challenges make a technological aware management imperative, leading the implementation of necessary I 5.0 infrastructure [3,41]. Furthermore, this infrastructure implies vulnerability against cyberattacks, thus making cyber security one major point of concern [1,3,46]. Especially the IIoT should be built upon state of the art protocols and layer architectures, thus reducing the risk of successful cyberattacks [1,46]. Following the successful implementation, the enterprise as well as the entire value chain benefit from higher productivity, efficiency, competitiveness as well increasing customer satisfaction and reduction of waste, following the premises of lean production [1,3,4,7,27,34,36,41,47]. Ultimately, the implementation of Q 5.0 is highly individual with respect to the corresponding process, product, environment as well as available infrastructure and resources [33].

4   CONCLUSION AND OUTLOOK

This paper explored the different enabler technologies, applications and challenges of Q 5.0. Furthermore, the different aspects and goals were highlighted.

Based on this, the initial challenge in order to implement a holistic and resilient Q 5.0 system is a well working I 5.0 infrastructure. Therefore, the human, intellectual and technological as well as financial resources have to be considered. Depending on the enterprise, either classifying them as small and medium enterprises (SME) or big enterprises, have to overcome different obstacles in the aforementioned aspects depending on their digital maturity. Especially SMEs face obstacles in these terms, thus making special support imperative to enable a successful digital transformation of SME businesses and furthermore value chains. In order to ensure the implementation of every enterprise along a value chain, digitalization standards have to be established, enabling a standardized communication. Therefore, frameworks such as RAMI 4.0 represent suitable options, ensuring standardized communication in digitalization as well as in data and data integration along the entire value chain. Hereby, the RAMI 4.0 framework should undergo further specification regarding protocols, data and technologies, facilitating the digital transformation for SMEs. Regarding the enabler technology Big Data, further focus has to be put on the accessibility of Cloud Computing resources. Here, SME face major obstacles in all of the aforementioned terms, as these enterprises often do not

have the necessary infrastructure, human and/or financial resources. Therefore, emphasis has to be put on the future availability and possibility of outsourcing of computing resources. Furthermore, to perform valuable data analysis using cloud computing resources, the data has to follow the 5Vs of Big Data, especially regarding Veracity and Value. Thus, the data has to be trustworthy in order to create information of value, making sanity or cross checks of sensors and data.

To support the success and continuous improvement of Q 5.0, the already implemented quality management methods must undergo automation and digitalization, further refining them with ML. Hereby, ML like Support Vector Machines (SVM) can be used to analyze time series data and other processes variables, deciding about the quality compliance of the product. Thus, gathering more data about processes and products complying with the desired quality, the ML can be refined with the growing amount of available training data, further supporting the premises of Q 5.0 in terms of optimization and reduction of waste and costs along the entire value chain. Besides, the data gathering should undergo analysis in the context of usefulness, as the storage and processing of a huge amount of data using cloud computing services, requires corresponding recourses, therefore standing in conflict with a more sustainability production.

Another important point of view is that of security. Hereby, a differentiation has to be made between the security of intellectual property and cyber security. As proposed previously, cyber security is a point of major concern, as cyberattacks can lead to long lasting downtime or malfunctions, thus leading to delays in the supply chain and loss of profits. Moreover, data manipulation could lead to similar events, e.g., ML relying on faulty, manipulated data. Therefore, referring to aforementioned techniques like cross and sanity checks. Henceforth, the development of the blockchain and quantum computer technologies may serve as a major contributor to cyber security and computing resources, therefore driving I 5.0 and Q 5.0 advancements. On the other hand, the security of intellectual property has to be further refined. As in the case of data theft, regarding multinational enterprises and decentralized cloud computing resources, the jurisdiction of respective nations should undergo a standardization, supporting international collaborations and exchange.

Coming back to the financial hurdles SME might face, the digitalization of quality management processes should also follow a low-cost approach, using open-source software and brownfield approaches, equipping existing machines with suitable digitalization technologies. As a result, the implemented software and hardware has to fulfil the point of connectivity, allowing the data integration into Manufacturing Execution Systems (MES), Enterprise Resource Planning (ERP) systems and databases of the respective enterprises and along the entire value chain.

Moreover, the already existent shortage of skilled employees could pose as an increasing obstacle intensifying in future years. In general, employees

capable of handling the versatile and demanding tasks linked to I 5.0 and Q 5.0 will be harder to find. Therefore, further focus has to be set on the engineering education in the field of digitalization, as proposed by [48–50]. Henceforth, the HMI support on all hierarchy levels assists decision-making, thus facilitating certain tasks and improving the overall product and process quality, as well as the working environment itself. Focusing on the customers, Q 5.0 benefits from the increasing involvement between product and customer, thus collecting customer impressions, data, experiences and feedback in order to incorporate them into the design process of the product, leading to further improvements. Hereby, social media and new digital media like the Metaverse can be seen as major contributors in deepening customer relationships, gathering product specific data and customer experiences.

Eventually, all of the aforementioned statements support the ultimate goal of an efficient and sustainable production, driving towards the ultimate goal of zero waste. Previously, [7] concluded the negative impact of current quality management practices on green innovations, therefore putting additional expectations on Q 5.0. Thus, the incorporation of I 5.0 technologies in Q 5.0, the gathering of data from customer, product and processes, followed by data analysis and an overarching data sharing and integration along the value chain, this premise of a green and sustainable production is supported. Therefore, the more data is gathered and analyzed, the more correlations between various product and processes variables are found, improving both products and processes, leading to a reduction of costs and waste. Done steadily and thoughtful over a long period of time, steadily decreasing waste can be achieved.

5 REFERENCES

1. Sorger, M.; Ralph, B.J.; Hartl, K.; Woschank, M.; Stockinger, M. Big Data in the Metal Processing Value Chain: A Systematic Digitalization Approach under Special Consideration of Standardization and SMEs. *Applied Sciences* **2021**, *11*, 9021, doi:10.3390/app11199021.
2. Nahavandi, S. Industry 5.0—A Human-Centric Solution. *Sustainability* **2019**, *11*, 4371, doi:10.3390/su11164371.
3. Sader, S.; Husti, I.; Daroczi, M. A review of quality 4.0: definitions, features, technologies, applications, and challenges. *Total Quality Management & Business Excellence* **2021**, 1–19, doi:10.1080/14783363.2021.1944082.
4. Sariyer, G.; Mangla, S.K.; Kazancoglu, Y.; Ocal Tasar, C.; Luthra, S. Data analytics for quality management in Industry 4.0 from a MSME perspective. *Ann Oper Res* **2021**, doi:10.1007/s10479-021-04215-9.
5. Goecks, L.S.; Santos, A.A.d.; Korzenowski, A.L. Decision-making trends in quality management: a literature review about Industry 4.0. *Prod.* **2020**, *30*, doi:10.1590/0103-6513.20190086.
6. López Martínez, P.; Dintén, R.; Drake, J.M.; Zorrilla, M. A big data-centric architecture metamodel for Industry 4.0. *Future Generation Computer Systems* **2021**, *125*, 263–284, doi:10.1016/j.future.2021.06.020.
7. Li, D.; Zhao, Y.; Zhang, L.; Chen, X.; Cao, C. Impact of quality management on green innovation. *Journal of Cleaner Production* **2018**, *170*, 462–470, doi:10.1016/j.jclepro.2017.09.158.
8. Ralph, B.J.; Stockinger, M. *Digitalization and Digital Transformation in Metal Forming: Key Technologies, Challenges and Current Developments of Industry 4.0 Applications*, 2020.
9. Müller, J.M. Contributions of Industry 4.0 to quality management - A SCOR perspective. *IFAC-PapersOnLine* **2019**, *52*, 1236–1241, doi:10.1016/j.ifacol.2019.11.367.
10. Yadav, N.; Shankar, R.; Singh, S.P. Critical success factors for lean six sigma in quality 4.0. *IJQSS* **2021**, *13*, 123–156, doi:10.1108/IJQSS-06-2020-0099.
11. Sony, M.; Antony, J.; Douglas, J.A. Essential ingredients for the implementation of Quality 4.0. *TQM* **2020**, *32*, 779–793, doi:10.1108/TQM-12-2019-0275.
12. Ammar, M.; Haleem, A.; Javaid, M.; Walia, R.; Bahl, S. Improving material quality management and manufacturing organizations system through Industry 4.0 technologies. *Materials Today: Proceedings* **2021**, *45*, 5089–5096, doi:10.1016/j.matpr.2021.01.585.
13. Sader, S.; Husti, I.; Daróczi, M. Industry 4.0 as a Key Enabler toward Successful Implementation of Total Quality Management Practices. *Period. Polytech. Soc. Man. Sci.* **2019**, *27*, 131–140, doi:10.3311/PPso.12675.
14. Ralph, B.J.; Sorger, M.; Hartl, K.; Schwarz-Gsaxner, A.; Messner, F.; Stockinger, M. Transformation of a rolling mill aggregate to a cyber physical production system: from sensor retrofitting to machine learning. *J Intell Manuf* **2022**, *33*, 493–518, doi:10.1007/s10845-021-01856-2.
15. Ralph, B.J.; Sorger, M.; Schödinger, B.; Schmölzer, H.-J.; Hartl, K.; Stockinger, M. Implementation of a Six-Layer Smart Factory Architecture with Special Focus on Transdisciplinary Engineering Education. *Sensors (Basel)* **2021**, *21*, doi:10.3390/s21092944.
16. Ralph, B.J.; Hartl, K.; Sorger, M.; Schwarz-Gsaxner, A.; Stockinger, M. Machine Learning Driven Prediction of Residual Stresses for the Shot Peening Process Using a Finite Element Based Grey-Box Model Approach. *JMMP* **2021**, *5*, 39, doi:10.3390/jmmp5020039.
17. Albers, A.; Gladysz, B.; Pinner, T.; Butenko, V.; Stürmlinger, T. Procedure for Defining the System of Objectives in the Initial Phase of an Industry 4.0 Project Focusing on Intelligent Quality Control

Systems. *Procedia CIRP* **2016**, *52*, 262–267, doi:10.1016/j.procir.2016.07.067.

18. Pisching, M.A.; Pessoa, M.A.; Junqueira, F.; dos Santos Filho, D.J.; Miyagi, P.E. An architecture based on RAMI 4.0 to discover equipment to process operations required by products. *Computers & Industrial Engineering* **2018**, *125*, 574–591, doi:10.1016/j.cie.2017.12.029.

19. Santos, G.; Sá, J.C.; Félix, M.J.; Barreto, L.; Carvalho, F.; Doiro, M.; Zgodavová, K.; Stefanović, M. New Needed Quality Management Skills for Quality Managers 4.0. *Sustainability* **2021**, *13*, 6149, doi:10.3390/su13116149.

20. Carvalho, A.V.; Enrique, D.V.; Chouchene, A.; Charrua-Santos, F. Quality 4.0: An Overview. *Procedia Computer Science* **2021**, *181*, 341–346, doi:10.1016/j.procs.2021.01.176.

21. Ramezani, J.; Jassbi, J. Quality 4.0 in Action: Smart Hybrid Fault Diagnosis System in Plaster Production. *Processes* **2020**, *8*, 634, doi:10.3390/pr8060634.

22. Nenadál, J. The New EFQM Model: What is Really New and Could Be Considered as a Suitable Tool with Respect to Quality 4.0 Concept? *QIP Journal* **2020**, *24*, 17, doi:10.12776/qip.v24i1.1415.

23. Küpper, D.; Knizek, C.; Ryeson, D.; Noecker, J. *Quality 4.0 Takes More Than Technology*, 2019. Available online: https://www.bcg.com/publications/2019/quality-4.0-takes-more-than-technology.

24. Javaid, M.; Haleem, A.; Pratap Singh, R.; Suman, R. Significance of Quality 4.0 towards comprehensive enhancement in manufacturing sector. *Sensors International* **2021**, *2*, 100109, doi:10.1016/j.sintl.2021.100109.

25. Abbas, J. Impact of total quality management on corporate sustainability through the mediating effect of knowledge management. *Journal of Cleaner Production* **2020**, *244*, 118806, doi:10.1016/j.jclepro.2019.118806.

26. Illés, B.; Tamás, P.; Dobos, P.; Skapinyecz, R. New Challenges for Quality Assurance of Manufacturing Processes in Industry 4.0. *SSP* **2017**, *261*, 481–486, doi:10.4028/www.scientific.net/SSP.261.481.

27. Fonseca, L.; Amaral, A.; Oliveira, J. Quality 4.0: The EFQM 2020 Model and Industry 4.0 Relationships and Implications. *Sustainability* **2021**, *13*, 3107, doi:10.3390/su13063107.

28. Sader, S.; Husti, I.; Daroczi, M. Quality Management Practices in the Era of Industry 4.0. *ZNPCZ* **2019**, *35*, 117–126, doi:10.17512/znpcz.2019.3.10.

29. Pambreni, Y.; Khatibi, A.; Azam, S.M.F.; Tham, J. The influence of total quality management toward organization performance. *10.5267/j.msl* **2019**, 1397–1406, doi:10.5267/j.msl.2019.5.011.

30. Rahmatov, N.; Paul, A.; Saeed, F.; Hong, W.-H.; Seo, H.; Kim, J. Machine learning–based automated image processing for quality management in industrial Internet of Things. *International Journal of Distributed Sensor Networks* **2019**, *15*, 155014771988355, doi:10.1177/1550147719883551.

31. Chiarini, A. Industry 4.0, quality management and TQM world. A systematic literature review and a proposed agenda for further research. *TQM* **2020**, *32*, 603–616, doi:10.1108/TQM-04-2020-0082.

32. Villalba-Diez, J.; Schmidt, D.; Gevers, R.; Ordieres-Meré, J.; Buchwitz, M.; Wellbrock, W. Deep Learning for Industrial Computer Vision Quality Control in the Printing Industry 4.0. *Sensors (Basel)* **2019**, *19*, doi:10.3390/s19183987.

33. Závadská, Z.; Závadský, J. Quality managers and their future technological expectations related to Industry 4.0. *Total Quality Management & Business Excellence* **2020**, *31*, 717–741, doi:10.1080/14783363.2018.1444474.

34. Yadav, N.; Shankar, R.; Singh, S.P. Hierarchy of Critical Success Factors (CSF) for Lean Six Sigma (LSS) in Quality 4.0. *JGBC* **2021**, *16*, 1–14, doi:10.1007/s42943-020-00018-0.

35. Gunasekaran, A.; Subramanian, N.; Ngai, W.T.E. Quality management in the 21st century enterprises: Research pathway towards Industry 4.0. *International Journal of Production Economics* **2019**, *207*, 125–129, doi:10.1016/j.ijpe.2018.09.005.

36. Mrugalska, B.; Wyrwicka, M.K. Towards Lean Production in Industry 4.0. *Procedia Engineering* **2017**, *182*, 466–473, doi:10.1016/j.proeng.2017.03.135.

37. Shin, W.S.; Dahlgaard, J.J.; Dahlgaard-Park, S.M.; Kim, M.G. A Quality Scorecard for the era of Industry 4.0. *Total Quality Management & Business Excellence* **2018**, *29*, 959–976, doi:10.1080/14783363.2018.1486536.

38. Quesado, P.; Aibar Guzmán, B.; Lima Rodrigues, L. Advantages and contributions in the balanced scorecard implementation. *IC* **2018**, *14*, 186, doi:10.3926/ic.1110.

39. Pipiay, G.T.; Chernenkaya, L.V.; Mager, V.E. Quality Indicators of Instrumentation Products According to the «Quality 4.0» Concept. In *2021 IEEE Conference of Russian Young Researchers in Electrical and Electronic Engineering (ElConRus)*. 2021 IEEE Conference of Russian Young Researchers in Electrical and Electronic Engineering (ElConRus), St. Petersburg, Moscow, Russia, 26–29 Jan. 2021; IEEE, 1262021; pp 1032–1036, ISBN 978-1-6654-0476-1.

40. Uniserv. Data Quality Scorecard. Available online: https:www.uniserv.com/services/data-quality-scorecard/ (accessed on 4 February 2022).

41. Fundin, A.; Bergquist, B.; Eriksson, H.; Gremyr, I. Challenges and propositions for research in quality management. *International Journal of Production Economics* **2018**, *199*, 125–137, doi:10.1016/j.ijpe.2018.02.020.

42. Bouranta, N.; Psomas, E.; Suárez-Barraza, M.F.; Jaca, C. The key factors of total quality management in the service sector: a cross-cultural study. *BIJ* **2019**, *26*, 893–921, doi:10.1108/BIJ-09-2017-0240.

43. Kamble, S.S.; Gunasekaran, A. Big data-driven supply chain performance measurement system: a review and framework for implementation. *International Journal of Production Research* **2020**, *58*, 65–86, doi:10.1080/00207543.2019.1630770.

44. *What is Quality 4.0 in the era of Industry 4.0?;* 3rd International Conference on quality of life, Ed. In Proceedings of the 3rd International Conference on Quality of Life, Kopaonik, Serbia, 28–30 November 2018, 2018.

45. Escobar, C.A.; McGovern, M.E.; Morales-Menendez, R. Quality 4.0: a review of big data challenges in manufacturing. *J Intell Manuf* **2021**, *32*, 2319–2334, doi:10.1007/s10845-021-01765-4.

46. Jaloudi, S. Communication Protocols of an Industrial Internet of Things Environment: A Comparative Study. *Future Internet* **2019**, *11*, 66, doi:10.3390/fi11030066.

47. van Kemenade, E.; Hardjono, T.W. Twenty-first century Total Quality Management: the Emergence Paradigm. *TQM* **2019**, *31*, 150–166, doi:10.1108/TQM-04-2018-0045.

48. Ralph, B.J.; Schwarz, A.; Stockinger, M. An Implementation Approach for an Academic Learning Factory for the Metal Forming Industry with Special Focus on Digital Twins and Finite Element Analysis. *Procedia Manufacturing* **2020**, *45*, 253–258, doi:10.1016/j.promfg.2020.04.103.

49. Ralph, B.J.; Pacher, C.; & Woschank, M. Conceptualization of the Lecture 'Digitalization and Digital Transformation in Metal Forming'based on Implications from Contemporary Teaching and Learning Theories. *Proceedings of the 2nd African International Conference on Industrial Engineering and Operations Management, Harare, Zimbabwe* **2020**, 7–10.

50. Ralph, B.J.; Woschank, M.; Pacher, C.; Murphy, M. Evidence-based redesign of engineering education lectures: theoretical framework and preliminary empirical evidence. *European Journal of Engineering Education* **2022**, *81*, 1–28, doi:10.1080/03043797.2021.2025341.

A 3   Publication 3

Author contributions:

1. B.J. Ralph: Conceptualization, Methodology, Writing - Original Draft, Writing - Review & Editing
2. M. Woschank: Conceptualization, Methodology, Writing - Original Draft, Writing - Review & Editing
3. P. Miklautsch: Writing - Original Draft, Writing - Review & Editing
4. Kaiblinger: Writing - Original Draft, Writing - Review & Editing
5. Pacher: Writing - Original Draft, Writing - Review & Editing
6. M. Sorger: Writing - Original Draft, Writing - Review & Editing
7. H. Zsifkovits: Supervision
8. M. Stockinger: Supervision

30th International Conference on Flexible Automation and Intelligent Manufacturing (FAIM2021)
15-18 June 2021, Athens, Greece.

MUL 4.0: Systematic Digitalization of a Value Chain from Raw Material to Recycling

Benjamin James Ralph[a], Manuel Woschank[b]*, Philipp Miklautsch[b], Alexander Kaiblinger[b], Corina Pacher[c], Marcel Sorger[a], Helmut Zsifkovits[b], Martin Stockinger[a]

[a]Chair of Metal Forming, Montanuniversitaet Leoben, Austria
[b]Chair of Industrial Logistics, Montanuniversitaet Leoben, Austria
[c]Life Long Learning, Graz University of Technology, Austria

* Corresponding author. Tel.: +433842 402-6023. *E-mail address:* manuel.woschank@unileoben.ac.at

Abstract

The digital revolution, also known as Industry 4.0, offers a variety of new technologies and technological concepts for the continuous optimization of production and logistics processes in manufacturing enterprises. Up to now, a multitude of scholars have investigated potential opportunities, barriers, threads, and necessary enablers of Industry 4.0 initiatives. However, most of the recent Industry 4.0 approaches can still not resist practical tests due to their limited view on a small range of relevant topics. This paper introduces the research project 'MUL4.0' which aims to digitalize an entire value chain, from raw material to recycling. Based on an action-research-orientated approach, the authors use a multi-case-study design to investigate the potential of digitalization approaches within production and logistics processes. Furthermore, the authors present future research activities and discuss the therefore necessary prerequisites, from a materials science, mechanical engineering, metallurgical, logistics engineering, and management perspective.

1. Introduction

Industry 4.0, as the ongoing revolution of the manufacturing industry around the world, focuses on the integration of emerging information and communication technologies in traditional production and logistics processes [1]. Thereby, according to recent literature, current studies on digitalization in production and logistics can be divided into the clusters of 1) technologies and technologies concepts, 2) enablers of digitalization, 3) risks of digitalization, and 4) opportunities of digitalization. Thereby, cluster 1 listed data science, virtual environments, IoT devices, automatic identification, CPS, location (technologies), interfaces, and decentralized applications as the main technologies and technological concepts within the framework of Industry 4.0 [2].

However, from a methodological point of view, it must be noted that most studies can be assigned to the research type of conceptual studies, preliminary laboratory experiments, or single case studies leading to a limited external validity of the established research findings. Therefore, the authors conclude that, despite some fruitful insights, most studies provide only a limited view on the 'realistic' system behavior in economic practice.

To increase the generalizability and transferability of research results to manufacturing enterprises, the authors introduce the research project 'MUL 4.0' which aims to investigate an entire value chain, from raw material to recycling, based on a combination of quantitative and qualitative research methods. Moreover, this paper discusses the necessary prerequisites from a material science, mechanical engineering, metallurgical, logistics engineering and

management point of view and concludes with a summary of potential future research initiatives.

2. Research methodology and concept overview: MUL 4.0

Based on the implications of relevant strategy papers from the European Commission, which are generally aiming at increasing the competitiveness of companies as micro-economic entities through the implementation of Industry 4.0 technologies, Austria's first digital learning factory is to be established in a cooperative project of four institutes or chairs of the Montanuniversitaet Leoben within the framework of a multitude of research projects. This learning factory represents an isomorphic representation of a fully digitalized value chain and should also be able to dynamically optimize processes based on the latest Industry 4.0 technologies. For the first time, in contrast to the mostly isolated basic concepts of Industry 4.0, holistic and sustainable measures of a digital learning factory derived from the fields of action 1) digitization and artificial intelligence, 2) resource-efficient production-oriented to concepts of the circular economy, and 3) human-machine interaction will be designed, implemented, and scientifically investigated. Therefore, Fig. 1 shows an overview of the production process and involved parties within this project.
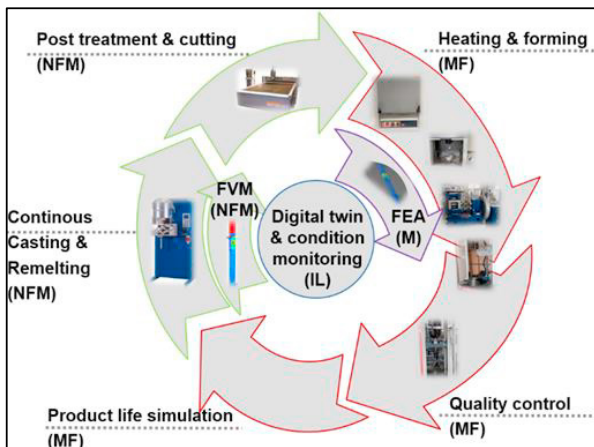
Fig. 1. Overview and responsibilities of respective process steps in the MUL 4.0 concept [3].

The starting point of the digital learning factory is the continuous casting plant at the Chair of Nonferrous Metallurgy (NFM). At the NFM, a previously specified aluminum alloy is casted with varying process parameters and geometries and prepared for subsequent process steps (Fig. 1, green). From the beginning of the casting process, continuous identification and automated data acquisition (DAQ) is performed by the higher-level tracking system, which processes the product, process, and logistics data (e.g., location, throughput time, etc.) and passes on information to the subsequent process steps. The processed workpiece is then transported from the NFM to the Chair of Metal Forming (MF), where it is first preheated and then formed into its final shape in two or more subsequent forming processes, with the possibility of reheating between each step. The transport itself from the NFM to the MF will be captured in real-time by the implemented tracking software.

The most important process steps in terms of mechanical engineering, metallurgy, and materials science are mapped in real-time using finite element analysis (FEA) and finite volume analysis (FVA). Based on this FEA and FVA, real-time adaptations for active intervention in involved processes should then be possible. The Institute of Mechanics (M) (Fig. 1, violet) is mainly responsible for the development of the FEA-based digital twins based on real physical data together with the MF. Here, attention is also paid to the influence of thermo-kinetics, which leads to highly informative and accurate results about the current condition of the respective workpiece. The results of these simulations are validated and calibrated with the aid of appropriate quality management carried out at the NFM and MF. The adapted process data is fully automated and continuously transmitted to a Supervisory Control and Data Acquisition (SCADA) system already implemented at the MF, pre-processed, and then transferred to the higher-level tracking system. A similar suitable SCADA system is currently in development at the NFM. After quality management has been carried out (on a statistical basis and as far as possible on a practical basis), the finished components can be put to further use. During almost all process steps, there is material waste, which is also fully tracked from the point of origin and systematically returned to the NFM. This closes the cycle of the (digitalized) value chain.

Besides the tracking system, additional simulations are carried out in logistics processes to be able to continuously optimize inventories, throughput times, adherence to schedules, and machine utilization. As a result, an ideal maintenance strategy can be systematically derived based on the system's behavior. The discrete event simulation used for this purpose can also be displayed three-dimensionally and, in combination with modern augmented reality technologies, is, thus, an important component of advanced teaching. The Chair of Industrial Logistics (IL) is mainly responsible for this image of the digital learning factory as well as the implementation, maintenance, and optimization of the tracking and condition monitoring system (Fig. 1, blue). The mainly used open-source and low-cost hardware and software also offers the possibility to educate a broad variety of engineering students of different disciplines as well as external parties under the premise of the transdisciplinary engineering education concept, which is displayed in Fig. 2 [4,5,6].
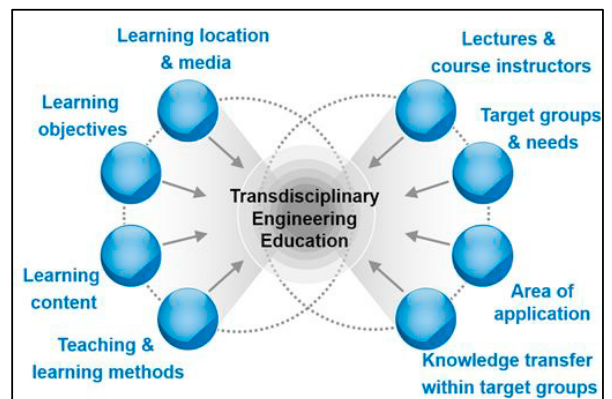

Fig. 2. Transdisciplinary Engineering Education concept [4,5,6].

Fig. 2 illustrates the variety of complex influencing factors that affect transdisciplinary learning processes. Different causal mechanisms intervene in teaching and learning processes, and, therefore, must be considered when planning, implementing, and evaluating it. On the one hand, endogenous factors, such as previous experience, expectations, or motivation of teachers and participants, affect the micro-level, as the respective learning unit. On the other hand, exogenous factors, such as legal foundations, living conditions, or higher-level goals at the meso- and macro-levels, further have a significant impact on the learning process. This transdisciplinary engineering concept will also be an integral part of a transdisciplinary engineering lecture, which mainly focuses on digitalization and its underlying technologies [4,5,6].

3. A holistic concept of the process value chain

In a prior analysis, several gaps in current research about digitization and digitalization in industrial logistics were found [1]:

- Many approaches to use new technologies or technological concepts in logistics processes do not go beyond a conceptual stage or theoretical validation and, thus, open up the demand for implementation and validation of the concepts in practice.
- A common method for examining the complex behavior of logistical processes is the usage of discrete event simulation. However, the literature review shows a lack of attention to the use of digital twins in the field of industrial logistics. The combination of real-time production data and a discrete event simulation can fill this gap. Nevertheless, the potential benefits of such systems, as well as development challenges, need to be addressed.
- The authors state that, even though current literature agrees on the positive impact of digitization on sustainability performance, research does not focus on the achievement of general objectives such as the Sustainable Development Goals (SDGs). In addition to this, small- and medium-sized enterprises (SMEs) face several barriers when implementing sustainability reporting (SR) in general [7]. Due to a lower market value, SMEs seem to have a lower SR quality. This circumstance is a result of an existing positive correlation between a company´s market value and the quality of SR [8].
- In physical as well as in digital processes, (IT-) security issues are a widely discussed topic [9]. Increased data sharing involves risks of cyber-attacks and the interest of certain parties to manipulate data.

The MUL 4.0 lab offers several opportunities to implement and assess newly developed models, frameworks, or technologies, which have only been theoretically approved in the examined literature. According to the authors, the main contribution to research is the development and implementation of a holistic near-real-time digital twin that extends material science and engineering-based simulations with simulation and visualization of the logistical processes.

Potentially, the above-mentioned research gaps can be closed due to practical implementation of the technologies in the laboratory to

- use real-time data to simulate logistics processes and forecast their output,
- use real-time data to evaluate different scenarios, based on the current status in the production, which enables the realization of decision support systems for logistical purposes,
- use real-time data to assess the environmental impacts of the process as well as the products and
- visualize real-time quality, sustainability, and process metrics in a production data cockpit.

Due to the laboratory character of the manufacturing system, the comparability and implementation of the gathered results into industrial environments with large-scale production and highly automated systems would lack of accuracy. Instead, the authors expect a similarity to environments of manufacturing SMEs, whose production resembles semi-automated workshop production. The implementation of the near-real-time digital twin described above offers new possibilities to evaluate production plans and schedules on the fly, more precise forecasting, and faster exception handling during the manufacturing process, resulting in a more realistic factory planning. Furthermore, both a dynamic allocation of transport tasks and a dynamic routing through the production can be achieved. Due to the virtual environment of the production, reinforcement learning algorithms can be used.

An environment to assess and visualize sustainability and quality indicators of the production on the product-level in near real-time in workshop manufacturing could enable higher SR quality and shorter reaction times in case of an exceptional waste of energy or material. Furthermore, agent-based production planning and scheduling could be implemented, which focuses on the reduction of lead times of products with lower environmental impacts. Overall, material and energy efficiency could be increased due to new, realistic, and live insights in the production process and the creation of incentives to buy environmentally better products could be more feasible to potential customers due to reduced process-related costs. Also, secure mechanisms to save and share recorded data across the supply chain could support efficient compliance with a potential supply chain act.

To enable the proposed logistics digital twin, the assessment and the implementation of several technologies are necessary:

- To create a valid 3D-simulation for simulating the material flow, a 3D-model of the laboratory setting must be generated. This could be achieved by new 3D-scanning methods such as LIDAR-sensors or smart cameras (e.g., Azure Kinect).
- Indoor Positioning Systems (IPS) have to be installed in the laboratory, including a continuous identification of the material flows by Auto-ID technologies. This should ensure the complete traceability of the material

flow and the localization of the means of transportation.

- A suitable integration of logistics applications into the proposed layer structure of the FEA and FVA must be defined. The establishment of interfaces is necessary for fast and reliable information exchange between the applications.
- The creation of a resilient software architecture for the integration of real-time data or a real-time initialization of discrete event simulations is crucial.
- The scope of the sustainability assessment has to be defined. According to this scope, valid input data, emissions factors, etc., must be available.
- Metrics that represent the environmental impact of the produced goods and IIoT-sensors to measure these metrics are to be found and implemented, e.g., GHG emissions during production, which arise because of energy usage. To capture this, electricity and gas meters have to be installed and integrated into the infrastructure.
- Security of information sharing has to be guaranteed to create unalterable data that are available to all necessary parties in near real-time.
- Recording production times for different products and their distributions, to create different production plans and for further investigations has to be carried out.

4. SCADA and numerical simulation integration

The following subchapters describe the data gathering at the most important aggregates within the digitalized supply chain. The focus lies on the interaction between the physical machining processes and resulting sensor data with near real-time integration of corresponding numerical simulations. Therefore, the main objective is the prediction of material behavior with upcoming process steps, which allows the superordinate logistics digital twin system to optimize the logistic chain in terms of lead time and general production planning. To achieve this efficiently and effectively, a variety of numerical simulations were designed. Based on the results of these simulations, process steps will be automatically adapted. Despite the positive effect on logistics, desired material quality can be optimized, and out coming parts that don't fulfill the quality requirements can be reduced [10].

4.1. Thermo-mechanical process route

The numerical process chain starts at the continuous casting unit, which produces slabs with defined geometry made from raw material, followed by a cutting operation on another aggregate. The resulting workpieces are heated to a defined temperature and pre-formed in a hydraulic press or alternatively rolling mill aggregate, which results in either bulk or sheet metal-based products. Depending on the desired final shape and mechanical material properties, additional reheating steps can be performed and additional forming steps within the same aggregates can be taken. After quality control and simulated usage, the specimen is transported to the NFM, refined, and finally re-melted (Fig. 1). All machines are equipped with sensors matched to the measured parameters to be able to record

the most important machine and process parameters qualitatively and quantitatively.

4.2. Aggregates with coupled numerical simulations

The Indutherm CC3000 continuous casting plant at the NFM is equipped ex works with a variety of different sensors (Fig. 3). These sensors record the crucible temperature, die temperature, draw path, time step of the draw path, reversing draw path, timestep of the reversing draw path, and resulting drawing force.

Fig. 3. Continuous casting aggregate at the NFM [10].

Two die shapes with dimensions 6x75mm and 30x110mm can be distinguished to produce specimens with different dimensions. These determine the width b and height h of the specimen. The casted slab is then separated into several specimens of length l. The temperature in the crucible and the mold temperature are measured with a thermocouple of Type K (NiCr-Ni) or Type S (PtRh-Pt) (Tab. 1).

Table 1. Sensors of the continuous casting plant [11].

Measurement	Sensor	Range
Crucible temperature [°C]	Thermocouple Type K or Type S	0-1200°C
		0-1500°C
Die temperature [°C]	Thermocouple Type K or Type S	0-1200°C
		0-1500°C
Draw path [mm]	N/A	N/A
Timestep of draw path [s]	N/A	N/A
Reversing draw path [mm]	N/A	N/A
Timestep of reversing draw path [s]	N/A	N/A
Draw force [N]	Load cell	N/A
Process time [s]	Processed by programming	Processed by programming

Due to the separate location of the continuous casting plant and the aggregates for the next process steps, which are carried out at the MF (approximately eight minutes transportation time), there is a significant drop in the temperature of the specimens during transport. To achieve desired material behavior, the specimens are reheated in a furnace at the MF in the next process step to set the specimen temperature required for the following forming operations. To determine the necessary temperature and time, a Type K thermocouple (NiCr-Ni) is added to the furnace by the retrofitting method, which has been adjusted to the maximum temperatures occurring in the furnace of up to 1200°C (Tab. 2).

Table 2. Sensors of the furnace.

Measured quantity	Sensor	Range
Temperature [°C]	Thermocouple Type K	0-1200°C
Process time [s]	Processed by programming	Processed by programming

The used main forming aggregate for bulk-forming, a hydraulic press, is placed next to the furnace to keep the transport distance and transport time and the associated temperature loss of the specimen as low as possible (Fig. 4). The sensor technology of this aggregate records the temperature of the specimen using a ratio pyrometer (also known as a comparison pyrometer) as well as the upsetting force applied during the upsetting process utilizing a load cell (Tab. 3). A special advantage of the ratio pyrometer is its ability to measure correct temperatures at the surface of the specimen without having to know the emission of the underlying material. By measuring with two different spectra, the temperature of the measured object can be determined from their quotient, the radiation ratio [12]. This principle results in a further advantage, which is particularly relevant for harsh operating and environmental conditions - the insensitivity to interference, e.g., smoke and dirt between the measuring object and the ratio pyrometer [13].

Fig. 4. Hydraulic press with control unit (left), furnace (right).

The rolling mill at the MF (Fig. 5) was equipped with suitable sensor technology to record the process parameters relevant to the rolling process (Tab. 4).

Table 3. Sensors of the hydraulic press.

Measured quantity	Sensor	Range
Die force [N]	Load cell	0-1MN
Die position [mm]	LVDT	0-600mm
Temperature of specimen [°C]	Pyrometer	0-1200°C
Process time [s]	Processed by programming	Processed by programming

As a result, the mill can be incorporated into the process chain to roll specimens and collect further information on texture or formability. Two load cells, one on each side of the work rolls, measure the resulting rolling force and sum to give the total force, which has the advantage of collect data regarding eccentricity directly in the roll gap. A Linear Variable Differential Transformer (LVDT) sensor, which has a very high resolution and low deviation from linearity, measures the height of the roll gap as well as the deflection of the roll gap during forming.

Fig. 5. Rolling mill system at the MF (300 kN).

Table 4. Sensors of the rolling mill.

Measured quantity	Sensor	Range
Rolling force [N] (left guide rail)	Load cell	0-150kN
Rolling force [N] (right guide rail)	Load cell	0-150kN
Roll gap [mm]	LVDT	0-25mm
Gear angle [°]	Magnetic multi turn encoder	0-360° x 32 turns
Process time [s]	Processed by programming	Processed by programming

4.3. IT-infrastructure and integration of numerical simulation

The DAQ of the sensors from the forming and heating aggregates is carried out within the CMs' internal network using the Wago controller of the XTR-series suited for harsh environmental conditions. Due to the usage of compatible I/O modules, the DAQ can be easily and flexibly adapted to a variety of analog and digital signals from the respective sensors, e.g., voltages, current, bits. The acquired signals are

internally processed by the respective controller and converted into a digital signal that can be used for further computer-based processing and fed into a new set-up production network, which is accessible only for respective stakeholders of the MUL 4.0 project. After initial calibration of all respective sensors, calibration curves varying between third and sixth-order were directly programmed into the corresponding controller in structured text, which results in the direct conversion of sensor signals into corresponding physical quantity. For the connection of the aggregates used at the NFM, the proprietary software of the continuous caster will be used, resulting in txt files automatically stored at the MUL 4.0 production network. The preparation and further processing of the process data from both chairs are carried out in an additional layer with the open-source programming language Python, which was chosen to prevent an isolated solution. Using suitable frameworks, the data in the network are collected, processed, and evaluated to make them available for analysis and automatic feeding into FVA and FEA-based simulations [14].

As soon as data are supplied from the continuous caster, the simulation of the upsetting forming process of the hydraulic press and/or rolling mill is automatically set up and started with Python. This provides the sample temperature to be set for the desired degree of forming. As a result, the temperature to be set as well as corresponding heating time will automatically be adapted. In the case of the bulk-forming processes, an additional thermal simulation of the temperature gradients within the specimen is carried out to ensure that all samples are heated thoroughly and homogeneously. The process steps 'reheating' and 'forming' can be repeated several times, with each of these process steps being automatically simulated again. Furthermore, text (txt) files containing the relevant time steps, such as process start, and end, are stored in the network to provide the most important results of the simulation for further processing at the IL. The obtained data are automatically fed into a SQL database using Python, which is shared between all cooperating chairs and institutes via the network. The simulation of continuous casting and the associated implementation of a digital twin (DT) will be carried out by the NFM. The simulation of the continuous casting process will be performed using common FVA programs. If the required computational time cannot be achieved using FVA, a sophisticated abstraction using FDM will be designed.

The implementation of the three DTs and setup of the simulation using FEA for the furnace, rolling mill, and hydraulic press will be performed by the MF. Fig. 6 shows the resulting material and data flow within the numerical simulation optimized aggregates in the value chain. All numerical simulations are supplied with input parameters and deliver output parameters, which are passed on to the simulation of the next process step according to the process chain (Fig. 1), to digitally represent the process chain in the best possible way. Tab. 5 shows an overview of the resulting input and output parameters. The automatic input data transfer and starting of the simulation is realized by Python (Fig. 7).

As demonstrated in Fig. 7, a python script is written, which serves as the basis for the automatic creation of an input (inp) file for the simulation with the FE program Abaqus (abq).
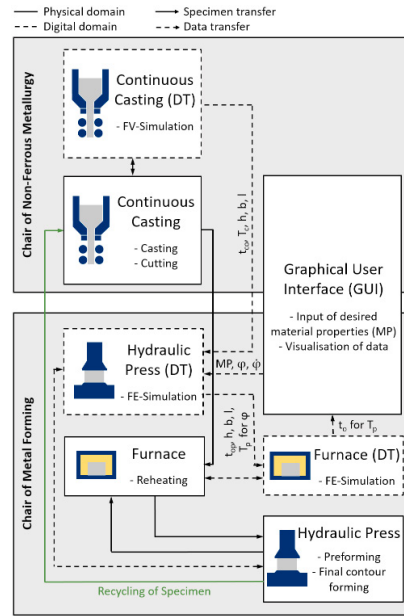

Fig. 6. Overview of the material and data flow corresponding to the numerical simulation-based DTs'.

Table 5. Input and output parameters of the coupled numerical simulations.

Machine	Type of Simulation	Input	Output
Continuous Casting	FVA (FDM)	CP, MP	t_{co}, T_c, h, b, l
Oven	FEA	CP, MP, t_{co}, T_c, h, b, l, φ, φ̇	t_o for T_p
Press	FEA	t_{co}, T_c, h, b, l, MP, φ, φ̇	t_{op}, h, b, l, T_p for φ

This inp file contains all required information and data, e.g., CP, MP, geometries, to perform an FEA with Abaqus.
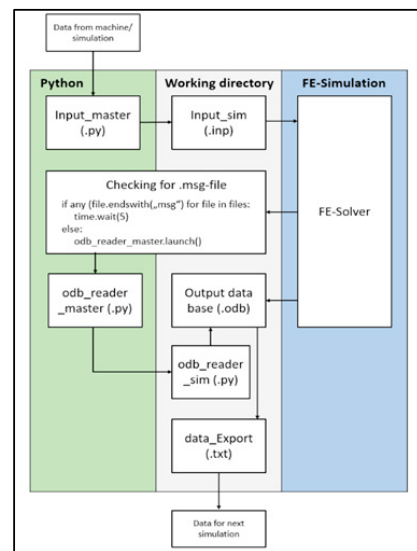

Fig. 7. Scheme of automated FE-Simulation with Python.

With Python, the input data from the previous process step is automatically transferred into the inp file and the simulation is started. During calculation, Python checks in defined time increments if certain files are present in the working directory, e.g., the message (msg) file, which is only present during and automatically deleted after completion of the respective simulation. If the script cannot find such an msg file, it automatically reads out the output database (odb) file using another Python (py) script. It is important to note that the automated data extraction from the used FEA-program does not work within the used PyCharm IDE, as the extraction from the proprietary odb format must be carried out with a specific library only available within the abq environment. Therefore, the py Masterfile executes an abq-specific py file with the imported library and underlying methods directly in the abq environment using the abq command window.

The resulting abq odb file contains the output parameters defined in the inp file at all selected nodes, depending on the previous definition in the inp file. To make the resulting odb data usable for the simulation of the next process step, the master file transfers the odb data into a txt file and transfers it automatically into the next inp file, followed by the start of the upcoming simulation. A similar approach, depending on the decided FVA software will be carried out for the integration of FVA by the NFM.

5. Results and discussion

The cooperation between the involved chairs and institutes results in an interdisciplinary digitalization framework demonstrated in Fig. 8. One advantage of the presented framework was the transdisciplinary development approach used, considering different points of view from automation, mechanical engineering, materials science, metallurgy, and industrial logistics perspectives. Furthermore, every party was involved, from the initial conception to the following adaption phases, allowing each different discipline to include specific knowledge from the very beginning.

Therefore, the resulting framework (Fig. 8) has the main advantage of being planned from scratch to create a low-cost open-source solution for the digitalization and digital transformation of low volume and high variety manufacturing environments. Proprietary solutions, resulting in heterogeneous data sources for the DAQ and functional domains, were avoided. The inclusion of numerical simulation domain experts from the beginning of this project avoided over-engineering in terms of (in practice not particularly needed) accuracy for the cost of higher computational times. The exchange between logistics experts and involved process engineers leads to various adaptions in implemented sensor technology, as the integration of a logistics digital twin requires additional hardware, which to a significant extent must be implemented within the retrofitting process. The delocalized structure of the physical entities also made it necessary to include different IT-infrastructures from the beginning. Therefore, the implementation of a shared production network leading to a unified database structure was of utmost importance. The MF and NFM also included their respective shop floor workers in the concept, giving regular updates on the project status to avoid refusal from coworkers who will have to work with the introduced framework regularly soon.
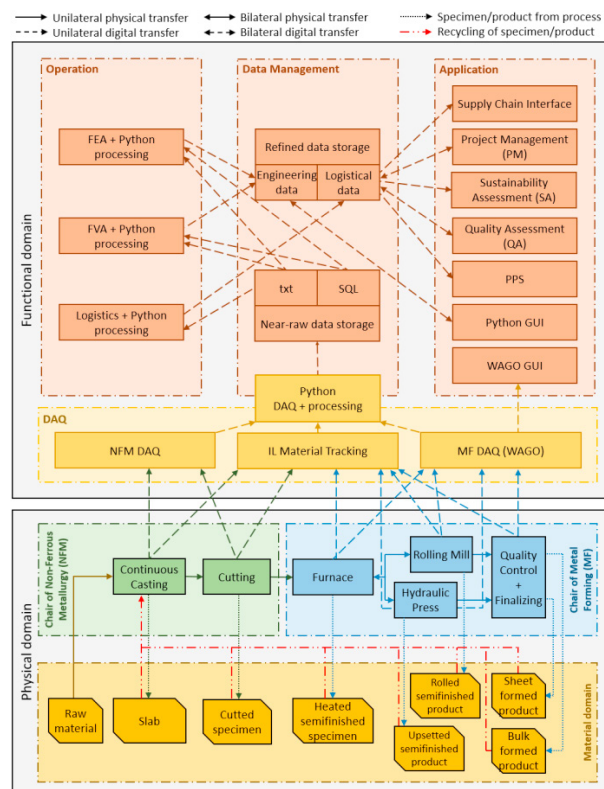

Fig. 8. MUL 4.0: physical and functional domain blueprint.

6. Conclusion and outlook

The framework presented in this paper is already in the implementation phase. The necessary retrofitting of involved aggregates is determined and will be completely implemented within this year. One of the main aggregates, the rolling mill at the MF is already fully integrated within the superordinate DAQ and Python layer and serves as a case study for further implementation in the Wago DAQ environment at the MF. The designed production network is planned, and necessary IT infrastructure is implemented. The first numerical digital twin is already in the final development phase and should be completed within mid of this year. The designed databases are defined, and corresponding python interfaces are programmed. Until next year, the complete implementation of the framework is planned, whereas potential delays, e.g., due to delivery delays, are included in the defined time horizon.

To extend the transdisciplinary engineering education approach, an extension of the involved parties within the end of next year is planned. The main objective is to include further numerical simulation experts regarding FVA as well as ferrous metallurgists to be able to vary between nonferrous and ferrous input material for the upcoming forming processes, which adds more variety in the production planning and coupled numerical simulations. From a logistics point of view, the implementation of different materials also results in another location that must

be tracked, as the production of casted steel grades, similar to the nonferrous counterpart, happens at a different location.

From a techno-economics perspective, on the long term, the introduced digitalization approach aims to serve future engineering experts as well as manufacturing SMEs as a practical case study, supporting knowledge and know-how transfer from the academic to the practical manufacturing environment [15].

CRediT author statement

Benjamin James Ralph: Conceptualization, Methodology, Writing - Original Draft, Writing - Review & Editing. Manuel Woschank: Conceptualization, Methodology, Writing - Original Draft, Writing - Review & Editing. Philipp Miklautsch: Writing - Original Draft, Writing - Review & Editing. Alexander Kaiblinger: Writing - Original Draft, Writing - Review & Editing. Corina Pacher: Writing - Original Draft, Writing - Review & Editing. Marcel Sorger: Writing - Original Draft, Writing - Review & Editing. Helmut Zsifkovits: Supervision. Martin Stockinger: Supervision.

Acknowledgments

References

[1.] Matt DT, Modrák V, Zsifkovits H (eds). Industry 4.0 for SMEs, Cham: Springer International Publishing; 2020.
[2.] Woschank M, Kaiblinger A, Miklautsch P. Digitalization in Industrial Logistics: Contemporary Evidence and Future Directions. Proceedings of the of the International Conference on Industrial Engineering and Operations Management. Singapore, March 9–11. p. 1–12; 2021.
[3.] Thomas BG. Review on Modeling and Simulation of Continuous Casting. Steel Research Int. 89. p. 1700312; 2018.
[4.] Woschank M, Pacher C. Fostering Transformative Learning Processes in Industrial Engineering Education. Proceedings of the 5th NA International Conference on Industrial Engineering and Operations Management. Detroit, Michigan, USA, August 10–14. p. 2022–2029; 2020.
[5.] Ralph BJ, Pacher C, Woschank M. Conceptualization of the Lecture 'Digitalization and Digital Transformation in Metal Forming' based on Implications from Contemporary Teaching and Learning Theories. Proceedings of the 2nd African International Conference on Industrial Engineering and Operations Management. p. 703–712; 2020.
[6.] Reich-Claasen J, von Hippel A. Programm- und Angebotsplanung in Erwachsenenbildung. In: Tippelt R, von Hippel A (eds.). Handbuch Erwachsenenbildung, Weiterbildung. Wiesbaden: Springer; 2018. p. 1405–1425.
[7.] Kassem E, Trenz O. Automated Sustainability Assessment System for Small and Medium Enterprises Reporting. Sustainability. 12. 14. p. 5687; 2020.
[8.] Loh L, Thomas T, Wang Y. Sustainability Reporting and Firm Value: Evidence from Singapore-Listed Companies. Sustainability. 9. 11. p. 2112; 2017.
[9.] Zheng T, Ardolino M, Bacchetti A, Perona M. The applications of Industry 4.0 technologies in manufacturing context: a systematic literature review. International Journal of Production Research. 59. 6. p. 1–33; 2020.
[10.] Ralph BJ, Schwarz A, Stockinger M. An Implementation Approach for an Academic Learning Factory for the Metal Forming Industry with Special Focus on Digital Twins and Finite Element Analysis. Procedia Manufacturing. 45. p. 253–258; 2020.
[11.] Indutherm Erwärmungsanlagen GmbH. Technical Documentation Continuous-Casting-Machine (V)CC1000 / (V)CC3000 with PM-generator. Indutherm Erwärmungsanlagen GmbH. 3. p. 1–77; 2017.
[12.] Hahn JW, Rhee C. Reference wavelength method for a two-color pyrometer. Appl. Opt. 26. p. 5276–5279; 1987.
[13.] Lowe D, Machin G, Sadli M. Correction of temperature errors due to the unknown effect of window transmission on ratio pyrometers using an in situ calibration standard. Measurement. 68. p.16–21; 2015.
[14.] van der Walt S, Colbert SC, Varoquaux G. The NumPy Array: A Structure for efficient Numerical Computation. Computing in Science & Engineering. 13. p. 22–30; 2011.
[15.] Zunk B. M. Positioning "Techno-Economics" as an interdisciplinary reference frame for research and teaching at the interface of applied natural sciences and applied social sciences: An approach based on Austrian IEM study programmes. International Journal of Industrial Engineering and Management. 9. 1. p. 17–23; 2018.

A 4 Publication 4

Author contributions:

1. B.J. Ralph: Conceptualization, Methodology, Software, Validation, Formal Analysis, Data Curation, Writing - Original Draft, Writing - Review & Editing, Visualization, Supervision, Project Administration
2. M. Sorger: Software, Validation, Formal Analysis, Data Curation, Visualization
3. B. Schödinger: Software
4. H.-J. Schmölzer: Software
5. K. Hartl: Writing - Original Draft, Writing - Review & Editing
6. M. Stockinger: Resources, Supervision

Implementation of a Six-Layer Smart Factory Architecture with Special Focus on Transdisciplinary Engineering Education

Benjamin James Ralph *, Marcel Sorger, Benjamin Schödinger, Hans-Jörg Schmölzer, Karin Hartl and Martin Stockinger

Chair of Metal Forming, Montanuniversität Leoben, Franz Josef Str. 18, 8700 Leoben, Austria; marcel.sorger@unileoben.ac.at (M.S.); benjamin.schoedinger@unileoben.ac.at (B.S.); hj.schmo@gmail.com (H.-J.S.); karin.hartl@unileoben.ac.at (K.H.); martin.stockinger@unileoben.ac.at (M.S.)
* Correspondence: benjamin.ralph@unileoben.ac.at; Tel.: +43-384-2402-5611

Abstract: Smart factories are an integral element of the manufacturing infrastructure in the context of the fourth industrial revolution. Nevertheless, there is frequently a deficiency of adequate training facilities for future engineering experts in the academic environment. For this reason, this paper describes the development and implementation of two different layer architectures for the metal processing environment. The first architecture is based on low-cost but resilient devices, allowing interested parties to work with mostly open-source interfaces and standard back-end programming environments. Additionally, one proprietary and two open-source graphical user interfaces (GUIs) were developed. Those interfaces can be adapted front-end as well as back-end, ensuring a holistic comprehension of their capabilities and limits. As a result, a six-layer architecture, from digitization to an interactive project management tool, was designed and implemented in the practical workflow at the academic institution. To take the complexity of thermo-mechanical processing in the metal processing field into account, an alternative layer, connected with the thermo-mechanical treatment simulator Gleeble 3800, was designed. This framework is capable of transferring sensor data with high frequency, enabling data collection for the numerical simulation of complex material behavior under high temperature processing. Finally, the possibility of connecting both systems by using open-source software packages is demonstrated.

Keywords: engineering education; smart factory; digitalization; industry 4.0; metal processing; layer architecture

1. Introduction

Since the beginning of the fourth industrial revolution, a paradigm change within the manufacturing environment can be observed [1–6]. As an integral part of this revolution, the Reference Architecture Model Industry 4.0 (RAMI 4.0) was introduced [7]. RAMI 4.0 is an extension of the Smart Grid Architecture Model (SGAM) to meet the initial requirements of Industry 4.0 [8,9]. Within this model, information type, system hierarchy as well as asset lifecycle is considered within an administration shell, responsible for the communication between these sections [10]. The inclusion of these key factors is especially important for the development of a smart factory [8,11]. This kind of abstract reference model for layer architectures is not a new concept [12–14], but it has a superior advantage due to international standardization. The high amount of the current literature regarding layer architectures demonstrates the importance of this topic among different disciplines in the manufacturing environment, e.g., in [15], Zyrianoff et al. focused the implementation of layered internet of things (IoT) solutions for the development and further enhancement of smart agriculture and smart cities; in [16], Ungurean and Gaitan describe a further concretization of the reference model with a special focus on industrial internet of things (IIoT) solutions; in [17], Gonzalez et al. present the utilization of Modbus

TCP to overcome proprietary automation solutions for smart microgrids in the photovoltaic sector. Despite the high academic as well as industrial research activities within the last years [1,2,18], numerous new concepts and developments are not suitable for small and medium sized enterprises (SMEs) operating in the manufacturing environment [19,20]. High investment costs, a high level of standardization in conducted processes (e.g., by lean management approaches) as well as advanced internal IT and data management/digitalization know-how is required for a majority of solutions recommended in the literature [21–27]. The vast majority of high specialized SMEs do not fulfill these requirements because they have a huge variety as well as low volumes within the production plans. Another characteristic of these businesses is a lower degree of process automation, combined with generally less standardized process management [28,29]. Nevertheless, the economic contribution of SMEs in this sector is not negligible and provides employment opportunities for many current and future graduates of academic institutions [30–32]. To ensure sustainable economic development in these companies, variable low-cost digitalization solutions can add major advantages [33,34]. Therefore, interdisciplinary expertise from current and future employees is required in order to achieve this objective [35–37]. For this reason, an academic smart factory environment [38] was developed, which serves students and therefore future experts as a practical learning environment to deepen their knowledge in digitalization technologies. In comparison to similar learning factories [39–44], the framework discussed in this paper has the advantage of consideration of real physical processes and material parameters (e.g., the possibility of integrating numerical simulation, prediction of microstructure of examined specimens). Furthermore, it supports SMEs by demonstrating low-cost possibilities of digitization and digitalization approaches within the metal processing industry. Despite the hardware solutions, the usage of open source and, more importantly, highly integrative software solutions is of crucial significance. Furthermore, the effort of learning, implementing and updating of such a programming environment must be reasonable. For this reason, Python (Version 3.8) was chosen for the majority of data processing operations described in this case study, using the open source PyCharm Integrated Development Environment (IDE). Python's increasing popularity in the manufacturing as well as academic world was an additional driver for this decision [45,46]. In addition to the free availability as an open-source product, the increasing popularity is due to the multitude and diversity of the frameworks and their continuous improvement and expansion. Popular frameworks such as pandas enable the preprocessing and manipulation of data [47], Matplotlib visualizes the data [48], and Numpy as well as Scipy allow the elaboration of mathematical operations and machine learning algorithms [49]. Additional frameworks permit the fast assembly of versatile GUIs, e.g., PyQt [50].

For the development of a smart factory layer architecture, efficient and effective data management is key. Digital data storage allows a more efficient, secure and accessible data administration and preservation. Databases are practical for storing and managing data and facilitating the retrieval of specific information. In addition, many databases determine which people or programs can access data depending on the respective permissions. In order to facilitate such a permission system, a database management system (DBMS) is used. For this case, the Structured Query Language (SQL)-based relational DBMS MySQL (Version 8.0.23) was chosen because it is an open source product exhibiting a high compatibility with Python and is simple to learn for engineering students [51]. Furthermore, it provides a straightforward connection to Hypertext Preprocessor (PHP), another widely used open source language for the development of advanced Web applications [52]. Additionally, the hosting can be outsourced to an external server provider or done on in-house servers.

Because there is no all-encompassing solution available for the implementation, suitable for the majority of entrepreneurs, two different layer architectures were developed, depending on the existing IT-infrastructure as well as degree of automation

within the respective machine systems. Despite retrofitting approaches, which involve a major proportion of old machine systems with a poor degree of automation, the integration of state of the art machines that already possess a specific digital interface into a not-proprietary IT-framework is of utmost importance [34]. A lot of these systems do not exhibit a standardized open source interface, leading to highly functional, but in most cases isolated, applications [53]. Because the full potential of digitalization and digital transformation lies in the integration of these stand-alone solutions, machine manufacturers commonly offer high cost solutions for the coupling of their individual data acquisition (DAQ) system with other foreign applications [54]. Especially for small and medium-sized enterprises, it is common to avoid these cost-intensive solutions by independently developing efficient solutions.

The following work shows two possibilities of methods capable of gathering and processing necessary data for condition monitoring, maintenance interval optimization and machine learning approaches for engineering education purposes. A special focus lies on the integration of different heterogeneous interfaces as well as easy-to-use human machine interfaces (HMIs) [55–57]. Another important attribute of the presented layer architectures is the resilience regarding a harsh manufacturing environment, achieved with the inclusion of data mirroring and strict access right policy [58]. The possibility of adding new layers, e.g., real time numerical simulation as well as a possible interface to an enterprise resource planning (ERP) system was additionally considered.

2. Transdisciplinary Engineering Education 4.0: Target Groups and Learning Outcomes

As a result of the fourth industrial revolution and corresponding digitalization and digital transformation in the metal processing environment, required competencies and skills for engineers in this field have changed significantly [59–61]. The increase in inter- and transdisciplinary skills necessary to work within this digitalized manufacturing environment must substantially affect the curricula of traditional secondary and tertiary engineering education in order to ensure long-term employability [62–64]. For this reason, a new transdisciplinary lecture at the Montanuniversität Leoben was designed. This lecture aims to introduce engineering students of different disciplines into the fundamentals of digitalization and digital transformation in the metal processing environment. Table 1 gives a general overview about affected disciplines at the academic institution.

Table 1. Main target engineering disciplines at the Montanuniversität Leoben.

Engineering Focus	Associated Programs at the Montanuniversität Leoben
Energy	Industrial Energy Technology
Materials	Materials Science
Process and Product	Metallurgy; Mechanical Engineering; Industrial Logistics
Recycling	Industrial Environmental Protection and Process Technology; Recycling

Students of industrial energy technology, mechanical engineering, industrial logistics, recycling and process technology are heavily affected by the changes in the process and production environment. Therefore, fundamentals of smart-factory-related layer architectures are mandatory for their future careers. Material scientists additionally need to be aware of digitalization in the research and development field. This especially includes know-how about technology-enabled advances in material testing and how this discipline can profit from recent Industry 4.0 related technologies and corresponding advances in sensor technologies. Metallurgists and materials-science-interested mechanical engineers should be aware of developments in both sectors mentioned.

As an integral part to fulfill these requirements, two different layer architectures were developed. The first development focuses on the fundamentals of digitization and

digitalization and is based on a low-cost layer architecture, often used in an SME environment (Section 3). Additionally, to point out the importance of such a framework for material scientists, mechanical engineers and metallurgists, the possibilities of including complex FEA into this architecture is elaborated in Section 5. To also demonstrate the potentials and advantages of higher frequency measurement methods for material testing and characterization, a second layer system including fiber optic measurement technologies is implemented on a state-of-the-art thermomechanical treatment simulator. Both architectures transmit data by the Modbus TCP/IP protocol widely used in industrial practice to the internal server system.

3. Digitalization and Low-Cost Layer Architecture: Structure and CNC-Lathe Integration

The DAQ is performed by a Wago PFC200 G2 2ETH RS controller, which executes PLC control tasks and internally processes analog and digital signals supplied by input/output (I/O) modules. The I/O modules used are analog input modules that receive analog signals from the CNC-lathe and forward them to the controller in order to convert these analog signals into digital ones that are required for further computer-aided processing (Figure 1).
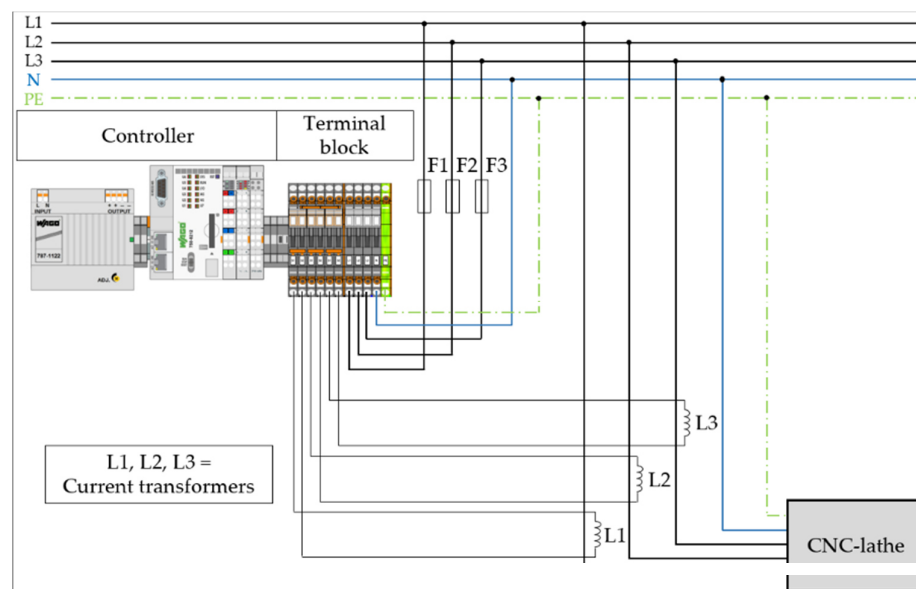

Figure 1. Circuit diagram for the connection of the CNC-lathe to the superordinate system.

By connecting three-phase currents measured by a current transformer as well as voltages, the Wago 750-494 analog input module, a three-phase power measurement module, enables real-time measurement of reactive power, apparent power, active power, energy consumption, power factor, phase angle and frequency. The corresponding circuit diagram from the power module point of view is visualized in Figure 2.

Figure 3 shows the implemented measurement and DAQ module. The selected controller is further capable of storing data directly on a SDHC device, serving as an additional security layer. If network transfer would fail, e.g., due to a server maintenance or other, nonplanned downtimes, the processing data is still automatically stored within the memory device.
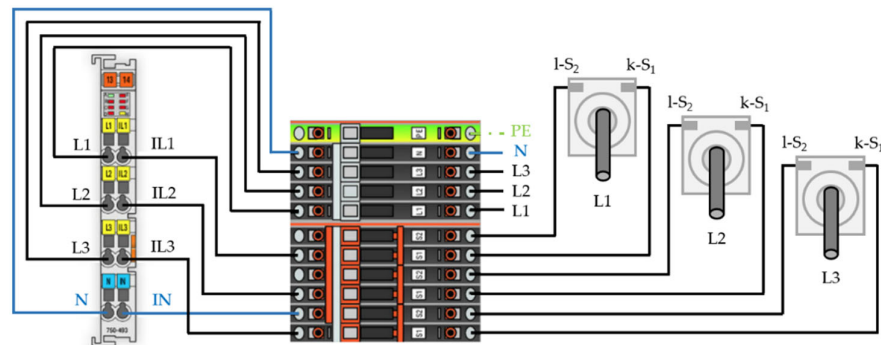
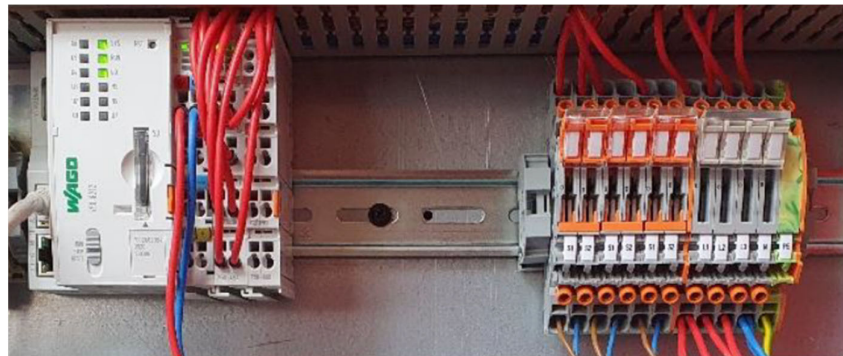**Figure 2.** Circuit diagram: power module side.

Figure 3. Controller (left) and terminal block (right) with wiring.

While the analog module automatically stores the measurement data, additional measurements can be manually added for the purpose of calibration or further specific analysis of defined indicators (e.g., with higher frequency). These measurements can be started and stopped with a graphical user interface (GUI), (Figure 4, dash button 'Electrical Measurement'), created with the Wago e!Cockpit software suite, which, moreover, allows real-time monitoring of the system parameters.

To apply various data processing programs to acquired data and minimize storage space to a reasonable size, all signals are converted and saved as pre-sorted text-files by an automatically working data transfer protocol, running simultaneously on two local computers. The SD-memory is checked for differences between its storage and the server storage every 24 h. If a deviation is detected (more/different data on the SDHC in comparison to the local raw data file storage), the raw data will be overwritten. In order to avoid a malfunction in the SDHC device, the stored raw data on the server is automatically mirrored, enabling the administrator to investigate potential errors after their occurrence. Because space on the memory card is limited to 32 GB, the card is automatically cleared after exceeding of 80% internal memory space. To guarantee no loss of data, the server storage is mirrored within each 24 h and stored to a SQL database, which operates on a different server partition.

The recorded data set contains the timestamp, active, reactive and apparent powers, currents, voltages, power factors and the quadrants of the three phases (Figure 4, yellow frame). The automatic measurement data recording is realized with a sampling frequency of 2 Hz, which was found to be sufficient from previous evaluations. A preprocessing algorithm also calculates the resulting machine costs according to the consumed apparent power (Figure 4, red frame), serving as a basis for the project management tool.
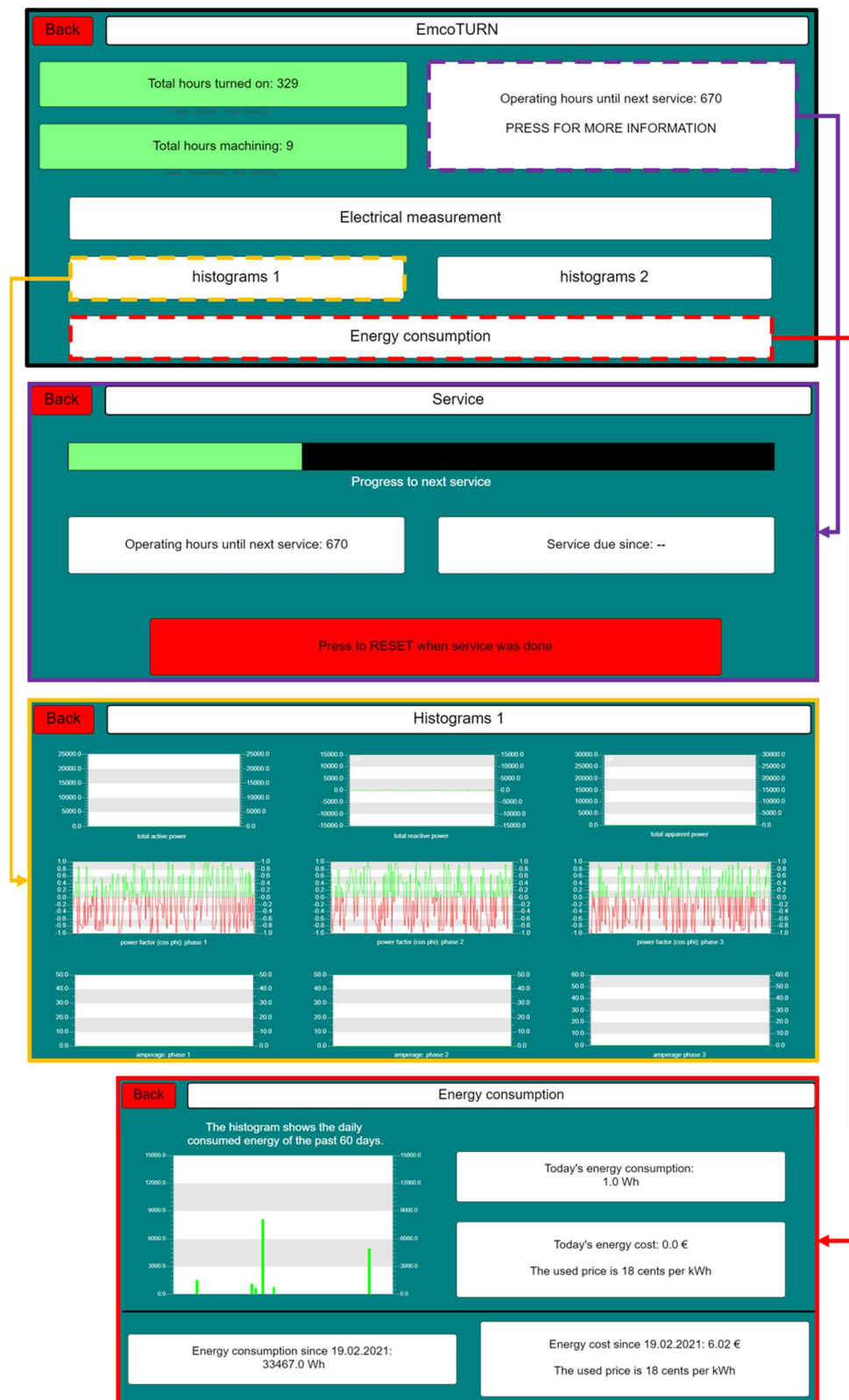
Figure 4. Wago GUI for measurement control (CNC-lathe).

Figure 5 shows the main GUI for the Python processing layer, which visualizes the non-idle machine hours from the recorded data, analyzed by the embedded programming

algorithm [65]. In order to minimize data access time, previously refined data is stored for accounting and general project management purposes in the network within a second mySQL database, and it is made available to technicians and students.
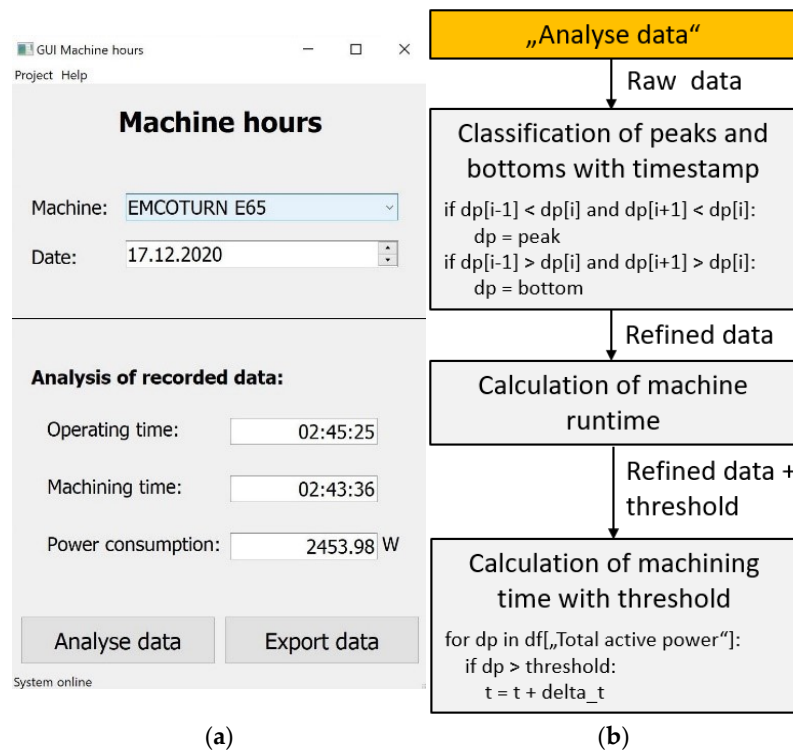

Figure 5. Python logic for machine hour counting: (**a**) visualization, programmed in QtPy; (**b**) back end logic for the GUI.

Figure 6 summarizes the first four layers of the low-cost layer architecture for the CNC-lathe, from implemented sensors to the main processing layer.

Table 2 shows the implemented roles and corresponding rights regarding viewing and changing settings within the PHP GUI for an exemplary project. The second SQL database, including the refined data as a result of the main processing layer, serves as an underlying fundamental for this GUI. Within the Python programming environment, input data from the PHP GUI (e.g., new projects or involved coworkers within a specific project) is stored automatically within the refined SQL-database. For the education of engineering students, the developed PHP GUI was duplicated and set up with realistic values to enable a comprehensive experimental setup without disturbing the workflow of respective employees. For this replica, students receive logins for every role, thus enabling them to work with existing roles and corresponding rights. This approach also enables the possibility to change the underlying logic in the back-end of the project management tool, giving deeper insights into PHP-based programming.

The visualization and publishing of refined data for the interactive project management tool is done within the internal network using PHP programming, with a special focus on IT security due to the implementation of different roles with different rights within the PHP GUI (Figure 7).
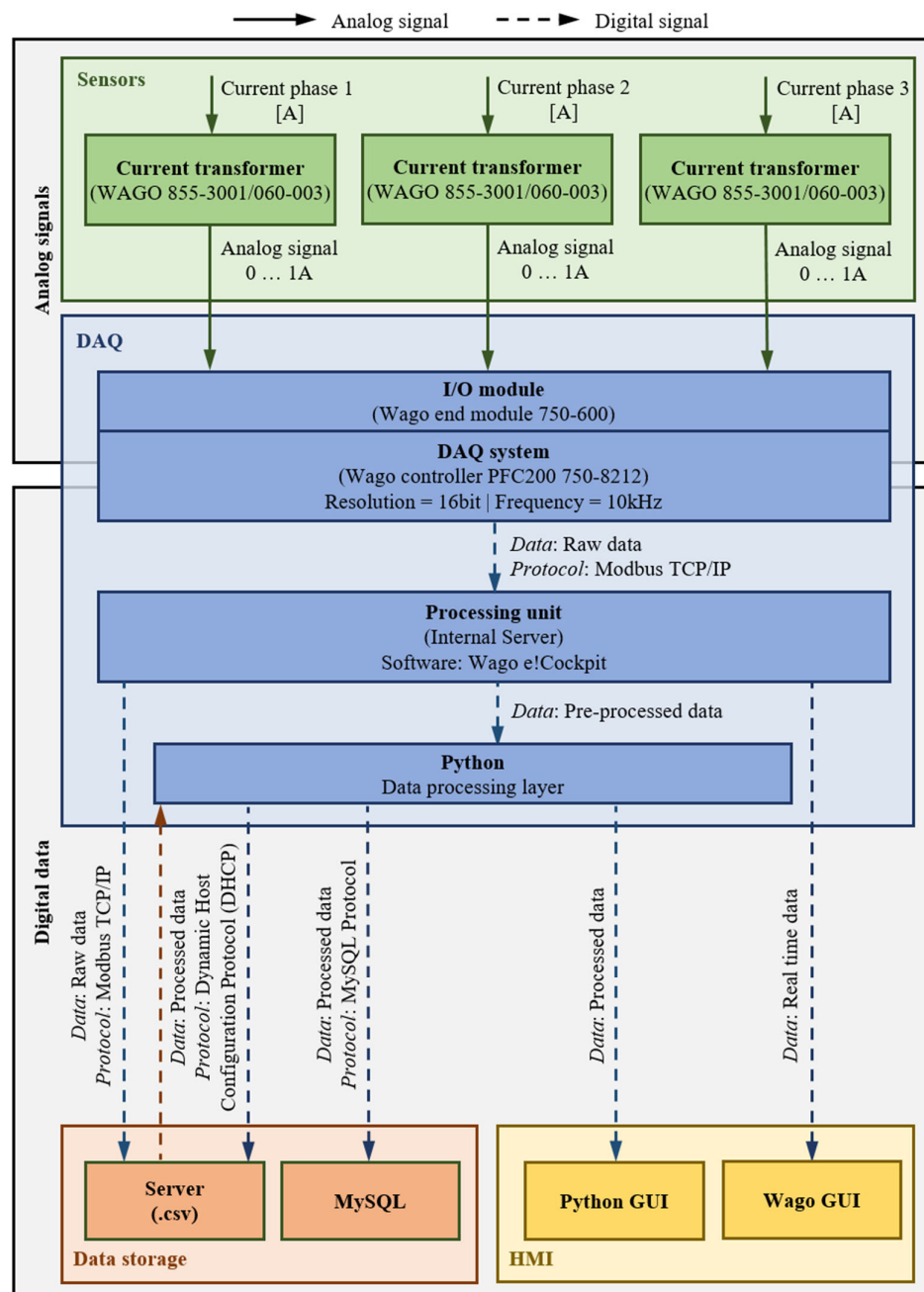
Figure 6. Data flowchart for the integration of the CNC-lathe into the low-cost layer architecture.

Table 2. Project management GUI: implemented roles and corresponding rights (E = employees/M = machines/P = project).

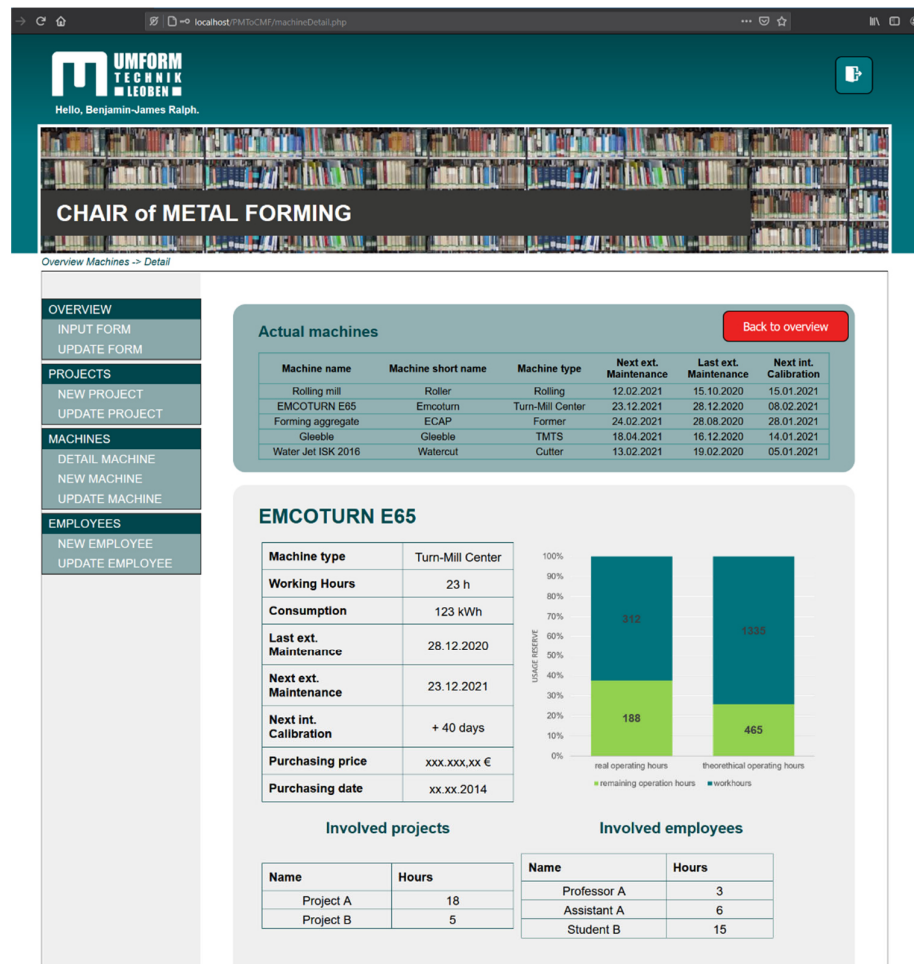| Role	Admin	Project Leader	Project Member	Technician	Other Personnel
Overview	X	X	X	X	X
Detail view	E/M/P	E/M/P	M/P	M	-
Set new project activities	X	X	-	-	-
Budget & cost details	X	X	-	-	-
Employee details	X	X	-	-	-
Change milestones	X	X	-	-	-
Change budget	X	-	-	-	-

Figure 7. Interactive project management tool, programmed in PHP and directly coupled to an underlying MySQL database. The SQL database is coupled within the Python logic presented in this work.

Figure 8 illustrates the resulting six-layer architecture. To sustain a resilient, adaptive and smooth working system, the machine park and corresponding machine sensors are divided into different nodes. The number of machines coupled to one node is depending on the number of sensors and therefore data transferred, as well as the frequency required. For node 1, two heterogeneous aggregates are coupled to controller 1, whereas the CNC-lathe transfers 25 different indicators with a frequency of 2 Hz, running continuously. This results in a low and steady CPU usage on the respective controller. The second aggregate submitting data through node 1 is a retrofitted cold rolling mill, which transfers data from four different sensors with a frequency of over 500 Hz when operating. This frequency is only achievable through writing data directly on the RAM of the controlling device, resulting in a temporary additional CPU load of more than 80% on the controlling unit. This load peak must be considered when planning digitalization solutions because an overload cannot be avoided persistently in most of low cost controllers. In this case, the necessary algorithm, programmed in structured text format, must also be implemented separately as the used controller initially merely provides up to 1 Hz of acquisition frequency.
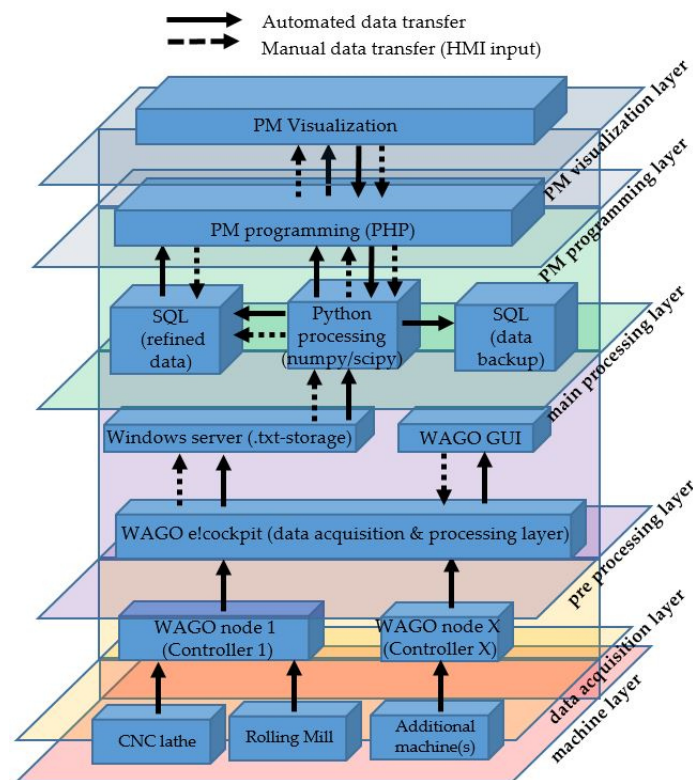
Figure 8. Resulting low-cost six-layer architecture.

4. Data Gathering for Initial Condition Monitoring and Further Analysis: A Case Study

As data science fundamentals become more important for future manufacturing experts, a simple case for the reproducible DAQ was defined and carried out. The objective of this approach was to collect data sets which can be easily edited by students on a basic level. Additionally, a simple state-of-the-art logic was implemented, serving as a basis for more sophisticated programming efforts within a supportive learning environment. The respective logic is initially able to distinguish between three states of the lathe system:

- Off;
- On but not working (idle time);
- Working (real machining time).

To be able to differentiate between real machining time (the CNC-lathe operates on a workpiece) and idle machine time (e.g., calibration, adjustment between two machining steps, set-up times), a pretest was carried out. In this pretest, idle mode, tool changer movements and main spindle rotations with different rpm without actually operating on a work piece were performed and analyzed to gain knowledge about the behavior of all recorded electrical parameters. This pretest exhibits the advantage of a low time consumption, allowing lecturers to demonstrate the data collection quickly and therefore enhance awareness of the comprehensive matter. Table 3 shows the 15 different settings investigated.

Table 3. Testing program for the identification of idle related change in electrical indicators.

Test no.	Type of Testing
1	X− transition of tool turret
2	X+ transition of tool turret
3	Z− transition of tool turret
4	Z+ transition of tool turret
5	Z− transition of tailstock
6	Z+ transition of tailstock
7	Counterclockwise rotation with 1000 rpm of main spindle
8	Clockwise rotation with 1000 rpm of main spindle
9	Counterclockwise rotation with 2000 rpm of main spindle
10	Clockwise rotation with 2000 rpm of main spindle
11	Counterclockwise rotation with 3000 rpm of main spindle
12	Clockwise rotation with 3000 rpm of main spindle
13	Counterclockwise rotation with 4200 rpm of main spindle
14	Clockwise rotation with 4200 rpm of main spindle
15	Full 360°rotation of tool turret

To analyze real machining time, a cylindrical workpiece (alloy steel, type 708M40) with a length of 250 mm and an initial diameter of 68 mm was axially turned at constant speed using a new cutting blade XMGC30 with an infeed of 0.5 mm per process step. An additional testing plan was created, consisting of constant machining parameters and using axial machining operations to reduce the base material in diameter (Table 4). In order to evaluate the influence of cooling on the power consumption of the machine, tests number 20 and 21 were carried out without the usage of the internal cooling system.

During the entire machining process, the measured sensor data was likewise recorded to identify the corresponding test data faster and figure out correlations between the machining time and the measured values. Another advantage of the control scheme is the opportunity to increase the frequency (simultaneously) while processing without interrupting the continuous DAQ process.

Table 4. Calibration plan and parameters for machining.

Test no.	Initial Diameter (mm)	End Diameter (mm)	Cooling	Rotational Speed (1/s)	Feed in (mm)	Cutting Speed (mm/s)
16	68.0	62.0	Yes	10	0.5	1.5
17	62.0	55.0	Yes	10	0.5	1.5
18	55.0	45.0	Yes	10	0.5	1.5
19	45.0	35.0	Yes	10	0.5	1.5
20	35.0	25.0	No	10	0.5	1.5
21	25.0	18.0	No	10	0.5	1.5
22	18.0	10.0	Yes	10	0.5	1.5

The analysis of all different types of electrical indicators shows that the total active power is the best suited indicator to distinguish between idle time and actual working time. Figure 9 shows the performed testing program according to Table 4, visualized using the Python matplotlib.py extension package.
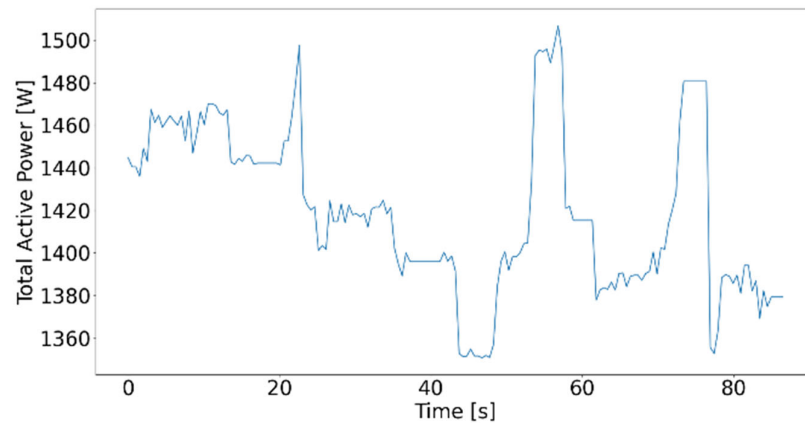
Figure 9. Total active power of idle tests carried out.

Figure 10 illustrates the total active power of test 13 and 14, a rotation of the main spindle with 4200 rpm. The power consumption does not significantly deviate for clockwise and counterclockwise rotation. For these tests, the average active power consumptions sum up to about 5100 W. This trend is also consistent with the results of paired tests at other speeds, i.e., test 7 and 8, 9 and 10, 11 and 12.
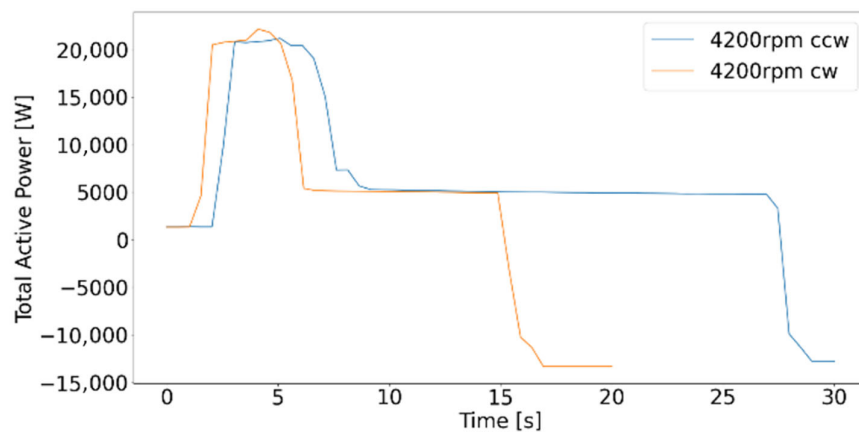

Figure 10. Total active power of tests 13 and 14.

Figure 11 shows the results of the tests with counterclockwise rotation at different speeds. As already shown in Figure 10, the power consumption remains constant after an initial peak. These plateaus increase in magnitude with speed. By analyzing the measurement data with Python, no trivial correlations or patterns were determined by reactive power, apparent power, phase current, phase voltage, power factor or phase angle. Through the visualization of the total active power, a comprehensible relationship can be established between the machining operation and the evaluated parameters.

As Figure 12 illustrates, a trend displayed by the dashed green line can be observed, which is a representative of the diameter and machined length. The negative measurement peaks, ranging from 50 to 550 W apart from the green trend line in terms of magnitude, represent the tool being set down from the workpiece and returned to the starting position to perform the next programmed process step.
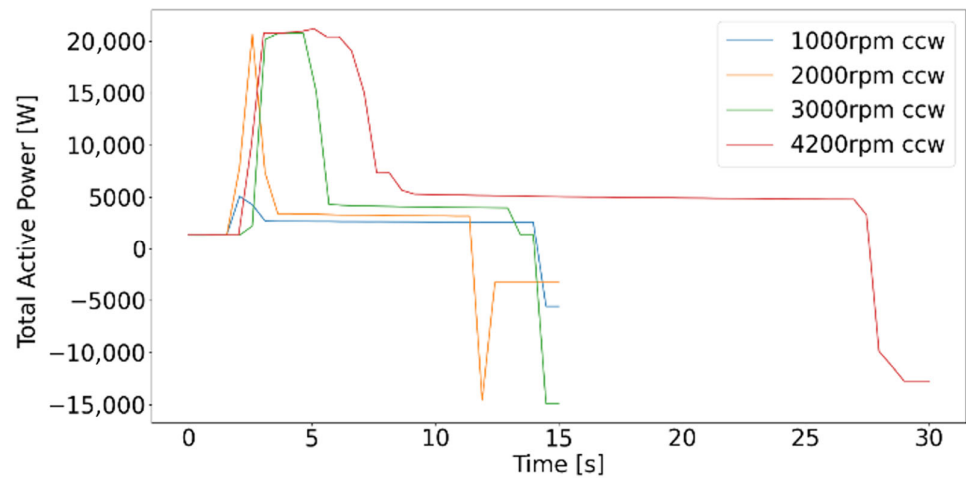
Figure 11. Total active power of tests 7, 9, 11 and 13.

To demonstrate the influence of adequate cooling, test numbers 20 and 21 were performed without cooling (Figure 12, red dashed line), resulting in a lower total active power in comparison to other test samples. The constant deviation from the green dashed trend line by an offset in magnitude can be explained as a result of decreasing power consumption due to unused aggregates for coolant supply. The number of negative peaks within Figure 12 is equivalent to the number of process steps for each test.

Figure 12. Total active power during axial machining.
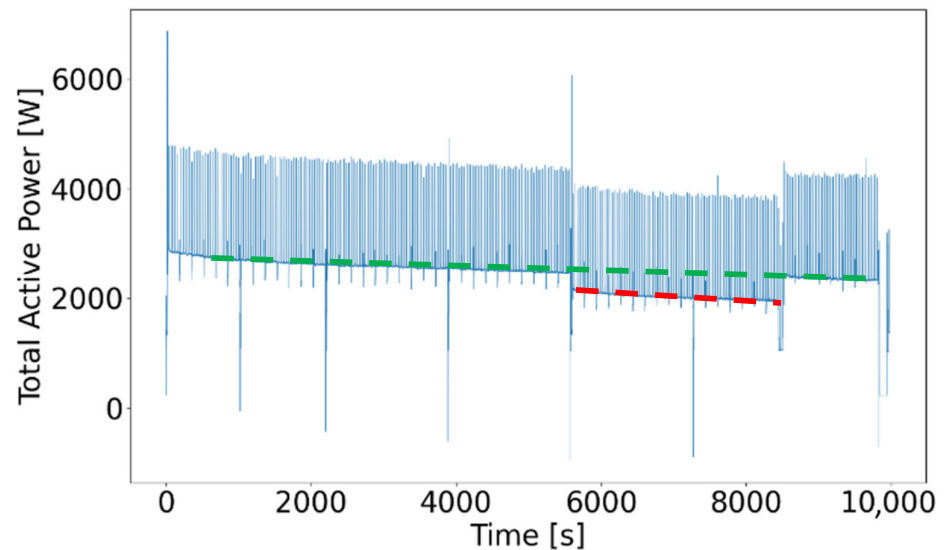
Figure 13 shows six of these smaller negative peaks that are equivalent to the number of processing steps of test number 16. If negative peaks fall below a total active power of 1500 W, the machinery is not operating—the time during which the total active power falls below this value does not contribute to machining and can be excluded from the machine-hours-counting algorithm.
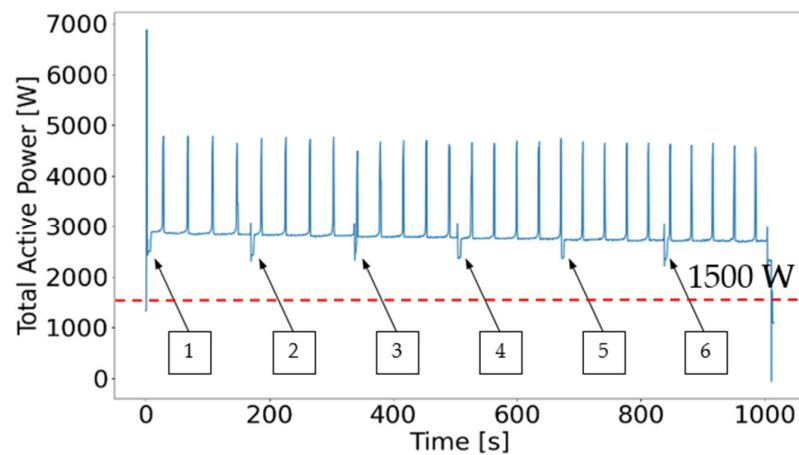
Figure 13. Total active power of test number 9.

Table 5 demonstrates the accuracy of the investigated behavior. A wrong classification of machining parameter data points is below 0.03%, which is not significant in terms of maintenance or machine hour calculations, and therefore, it is an activity-cost-based project management approach. If these tests were conducted more frequently, a higher number of heterogeneous datasets would be generated and simple machine learning algorithms for the classification of the respective data (e.g., Support Vector Machines, Decision Tree Analysis) can be instructed [66,67].

Table 5. Data point classification.

	Data Points Real Machining	Data Points Idle Machining
Sum	19,960	174
Right	19,440	173
Wrong	520	1
% Wrong	0.026	0.0057

Due to the relatively short recording time for test numbers 7 to 14 (20–30 s), higher mean values and standard deviations arise compared to machining tests 16 to 18. The shorter the recording time, the higher the influence of peaks at the beginning and the drop at the end of the data set (Figures 9 and 10), leading to the resulting deviation. This divergence also demonstrates the significance of encompassing statistics behind data-driven technology and the relationship between the amount of data and prediction accuracy.

Table 6 shows the calculated peak values, the mean values as well as the standard deviations of all test numbers listed in Tables 3 and 4. The precise identification of real machining and therefore actual wearing of the analyzed aggregate has several advantages. Before the development of the discussed architecture, ordinary maintenance was executed after specific time intervals, instead of considering the effective wear of the machine system. The implementation of this framework enables maintenance intervals to be determined on the basis of actual machine hours. This approach leads to lower maintenance costs because unnecessary servicing is minimized and additional necessary maintenance is recommended. As a result, periods with higher machine utilization are identified automatically and quantitatively. For a more efficient scheduling, the residual time until the next external service is calculated as a moving average. The exact predictability increases with the duration of the system's utilization. For a further cost reduction, a standardized internal calibration test was developed. After exceeding 25% of calculated machine hours until next external service, a standardized test, serving as an

indicator for possible malfunctions within the aggregate will be executed. The machining time left until the next internal service is implemented within the project management GUI (PHP/Python) as well as programmed Wago GUI (structured text). After internal or external service, the calculation can be reset within the corresponding GUI.

Table 6. Analysis of peak values, mean values and standard deviation of all tests.

Test No.	Peak (W)	Mean (W)	Standard Deviation (W)
1	1400.52	1373.97	22.45
2	1506.73	14,447.17	41.40
3	1470.10	1453.34	11.17
4	1497.68	1417.77	23.17
5	1480.63	1416.03	39.87
6	1394.20	1379.81	11.69
7	5081.58	2053.05	2198.34
8	10,064.27	2586.07	1864.12
9	20,644.23	1979.91	5508.34
10	20,754.51	2997.70	6094.99
11	20,723.80	4685.71	8261.15
12	20,752.01	607.02	10,746.6
13	21,175.08	5664.18	7751.18
14	22,137.44	3658.69	11,133.24
15	3374.98	1949.28	864.02
16	6879.55	2840.18	403.78
17	4655.05	2731.31	406.98
18	4590.80	2676.75	405.01
19	4929.11	2599.64	423.23
12	6070.17	2140.74	409.52
21	4245.32	2035.68	449.24
22	4556.87	2270.27	717.81

A substantially more precise calculation can be achieved by the developed project management GUI. As the system provides the real power consumption of the aggregate, internal as well as external projects can be calculated on a more reality-based manner. While the PHP interface authorizes respective project leaders to set up new projects and enter personnel costs with or without the usage of machines, the system also substitutes different manual working hour recordings, which were carried out for internal projects individually and more qualitatively until the implementation.

To ensure a learning experience that is as close to reality as possible by a reasonable data set from machine systems as well as the developed project management tool, the initial framework is also used on a daily basis by the personnel at the institution. When implementing new IT infrastructures with a higher level of automation, it is essential to involve the staff and identify their preferences at an early stage of the introduction. Therefore, all co-workers were briefed and asked about their opinion towards a project management system and what it is supposed to contain to facilitate the daily workflow. As a result, the PHP GUI was adapted several times, considering the preferences of respective employees. Moreover, the Wago as well as PHP GUI is available on every computer device within the local network of the academic institution, which allows all involved personnel to start measurements, overview specific machines and create or update projects independently from their specific location (depending on individual rights). Through secured VPN access, a completely remote condition monitoring is possible. This degree of freedom also offers students the possibility to engage with and refine the system remotely if access is given by respective lecturers.

5. Integration of Numerical Simulation and Implementation of a High Frequency DAQ Architecture

Due to the rise in computational capacity and speed within the last decades, the possibility of integrating real-time numerical simulation within the actual production process becomes more and more suitable among the manufacturing environment [68]. Therefore, the presented framework can be extended to include numerical simulation (near) real time in a variety of production processes.

Figure 14 visualizes the additional integration of a finite element analysis (FEA) program within the developed framework. In this example the Python GUI adapts different rolling steps within one rolling operation based on the results of a FEA, calculated during the time required for the previous process within the production operation and under consideration of processing and material properties.
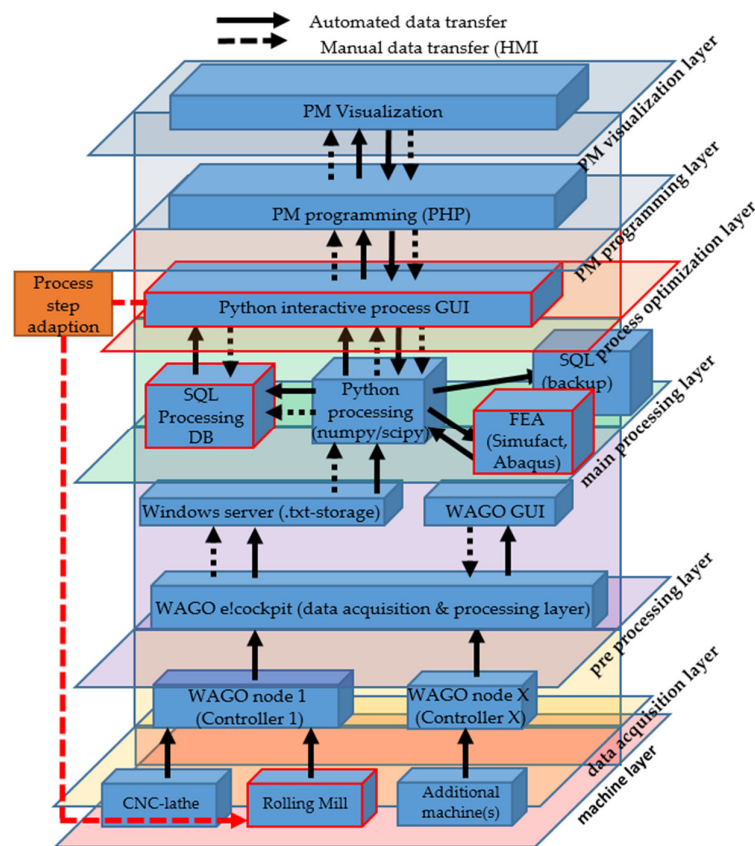

Figure 14. Six-layer architecture with integrated numerical simulation: FEA digital shadow for semi automatized process adaption (example rolling mill).

Based on the knowledge gained from the case study in Section 4, the integration of sophisticated numerical simulations into the framework derives in a broader understanding of the possible advantages of these technologies. Nevertheless, most material processing operations, especially high temperature forming processes, require constant surveillance of the material behavior under enhanced temperature and forming conditions. In order to be able to handle a forming process of a particular material, it is necessary to have a certain comprehension of microstructural changes. In general, extensive material parameter studies are indispensable for predicting the final microstructure resulting from the forming process, such as anisotropy and the resulting grain size or grain size distributions, as well as possible material damage influencing variables [69].

In an increasing number of cases, integrated microstructure models are used in the numerical simulation of a forming process as accompaniment, relating the occurring forming parameters (e.g., temperature gradient, strain rate) to the resulting microstructure changes such as static or (meta-) dynamic recrystallization as well as grain growth [70]. The required material parameters are commonly obtained in suitable thermomechanical simulators, that operate on a laboratory scale [71–75]. Since the processes proceed expeditiously, especially in the case of simultaneous forming at high strain rates, it is essential for material data acquisition to ensure a significantly higher sampling frequency of the system [76,77]. For this reason, an additional DAQ system provided by iba was implemented at the institution's thermo-mechanical treatment simulator (Type Gleeble 3800). This DAQ is widely used in industrial practice, offering different software packages and the possibility of significantly higher sensor sampling rates for further processing [78,79]. The connection between the sensors and the system is realized with a proprietary A/D converter, transferring digitized data by a fiber optic line with up to 100 kHz on four channels:

1. Temperature;
2. Dilation of the respective specimen;
3. Resulting Force;
4. Displacement.

The gathered data is preprocessed directly within the ibaAnalyzer software package and automatically submitted to a file system hosted by the internal server architecture of the institution.

The high sampling rate offers the possibility of investigating the influence of time-dependent changes in material behavior by measured values. The resulting data sets can be further used to develop and adapt numerical models to digital shadows and, in long instances, digital twins [80,81].

The Gleeble system, like a majority of highly specialized material testing aggregates, offers a proprietary software solution for resulting data analysis. By recording a hot tensile test of bainitic steel and comparing the results of both data sets, previous work of the authors revealed a significant difference in the gathered temperature data, which indicates an internal data preprocessing and correction of the proprietary software unit [38]. Due to the low output voltage signal of thermocouples used, a voltage fluctuation within 10^{-3} V results in a temperature deviation of 250 K. Figure 15 illustrates this deviation. These examples can be used to raise awareness about these kinds of potential inaccuracies.

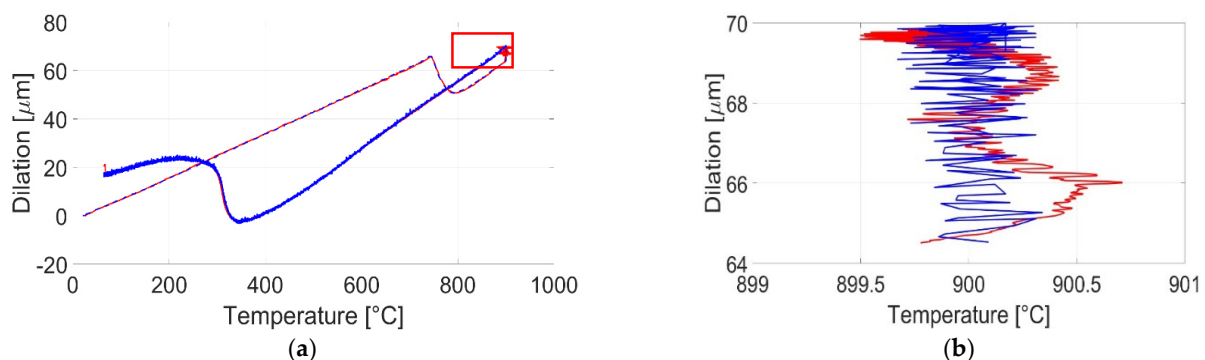**Figure 15.** Dilation curve for a tensile test of bainitic steel, carried out with the Gleeble system [38]: (**a**) temperature change with respect to dilation, blue line: Gleeble data set, red line: iba data set; (**b**) cutout area of deviation between both data sets from (**a**).

Figure 16 visualizes the resulting architecture, from the applied sensors to the (refined) data storage at the internal server.
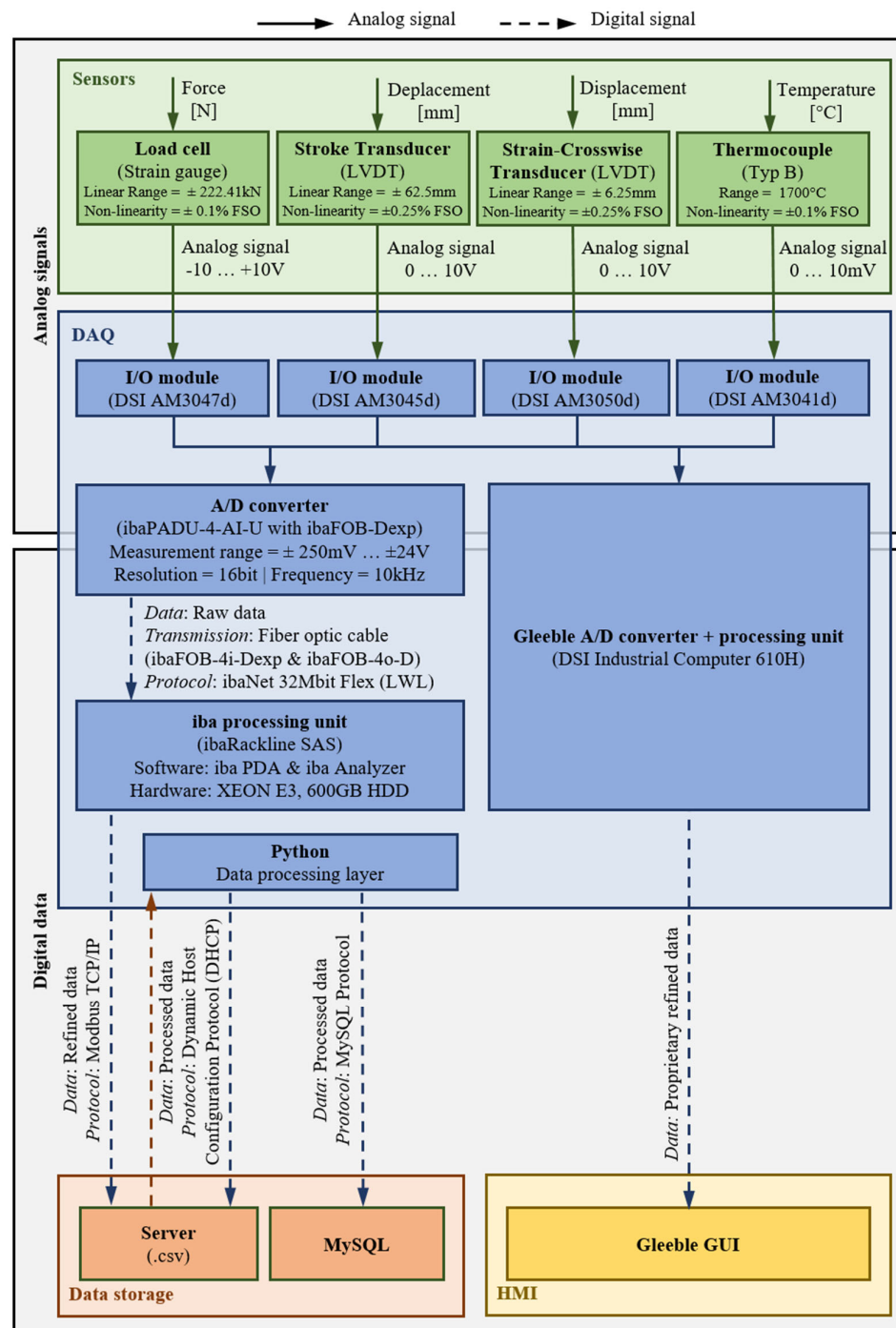
Figure 16. High frequency DAQ and data storage.

6. Results and Discussion

As a result of this work, a six-layer architecture was designed, concentrating deliberately on the use of a few selected products (open source if possible) in order to make application and modification by interested parties as simple as possible. Additionally, a second DAQ system was developed to give this group the opportunity to gain data for real physics-based numerical simulations. Besides, the most important objective was to create a smart factory layout that enables students and practitioners from the metal processing field to engage with different levels of digitization and digitalization,

reaching from analog signal to numerical simulation integration. The resulting layer architecture is highly adaptable in terms of the used programming languages (e.g., Python can be substituted with C++ or Java if preferred; mySQL can be substituted with flux). This architecture fulfills three purposes. First, a technical fundament for teaching students in manufacturing related disciplines was created, which allows the following:

- To gain an overview about the most important fundamentals of networking technologies and corresponding protocols in the manufacturing environment;
- To deepen knowledge on manufacturing related data science by working with different amounts and homogeneous as well as heterogeneous data sets;
- To be able to work with different types of DAQ systems used in industrial practice;
- To optimize interfaces and investigate interface-related efficiency and effectivity concerns in-person or remotely;
- To enhance knowledge about common programming languages and machine learning technologies in manufacturing by working with real data from machining processes;
- To obtain an overview of interactive project management and how (near) real-time adaption of required parameters (e.g., cost changes) can affect project outcomes;
- To raise awareness about the importance of transdisciplinary communication and education in the manufacturing field.

The second operational area of the implemented framework is the research and development of state-of-the-art digitalization technologies, based on this initial work by the following:

- Extending the framework with other, more complex machine systems (e.g., hydraulic presses, ovens);
- Extending the framework with more complex machine systems by developing predicting algorithms including thermo-mechanical properties of materials;
- Using this algorithms for the transformation of existing machine systems to Cyber Physical Production Systems (CPPS) based on the brownfield approach [82,83];
- Integrating further open-source-based logic between these CPPS, resulting in a superordinate Cyber Physical Logistic System [84–86].

The third purpose is the collaboration with interested parties from the industry, especially SMEs, who can use this framework within interdisciplinary projects. This approach has the main advantage of giving industrial experts the opportunity to deepen their knowledge or perform highly experimental tests. Additionally, engineering students are given the possibility to collaborate with these companies from an early stage, gaining additional practice and establishing networks already during their studies.

The presented architecture in Section 3 is an efficient and effective way of taking advantage of current information and communication technologies within a small volume and high-variety production environment. The tools and programs used are either low-cost or even completely free-of-charge, therefore providing an ideal basis for digitalization of small production facilities from scratch. To build up such a low-cost, resilient system, the following points must be considered:

1. How many different channels (different values from sensors, e.g., pressure, force, dilation, temperature) are needed for each respective machine system? (specification of needed input modules);
2. Which frequency is needed for each channel? (avoidance of aliasing, dependent on the process and respective material characteristics);
3. What kind of database is applicable within the respective company? (considering internal know-how and experience);
4. How resilient does the physical hardware and software have to be? (dirt, dust, temperature, accessibility, space);
5. What IT-infrastructure serves as a basis for the framework? (Windows, Linux, other server—OS);

6. What kind of GUI/HMI do respective employees favor?

The individual answer to (1) implies knowledge about all respective machine systems. In general, one can recommend starting with one system where all (from a present point of view) required sensors are already applied and the resulting data is understood.

Answering (2) seems more complex because the required frequency depends on the purpose. In the case of the rolling mill at the academic institution, a medium frequency is needed. In case of the discussed CNC lathe, a much lower frequency is applicable because the process itself is highly standardized trough the internal machine control unit. For high temperature or high-speed forming processes, a significantly higher sampling rate has to be ensured. In general, if the material behavior itself should be analyzed, higher frequencies are mandatory (e.g., considering microstructural changes due to applied or internal forces or as a function of the temperature gradient in case of an involved heat treatment).

Question (3) is dependent on the internal knowledge. If no specific database system is used, open-source programs can be recommended.

Question (4) is heavily dependent on the specific environment. If existing sensors are working within the environment, the sole important point to consider in this case is the resilience of the respective controller. Most Supervisory Control and Data Acquisition (SCADA) suppliers offer specific, more robust solutions (e.g., Wago XTR series).

Regarding (5), an efficient and stable interface between the resulting storage solution (server or PC) must be programmed. In this study, a regular windows system was used. One of the advantages that Python and its various extension packages offer is the very broad possibility of interface programming. There are different types of extensions for the coupling of different IT-systems to the controller system available. The controller system itself in this case produces txt-files, which then were automatically implemented in the SQL based database system as well as stored parallel on the used windows server system.

The answer to (6) is crucial for a successful implementation. Without considering the experience and preferences of involved employees on the shop floor, a well-planned digitalization solution is likely to fail. Including respective workers in the development of user interfaces at the earliest possible stage helps to successfully implement and sustain the change in working environment.

The second architecture should serve as an additional expansion to higher frequency DAQ technologies with a special focus on data gathering for numerical simulations. From a network technology and data science point of view, the most essential questions to answer, additionally, are as follows:

7. What sampling rate is sufficient to obtain enough data for an accurate material behavior prediction? (e.g., recrystallization behavior of the investigated material under defined process parameters)
8. How accurate are implemented DAQ systems? Is it possible to confirm resulting data?

These points should be considered intrinsic by each engineering student who strives for a career in a digitalized metal processing environment. This work should therefore give an experimental basis to concretize the answers given by the author for specific cases.

7. Conclusions and Outlook

This paper describes the development of a six-layer smart manufacturing architecture for the transdisciplinary engineering education. For this purpose, two DAQ systems—one to demonstrate fundamentals and possibilities of open-source low-cost digitalization solutions and a second for high frequency measurement applications—were developed and implemented. For both architectures, case studies were provided to enhance comprehensible teaching in a digitalized manufacturing environment. A major advantage of the proposed structure is the open-source components used wherever

possible. The selected technologies are already common in industrial practice, due to the high degree of connectivity, cost efficiency and practicability in the metal processing environment.

As measurement results of the high frequency architecture are stored within the same server architecture as the Wago DAQ system, respective data can be analyzed and further processed in the same Python environment. The Gleeble system coupled in this network is also a widely used simulators in the industrial practice, especially in the research and development field. By including this system into the layer architecture and coupling this architecture with a superordinate MES, the horizontal integration of different departments in the manufacturing environment can be simulated. Because the complexity in the academic institution's learning factory (14 heterogeneous machine systems with different initial degree of automation) can be defined as similar to those in SMEs, a low-cost open-source solution can be programmed and implemented to serve as MES. By using Python for this purpose, already-existing extensions for the coupling with an ERP program can be realized efficiently, allowing students and future manufacturing experts to use this framework for the simulation of manufacturing processes from initial digitization to the coupling with, e.g., corporate accounting or procurement. The Montanuniversität Leoben additionally launched the new bachelor's program Industrial Data Science, focusing on the transdisciplinary engineering education with special emphasis on data gathering and processing within the material processing environment. As additional machine systems are integrated within the frameworks, machine learning algorithms can be further implemented and optimized by interested engineers for data monitoring applications. The monitoring and malfunction detection as well as related IT-security issues, highly discussed in the current literature [87–89], can further be used for the deeper education of future industrial data scientists.

Author Contributions: Conceptualization, B.J.R.; methodology, B.J.R.; software, B.J.R., M.S. (Marcel Sorger), H.-J.S. and B.S.; validation, B.J.R. and M.S. (Marcel Sorger); formal analysis, B.J.R. and M.S. (Marcel Sorger); resources, M.S. (Martin Stockinger); data curation, M.S. (Marcel Sorger) and B.J.R.; writing—original draft preparation, B.J.R. and K.H.; writing—review and editing, B.J.R. and K.H.; visualization, M.S. (Marcel Sorger) and B.J.R.; supervision, B.J.R. and M.S. (Martin Stockinger); project administration, B.J.R. All authors have read and agreed to the published version of the manuscript.

Institutional Review Board Statement: Not applicable.

Informed Consent Statement: Not applicable.

Data Availability Statement: The data presented in this study are available on request from the corresponding author.

Conflicts of Interest: The authors declare no conflict of interest.

References

1. Culot, G.; Orzes, G.; Sartor, M.; Nassimbeni, G. The future of manufacturing: A Delphi-based scenario analysis on Industry 4.0. *Technol. Forecast. Soc. Chang.* **2020**, *157*, 120092, doi:10.1016/j.techfore.2020.120092.
2. Oztemel, E.; Gursev, S. Literature review of Industry 4.0 and related technologies. *J. Intell. Manuf.* **2020**, *31*, 127–182, doi:10.1007/s10845-018-1433-8.
3. Almada-Lobo, F. The Industry 4.0 revolution and the future of Manufacturing Execution Systems (MES). *J. Innov. Manag.* **2016**, *3*, 16–21, doi:10.24840/2183-0606_003.004_0003.
4. Frank, A.G.; Dalenogare, L.S.; Ayala, N.F. Industry 4.0 technologies: Implementation patterns in manufacturing companies. *Int. J. Prod. Econ.* **2019**, *210*, 15–26, doi:10.1016/j.ijpe.2019.01.004.
5. Stock, T.; Seliger, G. Opportunities of Sustainable Manufacturing in Industry 4.0. *Procedia CIRP* **2016**, *40*, 536–541, doi:10.1016/j.procir.2016.01.129.
6. Vaidya, S.; Ambad, P.; Bhosle, S. Industry 4.0—A Glimpse. *Procedia Manuf.* **2018**, *20*, 233–238, doi:10.1016/j.promfg.2018.02.034.
7. *DIN SPEC 91345:2016-04, Referenzarchitekturmodell Industrie 4.0 (RAMI4.0);* Beuth Verlag GmbH: Berlin, Germany, 2016.

8. Pisching, M.A.; Pessoa, M.A.; Junqueira, F.; dos Santos Filho, D.J.; Miyagi, P.E. An architecture based on RAMI 4.0 to discover equipment to process operations required by products. *Comput. Ind. Eng.* **2018**, *125*, 574–591, doi:10.1016/j.cie.2017.12.029.

9. Uslar, M.; Rohjans, S.; Neureiter, C.; Pröstl Andrén, F.; Velasquez, J.; Steinbrink, C.; Efthymiou, V.; Migliavacca, G.; Horsmanheimo, S.; Brunner, H.; et al. Applying the Smart Grid Architecture Model for Designing and Validating System-of-Systems in the Power and Energy Domain: A European Perspective. *Energies* **2019**, *12*, 258, doi:10.3390/en12020258.

10. Trunzer, E.; Calà, A.; Leitão, P.; Gepp, M.; Kinghorst, J.; Lüder, A.; Schauerte, H.; Reifferscheid, M.; Vogel-Heuser, B. System architectures for Industrie 4.0 applications. *Prod. Eng.* **2019**, *13*, 247–257, doi:10.1007/s11740-019-00902-6.

11. Mourtzis, D.; Gargallis, A.; Zogopoulos, V. Modelling of Customer Oriented Applications in Product Lifecycle using RAMI 4.0. *Procedia Manuf.* **2019**, *28*, 31–36, doi:10.1016/j.promfg.2018.12.006.

12. Schmid, H.A. Creating the architecture of a manufacturing framework by design patterns. *SIGPLAN Not.* **1995**, *30*, 370–384, doi:10.1145/217839.217876.

13. Williams, T.J.; Bernus, P.; Brosvic, J.; Chen, D.; Doumeingts, G.; Nemes, L.; Nevins, J.L.; Vallespir, B.; Vlietstra, J.; Zoetekouw, D. Architectures for integrating manufacturing activities and enterprises. *Comput. Ind.* **1994**, *24*, 111–139, doi:10.1016/0166-3615(94)90016-7.

14. Devedzic, V.; Radovic, D. A framework for building intelligent manufacturing systems. *IEEE Trans. Syst. Man Cybern. C* **1999**, *29*, 422–439, doi:10.1109/5326.777077.

15. Zyrianoff, I.; Heideker, A.; Silva, D.; Kleinschmidt, J.; Soininen, J.-P.; Salmon Cinotti, T.; Kamienski, C. Architecting and Deploying IoT Smart Applications: A Performance-Oriented Approach. *Sensors* **2019**, *20*, 84, doi:10.3390/s20010084.

16. Ungurean, I.; Gaitan, N.C. A Software Architecture for the Industrial Internet of Things-A Conceptual Model. *Sensors* **2020**, *20*, 5603, doi:10.3390/s20195603.

17. González, I.; Calderón, A.J.; Portalo, J.M. Innovative Multi-Layered Architecture for Heterogeneous Automation and Monitoring Systems: Application Case of a Photovoltaic Smart Microgrid. *Sustainability* **2021**, *13*, 2234, doi:10.3390/su13042234.

18. Culot, G.; Nassimbeni, G.; Orzes, G.; Sartor, M. Behind the definition of Industry 4.0: Analysis and open questions. *Int. J. Prod. Econ.* **2020**, *226*, 107617, doi:10.1016/j.ijpe.2020.107617.

19. Sommer, L. Industrial revolution—Industry 4.0: Are German manufacturing SMEs the first victims of this revolution? *J. Ind. Eng. Manag.* **2015**, *8*, 1512–1532, doi:10.3926/jiem.1470.

20. Moeuf, A.; Pellerin, R.; Lamouri, S.; Tamayo-Giraldo, S.; Barbaray, R. The industrial management of SMEs in the era of Industry 4.0. *Int. J. Prod. Res.* **2018**, *56*, 1118–1136, doi:10.1080/00207543.2017.1372647.

21. Cevik Onar, S.; Ustundag, A.; Kadaifci, Ç.; Oztaysi, B. The Changing Role of Engineering Education in Industry 4.0 Era. In *Industry 4.0: Managing the Digital Transformation*; Ustundag, A., Cevikcan, E., Eds.; Springer International Publishing: Cham, Switzerland, 2018; pp. 137–151, ISBN 978-3-319-57869-9.

22. Ghobakhloo, M.; Fathi, M. Corporate survival in Industry 4.0 era: The enabling role of lean-digitized manufacturing. *J. Manuf. Technol. Manag.* **2020**, *31*, 1–30, doi:10.1108/JMTM-11-2018-0417.

23. Hoellthaler, G.; Braunreuther, S.; Reinhart, G. Digital Lean Production An Approach to Identify Potentials for the Migration to a Digitalized Production System in SMEs from a Lean Perspective. *Procedia CIRP* **2018**, *67*, 522–527, doi:10.1016/j.procir.2017.12.255.

24. Hoellthaler, G.; Braunreuther, S.; Reinhart, G. Requirements for a methodology for the assessment and selection of technologies of digitalization for lean production systems. *Procedia CIRP* **2019**, *79*, 198–203, doi:10.1016/j.procir.2019.02.046.

25. Harteis, C. Machines, Change and Work: An Educational View on the Digitalization of Work. In *The Impact of Digitalization in the Workplace*; Harteis, C., Ed.; Springer International Publishing: Cham, Switzerland, 2018; pp. 1–10, ISBN 978-3-319-63256-8.

26. Kobus, J.; Westner, M.; Strahringer, S.; Strode, D. Enabling digitization by implementing Lean IT: Lessons learned. *TQM* **2018**, *30*, 764–778, doi:10.1108/TQM-02-2018-0026.

27. Branca, T.A.; Fornai, B.; Colla, V.; Murri, M.M.; Streppa, E.; Schröder, A.J. The Challenge of Digitalization in the Steel Sector. *Metals* **2020**, *10*, 288, doi:10.3390/met10020288.

28. Matt, D.T.; Modrák, V.; Zsifkovits, H. *Industry 4.0 for SMEs*; Springer International Publishing: Cham, Switzerland, 2020; ISBN 978-3-030-25424-7.

29. Peukert, S.; Treber, S.; Balz, S.; Haefner, B.; Lanza, G. Process model for the successful implementation and demonstration of SME-based industry 4.0 showcases in global production networks. *Prod. Eng.* **2020**, *14*, 275–288, doi:10.1007/s11740-020-00953-0.

30. Asgary, A.; Ozdemir, A.I.; Özyürek, H. Small and Medium Enterprises and Global Risks: Evidence from Manufacturing SMEs in Turkey. *Int. J. Disaster Risk Sci.* **2020**, *11*, 59–73, doi:10.1007/s13753-020-00247-0.

31. Chandler, V. The economic impact of the Canada small business financing program. *Small Bus. Econ.* **2012**, *39*, 253–264, doi:10.1007/s11187-010-9302-7.

32. Eniola, A.; Ektebang, H. SME firms performance in Nigeria: Competitive advantage and its impact. *Int. J. Res. Stud. Manag.* **2014**, *3*, doi:10.5861/ijrsm.2014.854.

33. Knol, W.H.; Slomp, J.; Schouteten, R.L.; Lauche, K. Implementing lean practices in manufacturing SMEs: Testing 'critical success factors' using Necessary Condition Analysis. *Int. J. Prod. Res.* **2018**, *56*, 3955–3973, doi:10.1080/00207543.2017.1419583.

34. Contreras Pérez, J.D.; Cano Buitrón, R.E.; García Melo, J.I. Methodology for the Retrofitting of Manufacturing Resources for Migration of SME Towards Industry 4.0. In *Applied Informatics*; Florez, H., Diaz, C., Chavarriaga, J., Eds.; Springer International Publishing: Cham, Switzerland, 2018; pp. 337–351, ISBN 978-3-030-01534-3.

35. Ho, T.C.; Ahmad, N.H.; Ramayah, T. Competitive Capabilities and Business Performance among Manufacturing SMEs: Evidence from an Emerging Economy, Malaysia. *J. Asia-Pac. Bus.* **2016**, *17*, 37–58, doi:10.1080/10599231.2016.1129263.

36. Benešová, A.; Tupa, J. Requirements for Education and Qualification of People in Industry 4.0. *Procedia Manuf.* **2017**, *11*, 2195–2202, doi:10.1016/j.promfg.2017.07.366.

37. Ralph, B.J.; Pacher, C.; Woschank, M. Conceptualization of the Lecture 'Digitalization and Digital Transformation in Metal Forming' based on Implications from Contemporary Teaching and Learning Theories. In Proceedings of the 2nd African International Conference on Industrial Engineering and Operations Management, Harare, Zimbabwe, 7–10 December 2020; pp. 703–712, ISBN 978-1-7923-6123-4.

38. Ralph, B.J.; Schwarz, A.; Stockinger, M. An Implementation Approach for an Academic Learning Factory for the Metal Forming Industry with Special Focus on Digital Twins and Finite Element Analysis. *Procedia Manuf.* **2020**, *45*, 253–258, doi:10.1016/j.promfg.2020.04.103.

39. Dobrilovic, D.; Brtka, V.; Stojanov, Z.; Jotanovic, G.; Perakovic, D.; Jausevac, G. A Model for Working Environment Monitoring in Smart Manufacturing. *Appl. Sci.* **2021**, *11*, 2850, doi:10.3390/app11062850.

40. Böhner, J.; Weeber, M.; Kuebler, F.; Steinhilper, R. Developing a Learning Factory to Increase Resource Efficiency in Composite Manufacturing Processes. *Procedia CIRP* **2015**, *32*, 64–69, doi:10.1016/j.procir.2015.05.003.

41. Faller, C.; Feldmüller, D. Industry 4.0 Learning Factory for regional SMEs. *Procedia CIRP* **2015**, *32*, 88–91, doi:10.1016/j.procir.2015.02.117.

42. Baena, F.; Guarin, A.; Mora, J.; Sauza, J.; Retat, S. Learning Factory: The Path to Industry 4.0. *Procedia Manuf.* **2017**, *9*, 73–80, doi:10.1016/j.promfg.2017.04.022.

43. Abele, E.; Metternich, J.; Tisch, M.; Chryssolouris, G.; Sihn, W.; ElMaraghy, H.; Hummel, V.; Ranz, F. Learning Factories for Research, Education, and Training. *Procedia CIRP* **2015**, *32*, 1–6, doi:10.1016/j.procir.2015.02.187.

44. Prinz, C.; Morlock, F.; Freith, S.; Kreggenfeld, N.; Kreimeier, D.; Kuhlenkötter, B. Learning Factory Modules for Smart Factories in Industrie 4.0. *Procedia CIRP* **2016**, *54*, 113–118, doi:10.1016/j.procir.2016.05.105.

45. Krill, P. Python Soars Past Java in Tiobe Language Index: Python Ranks as the Second Most Popular Programming Language in the November index, with C First and Java Slipping to Third Place. Available online: https://www.infoworld.com/article/3596069/python-soars-past-java-in-tiobe-language-index.html (accessed on 16 April 2021).

46. Martinez, P.; Ahmad, R.; Al-Hussein, M. A vision-based system for pre-inspection of steel frame manufacturing. *Autom. Constr.* **2019**, *97*, 151–163, doi:10.1016/j.autcon.2018.10.021.

47. Mckinney, W. *Python for Data Analysis*; O'reilly Editions: Sebastopol, USA, 2012; ISBN 978-1-449-31979-3.

48. Ari, N.; Ustazhanov, M. Matplotlib in python. In Proceedings of the 2014 11th International Conference on Electronics, Computer and Computation (ICECCO), Abuja, Nigeria, 29 September–1 October 2014; pp. 1–6, ISBN 978-1-4799-4106-3.

49. Ranjani, J.; Sheela, A.; Meena, K.P. Combination of NumPy, SciPy and Matplotlib/Pylab -a good alternative methodology to MATLAB—A Comparative analysis. In Proceedings of the 2019 1st International Conference on Innovations in Information and Communication Technology (ICIICT), Chennai, India, 25–26 April 2019; pp. 1–5, ISBN 978-1-7281-1604-4.

50. Summerfield, M. *Rapid GUI Programming with Python and Qt*: *The Definitive Guide to PyQt Programming*, 1st ed.; Addison-Wesley Professional: Boston, USA, 2015; ISBN 978-0-13-235418-9.

51. Krogh, J.W. *MySQL Connector/Python Revealed*: *SQL and NoSQL Data Storage Using MySQL for Python Programmers*; Apress: Berkeley, CA, USA, 2018; ISBN 978-1-4842-3694-9.

52. Okulicz, K. Virtual reality-based approach to manufacturing process planning. *Int. J. Prod. Res.* **2004**, *42*, 3493–3504, doi:10.1080/00207540410001699426.

53. Galambos, P.; Csapó, Á.; Zentay, P.; Fülöp, I.M.; Haidegger, T.; Baranyi, P.; Rudas, I.J. Design, programming and orchestration of heterogeneous manufacturing systems through VR-powered remote collaboration. *Robot. Comput. Integr. Manuf.* **2015**, *33*, 68–77, doi:10.1016/j.rcim.2014.08.012.

54. Kusiak, A. Smart manufacturing must embrace big data. *Nature* **2017**, *544*, 23–25, doi:10.1038/544023a.

55. ElMaraghy, H.A. Flexible and reconfigurable manufacturing systems paradigms. *Int. J. Flex. Manuf. Syst.* **2005**, *17*, 261–276, doi:10.1007/s10696-006-9028-7.

56. Körner, U.; Müller-Thur, K.; Lunau, T.; Dragano, N.; Angerer, P.; Buchner, A. Perceived stress in human-machine interaction in modern manufacturing environments-Results of a qualitative interview study. *Stress Health* **2019**, *35*, 187–199, doi:10.1002/smi.2853.

57. Pacaux-Lemoine, M.-P.; Trentesaux, D.; Zambrano Rey, G.; Millot, P. Designing intelligent manufacturing systems through Human-Machine Cooperation principles: A human-centered approach. *Comput. Ind. Eng.* **2017**, *111*, 581–595, doi:10.1016/j.cie.2017.05.014.

58. Werner, M.R.; Fahrner, W.R. Review on materials, microsensors, systems and devices for high-temperature and harsh-environment applications. *IEEE Trans. Ind. Electron.* **2001**, *48*, 249–257, doi:10.1109/41.915402.

59. Fomunyam, K.G. Education and the Fourth Industrial Revolution: Challenges and Possibilities For Engineering Education. *Int. J. Mech. Eng. Technol. (IJMET)* **2019**, *10*, 23–25.

60. Kovacs, O. The dark corners of industry 4.0—Grounding economic governance 2.0. *Technol. Soc.* **2018**, *55*, 140–145, doi:10.1016/j.techsoc.2018.07.009.

61. Sony, M. Industry 4.0 and lean management: A proposed integration model and research propositions. *Prod. Manuf. Res.* **2018**, *6*, 416–432, doi:10.1080/21693277.2018.1540949.

62. Ramirez-Mendoza, R.A.; Morales-Menendez, R.; Iqbal, H.; Parra-Saldivar, R. Engineering Education 4.0:—proposal for a new Curricula. In Proceedings of the 2018 IEEE Global Engineering Education Conference (EDUCON), Tenerife, Canary Islands, Spain, 17–20 April 2018; pp. 1273–1282, ISBN 978-1-5386-2957-4.

63. Brougham, D.; Haar, J. Smart Technology, Artificial Intelligence, Robotics, and Algorithms (STARA): Employees' perceptions of our future workplace. *J. Manag. Org.* **2018**, *24*, 239–257, doi:10.1017/jmo.2016.55.

64. Ghobakhloo, M. Industry 4.0, digitization, and opportunities for sustainability. *J. Clean. Prod.* **2020**, *252*, 119869, doi:10.1016/j.jclepro.2019.119869.

65. van der Walt, S.; Colbert, S.C.; Varoquaux, G. The NumPy Array: A Structure for Efficient Numerical Computation. *Comput. Sci. Eng.* **2011**, *13*, 22–30, doi:10.1109/MCSE.2011.37.

66. Rostami, H.; Dantan, J.-Y.; Homri, L. Review of data mining applications for quality assessment in manufacturing industry: Support vector machines. *Int. J. Metrol. Qual. Eng.* **2015**, *6*, 401, doi:10.1051/ijmqe/2015023.

67. Kim, A.; Oh, K.; Jung, J.-Y.; Kim, B. Imbalanced classification of manufacturing quality conditions using cost-sensitive decision tree ensembles. *Int. J. Comput. Integr. Manuf.* **2018**, *31*, 701–717, doi:10.1080/0951192X.2017.1407447.

68. Bergman, G.; Oldenburg, M. A finite element model for thermomechanical analysis of sheet metal forming. *Int. J. Numer. Methods Eng.* **2004**, *59*, 1167–1186, doi:10.1002/nme.911.

69. Bontcheva, N.; Petzov, G. Microstructure evolution during metal forming processes. *Comput. Mater. Sci.* **2003**, *28*, 563–573, doi:10.1016/j.commatsci.2003.08.014.

70. Pietrzyk, M. Through-process modelling of microstructure evolution in hot forming of steels. *J. Mater. Process. Technol.* **2002**, *125–126*, 53–62, doi:10.1016/S0924-0136(02)00285-6.

71. Bennett, C.J.; Leen, S.B.; Williams, E.J.; Shipway, P.H.; Hyde, T.H. A critical analysis of plastic flow behaviour in axisymmetric isothermal and Gleeble compression testing. *Comput. Mater. Sci.* **2010**, *50*, 125–137, doi:10.1016/j.commatsci.2010.07.016.

72. Chobaut, N.; Carron, D.; Arsène, S.; Schloth, P.; Drezet, J.-M. Quench induced residual stress prediction in heat treatable 7xxx aluminium alloy thick plates using Gleeble interrupted quench tests. *J. Mater. Process. Technol.* **2015**, *222*, 373–380, doi:10.1016/j.jmatprotec.2015.03.029.

73. Hsieh, R.-I.; Liou, H.-Y.; Pan, Y.-T. Effects of Cooling Time and Alloying Elements on the Microstructure of the Gleeble-Simulated Heat-Affected Zone of 22% Cr Duplex Stainless Steels. *J. Mater. Eng. Perform.* **2001**, *10*, 526–536, doi:10.1361/105994901770344665.

74. Liu, W.; Lu, F.; Yang, R.; Tang, X.; Cui, H. Gleeble simulation of the HAZ in Inconel 617 welding. *J. Mater. Process. Technol.* **2015**, *225*, 221–228, doi:10.1016/j.jmatprotec.2015.06.001.

75. Thomas, G.A.; Speer, J.G.; Matlock, D.K. Quenched and Partitioned Microstructures Produced via Gleeble Simulations of Hot-Strip Mill Cooling Practices. *Metall. Mater. Trans. A* **2011**, *42*, 3652–3659, doi:10.1007/s11661-011-0648-5.

76. Dour, G.; Dargusch, M.; Davidson, C. Recommendations and guidelines for the performance of accurate heat transfer measurements in rapid forming processes. *Int. J. Heat Mass Transf.* **2006**, *49*, 1773–1789, doi:10.1016/j.ijheatmasstransfer.2005.10.045.

77. Hauser, F.E. Techniques for measuring stress-strain relations at high strain rates. *Exp. Mech.* **1966**, *6*, 395–402, doi:10.1007/BF02326284.

78. Hu, S.Y.; Yu, H.B. Application of PDA Industry Data Acquisition System in Analysis of the Reason of Strip Blocked in Hot Mill. *AMR* **2012**, *591–593*, 1758–1761, doi:10.4028/www.scientific.net/AMR.591-593.1758.

79. Yi-bin, Q.; Xiao-jie, W.; Xiang-chao, L. Digital distance control system research and implementation. *Procedia Earth Planet. Sci.* **2009**, *1*, 1375–1379, doi:10.1016/j.proeps.2009.09.212.

80. Cimino, C.; Negri, E.; Fumagalli, L. Review of digital twin applications in manufacturing. *Comput. Ind.* **2019**, *113*, 103130, doi:10.1016/j.compind.2019.103130.

81. Kritzinger, W.; Karner, M.; Traar, G.; Henjes, J.; Sihn, W. Digital Twin in manufacturing: A categorical literature review and classification. *IFAC-PapersOnLine* **2018**, *51*, 1016–1022, doi:10.1016/j.ifacol.2018.08.474.

82. Wank, A.; Adolph, S.; Anokhin, O.; Arndt, A.; Anderl, R.; Metternich, J. Using a Learning Factory Approach to Transfer Industrie 4.0 Approaches to Small- and Medium-sized Enterprises. *Procedia CIRP* **2016**, *54*, 89–94, doi:10.1016/j.procir.2016.05.068.

83. Bader, S.R.; Wolff, C.; Vössing, M.; Schmidt, J.-P. Towards Enabling Cyber-Physical Systems in Brownfield Environments. In *Exploring Service Science*; Satzger, G., Patrício, L., Zaki, M., Kühl, N., Hottum, P., Eds.; Springer International Publishing: Cham, Switzerland, 2018; pp. 165–176, ISBN 978-3-030-00712-6.

84. Damianov, D.; Demirova, S. Principles of Designing Automated Logistics Systems—Hybrid Component of Cyber-Physical Systems. In Proceedings of the 2018 International Conference on High Technology for Sustainable Development (HiTech), Sofia, Bulgaria, 11–14 June 2018; pp. 1–4, ISBN 978-1-5386-7039-2.

85. Park, K.T.; Son, Y.H.; Noh, S.D. The architectural framework of a cyber physical logistics system for digital-twin-based supply chain control. *Int. J. Prod. Res.* **2020**, 1–22, doi:10.1080/00207543.2020.1788738.

86. Winkelhaus, S.; Grosse, E.H. Logistics 4.0: A systematic review towards a new logistics system. *Int. J. Prod. Res.* **2020**, *58*, 18–43, doi:10.1080/00207543.2019.1612964.

87. Phillips, B.; Gamess, E.; Krishnaprasad, S. An Evaluation of Machine Learning-based Anomaly Detection in a SCADA System Using the Modbus Protocol. In Proceedings of the ACM SE '20: 2020 ACM Southeast Conference, Tampa, FL, USA, 2–4 April *2020*; Chang, M., Lo, D., Gamess, E., Eds.; ACM: New York, NY, USA, 2020; pp. 188–196, ISBN 9781450371056.

88. Gu, X.; Liu, G.; Li, B. (Eds.) *Machine Learning and Intelligent Communications*; Springer International Publishing: Cham, Switzerland, 2018; ISBN 978-3-319-73446-0.

89. Li, S.-C.; Huang, Y.; Tai, B.-C.; Lin, C.-T. Using Data Mining Methods to Detect Simulated Intrusions on a Modbus Network. In Proceedings of the 2017 IEEE 7th International Symposium on Cloud and Service Computing (SC2), Kanazawa, Japan, 22–25 November 2017; pp. 143–148, ISBN 978-1-5386-5862-8.

A 5   Publication 5

Author contributions:

1. B.J. Ralph: Conceptualization, Methodology, Software, Validation, Formal Analysis, Data Curation, Writing - Original Draft, Writing - Review & Editing, Visualization, Supervision, Project Administration

2. M. Sorger: Methodology, Software, Validation, Formal Analysis, Data Curation, Writing - Original Draft, Writing - Review & Editing, Visualization

3. K. Hartl: Methodology, Formal Investigation, Writing - Original Draft

4. A. Schwarz-Gsaxner: Formal Investigation

5. F. Messner: Data Curation, Software

6. M. Stockinger: Resources, Supervision, Writing - Review & Editing

Transformation of a rolling mill aggregate to a cyber physical production system: from sensor retrofitting to machine learning

Benjamin James Ralph[1] · Marcel Sorger[1] · Karin Hartl[1] · Andreas Schwarz-Gsaxner[1] · Florian Messner[1] · Martin Stockinger[1]

Abstract

This paper describes the transformation of a rolling mill aggregate from a stand-alone solution to a fully integrated cyber physical production system. Within this process, already existing load cells were substituted and additional inductive and magnetic displacement sensors were applied. After calibration, those were fully integrated into a six-layer digitalization architecture at the Smart Forming Lab at the Chair of Metal Forming (Montanuniversitaet Leoben). Within this framework, two front end human machine interfaces were designed, where the first one serves as a condition monitoring system during the rolling process. The second user interface visualizes the result of a resilient machine learning algorithm, which was designed using Python and is not just able to predict and adapt the resulting rolling schedule of a defined metal sheet, but also to learn from additional rolling mill schedules carried out. This algorithm was created on the basis of a black box approach, using data from more than 1900 milling steps with varying roll gap height, sheet width and friction conditions. As a result, the developed program is able to interpolate and extrapolate between these parameters as well as different initial sheet thicknesses, serving as a digital twin for data-based recommendations on schedule changes between different rolling process steps. Furthermore, via the second user interface, it is possible to visualize the influence of this parameters on the result of the milling process. As the whole layer system runs on an internal server at the university, students and other interested parties are able to access the visualization and can therefore use the environment to deepen their knowledge within the characteristics and influence of the sheet metal rolling process as well as data science and especially fundamentals of machine learning. This algorithm also serves as a basis for further integration of materials science based data for the prediction of the influence of different materials on the rolling result. To do so, the rolled specimens were also analyzed regarding the influence of the plastic strain path on their mechanical properties, including anisotropy and materials' strength.

Keywords Cyber physical production system · Retrofitting · Digitalization · Digital twin · Machine learning · Smart Forming Lab · Industry 4.0

Introduction

The ongoing fourth industrial revolution forces manufacturers around the globe to face significant changes in their possibilities to plan and steer production processes and overlying operations (Zheng et al., 2021; Zhong et al., 2017). Despite all the advantages the connection and network technologies offer (e.g. digital value chain, one-piece flow concept, circular economy), there are crucial thresholds to overcome in order to implement digitalization technologies in a successful and sustainable way (Enyoghasi & Badurdeen, 2021; Gupta et al., 2021; Reiman et al., 2021). These thresholds can be divided into investment (economic related) and socio-cultural (management and psychology related) challenges. Regarding investment issues, especially SMEs face a serious problem, as most digitalization approaches are highly scalable, making the amortization time for necessary investments much longer for this kind of businesses (Müller et al., 2018). This also includes the required human capital to implement infrastructure changes within a company. To sustain the digital change in the manufacturing environment, responsible managers must be aware of potentials and possible threats on

✉ Benjamin James Ralph
   benjamin.ralph@unileoben.ac.at

[1] Chair of Metal Forming, Montanuniversität Leoben, Franz Josef Strasse 18, 8700 Leoben, Austria

Ⓢ Springer

the technical as well as working environment layer (Akkaya, 2019).

To contribute to the solution of these issues, this paper focusses on two main objectives:

a. Reducing the investment costs for smaller companies by using mainly open source software (SW) and cost-effective but suitablē hardware (HW),
b. Development of a resilient Cyber Physical Production System (CPPS) which can be used to educate engineering students and therefore future production managers as well as other interested parties from the manufacturing industry segment in the topic of digitalization and associated technologies.

In order to create a case study which fulfills the requirements of (a) and (b), an already existing metal forming aggregate at the Smart Forming Lab (SFL) at the Chair of Metal Forming (CMF) of the Montanuniversitaet Leoben was chosen (Ralph et al., 2020). For this purpose, the CMFs rolling mill aggregate was used, as it can serve as an ideal example of how retrofitting from sensor application up to implemented machine learning algorithms can be integrated successfully in a low-cost (LC) resilient digitalization layer architecture (Ralph et al., 2021a, 2021b, 2021c). This brownfield approach is also a common initial state within the metal forming and metallurgical environment, as the production asset life span tends to be significantly higher than in other industry segments (Ball et al., 2020; Elkins et al., 2004). Especially considering SMEs and their lower investment budget, brownfield approaches dominate when it comes to digitalization approaches in comparison to corresponding greenfield investments (Sorensen et al., 2019).

Further considering this financial restrictions, most SMEs face, LC solutions based on open-source software tend to be a suitable option for the implementation of Industry 4.0 related digitalization approaches (Buer et al., 2021; Denicolai et al., 2021; Dutta et al., 2021). Furthermore, as the metal forming industry heavily relies on process models to decrease the quality related costs, this software can support the integration of these models within the manufacturing operations, as most solutions tend to have more suitable interfaces to connect directly with simulation related program environments (Ralph et al., 2021a, 2021b, 2021c; Schwarz et al., 2021). One disadvantage of this approach are the required skill sets to maintain and adapt such open-source solutions, as IT skills remain a scarce resource especially in SMEs operating in the manufacturing environment (Dethine et al., 2020; Eller et al., 2020; Kergroach, 2020).

For this reason, this paper demonstrates a new approach for the transformation of outdated machine systems into CPPS, demonstrated by a rolling mill system initially put into operation in 1954. The novelty within this approach is the focus on suitable low-cost hardware and open-source software wherever applicable, to consider the limited financial capabilities of most SMEs and similar facilities. Furthermore, by taking into account the possible lack of IT-specialists within this environment, the user-friendliness in terms of operating and mainting this kind of CPPS was another special focus of this work. Based on the rolling mill example, this paper describes the most important principles of sheet metal rolling and an SME tailored CPPS approach in (2), followed by the initial setup before the transformation of the respective machine system in (3). Section 4 describes the required and applied sensor technology (4.1) as well as the digitization of the given sensor data (4.2), whereas the sensor selection was based on the principle of low-cost by maintaining sufficent accuracy, connectivity and reliability. In (5), the upfollowing digitalization approach including an appropriate HMI is discussed, based on the same requirements as in (4). Section 6 demonstrates the development, implementation and validation of the machine learning algorithm for the system including an additional GUI for the ML application. In (7), the resulting LC user-friendly CPPS is summarized and discussed, followed by a conclusion and a corresponding outlook in (8).

Fundamentals of the rolling process and CPPS

Within this chapter, the most important characteristics of the rolling process as well as a common definition of a CPPS are introduced. Based on these definitions, the case study will be elaborated, beginning with the initial state (3), followed by digitization (4) and digitalization (5) and the developed data driven (black box) digital twin setup (6) (Ralph & Stockinger, 2020).

The rolling process

According to DIN 8580, rolling belongs to the manufacturing processes of forming under compressive loads and to the group of direct forming processes. During the process, a sheet material is formed through the roll gap between at least two rotating rolls, leading to a reduction in the cross-section of the rolled material. (German Institute for Standardization).

During the rolling process, a force flow occurs through the roll stand as a result of the load applied to the processed material. All parts of the roll stand that are directly or indirectly affected from the force flow, undergo an elastic deformation (Wang et al., 2017). Affected parts are the rolls, roll bearings, load cells, adjusting elements and the roll stand itself. This elastic deformation causes the roll gap to increase, from the
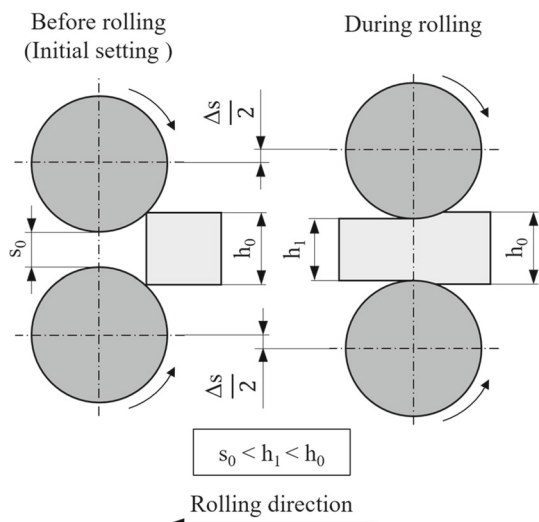
Fig. 1 Geometry change during rolling

Fig. 2 Work diagram for rolling for a defined s_0

initial (set) gap s_0 to s_1, whereas the difference between is defined as Δs (Fig. 1).

$$\Delta s = s_1 - s_0 \qquad (1)$$

The end thickness of the rolled sheet h_1 can be calculated according to the Gage-meter equation (Lee & Lee, 1999). The Gage-meter equation specifies the expected exit thickness of the rolled material h_1 depending on the initial roll gap height s_0 and the elastic deformation, which depends on the rolling force F_R and the stand modulus C. The elastic deformation of the aggregate is characterized by C and corresponds to the slope of the roll stand module in the rolling gap diagram.

$$h_1 = s_0 + \frac{F_R}{C} \qquad (2)$$

The rolling gap diagram shows the rolling force F_R over s_0 and initial material thickness h_0 (Fig. 2).

The point of intersection between the roll stand characteristic curve, defined by the slope C, and the materials characteristic curve, defined by the material module in the rolling gap diagram is called the working point (A). A provides information on the exit height of the rolled sheet h_1 as a function of F_R (Fig. 2).

It is important to note that the influence of sheet metal width is not considered as influencing factor of C, but included in the material module. The first hypothesis this paper aims to test can be stated as follows:

- The friction state and resulting rolling force deviations mainly depend on the initial sheet geometry.
  Therefore, the contact surface in the roll gap increases the resulting rolling force significantly more than the effect of
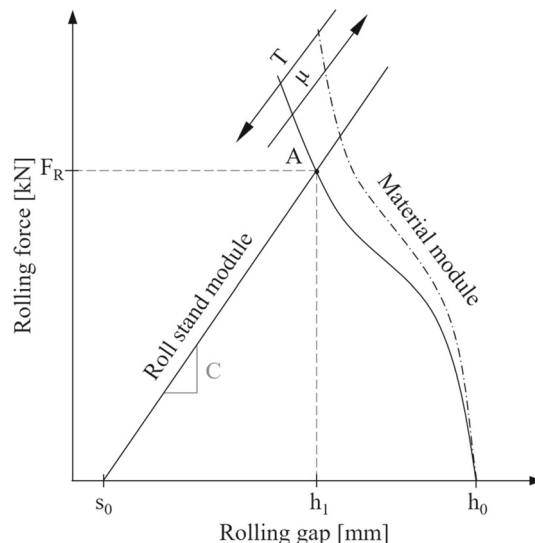
a rougher surface topology. In addition, the approximated linear behavior of C is given for one s_0.
The second hypothesis tested within this work and to be elaborate more deeply in Sect. 6 is defined as follows:

- The stand modulus C behaves non-linear as a function of varying s_0 and the overall difference between h_0 and h_1, Δh.

Similar to hypothesis 1, an influence on the material behavior (e.g. due to work hardening) can be observed, although the authors state that the force flow through the machine system also contributes significantly to the change in h_1, which as a consequence results in a dependency of C on Δh.

$$\Delta h = h_0 - h_1 \qquad (3)$$

Cyber physical production systems (CPPS)

CPPS can be defined as a derivative from Cyber Physical Systems (CPS), especially tailored to the production segment. Although CPS and CPPS are heavily researched in the past years, there is still no standardized definition for this technology framework (Wu et al., 2020).

According to Wu et al. (2020), the most accepted definition can be derived from the work of Cardin (2019) who extended a previous definition from Monostori et al. (2016) to the following statements:

1. CPPS are superordinate systems within systems.
2. CPPS consist of cooperative elements, those connect with each other situationally appropriate, on and between all different levels within the production environment, from

Table 1 LC user centered CPPS: further adaption and concretization by the authors (Wu et al., 2020)

	Criteria	Concretization
I	System in a system	Data exchange and process adaptions on other upcoming process steps based on gathered data from the rolling mill through a unified network layer
II	Situationally appropriate connection and data transfer on different layers	Change in data storage frequency based on actual machine status (on/off) and state dependent data publishing route within the layer system
III	Enhance decision making process in real time and state dependent	Implementation of a machine learning algorithm that predicts results of the actual process step and upcoming process steps in near real time including the capability of adaption of the prediction due to foreseen and unforeseen events
IV	User centered GUI	Two user friendly front end and two (IT-skilled) user friendly back end interfaces
V	LC and resilient design	Finding the optimum of cost-effective HW and SW solutions under the restriction of resilient, robust and easy to use solutions

the processes itself, through involved machines up to overlaying networks, e.g. MES or ERP-systems.

3. CPPS enhance decision making processes in real-time in a resilient and robust way, with respect to time as well as foreseen and unforeseen events (Wu et al., 2020).

The fulfillment of (1), (2) and (3) for the case study presented in this paper will be demonstrated in the following chapters. In order to do so, these very broad conditions have to be concretized. Despite this requirements, the practicability for learning purposes as well as financial restrictions (e.g. for the implementation in a SME or academic learning environment) were considered. Most important, the user friendliness of a CPPS will also be in focus of this study. Therefore, the development of shop-floor friendly, intuitive Human Machine Interfaces (HMIs) are a central point in this work. Additionally, LC solutions to avoid expensive maintenance and update plans were used wherever possible. Table 1 summarizes the specifications of the LC user centered CPPS developed within this paper.

Initial machine and digitalization set up

This chapter describes the initial state of the existing infrastructure at the SFL, whereas (3.1) focusses on the IT-layer structure and (3.2) shows the initial state of the rolling mill system to integrate into the layer architecture.

The six-layer architecture at the SFL

Figure 3 shows the initial layer system implemented at the SFL. Before the integration of the milling system, a CNC lathe (type EMCOTURN E65) was connected with a power measurement unit into a condition monitoring system, powered by a WAGO controller with integrated warm memory storage (type PFC200 G2 2ETH RS). The unrefined data (e.g. phase currents, voltages) is pre-processed, agglomerated and uploaded on the internal server structure at the SFL, using the structured text (STS) based WAGO e-cockpit SW, after A/D transmission via additional modules (type WAGO 750-494). Within the STS environment, an additional condition monitoring system and corresponding GUI was programmed. The server-stored data is extracted autonomously with a Python based script, running on the same server environment. This script extracts and transforms the data into a set up SQL database, from which most important project management (PM) data is published near real time on a PHP based PM tool (Ralph et al., 2021a, 2021b, 2021c).

The layer architecture was initially created with the purpose of connecting different machine systems at the SFL step by step, including not only condition monitoring and PM-related data, but also process data and, as final objective, resulting in different LC user centered CPPS. Therefore, the five criteria defined in Table 1 were already considered within the planning and development of this structure (Fig. 3).

The rolling mill system

The rolling mill system at the SFL at the CMF is a duo rolling mill and was built and put into operation in 1954. The hand wheel at the top of the rolling mill is used to adjust the height of the roll gap (Fig. 4) and rotates the guide spindle via gears, which increases or decreases the height of the rolling gap depending on the direction of rotation. An adjustment of 0.07 mm per gear tooth was used as a parameter for adjusting the roll gap height.

More than a decade ago, the machine was equipped with two load cells to measure the rolling force on the left and right guide spindle. Figure 5 shows the initial load cell mounted
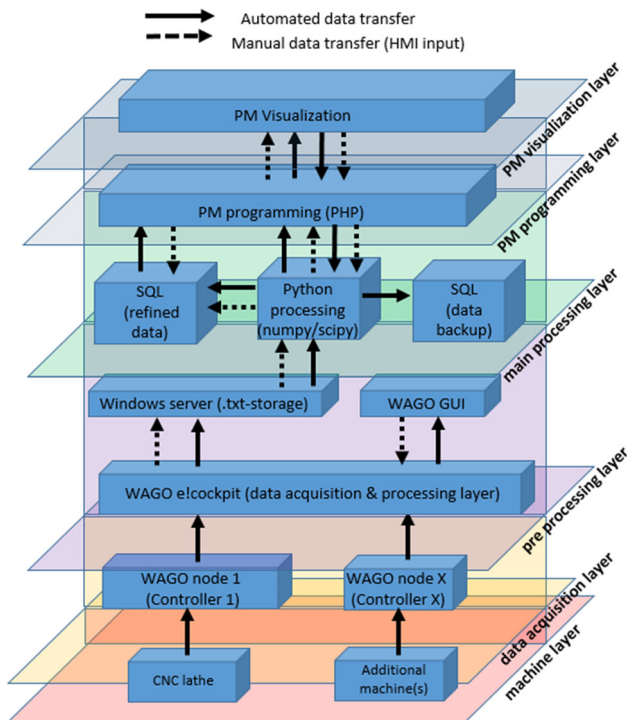
Fig. 3 Initial state of the six-layer architecture at the SFL (Ralph et al., 2021a, 2021b, 2021c)
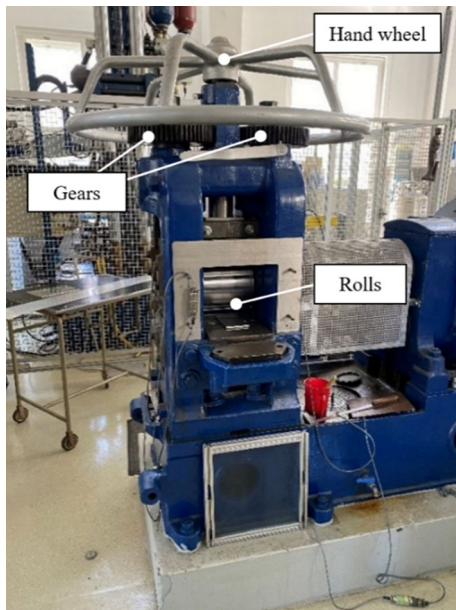

Fig. 4 Rolling mill system: initial state

between the left guide spindle and the roll chock. The data acquisition during a milling process, in order to obtain the actual F_R with corresponding time increments, was done with a proprietary Windows XP based DAQ system, with a maximum data transmission frequency of 22.5 Hz.
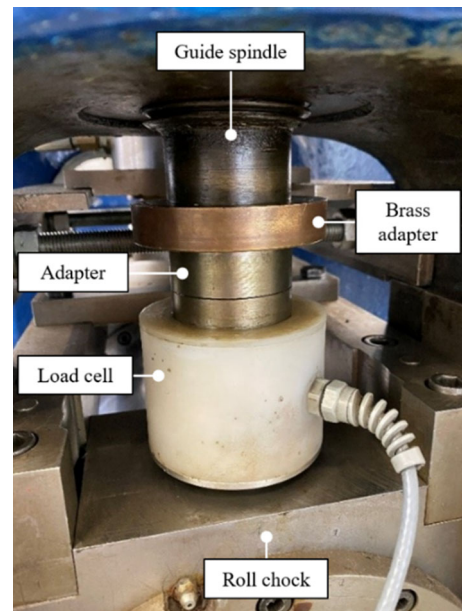

Fig. 5 Load cell of the left guide spindle: initial state

Retrofitting and digitization

The following subchapters describe the sensor retrofitting (4.1) as well as corresponding digitization (4.2) and therefore coupling of the calibrated sensors to the SFLs six-layer architecture. All actions taken for the sensor selection, calibration and implementation underly the assumptions made in (2.1) (the required physical quantities) and (3.2) (the physical limits of the machine system itself).

Sensor retrofitting

In order to choose appropriate sensors to meet the criteria of a LC user centered CPPS, the required specifications were defined in first instance. Based on these requirements, the sensor technology was selected. In addition to the required magnitude of the sensors, parameters such as linearity and resolution play a major role in the resulting quality of the recorded data and in the selection of suitable sensor technologies. Furthermore, the maximum resolution of the DAQ system must be taken into account, as in most terms the bottleneck is not the measurement of an analog signal or the signal transfer through an A/D converter but the buffering and writing of gathered data on the controlling unit (Fig. 3, data acquisition layer). In order to implement a machine learning algorithm based on Eqs. (1) and (2) and therefore satisfy condition III, Table 2 shows the minimum quantities to be measured to achieve such a system. The measurement range is a result of the rolling mill systems specifications.

For the measurement of F_R, the already existing load cells had to be replaced, as the maximum measurement range

Table 2 Quantities and corresponding range to be measured to ensure valid data gathering within the required operational range

System parameter	Measurement range
F_R	0–400 kN
s_0	0–20 mm

Table 4 External electronics and specifications from the sensors to be implemented

External electronics	Type	Sensor	Output
PR electronics 2261	mV transmitter	Load cell	0–20 mA
Waycon LV-S-25-300-KA05-L10	Integrated electronic (n/a)	LVDT	4–20 mA

of each cell was defined with 150 kN. Furthermore, after calibration and analysis of the resulting data, a significant deviation between both cells and high non-linearity in each measurement system was detected, indicating a malfunction within at least one of them.

For the new load cell measurement system, despite the specified range, the following requirements had to be fulfilled:

a. The measuring system must be able to withstand an overload to avoid measuring errors and shortened lifespan (Table 1, V).
b. The load cells must have a high linearity in order to be able to resolve the rolling force to a sufficient degree during the rolling process (Table 1) (III).

Additionally, the initial roll gap s_0 and with it, the change of the gap during the rolling process had to be measured with sufficient linearity and within the defined range. Based on heuristic knowledge and basic calculations, the deflection of the roll gap could be defined in the range of tenths of a millimeter, while the maximum height of the roll gap is constricted by the machines' geometry to 20 mm. Since the linearity of a sensor is specified as a percentage of the measuring range, two conditions must be met:

c. The sensor must be able to measure a distance greater than the maximum adjustable roll gap and
d. must have a high linearity in order to be able to resolve the deflection of the roll gap to a sufficient degree during rolling (Table 1, III).

To meet the requirements of (c), (d), and the defined measurement range in a cost-effective manner (Table 1, I), a linear variable differential transformer (LVDT) sensor was chosen. In addition, an angle sensor was attached to the gear of the hand wheel for demonstration purposes to students and other interested parties at the SFL.
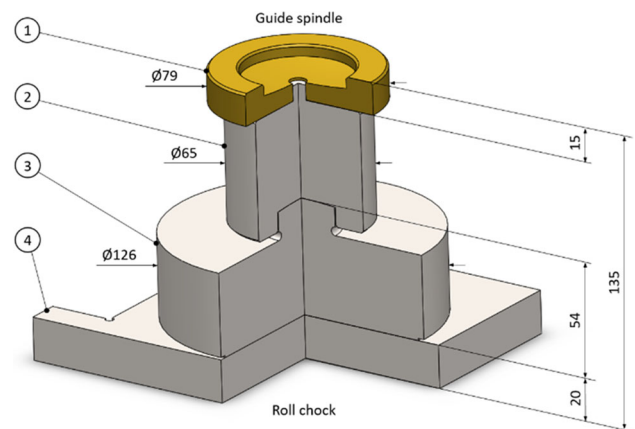

Fig. 6 Construction scheme of the new designed load measurement unit

Table 3 shows the finally selected sensors and their specifications.

Table 4 defines the external electronics used to transfer the sensor signals into a suitable analog signal for the DAQ system. For the LVDT sensor, the external electronics from the same manufacturer was used. External electronics from a third-party supplier were installed for the load cells. These mV transmitters can be individually configured to the specifications and requirements of the load cell and can therefore also be used if the load cells are replaced.

In order to mount the selected sensors on the rolling mill, mechanical adaptions had to be made. Since the diameter of the new load cells is larger than the width of the roller supports, the entire contact surface at the bottom of the load cell cannot be supported. This could lead to a falsification of the measurement results. In order to be able to use the entire contact surface of the new load cell, an intermediate plate was installed between the roll chock and the load cell. To connect the guide spindle with the load cell, an additional adaptor was designed to transmit the rolling force coaxially (Figs. 6, 7).

Table 3 Selected sensors and their specifications for the transformation of the rolling mill system according to the fundamental equations pointed out in Sect. 2

Sensor	Type	Range	Linearity	Output signal
Kern CR 20000-1Q1	Load cell	0–200 kN	0.1%	2 mV/V
Waycon LV-S-25–300-KA05-L10	LVDT	0–25 mm	0.1%	n/a
ASM PH36	Magnetic multiturn encoder	$31 \times 360°$	$\pm(2° + 0.015\%)$	4–20 mA
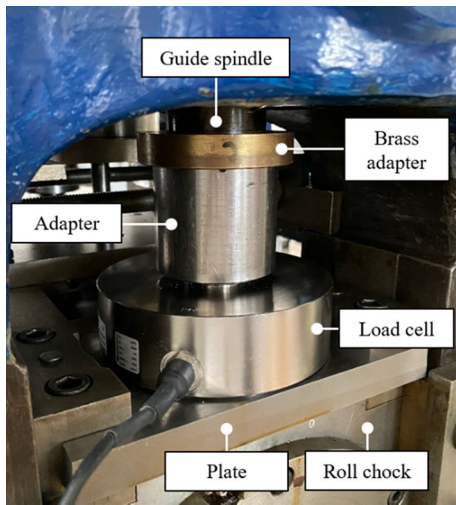
Fig. 7 Resulting implementation of the new designed load measurement unit

Fig. 8 Mounted LVDT sensor

Fig. 9 Mounted multiturn encoder
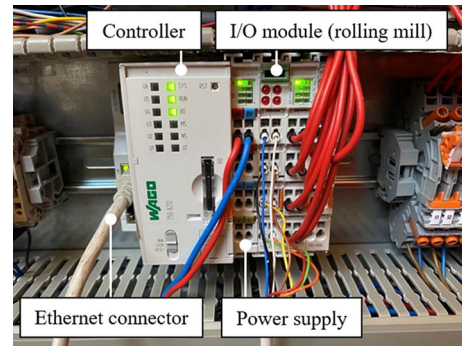
Fig. 10 Controller and I/O modules
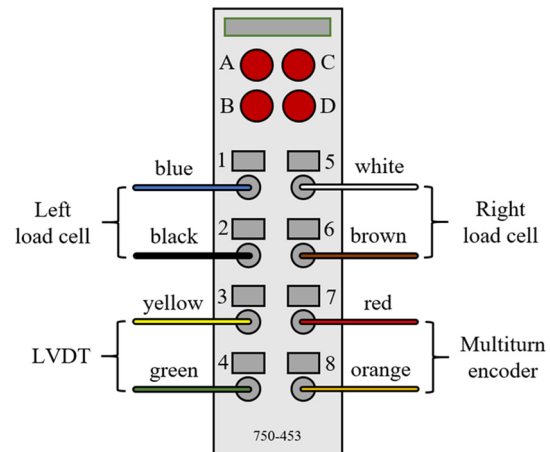
Fig. 11 Circuit diagram of the connection rolling mill sensors/DAQ
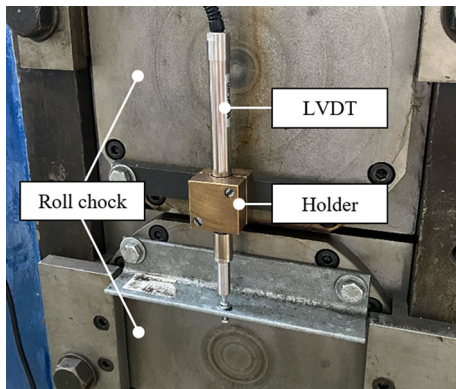
The LVDT sensor was mounted between the two roll chocks. In order to prevent interferences with the inductive measuring principle, the sensor holder is made of non-magnetic material (Fig. 8).

The multiturn encoder was mounted directly on the machine rack. The resulting angle after manual roll gap changing is derived via the connection of the sensor with one of the two main gears at the mill, which are connected to the hand wheel via a defined gear transmission ratio. To consider the surface roughness of the gear and therefore ensure contact between the sensor and the gear, a pre-stressed spring is applied to ensure continuous contact (Fig. 9).

Digitization

In order to convert the analog signals from the external electronics (Table 4) into signals suitable for computer-aided processing, the devices were connected to the already existing WAGO node 1 (Fig. 3, data acquisition layer). This node consists of a WAGO PFC200 G2 2ETH RS controller coupled with I/O modules (Fig. 10). The I/O modules used are from the same supplier (type 750-453) and are designed for transforming analog signals in the range of 0 to 20 mA. As already mentioned, the resolution depends on the DAQ, which can resolve the analog signals of the sensors in 15 bit, therefore the analog signal of each sensor can be resolved in 2^{15} equivalent steps.

Figure 11 shows the corresponding connections of the three mill sensors with the used I/O module.
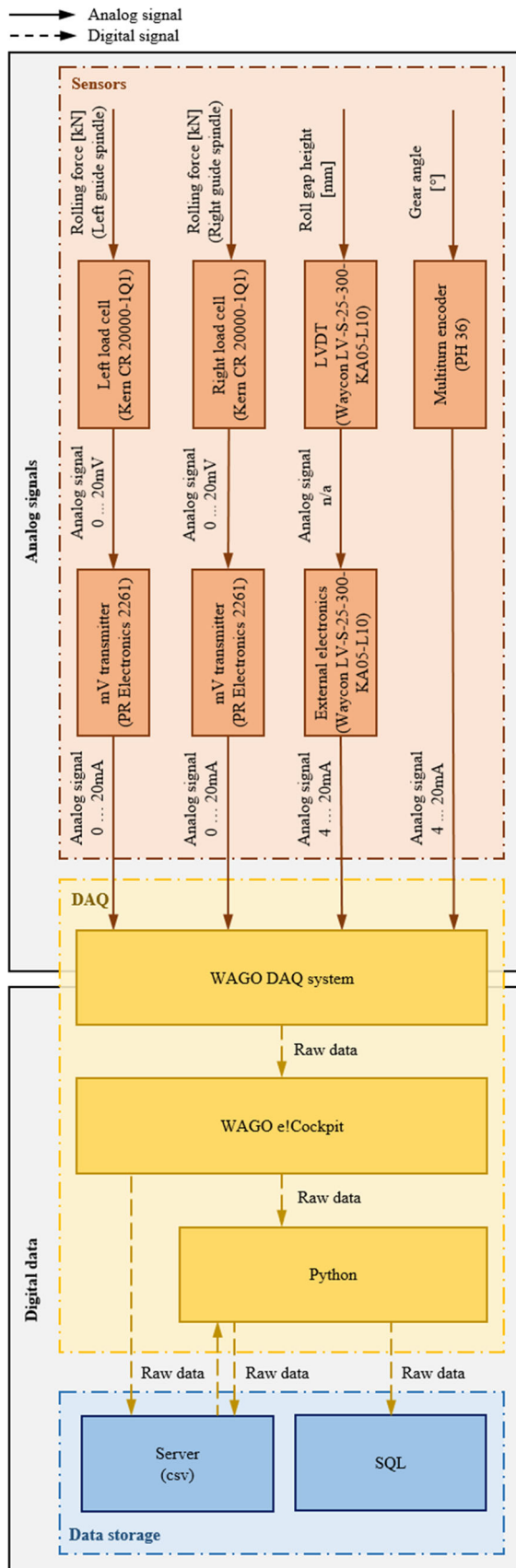
Fig. 12 Sensor connection and A/D conversion
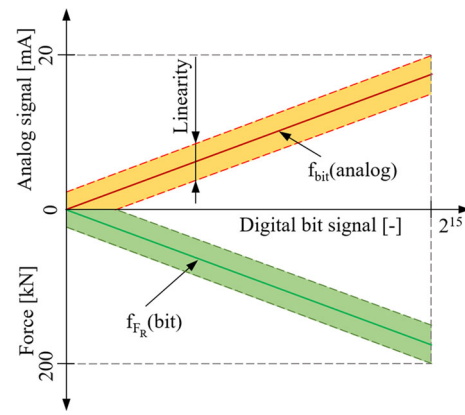
Fig. 13 A/D input signal to physical quantity transformation: example rolling mill
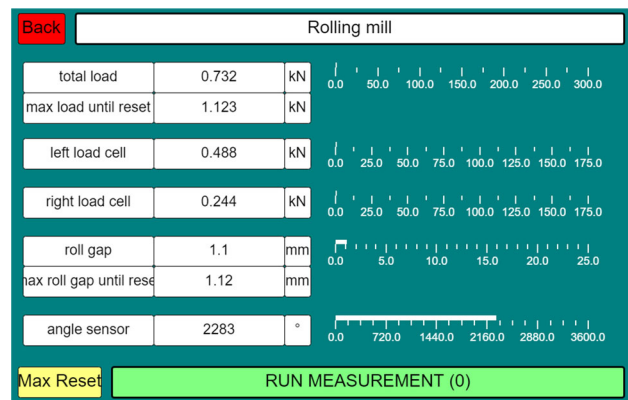
Fig. 14 Rolling mill layer of the WAGO GUI
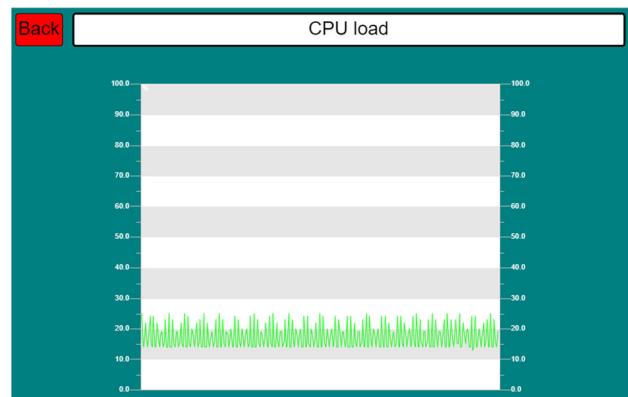
Fig. 15 CPU load layer of Node 1: connected machines turned off

Figure 12 shows the final digitization framework for all three sensor types, from the physical measurement entity to the implementation into the layer framework. It is important to note that the used WAGO DAQ system isn't the most cost efficient possibility to connect the machine within such a system (e.g. Arduino based microcontroller would have been a more LC alternative). Under consideration of practicability and longtime maintainability, the use of a stan-

Table 5 Coefficients for the linear characteristic curve of implemented sensors according to Tables 3 and 4

Physical quantity	a	b	Range
F_R (kN)	0.0	6.104E–3	0–200 kN
s_0, s_1 (mm)	6.5536E+3	9.537E–4	0–25 mm
deg (°)	6.5536E+3	4.257E–1	$0–31 \times 360°$

dardized framework which operates on industrial standards like the WAGO system or other comparable solutions was chosen. Another reason for this decision is the user friendly back end GUI, that comes within the SW and that allows non IT-personnel to supervise and even extend programmed functionalities with basic IT knowledge (e.g. the usage of predefined module blocks within the SW instead of STS coding). This advantages also apply for the first developed front end GUI, which is also based on the same framework.

Digitalization

This chapter describes the transformation of digitalized sensor data within the layer architecture. After A/D conversion, resulting digital signals have to be transformed into real physical quantities. This is done within the data preprocessing layer (Fig. 3) using STS based programming and an additional Python script. Additionally, state dependent data gathering frequency is set within this layer (5.1), fullfilling the requirements of I and II (Table 1). (5.2) describes the adaption of the first front-end GUI for the rolling mill setup (according to Table 1, IV).

Data pre-processing layer

Before working with the digitized signal data is possible, transformation of the resulting data into corresponding physical quantities has to be done. This operation is carried out within the data pre-processing layer (Fig. 3) using the STS environment provided by the WAGO SW. All three sensor types can be calibrated linearly under consideration of their characteristic linearity (Table 3). As a result, a linear equation was programmed for each input channel, whereas the two individual coefficients were derived as a result of the range restriction of the specific device.

$$f(physical quantity) = a + b * bit\_value \qquad (4)$$

Figure 13 visualizes the transformation of the current signal into its physical value on the example of the load cells used schematically.

Table 5 displays the resulting coefficients for all three sensor types on the basis of Eq. (4).

The resulting F_R is then obtained summarizing the values from both load cells within the STS environment. This approach also ensures that eccentric sheet insertion can be measured and do not result in a higher measurement error.

To fulfill requirement II. (Table 1), two different sampling rates for all rolling mill channels were defined. The first one is enabled continuously. In this case, 1 Hz was set within the STS. This low frequency is used to work as a simple condition monitoring system, giving warnings over the WAGO GUI (Sect. 5.2) whenever sensor values are out of calibrated range. For the actual processing, via a trigger that can be manually turned on within the GUI, a sampling frequency of 500 Hz was determined. In this case a Boolean variable is turned TRUE, which activates the higher rate, whereas the lower frequency stays enabled. After the actual process, the user can end the measurement again manually through the GUI, which sets the Boolean equal FALSE again. The major advantage through the manual activation is the possibility of measuring unconventional processes or trials, which would not be measured if the higher sampling rate would be activated by a force or dilation triggered algorithm (e.g. very thin sheets with low resulting F_R, very soft material with low Δs).While the continuous data gathered is directly stored on the CMFs' internal server, the actual 500 Hz measurements have to be refined additionally before data science and machine learning algorithms can be used on it. This refinement algorithm is carried out within a simple Python script, which deletes numerical artefacts and duplicates from the given raw data. Numerical artefacts are lines that may occur due to buffering issues on the used controller unit. As the controller is initially not able to obtain frequency rates above 100 Hz, a script that uses the controllers' RAM instead of warm memory was written and implemented in the STS environment. Nevertheless, the buffering operation stores data points until a defined extend, before submitting these data points to be actually written on the controllers' internal memory. During the writing process, doubled data points within the same time stamp occur. Additionally, lines with zeros or NaN values are a result of this procedure. To avoid errors at upcoming mathematical operations (6.2, 6.3), these data points and corresponding rows have to be filtered first.

WAGO based GUI

The already existing WAGO GUI was extended with an additional layer for the rolling mill system, taking into account the preferences of involved technicians on the shop-floor level. The GUI runs on the controlling unit and is available through the corresponding IPv4 address with all computing devices within the SFL network. Figure 14 shows the STS programmed rolling mill layer within the GUI. Additional to the two resulting loading force values and sum of both, another variable is visualized, which is named "max load until reset".

This variable returns the maximum value stored at a current measurement. If the "Max Reset" button is pressed, the variable is set to 0. The same function is given for the variable "max roll gap until reset", to be able to see the maximum height and force within a measurement, whereas all other variables defined return the real time value from the respective sensors. Depending on the status of the Boolean "Run Measurement", the sampling rate is whether 1 Hz (Boolean = FALSE, button = GREEN (Fig. 14) or 500 Hz (Boolean = TRUE, button = RED). The parenthesized integer next is coupled with a counter in the STS, which counts up for each measurement executed within the same day. If the day within the timestamp changes, the counter is reset to 0. As the automatic export of high frequency measurement data is done in single files, named "YEAR-MONTH-TRIAL-NR", the Python filter algorithm can easily distinguish between appending files within the defined folder. In order to prevent overloading of the rolling stand and power train, the visualization of force only contains a range of 0–300 kN. This ensures that the aggregate is not permanently operated at its load limit.

As mentioned in 5.2, the data storage from the I/O module is executed directly in the hot memory of the controller. Therefore, another layer was developed, which shows the actual CPU load of the respective controller. If this load exceeds 60%, writing and therefore accurate data gathering from connected sensors cannot be guaranteed. This value is reached within this setup if both connected aggregates are activated and the sampling frequency of the rolling mill exceeds about 0.560 kHz. If 60% are reached, another Boolean in the STS is set TRUE and a warning signal is shown at the main display. Figure 15 shows the CPU load GUI both connected machines disabled.

Machine learning algorithm and decision enhancing digital twin

After successful digitization (4) and digitalization (Sect. 5), III. (Table 1) has to be fulfilled. For this purpose, the connected rolling mill system had to be equipped with a suitable and efficient algorithm to support decision making within the milling process. As the correlation between the most important variables (Sect. 2.1) is rather complex in practice, a data driven modelling approach was chosen in first instance. This data driven model should be resilient, robust and easy to understand. Therefore, the complex and non-linear real-physical interrelationships between the machine system and processed material were discretized and transformed into a system of interdependent linear equations, calculated within the Python environment (Sect. 6.4). To avoid unrealistic or unreproducible results, a statistical approach was chosen (Sect. 6.1). Additionally, as the focus in this work lies on the

Table 6 Defined rolling schedules for data gathering, from high height reduction per process step (V_1) to moderate (V_3)

Nr	$s_0(V_1)$ (mm)	$s_0(V_2)$ (mm)	$s_0(V_3)$ (mm)
1	4.50	5.00	5.00
2	3.50	4.00	4.50
3	2.75	3.50	4.00
4	1.75	2.50	3.50
5	1.00	1.50	3.00
6	0.75	1.00	2.50
7	0.50	0.50	2.00
8	–	–	1.50
9	–	–	1.00
10	–	–	0.50

calibration of the stand module C with all relevant dependencies, a well characterized material (Sect. 6.2) was chosen for the first setup. As a result, the second front-end GUI mentioned initially in this paper is presented and explained (Sect. 6.5).

Experimental setup

According to hypothesis 1 and 2 (2.1), the stand module C is a function of the processed sheet width b as well as Δh and s_0. Despite this statement, another important influencing factor in practice is the usage of an appropriate lubricant. Therefore, the following dependencies have been investigated within this experiment:

$$C = C(s_0, b, \Delta h, \mu_{lubricant}) \qquad (5)$$

For the initial calibration, $\mu_{lubricant}$ describes the change between sufficient lubrication and no lubrication. To be able to develop a data driven prediction model for the rolling process, three different rolling schedules (V_1, V_2 and V_3) were defined (Table 6). The main objective of this setup was to get a broad set of data points for different $s_0(\Delta h)$, to investigate the influence of different combinations of these variables. To ensure comparability, an initial thickness of 6 mm and a final s_0 of 0.5 mm was defined for each rolling schedule.

By varying the rolling schedules according to Table 6, it is possible to investigate if different cumulated strain paths (Eq. 6) have an influence on the elastic behaviour of the mill stand and therefore C.

$$C(\Delta h_{ij}, s_{0_k}) =! C(\Delta h_{lm}, s_{0_n}) \qquad (6)$$

For the investigation of the influence of b, three widths for the initial test and calibration data setup were chosen. For the validation of the resulting equation system, two additional widths were defined, one between the three first and one

Table 7 Defined sheet widths and corresponding rolling schedules for data gathering

Nr	Width (mm)	Test/calibration	Validation
B_1	150.00	X	
B_2	100.00	X	
B_3	50.00	X	
B_4	74.50		Interpolation
B_5	30.10		Extrapolation

Table 8 Defined lubrication schemes for the corresponding rolling schedules and sheet widths defined in Tables 6 and 7

Test series	Description
T_1	Full lubrication
T_2	No lubrication

out of initial range, to be able to proof interpolation as well as extrapolation capabilities of the system (Table 7). For this validation experiments, rolling steps 1–4 from V_1 were used, followed by a direct height reduction from 1.75 to 0.75 mm (Table 6, $s_0(V_1)$). The fifth step was spared out to be able to see if the interpolation between known s_0 would obtain valid results within the developed machine learning algorithm.

To investigate the influence of lubrication on C, two different test series were defined, whereas test and calibration data sets were mirrored for both process friction states (Table 8).
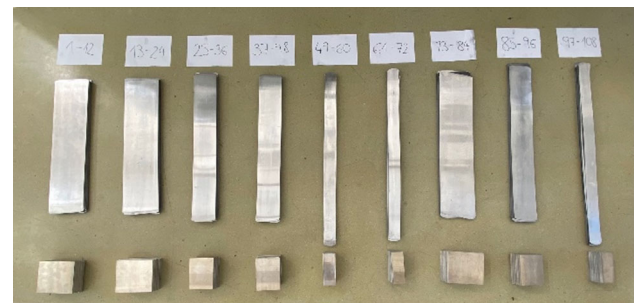
The sheet specimen for the rolling process has to be entered manually (Fig. 4). To avoid measuring errors due to deviations in the reproducibility of single process steps within the rolling schedule, a statistical approach has been chosen. For this experiment, twelve sheets for each tested rolling schedule, test series and width were cut out of two identical raw sheets. In sum, 216 sheets for the creation of test and calibration data were used, split into three different rolling schedules, three different widths and to different test series (Table 9). To ensure a smooth transition into the milling system, the initial length of each specimen was set to 135 mm. Additionally, each sheet was deburred and cleaned before treatment.

The configuration shown in Table 9 for each test series ensures a continuous reduction of s_0. In sum, 1736 milling process steps were carried out to gather the required test and calibration data. Figure 16 shows the processed specimens before and after rolling.

Table 10 shows the setup for the gathering of validation data. For this purpose, only 36 additional specimens were used and processed within T_1 (no lubrication) and rolling schedule V_1, whereas back up material was kept if the validation attempt in the resulting algorithm would fail. Including all process steps, a total of 1904 milling operations delivered output for the data driven modelling of the corresponding machine learning algorithm (Sect. 6.4).

Table 9 Specimen classification: resulting executed rolling schedules for the gathering of test/calibration data

Test series	Specimen nr	Rolling schedule	Sheet width
T_1	1–12	V_2	B_1
	13–24	V_3	B_1
	25–36	V_2	B_2
	37–48	V_3	B_2
	49–60	V_2	B_3
	61–72	V_3	B_3
	73–84	V_1	B_1
	85–96	V_1	B_2
	97–108	V_1	B_3
T_2	1–12	V_2	B_1
	13–24	V_3	B_1
	25–36	V_2	B_2
	37–48	V_3	B_2
	49–60	V_2	B_3
	61–72	V_3	B_3
	73–84	V_1	B_1
	85–96	V_1	B_2
	97–108	V_1	B_3

Fig. 16 Processed sheet specimens: rolled (T1, top); initial (T2, bottom)

Table 10 Specimen classification: rolling schedule, corresponding lubrication scheme and sheet with for the validation data

Test series	Specimen nr	Rolling schedule	Sheet width
T_2	109–124	V_1	B_4
(validation)	125–144	V_1	B_5

Deformation behavior of used material under rolling conditions

The material used in this study is EN AW-1050A, also referred to as Al 99.5, which is considered as technically pure aluminum due to its low content of constituents. Pure aluminum shows excellent ductility, exhibiting exceptionally good deformation behavior even after severe cold working. The hardening of the material introduced by forming can be attributed to the introduction and the multiplication of

dislocations during their migration. For deformations such as in a cold rolling process, the face-centered cubic (fcc) crystal structure determines the slip systems: primarily, slip is observed on {111}<110>-slip systems since the Peierl's stress is lowest in this direction. The stacking fault energy of about 170 mJm^{-2} in pure aluminum, which is comparatively high for fcc-structured metals, determines the predominant deformation mechanism of slip, rather than developing deformation twins (Simon, 1979).

The increase in strength introduced by cold working can be described in terms of increasing dislocation density. As a rough estimate, the dislocation density can be approximated by the increase in strength using Eq. (7).

$$\sigma = 0.5Gb\rho^{\frac{1}{2}} \tag{7}$$

In Eq. (7), σ is referred to as the strength, G is the shear modulus of the respective material, b is the burgers vector and ρ is the dislocation density. The higher the dislocation density, the lower the mean free path between the dislocations. As a result of their interaction, strength increases due to reduced mobility. The dislocation increase depends on the selected forming degrees, which are introduced into the material at certain height reductions Δh due to the rolling schedule. This increase in dislocations is opposed by certain softening processes since the condition including a high dislocation density is thermodynamically unstable. The most essential softening mechanisms represent recrystallization and recovery, the latter being crucial for aluminum due to the high stacking fault energy. For recrystallization to occur, both a critical degree of deformation and an elevated temperature of about 40% of the melting temperature are required, whereas both conditions are not met within this experimental setup (Gottstein, 2004).

During the rolling of a pure aluminum sheet, part of the applied forming energy is stored as deformation energy, the other, much larger part, dissipates in heat, driven by two phenomena: (1) the plastic deformation itself and resulting internal friction and (2) caused by tribological effects at the interface between the rolls and the sheet metal or the lubricant. These conditions favor the recovery processes which are characterized by facilitated cross-slipping of screw dislocations and climbing of step dislocations, thus causing annihilation of dislocations and therefore decreasing the dislocation density and the effect of cold working. These softening processes are diffusion-dependent, which occur at an accelerated rate under temperature increase, although room temperature is already sufficient to continue these processes to equilibrium when considering pure aluminum (Hasegawa & Kocks, 1979).

Therefore, strengthening due to cold working is already reduced at short time periods, leading to the conclusion that these processes do not have an effect on the corresponding
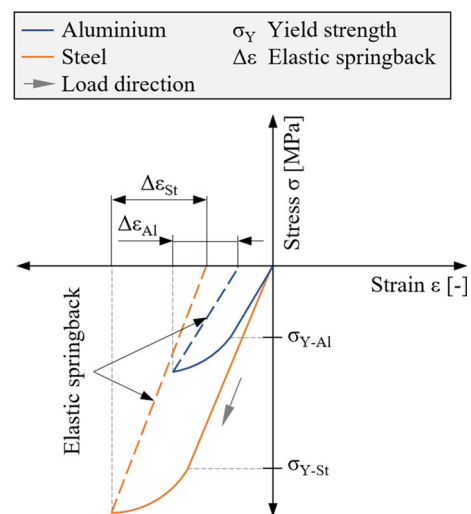

Fig. 17 Elastic stiffness and corresponding effect on h_1 during rolling

strength values. Despite the recovery effect, the heat transfer within the tribology system is of utmost importance for the rolling process within this case study.

Aluminum is furthermore characterized by its high thermal conductivity, which at approximately 220 W(mK)$^{-1}$ exceeds that of conventional steel grades by a factor of three. For this reason, the dissipated forming heat and heat generated by friction between the rolls and the sheet surface spreads rapidly over the entire specimen. As a result, the heat is more easily transferred to the lubricant and dissipated in this fluid. This phenomenon can have a substantial influence on the resulting behavior of the rolled specimen, especially considering different friction states (Ostermann, 2014).

Despite cold work hardening and thermal expansion, the elastic properties of the used material significantly contribute to the resulting process parameters in rolling. After the force is locally removed from the processed specimen, the elastic component of the strain applied results in an increase of the thickness h_1. As a result, materials with a lower Young's Modulus (YM) are increasing height after rolling significantly more than stiffer materials (Fig. 17).

Resulting experimental data

As expected from plastic deformation fundamentals, the resulting geometry changes of the tested specimens after rolling varies. The maximum bearable local plastic deformation wasn't exceeded at any specimen within the experiment, therefore the law of constant volume (Eq. 8) applies.

$$\ln \frac{l_1}{l_0} + \ln \frac{b_1}{b_0} + \ln \frac{h_1}{h_0} = \varphi_l + \varphi_b + \varphi_h = 1 \tag{8}$$

According to Eq. (8), l_1 can be obtained if b_1 and h_1 as well as the initial geometry is known. Before the resulting
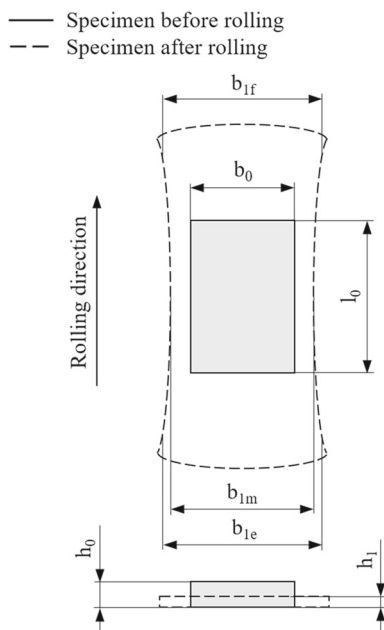
Fig. 18 Sheet width measurement after rolling

test and calibration data is analyzed from a black box point of view, a first indication about whether there is a difference between the two data series can be made after measuring the resulting sheet width of each specimen. This was made on three reproducible locations at each specimen, according to Fig. 18. Table 11 shows the mean value at each measured point for each calibration and validation series, additionally divided into test series T_1 and T_2.

As visualized in Table 11, the highest deviation in sheet width is 0.36%, which leads the authors to the statement that no differentiation between test and calibration data can be made. This also supports the theory, that the population of investigated specimens is valid. According to Sect. 6.2 and from a materials science point of view, there should also be no significant difference between sheets of same initial width that were rolled in different rolling schedules. Table 12 shows the standard deviation of all widths within a test series (V_1, V_2 and V_3).

Additional material related tests

To ensure that the definition of a CPPS according to Table 1 is fulfilled, additional validations were carried out (Condition III and V). The higher deviation between T_1 and T_2 within the same width indicates differences between the two test series, which, according to the authors, is the result of a changed tribology system. To investigate if this change significantly contributes to the resulting material behavior, tensile tests were carried out additionally. In order to characterize the mechanical anisotropy of the rolled sheets properly, a small but normed geometry was chosen to obtain stress–s-

Table 11 Specimen classification: resulting sheet widths of the exectuded rolling processes, measured at three points per sheet (test/calibration data)

T_1	Specimen nr	b_{1f} (mm)	b_{1m} (mm)	b_{1e} (mm)
Test data	1–6	150.93	150.82	150.95
Calibr. data	7–12	151.10	150.84	151.13
Dev. [%]		0.11	0.01	0.12
Test data	13–18	151.02	150.90	151.02
Calibr. data	19–24	151.08	150.90	151.15
Dev. (%)		0.04	0.00	0.09
Test data	25–30	101.06	100.86	100.76
Calibr. data	31–36	100.98	100.93	101.15
Dev. (%)		0.08	0.07	0.39
Test data	37–42	101.27	100.99	101.23
Calibr. data	43–48	101.11	100.90	101.09
Dev. (%)		0.16	0.08	0.14
Test data	49–54	51.71	51.35	51.68
Calibr. data	55–60	51.56	51.34	51.56
Dev. (%)		0.29	0.02	0.24
Test data	61–66	51.19	51.00	51.22
Calibr. data	67–72	51.29	51.07	51.25
Dev. (%)		0.19	0.13	0.07
Test data	73–78	151.00	150.84	151.06
Calibr. data	79–84	151.00	150.8	150.97
Dev. (%)		0.00	0.02	0.06
Test data	85–90	101.10	100.89	101.11
Calibr. data	91–96	101.06	100.80	101.11
Dev. (%)		0.04	0.09	0.00
Test data	97–102	51.33	51.27	51.46
Calibr. data	103–108	51.33	51.27	51.59
Dev. (%)		0.00	0.01	0.24
T_2				
Test data	1–6	151.42	151.14	151.51
Calibr. data	7–12	151.26	151.11	151.36
Dev. (%)		0.11	0.02	0.10
Test data	13–18	151.47	151.14	151.44
Calibr. data	19–24	151.45	151.10	151.53
Dev. (%)		0.01	0.03	0.06
Test data	25–30	101.08	100.79	101.24
Calibr. data	31–36	101.35	100.84	101.36
Dev. (%)		0.27	0.06	0.12
Test data	37–42	101.17	100.88	101.11
Calibr. data	43–48	101.25	100.97	101.18
Dev. (%)		0.08	0.09	0.07
Test data	49–54	51.55	51.11	51.45
Calibr. data	55–60	51.56	51.17	51.45
Dev. (%)		0.03	0.12	0.01
Test data	61–66	51.06	50.83	51.03
Calibr. data	67–72	51.15	50.79	51.01

Table 11 continued

T_1	Specimen nr	b_{1f} (mm)	b_{1m} (mm)	b_{1e} (mm)
Dev. (%)		0.17	0.07	0.03
Test data	73–78	151.54	151.14	151.53
Calibr. data	79–84	151.50	151.10	151.46
Dev. (%)		0.03	0.03	0.05
Test data	85–90	101.18	100.85	101.07
Calibr. data	91–96	101.28	100.95	101.16
Dev. (%)		0.11	0.10	0.09
Test data	97–102	51.70	51.25	51.65
Calibr. data	103–108	51.88	51.37	51.68
Dev. (%)		0.36	0.24	0.05

Table 12 Standard deviation of widths for T1 and T2 according to Table 11

Test series	Dev(b_{1f}) (mm)	Dev(b_{1m}) (mm)	Dev(b_{1e}) (mm)
T_1			
B_1	0.17	0.16	0.22
B_2	0.22	0.14	0.25
B_3	0.23	0.19	0.23
T_2			
B_1	0.14	0.13	0.15
B_2	0.14	0.12	0.27
B_3	0.31	0.26	0.29
B_4	0.22	0.14	0.30
B_5	0.15	0.15	0.09
$Dev(T_1/T_2)$			
B_1	0.26	0.20	0.28
B_2	0.19	0.13	0.26
B_3	0.28	0.24	0.26

Fig. 19 Tensile test: initial geometry (German Institute for Standardization)

Table 13 Statistical comparison of h_1 and resulting cross section for all tensile test specimens according to the initial rolling schedule

Specimen nr./schedule	Test series	Initial width	Thickness h_1 (mm)	Cross section (mm²)
2/V_2	T_1	B_1	1.34 ± 0.01	13.52 ± 0.12
2/V_2	T_2	B_1	1.50 ± 0.01	15.25 ± 0.15
14/V_3	T_1	B_1	1.33 ± 0.01	13.39 ± 0.09
14/V_3	T_2	B_1	1.46 ± 0.01	14.82 ± 0.13
26/V_2	T_1	B_2	1.20 ± 0.01	12.10 ± 0.10
26/V_2	T_2	B_2	1.37 ± 0.01	13.89 ± 0.21
38/V_3	T_1	B_2	1.20 ± 0.01	12.14 ± 0.18
38/V_3	T_2	B_2	1.35 ± 0.01	13.56 ± 0.16
50/V_2	T_1	B_3	1.01 ± 0.00	10.23 ± 0.06
50/V_2	T_2	B_3	1.17 ± 0.00	11.87 ± 0.04
62/V_3	T_1	B_3	1.01 ± 0.01	10.24 ± 0.10
62/V_3	T_2	B_3	1.13 ± 0.00	11.41 ± 0.02
74/V_1	T_1	B_1	1.22 ± 0.00	12.30 ± 0.12
74/V_1	T_2	B_1	1.33 ± 0.01	13.33 ± 0.13
86/V_1	T_1	B_2	1.10 ± 0.00	11.05 ± 0.11
86/V_1	T_2	B_2	1.21 ± 0.01	12.14 ± 0.20
98/V_1	T_1	B_3	0.95 ± 0.01	9.58 ± 0.16
98/V_1	T_2	B_3	1.03 ± 0.00	10.34 ± 0.03

train curves with 0°, 45° and 90° to the rolling direction for B_1 and B_2. For B_3, only 0° specimens could be realized with scientific validity. It is important to note that the resulting h_1 of each specimen varies as the final s_0 was kept constant but the resulting cumulated force diverges significantly and therefore, the elastic spring back behavior as well as work hardening and force related heat expansion of the used Aluminum alloy contributes to the final thickness to different extends (Fig. 19). Table 13 shows the initial properties of each specimen used for additional tensile tests. For each sheet, three tensile tests specimens for each examined direction were produced, one sheet per corresponding test data series for T_1 and T_2. Figure 19 shows the normed specimen geometry, according to DIN EN 10002-1 (German Institute for Standardization), for the performed tensile tests.

The higher deviation in the cross section is a result of the sample production, which were cut out with a water jet cutter at the CMF. More important, it can be stated that the resulting h_1 for sheets that undergo the same treatment, except friction state (T_1, T_2) vary significantly. For each state, the height of rolled sheets without lubrication is effectively higher than with. As a result of the higher F_R applied, the sum of elastic suspension of stand parts involved in the force flow during the rolling process is significantly higher. Therefore, the same degree of forming is not achieved as with the T_1 series, and the plate thickness of the T_2 series does not reach the same h_1 as that with lubrication, especially when large height reductions within the process were set. Figures 20 and 21 show the comparison of a specimen with B_1 (Fig. 20) and B_2 (Fig. 21) for both friction states. A small but reproducible effect on strength due to anisotropy can be observed.

To investigate the influence of friction, the following Figs. 22, 23, 24 show the direct comparison between a specific rolling direction and both investigated test series. Figure 22 compares different tensile test specimens for 0°, 45° and 90° to rolling direction, for specimen nr. 14 (B_1). The same comparison was made in Fig. 23 for specimen nr.
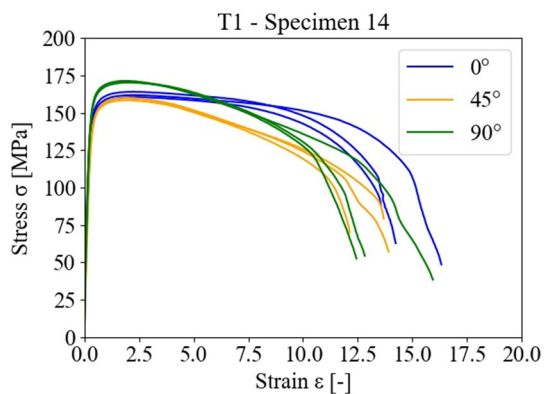
Fig. 20 Specimen nr. 14: mechanical anisotropy T1/T2

Fig. 21 Specimen nr. 86: mechanical anisotropy T1/T2

86 (B_2). In Fig. 24, the smallest width within the test and calibration series (specimen nr. 98, B_3) is compared in rolling direction.

The initial strip is commonly produced by hot rolling. This treatment already elongates the grains in the rolling direction, therefore the grains align themselves along a preferred orientation. The resulting microstructure exhibits a so-called rolling texture, as visualized in Fig. 25. The resulting anisotropy of the grain orientation also commonly affects the mechanical properties. The considerably larger number of grain boundaries to be overcome 90° to the rolling direction generally leads to an obstruction of the sliding processes. To determine the extent of anisotropy on sheet materials, tensile specimens are therefore regularly extracted and tested at 0°, 45° and 90° to the rolling direction. The recovery discussed in Sect. 6.2, however, leads to another phenomenon that is essential in explaining the low influence of anisotropy on macromechanical properties (Figs. 20 and 21), namely the polygonization of small-angle grain boundaries. This effect results in a substructure that forms globular sub grains. In optical microscopy images (OMI), this rearrangement is difficult to detect. In this case, the Barker electrolytic etching was used to visualize the microstructure (Figs. 25, 26, 27, 28), only showing the superposed deformation structure. It can be assumed that the progressed recovery stage in the
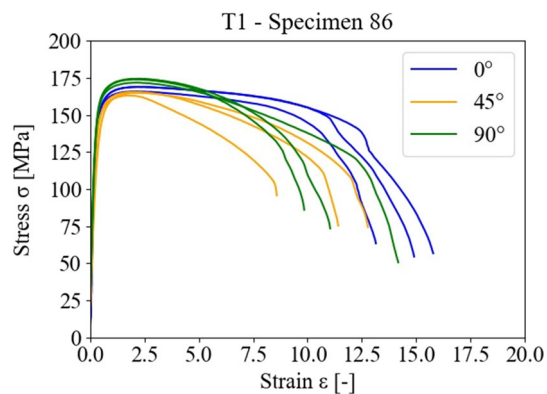
pure aluminum used in this experimental setup is most likely responsible for the similar deformation properties between the directions in the tensile test (Humphreys & Hatherly, 2007).

Table 14 summarizes the resulting ultimate tensile strength (UTS) of each tested specimen under consideration of tested degree to rolling direction.

The low but significant differences in UTS between different measured directions of one specimen can be explained as stated previously. The reproducible deviations in UTS between different specimens are a result of geometric differences, as specimens with different h_1 and therefore initial cross sections have different damage mechanisms dominating. The thinner the respective specimen, the more the plane stress state dominates, which results in higher resistance against damage and therefore slightly higher UTS values.

Data based experimental results

As stated in Sect. 6.4, the higher resulting friction within the tribological system of test series T_2 result in a higher elastic suspension of the stand components of the rolling aggregate. This phenomenon leads to a higher increase of h_0 as well as h_1 in T_2 compared to T_1. Despite the resulting higher h_1, the rolling mill and especially the mill stand has to apply higher
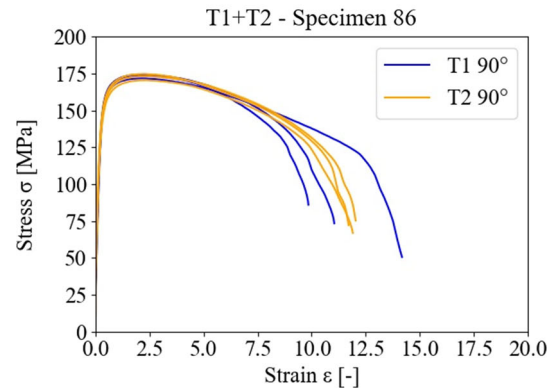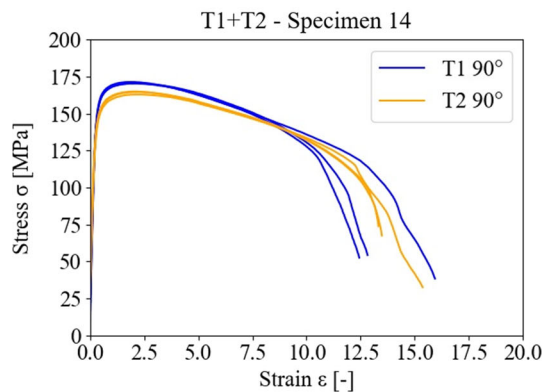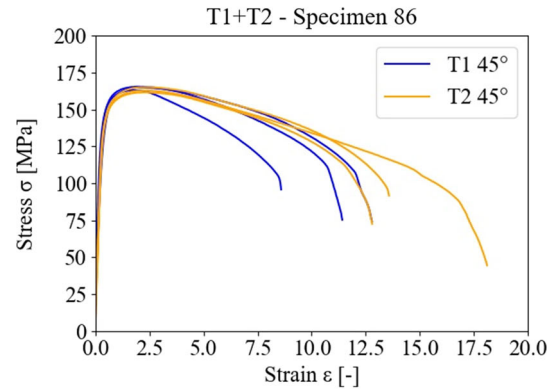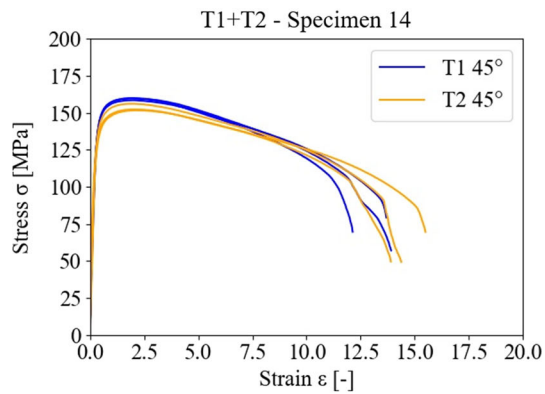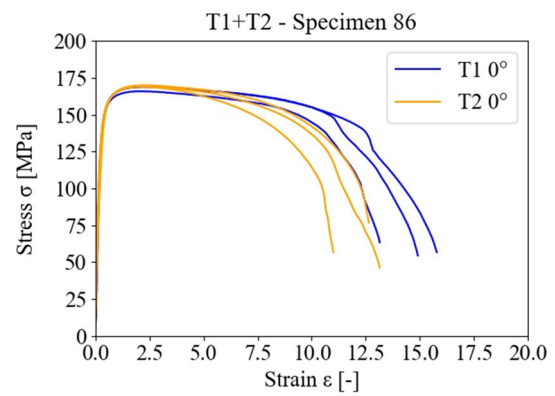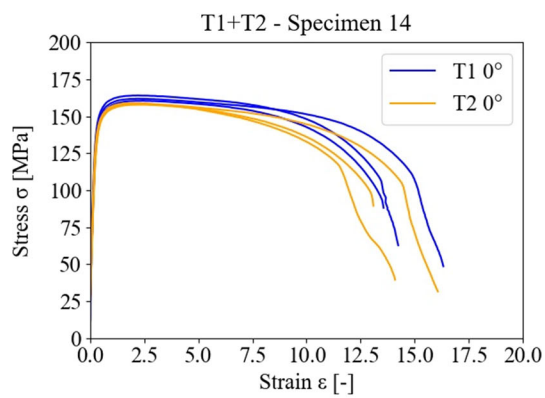
Fig. 22 Direct comparison: specimen nr. 14

Fig. 23 Direct comparison: specimen nr. 86

forces than in the tribologic system with adequate lubrication. Figure 29 demonstrates this effect on the resulting F_R on an exemplary rolling force hysteresis, where the same specimen from T_1 is compared with T_2. The effect of higher F_R for T_2 occurs in all different widths, as Figs. 30B_2 and 31B_3 demonstrate.

Figure 32 shows a direct comparison between B_1, B_2 and B_3 from the same rolling schedule and s_0, for T_1 (Fig. 32, top) and T_2 (Fig. 32, bottom).

The unnatural angular curve progression is a result of the sample rate during rolling (500 Hz). To obtain smoother results, a controlling unit (Sect. 4.2, Fig. 10) capable of higher frequency would have to be implemented. As this plot only

serves as a complementary visualization and the maximum valid sample rate is sufficient for the development of the machine learning algorithm (Sect. 6.6), the controlling unit is not changed within this case study.

For the development of the algorithm described in this paper, the maximum rolling force F_R is of importance, whereas the curve progression is not relevant for the resulting digital twin. The usage of the maximum resulting force as F_R can be seen as valid, as the deviation between this value and corresponding data points within the rolling process doesn't exceed 0.05%. Figure 33 shows an exemplary F_R(time) curve from a rolling process carried out.
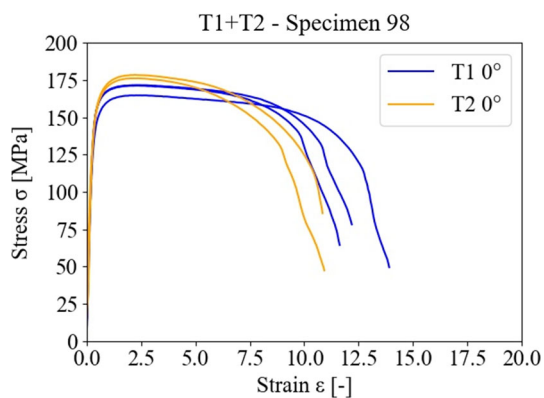
Fig. 24 Direct comparison: specimen nr. 98
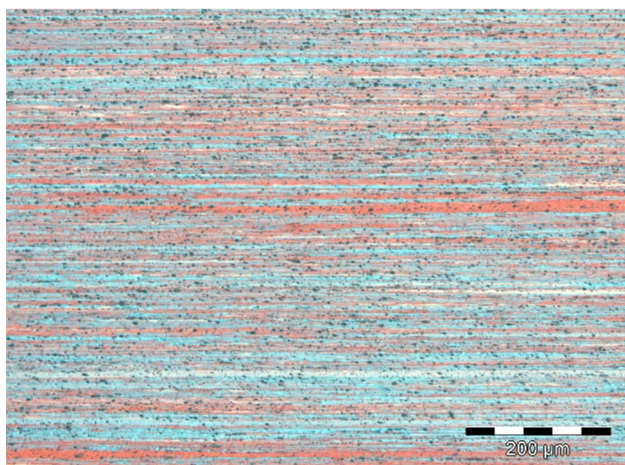
Fig. 25 Exemplary OMI: initial microstructure in rolling direction (T_1 /specimen nr. 86, 0°)
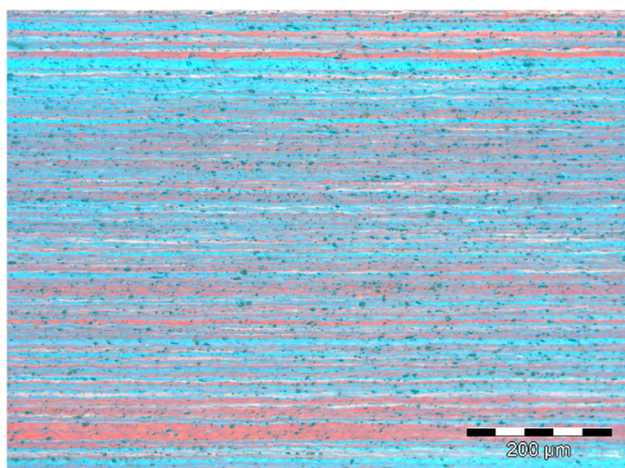
Fig. 26 Exemplary OMI: microstructure after the rolling process (T_1 /specimen nr. 86, 0°)

Fig. 27 Exemplary OMI: microstructure after the rolling process (T_1 /specimen nr. 86, 45°)
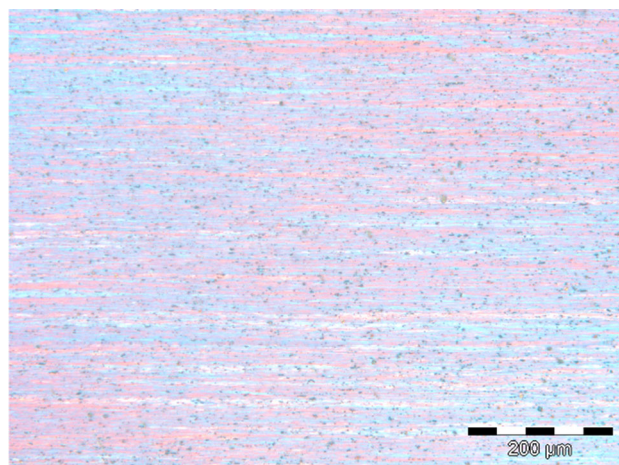
Fig. 28 Exemplary OMI: microstructure after the rolling process (T_1 /specimen nr. 86, 90°)

between F_R, $\Delta h(s_0)$, B_i and T_i can be identified. As expected, test and validation data points for the same B, V and T cannot be separated. Therefore, no difference between those sets will be made in the following visualizations.

As described in Sect. 6.4, a difference between the maximum roll gap (s) and the resulting h_1 of a specimen occurs. This effect can be demonstrated by plotting the same data points as a function of the maximum s (Figs. 35 and 36, yellow surface) and h_1 (Figs. 35 and 36, blue surface). As visualized in Fig. 34, the difference between T_1 (Fig. 35) and T_2 (Fig. 36) can be seen due the offset of data points to higher F_R with T_2. The dependencies described in Eq. (6) (Sect. 6.1) and the effect of cold working (Sect. 6.2) result in higher rolling forces with increasing Δh and decreasing s_0. As expected, the difference in the tribological system results in significantly higher F_R in T_2 in comparison to T_1. Also, higher F_R correlates with increasing initial sheet width. These

Figure 34 shows the resulting data points for each process step within the test and calibration data setup, divided in test series and initial widths. In this diagram, a clear correlation

Table 14 Statistical comparison of UTS for tensile test specimens according to the initial rolling schedule

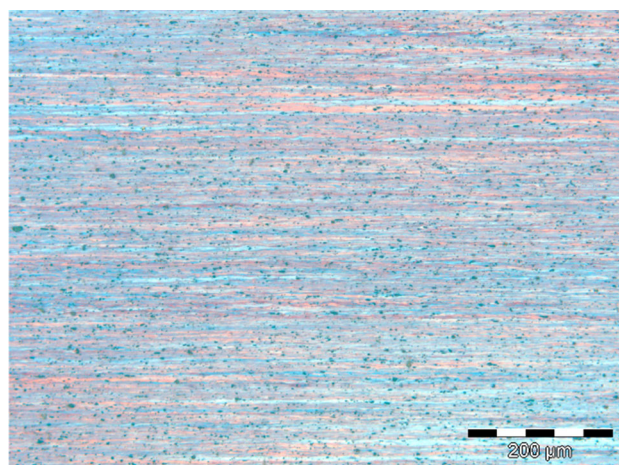| Nr./test series	UTS (0°) (MPa)	UTS (45°) (MPa)	UTS (90°) (MPa)
2/T_1	166.54 ± 1.82	160.98 ± 0.86	171.27 ± 1.23
2/T_2	162.35 ± 1.26	156.40 ± 0.46	164.10 ± 1.46
14/T_1	162.21 ± 1.48	159.41 ± 0.64	170.82 ± 0.45
14/T_2	158.53 ± 0.45	153.37 ± 1.97	164.18 ± 0.87
26/T_1	165.22 ± 1.28	162.41 ± 1.26	172.05 ± 0.56
26/T_2	163.94 ± 1.28	160.67 ± 1.80	167.75 ± 1.24
38/T_1	167.75 ± 1.02	160.28 ± 1.22	171.86 ± 0.41
38/T_2	162.29 ± 1.68	157.19 ± 2.30	167.47 ± 1.04
50/T_1	167.56 ± 0.64	–	–
50/T_2	170.85 ± 1.11	–	–
62/T_1	169.02 ± 1.24	–	–
62/T_2	169.76 ± 0.42	–	–
74/T_1	165.02 ± 0.93	163.23 ± 0.53	172.00 ± 0.72
74/T_2	169.76 ± 0.42	156.65 ± 2.08	164.96 ± 1.89
86/T_1	167.95 ± 1.45	164.54 ± 1.00	173.38 ± 1.13
86/T_2	169.39 ± 0.45	163.29 ± 1.43	172.80 ± 1.72
98/T_1	169.32 ± 2.15	–	–
98/T_2	177.61 ± 0.98	–	–
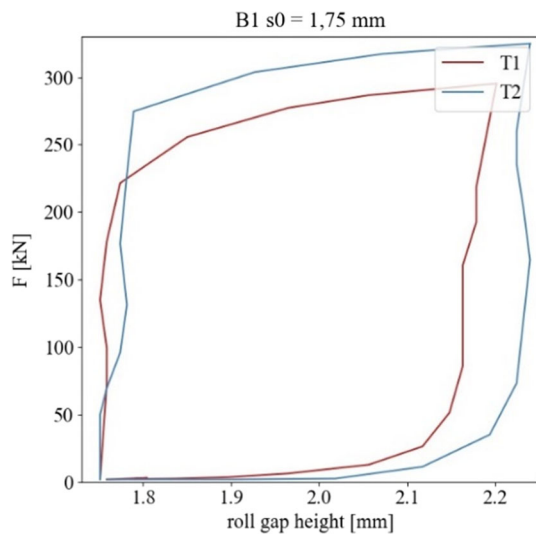
Fig. 29 Example of a rolling hysteresis: B_1 for $s_0 = 1.75$ mm

Fig. 30 Example of a rolling hysteresis: B_2 for $s_0 = 1.75$ mm
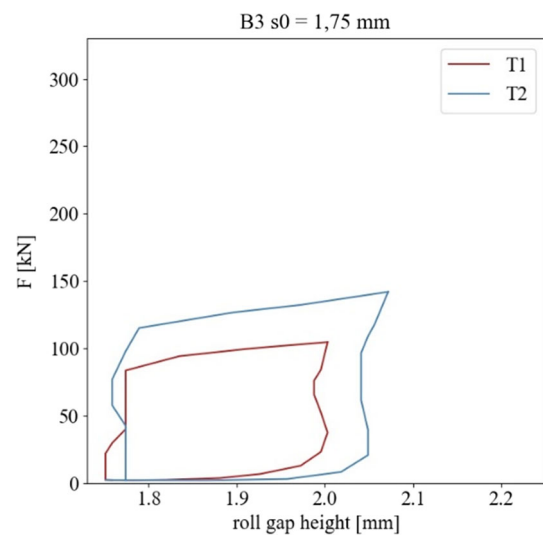
Fig. 31 Example of a rolling hysteresis: B_3 for $s_0 = 1.75$ mm

effects are cumulative, resulting in a maximum offset of F_R between B_1/T_2 and B_3/T_1 at maximum value of the product $\Delta h * s_0$.

In order to validate the stated hypotheses regarding the correlation of introduced variables, the validation data were implemented into the T_2 plane (Fig. 37). For a better visualization, only the V_1 rolling schedule for each introduced B was plotted within. The resulting diagram shows a clear linear correlation between different widths and the corre-

sponding s_0 of V_1. Furthermore, the modification of V_1 at $s_0 = 1.75$ mm (with a following s_0 of 0.75 mm instead of 1.00 mm) also supports the correlations stated by the authors within this paper.

Result based machine learning algorithm

According to the statements made in the last subsections of Sect. 6, the developed machine learning algorithm operates on linear interpolation and extrapolation of given test, calibration and validation data (Fig. 38). The first setup is based on the logic demonstrated in Fig. 2, whereas the material curve was also modeled linear. For each given F_R and corresponding h_1, the algorithm interpolates with linear weighting functions between the initial data to obtain the working point
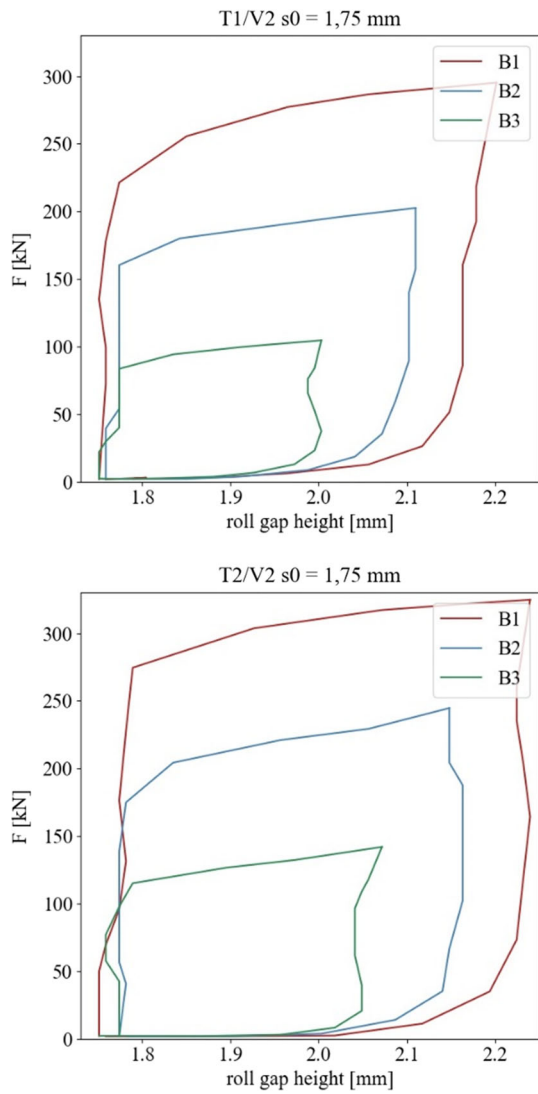
Fig. 32 Rolling hysteresis: resulting F_R as a function of initial sheet width: comparison between T_1 (top) and T_2 (bottom)
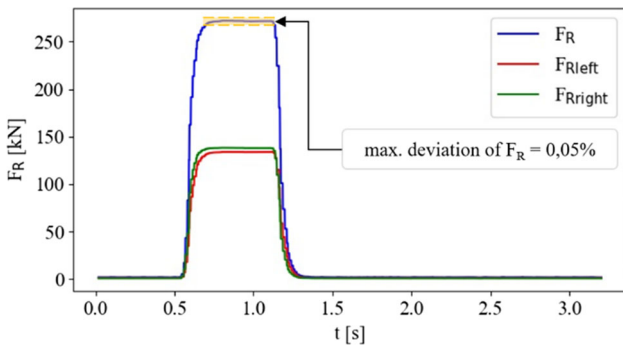
Fig. 33 Exemplary rolling force–time curve

A. This results in a new h_1, which is used as new input h_1 within a loop. As a result, a complete rolling schedule is obtained and in situ adapted during a carried out rolling pro-
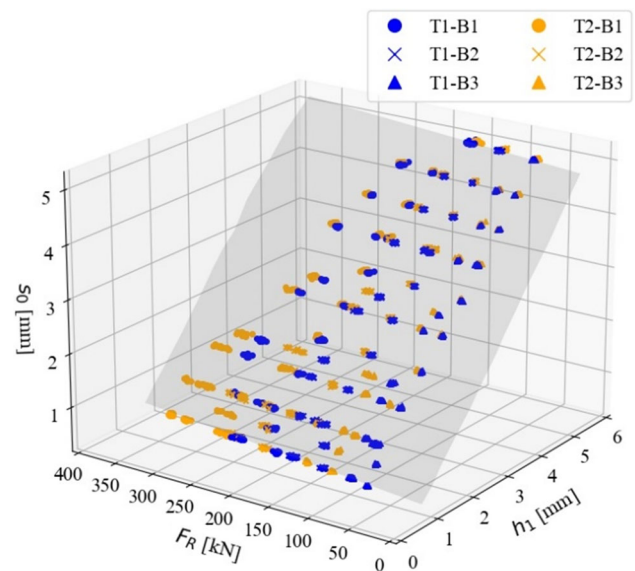
Fig. 34 Resulting data points (1736) from the test and calibration data series
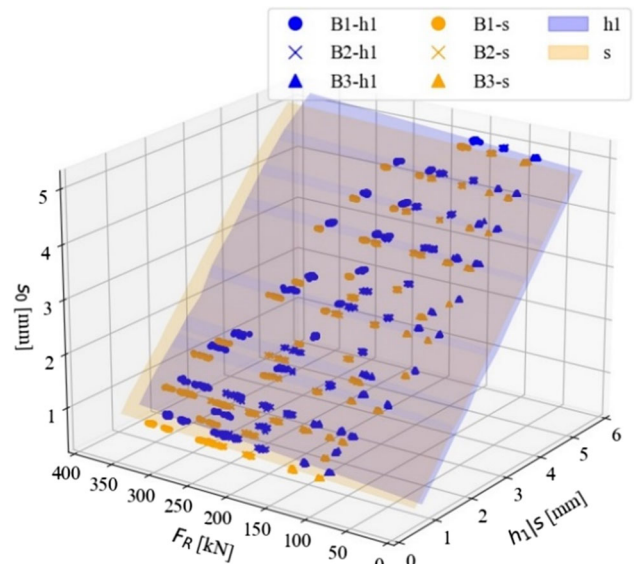
Fig. 35 Comparison between resulting s (yellow plane) and h_1 (blue plane) for B_1, B_2 and B_3 within test series T_1 (Color figure online)

cess. To develop this digital twin further and realize actual machine learning, final data of an executed rolling scheme is added to the respective initial data set (T_1 or T_2) resulting in an overall adaption of the linearized functions for the characteristic rolling mill and material curve. Although it would be possible to use predefined machine learning algorithms (e.g. using the sci.py kit available within the Python environment), this logic has the advantage of a simple adaptability for other materials. Furthermore, it is easy to understand and adapt for learning students and other interested parties within the SFL at the Montanuniversität Leoben.
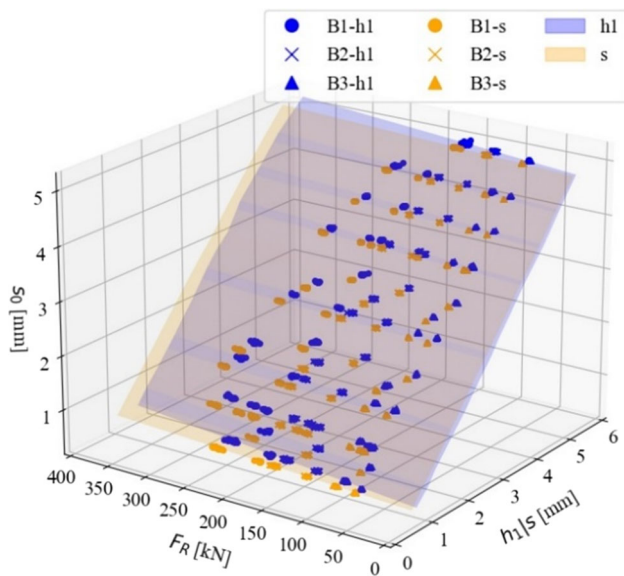
Fig. 36 Comparison between resulting s (yellow plane) and h_1 (blue plane) for B_1, B_2 and B_3 within test series T_2 (Color figure online)
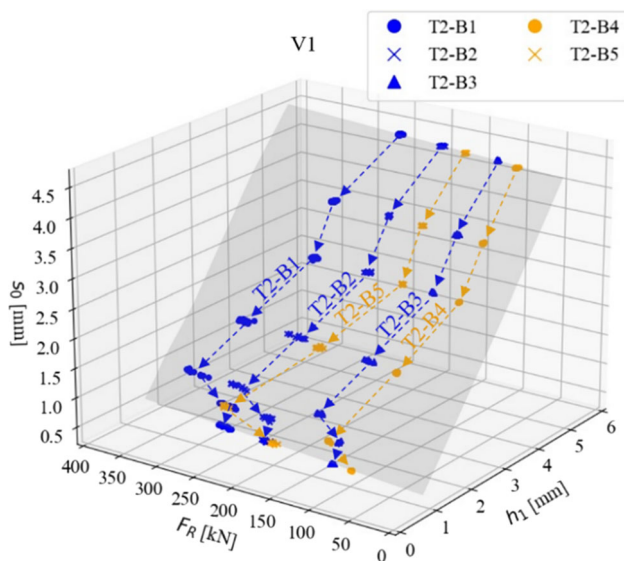
Fig. 37 Implementation of validation data: comparison with V_1 of test and calibration data sets

Machine learning GUI

The logic visualized in Fig. 38 (Sect. 6.6) serves as a basis for the second front end GUI (Table 1, IV). This GUI is also developed using the open source version of Qt Creator. The corresponding code was programmed using C++ and translated directly into Python within an appropriate translation framework (e.g. qtpy). As a result, the visualization can be started within the Python environment (e.g. using PyCharm or MS Visual Studio).

Figure 39 shows the resulting GUI for an exemplary rolling mill schedule. The possibility of including other materials is also considered.

The highlighted sequence (Fig. 39, green) indicates that no adaptions have been made and the generator calculated the complete scheme from the given input parameters (Fig. 39: Material, Rolling Force, h_0, demanded final h_1 after schedule, T_1 or T_2). After a rolling step, the real h_1 can be measured on two points (Fig. 39, End height front end h_1, End height back end h_1). Additionally, a change in width (according to Eq. (8), Sect. 6.3) or lubrication can be typed in, which also changes the result according to the fundamental logic (Fig. 38). Figure 40 demonstrates the influence of varying these parameters after a rolling step.

The user-given input parameters are triggering the machine logic. Furthermore, these parameters were also written into the initial database, which serves as fundament for the whole logic. Based on this data base extension, the logic is able to shift the boundaries for the extrapolation (if a B, s_0 out of the initial widths is given) or generate new interpolation data points within the given boundaries. Regardless which condition is met, the algorithm changes its final interpolation logic by changing material and stand related slopes and intercepts. As this adaption is made via linear weighting functions between a small step increment, the influence on the change is rapidly decreasing with increasing distance from the generated data points. As the point cloud gets denser with every data input, the prediction gets more accurate with each rolling process carried out. Figure 41 shows an overview of this loop.

Results and discussion

For the development of a LC user centered CPPS, the chosen forming equipment, a rolling mill aggregate built in 1954, was digitized and digitalized from the implementation of state of the art sensor technology to the integration of a self-learning digital twin with corresponding GUI. For all necessary development steps, cost efficient but robust solutions were chosen, in order to be able to use this case study as a possible framework for SMEs and (academic) learning factories to develop CPPS based on similar technologies and in alignment with the initial definition stated by the authors in (2.2). Another focus within this paper, a wide and high usability for all interested parties of the developed solution was realized with two different front end and two easy to understand back end GUIs. The usage of LC and mostly open source software solutions is another advantage of this framework, as continuous updates are made in the open source community and expensive software maintenance is not necessary. Figure 42 shows the final data flow at the rolling mill, from analog sensor signals to the Python logic.

1. Import of refined data

Import of refined data T_1 (with lubricant) and T_2 (without lubricant) from the database containing { Specimen nr. | V_i | B_i | $F_{R\,i}$ | $h_{1\,i}$ | $s_{0\,i}$ }

2. Linear Regression

Stand	Material

Stand — For every specimen n:

$$F(s) = a_{s\,n} \bullet s + b_{s\,n}$$

$$a_{s\,n} = \frac{F_R}{h_1 - s_0}$$

$$b_{s\,n} = -a_{s\,n} \bullet s_0$$

For each s_0 of every B:

$$a_{s\,median} \mid b_{s\,median}$$

Material — For every specimen n:

$$F(h) = a_{m\,n} \bullet h + b_{m\,n}$$

$$a_{m\,n} = \frac{F_R}{h_1 - h_0}$$

$$b_{m\,n} = -a_{m\,n} \bullet h_0$$

For each s_0 of every B:

$$a_{m\,median} \mid b_{m\,median}$$

3. Extrapolation of B

Stand	Material

Stand — Linear Regression of $a_{s\,median}$ and $b_{s\,median}$ for 400mm > B1 and B5 > 10mm to obtain $B_{ex\,(i)}$ > B_1 and $B_{ex\,(i+1)}$, < B_5

Material — Linear Regression of $a_{m\,median}$, $b_{m\,median}$ and h_0 for 400mm > B1 and B5 > 10mm to obtain $B_{ex\,(i)}$ > B_1 and $B_{ex\,(i+1)}$, < B_5

4. Interpolation of demanded b

Stand	Material

Calculation of weighting factor α between nearest neighbours of given widths B_i

$$\alpha = \frac{b - B_i}{B_{i+1} - B_i} \qquad B_{i+1} \geq b \geq B_i$$

Stand — Interpolation of slope a_s, intercept b_s with weighting factor α for every s_0:

$$a_s = a_{s\,i+1} + \alpha \bullet (a_{s\,i} - a_{s\,i+1})$$
$$b_s = b_{s\,i+1} + \alpha \bullet (b_{s\,i} - b_{s\,i+1})$$

Material — Interpolation of slope a_m, intercept b_m and resulting h_0 with weighting factor α for every s_0:

$$a_m = a_{m\,i+1} + \alpha \bullet (a_{m\,i} - a_{m\,i+1})$$
$$b_m = b_{m\,i+1} + \alpha \bullet (b_{m\,i} - b_{m\,i+1})$$
$$h_0 = h_{0\,i+1} + \alpha \bullet (h_{0\,i} - h_{0\,i+1})$$

$$F(s) = a_s \bullet s + b_s$$

$$F(h) = a_m \bullet h + b_m$$

Fig. 38 Fundamental logic for the Python based rolling schedule iterator

5. Extrapolation of s_0

Stand

Extrapolation of $a_{s\,max}$ for $20.0\,mm > s_{0\,ex} > s_{0\,max}$
Extrapolation of $a_{s\,min}$ for $s_{0\,min} > s_{0\,ex} < 0.1\,mm$

$s_{0\,max}$ = maximum s_0 obtained from data (5.0mm)
$s_{0\,min}$ = minimum s_0 obtained from data (0.5mm)

For $s_{0\,min} > s_{0\,ex} < 0.1\,mm$: $a_{s\,ex} = a_{s\,min}$
For $20.0\,mm > s_{0\,ex} > s_{0\,max}$: $a_{s\,ex} = a_{s\,max}$

Calculation of $b_{s\,ex}$ for corresponding $a_{s\,ex}$:
$$b_{s\,ex} = -a_{s\,ex} \bullet s_{0\,ex}$$

6. Extrapolation of h_0

Material

Extrapolation of $h_0(s_{0\,ex})$ with linear regression for
$s > s_{0\,max}$ and $s < s_{0\,min}$

Calculation of $b_{m\,ex}$ for corresponding $a_{m\,ex}$:
$$b_{m\,ex} = -a_{m\,ex} \bullet h_{0\,ex}$$

7. Interpolation of h_0 and rolling schedule iterator

Stand

Auxiliary variable γ
($0 \leq \gamma \leq 1; stepsize\ 5E-4$)

$$a_{s\,j} = a_{s\,i+1} + \gamma \bullet (a_{s\,i} - a_{s\,i+1})$$
$$b_{s\,j} = b_{s\,i+1} + \gamma \bullet (b_{s\,i} - b_{s\,i+1})$$

Calculation of roll gap height $s_{0\,j}$ height for rolling
schedule step j:

$$s_{0\,j} = \frac{a_{s\,j} \bullet h_{1\,j} - F_R}{b_{s\,j}}$$

Material

Calculation of weighting factor β between nearest
neighbours of h_0

$$\beta = \frac{h_0 - h_{0\,i}}{h_{0\,i+1} - h_{0\,i}} \qquad h_{0\,i+1} \geq h_0 \geq h_{0\,i}$$

$$a_{m\,j} = a_{m\,i+1} + \beta \bullet (a_{m\,i} - a_{m\,i+1})$$
$$b_{m\,j} = b_{m\,i+1} + \beta \bullet (b_{m\,i} - b_{m\,i+1})$$

Calculation of exit height $h_{1\,j}$ for rolling schedule
step j:

$$h_{1\,j} = \frac{F_R - b_{m\,j}}{a_{m\,j}} = h_{0\,j+1}$$

Fig. 38 continued

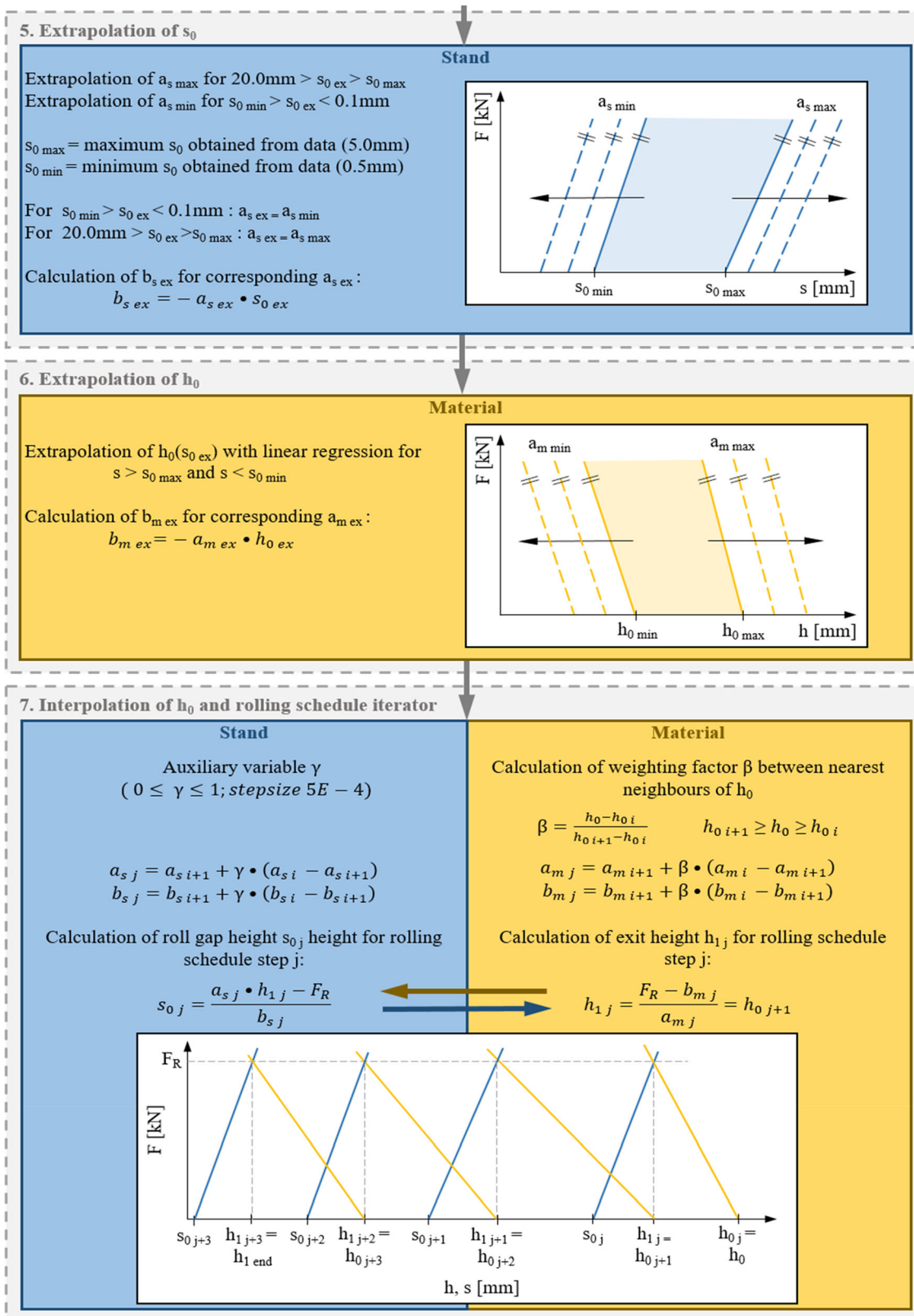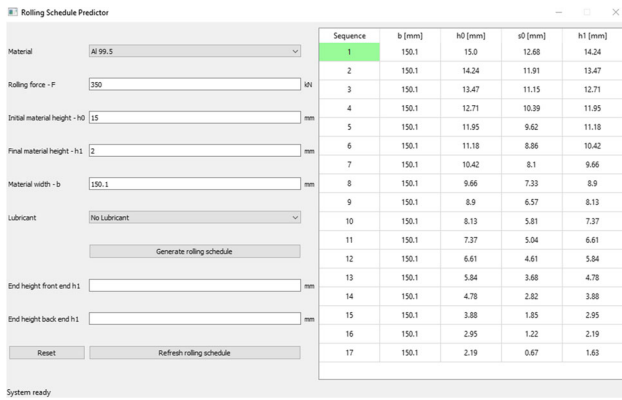**Fig. 39** Resulting front end GUI for the rolling scheme iterator

Fig. 40 Changed parameters based on Fig. 38 after the first rolling step: increased width and deviation between measured and predicted h_1

Fig. 41 Overview of the interaction between the database, the corresponding logic (back-end GUI) and visualization (front-end GUI)

To demonstrate the fulfilment of all criteria for a LC user-centered CPPS according to Table 1, Fig. 43 shows the final integration of the system in the layer architecture.

Fig. 42 Resulting data flow for the digitalized rolling mill

Fig. 43 Resulting layer architecture for the developed CPPS

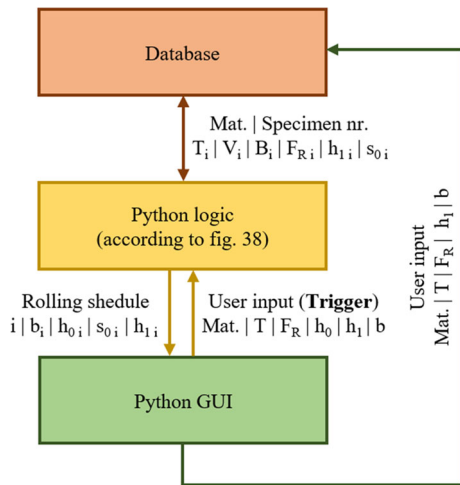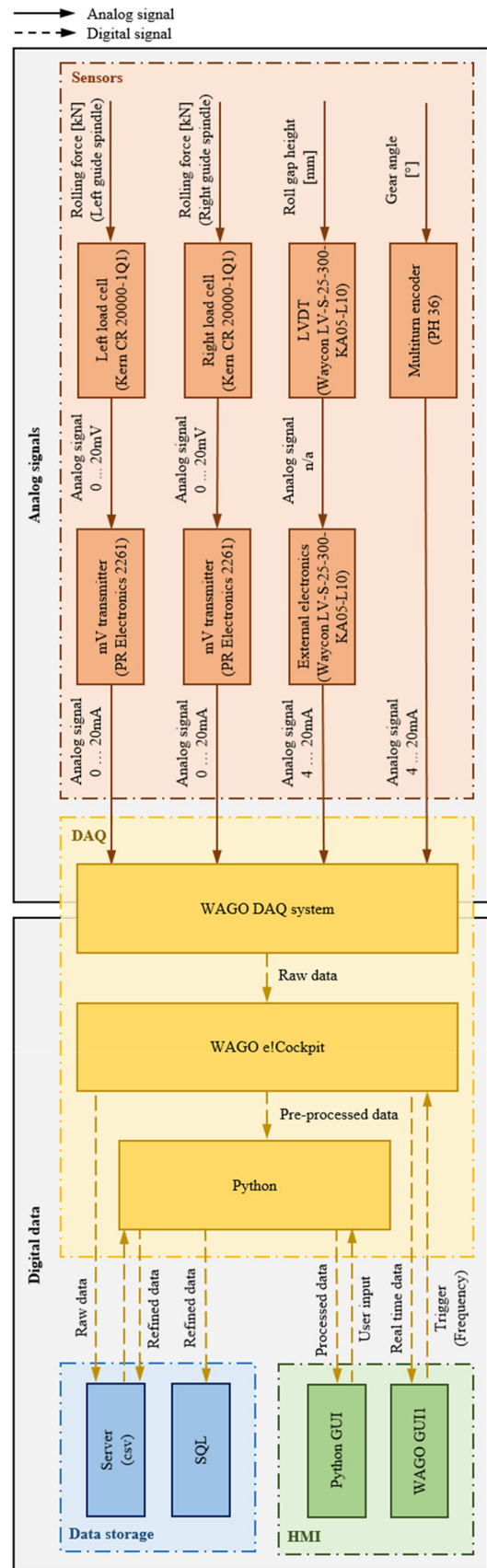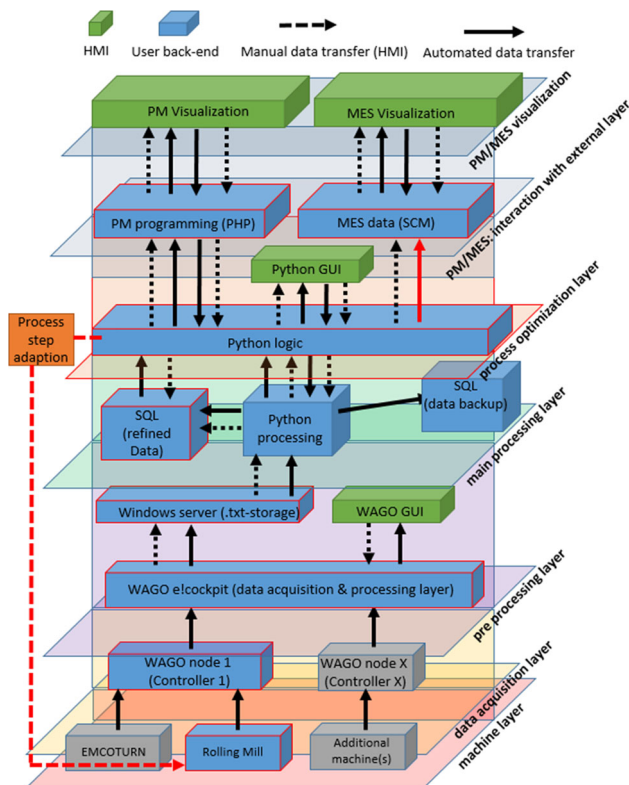ment Analysis software can additionally be connected to the system if the resulting complexity requires that. Another important advantage is that Python has a relatively low entrance barrier for respective workers (e.g. free/LC online tutorials), ensuring that no highly specialized IT-personnel is required for maintaining such an algorithm. In general, this approach can be used as a fundament for further adaption and optimization depending on the machine system and corresponding process to be transformed in a CPPS. The focus on LC technologies and digitization approaches based on a brownfield environment provides a reasonable method, especially but not restricted to SMEs, to accelerate their shopfloor digitalization and therefore remain competitive in a globalized and digitalized manufacturing environment.

Conclusion and outlook

This paper describes the successful transformation from a proprietary machine system to a LC user centered CPPS. Although the resulting integrated machine learning algorithm is based on a purely data-driven modeling approach, the respective material has to be and was considered. Without complementary experiments, the number of possible dependencies between input parameters would result in a far more complex system. The usage of a e.g. neural network based algorithms could be an alternative. A huge disadvantage of a more complex logic, however, would be the missing link between real physical effects and resulting prediction. Especially when considering different, more complex materials then the technical pure aluminum used in this case study, an overfitting effect could be the result. In general, a strict separation between material and machine parameters is not possible, as the dependencies and interactions are too complex to distinguish without a significant error or unreasonable computational and modeling efforts.

To extend the demonstrated framework for other material/process combinations, different alloys with different initial conditions will be implemented in the future. Furthermore, with the support of more advanced material characterization experiments (e.g. REM/EBSD), the prediction of grain size and corresponding anisotropy as a function of the thermomechanical treatment will be investigated. In general, the integration of temperature as an additional depended variable results in a far more complex equation system. To solve such a system in an adequate and reproducible way, the integration of finite element analysis connected to the framework within the Python logic will be investigated, whereas the reduction of computational time can be seen as most critical within such simulations. To decrease this parameter, direct coupling of

Depending on the state of the machine (measurement on: 500 Hz; measurement off: 1 Hz) a data flow into the MES is automatically enabled or not (Fig. 43, red arrow).

In general, both hypotheses stated initially can be defined as valid. According to the presented architecture, for a resilient and sustainable implementation of the proposed system, further adaptions depending on the existing infrastructure, available skill sets and budget have to be made. One major advantage of this LC approach is the utilization of industry standard software for the Level 2 automation of the resulting CPPS, which is crucial regarding to legal issues in case of a malfunction within the system in the operational industrial context. While the enhancing decision-making logic is provided by a LC open-source alternative within Python, the only direct machine connection is executed by a certified industrial standard software. This mixed-source approach also ensures the resilience of the machine system within the CPPS and additionally prevents unplanned downtimes due to possible malfunctions within the ML algorithm. As the process-material interaction becomes more complex, a simple numerical substitution as demonstrated in this work might also not be efficient anymore. By using Python and its available interfaces to other programs, e.g. Finite Ele-

Python based input and output files will be included. After successful coupling, the proposed extended algorithm will be able to predict micromechanical material properties as a function of the thermomechanical treatment. This information can be used to send recommendations into the MES-layer (Fig. 43), which can optimize necessary upstream or downstream heat treatment processes based on this information.

References

Akkaya, B. (2019). Leadership 5.0 in Industry 4.0. In J. Wang & J. C. Essila (Eds.), *Managing Operations Throughout Global Supply Chains* (pp. 136–158). IGI Global.

Ball, A., Gelman, L., & Rao, B. K. N. (Eds.). (2020). *Advances in Asset Management and Condition Monitoring*. Springer International Publishing.

Buer, S.-V., Strandhagen, J. W., Semini, M., & Strandhagen, J. O. (2021). The digitalization of manufacturing: Investigating the impact of production environment and company size. *Journal of Manufacturing Technology Management, 32*(3), 621–645.

Cardin, O. (2019). Classification of cyber-physical production systems applications: Proposition of an analysis framework. *Computers in Industry, 104*, 11–21.

Denicolai, S., Zucchella, A., & Magnani, G. (2021). Internationalization, digitalization, and sustainability: Are SMEs ready? A survey on synergies and substituting effects among growth paths. *Technological Forecasting and Social Change, 166*, 120650.

Dethine, B., Enjolras, M., & Monticolo, D. (2020). Digitalization and SMEs export management: Impacts on resources and capabilities. *Technology Innovation Management Review, 10*(4), 18–34.

Dutta, G., Kumar, R., Sindhwani, R., & Singh, R. K. (2021). Digitalization priorities of quality control processes for SMEs: A conceptual study in perspective of Industry 4.0 adoption. *Journal of Intelligent Manufacturing, 32*(6), 1679–1698.

Elkins, D. A., Huang, N., & Alden, J. M. (2004). Agile manufacturing systems in the automotive industry. *International Journal of Production Economics, 91*(3), 201–214.

Eller, R., Alford, P., Kallmünzer, A., & Peters, M. (2020). Antecedents, consequences, and challenges of small and medium-sized enterprise digitalization. *Journal of Business Research, 112*, 119–127.

Enyoghasi, C., & Badurdeen, F. (2021). Industry 4.0 for sustainable manufacturing: Opportunities at the product, process, and system levels. *Resources Conservation and Recycling, 166*, 105362.

Gottstein, G. (2004). *Physical Foundations of Materials Science*. Springer.

Gupta, H., Kumar, A., & Wasan, P. (2021). Industry 4.0, cleaner production and circular economy: An integrative framework for evaluating ethical and sustainable business performance of manufacturing organizations. *Journal of Cleaner Production, 295*, 126253.

German Institute for Standardization (2001). Manufacturing processes: Terms and definitions, division. Metallic materials - Tensile testing', DIN EN 10002-1:2001.

Hasegawa, T., & Kocks, U. (1979). Thermal recovery processes in deformed aluminum. *Acta Metallurgica, 27*(11), 1705–1716.

Humphreys, F. J., & Hatherly, M. (2007). *Recrystallization and Related Annealing Phenomena*. Elsevier.

Kergroach, S. (2020). Giving momentum to SME digitalization. *Journal of the International Council for Small Business, 1*(1), 28–31.

Lee, W. H., & Lee, S. R. (1999). Computer simulation of dynamic characteristics of tandem cold rolling process. *KSME International Journal, 13*(8), 616–624.

Monostori, L., Kádár, B., Bauernhansl, T., Kondoh, S., et al. (2016). Cyber-physical systems in manufacturing. *CIRP Annals, 65*(2), 621–641.

Müller, J. M., Buliga, O., & Voigt, K.-I. (2018). Fortune favors the prepared: How SMEs approach business model innovations in Industry 4.0. *Technological Forecasting and Social Change, 132*, 2–17.

Ostermann, F. (2014). *Anwendungstechnologie Aluminium*. Springer Vieweg.

Ralph, B. J., Schwarz, A., & Stockinger, M. (2020). An implementation approach for an academic learning factory for the metal forming industry with special focus on digital twins and finite element analysis. *Procedia Manufacturing, 45*, 253–258.

Ralph, B. J., & Stockinger, M. (2020). 'Digitalization and digital transformation in metal forming: Key technologies challenges and current developments of industry 4.0 applications. *XXXIX. Colloquium on Metalforming: Zauchensee, 2020*, 13–23.

Ralph, B. J., Hartl, K., Sorger, M., Schwarz-Gsaxner, A., et al. (2021a). Machine learning driven prediction of residual stresses for the shot peening process using a finite element based grey-box model approach. *Journal of Manufacturing and Materials Processing, 5*(2), 39.

Ralph, B. J., Sorger, M., Schödinger, B., Schmölzer, H.-J., et al. (2021b). Implementation of a six-layer smart factory architecture with special focus on transdisciplinary engineering education. *Sensors, 21*(9), 2944.

Ralph, B. J., Woschank, M., Miklautsch, P., Sorger, M., et al. (2021c). MUL 4.0: Systematic digitalization of a value chain from raw material to recycling. *Procedia Manufacturing, 2021*, 1–8.

Reiman, A., Kaivo-oja, J., Parviainen, E., Takala, E.-P., et al. (2021). Human factors and ergonomics in manufacturing in the industry 4.0 context: A scoping review. *Technology in Society, 65*, 101572.

Schwarz, A., Ralph, B. J., & Stockinger, M. (2021). Planning and implementation of a digital shadow for the friction factor quantification of the ECAP process using a grey box modeling approach and finite element analysis. *Procedia CIRP, 99*, 237–241.

Simon, J. P. (1979). A review of twin and stacking fault energies in Al, Mg and Be. *Journal of Physics F Metal Physics, 9*(3), 425–430.

Sorensen, D. G., Brunoe, T. D., & Nielsen, K. (2019). Brownfield development of platforms for changeable manufacturing. *Procedia CIRP, 81*, 986–991.

Wang, Q.-L., Sun, J., Liu, Y.-M., Wang, P.-F., et al. (2017). Analysis of symmetrical flatness actuator efficiencies for UCM cold rolling mill by 3D elastic–plastic FEM. *The International Journal of Advanced Manufacturing Technology, 92*(1–4), 1371–1389.

Wu, X., Goepp, V., & Siadat, A. (2020). 'Concept and engineering development of cyber physical production systems: A systematic literature review. *The International Journal of Advanced Manufacturing Technology, 111*(1–2), 243–261.

Springer

Zheng, T., Ardolino, M., Bacchetti, A., & Perona, M. (2021). The applications of Industry 4.0 technologies in manufacturing context: A systematic literature review. *International Journal of Production Research, 59*(6), 1922–1954.

Zhong, R. Y., Xu, X., Klotz, E., & Newman, S. T. (2017). Intelligent manufacturing in the context of industry 4.0: A review. *Engineering, 3*(5), 616–630.

Publisher's Note Springer Nature remains neutral with regard to jurisdictional claims in published maps and institutional affiliations.

A 6   Publication 6

M. Sorger, B.J. Ralph, K. Hartl, C. Waiguny, B. Schödinger, M. Schoiswohl, M. Stockinger: 'Transformation of a hydraulic press and furnaces into a Cyber Physical Production System: a brownfield approach from sensor retrofitting to Digital Shadow under special consideration of predictive maintenance and sustainability', in: *Journal of Intelligent Manufacturing* 2023, under review

Author contributions:

1. M. Sorger: Conceptualization, Methodology, Software, Formal Analysis, Investigation, Validation, Visualization, Data Curation, Writing - Original Draft, Writing - Review & Editing, Supervision, Project Administration

2. B.J. Ralph: Writing - Original Draft, Writing - Review & Editing

3. K. Hartl: Investigation, Visualization, Writing - Original Draft, Writing - Review & Editing

4. C. Waiguny: Software, Visualization

5. B. Schödinger: Data Curation

6. M. Schoiswohl: Data Curation

7. M. Stockinger: Supervision, Resources

Transformation of a hydraulic press and furnaces into a Cyber Physical Production System: a brownfield approach from sensor retrofitting to Digital Shadow under special consideration of predictive maintenance and sustainability

**Marcel Sorger[1]* , Benjamin James Ralph[1] , Karin Hartl[1] , Corinna Waiguny[1],
Benjamin Schödinger[1], Martin Schoiswohl[1], Martin Stockinger[1]**

[1]Chair of Metal Forming, Montanuniversität Leoben, Franz Josef Strasse 18, 8700 Leoben, Austria

* Corresponding author. Tel.: +43-3842-402-5604; fax: +43-3842-402-5604; *E-mail address:* marcel.sorger@unileoben.ac.at.

Abstract:

Cyber Physical Production Systems (CPPSs) are an integral part of Smart Factories, enabling the gathering, analysis, and integration of production data. Their implementation using a brownfield approach is especially sensible in the heavy industry due to the long life cycles of machines and aggregates. To demonstrate how these machine systems can transformed into a CPPS in an efficient and effective way, this paper describes the transformation of a hydraulic press from 1952 and two industrial furnaces into a fully interconnected CPPS. To measure and record process parameters, the respective machines and aggregates are retrofitted with suitable sensors and a data acquisition system. Furthermore, a Finite Element Analysis based Digital Shadow was implemented, to digitally map the process flow. These process steps include the preheating of respective specimens in a furnace, the transport from the furnace to the hydraulic press and the upsetting in the hydraulic press. For this purpose, a modular modeling approach using Python and Abaqus was applied, enabling simple and fast modification of simulations and process flows. To describe the material behavior of the used EN AW-6060 alloy during forming, the strain rates and temperature-dependent flow curves were experimentally evaluated, and the Johnson Cook and Hensel-Spittel material parameters were derived. To increase the user friendliness of the overall system, two types of front-end Graphical User Interfaces (GUIs) were programmed, one of which allows the execution of input specific simulations and validation of experiments. The second GUI is used for real-time visualization of process parameters to support decision-making on the shop floor, connected to a superordinate GUI environment, incorporating other digitalized machine systems at the Smart Forming Lab at the Chair of Metal Forming at the Montanuniversität Leoben. To support the applicability in small and medium sized enterprises and also in the academic environment of a learning factory, the best possible utilization of open-source software and state of the art, low-cost but resilient sensor technology was approached. As a result, students and other interested parties can use this open and low programming entrance barrier environment to deepen their understanding and knowledge of metal forming, the individual processes and digitalization.

KEYWORDS: Cyber Physical Production System; Industry 4.0; Digital Transformation; Digitalization; Smart Factory; Digital Shadow; Retrofitting; Metal Forming

1 Introduction

Since the rise of the fourth industrial revolution, the world of manufacturing undergoes significant changes concerning the incorporation of Industry 4.0 (I4.0) enabler technologies into established production processes (Zheng et al. 2021; Zhong et al. 2017). With the advancing digitalization and digital transformation in the manufacturing industry numerous advantages originate, enabling product and process optimization, continuous monitoring of all production stages along the entire value chain up to the product's quality control stage, and thus increasing sustainability (Nascimento et al. 2019; Reis and Gins 2017). On the other hand, this gives arise to new challenges and obstacles, especially for Small and Medium sized Enterprises (SMEs). To achieve a holistic digitalization and digital transformation, every enterprise along the entire value chain has to be implemented into a digital depiction of such (Sorger et al. 2021). Hereby, especially SMEs face obstacles that can be differentiated into economical, socio-cultural, and managerial resources (Ralph et al. 2022). As older machine systems often still exhibit good substance, a retrofitting approach seems beneficial from an economical point of view, especially for SMEs with restricted financial resources. Due to the high scalability of these digitalization technologies, the amortization time for such investments is longer for SMEs as for big enterprises, making low-cost digitalization a point of interest (Müller et al. 2018). Furthermore, the resources and capabilities necessary for implementing these I4.0 enabler technologies are less likely to be found in an SME as in comparison to a big enterprise. Therefore, managers have to be aware of I4.0 technologies, their potentials, threats, resilience as well as possibility of

outsourcing. Further, concerning socio-cultural thresholds, affected instances have to be sensitized to the newly implemented technologies (Akkaya 2019; Olsen and Tomlin 2020).

Therefore, this paper aims to contribute to the solution of the following SME specific issues:

a) Implementation of a Cyber Physical Production System (CPPS) suitable for an economic as well as educational application, therefore supporting future engineers in handling the challenges of I4.0

b) Demonstration of the potentials of the retrofitting of fundamentally different non-I4.0 compliant machines, transforming them into connected CPPSs.

c) Reduction of investment costs by using suitable low-cost hardware and open-source software

In the course of the MUL 4.0 project at the Montanuniversität Leoben, two furnaces and a hydraulic press at the Chair of Metal Forming (CMF) are transformed into CPPSs (Ralph, Woschank et al. 2021; Woschank et al. 2021). Regarding the objectives a) and b), these aggregates show resemblance to the situation in the manufacturing industry, therefore serving as an appropriate case study. Special focus is put on the applicability of such brownfield approaches for SMEs, opposing the financial obstacle of following a greenfield approach by purchasing a new machine replacing the old one. Therefore, special emphasis is put on low-cost but high-quality hardware as well as open-source software to the highest possible degree, emphasizing c). The pursued brownfield approach includes the retrofitting with suitable low-cost sensors, a Data Acquisition System (DAQ) and the integration into a production network, thus connecting the CPPSs with the Industrial Internet of Things (IIoT) (Lins and Oliveira 2020; Sorger et al. 2021). To promote the importance of Cyber Security, the production network was implemented as a Layer 2 network, preventing unauthorized access from outside the network. Hereby, an open-source software approach is followed, reflecting the financial limitations SMEs face. To further support the premises of I4.0 in terms of connectivity and the prevention of proprietary solutions, Python is used for automatic process modelling and data integration into the Finite Element Analysis (FEA) using Abaqus. Thus, both processes of heating and upsetting are modeled using a white box modelling approach based on real physical relationships. Additionally, Graphical User Interfaces (GUIs) were implemented, supporting the Human Machine Interaction (HMI) and decision-making process on the shop floor level, further advancing in Industry 5.0 territory (Nahavandi 2019; Özdemir and Hekim 2018).

To support a successful digitalization, the processes first have to be analyzed to set up an accurate white-box model, which is described for this case study in Section 2. Section 3 describes the initial state of the machines and the production network. Consequently, the digitalization approach by developing a Digital Shadow (DS) using a Python coupled FEA, is shown in Section 3 and 4. In Section 5, the experimental setup for the calibration and validation of the CPPSs is demonstrated. In Section 6, the resulting CPPSs, infrastructure and added value including the GUI is shown and discussed. Closing with Section 7, a summary of the outcome is given, followed by a conclusion and outlook.

2 Processes, FEA and CPPS fundamentals

The following chapter elaborates on the process fundamentals (2.1) and FEA material models (2.2), necessary for the retrofitting (Section 3) and implementation of a FEA based modelling approach (Section 4), followed by the definition of a CPPS (2.3).

2.1 The heating and upsetting process

The material behavior during forming is described by the flow stress curve. The flow stress curve represents the correlation of the flow stress k_f with the true strain φ. The true strain φ is defined as the natural logarithm of the ratio of the height after forming h_1 to the initial height h_0 of the specimen (Eq. (1)) (Doege and Behrens 2010; Hoffmann et al. 2012).

$$\varphi = \ln(\frac{h_1}{h_0}) \qquad (1)$$

The initial flow stress k_{f0} describes the stress necessary to initiate plastic deformation (yield point). Therefore, with increasing plastic deformation, thus increasing true strain φ, the flow stress k_f increases due to strain hardening, considered by the strain-hardening exponent n. The material specific constant K is referred to as strength coefficient. This formulation of the flow stress is also referred to as the Ludwik equation, shown in Eq. (2) (Doege and Behrens 2010; Hoffmann et al. 2012).

$$k_f = k_{f0} + K \cdot \varphi^n \qquad (2)$$

As shown in Fig. 1, the strain hardening, also referred to as work hardening, is more prevalent in cold forming than in warm forming, due to recovery and recrystallization processes of the material at higher temperatures. The strain hardening at increasing strains is due to dislocation multiplication and their mutual movement hindrance. If a certain dislocation density or degree of deformation is exceeded in relation to the prevailing temperature, this effect can be counteracted by softening processes. These effects refer on the one hand to recovery and on the other hand to recrystallization. Recovery is a result of softening due to the restructuring of the dislocations and the formation of a subgrain structure, whereas recrystallization embodies the new formation of nearly dislocation-free equiaxial grains. The effect of recovery can be observed already at lower temperatures, while the energy input required for recrystallization in terms of strain and temperature is higher (0.4 of the melting temperature). In contrast, the softening effect of recrystallization is much more pronounced, as visualized in Fig. 1.

Due to these processes, the flow curve has a different appearance at higher temperatures. While elevated temperatures reduce the yield point considerably, the occurrence of the above-mentioned effects in the yield curve can lead to a steady state area and to a subsequent decline in the flow curve, if the softening effects outweigh the hardening effects. The extent to which this occurs is dependent on the material, temperature and the process. Determining the course of a material's flow curve and its progression is therefore essential for metal forming processes.
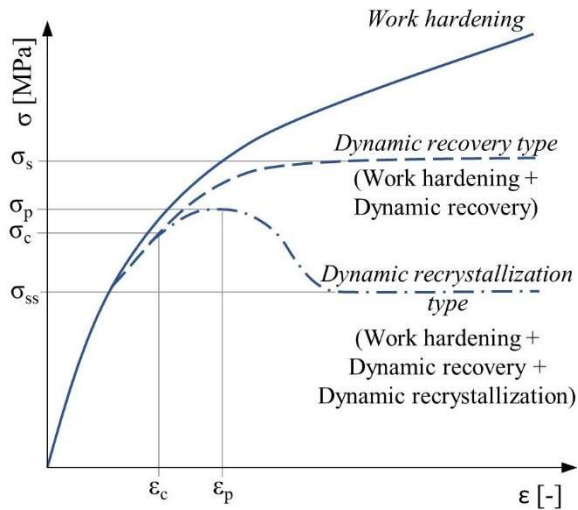

Fig. 1 Flow stress curve describing material behavior with increasing strain-hardening (Gottstein 2014)

According to DIN 8580, the upsetting process belongs to the subgroup of forming by pressure (Hoffmann et al. 2012). During upsetting, the specimen is compressed in axial direction between two parallel flat dies (Fig. 2). Due to the strain hardening of the material, the flow stress increases with the decreasing height of the specimen (Fig. 1), thus resulting in higher compression force. Furthermore, friction on the contact surface between die and specimen leads to a buckling of the specimen (Hoffmann et al. 2012).
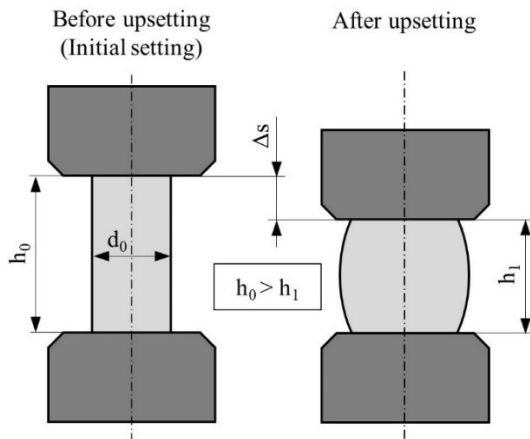

Fig. 2 Geometry change during upsetting

The EN AW-6060 material used in this study belongs to the 6xxx series with the alloying elements Mg and Si. The face-centered cubic lattice structure of aluminum contributes to good formability while the dispersion-forming elements Mg and Si serve as elements to enhance the age-hardening effect. The precipitation hardening effect of the wrought alloy is primarily determined by the β-phase Mg_2Si. These dispersions occur during a specific heat treatment route that includes solution annealing, quenching, and aging. In most cases, the fully artificially aged T66 condition is used. For forming processes such as hot forging, which is used in this investigation, the strength-enhancing precipitates dissolve again at higher temperatures and, depending on the prevailing temperature, remain partially present. This has a significant effect on the strength of the material and therefore on the flow curve. In addition, these precipitates have a grain boundary pinning effect, therefore recrystallization is suppressed. With a lower proportion of dispersions present, the impact of this effect is correspondingly reduced, hence recrystallization can occur to a greater extent. Nevertheless, aluminum has a strong tendency to recovery effects due to the high stacking fault energy, sometimes even at room temperature. Therefore, the energy introduced by forming which is converted into adiabatic heat can already lead to softening effects during cold forming (Ostermann 2014). To be able to describe the effect of metallurgical processes on the flow curve accurately, it is necessary to represent the material behavior for the FEA in terms of a material model, which considers these effects properly.

Beside the strain hardening and temperature dependency of the material's behavior, further dependency on the strain rate has to be considered. Popular models used to do this are the Johnson-Cook (JC) (Ralph, Hartl et al. 2021) and Hensel-Spittel material model (Hensel and Spittel 1978).

2.2 FEA material models

To perform an accurate FEA of the material's behavior during forming, a suitable material model is imperative. For this purpose, the commonly used JC model poses as an appropriate choice for dynamic problems, considering three important material effects – strain-hardening, strain rate dependency and thermal-softening (Eq. (3)) (Umbrello et al. 2007). The first term considers the strain-hardening of the material during forming, exhibiting the quasi-static yield strength A, the strain-hardening constant B, plastic strain φ_P and strain-hardening exponent n. Furthermore, the second term takes the material's strain rate dependency into account, incorporating the strain rate sensitivity constant C in dependence of the plastic strain rate $\dot{\varphi}_P$ divided by the quasi-static strain rate $\dot{\varphi}_0$. The third term, relates to the thermal softening behavior due to varying temperatures, including the current temperature T, reference temperature T_t, melting temperature T_m and thermal-softening exponent m (Johnson et al. 1983).

$$\sigma = \left(A + B\varphi_p^n\right)\left[1 + C\ln\left(\frac{\dot{\varphi}_p}{\dot{\varphi}_0}\right)\right]\left[1 - \left(\frac{T-T_t}{T_m-T_t}\right)^m\right] \quad (3)$$

The parameters A, B and n can be evaluated by neglecting the second and third term in Eq. (3), resulting in Eq. (4). Hereby, A can be taken from the flow curve under quasi-static conditions. By plotting the left term of Eq. (4) on the horizontal axis over logarithmic plastic strain on the vertical axis, the parameter n can be determined with a linear regression represented by the slope, and B is represented by the intercept with the vertical axis (Johnson et al. 1983). B can additionally be calculated by solving the exponential equation.

$$\ln(\sigma - A) = n \cdot \ln(B\varphi) \quad (4)$$

For the evaluation of C, the third term is neglected and rearranged, leading to Eq. (5). By plotting the left term on the vertical axis over the logarithmic strain rate ratio on the horizontal axis and applying a linear regression, the parameter C serves as the slope of the regression. Hereby, different strain rates $\dot{\varepsilon}_P$ with corresponding σ and ε have to be known, whereas A, B and n stay constant (Johnson et al. 1983).

$$\frac{\sigma}{(A + B\varphi^n)} = 1 + C \cdot \ln\left(\frac{\dot{\varphi}_P}{\dot{\varphi}_0}\right) \quad (5)$$

The parameter m can be derived from neglecting the second term of Eq. (3), leading to the rearrangement of Eq. (6). For the calculation of m, the parameters σ and ε for corresponding temperatures T have to be known (Johnson et al. 1983).

$$\ln\left(1 - \frac{\sigma}{(A + B\varphi^n)}\right) = m \cdot \ln\left(\frac{T-T_t}{T_m-T_t}\right) \quad (6)$$

To account for thermal softening effects due to recovery and recrystallization, the material modelling approach according to Hensel-Spittel can be applied (Hensel and Spittel 1978). Hensel-Spittel describes the occurring flow stresses with the material coefficients A, m_1, m_2, m_4, m_5, m_7, m_8, plastic strain φ, strain rate $\dot{\varphi}$ and temperature T (Eq. (7)) (Chen et al. 2021).

$$\sigma = A \cdot e^{m_1 \cdot T} \cdot \varphi^{m_2} \cdot e^{\frac{m_4}{\varphi}} \cdot (1+\varphi)^{m_5 \cdot T} \cdot e^{m_7 \cdot \varphi} \cdot \dot{\varphi}^{m_8 \cdot T} \quad (7)$$

To determine the material coefficients A and m_1 to m_8, the univariate method can be applied, shown in (Eq. (8)) (Chen et al. 2021).

$$\ln\sigma = \ln A + m_1 \cdot T + m_2 \cdot \ln\varphi + \frac{m_4}{\varphi} + m_5 \cdot T \cdot \ln(1+\varphi) + m_7 \cdot \varepsilon + m_8 \cdot T \cdot \ln\dot{\varphi} \quad (8)$$

By keeping the strain and temperature constant and thus introducing the constant k_1, the material coefficient m_8 are determined, leading to Eq. (9) (Chen et al. 2021).

$$\ln\sigma = k_1 + m_8 \cdot T \cdot \ln\dot{\varphi} \quad (9)$$

Consequently, the material coefficients m_1 and m_5 are calculated by keeping the strain and strain rate constant, introducing the constant k_2, shown in Eq. (10) (Chen et al. 2021).

$$\ln\sigma = k_2 + (m_1 + m_5 \cdot \ln(1+\varphi) + m_8 \cdot \ln\dot{\varphi}) \cdot T \quad (10)$$

Eventually, the material coefficients m_2, m_4 and m_7 are determined using Eq. (11), introducing the constant k_4 as the strain rate and temperature are kept constant (Chen et al. 2021).

$$\ln\sigma = k_4 + m_2 \cdot \ln\varphi + \frac{m_4}{\varphi} + m_5 \cdot T \cdot \ln(1+\varphi) + m_7 \cdot \varphi \quad (11)$$

2.3 Cyber Physical Production Systems

CPPSs serve as an extension to Cyber Physical Systems (CPSs), adapted to the manufacturing industry (Ralph et al. 2022; Zhong et al. 2017). According to (Wu et al. 2020), a CPPS can be defined as a superordinate system within systems with connected and cooperative elements. Consequently, CPPS can communicate on every layer of the production environment via IIoT, enabling situationally appropriate adaption. Therefore, the classic automation pyramid can be restructured, resulting in the connection of the layers of the Programmable Logic Controllers (PLC), Supervisory Control and Data Acquisition (SCADA), Manufacturing Execution System (MES) and Enterprise Resource Planning (ERP) with the field level.(Fig. 3) (Rocca et al. 2020).

(a)　　　　　(b)
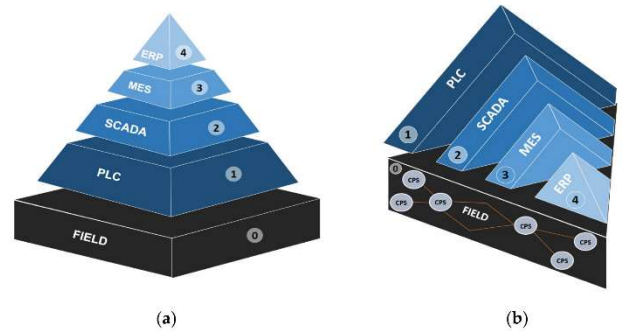
Fig. 3 Classic automation pyramid (a) and resulting automation network due to interconnected CPPS (b) (Rocca et al. 2020)

Based on (Wu et al. 2020), the authors (Ralph et al. 2022) concluded that a CPPS, especially for the application in SMEs, can be concretized by five criteria:
1. System in a system
2. Situationally appropriate adaption and multi-layer data transfer
3. Real time and state dependent support of decision-making process
4. User centered Graphical User Interface (GUI)

5. Resilient and low-cost design

In this case study, to fulfil (1), the resulting CPPS of the furnace and hydraulic press will be implemented in the production network, enabling the data transfer between other integrated CPPS imperative for process adaptions and process planning. Thus, contributing to (2), the implementation of the CPPS into the production network, the multi-layer data transfer is enabled. Furthermore, the sampling rate is attuned to the machine status of either machining or not machining, thus adapting situationally appropriate. For the fulfilment of (3) and (4), an FEA will predict the necessary process parameters of the current and upcoming process steps in near real-time, therefore also being adaptable to prevailing circumstances. The HMI is enhanced with the use of GUIs, allowing the visualization of current process parameters and FEA results, thus supporting human decision-making on the shop floor. For (5), a low-cost approach is chosen, using low-cost but high-quality hardware and open-source software to the best possible extend, responsive to the needs of an SME.

3 Initial setup, retrofitting and digitization

The following chapter presents the initial setup at the CMF. Hereby, (3.1) outlines the IT infrastructure, followed by the initial state and retrofitting of the furnaces and hydraulic press in (3.2), followed by the digitization and digitalization approach in (3.3).

3.1 Production network

The advancing of the digitalization and digital transformation led to cyber security significantly gaining importance (Buehler et al. 2020). To counteract cyber-attacks in the best possible way, a two-layer production network was implemented. As described in previous work (Sorger et al. 2021), an IT-layer architecture was already designed and implemented, shown in Figure 4. Hereby, the IIoT data from incorporated devices can only be transferred via the NodeRed server and the MariaDB database from layer 2 to layer 3, thus acting as a closed system. Furthermore, layer 3 is only accessible by the client with an authorized workstation. Hereby, the authorized workstation hosts the remote admin host, the webserver dashboard, the low-cost ERP Next and the virtual fileserver. To further increase the cyber security of the layer architecture, a firewall was implemented between layer 2 and 3, allowing layer 3 to query layer 2.
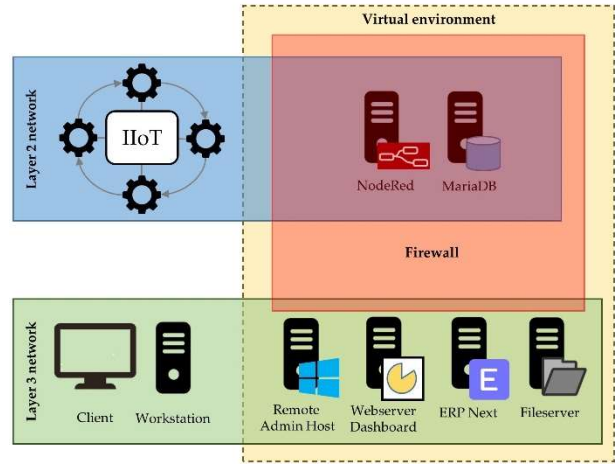
Fig. 4 MUL 4.0 production network with layers and corresponding instances (Sorger et al. 2021)

The IIoT-network contains all incorporated devices, such as DAQs and tablet computers. To expend the existing IIoT-network and implement the new machines, a RevPi Connect+ featuring CODESYS was integrated. Hereby, the RevPi acts as a DAQ of the new machines, gathering data from the machine's respective sensors. First, the unrefined sensor data is fed into the MariaDB for pre-processing. In addition, unrefined and refined data is stored on the fileserver, sharing data for the FEA and further post processing on the workstation. The real-time visualization of the sensor data and other relevant features, such as the start of a measurement, is realized with a browser-based GUI, which can be accessed by IIoT devices, e.g., tablets and laptops. Here, the RevPi communicates chosen parameters via MODBUS into the network, which is then visualized with the already previously implemented CODESYS based WAGO e!COCKPIT software (Ralph et al. 2022).

3.2 Sensor retrofitting

Due to their robust design, decades-old machines and aggregates are still used in heavy and manufacturing industry. Especially for SMEs, their replacement is difficult due to the high costs, and the robust design makes a retrofitting of appropriate sensors and digitalization technology economically more sensible than a purchase of a new machine (Müller et al. 2018; Ralph et al. 2022). Therefore, the initial step has to be the definition of the relevant process parameters, environmental requirements and financial restrictions. In the next step, the range of the measurements as well as the required resolution of the process parameters must be defined. The range of the measurement refers to the minimum and maximum of the physical quantity to be measured. Furthermore, a high linearity is imperative to accurately represent the actual measurement value. In the field of sensor technology, this is referred to as linearity or non-linearity, characterizing the deviation from the actual measurement, resulting in a scatter band of the ideal characteristic curve. The linearity is given as a percentage of the sensor's measurement

range, wherefrom the deviation and thus the minimum and maximum scattering value is calculated. Based on these requirements, the sensor selection is conducted. These requirements represent the minimum requirements that have to be fulfilled, thus the sensors must be able to measure below the minimum and above the maximum of the measurement range and possess a linearity higher than the minimum linearity. Furthermore, the sensor must be able to withstand the environmental conditions in order to avoid errors and expand the lifespan, therefore supporting the longevity and thus sustainability. Thereupon, the sensor technology for the incorporated machines were chosen (Ralph et al. 2022).

In addition, the process sequence must also be defined in order to identify possible influencing variables and process parameters. The process under consideration consists of the first step of heating the specimen in one of the two furnaces, followed by the second step of transporting the specimen from the furnace to the hydraulic press using tongs. In the third step, the specimen is placed on the lower die of the hydraulic press and is then compressed in the fourth and final step.

The CMF houses two furnaces capable of different maximum temperatures. Furnace 1 is lined with 1.4301, capable of temperatures of up to 600 °C, whereas the refractory material lined furnace 2 is capable of temperatures of up to 1400 °C (Fig. 5-7). The standard control of furnace 1 is realized with Eurotherm 2132 and 3216 elements, whereas furnace 2 uses Eurotherm 2132, 2216e and 2416 elements. Furthermore, the thermocouples used by the Eurotherm elements were already built in as standard. To support the low-cost approach, suitable thermocouples were retrofitted to the respective machines without intervening with the existing controls, thus avoiding costly modifications. With the specification of the temperature ranges (Table 1), suitable thermocouples (Table 2) and external electronics (Table 3) were chosen. Hereby, the external electronics transform the analog signal of the thermocouples into another analog signal, suitable for the DAQ. The external electronics shown in Table 2 can be individually configured, making them compatible with other types of thermocouples and therefore can be used with potential replacements or alternatives.

Fig. 5 Furnace 1 (right) capable of 600°C and furnace 2 (left) capable of 1400°C
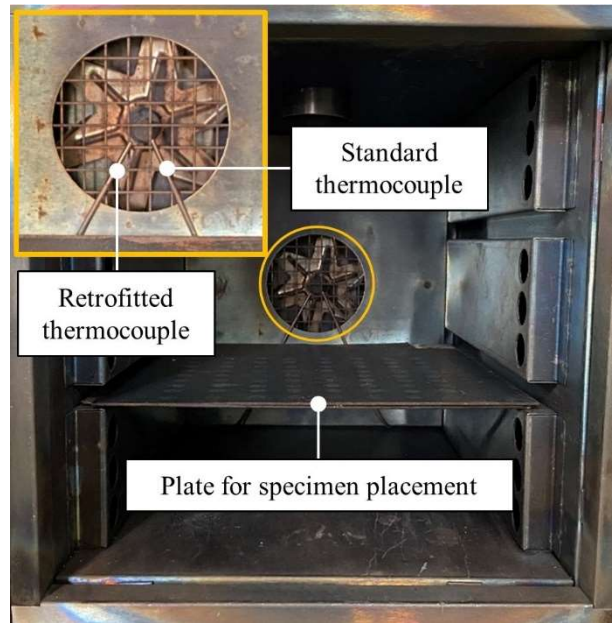
Fig. 6 Retrofitted thermocouple Type K of furnace 1
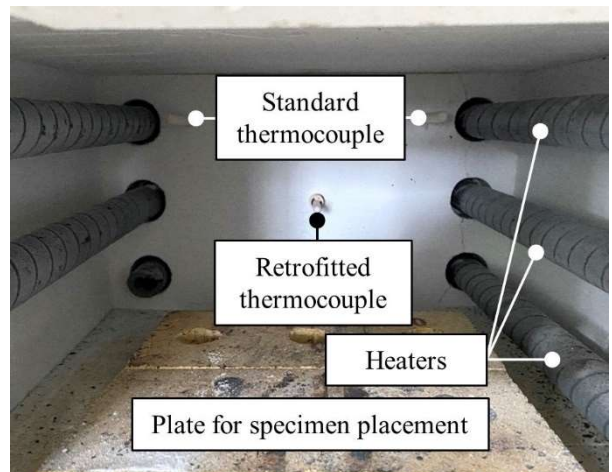
Fig. 7 Retrofitted thermocouple Type K of furnace 2

The second type of machine at the CMF is a hydraulic press from 1952 (Fig. 8). The press is capable of a maximum opening height of 345 mm, reduced by the implemented dies and tools. Furthermore, the limit of the one-sided press force is 1 MN with a maximum pressing speed of 6.3 mm/s (Table 1). The initial state of the press already included a load cell located between the base plate and the bottom die to measure the force and a Linear Variable Differential Transformer (LVDT) sensor to measure the distance between top piston and base plate.

Due to the non-uniformity of the contact surface between load cell and worktable, the initial load cell showed plastic deformation leading to a falsification of the measurement. Therefore, a base plate was designed to ensure a uniform contact surface and consequently the accuracy of measurements as well as the longevity of the new load cell (Fig. 9). For this retrofitting approach, a load cell

compatible with the existing external electronics was chosen, (Table 3), supporting the low-cost brownfield approach. This cell has a linearity of 0.05%, enabling the accurate measurement of forces from 0-1 MN. Besides eliminating the necessity of interchanging between different load cells depending on the maximum accruing process forces, the probability of damaging the load cell is significantly reduced.

To measure the distance between the piston and base plate, an already existing LVDT sensor was tested and recalibrated, showcasing the prescribed accuracy as indicated on the data sheet. Thus, the testing, recalibration and further utilization of the sensor supports the applied low-cost approach. The mounting of the LVDT sensor is located at the back of the hydraulic press with non-magnetic material, thus preventing an interference with the inductive measuring principle of the sensor (Fig. 10). As in the case of the load cells, the use of the LVDT (Table 2) enables the further utilization of the already implemented external electronics (Table 3). To measure the specimen temperature in-line during upsetting, a pyrometer (Table 2) calibrated to the respective specimen material is positioned at the back of the press between the upper and lower die (Fig. 9). To protect the sensitive optic of the pyrometer, an enclosure is implemented to prevent possible damage and ensure accurate measurements. Additionally, a thermocouple Type K (Table 2) with corresponding external electronics (Table 3) was implemented, to measure the temperature of a hot specimen on contact for the determination of the corresponding emissivity coefficient and characteristic curve of the tested material. The same thermocouple was used to measure the ambient temperature T_a. The emissivity coefficient and other software parameters of the pyrometer for each respective material can be set via MODBUS without using the software. Due to the difficult determination of the emissivity coefficient of aluminum and the respective surface, a material and surface specific temperature characteristic curve was evaluated and implemented in CODESYS, also accounting for environmental influences in to obtain the most accurate temperature measurement possible under given restrictions.
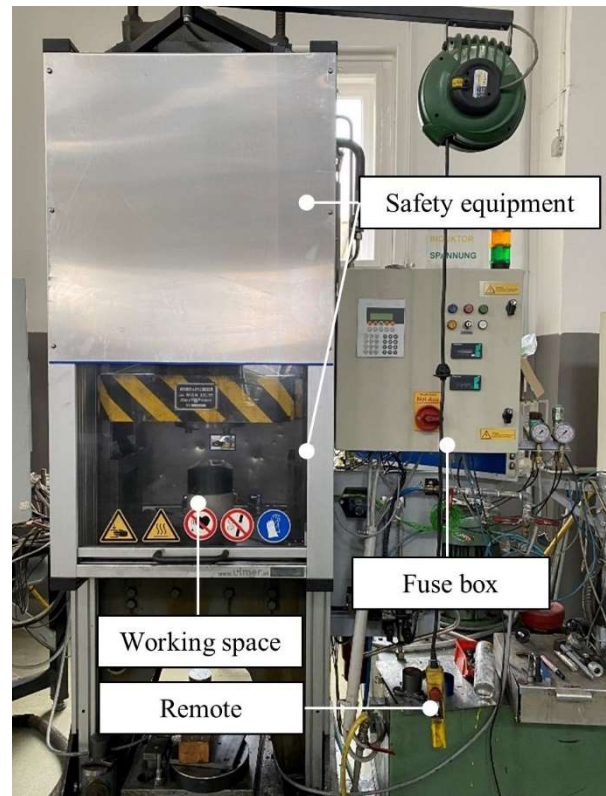

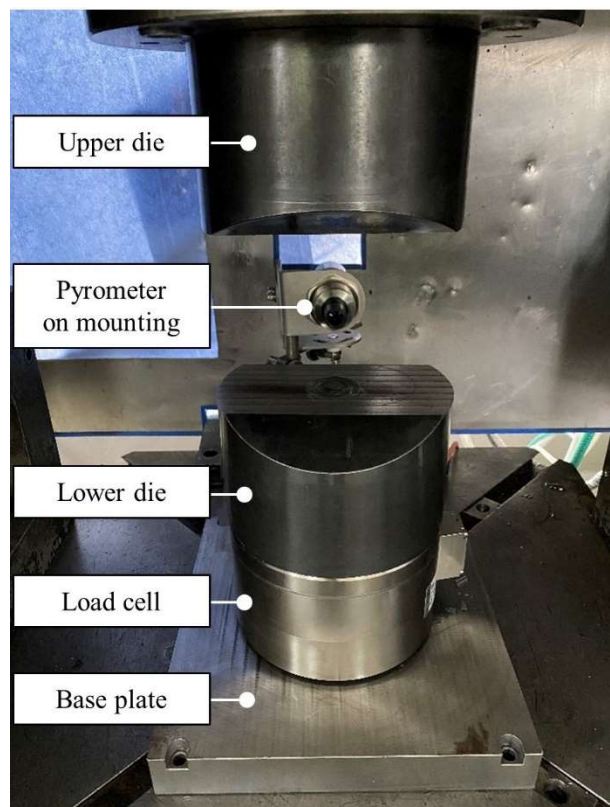**Fig. 8** Hydraulic press with retrofitted safety door and housing

Fig. 9 Replaced load cell with base plate to ensure uniform load and therefore accurate measurements, and mounted Pyrometer for in-line measurement of specimen temperature during upsetting
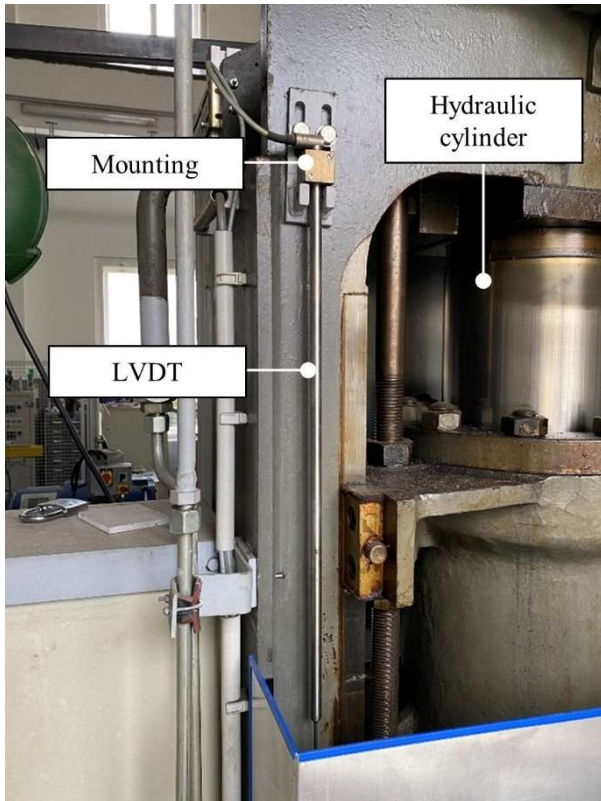
Fig. 10 Recalibrated LVDT sensor at the back of the hydraulic press

Table 1 Machines and system parameters to be measured including the respective ranges of the measurements

Machine	System Parameter	Range
Furnace 1	T_{F1}	25-600 °C
Furnace 2	T_{F2}	25-1400 °C
Hydraulic press	F_P	0-1 MN
	h_{ud}	0-345 mm
	T_a (°C)	25-600 °C
	T_{pyro}	20-850 °C

Table 2 Machines and selected sensors with respective specifications based on the system parameters and requirements

Machine	Sensor	Type	Range	Linearity	Output signal
Furnace 1	Thermo couple Type K	Thermo couple	-40-1050 °C	n/a	n/a
Furnace 2	Thermo couple Type S	Thermo couple	0-1400 °C	n/a	n/a
Hydraulic press	HBM C6B	Load cell	0-1 MN	0,05%	2.35 mV/V
	Gefran PC-B-500	LVDT	0-500 mm	0,05%	4-20 mA
Hydraulic press	Thermo couple Type K	Thermo couple	-40-1050 °C	n/a	n/a
Hydraulic press	PMR Pyrospot DA 44M	Pyrometer	20-850 °C	0,6%	0/4-20 mA

Table 3 External electronics with specifications for the selected sensors of the respective machines

Machine	External electronics	Type	Sensor	Output
Furnace 1	PMR PMD universal Measuring transducer - Isolating transducer	integrated electronic (n/a)	Thermocouple Type K	4-20 mA
Furnace 2	PMR PMD universal Measuring transducer - Isolating transducer	integrated electronic (n/a)	Thermocouple Type S	4-20 mA
Hydraulic press	HBM AE 301	mV transmitter	Load cell	±10V
	HBM AE 501	integrated electronic (n/a)	LVDT	±10V
	PMR PMD universal Measuring transducer - Isolating transducer	integrated electronic (n/a)	Thermocouple Type K	4-20 mA

3.3 Digitization and Digitalization

To process the resulting analog sensor signals, a conversion to digital signals has to be carried out, making the signals applicable for computer-aided processing. Therefore, a uniform analog signal of 4-20 mA was preferred, as electric current exhibits noise immunity and lower sensitivity to the increasing cable length in comparison to voltage (Fraden 2010; Johnson 2009, 2006). Therefore, the analog signal would not be affected significantly in the case of relocation of the PLC, thus being suitable for the long-distance transmission. The analog output signal is either directly provided by the sensor (Table 2) or transformed by supporting external electronics (Table 3), providing the selected output signal for the I/O modules of the PLC. For the PLC, a RevPi Connect+ feat. CODESYS and corresponding RevPi AIO I/O modules powered by 24 V power supply were utilized (Fig. 11). In addition, an electronic fuse was implemented, to protect the sensors, external electronics and DAQ from electrical malfunctions. The inputs of the AIO modules can be configured individually to each analog signal, enabling the utilization of the full resolution of the signal. Hereby, the resolution of the analog measurement signal is defined by the DAQ. In the case of the RevPi, each analog system can be resolved in 14 bit, thus resulting in 2^{14} equivalent increments. To convert the analog signal into a digitized signal equivalent to the physical quantity, a linear characteristic curve for each sensor has to be determined. Therefore, the bit signal in the range from 0 to 2^{14} is multiplied with the slope a, resulting in the physical quantity of the respective signal (Eq. (12)). In addition, the intercept b is taken into account in order to compensate deviations from the ideal state of the sensor, e.g., assembly inaccuracies. The coefficients of Eq. (12)

of all machine parameters and respective physical quantities are listed in Table 4.

$$value_{physical\ quantity} = a \cdot signal_{bit} + b \qquad (12)$$

Table 4 Machine parameters and coefficients of the linear characteristic curve

Machine	Physical quantity	Range	a (-)	b (-)
Furnace 1	T_{F1} (°C)	25-600	0.090625	-362.5
Furnace 2	T_{F2} (°C)	25-1400	0.04375	-175.0
Hydraulic press	F_P (MN)	0-1	0.1	0.0
	h_{ud} (mm)	0-345	0.0347	-1.804
	T_a (°C)	25-1400	0.04375	-175.0

The programming for the DAQ including the embedding of the characteristic curves (Table 4) is realized with CODESYS. In contrast to the linear characteristic curves in Table 4, the material and surface-specific pyrometer characteristic curve was experimentally evaluated as described in Section 3.2 and implemented as an eighth-order function for the determination of T_{pyro}. The structured text (ST)-based programming language CODESYS operates on the RevPi and runs the code for gathering, pre-processing and integrating the data into the production network. An alternative programing approach with Python would support the open-source approach, but was neglected because of the higher resilience of CODESYS. Therefore, the open-source approach is not applicable, but due to the relatively low cost of the software, the low-cost premise of requirement (5) is fulfilled. To enable the situationally appropriate adaption and contribute to requirement (2), two different sampling rates were defined. Furthermore, a continuous sampling rate for condition monitoring of 1 Hz was set, showing warnings on the GUI in case of needed sensor recalibration due to a possible exceeding of the calibration range. The second sampling rate of 100 Hz is triggered with the GUI, by switching a Boolean variable from False to True by the press of a button. Hereby, the higher sampling rate is imperative to gather a sufficient amount of data points during the processes to accurately depict them. As shown in Figure 13, the visualization of process parameters and the initialization of a measurement is realized with a WAGO based GUI, thus fulfilling requirement (4). Using MODBUS, the RevPi publishes specific process parameters into the network, allowing the visualization on the GUI, therefore enabling a superordinate GUI of different systems using different DAQs (Fig. 12). This approach also avoids workers to have to operate with a multitude of separate visualization solutions. As previously mentioned, the data of all systems is stored in parallel in a MariaDB and on a file server, ensuring availability for the FEA and post processing, thus fulfilling requirements (1) and (2). The resulting hardware and software structure resulting from the retrofitting approach is shown in Fig. 14.
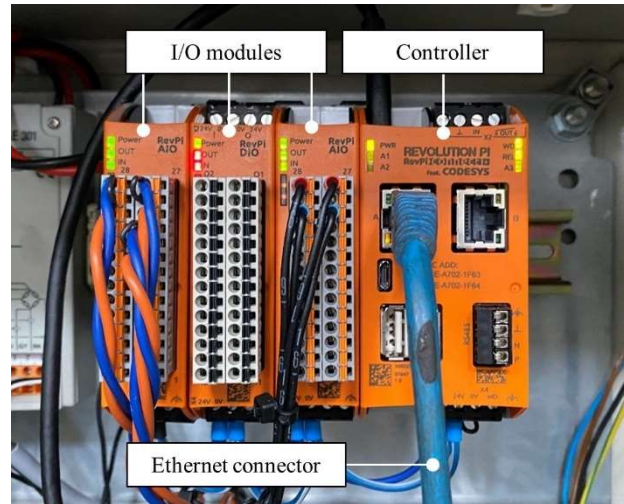
Fig. 11 RevPi Connect+ feat. CODESYS with AIO modules and sensor inputs
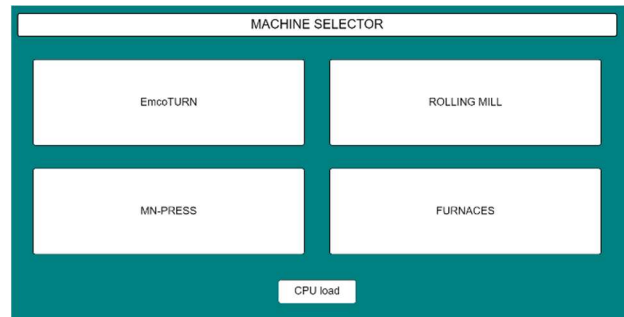
Fig. 12 Superordinate WAGO GUI for uniform implementation of other CPPS into the production network and visualization environment
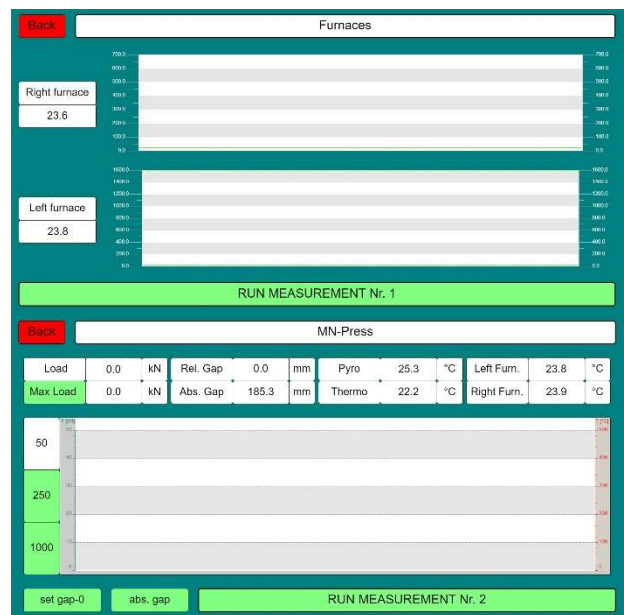
Fig. 13 Individual GUIs of the furnaces (top) and the hydraulic press (bottom), allowing the independent operation as stand-alone CPPS
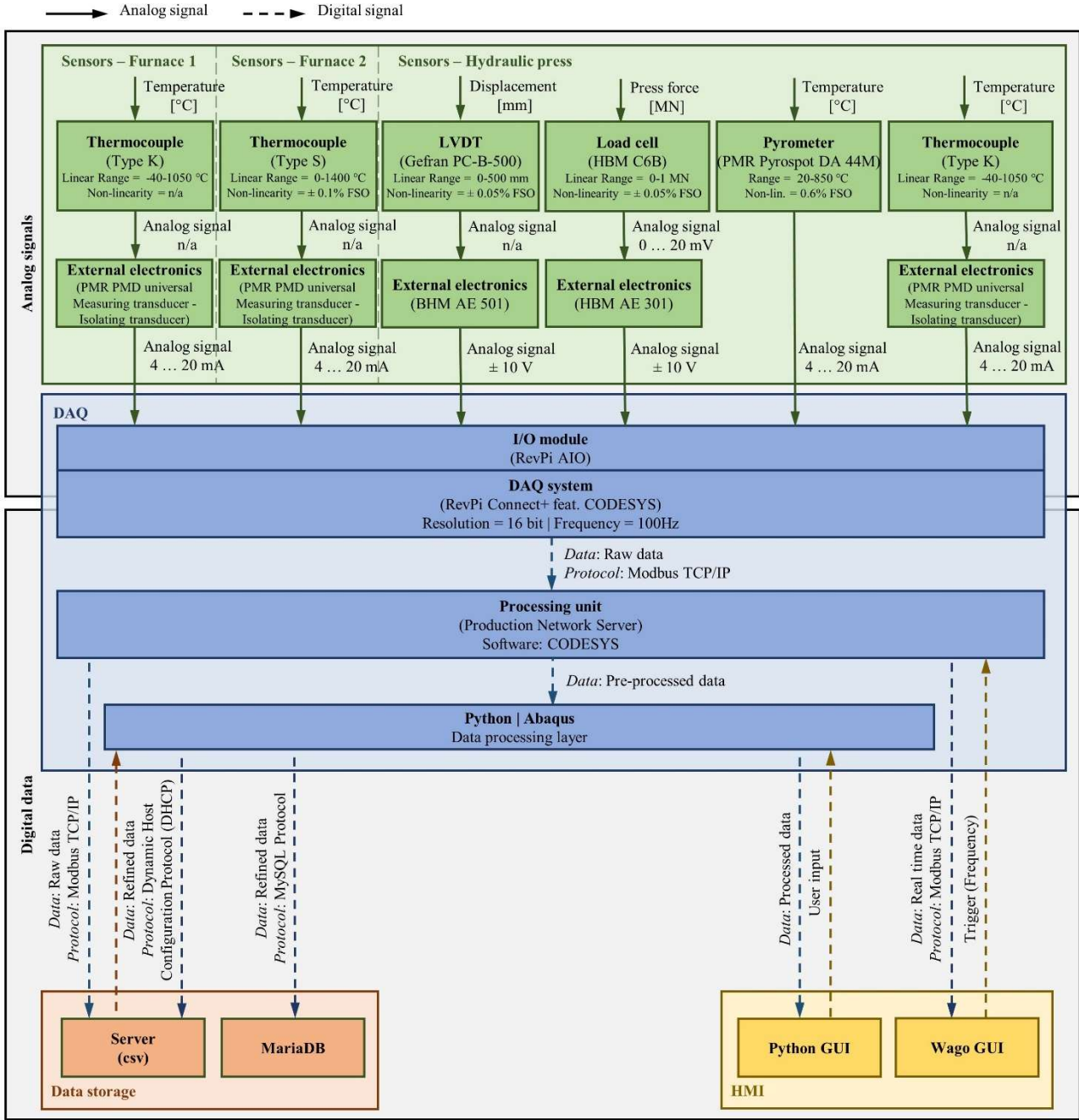
Fig. 14 Sensors, signals, connectivity and resulting signal path

4 Digital Shadow development

In this chapter, the FEA development of the individual processing steps and the respective process and material parameters are outlined (4.1-4.3), followed by the connectivity of the simulations for the development of the DS (4.4).

4.1 FEA of the furnaces

Both furnaces were modeled as three-dimensional rigids with DC3D8 elements, as the temperature field is the only desired output of this thermal analysis. The dimensions of furnace 1 are defined by the height h_{F1} x width w_{F1} x depth

d_{F1}, measuring 300 x 260 x 300 mm. Similarly, the dimensions of furnace 2 are defined by the height h_{F2} x width w_{F2} x depth d_{F2}, measuring 240 x 300 x 450 mm. For the FEA, furnace 1 is meshed with the predefined seed size s_{F1}, whereas furnace 2 uses a predefined seed size s_{F2}. By inputting a specific user defined furnace temperature T_F, the respective preheating time of furnace 1 t_{F1}, using equation Eq. (13), and furnace 2, using equation Eq. (14), is calculated. Subsequently, T_F is set as a boundary condition (BC) in the FEA (Fig, 15).

$$t_{F1} = 7.446 \cdot 10^{-8} \cdot T_F{}^3 + 1.474 \cdot 10^{-4} \cdot T_F{}^2 + 0.1282 \cdot T_F - 22.78 \quad (13)$$

$$t_{F2} = 1.034 \cdot 10^{-6} \cdot T_F{}^3 + 7.115 \cdot 10^{-4} \cdot T_F{}^2 \\ + 0.2692 \cdot T_F - 3.804 \qquad (14)$$

Similar to the furnaces, the specimen was modeled using three-dimensional rigids and DC3D8 elements, whereby the cylindrical specimen is defined by the initial diameter d_0 and initial height h_0 meshed with a defined seed size s_m. Furthermore, the initial specimen temperature T_0 is defined as the ambient temperature T_a, evaluated from the thermocouple Type K of the hydraulic press. To map the heating process, surface-to-surface contact between the specimen and the furnace was defined, considering convection, emissivity and contact conduction in the contact area of specimen and furnace. For the mapping of the heat transfer between the furnace and the specimen, a convention coefficient h_{c1} of 0.025 W/m²K (Han 2012; Marek and Nitsche 2019) and contact conductance as a function of clearance k_{c1} was defined, employing 0.3 W/m²K at contact and 0.0 W/m²K at a distance of 0.01 mm (Rosochowska et al. 2003). Depending on the surface properties of the analyzed specimen, the emissivity coefficient can vary significantly. According to literature, the emissivity coefficient for aluminum can range from 0.02 for polished aluminum to 0.9 for anodized aluminum (Willems 2017). For the CNC machined surface of the used specimens, an emissivity coefficient of 0.3 was fitted, achieving accurate results in the FEA (Table 5). For stainless steels like 1.4301, used for the lining of furnace 2, the emissivity coefficient can vary from 0.6 to 0.9 for matte or rough surfaces (Modest and Mazumder 2022). For the FEA, an emissivity coefficient of 0.68 was chosen (Table 5). The generated output of this simulation is the node temperatures of the specimen T_{1end}, also indicating whether the specimen has been heated through.
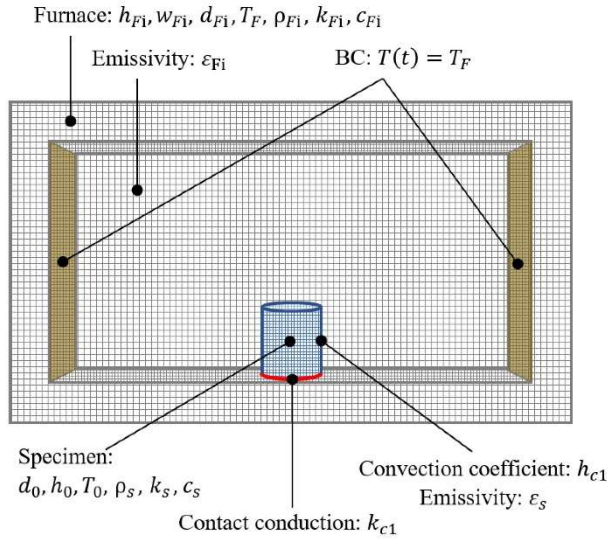
Fig. 15 Schematic FEA of the furnace and specimen with respective parameters and BC

4.2 Transport simulation

To map heat transfer during the transport of the specimen from the furnace to the hydraulic press for the positioning on the bottom die, initial FEAs were set up to simulate the cooling process. For the transport, the specimen with T_{1end} is manipulated with tongs at T_a, resulting in further heat transfer between the contact surface of the tongs and specimen over a defined time period t_{trans}. The resulting heat transfer is taken into account by the fitted convection coefficient h_{c2} of 0.255 W/m²K. Based on the approach by (Kashani et al. 2017), a Python based model was implemented to improve the computational efficiency of the cooling process using a finite differences approach, calculating the heat transfer in cylindrical coordinates. The consistent underlying physics were fitted in the Python application to represent the cooling behavior of the EN AW-6060 specimen according of the FEAs but can be replaced with other material parameters automatically by the GUI. As in the FEA, the additional heat transfer between the line-shaped contact surface of the tongs and the specimen was considered by the parameter fitting. Both modelling approaches produce similar outputs for node temperatures and return the specimen node temperatures after the transport T_{2end}.

4.3 FEA of the hydraulic press

For the FEA of the upsetting process, the simulation was modeled as three-dimensionally rigids and divided into two steps. For both dies a cylindrical geometry with the diameter d_p and height h_p was chosen. In the first step, the cooling in the defined resting time of the specimen t_{rest} with T_{2end} (Section 4.2) while resting on the bottom die at T_a is simulated. Here, convection, emissivity and contact conduction between the contact surface of specimen and bottom die is taken into account. The heat transfer of the specimen is accounted by the convection coefficient h_{c3} of 0.04 W/m²K (Han 2012; Marek and Nitsche 2019) and contact conductance as a function of clearance k_{c3} of 2.0 W/m²K at contact and 0.0 W/m²K at a distance of 0.01 mm (Rosochowska et al. 2003). The emissivity coefficients of the dies made from tool 1.4301 ranges from 0.3 to 0.5 for smooth or oxidized surfaces (Palik 1997). Consequently, an emissivity coefficient of 0.3 was chosen for the dies. For the contact definition, general contact is applied using hard contact in normal direction and a penalty friction formulation with a constant friction coefficient μ of 0.3 in tangential direction. Consequently, the generated output of this simulation are the node temperatures of the specimen and lower die T_{3end}. After t_{rest} has elapsed, the second step is initiated with the top die moving down. Therefore, all degrees of freedom of the bottom die are constrained to keep it in position. For the movement of the top die, a coupled reference point with a time-displacement BC equal to the real velocity of the hydraulic press was applied over the upsetting time, constraining transitional and rotational degrees of freedom. Furthermore, inelastic heat fraction of 0.9 (Chen et al. 2017; Groche and Krech 2017), convection, emissivity and contact conduction at T_a between the

contact surfaces of specimen and the upper and bottom die is determined (Table 5). For the contact conductance k_{c4}, 10.0 W/m²K at contact and 0.0 W/m²K at a distance of 0.01 mm were used (Rosochowska et al. 2003). As shown in Fig. 2, the top die is lowered until the end height h_1 is reached, completing the upsetting simulation. To accurately represent the upsetting process, both specimen and dies were defined with their respective thermo-mechanical properties (Table 5, 6). For the specimen as well as for both dies, C3D8RT elements with a seed size s_p were used. To represent the forces due to deformation of the specimen, three material models were experimentally evaluated, validated, and implemented. The material model parameters were determined according to Section 5.2 and are listed in Table 9. The flow curve, JC and Hensel-Spittel material models were used for the calculation of the deformation forces. The output of the FEA contains the node temperatures, corresponding forces and displacements of the respective entities.
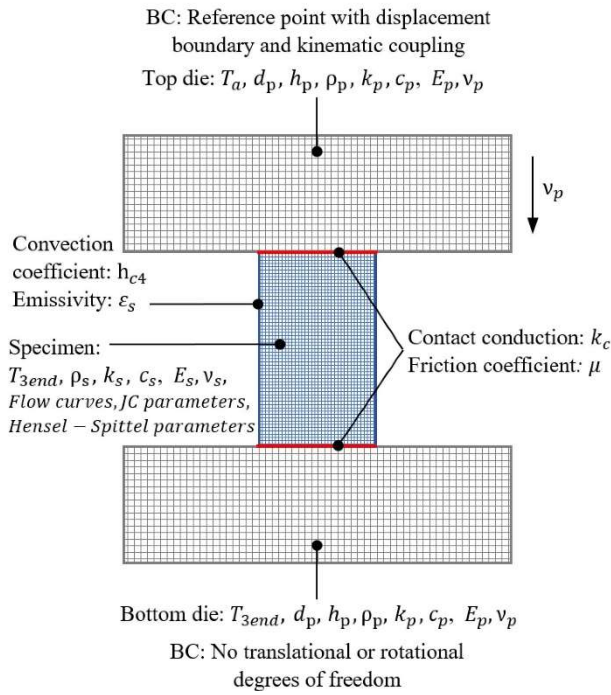
Fig. 16 Schematic FEA of the hydraulic press and specimen with respective parameters and BCs

4.4 Connectivity

Due to the focus on low-cost and open-source software solutions, Python was used to connect the individual FEAs. All simulations were scripted with Python, automatically transferring the relevant parameters to the subsequent simulation after their completion, enabling a fully automated and holistic process mapping, as visualized in Fig. 17. The execution of the main script launches the DS, starting the automated process sequence

simulation. First, the simulation "furnace.py" (Section 4.1) is initialized, using the respective user input and predefined parameters, specifying the desired temperature and the type of furnace. The results of this heating simulation are the node temperatures of the specimen, saved in an odb-file, which data is consequently extracted with Python to pass them to the following simulation. Subsequently, the second Python-based simulation "transport.py" (Section 4.2) is started, using the specimen node temperatures from the previous simulation, evaluating the node temperatures after the transport. Next, the third simulation "hypr_resting.py" (Section 4.3) is launched with the new specimen node temperatures, also delivering specimen node temperatures in the odb-file format, as previously described. In addition, the odb-file data is extracted and saved in a csv-file for further data processing and analysis. Last, the fourth simulation "hypr_upsetting.py" (Section 4.3) is launched, using the node temperatures of the specimen and bottom die, eventually outputting the defined simulation parameters of force, displacement, and node temperatures. Simultaneously, the data is extracted and saved.
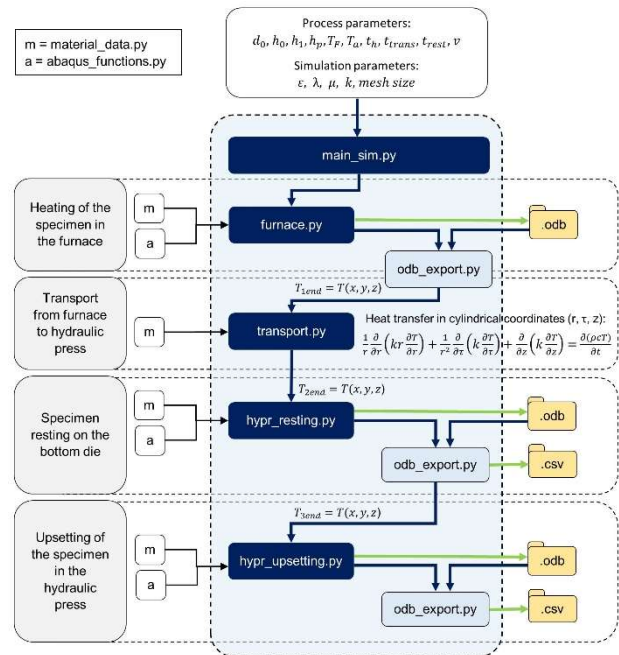
Fig. 17 Modular process flow with respective input and output

Table 5 Thermal material parameters of the specimen (Martienssen and Warlimont 2011), furnace 1 (KLEIBER Infrared GmbH; Stephan et al. 2019), furnace 2 (Simufact Engineering GmbH 2023) and hydraulic press (Simufact Engineering GmbH 2023)

Section	Material	Specific heat capacity c (J/kg·K)	Thermal Conductivity k (W/m·K)	Temperature T (K)	Emissivity coefficient ε (-)	Temperature T (K)
Specimen	EN AW 6060	904.1	211.6	293.15	0.3	
		916.4	215.8	323.00		
		928.6	220.0	373.00		
		940.9	224.0	423.00		
		953.2	228.3	473.00		
		965.4	232.4	523.00		
		977.7	236.6	573.00		
		990.0	240.7	623.00		
		1002.2	244.9	673.00		
		1014.5	249.0	723.00		
		1026.8	253.2	773.00		
Furnace 1	1.4301	430.0	15.0	323.15	0.68	
		502.0	16.3	373.15		
		503.0	16.7	423.15		
		519.0	17.2	473.15		
		533.0	17.6	523.15		
		558.0	18.4	573.15		
		587.0	19.3	526.15		
		591.0	20.5	673.15		
		582.0	20.9	723.15		
		595.0	21.8	773.15		
		630.0	23.0	823.15		
		628.0	23.4	873.15		
		513.0	24.7	923.15		
		514.0	25.5	973.15		
		598.0	26.4	1023.15		
Furnace 2	Silica	915.0	1.20	673.15	0.88	293.15
		944.0	1.36	873.15	0.77	603,15
		961.0	1.51	1073.15	0.58	1003.15
		969.0	1.64	1273.15	0.28	2003.15
		979.0	1.76	1473.15		
Hydraulic press	1.2343	439.0	31.9		0.3	

Table 6 Density and elastic material parameters of the specimen (Simufact Engineering GmbH 2023), furnace 1 (Stephan et al. 2019), furnace 2 (Simufact Engineering GmbH 2023) and hydraulic press (Simufact Engineering GmbH 2023)

Section	Material	Density ρ (kg/m³)	Poisson's ratio ν (-)	Young's Modulus E (MPa)	Temperature T (K)
Specimen	EN AW 6060	27000.0	0.34	69500.0	293.15
				69000.0	323.00
				68000.0	373.00
				65000.0	423.00
				63000.0	473.00
				60000.0	523.00
				58000.0	553.00
				55000.0	623.00
				53000.0	673.00
				51000.0	723.00
				50000.0	773.00
				48000.0	823.00
Furnace 1	1.4301	7850.0			
Furnace 2	Silica	1820.0			
Hydraulic press	1.2343	7890.0	0.30	210000.0	

5 Experimental setup, calibration, and validation for DS and CPPS development

In this section, the experimental setup for the evaluation of the material model parameters of the EN AW-6060 is outlined in (5.1). Furthermore, the calibration and validation of the parameters used in FEAs are described in detail in (5.2). In addition, material related tests to validate the material models are elaborated in (5.3).

5.1 Evaluation of material data and material model parameters

To evaluate the JC parameters of EN AW 6060, a Servotest thermomechanical treatment simulator was used. This testing machine is capable of reproducing multi-stage forming processes with high temperatures up to 1300°C as well as strain rates as they can occur e.g. in rolling mills or forges. The manipulator can transport a specimen, to which thermocouples are attached, via an

inductively heated furnace to subsequent presses, which compress the specimen to a defined final height with a force of up to 500 kN at a corresponding strain rate. It is possible to set tool speeds of up to 1 m/s and strain rates of up to 200 s⁻¹. As a result, the flow curves in dependency of various strain rates and temperatures, imperative for the JC material model and thus for upsetting process can be recorded. Concerning the experimental setup shown in Figure 18, the specimen is compressed longitudinal to the extrusion direction of the specimen. To reduce friction in the contact are between the specimen and the anvil, glass powder was used, furthermore ensuring a uniform stress state. The conducted experiments were carried out with the temperatures and strain rates shown in Table 7, using EN AW-6060 specimens manufactured from rod material, whereby the specimen exhibited an initial diameter d_0 of 10 mm and an initial height h_0 of 15 mm. Due to the high reproducibility of the flow curve measurement and its results, five specimens of each combination of temperature and strain rate were examined, resulting in a total of 240 specimen. The statistical evaluation of the resulting flow curve parameters are listed in Table 8.
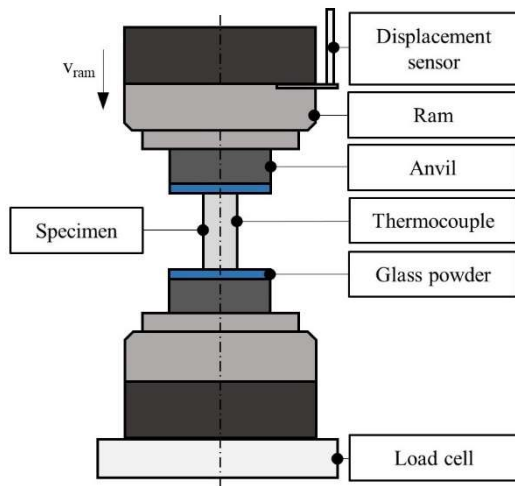
Fig. 18 Schematic experimental setup of the Servotest for the evaluation of the flow stresses in dependence of different temperatures and strain rates.

Table 7 Experimental setup for the Servotest with five specimens of each parameter combination resulting in a total 240 specimen for the evaluation the JC parameters

T (°C)	$\dot{\varepsilon}_P$ (1/s)
25	0.01
50	0.1
75	1
100	10
125	
150	
175	
200	
250	
300	
350	
400	

Table 8 Resulting experimental plan and respective results from the Servotest experiments

T (°C)	$\dot{\varepsilon}_P$ (s⁻¹)	k_{f0} (MPa)	K (MPa)	n (-)
25	0.01	187.540 ± 7.263	167.746 ± 15.461	0.587 ± 0.027
25	0.1	186.833 ± 5.117	159.081 ± 6.311	0.555 ± 0.013
25	1	186.973 ± 3.291	142.228 ± 8.349	0.472 ± 0.019
25	10	163.107 ± 16.647	151.072 ± 11.007	0.332 ± 0.061
50	0.01	187.060 ± 7.846	157.382 ± 12.258	0.597 ± 0.047
50	0.1	178.667 ± 2.568	164.556 ± 10.856	0.575 ± 0.018
50	1	188.413 ± 5.240	119.492 ± 6.982	0.454 ± 0.024
50	10	176.453 ± 5.203	137.274 ± 7.971	0.416 ± 0.097
75	0.01	178.320 ± 7.727	144.009 ± 10.097	0.573 ± 0.035
75	0.1	175.947 ± 10.739	146.725 ± 10.793	0.546 ± 0.027
75	1	186.480 ± 5.347	112.661 ± 8.474	0.452 ± 0.022
75	10	145.080 ± 8.207	144.007 ± 15.412	0.301 ± 0.087
100	0.01	176.200 ± 5.442	138.827 ± 10.369	0.613 ± 0.034
100	0.1	180.567 ± 5.642	120.954 ± 11.946	0.555 ± 0.030
100	1	180.073 ± 7.213	97.814 ± 10.317	0.411 ± 0.028
100	10	165.127 ± 8.217	110.963 ± 10.892	0.325 ± 0.030
125	0.01	169.753 ± 2.612	111.982 ± 9.866	0.586 ± 0.034
125	0.1	174.880 ± 5.748	109.503 ± 15.440	0.546 ± 0.034
125	1	175.073 ± 5.901	81.872 ± 6.750	0.353 ± 0.024
125	10	173.793 ± 6.776	92.325 ± 8.382	0.320 ± 0.018
150	0.01	167.167 ± 4.015	87.320 ± 7.199	0.559 ± 0.039
150	0.1	169.767 ± 4.019	87.171 ± 6.407	0.492 ± 0.039
150	1	172.293 ± 4.920	74.822 ± 7.914	0.343 ± 0.032
150	10	164.440 ± 9.390	81.280 ± 6.290	0.293 ± 0.043
200	0.01	122.827 ± 14.417	67.837 ± 7.462	0.387 ± 0.054
200	0.1	153.827 ± 3.575	43.129 ± 8.247	0.336 ± 0.064
200	1	159.727 ± 4.175	128.459 ± 15.923	0.532 ± 0.0632
200	10	158.927 ± 7.729	148.291 ± 5.921	0.613 ± 0.134
250	0.01	103.320 ± 8.661	34.859 ± 7.091	0.313 ± 0.057
250	0.1	134.067 ± 2.095	37.186 ± 3.445	0.422 ± 0.058
250	1	138.913 ± 1.553	90.815 ± 9.069	0.642 ± 0.150
250	10	143.253 ± 3.764	131.248 ± 5.560	0.674 ± 0.129
300	0.01	78.593 ± 1.963	35.569 ± 4.632	0.709 ± 0.208
300	0.1	87.067	41.598	0.597

		± 2.353	± 6.039	± 0.147
300	1	94.873	40.577	0.452
		± 0.883	± 4.481	± 0.209
300	10	98.087	33.425	0.253
		± 2.581	± 0.772	± 0.042
350	0.01	42.922	11.095	0.559
		± 1.225	± 4.150	± 0.125
350	0.1	49.667	18.306	0.451
		± 0.775	± 3.596	± 0.161
350	1	54.913	23.821	0.315
		± 1.282	± 1.921	± 0.035
350	10	51.347	45.698	0.311
		± 4.439	± 5.149	± 0.034
400	0.01	21.907	9.152	0.457
		± 0.419	± 1.646	± 0.043
400	0.1	22.487	28.985	0.390
		± 1.074	± 4.060	± 0.070
400	1	35.933	23.949	0.339
		± 0.823	± 4.767	± 0.094
400	10	31.140	51.807	0.319
		± 3.518	± 8.619	± 0.028

The evaluated JC and Hensel-Spittel material parameters (Table 9) from the experimental results (Table 8) follow the evaluation procedure in (2.2), whereas the derivation was fully automated using Python. Consequently, this enables the automated determination of new material model parameters of new materials and their implementation into a material database, pointing out the scalability of this approach.

Table 9 Evaluated material parameters for the JC and Hensel-Spittel material models used in the FEAs

Material model	Abr.	Unit	Quantity
JC	A	(MPa)	136.113
	B	(MPa)	111.80
	C	(-)	3.027E-3
	n	(-)	0.248
	m	(-)	0.942
	T_t	(°C)	25.00
	T_m	(°C)	550.00
	$\dot{\varepsilon}_0$	(s^{-1})	0.01
Hensel-Spittel	A	(MPa)	352.347
	m_1	(-)	-1.623E-3
	m_2	(-)	4.396E-2
	m_4	(-)	-5.729E-3
	m_5	(-)	-4.742E-3
	m_7	(-)	-2.893E-3
	m_8	(-)	6.637E-4

5.2 Practical experiments and validation

For the practical experiments necessary to validate the FEA, a total of 648 EN AW-6060 specimen were heated in a furnace and compressed with the hydraulic press. To avoid size effects, the same specimen geometry of d_0 and h_0 as with the Servotest experiments was used. In the first step, the specimens were heated in the one of the furnaces until a homogeneous temperature field was reached, whereby the furnace temperature was measured with a thermocouple, according to Table 2. For this purpose, the respective furnace was preheated according to the Eq. (13) or Eq. (14) for a calculated time depending on the defined condition of the desired furnace temperature T_f, as shown in Table 10. After reaching the defined temperature, the specimens were placed in the furnace and heated through according to the FEA. Subsequently, a specimen was taken out of the furnace with metallurgical tongs and transported to the hydraulic press in a defined transport time t_{trans} (Table 10). Due to the transport from the furnace to the hydraulic press, a holistic measurement of the specimen temperature is not possible, schematically illustrated in Fig. 22. Thus, when the specimen reaches the press, the specimen was held between the upper and lower punches in a floating position while measuring the specimen temperature with the pyrometer, avoiding cooling due to the contact of the specimen and the bottom die. In the next step, the specimen is placed on the bottom die for a defined resting time t_{rest}, during which heat transfer occurs between the bottom die and the specimen, marking the time t_1. As shown in Fig. 20, the pyrometer measures the punctual specimen with the differential height h_{pyro} from the bottom die while the top die was positioned 37.3 mm above the bottom die. After reaching t_{rest}, the control of the hydraulic press is started manually, whereas the top die automatically descends at a constant speed of 6.3 mm/s, contacting the specimen at t_2, and reaching its end position at t_3, upsetting the specimen to the end height h_1, according to Table 10 and Fig. 22. The movement of the bottom die is controlled by the internal control unit of the hydraulic press, resulting in a high reproducibility of the process. During the upsetting process, both dies are in contact with the specimen and heat transfer occurs between contact surfaces of the specimen and the two dies, resulting in a heat transfer and corresponding temperature change which is measured in-situ with the pyrometer (Fig. 21). As described in section 3.2, the force is measured in-situ with a load cell (Table 2) and the top die position is measured with an LVDT (Table 2). After reaching h_1, the upper die returns to its initial position and the specimen is removed. This approach also includes time delays due to extrinsic inaccuracies and influences in removing the specimen from the furnace, placing it in the hydraulic press, as well as initiating the start-up process for the upsetting. Nonetheless, these human inconsistencies can be quantified with the gathered data and incorporated into simulation and data analysis for the optimization processes.
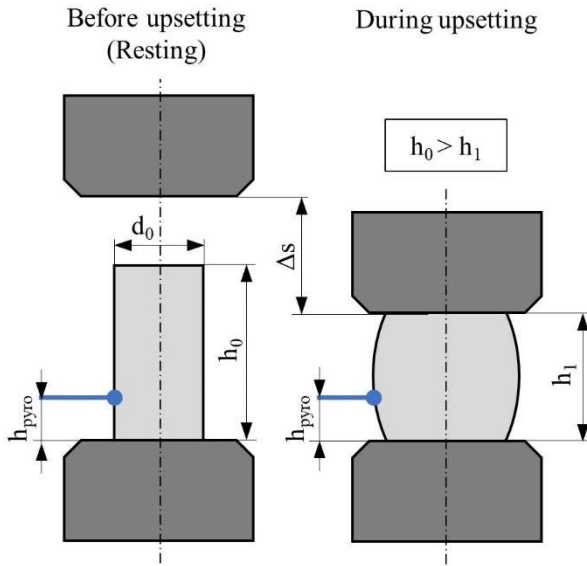
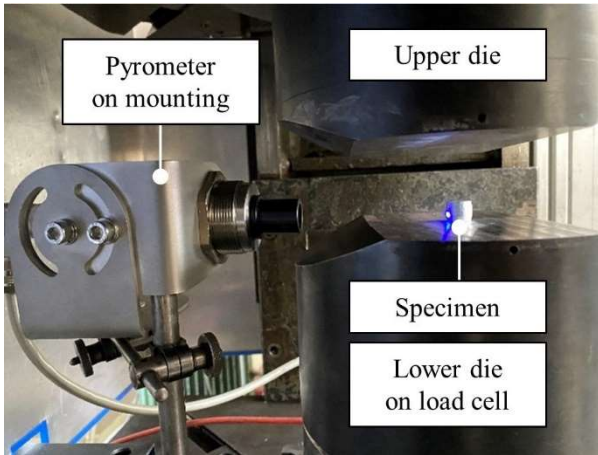Fig. 20 Schematic experimental setup for the upsetting process

Fig. 21 Experimental setup with pyrometer and specimen with pyrometer laser (blue) with a distance of 70 mm
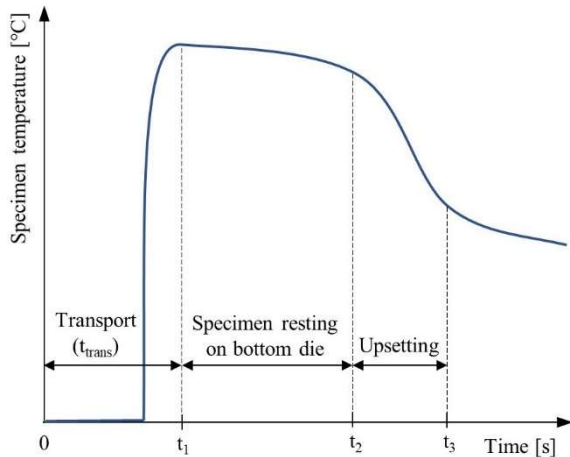
Fig. 22 Quantitative pyrometer measurements as a result of the experimental setup and order of processing steps

Table 10 Experimental setup for the hydraulic press with eight specimens of each parameter combination resulting in a total 846 specimen for the calibration and validation

T_F (°C)	t_{trans} (s)	h_1 (mm)
100	7	5.0
150	10	7.5
200	13	10.0
250		
300		
350		
400		
450		
500		

The results of the experimental plan from Table 10 are shown in Table 11.

Table 11 Resulting experimental plan for the practical experiments and respective results

T_F (°C)	t_{trans} (s)	h_1 (mm)	F_{max} (kN)	T (at t_3) (°C)	h_{1exp} (mm)	d_{1exp} (mm)
100	7	5.0	68.38 ± 1.75	71.52 ± 2.75	5.21 ± 0.05	17.37 ± 0.10
100	7	7.5	39.63 ± 0.41	77.01 ± 7.34	7.62 ± 0.05	14.40 ± 0.05
100	7	10.0	28.43 ± 0.52	63.96 ± 4.46	9.91 ± 0.08	12.67 ± 0.06
100	10	5.0	66.68 ± 0.83	80.49 ± 9.17	5.26 ± 0.05	17.31 ± 0.06
100	10	7.5	39.41 ± 0.50	78.61 ± 9.88	7.64 ± 0.06	14.41 ± 0.06
100	10	10.0	28.29 ± 0.37	68.16 ± 3.86	9.92 ± 0.04	12.69 ± 0.03
100	13	5.0	67.37 ± 1.54	79.81 ± 5.87	5.20 ± 0.07	17.39 ± 0.10
100	13	7.5	39.53 ± 0.46	70.55 ± 6.99	7.67 ± 0.05	14.40 ± 0.05
100	13	10.0	28.37 ± 0.27	80.56 ± 14.35	9.92 ± 0.04	12.67 ± 0.04
150	7	5.0	65.07 ± 1.18	86.14 ± 6.94	5.29 ± 0.06	17.27 ± 0.10
150	7	7.5	39.43 ± 0.40	86.74 ± 11.79	7.53 ± 0.07	14.55 ± 0.06
150	7	10.0	27.66 ± 0.16	90.99 ± 3.80	9.85 ± 0.06	12.73 ± 0.03
150	10	5.0	64.19 ± 1.05	86.25 ± 8.34	5.32 ± 0.05	17.23 ± 0.09
150	10	7.5	39.41 ± 0.50	92.53 ± 4.15	7.55 ± 0.08	14.54 ± 0.09
150	10	10.0	27.58 ± 0.27	87.45 ± 3.41	9.93 ± 0.05	12.68 ± 0.03
150	13	5.0	64.99 ± 1.55	91.96 ± 11.14	5.28 ± 0.08	17.29 ± 0.10
150	13	7.5	39.23 ± 0.39	87.96 ± 14.79	7.56 ± 0.06	14.52 ± 0.06
150	13	10.0	27.59 ± 0.54	93.16 ± 14.74	9.88 ± 0.05	12.66 ± 0.16
200	7	5.0	65.70 ± 1.32	100.89 ± 10.08	5.30 ± 0.05	17.28 ± 0.07
200	7	7.5	37.96 ± 0.38	108.14 ± 7.08	7.60 ± 0.06	14.55 ± 0.07
200	7	10.0	26.81 ± 0.28	106.42 ± 5.44	9.97 ± 0.05	12.73 ± 0.03
200	10	5.0	66.27 ± 0.80	97.88 ± 3.66	5.29 ± 0.04	17.32 ± 0.06
200	10	7.5	37.93 ± 0.56	103.79 ± 9.41	7.63 ± 0.06	14.52 ± 0.06
200	10	10.0	26.86 ± 0.42	108.35 ± 4.56	9.98 ± 0.05	12.69 ± 0.06

200	13	5.0	66.48 ± 1.27	109.86 ± 10.43	5.31 ± 0.04	17.29 ± 0.07
200	13	7.5	38.54 ± 0.53	102.25 ± 3.13	7.60 ± 0.03	14.56 ± 0.04
200	13	10.0	26.95 ± 0.29	108.08 ± 11.37	10.03 ± 0.07	12.67 ± 0.06
250	7	5.0	59.83 ± 1.14	102.31 ± 1.78	5.18 ± 0.07	17.52 ± 0.10
250	7	7.5	30.50 ± 0.56	115.11 ± 5.74	7.50 ± 0.06	14.71 ± 0.07
250	7	10.0	19.77 ± 0.43	126.05 ± 4.03	9.88 ± 0.07	12.81 ± 0.05
250	10	5.0	59.83 ± 1.19	103.29 ± 2.87	5.18 ± 0.06	17.53 ± 0.10
250	10	7.5	30.31 ± 0.73	114.10 ± 6.91	7.50 ± 0.03	14.71 ± 0.04
250	10	10.0	19.76 ± 0.32	125.06 ± 10.87	9.85 ± 0.06	12.83 ± 0.04
250	13	5.0	58.70 ± 0.77	101.48 ± 5.22	5.23 ± 0.02	17.45 ± 0.06
250	13	7.5	30.28 ± 0.53	113.27 ± 5.55	7.43 ± 0.05	14.76 ± 0.05
250	13	10.0	20.01 ± 0.25	117.90 ± 7.17	9.84 ± 0.03	12.83 ± 0.03
300	7	5.0	44.80 ± 1.24	96.68 ± 7.76	5.20 ± 0.05	17.46 ± 0.11
300	7	7.5	23.39 ± 0.25	113.70 ± 12.02	7.49 ± 0.06	14.69 ± 0.05
300	7	10.0	15.24 ± 0.14	125.58 ± 5.23	9.93 ± 0.04	13.09 ± 0.87
300	10	5.0	45.47 ± 1.14	91.80 ± 3.93	5.19 ± 0.05	17.51 ± 0.06
300	10	7.5	23.68 ± 0.36	108.58 ± 5.98	7.47 ± 0.07	14.73 ± 0.07
300	10	10.0	15.26 ± 0.26	127.95 ± 9.37	9.95 ± 0.05	12.75 ± 0.03
300	13	5.0	45.84 ± 0.69	93.82 ± 4.43	5.18 ± 0.04	17.52 ± 0.05
300	13	7.5	23.61 ± 0.43	103.55 ± 6.97	7.51 ± 0.06	14.70 ± 0.05
300	13	10.0	15.39 ± 0.15	124.68 ± 11.44	9.92 ± 0.05	12.76 ± 0.07
350	7	5.0	42.10 ± 1.17	107.28 ± 3.69	5.22 ± 0.06	17.46 ± 0.11
350	7	7.5	22.09 ± 0.50	124.55 ± 6.92	7.45 ± 0.05	14.76 ± 0.05
350	7	10.0	13.55 ± 0.14	142.66 ± 4.77	9.95 ± 0.06	12.76 ± 0.04
350	10	5.0	41.74 ± 0.97	107.50 ± 4.78	5.24 ± 0.05	17.43 ± 0.09
350	10	7.5	22.03 ± 0.47	119.81 ± 3.96	7.45 ± 0.06	14.75 ± 0.07
350	10	10.0	13.99 ± 0.22	140.11 ± 12.29	9.91 ± 0.05	12.79 ± 0.03
350	13	5.0	42.93 ± 0.86	101.47 ± 3.01	5.20 ± 0.04	17.50 ± 0.08
350	13	7.5	22.31 ± 0.11	120.97 ± 8.37	7.47 ± 0.06	14.73 ± 0.07
350	13	10.0	13.97 ± 0.24	135.63 ± 4.86	9.96 ± 0.06	12.74 ± 0.02
400	7	5.0	42.31 ± 1.04	114.97 ± 10.57	5.17 ± 0.07	17.55 ± 0.11
400	7	7.5	20.21 ± 0.39	138.25 ± 7.84	7.56 ± 0.06	14.66 ± 0.06
400	7	10.0	12.33 ± 0.25	153.14 ± 7.43	9.91 ± 0.03	12.79 ± 0.04
400	10	5.0	42.29 ± 0.61	111.98 ± 3.35	5.18 ± 0.03	17.54 ± 0.07
400	10	7.5	20.75 ± 0.43	127.75 ± 3.68	7.51 ± 0.04	14.71 ± 0.06
400	10	10.0	12.59 ± 0.25	155.63 ± 20.24	9.88 ± 0.06	12.80 ± 0.05
400	13	5.0	42.88 ± 1.50	110.75 ± 4.53	5.15 ± 0.07	17.54 ± 0.16
400	13	7.5	20.71 ± 0.41	129.94 ± 5.20	7.55 ± 0.07	14.64 ± 0.06
400	13	10.0	12.89 ± 0.36	142.46 ± 5.73	9.93 ± 0.07	12.75 ± 0.05
450	7	5.0	42.49 ± 1.04	127.12 ± 4.77	5.18 ± 0.03	17.55 ± 0.06
450	7	7.5	20.34 ± 0.35	154.66 ± 13.83	7.54 ± 0.06	14.69 ± 0.05
450	7	10.0	11.99 ± 0.17	177.69 ± 8.51	9.90 ± 0.06	12.83 ± 0.05
450	10	5.0	43.55 ± 1.13	122.84 ± 3.20	5.15 ± 0.05	17.58 ± 0.07
450	10	7.5	20.71 ± 0.53	144.16 ± 5.22	7.54 ± 0.04	14.68 ± 0.07
450	10	10.0	12.43 ± 0.17	173.94 ± 14.94	9.93 ± 0.06	12.79 ± 0.06
450	13	5.0	43.06 ± 0.77	121.81 ± 5.08	5.16 ± 0.05	17.50 ± 0.12
450	13	7.5	21.24 ± 0.24	137.10 ± 2.67	7.58 ± 0.07	14.63 ± 0.07
450	13	10.0	13.20 ± 0.41	156.38 ± 8.11	9.91 ± 0.06	12.77 ± 0.04
500	7	5.0	44.73 ± 1.42	138.73 ± 4.31	5.18 ± 0.05	17.57 ± 0.09
500	7	7.5	21.69 ± 0.60	162.67 ± 3.12	7.49 ± 0.05	14.74 ± 0.16
500	7	10.0	12.86 ± 0.36	190.87 ± 10.80	9.86 ± 0.05	12.90 ± 0.03
500	10	5.0	45.43 ± 0.92	133.06 ± 3.09	5.18 ± 0.04	17.55 ± 0.07
500	10	7.5	22.47 ± 0.54	160.92 ± 3.52	7.46 ± 0.07	14.79 ± 0.08
500	10	10.0	13.38 ± 0.50	185.62 ± 10.19	9.88 ± 0.08	12.87 ± 0.07
500	13	5.0	45.58 ± 1.37	135.57 ± 5.08	5.21 ± 0.06	17.51 ± 0.08
500	13	7.5	23.00 ± 0.58	156.04 ± 5.57	7.47 ± 0.06	14.74 ± 0.08
500	13	10.0	13.88 ± 0.51	174.36 ± 7.84	9.87 ± 0.07	12.83 ± 0.08

As statistically evaluated in Table 11 and exemplarily visualized in Figure 23, the experiments depict a high reproducibility in terms of force, temperature control and final geometry, proving the validity of the collected experimental data.
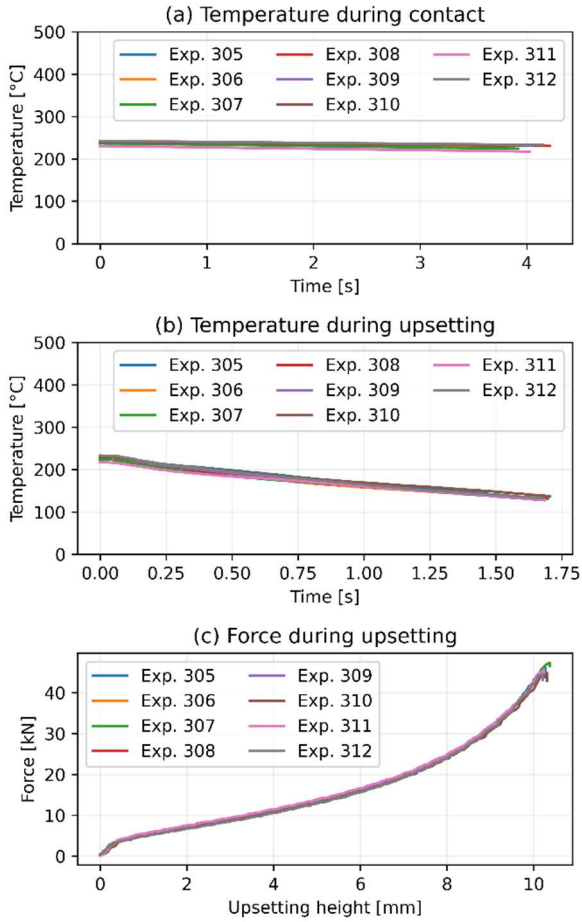
Fig. 23 Experimental results of the (a) specimen temperature during contact with the lower, (b) specimen temperature during upsetting, and (c) the force over the upsetting height h_0-h_1, of the parameters combination T_F = 500 °C, h_1 = 5 mm, t_{trans} = 10 s, and t_{rest} = 3 s.

To compare and validate experiment and simulation, the Pearson correlation coefficient (PCC) (Benesty et al. 2009) is computed, comparing the shape of the curves from the simulation and experiment by calculating the strength of the linear correlation between two vectors, represented by the time series data (Eq. (15)). The PCC is a single value, ranging from -1 to +1 indicating the strength of the linear relationship between to variables or vectors with the same length. Hereby, $\bar{x}$ and $\bar{y}$ represent the means of the vectors x and y (Rodgers and Nicewander 1988; Zhou et al. 2016).

$$PCC = \frac{\sum(x_i - \bar{x}) \cdot \sum(y_i - \bar{y})}{\sqrt{\sum(x_i - \bar{x})^2} \cdot \sqrt{\sum(y_i - \bar{y})^2}} \qquad (15)$$

For the calculation of the PCC, the load was used as y-component of the vector, whereas the corresponding the position of the upper die was used as the x-component of the vector. Accordingly, the PCCs between the measured values during the experiment and each of the material models with the flow curve, JC, and Hensel-Spittel material model were calculated. A similar approach was

conducted using the specimen temperature measured with the pyrometer. Here, the specimen temperature was used as y-component of the vector, and the corresponding the position of the upper die was used as the x-component of the vector. Subsequently, the PCCs of the load and specimen temperature are compared with the defined PCC residuals to validate the experiment, generating a Boolean response of True, when the calculated PCC exceeds the defined PCC residual, or otherwise False.

5.3 Material related tests and material model validation

As already mentioned, for aluminum alloys, such as the EN AW-6060 used in this study, there are many influencing parameters, such as the quantity and condition of the precipitates, which determine the strength as well as the behavior during the process. When steel or titanium grades are used, phase transformations or the phase fractions in the microstructure are additional factors. Apart from these special material properties, all metals exhibit the enormous influence of grain size on formability. According to the Hall-Petch relationship, grain refinement leads to an improvement in mechanical properties, both in strength and ductility. With corresponding grain growth (e.g. secondary recrystallization), this leads to lower tensile strength. This results in a benefit for the stamping force, although it often exhibits negative effects on the part performance. An estimation of the energy minimization requires detailed comprehension of the applied forming forces and the microstructural effect on the component. Therefore, in many cases, heat treatments are appended after the forming process for the adjustment of the desired grain size. Nevertheless, there are requirements for a minimum dislocation density and a corresponding choice of annealing temperatures and the duration. In the case of certain aluminum alloys, precipitation hardening followed by ageing needs to be specified. This demands an extensive amount of preliminary and subsequent investigations and characterizations when these are performed ex-situ e.g. using optical microscopy or performing mechanical tests (Hansen 1977; Lloyd 1980; Song et al. 2019)

As an example, the material analysis was carried out here to a certain extend and is illustrated in extracts in the following figures. Since it is not possible to perform tensile tests on upsetting specimen, the correlation to tensile strength was covered in this case by performing a hardness test. This was carried out using the Vickers HV1 test method on upsetting specimens from room temperature up to 400°C. In Fig. 24, the influence of the dissolution behavior of the precipitates as well as the recovery and recrystallization become clearly visible. Up to a temperature of 125°C the hardness values remain almost constant, from 150°C the values decrease continuously to about half.
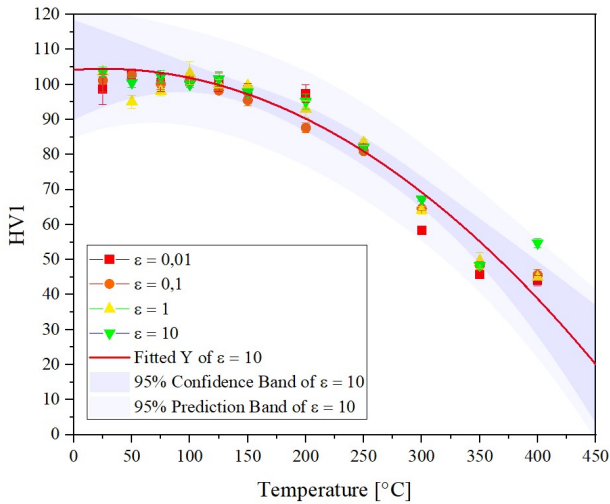
Fig. 24 Evolution of hardness results from room temperature up to 400°C

This is attributable to the aforementioned strength-reducing effects at elevated temperature. It is further illustrated by extracts of the microstructure, which was prepared metallographically and revealed by Barker color etching. As an example, Fig. 25 shows the microstructure at room temperature for a strain rate of $0.01 \ s^{-1}$ and a strain rate of $10 \ s^{-1}$.

a)

b)

Fig. 25 Visualization of the resulting microstructure of the upsetting specimen at room temperature for a strain rate of a) $0.01 \ s^{-1}$ and b) $10 \ s^{-1}$

Here it can be seen that the grains appear more isotropic in certain areas at $0.01 \ s^{-1}$ than at the high strain rate. This can be explained by diffusion processes, which are more pronounced at lower strain rates. The reason for this is the possibility of the formation of substructures due to the longer period of forming time. At the higher strain rate, the anisotropic deformation structure is still clearly visible after compression. At higher temperatures, the situation deteriorates. As a consequence of the high energy in form of heat quantity at higher temperatures, the diffusion processes are accelerated to a large extent, resulting in recrystallization. The resulting microstructure at 250°C is again shown in Fig. 26 for the lowest and highest strain rates.

a)

b)

Fig. 26 Visualization of the resulting microstructure of the upsetting specimen at 250°C for a strain rate of a) $0.01 \ s^{-1}$ and b) $10 \ s^{-1}$

In this case, likewise, the deformation structure is still recognizable, but already to a lesser extent. As shown in Fig. 27, the effect of different recrystallization kinetics dependent on the strain rate at a temperature of 400°C is clearly evident.

a)

b)

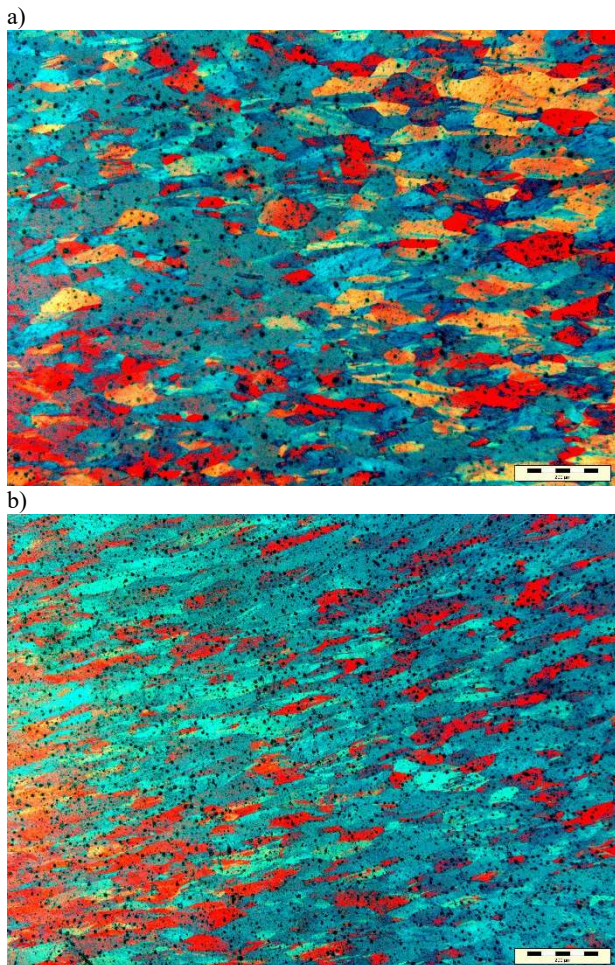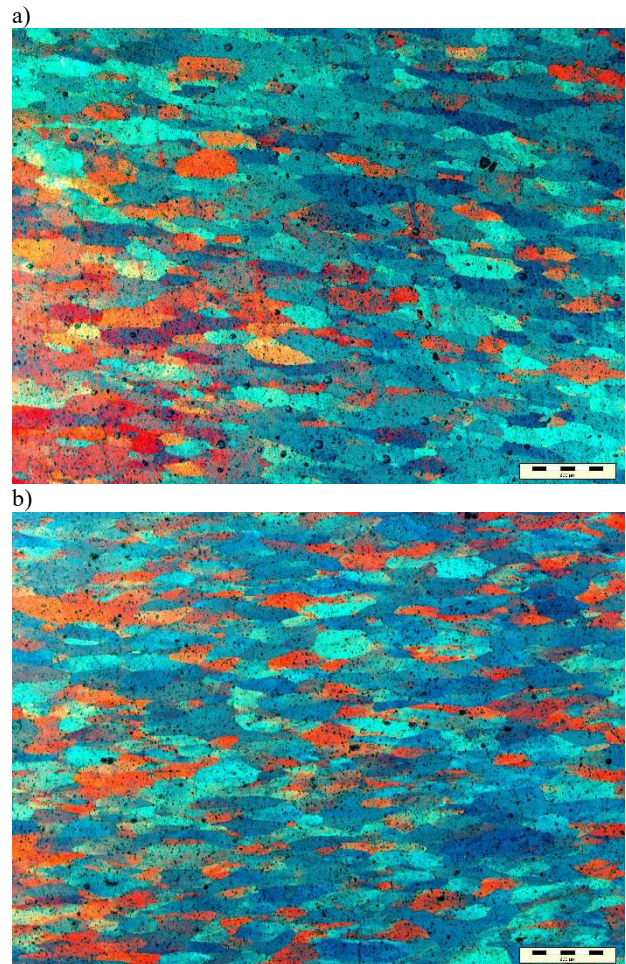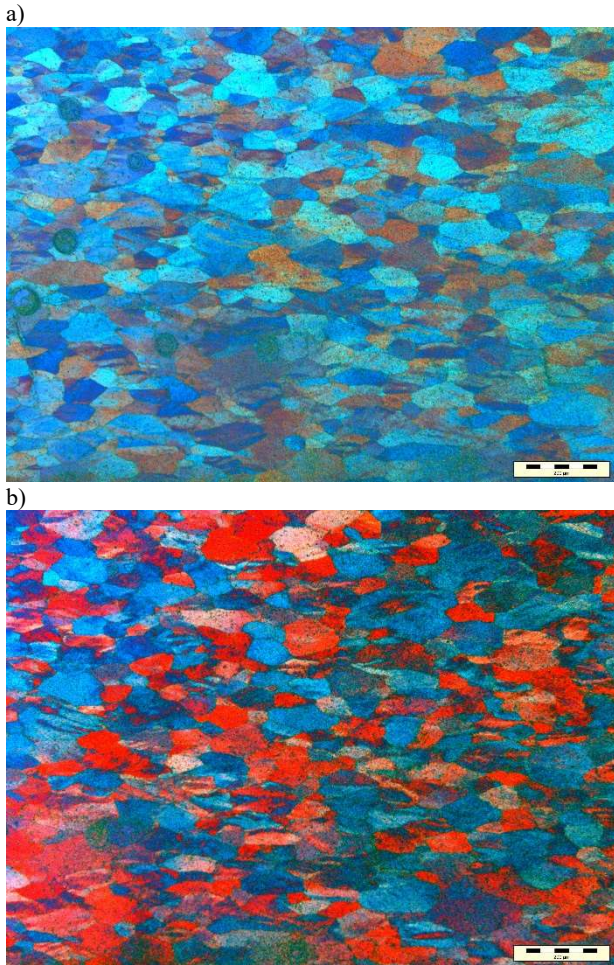**Fig. 27** Visualization of the resulting microstructure of the upsetting specimen at 400°C for a strain rate of a) 0.01 s^{-1} and b) 10 s^{-1}

As described, the presence and influence of recrystallization for this material is clearly proven, validating the application of the material models and their consideration of these effects.

6 Results and discussion

To advance the shop floor digitization, a hydraulic press from 1952 and two industrial furnaces were transformed into a CPPS by applying a retrofitting approach. To meet the defined requirements, strong focus was set on the utilization of state-of-the-art sensor technology, DAQ and open-source software, also focusing on low-cost but resilient design to be economically applicable in an academic learning factory as well as in SMEs. To avoid a proprietary software solution, the DS was programmed and implemented with Python and Abaqus, enabling the modularized scripting of the FEAs, and thus an automated data flow. As a consequence of the relatively low programming entrance barrier and the modular Python-scripted FEA approach, the individual FEAs can be modified easily, and the entire process can be changed with low afford. As a result of the combination the digitalization approach (Section 3) and the developed DS (Section 4), a CPPS conform structure was developed and

implemented, according to the visualization shown in Fig. 28. The superordinate modular and thus more easily modifiable approach was realized with Python.
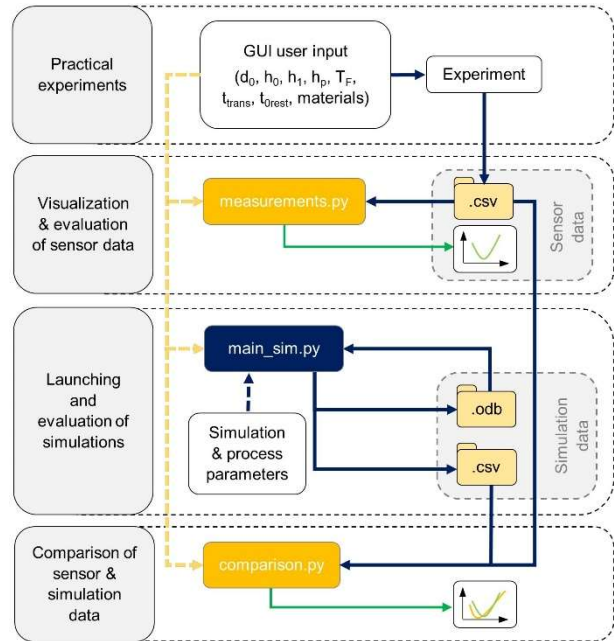
Fig. 28 Implemented CPPS structure with interconnected steps (yellow), data flows (blue), and processed results (green)

In order to support the usability and the decision-making process on the shop floor, two types of GUIs were implemented, enhancing the HMI and enabling the visualization of machine and process parameters, as well as the interaction of the front-end user with the back-end FEAs. In addition to the superordinate WAGO GUI system (Section 3), a Python GUI was developed (Figure 29).

On the left side of the GUI, the user is enabled to input the desired process parameters into four sections, corresponding to the individual process steps. In the first section "Specimen", the user defines the material of the specimen, the initial geometry with d_0 and h_0, and the desired end height after upsetting h_1. By gathering more material data and evaluating the material model parameters following the approach presented in Section 5 and 2, the material database can be expanded, allowing the automatic simulation of various materials. These can then be chosen in the dropdown menu "Material". In the second section "Furnace", the type of furnace and furnace temperature is chosen, whereby a sanity check is applied, that the input furnace temperature does not exceed the maximum furnace temperature. Similar to the previous section, additional furnaces can be added to a database, enabling the incorporation of more furnaces into the CPPS. In the section "Transport of specimen", the estimated t_{trans} and t_{rest} is specified. Concluding in section "Hydraulic press", the materials of the upper and lower die is chosen, enabling the utilization of different tools. Furthermore, the distance of the pyrometer from the lower die h_{pyro} is specified, needed for the comparison of the

specimen temperature of the simulation and experiment. With the means of a GUI, the simulations are launched sequentially with the user input parameters by the push of the button "Start simulation", also creating a uniform directory structure to facilitate standardized data management. To compare the simulation and the experiment, the Section "Comparison and Validation" enables the user to either compare a specific experiment by choosing the corresponding date and number of the experiment, or the latest measured experiment.
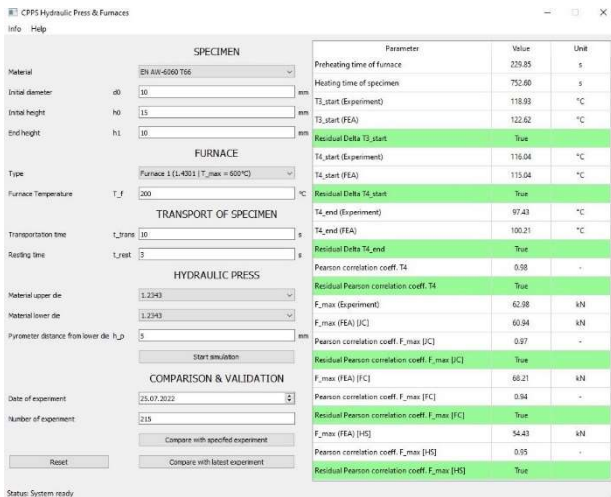

Fig. 29 Python GUI for the support of the decision-making process

To launch the CPPS, the user input process parameters are taken from the GUI after pushing "Start simulation", followed by the launching of the simulation sequence with "main_sim.py". Subsequently, the practical experiments are carried out with the parameters shown on the GUI. After the completion of both simulations and experiments, the data of the sensors gathered during the experiments is evaluated with "measurments.py and compared with the simulation results, using the module "comparison.py". Hereby, the resulting data sets are compared by several metrics and thereby validated. By comparing FEA results and real sensor data, practical conclusions can be drawn about the correct execution of the process. For a process sequence to be considered valid, the temperature of the furnaces and the temperature of the specimen when placed in the hydraulic press must lie within a certain range within a defined residual. In addition, the force curve during upsetting is compared with the results of all three FEA material models. An upsetting process is considered valid when at least two of three force curves resulting from the FEA match the real one within the defined residuals.

The first metric is the relative deviation between the maximum forces ΔF_{max} of the upsetting FEA with the respective material model and the experiment. Furthermore, the relative deviations between the simulated and measured specimen temperatures are computed. Hereby, the relative temperature deviations are calculated at the start of the contact between the lower die

and the specimen ΔT_{3_start} (Fig. 22, t_1), at the beginning of the upsetting process ΔT_{4_start} (Fig. 22, t_2), and at the end of the upsetting process ΔT_{4_end} (Fig. 22, t_3). For the determination of the residuals, the results of the statistical evaluation in Table 11 and the benchmark test (Fig. 31) were used. For the residual of ΔF_{max}, a value of $\pm$ 17.0 % from the experimental force were defined, applicable to all three material models. For the relative temperature residual ΔT_{3_start}, ΔT_{4_start} and ΔT_{4_end} a value was defined as $\pm$ 15.0 °C.

For the residual of the load PCC for the flow curve, JC and Hensel-Spittel material models, and a value of 0.92 was defined, as the benchmark test revealed a highly linear correlation the datasets. The specimen temperature PCC was set as 0.94 also exhibiting a high linear correlation between the measurement and the simulation. When the residual condition is met, the Boolean response of True is visualized in the Python GUI, by highlighting the respective line in the result section in green, enhancing the intuitiveness of the GUI (Fig. 29). If, due to the mathematical formulation of the material behavior, a material model cannot adequately represent the real material behavior, a condition was introduced, considering the experiment valid if two of three PCC residuals are met. In this case, the respective line in the GUI is highlighted in orange. As a result, the comparison of both datasets is enabled, also resulting in the possibility of sanity checks of sensor data and the warning in case of mismatch of simulation and measurement results. As shown in Fig. 30, the results of the comparison are visualized and highlighted on the right side of the GUI, supporting the decision-making on the shop floor, and therefore support situationally appropriate action taking.
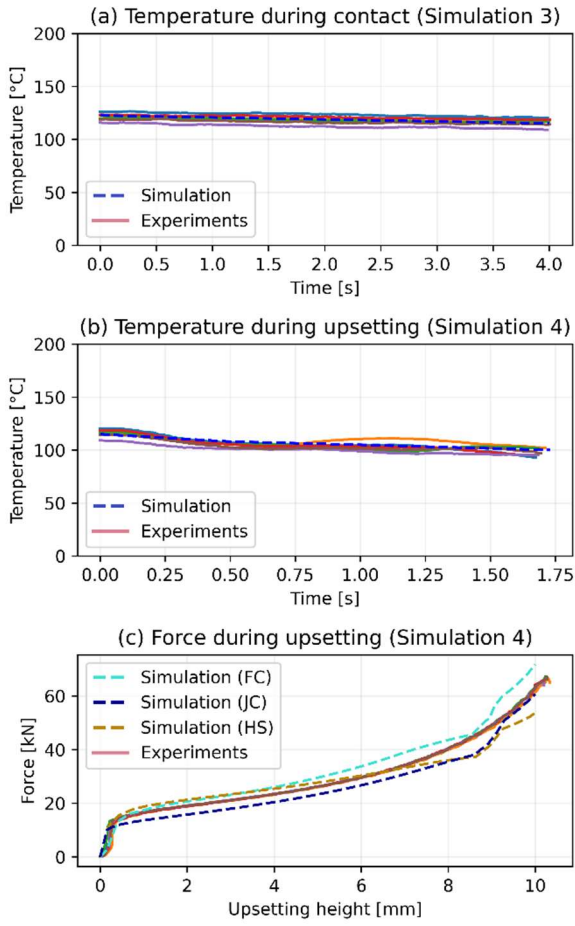
Fig. 30 Comparison of the simulation and experimental results of the (a) specimen temperature during contact with the lower, (b) specimen temperature during upsetting, and (c) the force over the upsetting height h_0-h_1, of the parameters combination $T_F = 200\ °C$, $h_1 = 5$ mm, $t_{trans} = 10$ s, and $t_{rest} = 3$ s.

To optimize the DS, a benchmark test was performed and optimized in terms of accuracy in comparison to the sensor data and computation time to enable a near in-situ application of each individual process. As shown in Table 12, four identical simulations were performed for each

experimental setup from Section 5 and compared with the real experimental results. In the simulations, the element sizes of the respective sections were varied in order to find the best possible compromise between accuracy and computing time. For the execution, a workstation equipped with a 11th Gen Intel(R) Core(TM) i7-11700K @ 3.60GHz with 64GB RAM was used, whereby eight cores were utilized.

Table 12 Parameters for the variations of the FEA benchmark with a uniform of t_{rest} of 3 s

Seed size specimen s_s (mm)	Seed size furnace s_f (mm)	Seed size dies s_p (mm)
1.0	10	3
1.5	15	6
2.0	20	9
2.5	25	12
3.0	30	15
3.5		
4.0		
4.5		
5.0		

As a result, the parameter combination of $s_s = 2.5$ mm, $s_f = 30$ mm, $s_p = 6$ mm the best compromise of computation and accuracy was chosen as the most suitable parameter combination (Figure 31). In terms of accuracy all simulations showed relative deviation between the simulated and measured maximum upsetting force of 16.5 % and a PCC of at least 0.93. The specimen temperature PCC was slightly higher with at least 0.95. The computation times with this parameter combination results in a computation time of 95.55 ± 10.96 s for simulation 1, 2.03 ± 0.14 s for simulation 2, and 2.20 ± 0.28 s for simulation 3. For the upsetting process in simulation 4, the computation time incorporating the JC material model was 55.75 ± 3.32 s, and 52.85 ± 6.01 s for the Hensel-Spittel approach. Due to the necessity of interpolation in the flow curve model, the computation time of 81.90 ± 10.47 s is comparatively higher. By improving the FEA performance and enabling the in-situ application, an in-situ process monitoring was implemented.
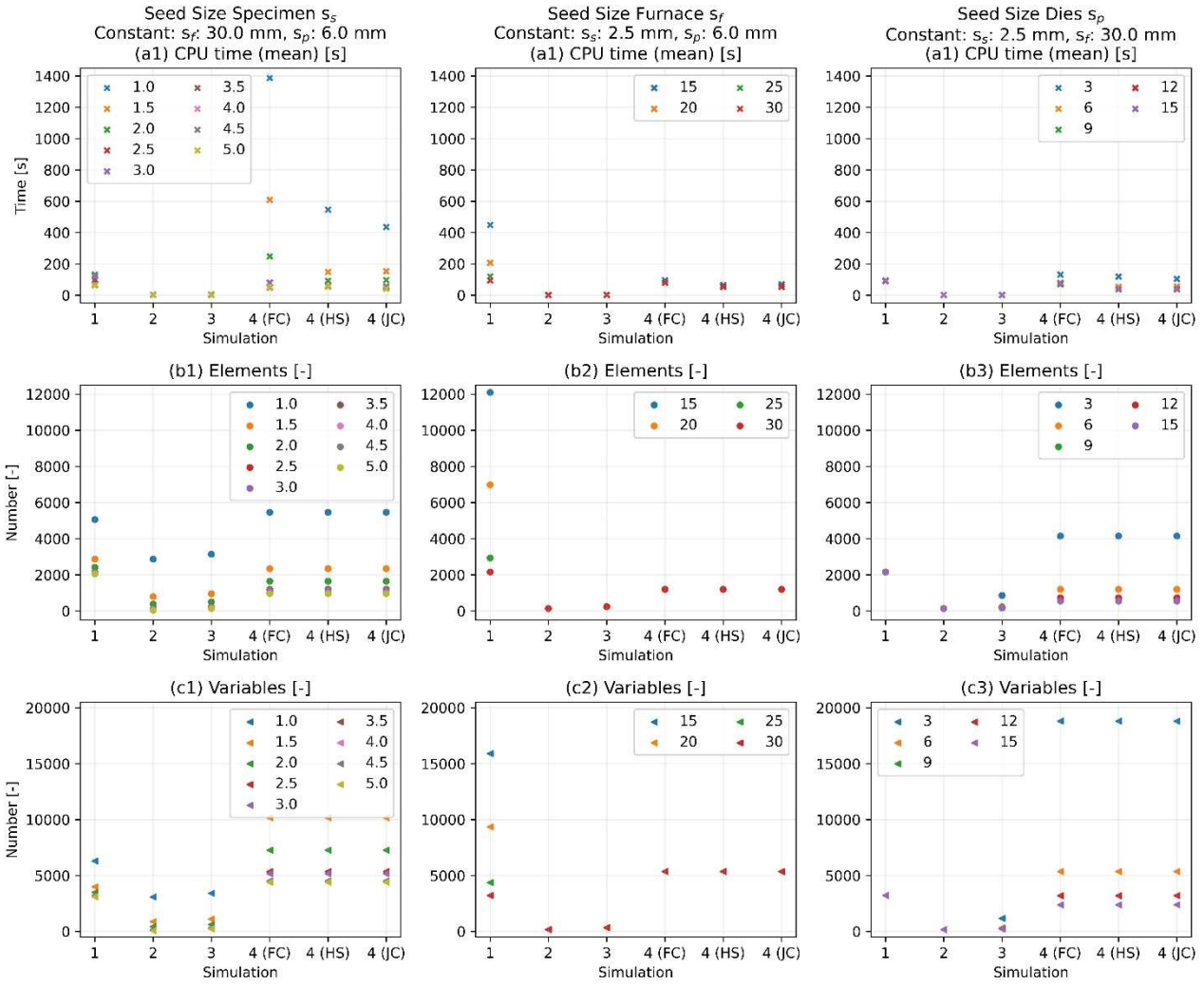
Fig. 31 Visualization of the benchmark test results for the computation time (CPU time), number of elements and number of variables, varying s_s (a1-c1), s_f (a2-c2) and s_p (a3-c3)

Based on the supervised ML approach elaborated by (Ralph, Hartl et al. 2021), data from valid processes are continuously fed into the model to improve the defined residuals, acting a Quality Control (QC) approach and resulting in a reduction of waste, supporting the premise of sustainability.

As an additional production assistance tool resulting from the in-situ DS, the decision-making process on the shop floor is further improved, visualizing near real-time information on the GUI (Fig. 13) about the process to the frontend user. Therefore, a situationally appropriate action taking in and between the individual process steps is promoted to increase the process stability and quality, subsequently reducing the waste and promoting sustainability. Regarding the application of Artificial Intelligence (AI) compared to real-physical based simulations in the context of manufacturing SMEs, the inner workings and results simulations are easier explainable and thus more transparent. For this reason, the effects of different parameters and parameter combinations are more adjustable and thus better support

the optimization process of product and process. Especially manufacturing SMEs often perform low-volume high-complexity tasks and cannot generate enough data to train an AI model in a justifiable time. The time and resources used for the data generation and AI model implementation, also require financial expenditures that could be considered as an additional obstacle. Especially in the context of low-volume high-complexity tasks, simulation can offer significant advantages in terms of flexibility and optimization potential for complicated component geometries. Nevertheless, this is accompanied by a certain amount of computing time, which can be reduced through optimization, but is still computationally and time intensive. When dealing with large amounts of data, AI can offer advantages in this regard, provided that the model is appropriately trained.

Additionally, a predictive maintenance approach with failure investigation diagnostics was implemented using the RevPi. If measured values occur in the process that reside outside the defined error residual, the user is informed, the frontend user is informed via the GUI,

enabling situationally appropriate action taking. Subsequently, the machines and specimen can be checked to avoid errors and to ensure proper working of the entire system. Additionally, an automated omnipresent sanity check was implemented, informing the frontend user via the GUI about malfunctions of sensors, delivering implausible out of range data.

To ensure the resilience and security of the production network and thus also of the entire value chain, a layer 2 network was further expanded, into which the CPPS was integrated. Consequently, the vulnerability to cyberattacks has been reduced, minimizing potential downtime and outages of individual CPPS and other value chain entities. This production network, implemented as part of MUL 4.0, allows the expansion and linking of further CPPS into the network, whose data can be collected, exchanged, analyzed and interlinked authorized parties, using the database. Furthermore, this connective open-source approach and the integration into the production network, the data integration into a MES and ERP was enabled for future research purposes. The real-time data gathering and integration in the superordinate MES can be used to monitor the value chain and optimize production flows and processes, and thus increase the overall efficiency and reduce costs. In conjunction with an ERP, inventory and process planning can also be better controlled and optimized, being beneficial for the value and supply chain.

As a result, this work represents a representative case study for the applicability of a brownfield approach implementation of a CPPS in the manufacturing industry, suitable for an academic learning environment (Ralph, Sorger et al. 2021) as well as in the context of SMEs. For these reasons, this interconnected, low-cost, open-source, modular and easily modifiable digitalization approach enables an interactive academic learning experience to prepare the tech talents of the future for new digital challenges. Furthermore, a framework for SMEs in the metal forming and manufacturing industry was elaborated, to increase the digital maturity of this field, and thus to stay competitive in an increasingly digitalized global value chain.

7 Conclusion and outlook

This paper describes the transformation of three isolated machine and aggregate systems to an interconnected CPPS, applicable for the I4.0 utilization. Consequently, this modular framework also allows the substitution of the cylindrical specimen with more complex product geometries into the DS, for example by importing a CAD file. Furthermore, the modularity enables the modification of process sequences, or other intermediate steps, such as rolling (Ralph et al. 2022). Within this case study, the use of low-cost hardware and open-source software could be successfully applied in the manufacturing context, proving the applicability for SMEs. In the future, the developed frameworks and respective application examples will also be included in the academic learning

factory to further sharpen the focus of digitalization and digital transformation of interested parties.

In addition, the diversity of complex materials significantly increases the selection and modeling of a material model and the associated experimental effort to determine the respective material model parameters. For this purpose, precipitation and recrystallization behavior of EN AW-6060 could be further quantified for this material model in order to further adapt the simulation results to those of the real process. For this reason, an iterative process can be used to find the optimum between a data-driven black box model and a real physical white box model, resulting in a more resource-efficient grey box model optimized for in-situ process mapping.

An essential part of the value chain of a manufactured component is the material and component quality inspection before and after the manufacturing process. Since the input material has an immense influence on the process stability as well as subsequently on the product quality, it is essential for in-line production monitoring to identify the initial condition of the material used. The material tests used and described in this work illustrate the high experimental effort required for the microstructural and mechanical analysis of the samples. In-situ material characterization methods on the other hand offer a great possibility to reduce this resource and time expenditure significantly. A progressively more established method, both in academic and industrial R&D, is the laser ultrasonic (LUS) method. The high-frequency in-situ material analysis during thermal and thermo-mechanical processes allows a large number of relevant material parameters to be determined on the basis of a single measurement. The LUS can be combined with a thermomechanical treatment simulator, such as a dilatometer or a Gleeble, to draw conclusions about grain size evolution, recrystallization, texture, Young's modulus, dislocation density and much more (Hartl et al. 2023). By integrating such a measuring unit, as envisaged in the MUL 4.0 project, into the SFL, both the incoming material and the manufactured product can be characterized in detail and the best subsequent heat treatment can be recorded. The main advantage of such a methodology is the low barrier to material parameters for the certain batch that is about to be processed. By automatically integrating the real parameters of this batch, improved and more realistic microstructure simulations can be carried out and the DS can be optimized accordingly. In addition, it is possible to judge a batch as a good or bad part prior to the process route and, if necessary, to exclude it from production. This control at the beginning of a process route prevents a lot of rejects that would possibly have been recorded at the finished part. These quality controls along the value chain significantly contribute to scrap and energy reduction and therefore to sustainability.

Author Contributions Conceptualization: Marcel Sorger; Data curation: Marcel Sorger, Martin Schoiswohl and Benjamin Schödinger; Formal analysis: Marcel

8   Compliance with ethical standards

Conflict of interest The authors declare that they have no conflict of interest.

9   References

Akkaya, B. (2019). 'Leadership 5.0 in Industry 4.0'. In: J. Wang and J. C. Essila (eds) *Managing Operations Throughout Global Supply Chains*:, pp. 136–58: IGI Global.

Benesty, J., Chen, J., Huang, Y. and Cohen, I. (2009). 'Pearson Correlation Coefficient'. In: I. Cohen, Y. Huang, J. Chen and J. Benesty (eds) *Noise Reduction in Speech Processing*:, pp. 1–4. Berlin, Heidelberg: Springer Berlin Heidelberg.

Buehler, K., Anant, V., Bailey, T. and Kaplan, J. *et al.* (2020) *Cybersecurity in a Digital Era*, <https://www.mckinsey.com/~/media/McKinsey/Business%20Functions/Risk/Our%20Insights/Cybersecurity%20in%20a%20digital%20era/Cybersecurity%20in%20a%20Digital%20Era.pdf> accessed 23 Feb 2023.

Chen, X., Du, Y., Du, K. and Lian, T. *et al.* (2021) 'Identification of the Constitutive Model Parameters by Inverse Optimization Method and Characterization of Hot Deformation Behavior for Ultra-Supercritical Rotor Steel', *Materials (Basel, Switzerland)*, 14/8.

Chen, X., Peng, Y., Peng, S. and Yao, S. *et al.* (2017) 'Flow and fracture behavior of aluminum alloy 6082-T6 at different tensile strain rates and triaxialities', *PloS one*, 12/7: e0181983.

Doege, E. and Behrens, B.-A. (2010) *Handbuch Umformtechnik*: *Grundlagen, Technologien, Maschinen*. Berlin, Heidelberg: Springer.

Fraden, J. (2010) *Handbook of Modern Sensors*. New York, NY: Springer New York.

Gottstein, G. (2014) *Materialwissenschaft und Werkstofftechnik*. Berlin, Heidelberg: Springer Berlin Heidelberg.

Groche, P. and Krech, M. (2017) 'Efficient production of sensory machine elements by a two-stage rotary swaging process—Relevant phenomena and numerical modelling', *Journal of Materials Processing Technology*, 242: 205–17.

Han, J.-C. (2012) *Analytical Heat Transfer*. Hoboken: CRC Press.

Hansen, N. (1977) 'The effect of grain size and strain on the tensile flow stress of aluminium at room temperature', *Acta Metallurgica*, 25/8: 863–9.

Hartl, K., Sorger, M. and Stockinger, M. (2023) 'The Key Role of Laser Ultrasonics in the Context of Sustainable Production in an I 4.0 Value Chain', *Applied Sciences*, 13/2: 733.

Hensel, A. and Spittel, T. (1978) *Kraft- und Arbeitsbedarf bildsamer Formgebungsverfahren*: Deutscher Verlag für Grundstoffindustrie.

Hoffmann, H., Neugebauer, R. and Spur, G. (eds) (2012) *Handbuch Umformen*. München: Hanser.

Johnson, C. D. (2009, 2006) *Process control instrumentation technology*. New Delhi: PHI Learning.

Johnson, G. R., Hoegfeldt, J. M., Lindholm, U. S. and Nagy, A. (1983) 'Response of Various Metals to Large Torsional Strains Over a Large Range of Strain Rates—Part 1: Ductile Metals', *Journal of Engineering Materials and Technology*, 105/1: 42–7.

Kashani, M. M., Movahhedy, M. R., Ahmadian, M. T. and Razavi, R. S. (2017) 'Analytical Solution of Transient Three-Dimensional Temperature Field in a Rotating Cylinder Subject to a Localized Laser Beam', *Journal of Heat Transfer*, 139/6.

KLEIBER Infrared GmbH *Emissionsgradtabelle*, <https://www.kleiberinfrared.com/index.php/de/amanwendungen/emissionsgrade.html> accessed 23 Feb 2023.

Lins, T. and Oliveira, R. A. R. (2020) 'Cyber-physical production systems retrofitting in context of industry 4.0', *Computers & Industrial Engineering*, 139: 106193.

Lloyd, D. J. (1980) 'Deformation of fine-grained aluminium alloys', *Metal Science*, 14/5: 193–8.

Marek, R. and Nitsche, K. (2019) *Praxis der Wärmeübertragung*: *Grundlagen - Anwendungen - Übungsaufgaben : mit 778 Abbildungen, 62 Tabellen, 50 vollständig durchgerechneten Beispielen sowie 168 Übungsaufgaben mit über 300 Seiten ausführlicher Lösungen zum Download*. München: Hanser.

Martienssen, W. and Warlimont, H. (2011) *Part 2: Non-ferrous Alloys - Light Metals*. Berlin, Heidelberg: Springer Berlin Heidelberg.

Modest, M. F. and Mazumder, S. (2022) *Radiative heat transfer*. London, San Diego, CA: Academic Press, an imprint of Elsevier.

Müller, J. M., Buliga, O. and Voigt, K.-I. (2018) 'Fortune favors the prepared: How SMEs approach business model innovations in Industry 4.0', *Technological Forecasting and Social Change*, 132: 2–17.

Nahavandi, S. (2019) 'Industry 5.0—A Human-Centric Solution', *Sustainability*, 11/16: 4371.

Nascimento, D. L. M., Alencastro, V., Quelhas, O. L. G. and Caiado, R. G. G. *et al.* (2019) 'Exploring

Industry 4.0 technologies to enable circular economy practices in a manufacturing context', *Journal of Manufacturing Technology Management*, 30/3: 607–27.

Olsen, T. L. and Tomlin, B. (2020) 'Industry 4.0: Opportunities and Challenges for Operations Management', *Manufacturing & Service Operations Management*, 22/1: 113–22.

Ostermann, F. (2014) *Anwendungstechnologie Aluminium*. Berlin, Heidelberg: Springer Berlin Heidelberg.

Özdemir, V. and Hekim, N. (2018) 'Birth of Industry 5.0: Making Sense of Big Data with Artificial Intelligence, "The Internet of Things" and Next-Generation Technology Policy', *Omics : a journal of integrative biology*, 22/1: 65–76.

Palik, E. D. (1997) *Handbook of Optical Constants of Solids*. s.l.: Elsevier professional.

Ralph, B. J., Hartl, K., Sorger, M. and Schwarz-Gsaxner, A. *et al.* (2021) 'Machine Learning Driven Prediction of Residual Stresses for the Shot Peening Process Using a Finite Element Based Grey-Box Model Approach', *Journal of Manufacturing and Materials Processing*, 5/2: 39.

Ralph, B. J., Sorger, M., Hartl, K. and Schwarz-Gsaxner, A. *et al.* (2022) 'Transformation of a rolling mill aggregate to a cyber physical production system: from sensor retrofitting to machine learning', *Journal of Intelligent Manufacturing*, 33/2: 493–518.

Ralph, B. J., Sorger, M., Schödinger, B. and Schmölzer, H.-J. *et al.* (2021) 'Implementation of a Six-Layer Smart Factory Architecture with Special Focus on Transdisciplinary Engineering Education', *Sensors (Basel, Switzerland)*, 21/9.

Ralph, B. J., Woschank, M., Miklautsch, P. and Sorger, M. *et al.* (2021) 'MUL 4.0: Systematic Digitalization of a Value Chain from Raw Material to Recycling', *Procedia Manufacturing*, 52: 1–8.

Reis, M. and Gins, G. (2017) 'Industrial Process Monitoring in the Big Data/Industry 4.0 Era: from Detection, to Diagnosis, to Prognosis', *Processes*, 5/4: 35.

Rocca, R., Rosa, P., Sassanelli, C. and Fumagalli, L. *et al.* (2020) 'Integrating Virtual Reality and Digital Twin in Circular Economy Practices: A Laboratory Application Case', *Sustainability*, 12/6: 2286.

Rodgers, J. L. and Nicewander, W. A. (1988) 'Thirteen Ways to Look at the Correlation Coefficient', *The American Statistician*, 42/1: 59.

Rosochowska, M., Balendra, R. and Chodnikiewicz, K. (2003) 'Measurements of thermal contact conductance', *Journal of Materials Processing Technology*, 135/2-3: 204–10.

Simufact Engineering GmbH (2023) *Simufact Forming 2021: Simufact Material 2022*: Hexagon AB.

Song, Y., Yeon, J. and Na, B. (2019) 'Numerical Simulations of the Hall–Petch Relationship in Aluminium Using Gradient-Enhanced Plasticity Model', *Advances in Civil Engineering*, 2019: 1–9.

Sorger, M., Ralph, B. J., Hartl, K. and Woschank, M. *et al.* (2021) 'Big Data in the Metal Processing Value Chain: A Systematic Digitalization Approach under Special Consideration of Standardization and SMEs', *Applied Sciences*, 11/19: 9021.

Stephan, P., Kabelac, S., Kind, M. and Mewes, D. *et al.* (2019) *VDI-Wärmeatlas*. Berlin, Heidelberg: Springer Berlin Heidelberg.

Umbrello, D., M'Saoubi, R. and Outeiro, J. C. (2007) 'The influence of Johnson–Cook material constants on finite element simulation of machining of AISI 316L steel', *International Journal of Machine Tools and Manufacture*, 47/3-4: 462–70.

Willems, W. M. (ed.) (2017) *Lehrbuch der Bauphysik: Schall - Wärme - Feuchte - Licht - Brand - Klima*. Wiesbaden, Heidelberg: Springer Vieweg.

Woschank, M., Ralph, B. J., Kaiblinger, A. and Miklautsch, P. *et al.* (2021) 'MUL 4.0 – Digitalisierung der Wertschöpfungskette vom Rohmaterial bis hin zum Recycling', *BHM Berg- und Hüttenmännische Monatshefte*, 166/6: 309–13.

Wu, X., Goepp, V. and Siadat, A. (2020) 'Concept and engineering development of cyber physical production systems: a systematic literature review', *The International Journal of Advanced Manufacturing Technology*, 111/1-2: 243–61.

Zheng, T., Ardolino, M., Bacchetti, A. and Perona, M. (2021) 'The applications of Industry 4.0 technologies in manufacturing context: a systematic literature review', *International Journal of Production Research*, 59/6: 1922–54.

Zhong, R. Y., Xu, X., Klotz, E. and Newman, S. T. (2017) 'Intelligent Manufacturing in the Context of Industry 4.0: A Review', *Engineering*, 3/5: 616–30.

Zhou, H., Deng, Z., Xia, Y. and Fu, M. (2016) 'A new sampling method in particle filter based on Pearson correlation coefficient', *Neurocomputing*, 216: 208–15.

A 7   Publication 7

Author contributions:

1. B.J. Ralph: Conceptualization, Data curation, Methodology, Project administration, Software, Validation, Visualization, Writing – Original Draft, Writing – Review and Editing
2. K. Hartl: Investigation, Writing – Original Draft, Writing – Review and Editing
3. M. Sorger: Data Curation, Formal Analysis, Software, Visualization
4. A. Schwarz-Gsaxner: Investigation, Writing – Review and Editing
5. M. Stockinger: Resources, Supervision

Article

Machine Learning Driven Prediction of Residual Stresses for the Shot Peening Process Using a Finite Element Based Grey-Box Model Approach

Benjamin James Ralph *[ID], Karin Hartl, Marcel Sorger, Andreas Schwarz-Gsaxner and Martin Stockinger[ID]

Chair of Metal Forming, Montanuniversität Leoben, Franz Josef Str. 18, 8700 Leoben, Austria;
karin.hartl@unileoben.ac.at (K.H.); marcel.sorger@unileoben.ac.at (M.S.);
andreas.schwarz-gsaxner@unileoben.ac.at (A.S.-G.); martin.stockinger@unileoben.ac.at (M.S.)
* Correspondence: benjamin.ralph@unileoben.ac.at; Tel.: +43-384-2402-5611

Abstract: The shot peening process is a common procedure to enhance fatigue strength on load-bearing components in the metal processing environment. The determination of optimal process parameters is often carried out by costly practical experiments. An efficient method to predict the resulting residual stress profile using different parameters is finite element analysis. However, it is not possible to include all influencing factors of the materials' physical behavior and the process conditions in a reasonable simulation. Therefore, data-driven models in combination with experimental data tend to generate a significant advantage for the accuracy of the resulting process model. For this reason, this paper describes the development of a grey-box model, using a two-dimensional geometry finite element modeling approach. Based on this model, a Python framework was developed, which is capable of predicting residual stresses for common shot peening scenarios. This white-box-based model serves as an initial state for the machine learning technique introduced in this work. The resulting algorithm is able to add input data from practical residual stress experiments by adapting the initial model, resulting in a steady increase of accuracy. To demonstrate the practical usage, a corresponding Graphical User Interface capable of recommending shot peening parameters based on user-required residual stresses was developed.

Keywords: python scripting; residual stresses; shot peening; finite element analysis; digitalization; machine learning; smart factory

1. Introduction

For the design of dynamically load-bearing components, a certain safety risk is minimized by increasing the service life and improving its estimation. A key aspect in this context is the selected material and its long-term stability under dynamically oscillating loads [1–3]. Numerous machining end contour processes included in the manufacturing of critical components such as milling, turning, or drilling lead to residual tensile residual stresses on the surface. These stresses are counterproductive for the fatigue resistance; therefore, further surface treatment is essential for these components.

There are several mechanical surface treatment technologies available today, pursuing the objectives of implementing residual compressive stresses close to the surface, as well as introducing a work hardened layer. A well-known example is deep rolling, a low-cost method that achieves a comparatively smooth surface, but is limited to elementary, usually rotation-symmetrical geometries [4]. This technique is mainly used for components that require frictionless sliding, where good surface quality is critical for wear. Another alternative is laser shock peening, an efficient method to introduce compressive residual stresses at four times the depth of shot peening [5]. This is achieved by high-energy laser pulses that introduce a shock wave into the material that exceeds the material's yield strength and causes localized deformation. Although this method is gaining popularity, the

investment in such a system is a high-cost proposition. Moreover, the long process times are currently not suitable for an efficient application in production [6]. Additionally, the ball burnishing or roller burnishing method produces a particularly smooth surface [5,7–9]. A related method developed by Lambda Technologies Group is low plasticity burnishing, which is capable to introduce significant residual compressive stresses while initiating comparatively low work hardening. This assists in ensuring permanent compressive stresses when components are used in higher temperature applications. This method has the further advantage that it can be integrated into a variety of machining systems, e.g., CNC lathes [10–14].

Even though there is a strong effort in establishing new and optimizing well-known surface treatment methods, shot peening still is the standard procedure in the manufacturing environment. Irrespective of the mechanical surface treatment chosen, specific knowledge and therefore respective data about suitable process parameters is mandatory to obtain the required results.

To receive a comprehensive data set for the shot peening process, it is mandatory to obtain a significant amount of valid data. This approach requires the execution of an unreasonable amount of practical experiments per workpiece material/sphere material combination. Furthermore, the same amount of upfollowing experiments to receive valid residual stress profiles would have to be carried out. By substituting practical tests with Finite Element Analysis (FEA)-based simulations, this disproportionate effort can be avoided.

The effectiveness of FEA for production processes can be further increased by using state of the art digitalization technologies, taking into account user, processes, and materials [15–17]. One possibility to achieve this objective is the implementation of robust machine learning algorithms. In order to do so, a first decision has to be made regarding the nature of the respective algorithm. In general, three methods are defined: reinforcement learning (RL), unsupervised learning (UL), and supervised learning (SL) [18]. According to more recent work, there are different subordinate algorithms available, which can be used within one or more of these three main techniques [19,20]:

RL: Genetic Algorithms, Simulated Annealing, and Estimated Value Functions;

UL: Decision Tree Analysis (DTA), Rule-Based Learners, Instance-Based Learners, Artificial and Bayesian Neural Networks (NN), as well as Naïve Bayesian Approaches;

SL: Support Vector Machines, DTA, Rule-Based Learners, Instance-Based Learners, Genetic Algorithms, Artificial and Bayesian NN, and Naïve Bayesian Approaches.

For the prediction of residual stresses after the shot peening process, the authors decided to use a SL algorithm, as the nature of this technique is a continuous learning from data provided by an external knowledgeable source. The accuracy of this algorithm depends on internal knowledge about the expected results and, most important, comprehensible input data [19,21,22].

To achieve accurate data sets serving as an input for this kind of simulation, a suitable material model based on reliable material data from practical experiments must be chosen. Therefore, it is essential to implement real-physics-based input variables, which must be obtained under similar conditions as the process to be modeled.

2. Fundamentals of the Shot Peening Process and Corresponding FEA

In order to increase the fatigue strength, shot peening is applied as a standard procedure in the production process for structural materials. This method contributes to the service life enhancement of cyclic loaded components [23]. The most notable advantages of shot peening compared to other surface hardening treatments are the good process quality, reproducibility, and applicability to a wide range of materials and component geometries [3]. During the process, the surface of the component is impacted by spheres at high velocities. As a result of the momentum transfer, work hardening is increased directly on the surface which reduces the probability of crack initiation. The plastic deformations induced by the spheres also generate residual compressive stresses in the material to a certain

depth. These stresses are the main inhibitors of crack propagation due to the prevention of crack tip opening and thus increase the fatigue strength. However, this surface treatment does not always contribute to a work piece's service life extension rather than a reduction, as König investigated for Waspalloy in [24]. Although increasing the degree of coverage from the impacting spheres can increase the magnitude of resulting residual stresses, this additional loading for higher strength materials at the surface may contribute to a higher probability of initiating cracks. Therefore, it is crucial to be aware of the influential variables of the process before it is applied in practice. The process itself is variable in numerous aspects, such as the sphere's material and geometry, as well as the impact velocity and the coverage [25,26]. The average sphere radius is about 0.4 mm and they are commonly made of glass, ceramic, cast iron, or steel. A prerequisite for the sphere's material is the higher hardness compared to the shot-peened material. A higher difference between the sphere's and the target's hardness yield higher resulting residual compressive stresses [27]. Additionally, larger sphere radii result in the maximum compressive stresses occurring deeper in the material [28].

In order to achieve the maximum effect on service life extension through this process, these parameters must be optimally adjusted to the material. The maximum achievable residual compressive stresses and the depth of penetration into the material are decisive, since the residual compressive stresses inside the material are balanced by tensile residual stresses in a certain depth. Additionally, the dislocation density introduced by this surface treatment needs to be observed concerning the resulting material behavior. On the one hand, this can prevent the crack initiation [29], on the other hand, it may contribute to the brittleness of certain materials and thus drastically reduce their service life, especially in corrosive environments [30]. To experimentally analyze the residual stresses inside the material, destructive and therefore expensive examinations based on X-ray diffraction (XRD) or using the hole drilling method have to be performed in practice. A time and cost-saving alternative to physical experiments is the numerical simulation, which allows the determination of favorable parameters for the optimal result in advance. In addition, stresses on the surface and in depth of the material can be analyzed to provide a better comprehension of the effectiveness of the process. Several studies have been carried out using FEA to simulate the shot peening treatment. The approaches to simulate this process vary widely in different publications. In [31], Edberg et al. designed a three-dimensional FEA simulation, comparing a visco-plastic strain hardening formulation to a elasto-plastic one analyzing a single shot. This study revealed that the visco-plastic model overestimated the resulting residual stresses by a factor of 1.5. In [32], Majzoobi et al. used a three-dimensional set up applying multiple shot impacts and investigated the shot velocity and coverage effects on the resulting residual stresses. The investigations of Meguid et al. in [33] included the separation distance of the spheres and its impact on the residual stress profile as well as the frictional behavior of AISI 4340. A comparison between the resulting values of an axisymmetric and a three-dimensional numeric model on an aluminum target was conducted by Han et al. in [34] where high emphasis was attached to the interaction of the sphere and the target as well as suitable boundary conditions for the FEA. In [35], Schwarzer et al. investigated the influence of the sphere's impact angle on the resulting residual stresses while Hong et al. focused on the loss of kinetic energy of the spheres as a result of alternating impact angles in [36]. In [37], Mylonas and Labeas addressed a reasonable relation between the quantity of impacts needed in order to receive the results of experimentally obtained residual stress profiles but still reduce computational time. The approach of reducing computational time is also applied in this study by the usage of a two-dimensional setup for the simulation, in order to provide a beneficial tool for the industry, taking into account the results of previous works mentioned in this section.

3. Fundamentals and Behavior of EN-AW-6082 T6 under Dynamic Conditions

The material investigated in this study is the age-hardenable EN-AW-6082 aluminum alloy, which is one of the most essential alloying systems for the usage in lightweight

construction due to its balanced properties and good formability. The chemical composition of the used alloy is shown in Table 1.

Table 1. Chemical composition of examined aluminum alloy EN-AW-6082.

Chemical Composition of EN-AW-6082 (wt. %)							
Si	Fe	Cu	Mn	Mg	Cr	Zn	Ti
0.87	0.42	0.08	0.57	0.66	0.02	0.2	0.02

The alloy achieves its strength values primarily through the precipitation of the so-called β-Phase Mg_2Si, and further phases such as $AlSi_6Mg_3Fe$ and $Al_{15}(FeMn)_3Si_2$ with suitable ageing after solution heat treatment. Since particularly Mn particles increase the strength of the alloy, while negatively influencing ductility, a homogenization annealing is carried out before forming in practice [38]. The duration of homogenization annealing increases the effect on the reshaping and distribution of particles and therefore reduces the yield stress for extrusion [39]. The highest strength is achieved with the T6 treatment, which consists of a solution heat treatment between 793 K and 813 K for 30 min to one hour in order to dissolute the alloying elements in the matrix. Subsequent quenching creates a supersaturated condition which is immediately followed by the artificial heating treatment, ranging between 423 K and 443 K for 5–20 h, resulting in a peak of precipitation [40–45]. It is common to consider strain-rate sensitivity for the determination of processing parameters and processing maps, as it has a significant impact on fracture behavior [46]. However, the existence of metastable precipitates causes a change in mechanical properties to higher strength values with a reduction in ductility.

EN-AW-6082 also exhibits deficiencies, especially with regard to fatigue resistance under cyclic loading. When used as a component in a chlorine-containing environment such as near industrial production facilities, the corrosion-resistant passive coating cannot withstand the incorporation of chlorine ions in the passive layer. This increases the probability of pitting corrosion. The crack initiation enhanced by this effect leads to a facilitated crack growth under dynamic loading [2]. In order to increase the fatigue strength, shot peening is applied as a standard procedure in the production process for this alloy.

The initial microstructure of the investigated material is shown in Figure 1. The specimen was prepared by electrolytic polishing using the Barker etching method [47]. The microstructure shows a non-textured grain structure with uniform grain size. The emphasis on the age-hardened condition, which is investigated in the present case, is essential in the case of shot peening, since this treatment is applied as a last processing step after heat treatment.
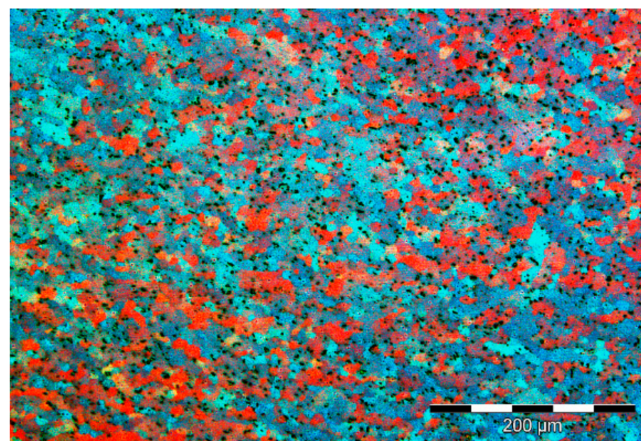

Figure 1. Initial microstructure of the EN-AW-6082 specimens investigated.

4. The Johnson–Cook Material Model

In order to simulate impact problems such as shot peening, material models are commonly used to represent the material's behavior in the most accurate possible way. Especially for high dynamic impacts, using FEA to model this process is an efficient and effective solution. The most important aspect in this context is the strain rate dependency of a material. Many constitutive models deal with material behavior by dislocation motions and their interactions with lattice defects. For many industrial processing related applications, these models are exceedingly complex and require material data with limited accessibility. Others, such as the Zerilli–Armstrong model, contain a simpler structure, but still include factors that are elaborate to determine, such as initial grain size [48]. In order to provide simplicity and convenience to the user, the Johnson–Cook (JC) material model is establishing itself as the most commonly used material model for impact problems, since it takes both strain rate and thermal softening behavior into account. Nevertheless, it is kept simple, consisting of three terms and five material parameters which are arranged as visualized in (1) [49].

$$\sigma = \left(A + B\varepsilon_p^n \right) \left[1 + C \ln \left(\frac{\dot{\varepsilon}_p}{\dot{\varepsilon}_0} \right) \right] \left[1 - \left(\frac{T - T_t}{T_m - T_t} \right)^m \right] \tag{1}$$

The first term refers to strain hardening during plastic deformation including the plastic strain ε_p, the yield strength of the quasi-static condition A, the strain hardening constant B, as well as strain hardening exponent n. The second term relates to the material's behavior under different strain rates with the strain rate sensitivity coefficient C as a result of different strain rates $\dot{\varepsilon}_p$ normalized to a quasi-static strain rate $\dot{\varepsilon}_0$. The third term describes the material behavior under temperature influence including the reference temperature T_t, the melting temperature T_m, and the thermal softening exponent m [49]. The localized strain acquired through the shot peening process is limited, resulting in a small energy input due to the deformation process, even at high strain rates. For this reason, the thermal input due to the plastic deformation of the impinging spheres at the surface is neglected in the JC material model for this framework. Therefore, (1) can be reduced by the third term, resulting in (2).

$$\sigma = \left(A + B\varepsilon_p^n \right) \left[1 + C \ln \left(\frac{\dot{\varepsilon}_p}{\dot{\varepsilon}_0} \right) \right] \tag{2}$$

The parameters of the first term can be determined by using (3).

$$\ln(\sigma - A) = n \cdot \ln(B\varepsilon) \tag{3}$$

A can be derived from the initial flow curve under quasi-static conditions. The slope n can be determined graphically by plotting a trend line while B can be expressed by solving the exponential function. The parameter C includes tests for higher strain rates. To receive C, (2) has to be arranged as demonstrated in (4).

$$\frac{\sigma}{(A + B\varepsilon^n)} = 1 + C \cdot ln \left(\frac{\dot{\varepsilon}}{\dot{\varepsilon}_0} \right) \tag{4}$$

By plotting the left term of (4) against the logarithmic strain rate ratio, C can be obtained directly from the resulting trend line.

Particular attention is required for the comparison of the determined material parameters with literature values, especially the quasi-static strain rate used ($\dot{\varepsilon}_0$), as this value often varies in a range between 10^{-4} and 1 s^{-1}. Another disadvantage regarding literature-based JC parameters is the test setup used to determine these values. For quasi-static stresses, the tensile test is usually selected in literature for the simplicity of the method. For particularly high strain rates, the strain rate sensitivity is frequently determined using the Split-Hopkinson pressure or tensile bar [50]. It should be noted that the stress states

differ in these test methods. The main disadvantage of tensile tests is the instability of the deformation due to geometric deconsolidation processes after the ultimate tensile strength is reached. In contrast, the upsetting test provides steady strain hardening. The critical aspect here, in addition to the frictional conditions at the dies, is the barreling of the specimen. As a result of this phenomenon, the uniaxial load state cannot be ensured [51]. The comparison of the determined material parameters with those from literature revealed deviations in the values. One reason might be that some of the tests performed were carried out under tensile stress conditions. Besides, there might be differences between the chemical compositions of the materials studied. Slight differences in the heat treatment route for the T6 condition could also be responsible for these divergences. For this reason, separate tests should be carried out with the specific material used, in order to eliminate these variations. The different parameters from the literature are listed in Table 2, whereas temperature is not listed due to the lack of definition within the investigated publications. Accordingly, it is essential to arrange the test setup in such a way that it comes closest to real conditions of usage. For the simulation of shot peening processes, the upsetting test is most similar to the compressive stresses introduced by the spheres at the surface. For low degrees of deformation, uniaxial deformation can be also provided, which is why the experiments carried out in this study are based on this principle.

Table 2. Material parameters for the JC model for EN-AW-6082 T6 from literature sources.

	A [MPa]	B [MPa]	C [-]	n [-]	m [-]	$\dot{\varepsilon}_0$ [s^{-1}]
[52]	250.00	243.60	7.47×10^3	0.17	1.31	1.0
[53]	305.72	304.90	4.37×10^3	0.68	-	10^{-3}
[50]	277.33	307.93	3.2×10^3	0.69	1.28	10^{-4}

5. Experimental Setup

For the determination of the material parameter of the investigated alloy EN-AW-6082 T6, cylindrical samples with a diameter of 8 mm and an initial height of 12 mm were obtained from an extruded rod material. To receive the T6 condition, all specimens were solution-annealed at 803 K for one hour, followed by water quenching. After these steps, age hardening at 443 K for another five hours was carried out. For the determination of realistic material parameters, the specimens were compressed longitudinal to the extrusion direction at room temperature on the Gleeble 3800 thermal-mechanical Simulator, using the Hydrawedge module at constant strain rates of $1 \, \mathrm{s}^{-1}$, $10 \, \mathrm{s}^{-1}$, and $100 \, \mathrm{s}^{-1}$. The Hydrawedge module is especially designed for the simulation of forging and forming processes requiring a high strain rate, as it is capable of significantly reducing ringing of the hydraulic ram. The capability of high-speed deformations allows the generation of flow curves, which are relevant for the shot peening process. As shown within Figure 2, a graphite foil was additionally placed between both contact surfaces to reduce the friction between specimen and anvil, thus ensuring a uniform stress state during compression.
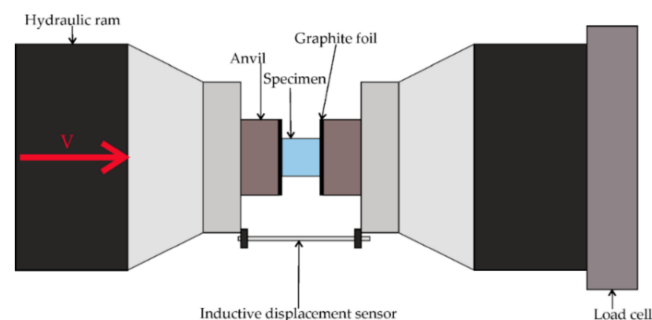

Figure 2. Experimental setup for the obtainment of JC material parameters.

Table 3 shows the resulting JC parameters, derived from the practical experiments and calculated according to Section 4. The experiments were carried out until a strain of 0.035 was reached, as higher strains are not relevant considering the shot peening process.

Table 3. Material parameters for the JC model for EN-AW-6082 T6 obtained from practical experiments.

A [MPa]	*B* [MPa]	*C* [-]	*n* [-]	*m* [-]	$\dot{\varepsilon}_0$ [s^{-1}]
385.02	116.01	7.97×10^3	0.50	-	1.0

6. FEA Setup and Resulting Data Mining Algorithm

For the implementation of the initial state white box model, a fundamental Abaqus input script was defined in first instance. This script contains all necessary input parameters for the simulation model to be automated and is scripted within the Abaqus Python environment. Table 4 shows a brief overview of the most important variables changeable within this input script.

Table 4. Variables changeable within the Python input script.

Input Variable	Functionality
Radius	Possible variation in sphere radius
x_specimen	Width of investigated specimen
y_specimen	Depth of investigated specimen
rows	Number of rows of spheres
angle	Angle of sphere impact (initially 90°)
number_spheres	Number of spheres (per defined rows)
delta_x	Horizontal distance between each sphere
delta_y	Vertical distance between each sphere
row_offset	Offset between different rows
step_time_shot	Step time related to the impact phase
dens_mat; YM; pois;	Density and elastic behavior of investigated material
A; *B*; *n*;	JC material parameters for the investigated material
C; eps_dot_0	Strain hardening parameters according to the JC model
damping_time	Additional step time for stress oscillation analysis
friction_coefficient	Defined friction state between specimens and impacting spheres
field frames	Number of field output frames within each step
v_shot	Shot velocity of spheres
mat	Density of spheres (depending on the material)
fine_mesh_region	Mesh size of direct impact zone
ground_mesh_region	Mesh size of the remaining geometry
RS_node	Node set definition for the residual stress analysis

In order to keep the number of degrees of freedom (dof) for the upstream data analysis reasonable, only the variables v_shot, radius, mat, elastic, and JC parameters of the investigated material (Section 3) were changed. For a further extending of simulation dof, a link between the Python input script and the overlaying automation layer is prepared. The fundamental FEA is defined as dynamically explicit, with widely used element type CPS4R (mesh size 0.01 mm) and a steady friction coefficient of 0.3. To achieve a high shot peening coverage rate on the specimen's surface, 90 spheres within three different rows were created, with a horizontal and vertical distance of 0.025 mm and a vertical offset between each row of 0.02 mm. The specimen's length as well as width was defined with 1.0 mm. Additionally, the impact angle was set to 90° and not changed in this study. To avoid contact definition dependent errors, a loop within the script automatically defined a surface-to-surface contact between each sphere and the target. Table 5 shows the resulting parameters varied within this paper.

Table 5. Varied variables within this case study.

Varied Input Variable	Range (Step)
mat	Mat 1.0 (steel spheres)/Mat 2.0 (glass beads)
Radius	0.1–0.5 mm (0.05)
v_shot	30–200 m/s (10)
A; *B*; *n*; *C*; eps_dot_0	Literature value (Table 2, [53]) and values obtained (Table 3)

Figure 3 shows the visualization of an exemplary setup for one defined sphere radius. Depending on the varying radii of the respective spheres, the resulting point mass of each sphere changes. To reduce computational time for the required simulations, the spheres were defined as rigid. For the automated data generation, the Abaqus GUI was excluded from the solver operation.

Figure 3. Visualization of the experimental setup and definition of geometric variables.

For the development of the white-box model, an initial database with all resulting residual stresses for each node included in the RS_node node set has to be created. This database also includes the different impact velocities and sphere diameters and serves as a basis for the initial GUI. In order to receive the steady-state residual stresses, the resulting amplitude at each respective node within the node set was analyzed. To consider a residual stress value for a node within RS_node as steady, the residual stress amplitude $\Delta\sigma$ for this node at a specific time increment has to be underneath 10 MPa (Figure 4). The fulfillment of this condition is checked within the initial Python algorithm. In this case, for a step time of 10^{-3} s, the condition is valid for each node within all performed simulations. The steady-state residual stress was returned and stored in the master database. As a result, one stress value for every 10 μm in each simulation is obtained.

Figure 5 visualizes the programming logic for the creation of this database, starting by the initial input script.
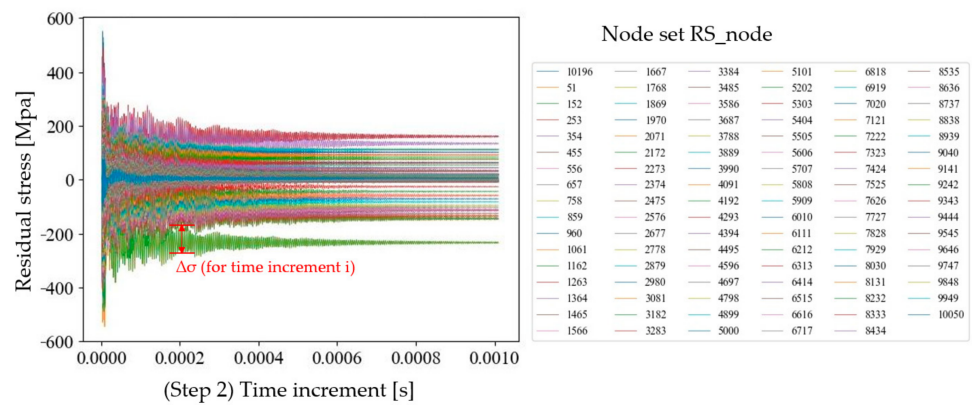
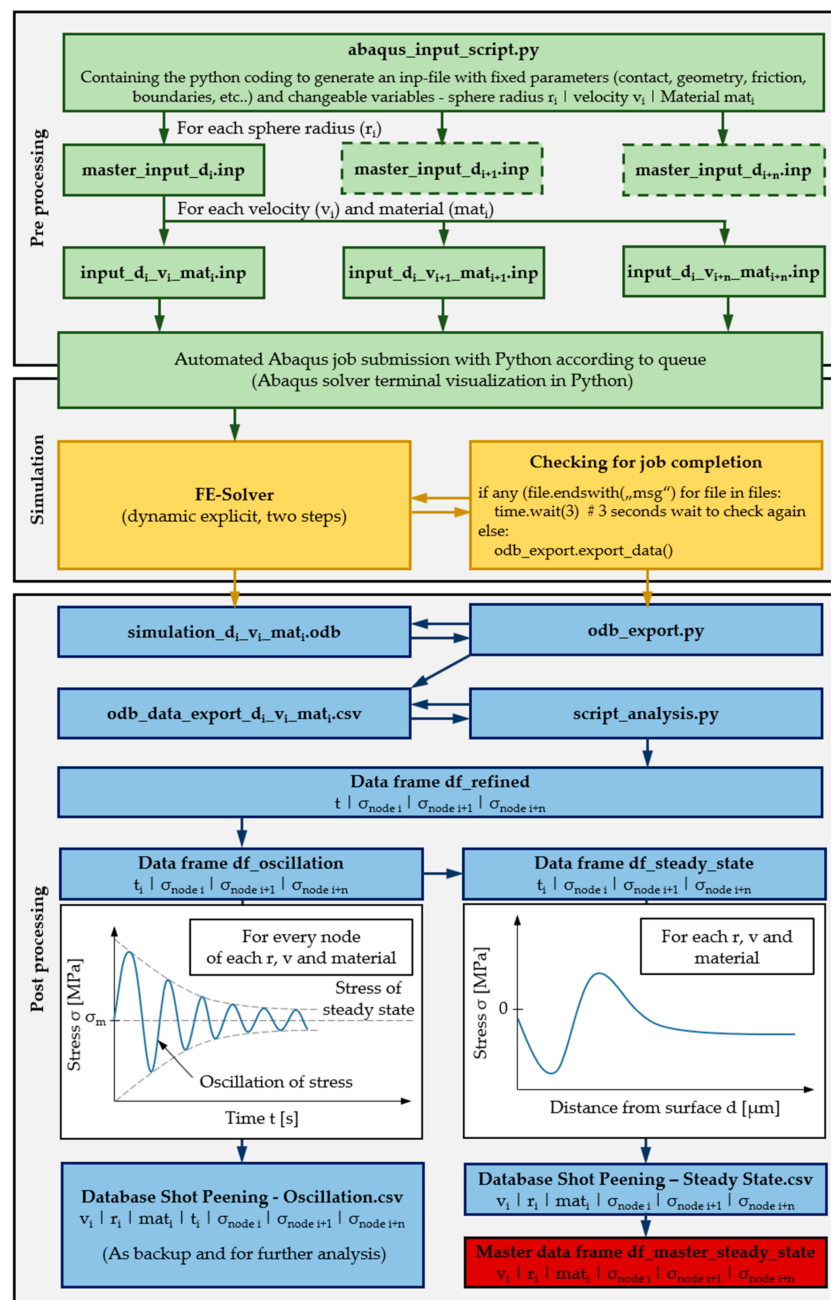**Figure 4.** Exemplary residual stress amplitudes over step time with included nodes in RS_node.

Figure 5. Programming logic for the obtainment of the database and master data frame from FEA data.

The master data frame extracted from the steady-state database contains all necessary information for further analysis and implementing the initial white-box-model-based logic. Figure 6 shows the comparison between different velocities for one exemplary sphere diameter (0.4 mm), whereas both investigated sphere materials (steel (red) and glass beads (blue)) are visualized. Additionally, the results for the JC material parameters from [53] are shown (steel spheres (green) and glass beads (orange)).
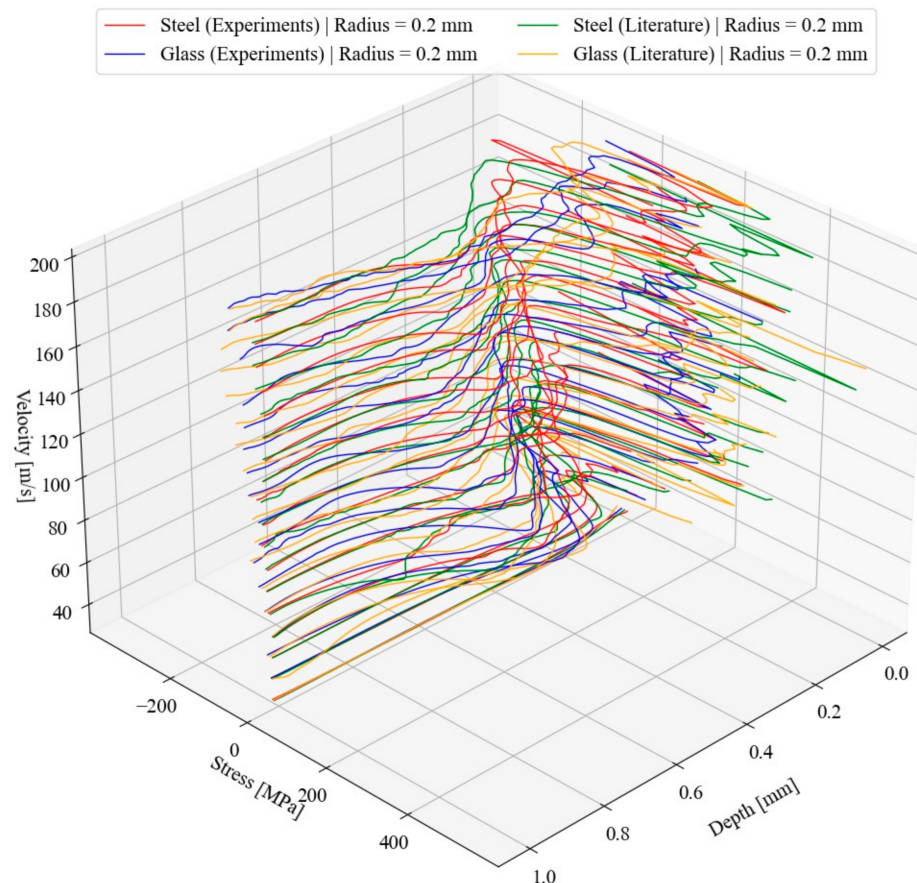
Figure 6. Resulting residual stress profile for a defined sphere diameter (0.4 mm) for the JC parameters obtained experimentally (steel spheres (red), glass beads (blue)) and alternative parameters derived from [53] (steel spheres (green), glass beads (orange)).

As demonstrated in Figure 6, a significant difference between the JC parameters determined from literature and own experiments can be seen, for the reasons explained previously in Section 4. In general, the impact of steel spheres results in higher residual stresses within comparable velocities and diameters. This effect can be explained by the higher resulting momentum of the iron-based sphere material, as the density is 3.1 times higher than the density of glass. The observed tensile stresses at the surface are a result of the material flow through adjacent impacts. This effect can be enhanced by the rigid definition of the spheres as well as the chosen mesh size. As the main objective of this framework is to obtain valid residual stress minima under reasonable computational time, this divergence was not considered any further [54].

Figure 7 shows the same sphere material and material parameter variation for a steady velocity (100 m/s) with varying sphere diameters (0.2–1.0 mm). The increase in maximum negative residual stresses with bigger sphere diameter can be explained again by the higher resulting momentum for a steady velocity [28].

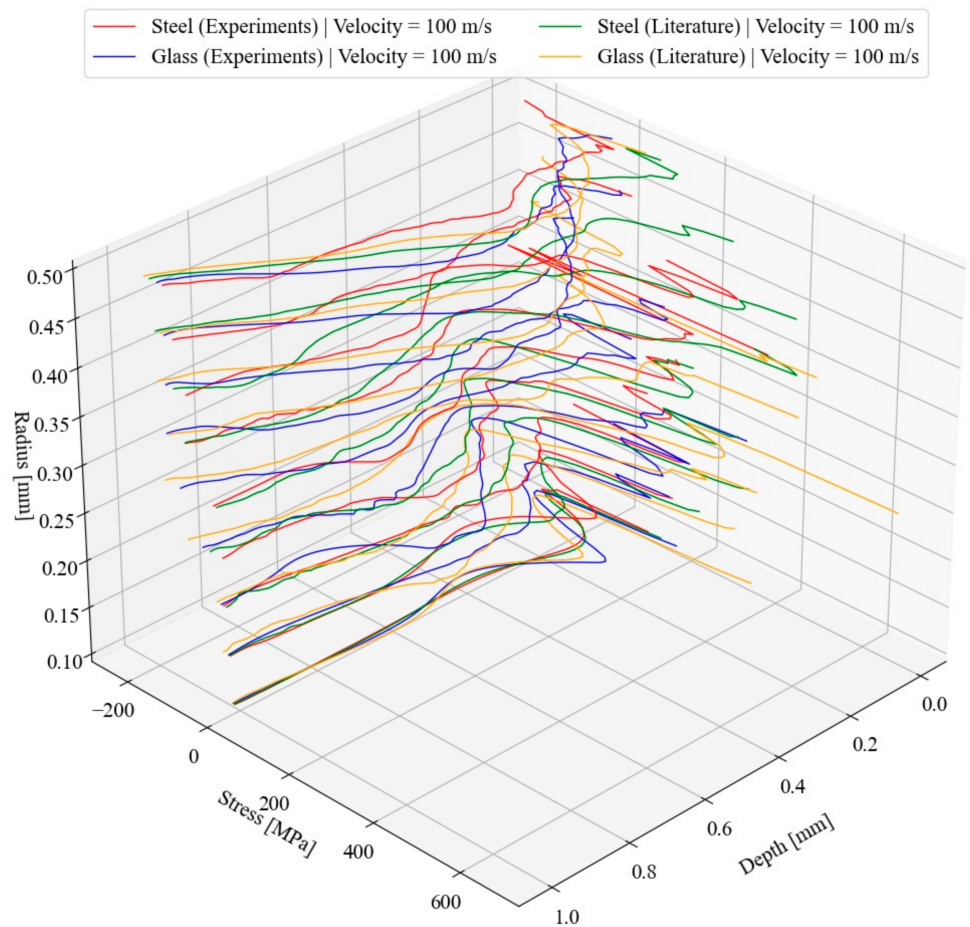**Figure 7.** Resulting residual stress profiles for a defined velocity (100 m/s) for the same variations defined within Figure 7.

Figure 8 illustrates the difference between literature values and the data obtained from the experiment exemplarily.
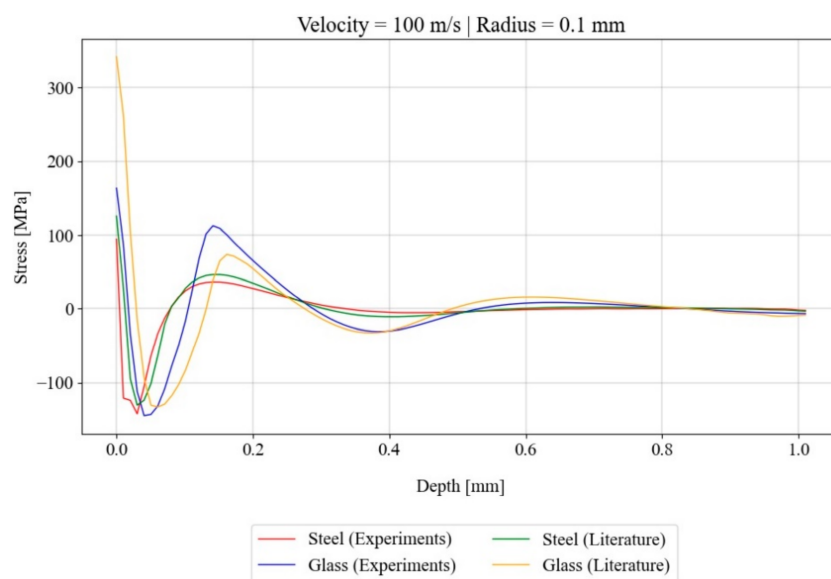

Figure 8. Resulting residual stress profiles for velocity = 60 m/s and a sphere diameter of 0.4 mm for literature and experimental data.

7. Development of the Initial White-Box Model for the Residual Stress Prediction

Figure 9 visualizes the initial white-box logic, beginning with the input parameters defined by the respective user to the final values returned from the algorithm.
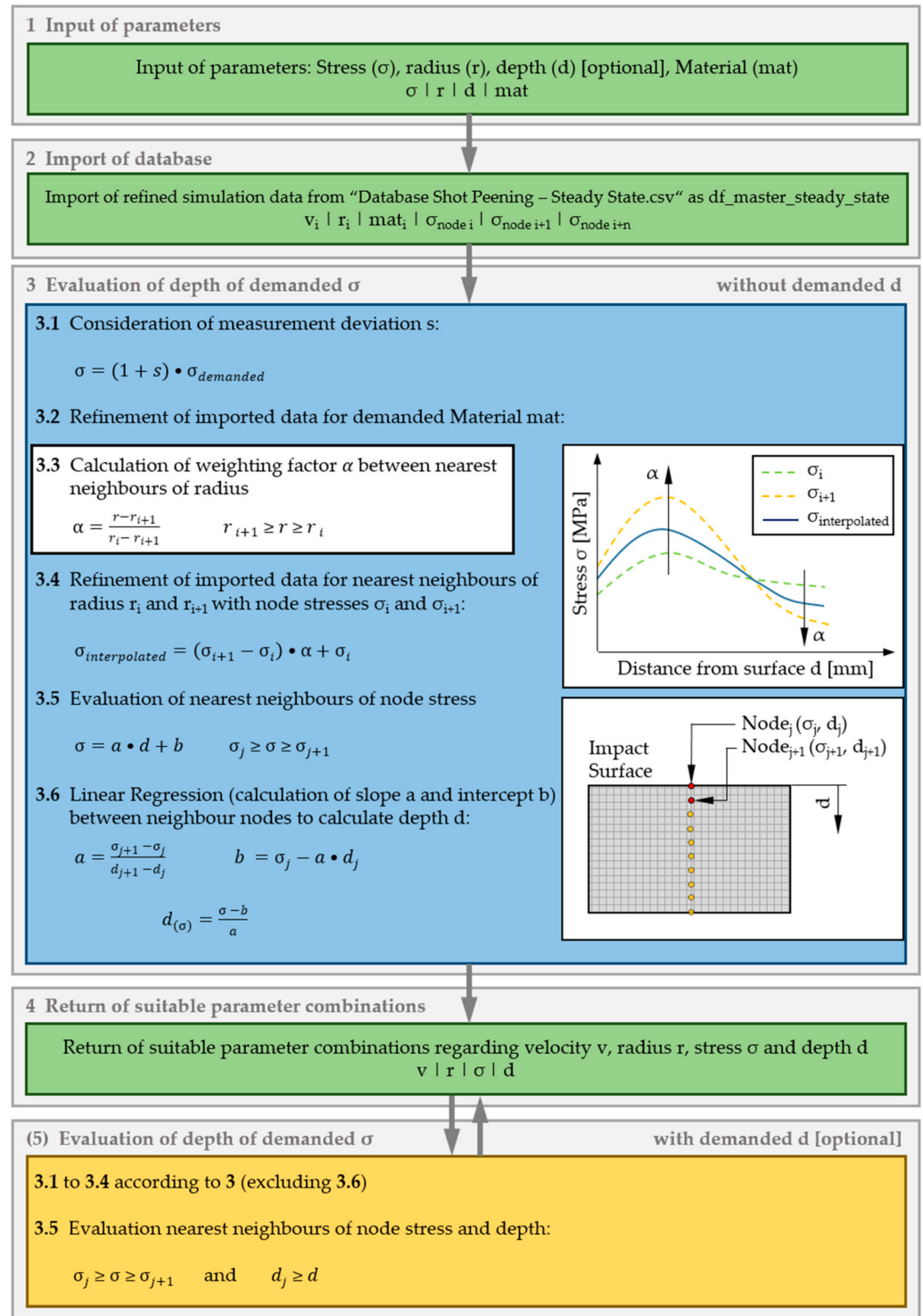

1 Input of parameters

Input of parameters: Stress (σ), radius (r), depth (d) [optional], Material (mat)
σ | r | d | mat

2 Import of database

Import of refined simulation data from "Database Shot Peening – Steady State.csv" as df_master_steady_state
v_i | r_i | mat_i | $\sigma_{node\,i}$ | $\sigma_{node\,i+1}$ | $\sigma_{node\,i+n}$

3 Evaluation of depth of demanded σ   without demanded d

3.1 Consideration of measurement deviation s:

$$\sigma = (1 + s) \bullet \sigma_{demanded}$$

3.2 Refinement of imported data for demanded Material mat:

3.3 Calculation of weighting factor α between nearest neighbours of radius

$$\alpha = \frac{r - r_{i+1}}{r_i - r_{i+1}} \qquad r_{i+1} \geq r \geq r_i$$

3.4 Refinement of imported data for nearest neighbours of radius r_i and r_{i+1} with node stresses σ_i and σ_{i+1}:

$$\sigma_{interpolated} = (\sigma_{i+1} - \sigma_i) \bullet \alpha + \sigma_i$$

3.5 Evaluation of nearest neighbours of node stress

$$\sigma = a \bullet d + b \qquad \sigma_j \geq \sigma \geq \sigma_{j+1}$$

3.6 Linear Regression (calculation of slope a and intercept b) between neighbour nodes to calculate depth d:

$$a = \frac{\sigma_{j+1} - \sigma_j}{d_{j+1} - d_j} \qquad b = \sigma_j - a \bullet d_j$$

$$d_{(\sigma)} = \frac{\sigma - b}{a}$$

4 Return of suitable parameter combinations

Return of suitable parameter combinations regarding velocity v, radius r, stress σ and depth d
v | r | σ | d

(5) Evaluation of depth of demanded σ   with demanded d [optional]

3.1 to **3.4** according to **3** (excluding **3.6**)

3.5 Evaluation nearest neighbours of node stress and depth:

$$\sigma_j \geq \sigma \geq \sigma_{j+1} \quad \text{and} \quad d_j \geq d$$

Figure 9. Algorithm for the transformation of user input data (real sphere diameter and desired residual stress, optionally required depth) into shot peening parameters (velocity options suitable for the defined input) by using the master data frame defined in Figure 6.

For the user to be able to adapt the initial sphere diameter to the real value, the model has to be capable of interpolating within the given data set. To achieve this, an interpolation scheme, including a linear weighting factor α which interpolates between given boundaries of the initial (FEA-based) data set, was defined. For the practical usage, the respective user is able to define the desired residual stress required for the individual case. Additionally, it is possible to define the desired depth in which the specified stress value should be obtained. If no depth is defined, the user gets a data frame which includes all shot velocities fulfilling the defined input value, including the depth in which the residual stress is reached first. To ensure that the calculated value will be reached in practice, a security factor s was set in the back end, which multiplies the input stress value with the factor 0.2.

8. Experimental Data-Driven Machine Learning Algorithm

As within every simulation, a deviation between the calculated results and experimentally determined data occurs. To close this gap in an efficient and sustainable way, the possibility of including actual test data in the model is considered, whereas the actual test data can be gained from different experiments (e.g., XRD measurements). In general, these results contain a few data points for each experiment carried out. To be able to adapt the initial FEA-based data cloud within the master data frame, at least four experiments have to be executed, analyzed, and transferred into the Python environment. These experiments have to be within a defined range of velocities ($\Delta v <= 30$ m/s) and sphere radii ($\Delta r <= 0.2$ mm). Based on this data set, non-linear functions with a sufficient amount of respective supporting grid points (initially 100 per three original data points) are created. For more complicated residual stress profiles, this range must be decreased to ensure accuracy. Based on this additional data, the curves received from the FEA within the range of the experimental data sets are overruled and excluded from the master data frame and steady-state database. Furthermore, interpolations that include experimentally obtained curves change significantly. This procedure is carried out automatically within a Python algorithm, which leads to a steady increase of data-driven analytics. This data is not directly connected to real-physics, which includes black-box approaches within the initially white-box model, resulting in a grey-box model. Figure 10 demonstrates this paradigm change over increasing experimental data infeed.
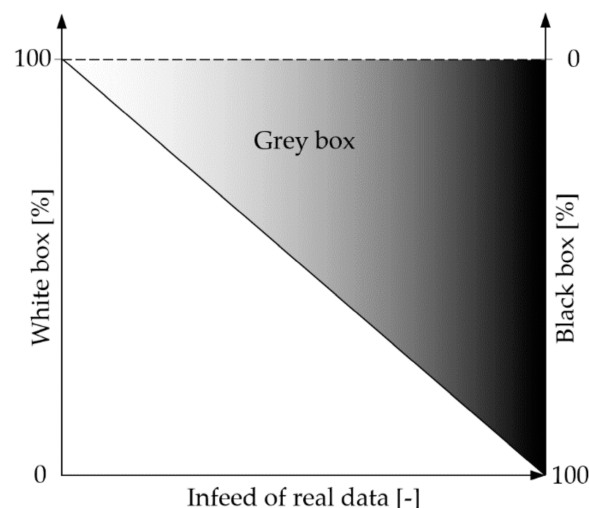

Figure 10. Change of model characteristics with increase of infeed data: the original FEA and real-physics-based model is overruled with more data from practical experiments.

Figure 11 shows the logic behind this machine learning approach, programmed within the same Python environment. To smoothen the resulting experimental data points without producing overfitting and therefore unrealistic behavior, a non-linear, second-order fitting approach between experimental data points was chosen. For the same purpose, a mean

value between two overlapping functions for the same data point was used. The resulting second order functions serve as boundaries for the creation of support data points, to be able to interpolate between the new resulting data sets with the same algorithm as for the initial white-box model.
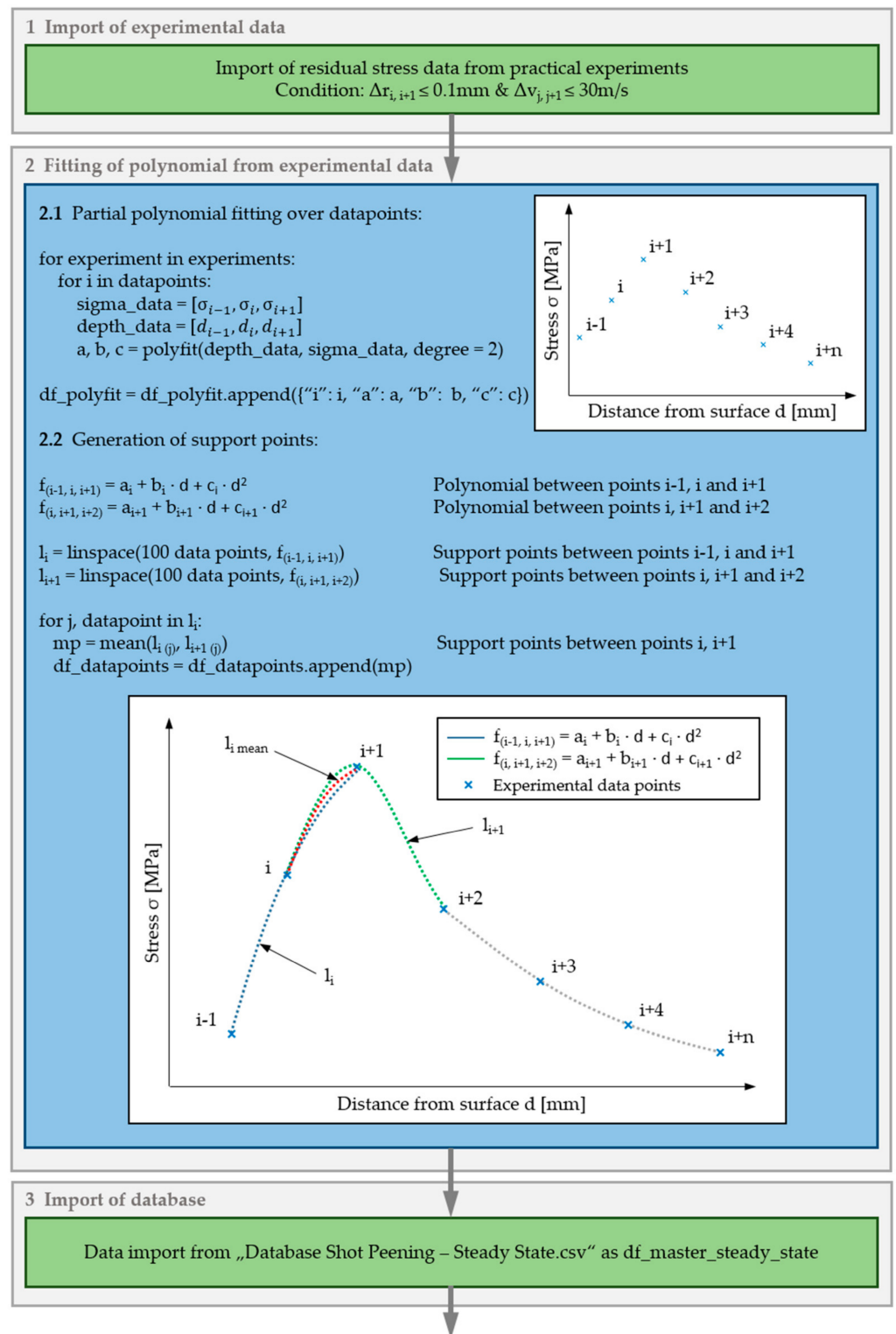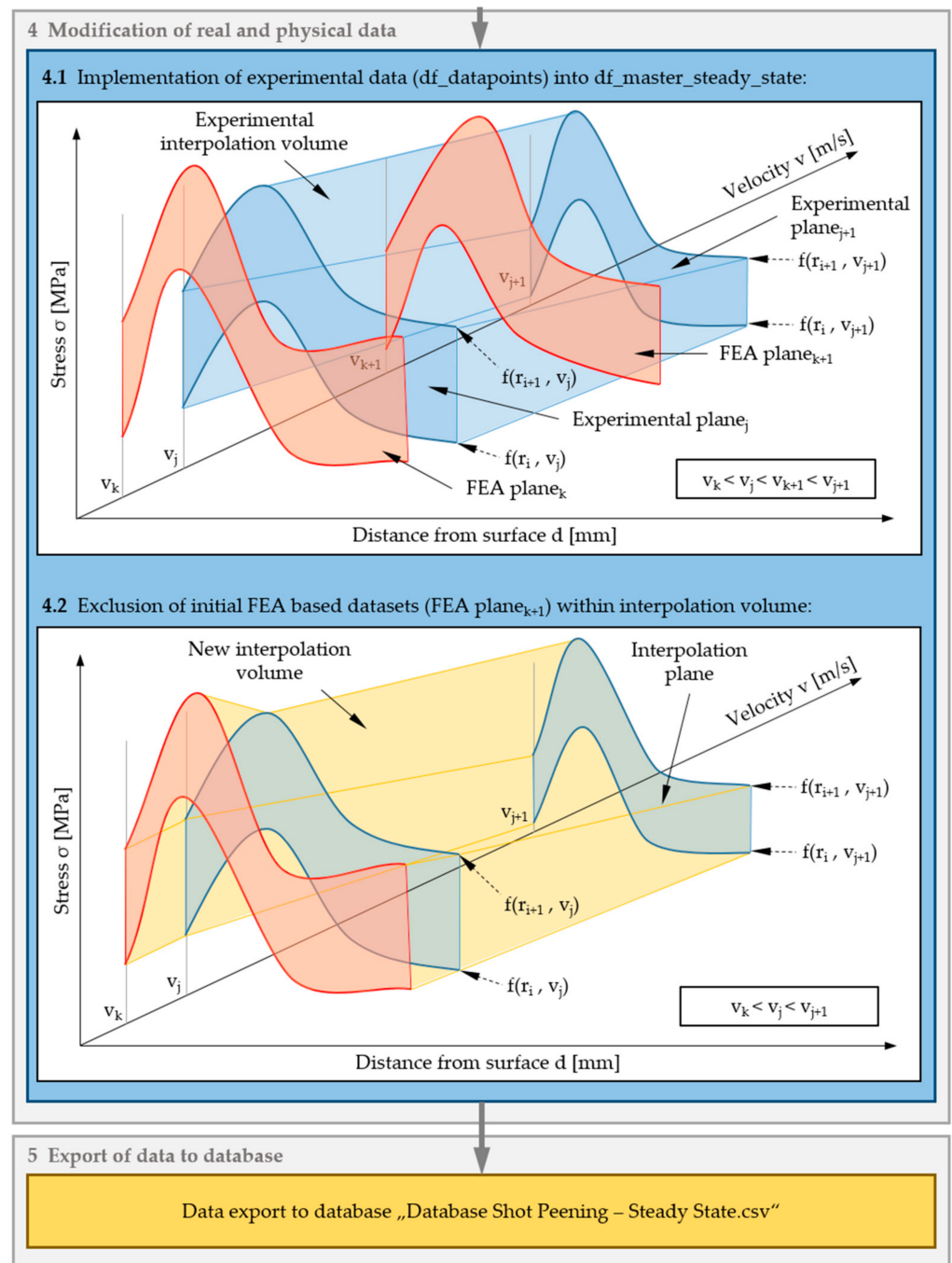

Figure 11. *Cont.*

Figure 11. Python logic implemented to adapt the initial FEA based white-box model by adding data from residual stress experiments. 1: Import data; 2: generation of support data points from experimental data and storage in a new data frame; 3: loading master data frame; 4: import data points from 2 and overrule data points of the master data frame to increase prediction efficiency; 5: overwrite master database with new data points.

9. Graphical User Interface

Based on the logic explained in Sections 7 and 8, a simple and user-friendly GUI was developed, using a C++ based open-source visualization environment. Due to an included library package within the Python environment, a direct programming within the same environment is possible. Figure 12 visualizes the automatic interaction between the resulting GUI and the algorithm developed.
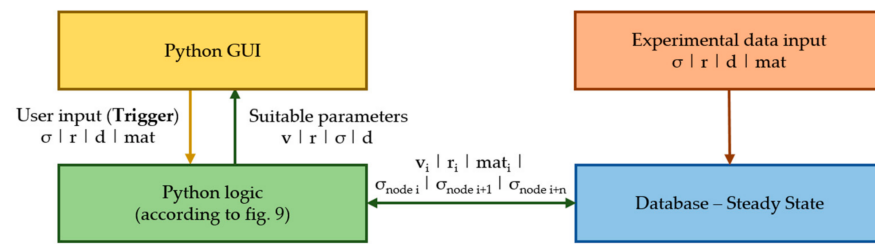
Figure 12. Interaction between the developed residual stress algorithm and GUI. To avoid confusion of respective users, the input of experimental data from practical experiments is excluded from this visualization.

Figure 13 shows the implemented GUI without optional definition of desired depth.

Figure 13. GUI with exemplary values for the prediction of residual stresses (without user-defined stress-corresponding depth).

As can be seen in Figure 13, a range of different velocities for the user-required residual stress is returned. If the stress value is necessary within a certain depth, the back-end algorithm changes, resulting in a recommendation for only those shot peening parameters, which result in a smaller depth while fulfilling the required stress (according to Figure 9). Figure 14 demonstrates this by using the same exemplary variables as in Figure 13.

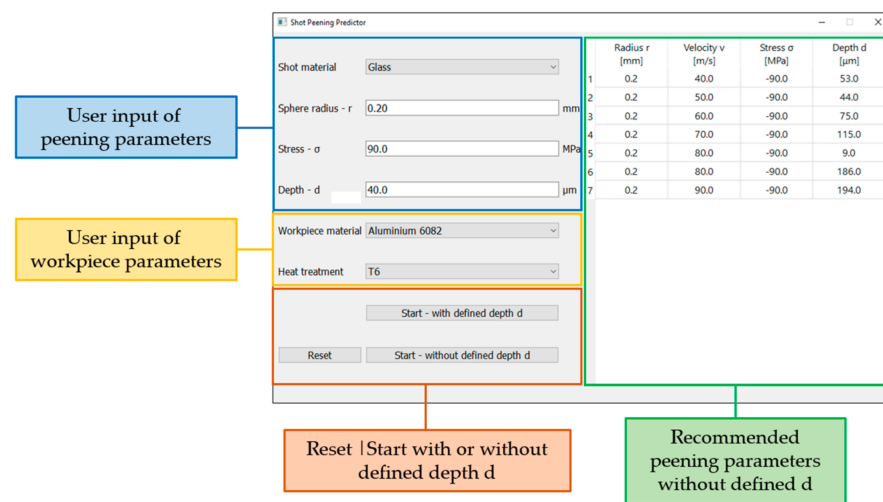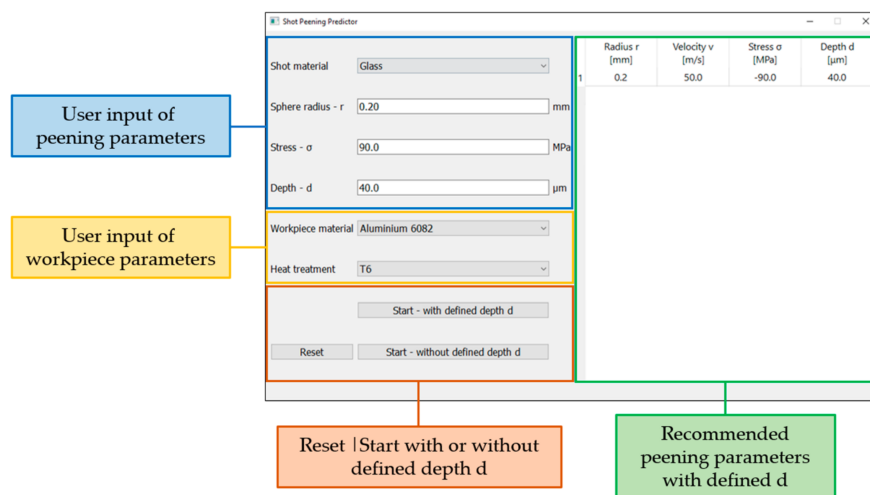**Figure 14.** GUI with exemplary values for the prediction of residual stresses (with user-defined stress-corresponding depth).

10. Results

This paper describes the development of a residual stress prediction module for the shot peening process. In order to demonstrate the logic implemented, an EN-AW 6082 T6 alloy was examined to obtain valid input parameters for the FEA simulation. This FEA model is set up according to literature [26,32,54–56], whereas the reduction of computational time without losing required accuracy was focused on. As a result, over 350 simulations with varying input parameters were automatically executed, resulting in residual stress profiles within common shot peening process ranges for two different sphere materials, 18 different velocities, and ten different sphere sizes. These simulations serve as a basis for the data mining algorithm introduced in Section 7. To enhance the predictor's accuracy, an algorithm for the implementation of experimental data from residual stress tests was additionally implemented. This algorithm is capable of overwriting the initial database within a defined range. For the usage in a production environment and for demonstration to interested parties, a user-friendly, front-end GUI was created, using the same open-source environment as for the logic introduced by the authors.

11. Discussion

Due to the ongoing fourth industrial revolution, the technologies implemented in the metal processing and manufacturing environment change significantly. Recent developments in automatic data exchange between production systems do not just increase the productivity within the production operation. The implementation of standardized interfaces additionally offers new possibilities to include other technologies into the process chain with reasonable effort. Numerical simulation, especially FEA, is a common tool in research and development, whereas the direct integration into the process chain is not state-of-the-art in practice. Nevertheless, the possibilities and potential advantages of FEA are pointed out recently in current literature [57,58]. The framework developed by the authors offers the possibility to be implemented into a digitalized production network. The algorithms introduced are programmed completely open-source, which allows interested companies the implementation without high economic barriers. Furthermore, the FEA solver used can be exchanged with every other software package suitable, as long as an interface to an open-source programming language is available. Despite the advantages of the ongoing digitalization and data-driven modeling, real-physics-based engineering has to be included to a certain extent. For the shot peening process, the relationship between workpiece and shot peening material as well as process parameters is complex. Using only black-box approaches would result in an unreasonable amount of required data from practical experiments to be obtained. On the other hand, using only real-physics-driven models often do not consider influences occurring in the manufacturing environment (e.g., sensor offset of respective aggregates, deviations from executed experiments due to different users). The combination of both techniques, although, can reduce the effort as well as deviations, offering an efficient and effective possibility to enhance the production process. Another advantage of the framework introduced in this work is the possibility of extension for all kinds of materials as well as according varieties in heat treatments, as already implemented in the respective GUI. Due to the possibility of changing the interpolation range within the machine learning algorithm, more complex residual stress profiles can be predicted with similar accuracy. However, it is important to note that smaller interpolation ranges result in a higher amount of required input data.

The GUI is designed under special consideration of user-friendliness, giving respective technicians the possibility to choose between two different initial options. Furthermore, the back-end programming carried out in Python ensures fast understanding and can therefore be used for educational purposes. The high connectivity provided within the Python environment allows easy coupling to superordinate networks, enabling users to connect the process simulation easily into a digitalized production system. For this purpose, the two-dimensional setup of the described FEA model should be the optimal compromise between accuracy and efficiency. Nevertheless, for more complex geometry (e.g., bevel,

material steps), a three-dimensional approach is recommended, as the difference between experiments and simulations for more complex geometries cannot be neglected. As the simulation model is based on Python, the implementation of such variations as well as the transformation to a 3-D model can be done shortly. Furthermore, by slightly adapting the initial post-processing, the resulting three-dimensional stress state can be easily obtained.

12. Conclusions and Outlook

In this article, a white-box-based framework for the prediction of residual stress profiles after shot peening treatments based on FEA simulations is presented. To include decisive influencing factors, the shot velocity, the sphere's diameter, and the material parameters were varied. According to this framework, a GUI was developed that enables the user in industrial environments to insert preferred residual stresses that should be obtained, receiving the optimal process conditions for this case. Due to the reduction of the simulation setup by using a two-dimensional FEA simulation that is based on the JC material model, the underlying algorithm presents a reasonable fit between efficiency and accuracy. The entries of the JC model can be extended for different materials based on a few practical experiments. The possibility to enhance accuracy of the predictions is given by the ability of the user to insert experimentally investigated resulting stress profiles, which the model adopts while cancelling imprecise entries.

To enhance the usage of the introduced algorithm, additional experiments to obtain valid input parameters from different materials are planned. Based on this additional data, other materials of interest will be inserted into the database. Further results from XRD-based residual stress experiments will also be included for the investigated material as well as additional materials, resulting in a significant increase of accuracy of the algorithm.

The model presented will be implemented within the Smart Forming Lab at the Chair of Metal Forming, connected with different types of Cyber Physical Production Systems by an open-source based MES. The main objective for this specific algorithm is to calculate accurate process parameters for processed workpieces, in order to increase the effectiveness and efficiency of the value chain, from casting to recycling. A possibility to extend this model is the incorporation of the resulting topology. This can be achieved by using the approach of Zeng et al. through comparative measurements, calculations, and adapted simulations [59]. Including the resulting mechanical properties and the expected hardness after shot peening would improve the model considerably. Due to the easy-to-implement logic of this framework, it is possible to apply this model to further mechanical surface treatments. Uprising technologies that are currently heavily investigated such as laser shock peening could be considered. A comparison of the three-dimensional FEA carried out by Li et al., also using the JC model to the two-dimensional model, will be considered [60]. Recent work from Dong et al. describes the development of a FEA for machining operations [61]. In this work, the effect on residual (tensile) stresses combined with a bimodal Gaussian function is used to predict existing stresses after machining and before mechanical surface treatment. This approach can be used to integrate the initial stress state of components to be shot peened. As a result, the accuracy of the initial white-box model presented in this work can be increased. Based on this combination, the number of practical experiments for the calibration of the algorithm can be further reduced. Recent work from Bock et al. [62] can additionally serve as a basis for the training of a physical data-driven artificial neural network.

Author Contributions: Conceptualization, B.J.R.; data curation, B.J.R. and M.S. (Marcel Sorger); formal analysis, M.S. (Marcel Sorger); investigation, K.H. and A.S.-G.; methodology, B.J.R. and M.S. (Marcel Sorger); project administration, B.J.R.; resources, M.S. (Martin Stockinger); software, B.J.R. and M.S. (Marcel Sorger); supervision, M.S. (Martin Stockinger); validation, B.J.R.; visualization, B.J.R. and M.S. (Marcel Sorger); writing—original draft, B.J.R. and K.H.; writing—review and editing, A.S.-G., B.J.R., and K.H. All authors have read and agreed to the published version of the manuscript.

Data Availability Statement: The data presented in this study are available on request from the corresponding author.

Conflicts of Interest: The authors declare no conflict of interest.

References

1. De Los Rios, E.R.; Walley, A.; Milan, M.; Hammersley, G. Fatigue crack initiation and propagation on shot-peened surfaces in A316 stainless steel. *Int. J. Fatigue* **1995**, *17*, 493–499. [CrossRef]
2. Hadzima, B.; Nový, F.; Trško, L.; Pastorek, F.; Jambor, M.; Fintová, S. Shot peening as a pre-treatment to anodic oxidation coating process of AW 6082 aluminum for fatigue life improvement. *Int. J. Adv. Manuf. Technol.* **2017**, *93*, 3315–3323. [CrossRef]
3. Hutmann, P. The Application of Mechanical Surface Treatment in the Passenger Car Industry. In *Shot Peening*; Wagner, L., Ed.; Wiley-VCH Verlag GmbH & Co. KGaA: Weinheim, Germany, 2003; pp. 1–12. ISBN 9783527606580.
4. Nalla, R.; Altenberger, I.; Noster, U.; Liu, G.; Scholtes, B.; Ritchie, R. On the influence of mechanical surface treatments—Deep rolling and laser shock peening—On the fatigue behavior of Ti–6Al–4V at ambient and elevated temperatures. *Mater. Sci. Eng. A* **2003**, *355*, 216–230. [CrossRef]
5. Tolga Bozdana, A. On the mechanical surface enhancement techniques in aerospace industry—A review of technology. *Aircr. Eng. Aerosp. Technol.* **2005**, *77*, 279–292. [CrossRef]
6. Gujba, A.K.; Medraj, M. Laser Peening Process and Its Impact on Materials Properties in Comparison with Shot Peening and Ultrasonic Impact Peening. *Materials* **2014**, *7*, 7925–7974. [CrossRef] [PubMed]
7. Travieso-Rodríguez, J.A.; Jerez-Mesa, R.; Gómez-Gras, G.; Llumà-Fuentes, J.; Casadesús-Farràs, O.; Madueño-Guerrero, M. Hardening effect and fatigue behavior enhancement through ball burnishing on AISI 1038. *J. Mater. Res. Technol.* **2019**, *8*, 5639–5646. [CrossRef]
8. Zhang, T.; Bugtai, N.; Marinescu, I.D. Burnishing of aerospace alloy: A theoretical–experimental approach. *J. Manuf. Syst.* **2015**, *37*, 472–478. [CrossRef]
9. Yen, Y.C.; Sartkulvanich, P.; Altan, T. Finite Element Modeling of Roller Burnishing Process. *CIRP Ann.* **2005**, *54*, 237–240. [CrossRef]
10. Preve´y, P.S.; Jayaraman, N.; Ravindranath, R. Fatigue Life Extension of Steam Turbine Alloys Using Low Plasticity Burnishing (LPB). In Proceedings of the ASME Turbo Expo 2010: Power for Land, Sea, and Air, Glasgow, UK, 14–18 June 2010; Volume 7, pp. 2277–2287, ISBN 978-0-7918-4402-1.
11. Scheel, J.E.; Hornbach, D.J.; Prevey, P.S. Mitigation of Stress Corrosion Cracking in Nuclear Weldments Using Low Plasticity Burnishing. In Proceedings of the 16th International Conference on Nuclear Engineering, Orlando, FL, USA, 11–15 May 2008; Volume 1, pp. 649–656, ISBN 0-7918-4814-0.
12. Avilés, R.; Albizuri, J.; Rodríguez, A.; López de Lacalle, L.N. Influence of low-plasticity ball burnishing on the high-cycle fatigue strength of medium carbon AISI 1045 steel. *Int. J. Fatigue* **2013**, *55*, 230–244. [CrossRef]
13. Rodríguez, A.; López de Lacalle, L.N.; Celaya, A.; Lamikiz, A.; Albizuri, J. Surface improvement of shafts by the deep ball-burnishing technique. *Surf. Coat. Technol.* **2012**, *206*, 2817–2824. [CrossRef]
14. Fernández-Lucio, P.; González-Barrio, H.; Gómez-Escudero, G.; Pereira, O.; López de Lacalle, L.N.; Rodríguez, A. Analysis of the influence of the hydrostatic ball burnishing pressure in the surface hardness and roughness of medium carbon steels. *IOP Conf. Ser. Mater. Sci. Eng.* **2020**, *968*, 12021. [CrossRef]
15. Kusiak, A. Smart manufacturing. *Int. J. Prod. Res.* **2018**, *56*, 508–517. [CrossRef]
16. Sjödin, D.R.; Parida, V.; Leksell, M.; Petrovic, A. Smart Factory Implementation and Process Innovation. *Res. Technol. Manag.* **2018**, *61*, 22–31. [CrossRef]
17. Zhong, R.Y.; Xu, X.; Klotz, E.; Newman, S.T. Intelligent Manufacturing in the Context of Industry 4.0: A Review. *Engineering* **2017**, *3*, 616–630. [CrossRef]
18. Monostori, L. AI and machine learning techniques for managing complexity, changes and uncertainties in manufacturing. *Eng. Appl. Artif. Intell.* **2003**, *16*, 277–291. [CrossRef]
19. Pham, D.T.; Afify, A.A. Machine-learning techniques and their applications in manufacturing. *Proc. Inst. Mech. Eng. Part B J. Eng. Manuf.* **2005**, *219*, 395–412. [CrossRef]
20. Wuest, T.; Weimer, D.; Irgens, C.; Thoben, K.-D. Machine learning in manufacturing: Advantages, challenges, and applications. *Prod. Manuf. Res.* **2016**, *4*, 23–45. [CrossRef]
21. Harding, J.A.; Shahbaz, M.; Srinivas; Kusiak, A. Data Mining in Manufacturing: A Review. *J. Manuf. Sci. Eng.* **2006**, *128*, 969–976. [CrossRef]
22. Kwak, D.-S.; Kim, K.-J. A data mining approach considering missing values for the optimization of semiconductor-manufacturing processes. *Expert Syst. Appl.* **2012**, *39*, 2590–2596. [CrossRef]
23. Harrison, J. Controlled shot-peening: Cold working to improve fatigue strength. *Heat Treat.* **1987**, *19*, 16–18.
24. König, G.W. Life Enhancement of Aero Engine Components by Shot Peening: Opportunities and Risks. In *Shot Peening*; Wagner, L., Ed.; Wiley-VCH Verlag GmbH & Co. KGaA: Weinheim, Germany, 2003; pp. 13–22. ISBN 9783527606580.
25. Bagherifard, S.; Ghelichi, R.; Guagliano, M. On the shot peening surface coverage and its assessment by means of finite element simulation: A critical review and some original developments. *Appl. Surf. Sci.* **2012**, *259*, 186–194. [CrossRef]

26. Xiao, X.; Tong, X.; Liu, Y.; Zhao, R.; Gao, G.; Li, Y. Prediction of shot peen forming effects with single and repeated impacts. *Int. J. Mech. Sci.* **2018**, *137*, 182–194. [CrossRef]

27. Kiefer, B. Shot Peening, Special Application and Procedure. International Scientific Committee for Shot Peening. shotpeener.com. Available online: https://www.shotpeener.com/library/detail.php?anc=1987088 (accessed on 20 April 2021).

28. Robertson, G. *The Effects of Shot Size on the Residual Stresses Resulting from Shot Peening*; SAE Technical Paper; International Scientific Committee on Shot Peening: Warrendale, PA, USA, 1987; pp. 46–48. [CrossRef]

29. Sharp, P.K.; Clayton, J.Q.; Clark, G. The fatigue resistance of peened 7050-T7451 aluminium alloy-repair and retreatment of a component surface. *Fatigue Frac. Eng. Mater. Struct.* **1994**, *17*, 243–252. [CrossRef]

30. Wagner, L.; Lütjering, G. Influence of shot peening parameters on the surface layer properties and the fatigue life of Ti-6Al-4V. In Proceedings of the Second International Conference on Shot Peening, Chicago, IL, USA, 14–17 May 1984; pp. 194–200.

31. Edberg, J.; Lindgren, L.-E.; Mori, K.-L. Shot peening simulated by two different finite element formulations. In *Simulation of Materials Processing: Theory, Methods and Applications Numiform 95*; Shen, S.-F., Dawson, P., Eds.; Balkema: Rotterdam, The Netherlands, 1995; pp. 425–430. ISBN 9054105534.

32. Majzoobi, G.H.; Azizi, R.; Alavi Nia, A. A three-dimensional simulation of shot peening process using multiple shot impacts. *J. Mater. Process. Technol.* **2005**, *164*, 1226–1234. [CrossRef]

33. Meguid, S.A.; Shagal, G.; Stranart, J.C. 3D FE analysis of peening of strain-rate sensitive materials using multiple impingement model. *Int. J. Impact Eng.* **2002**, *27*, 119–134. [CrossRef]

34. Han, K.; Peric´, D.; Owen, D.; Yu, J. A combined finite/discrete element simulation of shot peening processes—Part II: 3D interaction laws. *Eng. Comput.* **2000**, *17*, 680–702. [CrossRef]

35. Schwarzer, J.; Schulze, V.; Vöhringer, O. Finite Element Simulation of Shot Peening—A Method to Evaluate the Influence of Peening Parameters on Surface Characteristics. In *Shot Peening*; Wagner, L., Ed.; Wiley-VCH Verlag GmbH & Co. KGaA: Weinheim, Germany, 2003; pp. 349–354. ISBN 9783527606580.

36. Hong, T.; Ooi, J.Y.; Shaw, B. A numerical simulation to relate the shot peening parameters to the induced residual stresses. *Eng. Fail. Anal.* **2008**, *15*, 1097–1110. [CrossRef]

37. Mylonas, G.I.; Labeas, G. Numerical modelling of shot peening process and corresponding products: Residual stress, surface roughness and cold work prediction. *Surf. Coat. Technol.* **2011**, *205*, 4480–4494. [CrossRef]

38. Mazzolani, F.M. *Aluminium Alloy Structures*, 2nd ed.; CRC Press: Boca Raton, FL, USA, 2019; ISBN 9780367449292.

39. Bjørnbakk, E.B.; Sæter, J.A.; Reiso, O.; Tundal, U. The Influence of Homogenisation Cooling Rate, Billet Preheating Temperature and Die Geometry on the T5-Properties for Three 6XXX Alloys Extruded under Industrial Conditions. *MSF* **2002**, *396–402*, 405–410. [CrossRef]

40. Mohamed, M.S.; Foster, A.D.; Lin, J.; Balint, D.S.; Dean, T.A. Investigation of deformation and failure features in hot stamping of AA6082: Experimentation and modelling. *Int. J. Mach. Tools Manuf.* **2012**, *53*, 27–38. [CrossRef]

41. He, X.; Pan, Q.; Li, H.; Huang, Z.; Liu, S.; Li, K.; Li, X. Effect of Artificial Aging, Delayed Aging, and Pre-Aging on Microstructure and Properties of 6082 Aluminum Alloy. *Metals* **2019**, *9*, 173. [CrossRef]

42. Angella, G.; Bassani, P.; Tuissi, A.; Vedani, M. Aging Behaviour and Mechanical Properties of a Solution Treated and ECAP Processed 6082 Alloy. *Mater. Trans.* **2004**, *45*, 2282–2287. [CrossRef]

43. Das, S.; Pelcastre, L.; Hardell, J.; Prakash, B. Effect of static and dynamic ageing on wear and friction behavior of aluminum 6082 alloy. *Tribol. Int.* **2013**, *60*, 1–9. [CrossRef]

44. Lumley, R.N. Heat Treatment of Aluminum Alloys. In *Encyclopedia of Thermal Stresses*; Hetnarski, R.B., Ed.; Springer: Dordrecht, The Netherlands, 2014; pp. 2190–2203. ISBN 978-94-007-2738-0.

45. Ostermann, F. *Anwendungstechnologie Aluminium*; Springer: Berlin/Heidelberg, Germany, 2014; ISBN 978-3-662-43806-0.

46. Jonas, J.J.; Sellars, C.M.; Tegart, W.J.M. Strength and structure under hot-working conditions. *Metall. Rev.* **1969**, *14*, 1–24. [CrossRef]

47. Atkinson, H.V.; Burke, K.; Vaneetveld, G. Recrystallisation in the semi-solid state in 7075 aluminium alloy. *Mater. Sci. Eng. A* **2008**, *490*, 266–276. [CrossRef]

48. Zerilli, F.J.; Armstrong, R.W. Dislocation-mechanics-based constitutive relations for material dynamics calculations. *J. Appl. Phys.* **1987**, *61*, 1816–1825. [CrossRef]

49. Johnson, G.R.; Hoegfeldt, J.M.; Lindholm, U.S.; Nagy, A. Response of Various Metals to Large Torsional Strains Over a Large Range of Strain Rates—Part 1: Ductile Metals. *J. Eng. Mater. Technol.* **1983**, *105*, 42–47. [CrossRef]

50. Chen, X.; Peng, Y.; Peng, S.; Yao, S.; Chen, C.; Xu, P. Flow and fracture behavior of aluminum alloy 6082-T6 at different tensile strain rates and triaxialities. *PLoS ONE* **2017**, *12*, e0181983. [CrossRef]

51. Gottstein, G. *Materialwissenschaft und Werkstofftechnik*; Springer: Berlin/Heidelberg, Germany, 2014; ISBN 978-3-642-36602-4.

52. Ning, J.; Liang, S.Y. Inverse identification of Johnson-Cook material constants based on modified chip formation model and iterative gradient search using temperature and force measurements. *Int. J. Adv. Manuf. Technol.* **2019**, *102*, 2865–2876. [CrossRef]

53. Yibo, P.; Gang, W.; Tianxing, Z.; Shangfeng, P.; Yiming, R. Dynamic Mechanical Behaviors of 6082-T6 Aluminum Alloy. *Adv. Mech. Eng.* **2013**, *5*, 878016. [CrossRef]

54. Shivpuri, R.; Cheng, X.; Mao, Y. Elasto-plastic pseudo-dynamic numerical model for the design of shot peening process parameters. *Mater. Des.* **2009**, *30*, 3112–3120. [CrossRef]

55. Hu, D.; Gao, Y.; Meng, F.; Song, J.; Wang, Y.; Ren, M.; Wang, R. A unifying approach in simulating the shot peening process using a 3D random representative volume finite element model. *Chin. J. Aeronaut.* **2017**, *30*, 1592–1602. [CrossRef]
56. Wu, G.; Wang, Z.; Gan, J.; Yang, Y.; Meng, Q.; Wei, S.; Huang, H. FE analysis of shot-peening-induced residual stresses of AISI 304 stainless steel by considering mesh density and friction coefficient. *Surf. Eng.* **2019**, *35*, 242–254. [CrossRef]
57. Hürkamp, A.; Gellrich, S.; Ossowski, T.; Beuscher, J.; Thiede, S.; Herrmann, C.; Dröder, K. Combining Simulation and Machine Learning as Digital Twin for the Manufacturing of Overmolded Thermoplastic Composites. *J. Manuf. Mater. Process.* **2020**, *4*, 92. [CrossRef]
58. Vogel-Heuser, B.; Ribeiro, L. Bringing Automated Intelligence to Cyber-Physical Production Systems in Factory Automation. In Proceedings of the 2018 IEEE 14th International Conference on Automation Science and Engineering (CASE), Munich, Germany, 20–24 August 2018; pp. 347–352, ISBN 978-1-5386-3593-3.
59. Zeng, W.; Yang, J. Quantitative Representation of Mechanical Behavior of the Surface Hardening Layer in Shot-Peened Nickel-Based Superalloy. *Materials* **2020**, *13*, 1437. [CrossRef]
60. Li, X.; He, W.; Luo, S.; Nie, X.; Tian, L.; Feng, X.; Li, R. Simulation and Experimental Study on Residual Stress Distribution in Titanium Alloy Treated by Laser Shock Peening with Flat-Top and Gaussian Laser Beams. *Materials* **2019**, *12*, 1343. [CrossRef]
61. Dong, P.; Peng, H.; Cheng, X.; Xing, Y.; Tang, W.; Zhou, X. Semi-Empirical Prediction of Residual Stress Profiles in Machining IN718 Alloy Using Bimodal Gaussian Curve. *Materials* **2019**, *12*, 3864. [CrossRef]
62. Bock, F.E.; Keller, S.; Huber, N.; Klusemann, B. Hybrid Modelling by Machine Learning Corrections of Analytical Model Predictions towards High-Fidelity Simulation Solutions. *Materials* **2021**, *14*, 1883. [CrossRef]

A 8   Publication 8

K. Hartl, M. Sorger, H. Weiß, M. Stockinger: 'Machine learning driven prediction of mechanical properties of rolled aluminium and development of an in-situ quality control method based on electrical resistivity measurement', in: *Journal of Manufacturing Processes*, under review

Author contributions:

1. K. Hartl: Conceptualization, Methodology, Validation, Formal Analysis, Investigation, Validation, Visualization, Data Curation, Writing - Original Draft, Writing - Review & Editing, Project Administration

2. M. Sorger: Conceptualization, Methodology, Software, Validation, Formal Analysis, Investigation, Validation, Visualization, Data Curation, Writing - Original Draft, Writing - Review & Editing

3. H. Weiß: Supervision, Resources

4. M. Stockinger: Supervision, Resources

Machine learning driven prediction of mechanical properties of rolled aluminum and development of an in-situ quality control method based on electrical resistivity measurement

Karin Hartl[1]*, Marcel Sorger[1], Helmut Weiß[2], Martin Stockinger[1]

[1] Chair of Metal Forming, Montanuniversitaet Leoben, 8700 Leoben, Austria

[2] Institute of Electrical Engineering, Montanuniversitaet Leoben, 8700 Leoben, Austria

* karin.hartl@unileoben.ac.at, Franz Josef-Str. 18, 8700 Leoben, Austria

Keywords: in-situ quality control, machine learning, black box modelling, four point method

Abstract

As a result of the increasing digitization in the context of the fourth industrial revolution in the metal processing industry, the application of the associated possibilities has also entered the field of optimized in-situ material quality testing. In-line monitoring in the production of semi-finished products such as sheet metal in particular will be implemented and optimized to an increasing extent. For this purpose, this study presents a method that correlates the resulting mechanical properties to the electrical resistance of aluminum sheets during rolling for different rolling schedules and lubrication conditions by applying a non-contact measurement system. The four-point method, which was implemented for material testing on a tensile testing machine, can be further transferred to a rolling aggregate for an in-situ quality control step between the passes. Thus, using a black box machine learning approach, conclusions can be drawn about the prevailing mechanical properties as well as the anisotropic behaviour by measuring the electrical resistance. Furthermore, a graphical user interface was developed, which generates an optimized rolling schedule for desired mechanical properties. By integrating such a measurement equipment into the rolling process, predictions can be made about the resulting properties and labor-intensive subsequent quality checks as well as scrap can be significantly reduced. In addition, there is the possibility to specify desired mechanical properties for further sheet forming processes, whereupon the optimal rolling process route to achieve them is displayed.

Introduction

In recent years, there has been a steady increase in efforts to utilize the integration possibilities associated with the fourth industrial revolution (I 4.0) in the metalworking industry [1–4] . Due to the opportunity of collecting and processing data on the produced component throughout the entire value chain, data processing methods using artificial intelligence and machine learning (ML) algorithms are becoming increasingly important [5–7]. In addition to the manufacturing process itself, quality control of the processed component is an essential part of the production route. Especially for safety-relevant components, a large number of quality inspections and material testing methods are frequently carried out after production, in addition to the incoming semi-finished product inspection. In this area, the degree of automation is also steadily increasing as a result of the latest developments [8,9]. In-situ methods, which record mechanical, thermal, thermomechanical, microstructural and/or physical properties of the workpiece during a thermal, mechanical or thermomechanical testing

process, are of particular interest. In this context, those testing methodologies are advantageous which simultaneously record several properties and automatically create a data-driven correlation to other characteristics.

One of the most commonly tested physical properties of metals for quality control in a metal processing industry is the specific electrical conductivity or electrical resistance [10]. On the one hand, this has the advantage that it is easy to measure, but at the same time it correlates with a large number of other material properties, allowing numerous conclusions to be drawn about this measurand [11,12]. The best-known representatives of the measured quantities associated with electrical conductivity are, on the physical side, thermal conductivity and, on the microstructural level, lattice defects such as inclusions, voids, dislocations or grain boundaries [13]. In general, it is assumed that the electrical resistance increases with increasing temperature, which results from the stronger oscillation of the lattice atoms [14,15] .

Following the Matthiessen rule, the electrical conductivity is based on scattering processes of the electrons with various lattice defects or the thermally activated phonons and accumulates to a total electrical resistivity ρ according to

$$\rho = \rho_{th} + \rho_{res} \tag{1}$$

where the ρ_{th} describes the theoretical electrical resistance based on thermal activation and ρ_{res} the residual resistance consisting of impurities and lattice defects. This implies that the knowledge of the residual resistance at absolute zero allows to draw conclusions about the microstructure via the linear increase of the electrical resistance with temperature increase. However, this residual resistance is a superposition of a multitude of defects which, on the one hand, cannot be changed, such as impurities, but, on the other hand, can very well be changed via various processes. In addition to voids, this includes grain boundaries, which can be significantly changed by several processes [15]. Knowledge of grain boundaries, grain sizes or morphology is particularly essential for forming processes in the manufacture of semi-finished products or components. In forming processes such as rolling, dislocations are induced in the material while the grains are stretched in the rolling direction.

Basically, it is assumed that the forming energy is converted into stored energy of cold work (SECW) on the one hand and into adiabatic heating on the other hand. The coefficient of adiabatic heating, the Taylor-Quinney coefficient, can be calculated in principle by Eq.2:

$$\beta_{int} = \rho_{dens}C\Delta T / \int \sigma_{ij}d\varepsilon_{ij}^{P} = Q/W_{P} \tag{2}$$

In this context, ρ_{dens} corresponds to the material density, C to the heat capacity and ΔT to the temperature increase. The components in the denominator correspond to the stress and plastic strain tensors. In other words, the upper term can be summarized as the amount of heat dissipated and the lower term as the work input. The sum of the two components then corresponds to the initial forming energy [16].

While a large part of the energy input results in adiabatic heating in the workpiece, thus reducing the actual strain as well as enhancing diffusion processes, the decisive factor is the amount of undeformed strain prevailing in the material in the form of dislocation energy.

Furthermore, the amount of energy introduced as dislocations can be assumed by the formula

$$\sigma = 0.5Gb\rho_{dis}^{\frac{1}{2}} \tag{3}$$

Where σ corresponds to the stress, G to the shear modulus, b to the burgers vector, and ρ_{dis} to dislocation density [17].

The amount of dislocations introduced and their ability to move freely are critical to the deformation and corresponding to the strain hardening behaviour of the material. The strain hardening, in terms of the strain hardening exponent of a material, is likewise decisive for the further processability, for example by stretch forming processes.

In general, it is assumed that cold forming processes are primarily incorporated in the increase in dislocation density, which is proportional to the applied strain. Beyond a certain strain introduced into a material, this, in combination with thermal activation, can lead to recovery or recrystallization effects. Generally, this is not the case for most metals during cold forming, but considering aluminum, it cannot be completely precluded. Due to the high stacking fault energy of aluminum, this material has a strong tendency to recovery processes at a correspondingly high strain [18]. In the literature, a high value is usually assumed for the Taylor-Quinney factor, which means that even during cold forming of aluminum, the dissipated heat quantity is sufficient to force softening behavior due to (meta-) dynamic recovery as well as recrystallization and also their superposition. This again contrasts with the softening due to the increase in dislocation density, as the dislocations are thereby degraded again. Furthermore, it has been shown that the Taylor-Quinney factor can vary between 0.45 and 0.65 for pure aluminum, depending on the strain rate applied [19], although both the yield curve and the microstructural studies do not reveal any strain rate influence.

In addition, anisotropy becomes of predominant importance when considering rolled material. Due to the cold rolling process, the grains are stretched enormously in the rolling direction and remain in this arrangement, provided recrystallization has not occurred. This condition causes differences in the mechanical behavior in varying orientations and is particularly noticeable in sheet forming, such as deep drawing. In practice, it is therefore common to perform mechanical sampling in different directions in order to be aware of the extent of anisotropy [20].

Taking into account all these influencing factors for pure aluminum during cold forming renders a mathematical representation in terms of microstructure modeling, for instance, very complex. The implementation of a purely physical approach in a finite element analysis requires knowledge of all interactions at given parameters, which considerably complicates this approach. However, even the application of a semi-empirical material model requires an enormous amount of experimental effort, which is not least faced with the great challenge of separating all microstructural changes that can overlap simultaneously and developing the appropriate set of material parameters. This is further complicated by the fact that aluminum alloys can differ enormously from one another due to their diverse and multitude of precipitates [21,22].

Since microstructure simulation of aluminum turns out to be relatively difficult, simpler methods lend themselves to finding a correlation between the material, its mechanical and microstructural properties during forming.

For this purpose, it is suitable to consider the enablers of I 4.0. ML approaches offer an enormous facilitation in this respect, whereby the white-box or black-box method is in the focus in this context. While white-box ML algorithms are based on real-physical comprehensible models, the black-box method relies on data-driven models. A combination of these two modeling methods is offered by grey-box modeling. In this approach, real-physical data are used to provide supporting points, while data-driven algorithms predict an outcome [23].

In order to generate a simplification of the quality control of a rolled aluminum sheet, a data driven black-box model is developed in this study to establish a correlation between mechanical properties and the electrical resistivity of EN AW-1050A sheets for different rolling routes. For this purpose, tensile specimens are taken from aluminum sheets produced via different rolling schedules in the rolling direction (0°), 45° and transverse directions (90°) and examined by means of tensile tests. In addition, a four-point method is used to measure the change in electrical resistance during tensile testing. Based on this method, a data basis between mechanical properties depending on the spatial direction and the change of electrical resistivity is established. If this method is implemented in a forming process such as rolling, this can be integrated into a Cyber Physical Production System (CPPS) implemented in a Smart Production Lab at the Chair of Metal Forming at the Montanuniversitaet Leoben by combining it with grey box modeling and thus be used for non-destructive in-situ quality control of the semi-finished product [24–26].

Materials and Methods

EN AW-1050A

The material EN AW-1050A was selected as it is a material with a constant face-centered cubic (fcc) lattice structure, which does not exhibit allotropic transformation at elevated temperatures. It is a pure aluminum with limited impurity content, which is especially characterized by its excellent corrosion resistance. Therefore, it finds industrial application in the chemical or nourishment industry, as well as in container and apparatus construction. In addition, aluminum has excellent electrical and thermal conductivity [27].

Furthermore, this material was used because the lattice defects are limited to those occurring in pure metal, such as vacancies, dislocations, grain boundaries or stacking faults, without the presence of precipitations or additional phases. These would complicate the interpretation of electrical and thermal conductivity.

Due to the high stacking fault energy of aluminum, it shows a lower strengthening characteristic, resulting in a greater resistance to recrystallization than other metals. However, this results in the fact that there is also a very low tendency for twinning, which is why there is a smaller deviation between the compression and yield strengths in this material in the deformed state, as well as a low tendency for a bulking effect [18].

In addition, this material shows a pronounced dynamic recovery, due to the tendency to dominant transverse sliding of the screw dislocations caused by the high stacking fault energy. The dynamic recovery does not influence the grain structure, but reduces the strain hardening due to dislocation annihilation and the formation of a substructure [17,18]. The effect of the dynamic softening processes on the flow curve is shown in Figure 1.
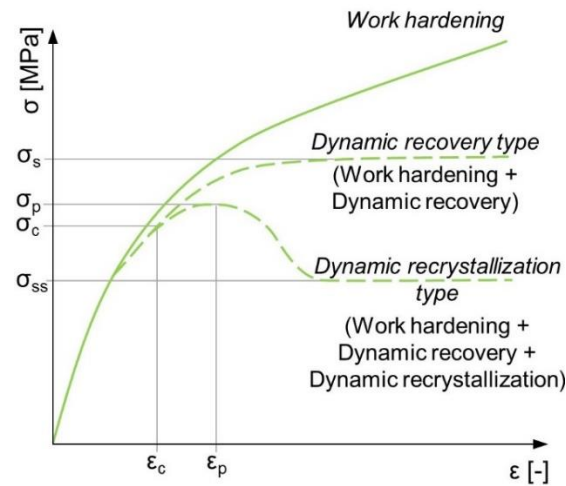
Figure 1: Characteristic flow curves of aluminum including softening processes cf. [17]

Initial condition of the material

The initial material for this investigation was EN AW-1050A sheet rolled from an initial height (h_0) of 6.0 mm to a thickness of 0.5 mm. These were rolled under different conditions in a rolling mill aggregate, which was transformed into a CPPS as described in [25]. Table 1 lists the different conditions of the rolling experiments.

Table 1: Different rolling conditions

T1	Full lubrication
T2	No lubrication
V1	„hard" rolling schedule
V2	„intermediate" rolling schedule
V3	„soft" rolling schedule

By varying the friction conditions, the influence on the rolling forces or on the mechanical properties of the sheets is to be investigated.

The gradations of the rolling schedules refer to the size of the pass reductions to achieve the final rolling thickness. This implies that V1 is associated with a lower number of passes but higher forces and thus hardening. The rolling schedules are summarized in Table 2.

Table 2: Height reductions during the different rolling schedules V1, V2 and V3

Nr.	s_0 (V$_1$) [mm]	s_0 (V$_2$) [mm]	s_0 (V$_3$) [mm]
1	4.50	5.00	5.00
2	3.50	4.00	4.50
3	2.75	3.50	4.00
4	1.75	2.50	3.50
5	1.00	1.50	3.00
6	0.75	1.00	2.50
7	0.50	0.50	2.00
8	-	-	1.50
9	-	-	1.00
10	-	-	0.50

These differences in the rolling schedules are intended to represent different stress paths and to determine their influence on the spring-back of the material and the rolling behavior. To determine whether these cumulative deformation paths have an influence on material behavior, in particular anisotropy, three flat tensile specimens were taken from each of the sheets at 0°, 45° and 90° to the rolling direction.

These were tested on the Zwick Z250 tensile testing machine where the stress-strain curves were evaluated via the associated testXpert software. The experiments were conducted in accordance with DIN EN 10002-1 (German Institute for Standardization). In addition, the development of electrical resistance during deformation up to fracture was also monitored on selected specimens using the four-point method.

Four-point Method

The four-point electrical resistance measurement method has been used in many studies to establish a correlation between strain, damage, dislocation density and the associated change in electrical resistance.

The basic principle behind the four-point method is that by using four probes to measure the voltage drop across a sample, it is possible to accurately measure the electrical resistance of the material, regardless of the resistance of the leads or contacts used to make the measurement.

The four-point measurement technique works by passing a known electrical current through two probes (referred to as the current probes) that are placed a known distance apart on the sample. Two additional probes (referred to as the voltage probes) are placed a known distance apart between the current probes, and the voltage drop across the sample is measured. By measuring the voltage drop using the two voltage probes, it is possible to calculate the electrical resistance of the sample using Ohm's law, which states that the resistance of a material is equal to the voltage drop across the material divided by the current passing through it. Because the current is known and the voltage drop is measured directly using the two voltage probes, the electrical resistance of the sample can be calculated accurately [28].

In this study, this method was applied to a non-contact in-situ test to record the changes in electrical resistance of the drawn specimens during tensile tests. For this purpose, as explained in [29], a voltage-controlled and current-regulated DC source was used, which generates a parallel current path across the tensile testing machine and the tensile specimen clamped on both sides. Thus, the voltage drop is measured over a certain length, which corresponds to the test length of the tensile specimen in addition to the strain during the test itself, via two pairs of contacts. The outer contact pair supplies a current of up to 30 amperes, while the inner registers this voltage drop.

These measured variables (current sensor signals, voltage drop) are visualized in the DewesoftX software during the test and recorded at a measurement frequency of 10 kHz. In order to achieve the correlation of the slope of the electrical resistance and an increase in the temperature of the sample, some experiments were also equipped with an additional temperature sensor Pt1000 with the possibility of integrating this measurement variable into the DAQ system as well. In this software it is possible to reduce signal noise by using various low pass filters.

One important advantage of the four-point probe technique is that it is relatively insensitive to variations in the contact resistance between the probes and the sample. This is because the

voltage probes are placed a known distance apart between the current probes, and so the voltage drop measured by the voltage probes is largely independent of the contact resistance. This allows for very accurate measurements of the electrical resistance of the sample, even if the contact resistance between the probes and the sample is relatively high.

Results and discussion

In this section, the results of the tensile tests and the four-point method are presented in the form of the resulting characteristic values for the experiments. At the beginning, the synchronization step is presented. Furthermore, an ML algorithm is presented which correlates the mechanical properties of the material with the electrical resistance. This results in synergies which do not require a background in real physics but nevertheless provide information about the obtained mechanical properties.

Digitization of two proprietary systems

To merge and synchronize the datasets of the two proprietary systems (testXpert & DewesoftX) without implementing further hardware, an open-source post-processing step using Python was developed, increasing the reliability and quality of the data. Both systems generate time series data in different formats with different sampling rates, whereby the tensile testing machine depicts a sampling rate of 50 Hz and the electrical resistivity system showcases a sampling rate of 10 kHz. The time of data synchronization was set at the time of the specimen failure. At the failure, the electrical circuit is broken and the current drops towards 0 A. If the current falls below a set threshold value of 0.15, the timestamp of the last data point and of the tensile test dataset is set equal to the timestamp of the last data point of the electrical resistivity dataset. Consequently, both data sets are merged from this common synchronization point.

Results of the mechanical properties

Figure 2 shows the ultimate tensile strength (UTS) results as a function of the rolling schedule, lubrication condition and extraction orientation.
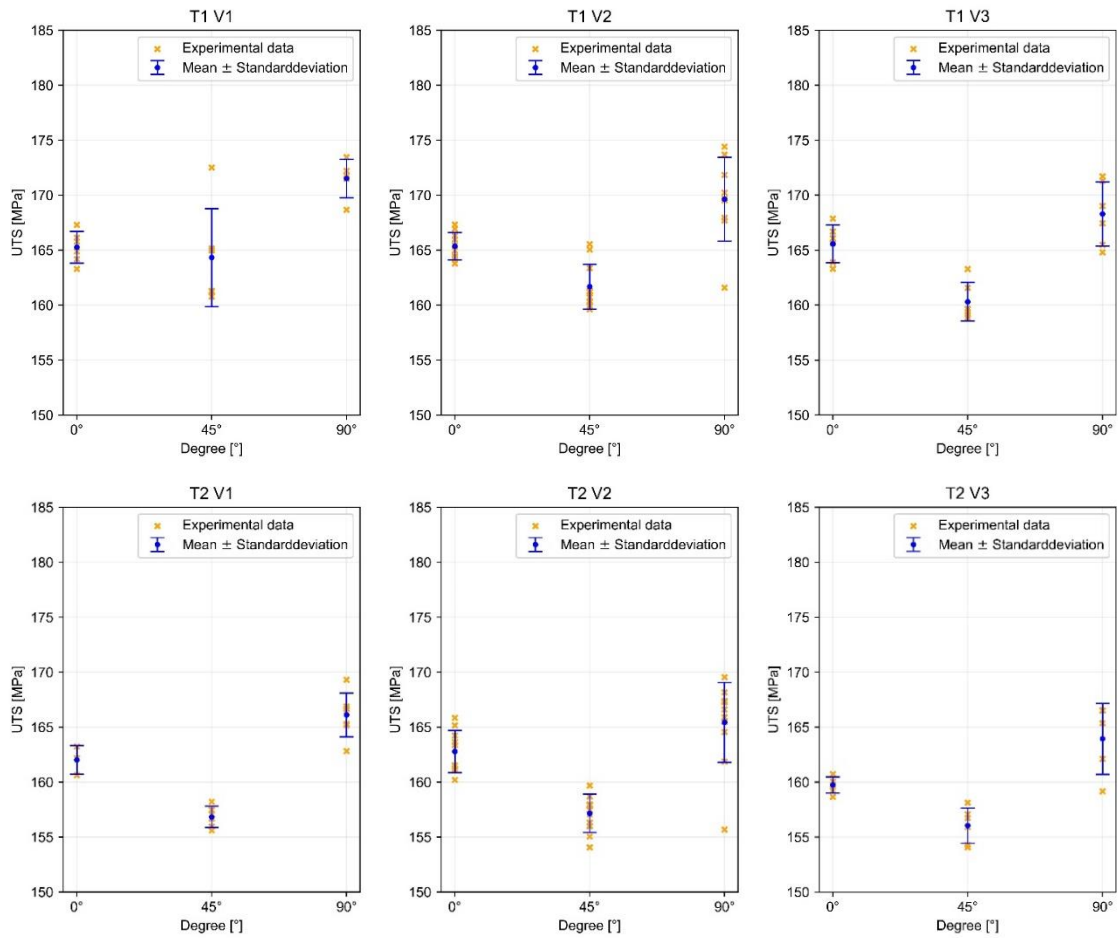
Figure 2: Comparison of UTS for different rolling schedules, friction conditions and extraction directions

The results for yield strength (YS) (proportional limit at 0.2%) as a function of lubrication and rolling schedules are shown in Figure 3.
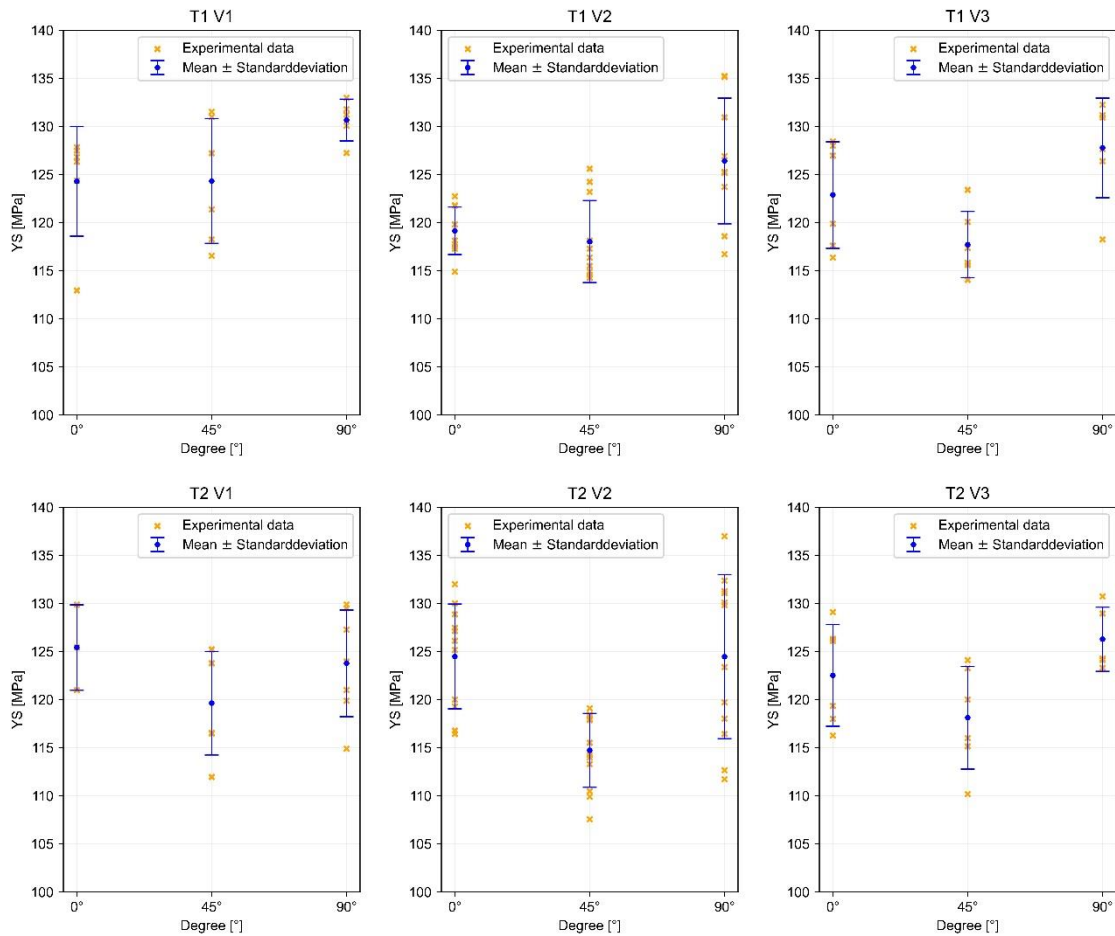
Figure 3: Comparison of YS for different rolling schedules, friction conditions and extraction directions

For both of these strength values (YS and UTS) of the stress-strain diagram, there is a tendency towards higher strength values in the rolling direction than in the 45° orientation. The highest values tend to occur in the transverse direction.

The absolute values of UTS are in a relatively similar range for all three rolling schedules, regardless of the prevailing lubrication condition. In addition, the values for 0° are in a relatively narrow scatter range.

The deviation from the common opinion that the mechanical properties are worse in the transverse direction than in the rolling direction can be explained by the choice of alloy. When the grains are stretched in the rolling direction, the dislocations mobilized by the uniaxial deformation during the tensile test do not have to change their preferred slip plane/direction (preferably {111} <110> for aluminum) as often due to the small number of grain boundaries, which is why there is less accumulation of dislocations at grain boundaries. Therefore, even in theory, the rolling direction would tend to have lower strength.

However, for alloys that have inclusions, precipitates or other impurities that preferentially accumulate at grain boundaries, the likelihood of detachment at these particles, and thus preferential pore formation, is higher in the transverse direction than in the rolling direction.

Since EN AW-1050A is a rather pure grade in which precipitations are not expected, this leads to a rather theoretical behavior of the mechanical properties, therfore the transverse direction shows higher strengths.

On the other hand, the strength values behave approximately similar to the values of the uniform elongation (e_u), which are shown in Figure 4. In the case of lubrication condition T1, thus with the presence of the lubricant, the specimens in the rolling direction tend to exhibit higher elongation than those in the 45° or 90° direction. The tendency of the higher elongation values at 0° and 90° is maintained.

For the non-lubricated rolled specimens (T2), the results for all pass schedules provide a relatively large scatter. The value ranges for V2 and V3 are in a rather lower range than for the "hard" stitch plan V1.

It should be noted here that the lubrication conditions on the one hand affect the amount of forming energy introduced and on the other hand influence the heat generation in the system.
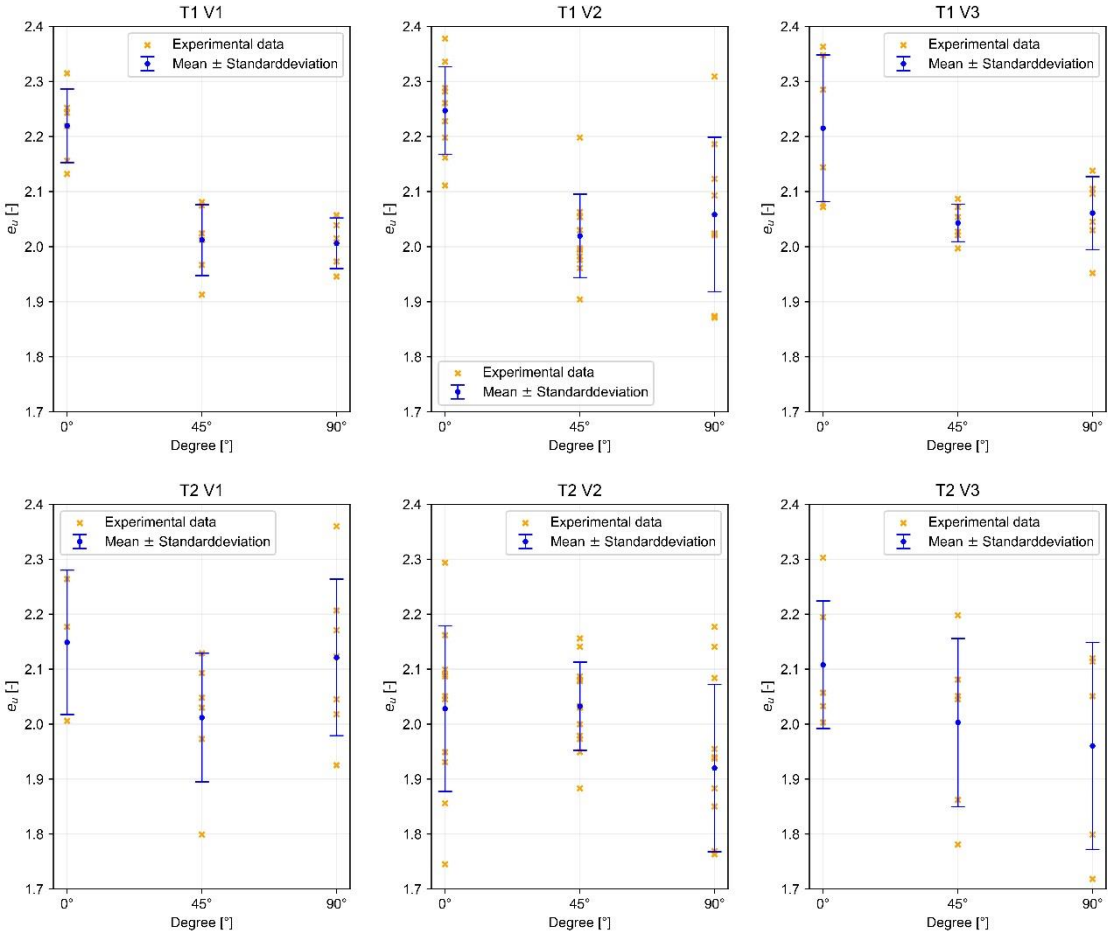

Figure 4: Comparison of e_u for different rolling schedules, friction conditions and extraction directions

Figure 6 plots the slope of the resistance (k_Ω) for the different conditions. This slope is linear to the strain in the tensile test for all specimens, as depicted for a representative measurement in Figure 5.
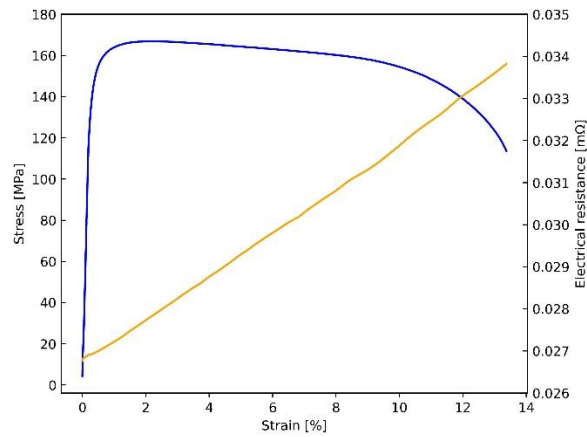
Figure 5: Representation of the evolution of the electrical resistance during tensile testing
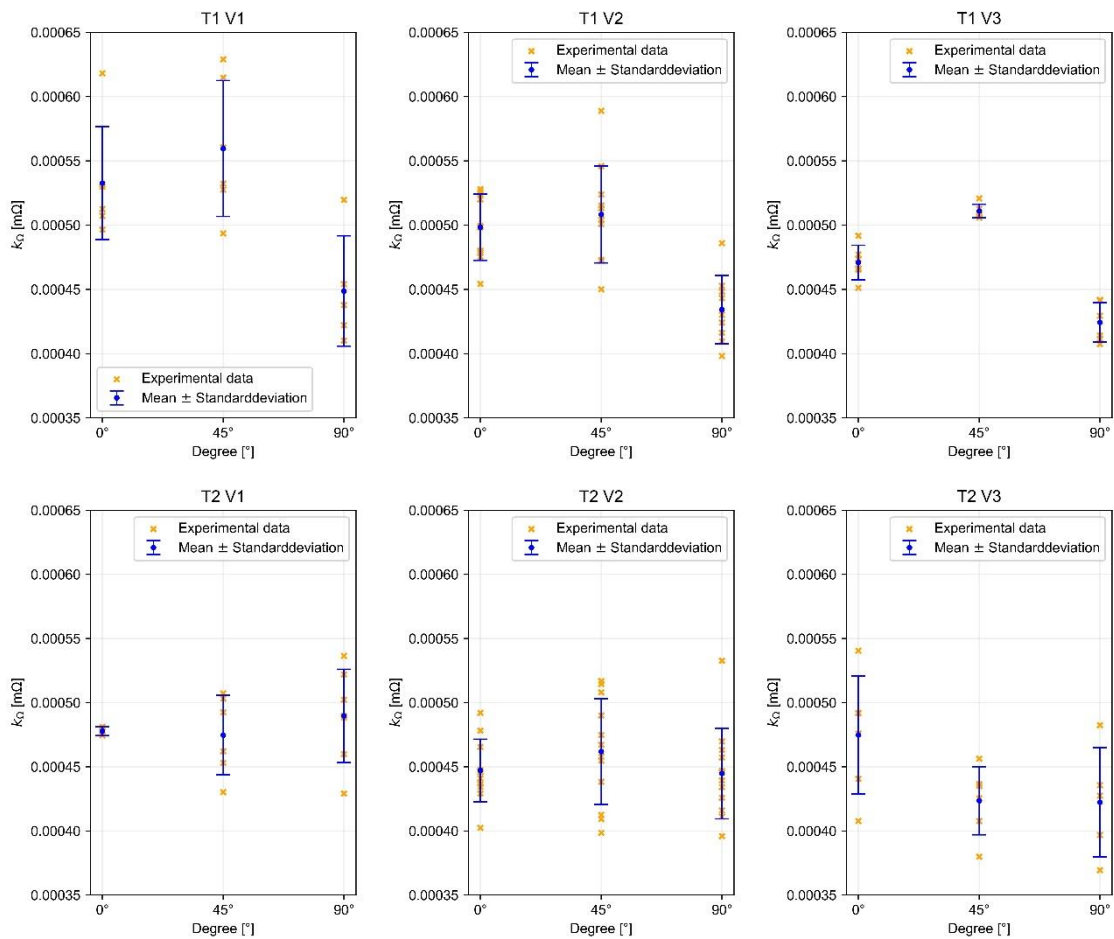
Figure 6: Comparison of k_Ω for different rolling schedules, friction conditions and extraction directions

This evaluation revealed a high linearity of the slope of the electrical resistance with the mechanical strain of the specimen until rupture. For a T1 condition, it is noticeable that the slope of the electrical resistance tends to be higher for the 45° specimens than for 0°, regardless of the rolling schedule, and this in turn is higher than for 90°. This indicates an indirect proportionality to the strength values.

If the lubricant is excluded, it is impossible to deduce any pattern. This would suggest an undefinable thermal condition, which, due to the higher heat dissipation, would imply different retention times for the diffusion of dislocations in the sense of recovery (healing of dislocations and formation of a substructure) depending on the rolling schedule.

In addition to the slope of the electrical resistance, the initial state d_Ω of the electrical resistance at the start of the tensile test was additionally analyzed and visualized in Figure 7. According to the Matthiessen rule, this would imply a measurement of the initial microstructure under the same material conditions, each with the same lubrication and stitch plan constraints. Due to the anisotropy of the rolled sheet, the comparison of the three different directions here indicates the accumulated resistance of theoretical (residual) resistance with that caused by dislocation density and grain boundaries.
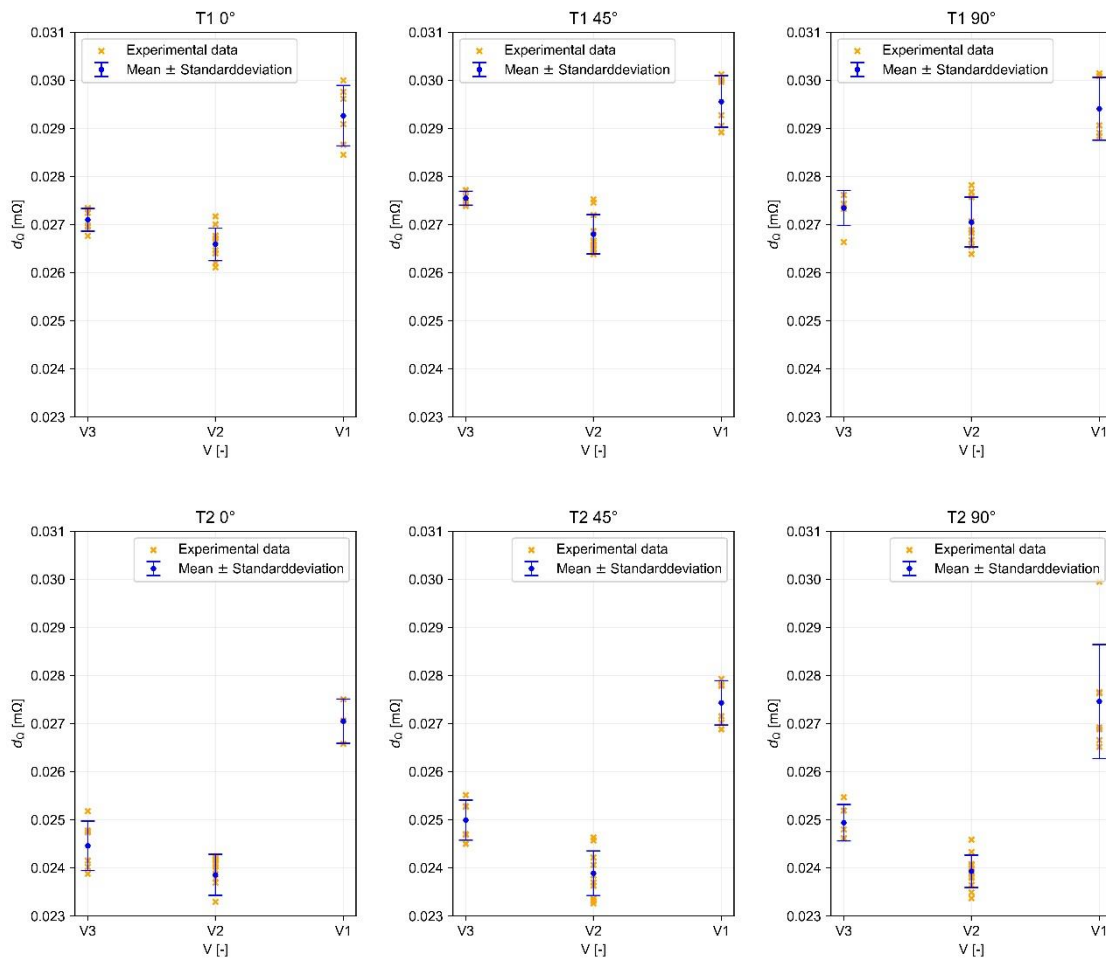
Figure 7: Comparison of d_Ω for different rolling schedules, friction conditions and extraction directions

Here the effects of the different rolling schedules and lubrication conditions are clearly visible. Under both conditions, T1 and T2, the V1 rolling schedule exhibits a significantly higher initial electrical resistance in all directions. In this regard, the rolling schedule V3 has the lowest initial resistance, although it is relatively close to V2. These conditions are largely unaffected by the tested directions. In contrast, the absolute values of the T1 condition are always higher than those of the T2 condition.

That suggests that it is essentially the introduced dislocation density which act as obstacles to electron movement. Since the V1 state assumes a considerably higher value, this will be due to the "hard" rolling plan and the associated high work hardening, in other words high stored

dislocation density. Accordingly, the V2 rolling schedule should be in a higher range than V3, but since V3 requires more passes to generate the same sheet thickness, the higher dislocation density may be a consequence of the number of passes. Due to the fact that the values of the initial electrical resistivity do not vary statistically for the tested orientations, it is obvious that the influence of the scattering of electrons at the grain boundaries has to be estimated as rather small.

The influence of lubrication conditions here will be due to heat generation or deviation. In the case of an unlubricated condition, the forming by rolling occurs apparently by solid state friction. This leads to a higher heat development in the material. In addition, the heat dissipation introduced by the forming energy is first dissipated along the material itself instead of to the gaseous ambient air. As a result, more energy is stored in the material in the form of heat, and thus the diffusion-controlled softening mechanisms, such as recovery, occur primarily.

On the other hand, the energy dissipation acting due to the application of a lubricating film is absorbed by the film itself, resulting in the cooling of the sheet and thus minimizes the driving force for dislocation annihilation and subgrain formation. Therefore, in this state, the dislocation density introduced is comparatively maintained and therefore results in a higher initial electrical resistance.

This is a significant parameter with a good correlation to the different pass schedules, directions and lubrication conditions. In addition, this variable is relatively easy to measure in-situ during rolling and to assign to the other mechanical values.

Therefore, this measured quantity (the electrical resistivity) as a function of the pass schedule, the spatial directions and the lubrication condition corresponds to a measured quantity that can preferably be processed in a black box model.

Another variable that can be generated from the values obtained is the strain hardening exponent n. This is a criterion for the stretch formability of a sheet and therefore an essential variable for the further processability of the sheet.

The n- value is a measure of the rate at which a material hardens when it is deformed plastically, such as during rolling or bending. It is a dimensionless value that characterizes the relationship between the true stress and true strain during plastic deformation.

It can be calculated from the stress-strain curve of a material during plastic deformation using the following equation:

$$n = d(\log(\sigma))/d(\log(\varepsilon))$$

(4)

where σ represents the true stress and ε is the true strain.

The value of the strain hardening exponent can provide information about the mechanical properties of the material, such as its ductility and work hardening behavior and are represented in Figure 8.
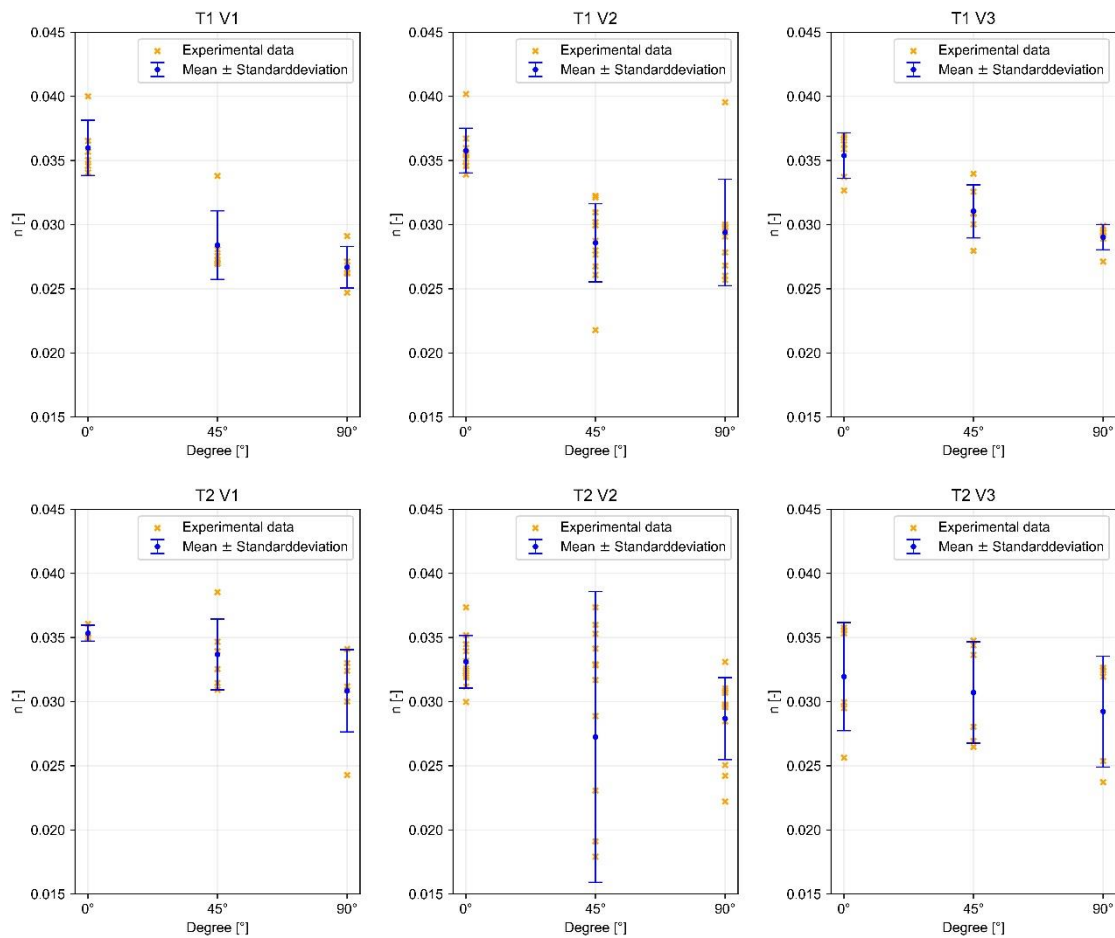
Figure 8: Comparison of n for different rolling schedules, friction conditions and extraction directions

Despite aluminum being a fairly isotropic material, any significant expression of anisotropy is not anticipated. A decreasing tendency of the n-values from 0° to 90° can be observed for the T1 condition for all rolling schedules.

The decrease of the n-value can be explained by the elongated grain structure of the rolled sheets, creating a preferred crystallographic orientation. This orientation leads to higher dislocation density and more pronounced dislocation interactions, such as pile-ups and cell formation in the rolling direction compared to the transverse direction, resulting in greater strain hardening.

In the T2 state, this phenomenon is also present, but the values are scattered, especially in V2 at 45°.

Furthermore, during selected tensile tests, the temperature development was additionally measured using Pt1000 temperature sensors on the specimen. The results of the temperature rise during deformation (the slope) is represented in Figure 9.

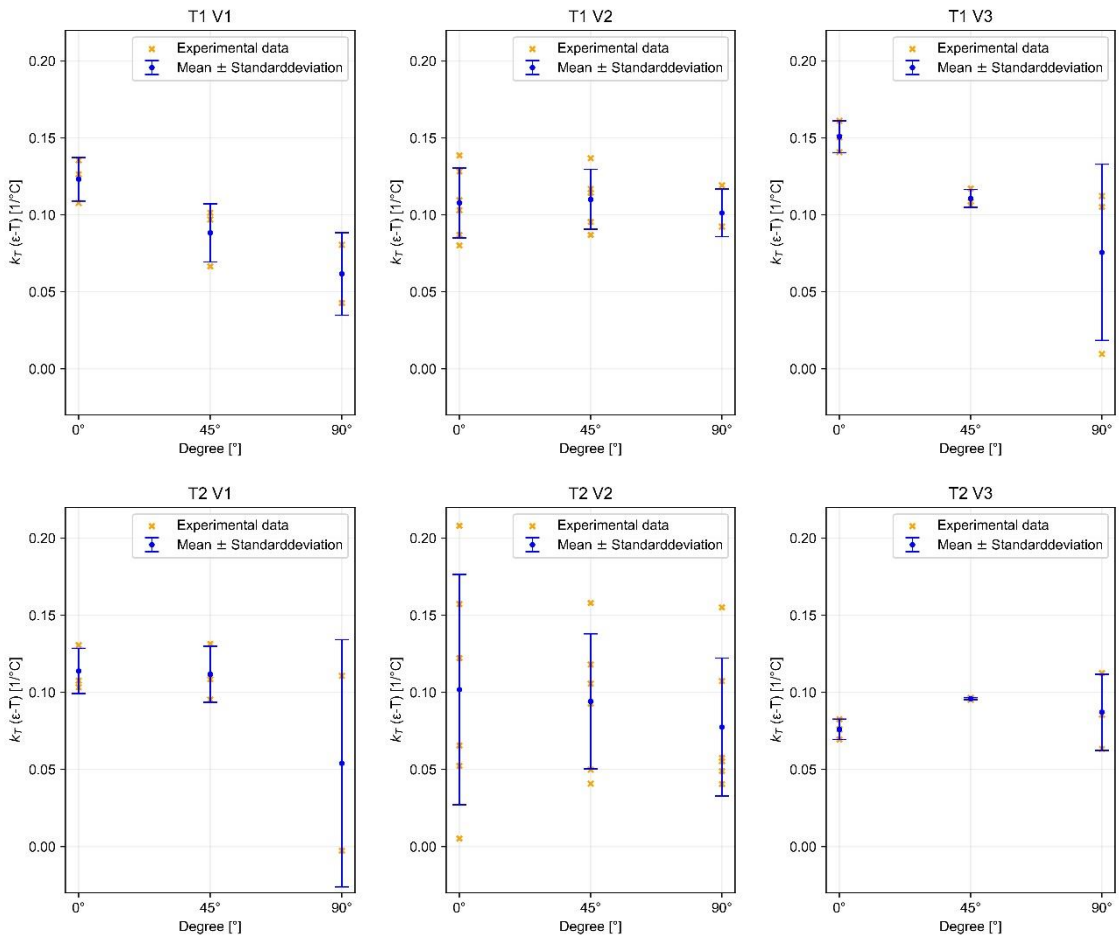*Figure 9: Comparison of the slope of temperature versus the slope of the elongation for different rolling schedules, friction conditions and extraction directions*
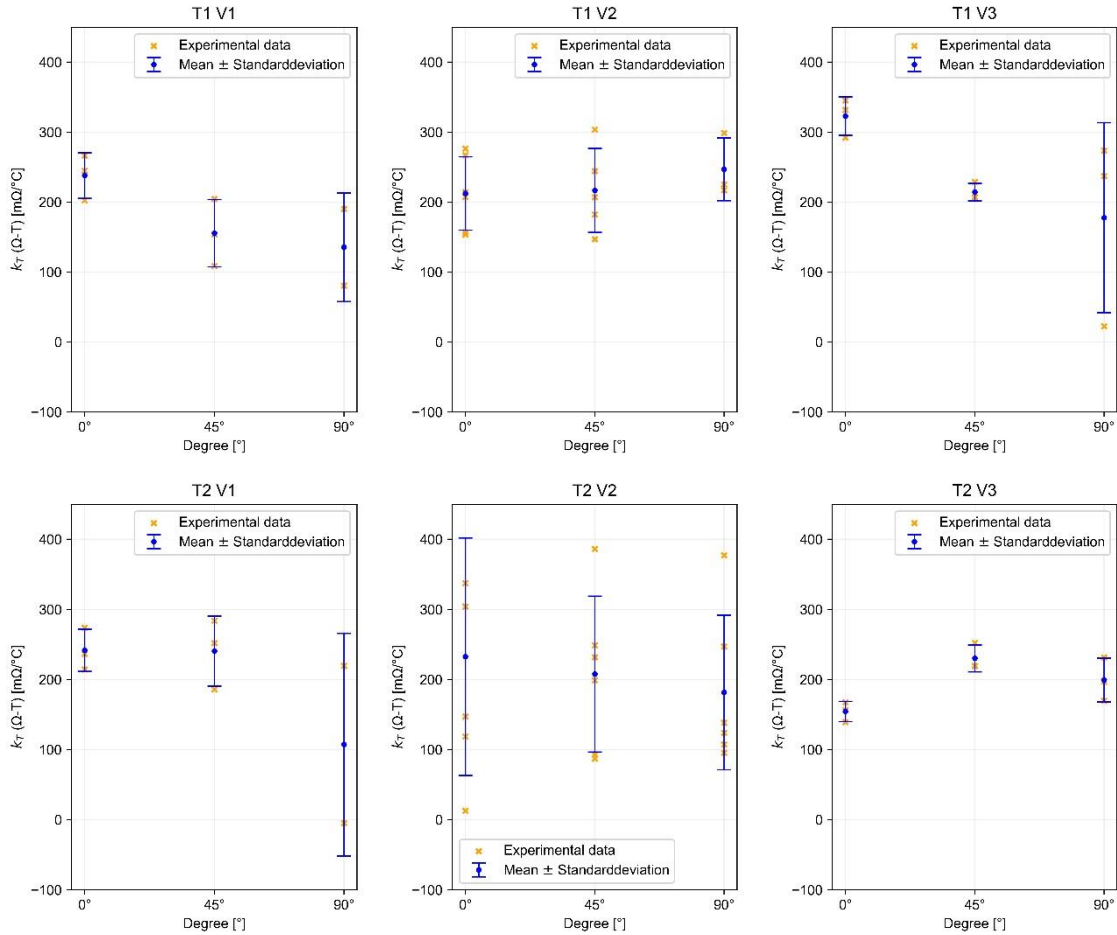
Figure 10: Comparison of the slope of temperature versus the slope of the electrical resistivity for different rolling schedules, friction conditions and extraction directions

A decreasing tendency from 0° to 90° can be found for both assignments of the temperature gradient for the T1 condition. This cannot be found for the T2 condition.

Table 3 contains the evaluated results of the measurements performed. For the studied slopes, the intersection with the y-axis was furthermore evaluated but were not described due to the lack of significance.

Table 3: Results of the tensile tests and electrical resistivity measurements

T	V	sheet no.	Grad	YS	e_u	UTS	e_{break}	n	d_n	k_Ω	d_Ω	k_T	d_T
T1	V1	73	0°	122.756 ±8.5	2.259 ±0.05	165.744 ±1.556	11.146 ±2.276	0.0369 ±0.0027	5.2771 ±0.0052	0.000549 ±0.000063	0.02874 ±0.00032		
T1	V1	73	45°	118.733 ±2.452	2.037 ±0.033	161.1 ±0.286	8.685 ±2.154	0.0294 ±0.0038	5.2098 ±0.0219	0.00054 ±0.000018	0.02908 ±0.00018		
T1	V1	73	90°	130.08 ±2.474	2.015 ±0.042	172.474 ±0.867	9.231 ±0.291	0.0272 ±0.0017	5.2746 ±0.0053	0.000434 ±0.000022	0.02894 ±0.00011		
T1	V1	76	0°	125.84 ±1.305	2.18 ±0.063	164.772 ±1.425	8.807 ±4.077	0.03506 ±0.0013	5.26422 ±0.00383	0.000517 ±0.000012	0.02979 ±0.00019	0.12324 ±0.01419	23.47392 ±0.04528
T1	V1	76	45°	129.913 ±2.347	1.987 ±0.086	167.548 ±4.3	10.104 ±0.69	0.02737 ±0.0006	5.24604 ±0.02461	0.000579 ±0.000074	0.03003 ±0.00008	0.08832 ±0.01892	23.60461 ±0.11557
T1	V1	76	90°	131.528 ±2.046	1.993 ±0.066	170.084 ±1.987	10.067 ±0.352	0.02591 ±0.00171	5.25589 ±0.0189	0.000471 ±0.000069	0.03012 ±0.00004	0.06169 ±0.02675	23.71194 ±0.26287
T1	V2	1	45°	116.668 ±1.859	1.995 ±0.035	160.394 ±0.851	9.541 ±3.991	0.0286 ±0.0014	5.2074 ±0.0106	0.000496 ±0.000022	0.02655 ±0.00008		
T1	V2	1	90°	120.158 ±4.442	2.068 ±0.222	165.741 ±3.596	9.019 ±3.898	0.0289 ±0.001	5.2424 ±0.0193	0.000455 ±0.000028	0.02682 ±0.00026		
T1	V2	4	0°	116.555 ±1.442	2.224 ±0.06	165.071 ±1.155	10.105 ±5.332	0.0361 ±0.0006	5.2701 ±0.0097	0.000478 ±0.000023	0.02643 ±0.00033		

T1	V2	4	45°	115.377 ±1.069	2.033 ±0.044	160.48 ±0.666	12.323 ±1.018	0.0299 ±0.0011	5.2112 ±0.0057	0.000507 ±0.000005	0.02648 ±0.00009		
T1	V2	4	90°	125.304 ±1.59	2.134 ±0.047	170.591 ±1.109	9.947 ±4.065	0.0331 ±0.0056	5.2898 ±0.0322	0.000437 ±0.000019	0.02665 ±0.00025		
T1	V2	5	0°	118.56 ±1.089	2.259 ±0.03	165.89 ±1.281	16.247 ±2.485	0.03679 ±0.00298	5.2763 ±0.01297	0.000508 ±0.000029	0.02651 ±0.00013	0.09993 ±0.01156	22.52516 ±0.23065
T1	V2	5	45°	114.599 ±0.438	2.097 ±0.142	160.963 ±0.365	13.652 ±1.215	0.03218 ±0.00008	5.22533 ±0.00234	0.000509 ±0.000052	0.02677 ±0.00014	0.11562 ±0.00177	22.55969 ±0.01289
T1	V2	6	0°	121.46 ±1.488	2.229 ±0.136	165.529 ±1.603	10.382 ±4.04	0.03465 ±0.00079	5.26681 ±0.01307	0.000499 ±0.000021	0.02696 ±0.00023	0.11575 ±0.03121	23.03741 ±0.11506
T1	V2	6	45°	124.343 ±1.2	1.978 ±0.075	164.651 ±1.137	10.499 ±0.688	0.02487 ±0.0027	5.21648 ±0.01062	0.000521 ±0.000069	0.02739 ±0.00017	0.10648 ±0.02662	23.05508 ±0.08117
T1	V2	6	90°	133.778 ±2.46	1.973 ±0.086	172.542 ±2.638	10.545 ±0.356	0.02618 ±0.00058	5.27132 ±0.01306	0.000411 ±0.000013	0.02769 ±0.00012	0.10135 ±0.01551	23.11543 ±0.02132
T1	V3	16	0°	117.957 ±1.795	2.332 ±0.041	164.276 ±1.205	8.049 ±1.56	0.0367 ±0.0004	5.2674 ±0.0081	0.000477 ±0.000013	0.02703 ±0.00029		
T1	V3	16	45°	115.159 ±0.976	2.032 ±0.038	159.385 ±0.272	11.23 ±0.59	0.0296 ±0.0015	5.2047 ±0.0077	0.000508 ±0.000002	0.02743 ±0.00004		
T1	V3	16	90°	125.273 ±6.529	2.057 ±0.035	169.276 ±3.89	10.311 ±0.522	0.0285 ±0.0012	5.2619 ±0.0212	0.000422 ±0.000016	0.02714 ±0.00043		
T1	V3	17	0°	127.805 ±0.756	2.098 ±0.04	166.884 ±0.907	4.369 ±0.243	0.0341 ±0.00165	5.2734 ±0.01228	0.000465 ±0.000013	0.02717 ±0.0002	0.15081 ±0.01025	23.12813 ±0.06533
T1	V3	17	45°	120.277 ±3.027	2.054 ±0.033	161.23 ±2.238	14.376 ±0.973	0.03248 ±0.00153	5.22889 ±0.01833	0.000514 ±0.000006	0.02767 ±0.00007	0.11076 ±0.00576	23.29566 ±0.02459
T1	V3	17	90°	130.275 ±2.368	2.065 ±0.099	167.314 ±1.77	12.421 ±0.531	0.02959 ±0.00028	5.25433 ±0.01225	0.000426 ±0.000017	0.02755 ±0.00011	0.07569 ±0.05727	23.48934 ±0.1827
T2	V1	73	0°	121.274 ±0.411	2.147 ±0.199	162.647 ±0.839	8.74 ±6.402	0.0354 ±0.0025	5.22648 ±0.0215	0.000507 ±0.000042	0.02662 ±0.00006		
T2	V1	73	45°	114.998 ±2.633	2.09 ±0.041	157.455 ±0.775	13.017 ±0.71	0.0353 ±0.003	5.2116 ±0.0147	0.000475 ±0.000039	0.02702 ±0.00014		
T2	V1	73	90°	123.719 ±3.704	2.167 ±0.175	167.082 ±2.046	9.02 ±4.894	0.0324 ±0.0021	5.2623 ±0.0153	0.000479 ±0.000017	0.02678 ±0.00022		
T2	V1	76	0°	127.651 ±3.128	2.22 ±0.061	161.407 ±1.091	13.31 ±1.754	0.03497 ±0.00005	5.24176 ±0.00737	0.00047 ±0.000015	0.0275 ±0.00043	0.11389 ±0.01467	23.56116 ±0.06334
T2	V1	76	45°	124.273 ±0.825	1.934 ±0.12	156.208 ±0.763	7.155 ±4.358	0.03211 ±0.00161	5.19447 ±0.01102	0.000466 ±0.000039	0.02852 ±0.00124	0.11177 ±0.01825	23.57839 ±0.10764
T2	V1	76	90°	125.267 ±6.015	2.066 ±0.199	163.996 ±1.661	10.306 ±0.394	0.02774 ±0.00488	5.22481 ±0.03115	0.000512 ±0.000014	0.02764 ±0.00002	0.05407 ±0.08013	23.71509 ±0.26905
T2	V2	1	0°	126.005 ±8.479	2.228 ±0.093	170.937 ±13.35	11.669 ±1.508	0.0353 ±0.003	5.2968 ±0.0919	0.000512 ±0.000029	0.02333 ±0.00005		
T2	V2	1	45°	111.468 ±2.227	2.11 ±0.067	157.328 ±2.025	9.03 ±4.507	0.0307 ±0.0072	5.192 ±0.0445	0.000475 ±0.000041	0.02386 ±0.00017		
T2	V2	1	90°	116.273 ±3.541	1.996 ±0.204	164.298 ±2.111	8.048 ±4.322	0.0304 ±0.0008	5.2375 ±0.0156	0.000421 ±0.000042	0.02405 ±0.00005		
T2	V2	4	0°	117.501 ±1.563	2.092 ±0.006	162.138 ±1.308	3.804 ±0.573	0.0341 ±0.0013	5.2414 ±0.0107	0.000455 ±0.0002	0.02389 ±0.00025		
T2	V2	4	45°	111.72 ±3.617	2.01 ±0.059	156.663 ±1.458	10.97 ±0.286	0.022 ±0.006	5.1479 ±0.0362	0.000456 ±0.000048	0.02409 ±0.00021		
T2	V2	4	90°	118.767 ±4.291	2.024 ±0.164	166.943 ±0.368	3.37 ±0.947	0.0297 ±0.0042	5.2495 ±0.0209	0.000474 ±0.000036	0.02378 ±0.00037		
T2	V2	5	0°	127.441 ±2.427	1.947 ±0.175	165.078 ±0.805	6.384 ±4.524	0.03262 ±0.00115	5.25338 ±0.00186	0.000435 ±0.000032	0.02364 ±0.00066	0.16254 ±0.04312	22.69885 ±0.31484
T2	V2	5	45°	118.599 ±0.442	2.066 ±0.031	158.787 ±0.858	16.656 ±2.347	0.03514 ±0.00093	5.22279 ±0.00928	0.000462 ±0.000026	0.0234 ±0.0002	0.06113 ±0.02771	22.90844 ±0.12501
T2	V2	5	90°	130.329 ±0.657	1.853 ±0.085	167.602 ±0.487	3.25 ±0.447	0.03012 ±0.00063	5.25727 ±0.00273	0.000418 ±0.000008	0.02365 ±0.00017	0.08446 ±0.06181	23.09845 ±0.20782
T2	V2	6	0°	127.488 ±1.376	1.912 ±0.049	161.545 ±1.634	3.092 ±0.327	0.0312 ±0.00124	5.22647 ±0.01333	0.000439 ±0.000009	0.02404 ±0.00022	0.04113 ±0.03172	23.32313 ±0.05981
T2	V2	6	45°	117.132 ±1.395	1.944 ±0.059	155.835 ±1.702	8.69 ±4.513	0.02119 ±0.02024	5.14514 ±0.09692	0.000444 ±0.000031	0.02447 ±0.00022	0.12728 ±0.02734	23.13613 ±0.09921
T2	V2	6	90°	133.547 ±3.024	1.837 ±0.129	166.666 ±2.575	2.741 ±0.221	0.02497 ±0.0032	5.22877 ±0.01448	0.000446 ±0.000012	0.02433 ±0.00025	0.07059 ±0.03201	23.31055 ±0.02981
T2	V3	16	0°	117.873 ±1.552	2.185 ±0.123	160.004 ±0.749	8.582 ±6.942	0.0356 ±0.0002	5.2344 ±0.0037	0.000463 ±0.000069	0.02402 ±0.00013		
T2	V3	16	45°	113.775 ±3.143	2.11 ±0.078	156.497 ±1.982	13.937 ±1.142	0.0343 ±0.0006	5.2042 ±0.0157	0.00043 ±0.000025	0.02463 ±0.00011		
T2	V3	16	90°	119.768 ±6.985	2.063 ±0.094	162.518 ±5.941	6.542 ±5.369	0.0316 ±0.0017	5.2308 ±0.044	0.000412 ±0.000022	0.02462 ±0.00001		
T2	V3	17	0°	127.17 ±1.669	2.031 ±0.027	159.484 ±0.743	10.587 ±1.144	0.02836 ±0.00237	5.20006 ±0.01083	0.000487 ±0.000009	0.0249 ±0.00024	0.07601 ±0.0066	23.42917 ±0.04648

| T2 | V3 | 17 | 45° | 122.467 ±2.168 | 1.896 ±0.135 | 155.573 ±1.36 | 9.89 ±4.052 | 0.02715 ±0.00081 | 5.16927 ±0.00653 | 0.000417 ±0.000032 | 0.02536 ±0.0014 | 0.09599 ±0.00066 | 23.43488 ±0.04279 |
| T2 | V3 | 17 | 90° | 127.938 ±3.431 | 1.856 ±0.174 | 162.603 ±3.713 | 5.374 ±4.67 | 0.02701 ±0.00436 | 5.21347 ±0.04023 | 0.000429 ±0.000057 | 0.02515 ±0.00034 | 0.08714 ±0.02462 | 23.42916 ±0.06495 |

Table 4 represents the corresponding R^2-values. This is is a statistical measure that represents the proportion of the variance in the dependent variable that is predictable from the independent variables. Therfore, R^2 indicates how well the data fits the regression model.

The R^2 values close to 0.9 or higher suggests that the regression model is a good fit for the data with high linearity.

Table 4: R²-values for the values listed

	n	ε_Ω	ε_T	Ω-T
Median	0.89494473	0.99865798	0.98398966	0.9736543
Mean	0.86378637	0.99746125	0.9494969	0.93920646

Microstructural Characterization

In addition to the data evaluation, metallographic investigations were further carried out to visualize the microstructure of individual tensile tests. For this purpose, specimens were prepared and treated with the Barker etching method in order to visualize the colored grain orientation. Figure 11 shows an example of the results. Here it can be seen that it is difficult to evaluate grain sizes or elongations by means of optical microscopy, which complicates data collection via microstructural evaluation. Furthermore, no clear differences in microstructure between sampling directions, stitch schedules, or lubrication conditions are apparent. However, the rolling-induced grain elongation is clearly evident for all specimens, which is why a clear anisotropy can also be concluded for this reason.
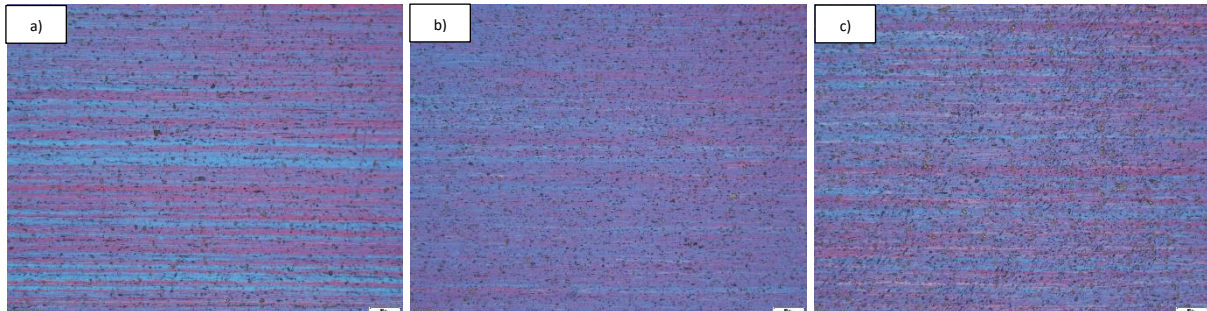

Figure 11: Exemplary representation of the microstructure in the optical microscope of a) T1 V1 0° b) T2 V2 45° and c) T1 V3 90°

To get a better insight into the underlying microstructure in a higher resolution, EBSD measurements would be necessary, which are rarely used for quality control and are more likely to be utilzed for research, especially since this kind of measurement is very laborious and time consuming. For this reason, a simple black box model approach is more suitable than a white box approach for the practical implementation of quality assurance in a metal processing facility.

Transition to practical application

By practically applying the relationship between the mechanical properties and the electrical resistance, the ML algorithm elaborated in [25] was enhanced by a subsequent quality control step without changing the basic principle. In summary, the rolling mill from 1954 in the Smart

Forming Lab of the Chair of Metal Forming at the Montanuniversitaet Leoben was upgraded to I 4.0 standard using a retrofitting approach, also implementing a supervised data-driven ML algorithm to generate rolling schedules, based on the roll gap diagram (Figure 12). The rolling gap diagram visualizes the relationship of the initial rolling gap s_0, initial material thickness h_0, the exit material height h_1, and rolling force F_R. Due to the occurring rolling force, the rolling mill is object to elastic deformation, accounted for by the roll stand modulus C, representing the slope of the roll stands characteristic curve. The intersection point of the roll stands characteristic curve and materials characteristic curve, is referred to as working point A and provides information of the maximum rolling force and h_1.
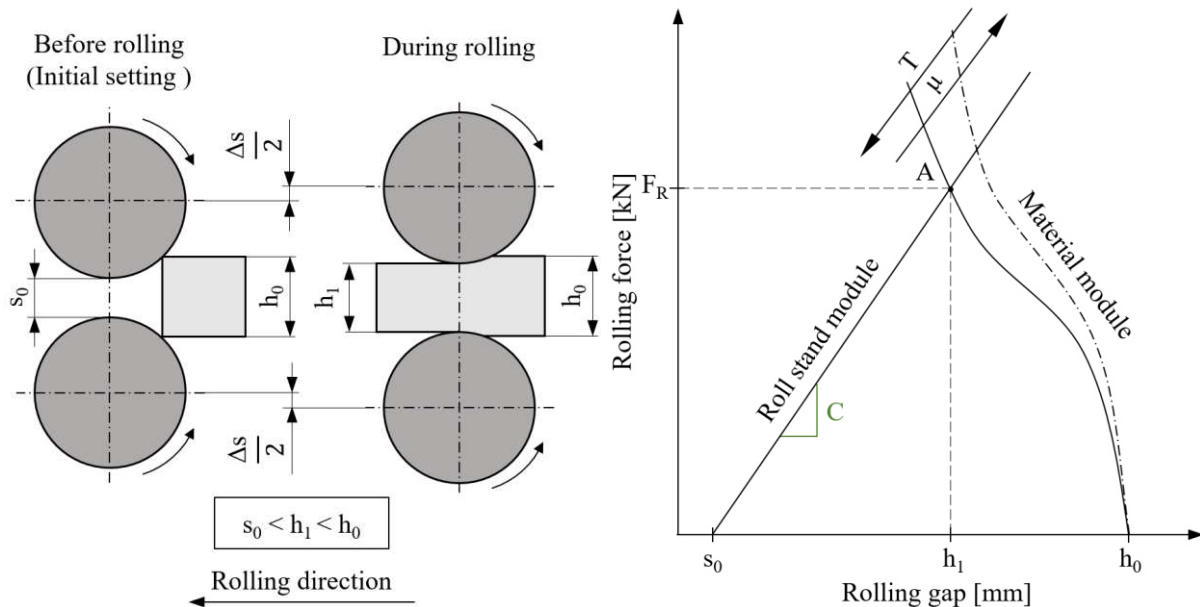

Figure 12: Rolling principle (left) and rolling gap diagram for rolling (right) [25]

Based on this principle, the initial ML algorithm was extended to generate a rolling schedule, also taking an additional input of desired mechanical properties into account. In the initial approach, the ML algorithm is given a h_0, h_1, F_R and with material width B of a specific material, also choosing the option of lubricant or no lubricant. Given h_0 and F_R, the algorithm performs interpolations using linear weighting functions between the experimentally generated data to evaluate A, resulting in a new h_1 for a specific rolling step. In the subsequent rolling step, the new h_1 is used as the new h_0, which is performed in an iterative process until the condition of the user-defined h_1 is reached, and thus obtaining a complete rolling schedule as shown in Figure 13. The performed experiments, data analysis and extension of the dataset enables the modification the algorithm to define desired mechanical properties for the rolled material. Additionally to the target value of h_1, YS, UTS and the relationship with d_Ω is applied to extend to obtain a suitable rolling schedule. After generating a rolling schedule, the experimental data is checked for d_Ω and the corresponding YS and UTS. If these values reside within a defined residual, the rolling schedule is considered valid, otherwise, another rolling schedule is generated. Here, a distinction between two cases is made. First, if d_Ω is too high, the strain hardening is assumed to be too high and a rolling schedule with a lower F_R is generated, consequently leading more rolling steps with a decreased h_1 for each individual rolling step. Second, if d_Ω is too low, the strain hardening is assumed to be too low and a rolling schedule with a higher F_R is generated, consequently leading to less rolling steps with an increased h_1 of each individual rolling step. In both cases, the interval bisection method is applied to the rolling force, resulting in a shift of A. Here, if d_Ω is too low, the interval bisection method is applied between the defined F_R and the maximum possible rolling force of 300 kN. For too high d_Ω, the

interval bisection method is applied between the defined F_R and 10-3 kN (or 0 kN) is applied, restarting with step 2. This process is iterated until the target values within the defined residuals are met and a valid rolling schedule is generated in step 7.

The user can enter the desired parameters for the rolling process as well as for the desired mechanical parameters through a user-friendly GUI and start the back-end ML algorithm at the push of a button (Figure 14). A successfully generated rolling schedule is displayed on the right side of the GUI and contains all the information necessary for the input parameter specific rolling schedule. If after some iterative steps no solution is found to achieve the mechanical properties, a message is displayed on the GUI informing the user that these cannot be achieved. This in-situ quality control solution also significantly supports and improves the decision-making process on the shop floor, resulting in less effort for necessary material testing and less waste, thus increasing sustainability.

1. Import of refined data

Import of refined data T_1 (with lubricant) and T_2 (without lubricant) from the database containing { Specimen nr. | V_i | B_i | $F_{R\,i}$ | $h_{1\,i}$ | $s_{0\,i}$ | UTS_i | YS_i | $e_{u\,i}$ | n_i | $d_{\Omega\,i}$ }

2. Linear Regression

Stand

For every specimen n:
$$F(s) = a_{s\,n} \bullet s + b_{s\,n}$$

$$a_{s\,n} = \frac{F_R}{h_1 - s_0}$$

$$b_{s\,n} = -a_{s\,n} \bullet s_0$$

For each s_0 of every B:
$$a_{s\,median} \mid b_{s\,median}$$

Material

For every specimen n:
$$F(h) = a_{m\,n} \bullet h + b_{m\,n}$$

$$a_{m\,n} = \frac{F_R}{h_1 - h_0}$$

$$b_{m\,n} = -a_{m\,n} \bullet h_0$$

For each s_0 of every B:
$$a_{m\,median} \mid b_{m\,median}$$

3. Extrapolation of B

Stand
Linear Regression of $a_{s\,median}$ and $b_{s\,median}$ for 400mm > B1 and B5 > 10mm to obtain $B_{ex\,(i)}$ > B_1 and $B_{ex\,(i+1)}$, < B_5

Material
Linear Regression of $a_{m\,median}$, $b_{m\,median}$ and h_0 for 400mm > B1 and B5 > 10mm to obtain $B_{ex\,(i)}$ > B_1 and $B_{ex\,(i+1)}$, < B_5

4. Interpolation of demanded b

Stand — **Material**

Calculation of weighting factor α between nearest neighbours of given widths B_i
$$\alpha = \frac{b - B_i}{B_{i+1} - B_i} \qquad B_{i+1} \geq b \geq B_i$$

Interpolation of slope a_s, intercept b_s with weighting factor α for every s_0:
$$a_s = a_{s\,i+1} + \alpha \bullet (a_{s\,i} - a_{s\,i+1})$$
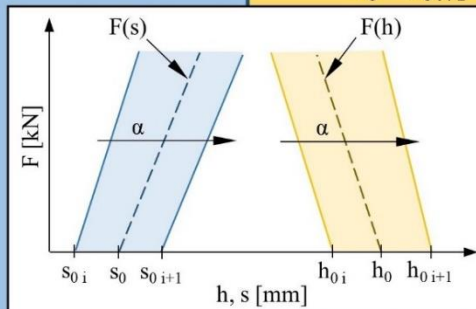$$b_s = b_{s\,i+1} + \alpha \bullet (b_{s\,i} - b_{s\,i+1})$$

Interpolation of slope a_m, intercept b_m and resulting h_0 with weighting factor α for every s_0:
$$a_m = a_{m\,i+1} + \alpha \bullet (a_{m\,i} - a_{m\,i+1})$$
$$b_m = b_{m\,i+1} + \alpha \bullet (b_{m\,i} - b_{m\,i+1})$$
$$h_0 = h_{0\,i+1} + \alpha \bullet (h_{0\,i} - h_{0\,i+1})$$

$$F(s) = a_s \bullet s + b_s$$

$$F(h) = a_m \bullet h + b_m$$

5. Extrapolation of s_0

Stand

Extrapolation of $a_{s\,max}$ for 20.0mm > $s_{0\,ex}$ > $s_{0\,max}$
Extrapolation of $a_{s\,min}$ for $s_{0\,min}$ > $s_{0\,ex}$ < 0.1mm

$s_{0\,max}$ = maximum s_0 obtained from data (5.0mm)
$s_{0\,min}$ = minimum s_0 obtained from data (0.5mm)

For $s_{0\,min}$ > $s_{0\,ex}$ < 0.1mm : $a_{s\,ex} = a_{s\,min}$
For 20.0mm > $s_{0\,ex}$ > $s_{0\,max}$: $a_{s\,ex} = a_{s\,max}$

Calculation of $b_{s\,ex}$ for corresponding $a_{s\,ex}$:
$$b_{s\,ex} = -a_{s\,ex} \bullet s_{0\,ex}$$

6. Extrapolation of h_0

Material

Extrapolation of $h_0(s_{0\,ex})$ with linear regression for $s > s_{0\,max}$ and $s < s_{0\,min}$

Calculation of $b_{m\,ex}$ for corresponding $a_{m\,ex}$:
$$b_{m\,ex} = -a_{m\,ex} \cdot h_{0\,ex}$$

F [kN]

$a_{m\,min}$ $a_{m\,max}$

$h_{0\,min}$ $h_{0\,max}$ h [mm]

7. Interpolation of h_0 and rolling schedule iterator

Stand

Auxiliary variable γ ($0 \leq \gamma \leq 1$; $stepsize\ 5E-4$)
$$a_{s\,j} = a_{s\,i+1} + \gamma \cdot (a_{s\,i} - a_{s\,i+1})$$
$$b_{s\,j} = b_{s\,i+1} + \gamma \cdot (b_{s\,i} - b_{s\,i+1})$$

Calculation of roll gap height $s_{0\,j}$ height for step j:
$$s_{0\,j} = \frac{a_{s\,j} \cdot h_{1\,j} - F_R}{b_{s\,j}}$$

Material

Calculation of weighting factor β between nearest neighbours of h_0
$$\beta = \frac{h_0 - h_{0\,i}}{h_{0\,i+1} - h_{0\,i}} \qquad h_{0\,i+1} \geq h_0 \geq h_{0\,i}$$
$$a_{m\,j} = a_{m\,i+1} + \beta \cdot (a_{m\,i} - a_{m\,i+1})$$
$$b_{m\,j} = b_{m\,i+1} + \beta \cdot (b_{m\,i} - b_{m\,i+1})$$

Calculation of exit height $h_{1\,j}$ for step j:
$$h_{1\,j} = \frac{F_R - b_{m\,j}}{a_{m\,j}} = h_{0\,j+1}$$

F [kN], F_R

$s_{0\,j+3}$ $h_{1\,j+3} = h_{1\,end}$ $s_{0\,j+2}$ $h_{1\,j+2} = h_{0\,j+3}$ $s_{0\,j+1}$ $h_{1\,j+1} = h_{0\,j+2}$ $s_{0\,j}$ $h_{1\,j} = h_{0\,j+1}$ $h_{0\,j} = h_0$

h, s [mm]

8. Checking of target values

$d_\Omega \geq d_{\Omega\,target} + d_{\Omega\,residual}$ d_Ω $d_\Omega \leq d_{\Omega\,target} - d_{\Omega\,residual}$

Interval bisection method applied to rolling force for iteration k

F_{max}, F [kN], $F_{R\,k}$, $F_{R\,new}$, 0, h, s [mm]

$$d_{\Omega\,target} - d_{\Omega\,residual} \leq d_\Omega \leq d_{\Omega\,target} + d_{\Omega\,residual}$$

Rolling schedule valid for defined mechanical properties
UTS | YS | e_u | n

Interval bisection method applied to rolling force for iteration k

F_{max}, $F_{R\,new}$, F [kN], $F_{R\,k}$, 0, h, s [mm]

$F_R = F_{R\,new}$ Restart at step 2. Linear Regression $F_R = F_{R\,new}$

Figure 13: Modified ML algorithm
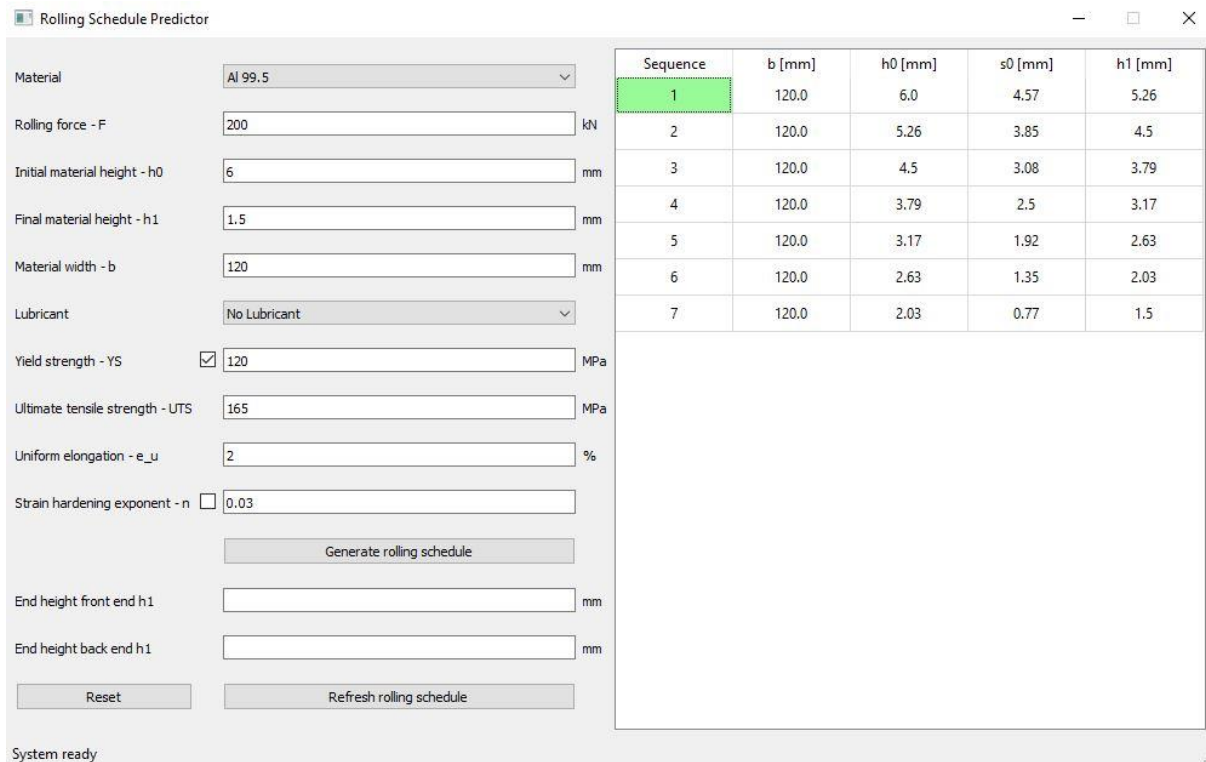
Figure 14: Corresponding GUI developed for the Rolling Mill Schedule Predictor

Sequence	b [mm]	h0 [mm]	s0 [mm]	h1 [mm]
1	120.0	6.0	4.57	5.26
2	120.0	5.26	3.85	4.5
3	120.0	4.5	3.08	3.79
4	120.0	3.79	2.5	3.17
5	120.0	3.17	1.92	2.63
6	120.0	2.63	1.35	2.03
7	120.0	2.03	0.77	1.5

Implementation of the approach in a rolling process

Using the data generation presented in this study, it should be possible in future to use this setup for in-situ measurement of mechanical properties via correlation with electrical resistance. For this purpose, the initial resistance after a rolling pass can be taken as shown in Figure 15 and the properties can be predicted via the ML algorithm. In order to optimize the data situation or to transfer this method to other materials and rolling schedules, the four-point method can be transferred aliquot to a tensile testing machine and the correlation of the mechanical properties with the electrical resistance can be extended.
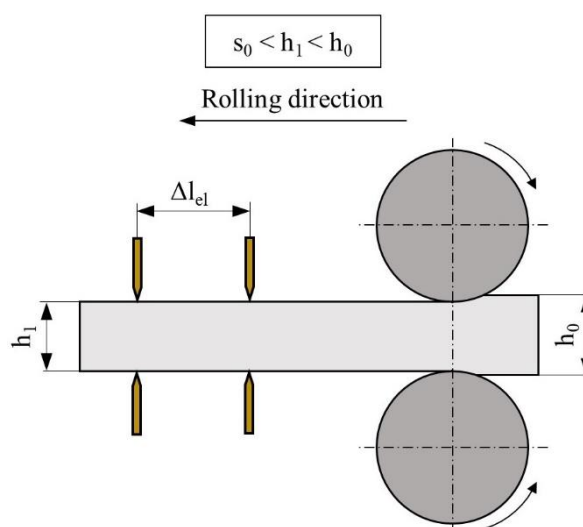
Figure 15: Schematic representation of the in-situ measurement of electrical resistance on a rolling mill aggregate

Discussion and Outlook

In this study, a data-driven black box model approach for correlating mechanical properties of aluminum sheets to measured electrical resistivity was presented. This model was created on the basis of a large number of experiments and does not capture real-physics background. Nevertheless, such an approach is often a better alternative to complex white box model approaches like FEA with integrated microstructural model, requiring an enormous knowledge about the material and its behavior. This ML algorithm can contribute to creating optimal rolling schedules for metals and predicting the mechanical properties. By implementing the measurement setup in the rolling line, the correlation of the electrical resistance with the mechanical properties can be used to control the quality in-situ, thus contributing to a reduction of scrap and a more sustainable production of semi-finished products. This approach is becoming increasingly important in a digitized environment, as it can provide fast, reliable predictions without the need for extensive research into material behavior characterization. The ability to capture, store and process huge amounts of data holds enormous potential even for small and medium-sized companies that do not have access to expensive equipment for materials characterization and quality control. The possibility of setting the desired mechanical properties before the forming process using a simple user interface enables a reproducible result that can be achieved independently of the operator. Furthermore, this allows the prediction of the suitability for subsequent forming processes such as stretching or deep drawing.

Through further data collection, this model can likewise be optimized and thus lead to increased resilience. Furthermore, this approach can be extended to include more real physical relations, which improves the understanding of the behavior of the material during rolling, proposing a grey box modelling approach.

In order to be able to integrate white box data into a model, several factors must be taken into account which simultaneously contribute to changes in electrical resistance. When implementing this method in a hot rolling process, for example, the temperature would have to be monitored simultaneously by means of pyrometer measurement. As mentioned earlier, the forming energy, or the Taylor-Quinney coefficient, determines the energy that is introduced into the material during forming. This is decisive for various microstructural transformations in the material in the form of recovery or recrystallization. Since the occurrence of grain boundaries is regarded as an obstacle for the electrons, the amount of these also determines the defect resistance. If recrystallization is initiated, the number of grain boundaries would be reduced, which results in a reduction of the electrical resistance. In addition, the resistance is also influenced by impurities. For both purposes, it is necessary to inspect the material in advance. The amount of impurities can be determined by chemical or metallographic analysis. Phenomena such as recrystallization and recovery represent a labor- and cost-intensive metallographic analysis, which is why in-situ material testing methodologies should be used in this area likewise. For example, laser-ultrasonic testing represents such an analysis method. When coupled with a thermomechanical treatment simulator, it can be used to detect in-situ microstructural changes such as those mentioned above at high temperatures and under harsh environmental conditions using non-contact ultrasound technology. By determining those material parameters, a specific microstructure model can be created, and the manufacturing process including microstructure monitoring can be simulated using FEA. This approach is driven by the integration of these measurement systems in the aforementioned Smart Forming Lab, which pushes the digital transformation of different material characterization and forming

processes to CPPS and fully integrates them into the production network as proposed in [6,24–26,30].

Declaration of interests

The authors declare that they have no known competing financial interests or personal relationships that could have appeared to influence the work reported in this paper.

References

[1] Ralph BJ, Stockinger M. Digitalization and Digital Transformation in Metal Forming: Key Technologies, Challenges and Current Developments of Industry 4.0 Applications. Proceedings of the 39th Colloquium of Metal Forming, Zauchensee:13–23; 2020.

[2] Zhong RY, Xu X, Klotz E, Newman ST. Intelligent Manufacturing in the Context of Industry 4.0: A Review. Engineering 2017;3(5):616–30. https://doi.org/10.1016/J.ENG.2017.05.015.

[3] Wang S, Wan J, Zhang D, Di Li, Zhang C. Towards smart factory for industry 4.0: a self-organized multi-agent system with big data based feedback and coordination. Computer Networks 2016;101:158–68. https://doi.org/10.1016/j.comnet.2015.12.017.

[4] Hagenah H, Schulte R, Vogel M, Hermann J, Scharrer H, Lechner M et al. 4.0 in metal forming – questions and challenges. Procedia CIRP 2019;79:649–54. https://doi.org/10.1016/j.procir.2019.02.055.

[5] Zheng T, Ardolino M, Bacchetti A, Perona M. The applications of Industry 4.0 technologies in manufacturing context: a systematic literature review. International Journal of Production Research 2021;59(6):1922–54. https://doi.org/10.1080/00207543.2020.1824085.

[6] Ralph BJ, Woschank M, Miklautsch P, Kaiblinger A, Pacher C, Sorger M et al. MUL 4.0: Systematic Digitalization of a Value Chain from Raw Material to Recycling. Procedia Manufacturing 2021;55:335–42. https://doi.org/10.1016/j.promfg.2021.10.047.

[7] Prates P, Pereira A. Recent Advances and Applications of Machine Learning in Metal Forming Processes. Metals 2022;12(8):1342. https://doi.org/10.3390/met12081342.

[8] Ammar M, Haleem A, Javaid M, Walia R, Bahl S. Improving material quality management and manufacturing organizations system through Industry 4.0 technologies. Materials Today: Proceedings 2021;45:5089–96. https://doi.org/10.1016/j.matpr.2021.01.585.

[9] Straat M, Koster K, Goet N, Bunte K. An Industry 4.0 example: real-time quality control for steel-based mass production using Machine Learning on non-invasive sensor data. In: 2022 International Joint Conference on Neural Networks (IJCNN). IEEE; 7182022, p. 1–8.

[10] SINGH Y. ELECTRICAL RESISTIVITY MEASUREMENTS: A REVIEW. Int. J. Mod. Phys. Conf. Ser. 2013;22:745–56. https://doi.org/10.1142/S2010194513010970.

[11] Omari MA, Sevostianov I. Estimation of changes in the mechanical properties of stainless steel subjected to fatigue loading via electrical resistance monitoring. International Journal of Engineering Science 2013;65:40–8. https://doi.org/10.1016/j.ijengsci.2013.02.006.

[12] Starke P, Klein M, Eifler D. Resistivity – a characteristic fingerprint of fatigue induced changes in the microstructure of metallic materials. Procedia Engineering 2011;10:698–703. https://doi.org/10.1016/j.proeng.2011.04.116.

[13] Andrews PV, West MB, Robeson CR. The effect of grain boundaries on the electrical resistivity of polycrystalline copper and aluminium. Philosophical Magazine 1969;19(161):887–98. https://doi.org/10.1080/14786436908225855.

[14] Fickett FR. Aluminum—1. A review of resistive mechanisms in aluminum. Cryogenics 1971;11(5):349–67. https://doi.org/10.1016/0011-2275(71)90036-1.

[15] Hummel RE. Electronic Properties of Materials. New York, NY: Springer New York; 2011.

[16] Lieou CK, Bronkhorst CA. Thermomechanical conversion in metals: dislocation plasticity model evaluation of the Taylor-Quinney coefficient. Acta Materialia 2021;202:170–80. https://doi.org/10.1016/j.actamat.2020.10.037.

[17] Gottstein G. Materialwissenschaft und Werkstofftechnik: Physikalische Grundlagen. 4th ed. Berlin, Heidelberg: Springer Berlin Heidelberg; Imprint; Springer Vieweg; 2014.

[18] Ostermann F. Anwendungstechnologie Aluminium. 3rd ed. Berlin, Heidelberg: Springer Berlin Heidelberg; 2015.

[19] Nieto-Fuentes JC, Osovski S, Venkert A, Rittel D. Reassessment of the Dynamic Thermomechanical Conversion in Metals. Phys Rev Lett 2019;123(25):255502. https://doi.org/10.1103/PhysRevLett.123.255502.

[20] Juul Jensen D, Hansen N. Flow stress anisotropy in aluminium. Acta Metallurgica et Materialia 1990;38(8):1369–80. https://doi.org/10.1016/0956-7151(90)90105-P.

[21] Miodownik MA. A review of microstructural computer models used to simulate grain growth and recrystallisation in aluminium alloys. Journal of Light Metals 2002;2(3):125–35. https://doi.org/10.1016/S1471-5317(02)00039-1.

[22] Sellars C, Zhu Q. Microstructural modelling of aluminium alloys during thermomechanical processing. Materials Science and Engineering: A 2000;280(1):1–7. https://doi.org/10.1016/S0921-5093(99)00648-6.

[23] Ralph BJ, Hartl K, Sorger M, Schwarz-Gsaxner A, Stockinger M. Machine Learning Driven Prediction of Residual Stresses for the Shot Peening Process Using a Finite Element Based Grey-Box Model Approach. JMMP 2021;5(2):39. https://doi.org/10.3390/jmmp5020039.

[24] Ralph BJ, Sorger M, Schödinger B, Schmölzer H-J, Hartl K, Stockinger M. Implementation of a Six-Layer Smart Factory Architecture with Special Focus on Transdisciplinary Engineering Education. Sensors (Basel) 2021;21(9). https://doi.org/10.3390/s21092944.

[25] Ralph BJ, Sorger M, Hartl K, Schwarz-Gsaxner A, Messner F, Stockinger M. Transformation of a rolling mill aggregate to a cyber physical production system: from sensor retrofitting to machine learning. J Intell Manuf 2022;33(2):493–518. https://doi.org/10.1007/s10845-021-01856-2.

[26] Hartl K, Sorger M, Stockinger M. The Key Role of Laser Ultrasonics in the Context of Sustainable Production in an I 4.0 Value Chain. Applied Sciences 2023;13(2):733. https://doi.org/10.3390/app13020733.

[27] Kaufman JG, Rooy EL. Aluminum alloy castings properties: Properties, processes and applications. Materials Park, OH: ASM International; 2004.

[28] Hájek M, Veselý J, Cieslar M. Precision of electrical resistivity measurements. Materials Science and Engineering: A 2007;462(1-2):339–42. https://doi.org/10.1016/j.msea.2006.01.175.

[29] Saberi S, Stockinger M, Stoeckl C, Buchmayr B, Weiss H, Afsharnia R et al. A new development of four-point method to measure the electrical resistivity in situ during plastic deformation. Measurement 2021;180:109547. https://doi.org/10.1016/j.measurement.2021.109547.

[30] Ralph BJ, Schwarz A, Stockinger M. An Implementation Approach for an Academic Learning Factory for the Metal Forming Industry with Special Focus on Digital Twins and Finite Element Analysis. Procedia Manufacturing 2020;45:253–8. https://doi.org/10.1016/j.promfg.2020.04.103.

A 9   Publication 9

Author contributions:

1. K. Hartl: Conceptualization, Writing – Original Draft, Writing – Review and Editing, Project Administration

2. M. Sorger: Conceptualization, Writing – Original Draft, Writing – Review and Editing, Visualization

3. M. Stockinger: Supervision, Project Administration, Resources

Review

The Key Role of Laser Ultrasonics in the Context of Sustainable Production in an I 4.0 Value Chain

Karin Hartl *, Marcel Sorger and Martin Stockinger

Chair of Metal Forming, Montanuniversität Leoben, Franz Josef Str. 18, 8700 Leoben, Austria
* Correspondence: karin.hartl@unileoben.ac.at; Tel.: +43-38424025603

Abstract: The advancement of laser ultrasonics has increased rapidly in recent years, providing applications for materials characterization as well as for industrial utilization, as a quality control device. The wide-ranging capabilities for high-temperature in-situ analysis of a variety of microstructural characteristics offers a multitude of possibilities for usage in R&D. To date, this is the only known method that has been successfully deployed for in-situ materials characterization, as well as in the harsh environment of the metalworking industry. Combined with the enablers, introduced by the fourth industrial revolution, and the conjunction of a laser ultrasonic system with a smart production lab, it has great potential to contribute to lower rejection rates, better recyclability, and consequently to a more sustainable production. In this review, the potential for systemic sustainability is explained throughout a part of the value chain, in the context of Industry 4.0. In addition, the integration of the methodology into a miniaturized Smart Production Lab is demonstrated, with the intention of incorporating it as a substantial part of the creation of a digital twin. Such a lab is designed to serve as an interface between laboratory and industry, in order to reveal the possibilities of digital transformation, Industry 4.0, and the application of highly flexible systems such as the laser-ultrasonic system for companies.

Keywords: laser ultrasonics; in-situ material testing; quality control; I 4.0; real-time monitoring; Smart Production Lab

1. Introduction

The onset of the fourth industrial revolution has led to substantive changes in many manufacturing sectors. For metal processing facilities in particular, the enablers, occurring in conjunction with the digital transformation, provide enormous opportunities to enhance the quality of products, while simultaneously improving the sustainability of production processes [1–4]. The increasing digitization and automation of manufacturing processes empowers a large amount of process data to be generated, while these can be increasingly processed by Artificial Intelligence (AI) and Machine Learning (ML) supported algorithms, and thus contribute to an extensive competitive advantage [5,6]. One aspect that offers great potential in this context is Quality Control (QC), which is one of the most important stages within a manufacturing route [7–12]. Especially for suppliers of the aerospace industry, which often require 100% component inspection, is a laborious procedure that is difficult to maintain. In the majority of cases, component inspection is solely performed at the end of the manufacturing process, before delivery. In the event of a quality defect in the product, it has to pass through the entire manufacturing process before being sorted out, which leads to high expenses, especially for cost-intensive materials and complex manufacturing routes, that are frequently used in this industry branch. Therefore, especially in these sectors, there are efforts to adapt the possibilities of the new era, and thereby optimize economical production.

For instance, process-integrated real-time monitoring, which automatically screens the process data for discrepancies, would indicate production divergences at an early stage, and forward them to a superordinate system. Additional in-line Quality Inspection Systems, investigating the component for deviations (e.g., geometry, cracks, voids, etc.) between or during the processing steps would allow the defects to be corrected in further process steps. A significant innovation therefore, would be the implementation of a Digital Model (DM), a Digital Shadow (DS), or even a Digital Twin (DT) [13,14]. The latter one is able to detect deviations in real time, on the basis of simultaneously performed calculations, usually with the usage of finite element analysis (FEA), proposing appropriate measures for subsequent process routes, to eliminate the error or to remove the defective component [15].

In the aerospace industry, in addition to non-destructive testing of any safety-relevant component, a simulation of the manufacturing process with an integrated microstructure model is often required in order to predict the resulting microstructure prevailing in a component in advance, in order to be able to estimate mechanical properties [16–19]. For the purpose of creating a valid microstructure model of a material, an extensive amount of material parameters is required to be able to describe the essential microstructural changes during thermal and thermomechanical treatments [20–22]. Traditionally, experiments are carried out in a thermomechanical treatment simulator (TMTS) to determine the material parameters for static, dynamic, and metadynamic recrystallization (RX) and recovery phenomena, as well as for primary and secondary grain growth at different temperatures, strains and strain rates for different time steps. The analysis is subsequently carried out by an ex-situ analysis of the microstructural evolution i.e., by optical evaluation methods [23–25]. Accordingly, the generation of a set of material parameters for a valid microstructure model takes an average of three years.

As this is the most common development scenario, it is abundantly evident that it is time-, material-, and resource-intensive. Obviously, this is contrary to the actual development plan, both governmental and self-imposed by the industry, which is to emphasize sustainability and responsible CO_2-saving production [26–28]. Therefore, alternative methods to detect microstructural changes in real-time, in-situ, and also at high temperatures, under the respective manufacturing conditions, are intensively investigated. Some of the methods developed so far, coupled with the enablers of I 4.0, have the potential to become very powerful, reliable QC systems that point the way to the future. If these techniques can be integrated into the production process while preserving human resources, these methods represent a path to a sustainable future and a revolution in the metalworking industry.

For both of the above-mentioned scenarios, either in-line QC as well as for R&D purposes, in-situ material testing methods can provide an essential facilitation, cost reduction, and time saving. The focus in this context lies on the laser ultrasonic (LUS) testing method, which can be implemented in-line in the manufacturing process, as well as for the determination of material parameters, when mounted on a TMTS. The main advantage of this method is the contactless introduction of ultrasonic waves, providing information about material properties or product characteristics, depending on attenuation and velocity of sound. In addition, this system can be used at high temperatures and is virtually insensitive to a production facility's harsh environment. Due to the flexible range of applications of the system, it has the potential to provide enormous improvements along the value chain. When integrated into a Smart Production Lab (SPL), such a system has the potential to exploit numerous possibilities for quality optimization and control. On the one hand, a multitude of microstructure data can be acquired rapidly when it is coupled to a TMTS. This material data in an automated workflow is capable of generating the required material parameters and integrating them into the microstructure model, which is used for the simulation of the manufacturing process. On this basis, a DM, DS, or even a DT can be

created and incorporated into the value chain. It then manages the task of real-time monitoring of the processes of component manufacturing, on the basis of real-time process parameters and a FEA evaluation, operating in the background.

In the following sections, the most important enablers of Industry 4.0 (I 4.0) are outlined, in addition to their potential integration in a value chain, to ensure quality control. Furthermore, other in-situ quality control systems will be explained, both inline and for R&D purposes. The emphasis here lies on the LUS system, describing its setup and operating principle, and the possibilities for in-line as well as for DT integration in a SPL.

2. Enablers of the Fourth Industrial Revolution

The digital transformation induced by the advancement of I 4.0 has led to the establishment of new enabler technologies in the manufacturing industry [29,30]: (I) Industrial Internet of Things (IIoT); (II) Cyber Physical Production System (CPPS); (III) Cloud Computing (CC); (IV) DM, DS, and DT; (V) AI and ML; and (VI) Big Data. Due to the interconnected nature of I 4.0, the fundamental requirement for the successful and sustainable implementation of I 4.0 technologies requires an appropriate Information and Communication Technology (ICT) infrastructure [29]. The IIoT (I) interconnects physical entities through the internet, enabling real-time data exchange [30]. Generally, a CPPS (II) refers to a system composed of interconnected physical and virtual components. A more detailed definition of CPPSs, according to [31–33], concludes five characteristics, defining them as (i) superordinate systems within systems; (ii) consisting of cooperative components, capable of adjusting data transfer between multiple production environment layers; (iii) acting situationally appropriate and supporting decision-making processes; (iv) providing Human Machine Interfaces (HMIs); and (v) showcasing resilient design. CC (III) provides on-demand computing resources separated from the production site by the CC providers [34]. Hereby, different CC models provide different services, from data storage and processing, up to AI and ML [29]. The DM, DS, and DT (IV) describe digital depictions of physical entities, however differ depending on the automation of data transfer between digital and physical entities [35,36]. Here, the DM has no automated data transfer between both entities, whereas the DS features unilateral and the DT features bilateral data transfer [36]. AI (V) attempts to replicate human intelligence with suitable algorithms, enabling autonomous decision-making, and thus situationally appropriate acting. As a sub-category of AI, ML (V) aims to develop learning data-driven computational algorithms with the goal of linking data, recognizing correlations, drawing conclusions, and optimization [29,37–39]. Big Data (VI) refers to large volumes of heterogeneously structured data being gathered, analyzed, and disturbed at high speeds in order to extract valuable and trustworthy information [40,41]. These characteristics are summarized in the 5Vs of Big Data: Volume, Velocity, Variety, Veracity, and Value [42].

In order to fully profit from the benefits of I 4.0, the interconnection of value chain participants is imperative, enabling the optimization of products and processes along the entire product lifecycle, thus reducing waste along the value chain and improving the sustainability of production [29,43]. Per definition, a value chain includes all value creating steps in order to create a final product [44]. As for I 4.0 enabler technologies, suitable ICT infrastructure serves as a fundamental requirement for the networking of enterprises. Henceforth, transparency concerning data governance has to be emphasized, allowing transparent data sharing between enterprises in a value chain [45]. As a result of the transparent data sharing, the analysis of product and process data can be used to find correlations and draw conclusions, leading to the optimization of both [43]. Furthermore, the I 4.0 enabled omnipresent real-time monitoring leads to a drastic change of traditional QC methods [43,46]. Whereby traditional QC uses statistical methods to project the quality of a product sample, onto the entire production population, the new omnipresent data-driven QC allows the evaluation of each individual product, also incorporating advanced technologies, such as AI and ML [43,46–48]. Therefore, the implementation of I 4.0 based QC methods in a state-of-the-art DT value chain using technologies, such as Big Data, AI

and ML, can result in a significant increase of flexibility, productivity, and sustainability of products and processes along the entire value chain and lifecycle of the product [46,49–51].

3. Quality Control Using In-Situ Methods

For in-line inspection, which in this context is regarded as QC in a manufacturing process, during or between the processing stages, there is a limited number of usable methods even today. While there are some established measuring systems for the quality inspection at the end of the component manufacturing route, which are also partially automated and connected in series, such as conventional ultrasonic technology, eddy current testing, etc., it is essential to find systems that include other restrictions.

The overriding goal of such systems is to observe the quality of a feedstock over the entire value chain until the finished component, in order to be able to react immediately in the event of any deviations. For this purpose, the targeted system requires complete networking and background calculations that can respond in real time, based on real process data. Computations of this kind can then decide, depending on the severity of the deviation, whether the existent deficiencies can be rectified by adjusting the production route, or whether it is rejected. Successful implementation of such systems can save a company an enormous amount of money, if a defective component is sorted out at an early stage. This does not only contribute to cost efficiency, but also to energy and resource efficiency, and thus leads to an enormous contribution to the sustainability of a company.

The criteria that a system has to fulfill in order to be a fundamental contributor are:

- Possibility of integration
- High measurement frequency
- Near real time data processing
- Robustness
- Reliability
- Innoxiousness
- Affordability
- Long service life

According to these criteria, most of the methodologies used for the final inspection are not suitable for an in-situ implementation, mainly due to the possibility of implementation, in combination with the low data acquisition frequency.

It is quite common for sensors to be installed in production facilities to monitor and control various process parameters in-situ, in a variety of ways. A decisive parameter in this case is the usually unavoidable temperature measurement, whether in the furnace, during the forming process, at the run-out table, or during galvanizing, to mention some examples. Pyrometers are mainly used for this purpose; thermal cameras are applied in rarer cases. Similarly developed are geometry measurements, which can also usually be checked in several manners, in a cost-effective manner, on the basis of a wide variety of measurement principles.

However, the situation is different when it comes to analyzing the microstructure prevailing in the component. For the quality of a component, there are several parameters that directly affect the material, which decide on good parts and rejects. On the one hand, for multiphase alloys or for composites, the phase composition or layer thickness inside would be an essential aspect. For correlating mechanical properties, grain size, aspect ratio, or orientation, is also essential. For thermomechanical treated steels, for example, it has been demonstrated that the prior austenite grain size and texture have an enormous influence on the morphology of the martensite produced in the cooling zone. This is ultimately reflected in the anisotropy of the mechanical properties (in rolling, normal, and transverse directions) [52]. In order to be able to determine the austenite grain size, which will not remain stable at lower temperatures, in the laboratory, elaborative stabilization procedures of the microstructure and complex microscopic analyses are often necessary.

Consequently, the research for possibilities to investigate the microstructure of materials at high temperatures and in-situ, e.g., during corresponding deformations, is intensified. This in turn is achieved by means of different physical or chemical properties of, for example, phases, lattice structures, grain sizes, or orientations, which can be measurably separated from one another. Methods that make use of such properties are still predominantly found in the laboratory for off-line testing. In most cases, these are used to investigate how materials behave under certain conditions, in order to obtain the best possible process parameters. Particular focus is often placed on finding material parameters that can be used for microstructure models. Most of the microstructure models used in this aspect are based on mathematical formulations of real-physics based microstructure changes (e.g., RX, recovery, grain growth, and phase transformation) with material specific parameters, which are determined by the use of such methods [21,23].

3.1. In-Line Quality Control

Due to the increasing possibilities of integrating algorithms into data processing systems, there are now a large number of different approaches for the QC of products during manufacturing. This is specifically being enforced by the increasing accessibility to the usage of ML, AI, and Big Data. For example, neural networks are in focus for the integration in different systems. Especially for visual inspection, these methods are progressively used in the metalworking industry [53–55].

Surface inspection systems are particularly important in this respect. These are designed to detect and classify defects on the surface of the material, on the basis of images. This is usually done by the usage of training data sets, which show various defects on the surface, and which class they belong to. For this purpose there are countless approaches, for example [56] where ML algorithms like the support vector machine are applied to classify the defects. Here it was shown that the classification speed is sufficient to achieve acceptable defect detection. Another possibility to implement a statistically based approach into a neural network is the Principal Components Analysis (PCA), which is not only able to detect a defect using a large variation of defect images as input data, but also to classify the defect in order to understand its history. Other approaches can eventually be found in [57–62].

However, this is a very complex endeavor, since the variety of defects can be very high for different steel products alone. The defects occurring in hot-rolled steel products, for instance, are divided into nine main and 29 secondary classes [63]. An exact classification based on images is therefore an enormous challenge. Furthermore, it is a major hurdle to use image processing systems, due to the high temperatures and the exit speed of the strip of up to 100 km/h [56]. Even with increasing image acquisition frequency and improved computer performance, this type of inspection can be suppressed by oxidation and the harsh environment [64].

While the surface inspection systems are designed only for the detection of defects on the surface, there is a method that can also determine the microstructure of the product in-line. The 3MA (Multiparameter Micromagnetic Microstructure and stress Analyzer) technique is based on four micromagnetic principles. The detection of Barkhausen noise, the incremental permeability, the eddy current, and the tangential magnetic field method, which together provide many parameters which are used to gain information about the prevalent microstructure. For example, by measuring the coercive field, remanence, and maximum permeability, the change in the hysteresis can be related to dislocation density, and thus to the prevailing strain. The implementation in a rolling mill in three directions relative to the rolling direction (0°, 45° and 90°) allows anisotropy parameters to be determined, in addition to the common mechanical parameters [65,66]. Although this method has already been implemented in some steel rolling mills and is a promising method for in-line QC, there are still some drawbacks. The operating temperature is currently still limited to 300 °C and can only be realized by intensive cooling of the probe head. In a rolling mill, the distance between the probe and the cold strip is decisive for measuring

accuracy. Therefore, the strip must be straightened by additional rollers to ensure an approximately constant lift-off. In addition, this method can only be used with ferromagnetic materials and requires complex calibration for each grade and strip thickness [65].

Eddy current inspection is a well-established method for detecting (near-) surface defects. In industry, these are also used for inline quality control, for example in wire rolling mills. Combined with high-speed cameras, they are able to detect manufacturing defects at temperatures of up to 1200 °C and wire speeds of up to 150 m/s. Here, a change in the signal recorded by the eddy current sensor triggers the camera, and a defect can be identified on the basis of the images. This system is likewise trained, as already discussed, with stored defect images and ML algorithms to detect defects autonomously [67].

The use of infrared (IR) cameras has increased in recent years due to their cheaper design. The advantage over visible-light imaging is that IR cameras are insensitive to smoke and can be used in dark environments. In addition, every object emits infrared radiation, and the intensity increases, the warmer the object is. In industry, these cameras are preferably used for temperature control as well as for defect detection, since a crack becomes detectable through a change in temperature. Especially for quality control in the field of welding and additive manufacturing, IR cameras are increasingly encountered. Another advantage is the image analysis, which can be adopted from the visible-light imaging [68,69].

In practice, some inspection methods based on X-rays are also employed. In particular, radioscopy and computed tomography (CT) have become widely established. The main difference lies in the two-dimensional image produced by radioscopy, while CT is used for more precise 3D analyses. The advantage of radioscopy is that image reconstruction is faster than CT, although it is not possible to determine the exact location or size of the defect, which is the case with CT. However, there are efforts to improve the use of CT in inline quality control by means of high speed area array detectors and a shorter exposure time [70,71].

3.2. In-Situ Methods for R&D Purposes

Approaches for the in-situ investigation of materials on a laboratory scale are widely existent. In order to characterize microstructural changes, the limiting factor is primarily the solution of applying measurement methodologies at elevated temperatures. One of the most prominent instruments in this case is dilatometry, which reproduces transformation kinetics via the abrupt change in thermal expansion. Phase fractions can also be determined by this technique. More comprehensive data can be obtained by structural analysis or high-resolution imaging instruments. Although the classical ultrasonic method is often used for microstructure characterization, the necessity of contacting the material restricts its use to low temperatures. The situation is similar for methodologies based on the eddy current principle. There are some approaches that equip established analytical methods like these with a heating chamber to apply the methodologies in-situ during heating, isothermal holding, or cooling. These are considered promising, as many are capable of simultaneously detecting and analyzing different changes in microstructure, but have certain limitations. Many of these methods can only be performed under vacuum or an inert gas atmosphere, are limited to surface examination, or can only be operated at a very low measurement frequency. Other methods, for example, based on synchrotron radiation or neutron scattering, have the disadvantage of limited accessibility. In the following, some promising methodologies for in-situ microstructure analysis are presented, which show great potential to analyze time- and temperature-resolved microstructural changes at high temperatures.

3.2.1. High Temperature X-ray Diffraction (HT-XRD)

This method is frequently used to perform in-situ qualitative or quantitative phase analysis, precipitation formation, as well as phase dissolution. The underlying principle is based on the classical XRD method, except that the sample can be heated in a heating

chamber and XRD scans are continuously generated during the heating or holding time. Using the time-resolved generated diffractograms, the characteristic peak intensities and the peak shifts for individual phases can be evaluated, providing information about phase composition, transformation, phase precipitation, or dissolution kinetics. The peak intensities can also be used to obtain information about the quantitative fractions. On the other hand, the crystallite size, as well as the dislocation density, can also be analyzed via selective peak profile analysis. These analyses are mostly performed using either the modified Williamson-Hall or the modified Warren-Averbach procedure [72–75]. Difficulties may arise in the analysis of the diffractograms due to the difference in peak positions between room temperature and higher temperatures, as a consequence of thermal expansion and therefore a peak profile shift. In addition, with the latter analysis methods, there can be an overlap of the residual stresses and the crystallite size, where both are analyzed based on the peak profile, while residual stresses dissipate at elevated temperatures, as the crystallite size increases. Therefore, the analysis requires enormous expertise for the interpretation of the data obtained [76]. This method is used in the laboratory scale for characterizing the above-mentioned effects of a material. Various verified reaction kinetics are used to create thermokinetic models for simulation software, such as MatCalc.

A major disadvantage of this method is that characterization can only be performed in the near surface region. Consequently, this can lead to difficulties, if oxidation reactions occur, or if there are local differences in the chemical composition. Also, a grain size below $10 \mu m$ and a statistical distribution is required for a reliable analysis. Furthermore, the sample preparation is a decisive criterion to ensure valid investigations [77].

3.2.2. High Temperature Scanning Electron Microscopy and Electron Backscatter Diffraction (HT-SEM/EBSD)

This method is also based on the classical SEM or EBSD method with an integrated heating chamber, where images are acquired at a certain frequency. In contrast to the HT-XRD method, actual images can be generated here, which are based on the interactions of the sample surface with the electron beam. This enables high-resolution imaging and tracking of changes in the microstructure. For example, the displacements of individual grain boundaries during grain growth or recrystallization phenomena or even twinning effects can be displayed [78]. By using the EBSD arrangement, the time- and temperature-resolved changes in grain size and grain orientation can be detected. In this context, the application of test facilities for the evaluation of mechanical properties and for the application at high temperatures is increasingly envisaged. To date, there are already a variety of mechanical testing equipment, such as tensile test equipment, which can be implemented in the chamber of an SEM. If such a setup is installed in a HT-SEM/EBSD, this opens up a wide range of new methods to apply mechanical properties in-situ, at high resolution [79–82]. Within the scope of deformation possibilities, such as the in-situ tensile test in the SEM, digital image correlation methods are also increasingly being used. By integrating camera systems, displacements of the previously applied patterns can be recorded with high precision, which allows conclusions to be drawn about strains in one or more spatial directions. Depending on the magnification adjusted in the SEM, strain localizations in the subgrain range can be determined. The combination of EBSD, for example, can also be used to identify the influence of the grain structure on the forming behavior [83,84].

The difficulty in this case is to obtain good image quality even at high temperatures. Similarly, as mentioned before, the sample preparation requires a lot of effort. Furthermore, the acquisition costs of such a system are enormously high.

3.2.3. In-Situ Methods Based on Synchrotron Radiation

The possibility to perform in-situ material characterization with High Energy X-rays opens up a great potential to investigate near-surface microstructural changes and to be able to investigate rapidly occurring processes in real time, due to high resolution capabilities at high measurement frequencies. One possibility involves implementing a TMTS, for example, in the form of a dilatometer that has windows mounted to transmit the High-Energy XRD (HEXRD) beam through the mounted specimen. The diffraction effects of the material can then be detected in complete Debye-Scherrer rings on a flat panel detector. Using such an arrangement, a variety of changes in microstructure (similar to HT-XRD) can be elicited simultaneously at high temperatures, and by using a deformation dilatometer, conclusions can also be made about the behavior during simultaneous deformation [85–87]. The main advantage of this method is that the high-energy radiation does not limit the investigation to the surface, but larger bulk materials can be investigated.

Another investigation method worth mentioning, which is often carried out with synchrotron radiation is Small-Angle X-Ray Scattering. Investigations based on this principle provide information on the size distribution and precipitation or dissolution kinetics of precipitates. These analyses can be performed in-situ rapidly and quantitatively, and with time and spatial resolution [88].

3.2.4. High Temperature Laser Scanning Confocal Microscopy (HT-LSCM)

This method combines the classical LSCM with an infrared heated high temperature chamber. A focused laser beam scans the surface of the sample selectively. The intrinsic radiation is blocked out by a He-Ne laser, allowing the investigation to be carried out up to the fluid state. The thermal etching of the laser enables the observation of grain growth during a defined time-temperature profile. Thus, the effects of precipitates on grain growth behavior can be investigated as well. The main disadvantage of this method remains the restriction of the analysis to surfaces only. In addition, the oxygen content in the high-temperature chamber must be kept meticulously low, since the slightest oxidation leads to reduced observability [89].

3.2.5. Bainite Sensor

Another field of application for eddy current based testing is the so-called bainite sensor. This consists of an excitation coil, which generates an electric field in the component to be tested. In addition to the eddy current, this field also generates a magnetic field, which in turn generates a field in the reverse order to the first field. Thus, magnetic as well as electrical signals can be obtained by a coil system in the sensor. The signals obtained are analyzed according to their harmonic spectrum. In-situ testing of material properties is carried out by implementation in a TMTS, like the Gleeble. This allows phase fractions as well as transformation kinetics to be recorded during heat treatment or deformation. This is based on the ferromagnetic to paramagnetic change of steel during the transformation from low-temperature phases to austenite in the steel. So far, this method has been used primarily to study the bainite transformation in steel, which gives rise to the designation. This represents a simple technique to obtain in-situ information on transformation behavior in materials with allotropic phase transformation. However, this method is limited to this kind of investigation [90,91].

4. The Key Role of LUS in a Smart Manufacturing Production Site

Despite the multitude of established methods for in-line in-situ quality inspection and off-line in-situ material characterization methods mentioned, there are hardly any inspection methods that provide a reasonable application for both fields.

One possibility to investigate in a contactless manner, in-situ, and at high temperatures is the LUS method. This measurement technique has been developed over the last decades for many fields of application and can be used in various different configurations.

This method can be applied to a variety of analyses known from the conventional ultrasonic technique. In particular, defect detection is one of the most common applications, especially the detection of defects in terms of pores, voids, or adhesion defects, especially in castings or welds [92]. However, such defect detections are also of great advantage in additive manufacturing. In this context, this method can also be applied in-situ, during the build-up process [93–95]. Furthermore, the ultrasonic method can also be used for the detection of corrosion phenomena and the associated fatigue analysis [77,96,97]. Damping analyses can be utilized to determine hardening depths in surface-hardened components. Most of the analysis options mentioned are based on approaches that can already be investigated with conventional ultrasonic measurement and are applied to static components not exposed to high temperatures.

Nevertheless, the important aspect here is the possibility for advanced in-situ microstructural characterizations at high temperatures or velocities, which is the core competence of LUS. Due to a high measurement frequency, this method can record time-resolved changes in the microstructure, even at temperatures above 1200 °C, thus providing a great contribution to an efficient characterization of metals, when implemented in-line for the inspection of e.g., dimensions, phase constitution, or grain size [98,99]. Unlike other systems, this method operates reliably in harsh environments as it is relatively insensitive to dirt and dust. The continuous development and improvement of the in-line system looks promising to extract progressively more microstructural information from, for example, hot-rolled steel strip and to contribute to a significant advance in QC. Currently tens of LUS systems are integrated in a production plant worldwide, the majority of them being oriented for wall thickness measurement in tube production plants, as described for in [100]. Recent LUS measurement devices are encountered in hot strip rolling mills. These are specialized for grain size measurement of austenite before the cooling section. The in-situ measurement of austenite grain size is an important factor in predicting the material properties of the steel strip. In [101], an example of a LUS system integrated in a hot strip mill is outlined. The excitation laser is a pulsed Q-switched laser operating at a frequency of 20Hz, up to 200 mJ, and a pulse length of 6 ns, at a wavelength of 532 nm. The detection laser operates at a wavelength of 1064 nm and a pulse duration of 100 s, at a power of 600 W. A GaAs two-wave mixing interferometer was used as the interferometer. The hot strip mill rolls the pre-rolled strips in six slabs to a thickness of 2-15 mm. The LUS system is mounted behind the slabs and in front of the runout table on a linear displacement and can move between two strip guide rollers, at a distance of about half a meter from the strip. The detection laser is located at a distance of a few meters. This measurement method is very promising and will certainly be found in several rolling mills in the future. Further literature about LUS Systems implemented in industry can be found in [102–106].

Furthermore, such a LUS system can be coupled to a TMTS to study in-situ microstructural changes of samples during thermal and thermomechanical treatments. In the context discussed here, the usage of the method in the relevant areas of quality testing and the determination of material parameters will be specifically addressed. This section is intended to outline the operating principle and the analyzing methods that allow conclusions to be drawn about the prevailing microstructure.

4.1. Operating Principle

The laser ultrasonic method is based on the contactless introduction and detection of ultrasonic signals in the material. The core of the system is an excitation laser and a detection laser—most commonly Nd:YAG lasers are used for both—and integrated interferometry, such as a Fabry-Perot or a two-wave mixing interferometer. The pulsed excitation laser transmits up to several mJ of energy to the material surface, where either thermoelastic excitation or ablative excitation occurs. Both variants generate a more or less intense stress field, resulting in a broadband ultrasonic signal (usually in the range of 500–50 MHz). In the case of thermoelastic excitation, mainly surface and plane waves are generated, while ablative excitation tends to produce more pronounced longitudinal waves.

These waves pass through the material and are reflected at the back side, creating an echo. The detection laser can be mounted either in transmission or reflection mode, where the smallest deflections of the surface, due to reflection lead to a frequency shift, which is processed by an interferometer into signals that can be evaluated [107]. Figure 1 shows a schematic visualization of a LUS system.
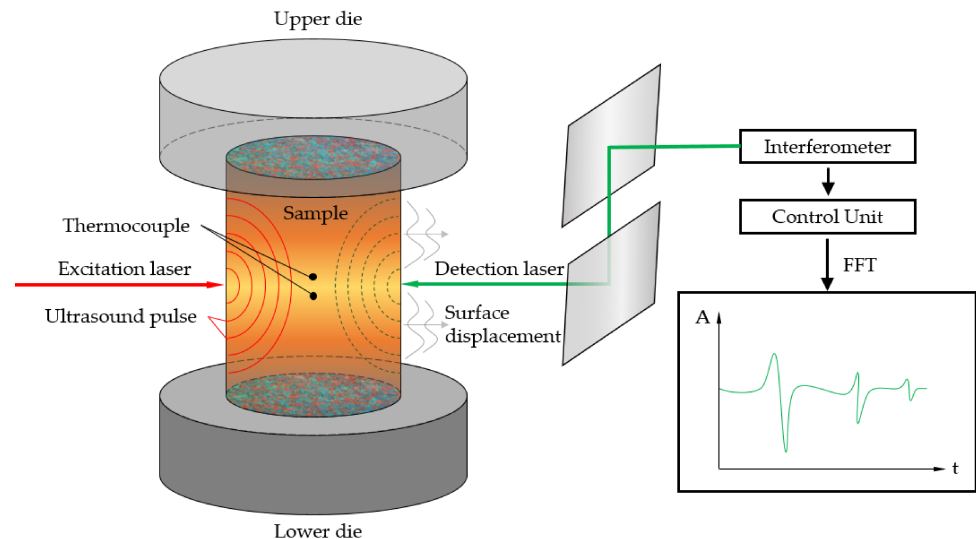

Figure 1. Schematic representation of the operating principle of a LUS System.

Apart from other types of waves generated by the excitation laser, such as surface waves or Lamb waves—an interaction of bulk waves occurring to (a-) symmetric vibrations in thin samples -, the essential ones here are the bulk waves. The bulk waves in a solid body can be subdivided depending on the mode of propagation. If the displacement of the involved particles is in the direction of propagation and results in compression, these waves are called longitudinal or compression waves; if the atomic motion is perpendicular to the direction of propagation, these waves are called transverse or shear waves. Bulk waves have the same frequency propagation, which means that they travel at the same speed, or in other words are non-dispersive. Since the compression waves propagate about twice as fast as the shear waves, these two types of waves can be clearly distinguished [107]. By analyzing the different types of waves in terms of propagation mode, direction and velocity, frequency and/or temperature dependence, or penetration depth into the material, different properties of the material can be determined.

The most important analysis parameters of the detected signals are the Time of Flight (ToF), i.e., the propagation velocity, and the amplitude or its decrease after passing through the material, i.e., the attenuation. These two parameters can be used to generate a wide range of information about the microstructural or geometric configuration of the component, by conducting suitable evaluation operations. The evaluation of the velocity of sound provides specific information about

- Geometry
- Phase transformation
- Phase composition
- Recrystallization
- Texture

    while the evaluation of the attenuation covers the aspects of

- Grain size and grain growth
- Phase constitution
- Dislocations

In the following subsections the underlying principles of gaining insight into microstructural changes are briefly described.

4.1.1. Ultrasonic Velocity

The propagation speed of ultrasonic waves (especially longitudinal c_L and shear waves c_T) depends on the density and the stiffness tensor [108]. Assuming a polycrystalline, isotropic material, with a small grain size in relation to the sample size, the following relationships between the speed of sound, density and elastic constants (K, S, v) for longitudinal and transverse waves can be assumed:

$$c_L = \sqrt{\frac{K}{\rho} \cdot \frac{1 - v}{(1 + v)(1 - 2v)}} \tag{1}$$

for the sound velocity of longitudinal waves and

$$c_T = \sqrt{\frac{S}{\rho}} \tag{2}$$

for that of transverse waves. K is referred to as the Compression Module, S is the Shear Module, and v is the Poisson ratio. In the simplest case, the propagation speed can be determined by ToF measurements. For a sample of thickness h, the propagation velocity can be derived from the time required for the wave to be reflected at the back of the sample and to be returned:

$$v = \frac{2h}{\Delta t} \tag{3}$$

If the density ρ of the inspected material is known, the Young's modulus (via known relationships with the compressive and shear moduli) or Poisson's ratio v can be determined very accurately over temperature, by measuring the speed of sound.

Since polycrystalline metals generally exhibit preferential grain orientations as a result of the manufacturing process (solidification and preferential dendrite growth or forming processes), it is of particular importance to be able to determine the predominant orientation.

Due to the high sensitivity of laser ultrasonic measurements with respect to the velocity of sound, individual entries of the elastic stiffness tensor can further be determined. Since the propagation velocity differs depending on the direction of propagation, the preferred direction can be determined using reference crystals. Conversely, orientation distribution coefficients (ODC) can also be calculated from ultrasonic signals.

Recrystallization phenomena, respectively the recrystallized fraction, can similarly be measured by measuring the changes in texture, and in turn the change in ultrasonic velocity. Since recrystallization is preceded by a certain strain and thermal activation, the changes in the measured sound velocity can be assigned to the recrystallized fraction via the Johnson-Mehl-Avrami (JMAK) function.

Especially for phase transformation or allotropic transformations of metals, a very precise prediction can be obtained with this measuring system. Since the acoustic velocity differs strongly depending on the crystal structure, the phase composition rule (lever rule) can provide an exact determination of the predominant fractions [109]. The speed of sound is also changed considerably during a transition from ferromagnetic to paramagnetic material (Curie temperature).

4.1.2. Attenuation

The second important aspect, which can be analyzed from the ultrasonic signals and related to microstructural properties of the material, is attenuation. This manifests itself in the reduction of the amplitudes of subsequent echoes. The total attenuation can be attributed to three significant phenomena and added as:

$$\alpha(f,T) = \alpha_{sc}(f,T) + \alpha_{IF}(f,T) + \alpha_D(f) \tag{4}$$

The three contributions are made by diffraction α_D, internal friction α_{IF}, and the contribution of grain scattering α_{sc}. The contribution of diffraction can be estimated qualitatively by the Fresnel parameter, while the contribution of internal friction (caused for example by magneto-mechanical damping, interstitial atoms, or dislocation motion) can be minimized by suitable algorithms, since this contribution is frequency independent to a large extent [110]. In turn, conclusions about recovery processes can be derived from the dislocation motion [111]. The contribution to be extracted is that of the grain boundary scattering, which provides information about the predominant grain size in the material. The contribution of grain scattering is primarily noticeable in metals with high elastic anisotropy and is the dominant contributor to the total damping, especially in metals of this type, such as steel, nickel, or cobalt. The grain size D is a temperature-dependent factor and damping increases as grain size increases. The contribution of the grain size to the total damping can be calculated via the power-law function

$$\alpha_{Sc}(f,T) = C(T)D^{n-1}f^n \tag{5}$$

where C corresponds to a temperature dependent material constant. The value of the exponent n depends on the ratio of the wavelength to the grain size. Below are the following three regimes:

Rayleigh regime $(\lambda \gg D)$: $\alpha_{Sc} = C_r D^3 f^4$
Stochastic regime $(\lambda \approx D)$: $\alpha_{Sc} = C_S D f^2$
Diffusion regime $(\lambda \ll D)$: $\alpha_{Sc} = C_D D^{-1}$

It is usually assumed that this ratio lies between the Rayleigh and the Stochasitic regime, which is why the value of 3 is usually chosen for n. However, this value can also be fitted specifically for a material, as described in [112].

To estimate the grain size, the power-law Formula (6) can be fitted into the measured attenuation curves:

$$a(f,T) = a + bf^n \tag{6}$$

Here, *a* represents a frequency-independent contribution that includes, for example, internal friction or external factors such as variations in laser intensity. The expression b represents the frequency dependent grain size contribution and can be assigned to the actual grain size via

$$b = \Gamma(T)D^{n-1} \tag{7}$$

with $\Gamma(T) = \sqrt{\frac{1}{C(T)}}$, which contains the material and temperature dependent Information.

Appropriate model calibration with ex-situ tests can be used to draw in-situ conclusions about grain size evolution in thermal and thermomechanical tests, based on the reference echo model or the single echo technique.

The correlations of damping as well as velocity with microstructure have been tested and published based on numerous investigations on a variety of materials. For example, grain size or grain growth investigations are discussed in [113–120]. Recrystallization effects can be found in [121–129], whereas texture measurements where conducted for instance in [130–132]. Further information of phase transformation and composition can be found in [133–137].

4.2. LUS in a Smart Production Lab

As already indicated, the LUS method is implemented to support the holistic construction of a SPL with regard to the creation of a DM/DS/DT, and to support it along the depicted value chain as a holistic auxiliary and quality inspection tool.

The MUL 4.0 project progressing at the Montanuniversität Leoben, in the form of a comprehensive SPL, encompasses parts of the holistic value chain. This value chain covers multiple technically different and geographically separated production sites, which are connected via a production network in order to transparently gather, store, and share data for analysis purposes. The starting point of the value chain, as depicted in Figure 2, is the Chair of Nonferrous Metallury (NFM), which specifically deals with aluminum alloys and has a miniature continuous casting facility. It enables the casting of a wide variety of common and newly developed alloys, as well as recycled material. This provides the feedstock for the Chair of Metal Forming (MF), where it is delivered. From here it can be further processed in a variety of methods both cold, or annealed to a specific temperature in a digitized industrial furnace. One possibility would be rolling in a miniature rolling mill that has been transformed into a CPPS. A black box machine learning approach allows rolling from a certain thickness to the desired final thickness in multiple passes, specifying the optimal pass schedule [32]. Another option would be forging in a hydraulic press capable of forces up to 1 MN. This press is being transformed into a fully integrated CPPS and is capable of recording data such as forces and temperature during upsetting, and automatically transferring them to a Supervisory Control and Data Acquisition (SCADA) system. The data is pre-processed and transmitted to a higher-level tracking system. Based on the raw material, this system can assign the process data to the respective product and provide information about the respective location. This data is additionally used throughout the value chain for input parameters for the FEA, in order to virtually represent the effects of the process conditions on the final product, and thus serve as a QC tool. Finally, the generated product can be heat treated to adjust the optimal material properties and then be machined to the final product. The value chain introduced here is illustrated in Figure 2.
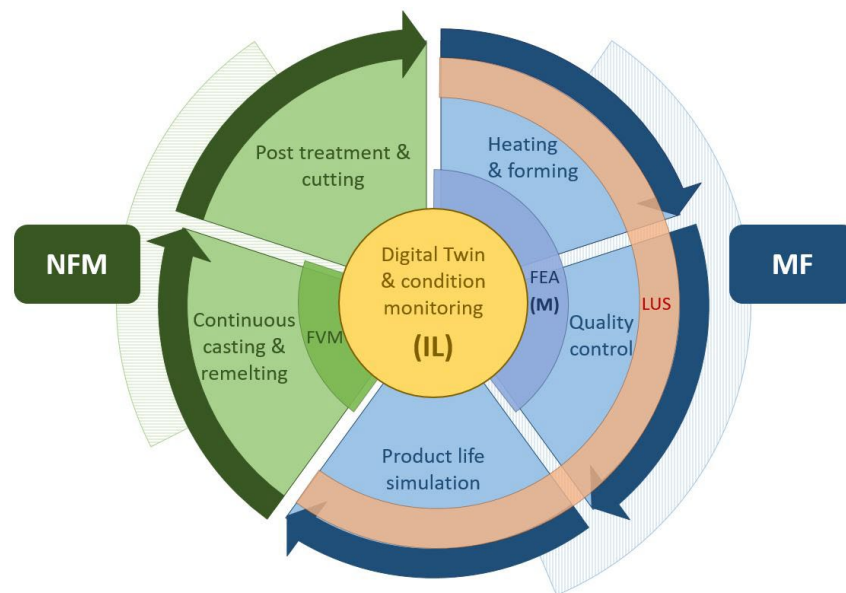

Figure 2. Visualization of the value chain covered in the SPL with the area covered by the LUS shown in orange.

The application of the LUS in the SPL is intended to provide a fundamental contribution to the creation of a DT. This consists of a FEA for the respectively considered heating or forming process of the specimen with microstructural information prevailing in the material. As already mentioned, the description of the microstructural behavior requires a large number of material parameters in order to be able to calculate various material responses as a function of strain, strain rate, and temperature, by means of a microstructure model. Therefore, the coupling of a LUS system with a TMTS, which records these

characteristic values of the deformation as well as the corresponding time, is inevitable. This coupling enables the acquisition of data of the forming process via the TMTS Gleeble 3800, as well as in-situ data of the microstructural processes by a trigger signal from the same time and its correlation. Although the LUS system only provides information on the velocity and attenuation of the ultrasonic waves, these can be automatically transferred to various microstructural changes using programmed evaluation routines, as exemplified in Section 4. This makes it possible to obtain information about grain size, recrystallization behavior, or phase transformations during the experiment. Based on the corresponding recording of the flow curve and the flow behavior, a microstructural change from the LUS data can be assigned to the corresponding flow curve parameters. For data acquisition from the LUS, a high-frequency Data Aqusition System (DAQ) will be implemented and integrated into the IIoT network, which can record the analog signals from the LUS, at a sufficiently high frequency to ensure high-resolution signal mapping. For this purpose, the fiber optic based ibaPADU-4-AI-I with ibaFOB-Dexp, in combination with the ibaRackline SAS was chosen, which has measurement frequencies of up to 10 kHz with a resolution of 16bit, and thus fulfills the minimum sampling rate of 400 Hz set by the LUS. Since this DAQ has only four analog inputs, which are already occupied by Gleeble sensors, an identical ibaPADU-4-AI-I is implemented in a parallel synchronous operation, which is combined on the iba processing unit ibaRackline SAS and the software iba PDA & iba Analyzer. For improved traceability of the data recording, the Hierarchical Data Format (HDF) HDF5 is implemented here to record the metadata of each data set, and thus to get a more holistic insight into each measurement. These datasets are automatically synchronized by an open-source approach using Python, on a file server shared with the production network at the MF, in its Data processing layer and consequently stored in the production network's relational open-source MySQL MariaDB database. This approach is visualized in Figure 3.
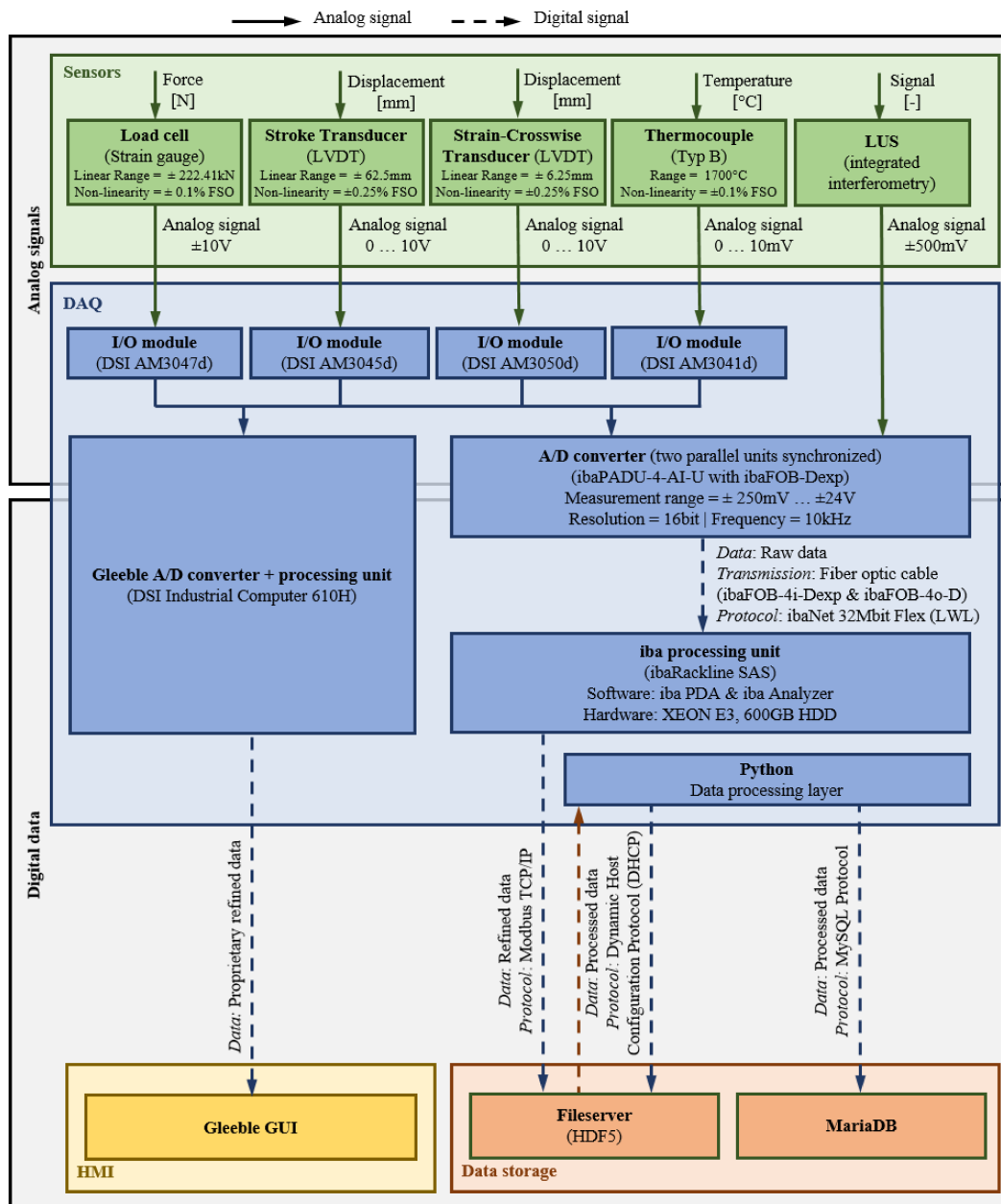
Figure 3. Visualization of the DAQ and data storage method.

Consequently, the data stored in the database is used for further post processing. The quintessence of the LUS data is the derivation of the material parameters essential for semi-empirical microstructure modeling. In addition to material-specific activation energies, etc., the associated forming conditions are necessary for the derivation of these. A typical set of formulas for the description of the material behavior in terms of static, dynamic, and metadynamic recrystallization, as well as grain growth and phase transformation, as a function of the temperature, as well as the corresponding flow curve, contains about 40 material constants [17,23] for the complete description of the microstructural processes. These are derived in a deposited evaluation script and are stored in a database. The subroutine required for FEA of the forming process, with corresponding microstructure simulation, can then extract these determined assigned material parameters from this database, and thus perform an accurate simulation of the process for the specific material under investigation. Since the computation time of a forming process with integrated microstructure simulation is too high for simultaneous computation, this results in a DM that is not applicable for the in-situ implementation. Nevertheless, to create a DS or DT

that can intervene in-situ in the process, several simulations with varying process parameters can be calculated, and the respective results in turn stored in a database for a number of process variations. These simulations can be performed locally or on a processing unit in the production network, in the form of CC, depending on the availability of computing resources required, and the results are always ultimately included in the superordinate database. For the implementation of a DS or DT, which is to intervene in-situ in a process, it is possible to fall back iteratively on the simulation results with the best-fitting process parameters, and to implement only individual data in the DS/DT. This saves an enormous amount of computational effort and still ensures an intervention in the process due to deviating microstructure conditions.

Furthermore, the LUS can be applied to characterize the raw material provided by NFM and the consequent material changes of the respective forming processes. Therefore, it can be used to rapidly identify significant deviations of a recycled material to a referenced primary material. In this way, it can be assured that the requirements for the use of a secondary metal meet specified tolerances, thereby contributing considerably to the avoidance of material waste. Thus, the LUS acts as an independent CPPS, capable of either using CC or local computing resources. As a result of the holistic data gathering, root causes of deviations in quality can be researched and evaluated, and thus be linked to the causing processes and parameters. In addition, ML can be applied in order to detect possible product quality deviations, due to unsuitable process parameters. Consequently, situationally appropriate decision-making is enhanced, and active measures can be taken, either adjusting the respective process or removing the affected specimen or product.

5. Conclusions and Outlook

The LUS method offers an immense variety of applications, whether in production, R&D, the laboratory or an interface, a so-called Smart Manufacturing Lab or SPL. In each of these areas, the method benefits from being applicable in-situ, contactless, at high temperatures, in harsh environments. By analyzing the resulting signals, a variety of different material or product characteristics can be derived in a rapid manner. Due to the constant further development, either of the internal systematics, for example, to increase the measuring frequency, or the more precise development of the models for the evaluation of any materials and alloys, the LUS will be indispensable for almost any scenario in the future. The possibility to reduce the development time of a microstructure model, including the whole required parameter set by about half, provides an enormous advantage. By implementing this methodology, it renders such microstructure models applicable, even in sectors where integration was not feasible for financial reasons. This development can provide a springboard for more economical and efficient production, since the effects of process conditions on the microstructure can be analyzed in advance.

Of course, the advantages on the production line are also of enormous importance. The possibility to inspect not only geometric parameters for tolerances in-line, but also to monitor the prevailing microstructure significantly, contributes to increasing efficiency and reducing scrap.

Especially the application as a CPPS in a digitalized production environment contributes to a considerable benefit. When combining the lab-scale utilization for a production facility, unimagined possibilities can still be considered with the assistance of the enablers of I 4.0. The interaction of DM, DS, and DTs and real-time process data integration with ML along the value chain can be a substantial contribution to the sustainable production of the future.

The main shortcomings in the implementation of the LUS in a SPL are that the evaluation of the obtained data is not yet mature for a variety of different materials. Even though a large number of investigations have already been carried out for microstructural changes of some various materials, it is necessary to investigate the behavior using the LUS for additional materials and alloys in a large-scale, creating a sub-ordinate database including microstructural data.

Institutional Review Board Statement: Not applicable.

Informed Consent Statement: Not applicable.

Data Availability Statement: Not applicable.

References

1. Zheng, T.; Ardolino, M.; Bacchetti, A.; Perona, M. The applications of Industry 4.0 technologies in manufacturing context: A systematic literature review. *Int. J. Prod. Res.* **2021**, *59*, 1922–1954. https://doi.org/10.1080/00207543.2020.1824085.
2. Govender, E.; Telukdarie, A.; Sishi, M.N. Approach for Implementing Industry 4.0 Framework in the Steel Industry. In Proceedings of the 2019 IEEE International Conference on Industrial Engineering and Engineering Management (IEEM), Macao, China, 15–18 December 2019.
3. Gajdzik, B.; Wolniak, R. Framework for R&D&I Activities in the Steel Industry in Popularizing the Idea of Industry 4.0. *JOItmC* **2022**, *8*, 133. https://doi.org/10.3390/joitmc8030133.
4. Hagenah, H.; Schulte, R.; Vogel, M.; Hermann, J.; Scharrer, H.; Lechner, M.; Merklein, M. 4.0 in metal forming—Questions and challenges. *Procedia CIRP* **2019**, *79*, 649–654. https://doi.org/10.1016/j.procir.2019.02.055.
5. Culot, G.; Orzes, G.; Sartor, M.; Nassimbeni, G. The future of manufacturing: A Delphi-based scenario analysis on Industry 4.0. *Technol. Forecast. Soc. Change* **2020**, *157*, 120092. https://doi.org/10.1016/j.techfore.2020.120092.
6. Oztemel, E.; Gursev, S. Literature review of Industry 4.0 and related technologies. *J. Intell. Manuf.* **2020**, *31*, 127–182. https://doi.org/10.1007/s10845-018-1433-8.
7. Ammar, M.; Haleem, A.; Javaid, M.; Walia, R.; Bahl, S. Improving material quality management and manufacturing organizations system through Industry 4.0 technologies. *Mater. Today Proc.* **2021**, *45*, 5089–5096. https://doi.org/10.1016/j.matpr.2021.01.585.
8. Beham, A.; Raggl, S.; Hauder, V.A.; Karder, J.; Wagner, S.; Affenzeller, M. Performance, Quality, and Control in Steel Logistics 4.0. *Procedia Manuf.* **2020**, *42*, 429–433. https://doi.org/10.1016/j.promfg.2020.02.053.
9. Straat, M.; Koster, K.; Goet, N.; Bunte, K. An Industry 4.0 example: Real-time quality control for steel-based mass production using Machine Learning on non-invasive sensor data. In Proceedings of the 2022 International Joint Conference on Neural Networks (IJCNN), Padua, Italy, 18–23 July 2022.
10. Souza, F.F. de; Corsi, A.; Pagani, R.N.; Balbinotti, G.; Kovaleski, J.L. Total quality management 4.0: Adapting quality management to Industry 4.0. *TQM* **2022**, *34*, 749–769. https://doi.org/10.1108/TQM-10-2020-0238.
11. Onyeiwu, C.; Yang, E.; Rodden, T.; Yan, X.-T.; Zante, R.C.; Ion, W. In-process monitoring and quality control of hot forging processes towards Industry 4.0. *Ind. Syst. Digit. Age Conf. 2017*, University of Strathclyde, UK,**2017**.
12. Maganga, D.P.; Taifa, I.W. Quality 4.0 conceptualisation: An emerging quality management concept for manufacturing industries. *TQM* **2022**, *ahead-of-print*. https://doi.org/10.1108/TQM-11-2021-0328.
13. Ashtari Talkhestani, B.; Jung, T.; Lindemann, B.; Sahlab, N.; Jazdi, N.; Schloegl, W.; Weyrich, M. An architecture of an Intelligent Digital Twin in a Cyber-Physical Production System. *Automatisierungstechnik* **2019**, *67*, 762–782. https://doi.org/10.1515/auto-2019-0039.
14. Ralph, B.J.; Schwarz, A.; Stockinger, M. An Implementation Approach for an Academic Learning Factory for the Metal Forming Industry with Special Focus on Digital Twins and Finite Element Analysis. *Procedia Manuf.* **2020**, *45*, 253–258. https://doi.org/10.1016/j.promfg.2020.04.103.
15. Kang, H.S.; Lee, J.Y.; Choi, S.; Kim, H.; Park, J.H.; Son, J.Y.; Kim, B.H.; Noh, S.D. Smart manufacturing: Past research, present findings, and future directions. *Int. J. Precis. Eng. Manuf. -Green Tech.* **2016**, *3*, 111–128. https://doi.org/10.1007/s40684-016-0015-5.
16. Sommitsch, C.; Radis, R.; Krumphals, A.; Stockinger, M.; Huber, D. Microstructure control in processing nickel, titanium and other special alloys. In *Microstructure Evolution in Metal Forming Processes*; Elsevier: Amsterdam, The Netherlands, 2012; pp. 337–383; ISBN 9780857090744.
17. Stockinger, M.; Tockner, J. Microstructure Modeling as a Tool to Optimize Forging of Critical Aircraft Parts. *MSF* **2004**, *467–470*, 683–688. https://doi.org/10.4028/www.scientific.net/MSF.467-470.683.

18. Stockinger, M.; Riedler, M.; Huber, D. Effect of Process Modeling on Product Quality of Superalloy Forgings. In *Superalloy 718 and Derivatives*; Ott, E.A., Groh, J.R., Banik, A., Dempster, I., Gabb, T.P., Helmink, R., Liu, X., Mitchell, A., Sjöberg, G.P., Wusatowska-Sarnek, A., Eds.; John Wiley & Sons, Inc: Hoboken, NJ, USA, 2010; pp 181–197; ISBN 9781118495223.

19. Whitmore, L.; Ahmadi, M.R.; Stockinger, M.; Povoden-Karadeniz, E.; Kozeschnik, E.; Leitner, H. Microstructural investigation of thermally aged nickel-based superalloy 718Plus. *Mater. Sci. Eng. A* **2014**, *594*, 253–259. https://doi.org/10.1016/j.msea.2013.11.037.

20. Brand, A.J.; Karhausen, K.; Kopp, R. Microstructural simulation of nickel base alloy Incone* 718 in production of turbine discs. *Mater. Sci. Technol.* **1996**, *12*, 963–969. https://doi.org/10.1179/026708396790122134.

21. Stockinger, M.; Tockner, J. Optimizing the Forging of Critical Aircraft Parts by the Use of Finite Element Coupled Microstructure Modeling. In Proceedings of the Sixth International Symposium on Superalloys 718, 625, 706 and Derivatives, Pittsburgh, United States, 2–5 October 2005; Loria, E.A., Ed.; Minerals Metals & Materials Society (TMS): Warrendale, PA, USA, 2005; pp. 87–95; ISBN 978-0-87339-602-8.

22. Medeiros, S.; Prasad, Y.; Frazier, W.; Srinivasan, R. Microstructural modeling of metadynamic recrystallization in hot working of IN 718 superalloy. *Mater. Sci. Eng. A* **2000**, *293*, 198–207. https://doi.org/10.1016/S0921-5093(00)01053-4.

23. Sellars, C.M.; Whiteman, J.A. Recrystallization and grain growth in hot rolling. *Met. Sci.* **1979**, *13*, 187–194. https://doi.org/10.1179/msc.1979.13.3-4.187.

24. Alimov, A.; Sizova, I.; Biba, N.; Bambach, M. Prediction of Mechanical Properties of Ti-6Al-4V Forgings Based on Simulation of Microstructure Evolution. *Procedia Manuf.* **2020**, *47*, 1468–1475. https://doi.org/10.1016/j.promfg.2020.04.326.

25. Gruber, C.; Raninger, P.; Stockinger, M.; Bucher, C. Multi-Class Grain Size Model for Forged Alloy 718 Aircraft Parts. *MSF* **2021**, *1016*, 499–508. https://doi.org/10.4028/www.scientific.net/MSF.1016.499.

26. Allwood, J.M.; Cullen, J.M.; Milford, R.L. Options for achieving a 50% cut in industrial carbon emissions by 2050. *Environ. Sci. Technol.* **2010**, *44*, 1888–1894. https://doi.org/10.1021/es902909k.

27. Milford, R.L.; Allwood, J.M.; Cullen, J.M. Assessing the potential of yield improvements, through process scrap reduction, for energy and CO_2 abatement in the steel and aluminium sectors. *Resour. Conserv. Recycl.* **2011**, *55*, 1185–1195. https://doi.org/10.1016/j.resconrec.2011.05.021.

28. Kumar, P. Implementation of industry 4.0 to achieve sustainable manufacturing in steel industry: A case study. *Sys. Lit. Rev. Meta. -Anl. J.* **2021**, *2*, 1–9. https://doi.org/10.54480/slrm.v2i1.10.

29. Sorger, M.; Ralph, B.J.; Hartl, K.; Woschank, M.; Stockinger, M. Big Data in the Metal Processing Value Chain: A Systematic Digitalization Approach under Special Consideration of Standardization and SMEs. *Appl. Sci.* **2021**, *11*, 9021. https://doi.org/10.3390/app11199021.

30. Boyes, H.; Hallaq, B.; Cunningham, J.; Watson, T. The industrial internet of things (IIoT): An analysis framework. *Comput. Ind.* **2018**, *101*, 1–12. https://doi.org/10.1016/j.compind.2018.04.015.

31. Cardin, O. Classification of cyber-physical production systems applications: Proposition of an analysis framework. *Comput. Ind.* **2019**, *104*, 11–21. https://doi.org/10.1016/j.compind.2018.10.002.

32. Ralph, B.J.; Sorger, M.; Hartl, K.; Schwarz-Gsaxner, A.; Messner, F.; Stockinger, M. Transformation of a rolling mill aggregate to a cyber physical production system: From sensor retrofitting to machine learning. *J. Intell. Manuf.* **2022**, *33*, 493–518. https://doi.org/10.1007/s10845-021-01856-2.

33. Wu, X.; Goepp, V.; Siadat, A. Concept and engineering development of cyber physical production systems: A systematic literature review. *Int. J. Adv. Manuf. Technol.* **2020**, *111*, 243–261. https://doi.org/10.1007/s00170-020-06110-2.

34. Alouffi, B.; Hasnain, M.; Alharbi, A.; Alosaimi, W.; Alyami, H.; Ayaz, M. A Systematic Literature Review on Cloud Computing Security: Threats and Mitigation Strategies. *IEEE Access* **2021**, *9*, 57792–57807. https://doi.org/10.1109/ACCESS.2021.3073203.

35. Kritzinger, W.; Karner, M.; Traar, G.; Henjes, J.; Sihn, W. Digital Twin in manufacturing: A categorical literature review and classification. *IFAC-Pap.* **2018**, *51*, 1016–1022. https://doi.org/10.1016/j.ifacol.2018.08.474.

36. Ralph, B.J.; Stockinger, M. *Digitalization and Digital Transformation in Metal Forming: Key Technologies, Challenges and Current Developments of Industry 4.0 Applications*. In XXXIX Colloquium on Metal Forming 2020; Montanuniversität: Leoben, Austria, 2020; pp. 13–23. ISBN 978-3-902078-26-1.

37. Ayvaz, S.; Alpay, K. Predictive maintenance system for production lines in manufacturing: A machine learning approach using IoT data in real-time. *Expert Syst. Appl.* **2021**, *173*, 114598. https://doi.org/10.1016/j.eswa.2021.114598.

38. Wu, D.; Jennings, C.; Terpenny, J.; Gao, R.X.; Kumara, S. A Comparative Study on Machine Learning Algorithms for Smart Manufacturing: Tool Wear Prediction Using Random Forests. *J. Manuf. Sci. Eng.* **2017**, *139*, 237. https://doi.org/10.1115/1.4036350.

39. Sharp, M.; Ak, R.; Hedberg, T. A Survey of the Advancing Use and Development of Machine Learning in Smart Manufacturing. *J. Manuf. Syst.* **2018**, *48 Pt C*, 170–179. https://doi.org/10.1016/j.jmsy.2018.02.004.

40. Ghasemaghaei, M. Understanding the impact of big data on firm performance: The necessity of conceptually differentiating among big data characteristics. *Int. J. Inf. Manag.* **2021**, *57*, 102055. https://doi.org/10.1016/j.ijinfomgt.2019.102055.

41. Zikopoulos, P.; Eaton, C. *Understanding Big Data: Analytics for Enterprise Class Hadoop and Streaming Data*; McGraw-Hill Osborne Media: New York, NY, USA, 2011; ISBN 978-0-07-179053-6.

42. Ishwarappa; Anuradha, J. A Brief Introduction on Big Data 5Vs Characteristics and Hadoop Technology. *Procedia Comput. Sci.* **2015**, *48*, 319–324. https://doi.org/10.1016/j.procs.2015.04.188.

43. Sorger, M. *Quality 5.—A Data-Driven Path towards Zero Waste.* XL. Colloquium on Metal Forming: Zauchensee, Austrian, 2022.

44. Lund, S.; Manyika, J.; Woetzel, J.; Bughin, J.; Krishnan, M.; Seong, J.; Muir, M. Globalization in Transition: The Future of Trade and Value Chains. Available online: https://www.mckinsey.com/featured-insights/innovation-and-growth/globalization-in-transition-the-future-of-trade-and-value-chains (accessed on 10 November 2022).

45. Lund, S.; Manyika, J.; Woetzel, J.; Barriball, E.; Krishnan, M.; Alicke, K.; Birshan, M.; George, K.; Smit, S.; Swan, D.; et al. Risk, Resilience, and Rebalancing in Global Value Chains. Available online: https://www.mckinsey.com/business-functions/operations/our-insights/risk-resilience-and-rebalancing-in-global-value-chains (accessed on 30 May 2022).

46. Sader, S.; Husti, I.; Daroczi, M. A review of quality 4.0: Definitions, features, technologies, applications, and challenges. *Total Qual. Manag. Bus. Excell.* **2022**, *33*, 1164–1182. https://doi.org/10.1080/14783363.2021.1944082.

47. Ralph, B.J.; Hartl, K.; Sorger, M.; Schwarz-Gsaxner, A.; Stockinger, M. Machine Learning Driven Prediction of Residual Stresses for the Shot Peening Process Using a Finite Element Based Grey-Box Model Approach. *JMMP* **2021**, *5*, 39. https://doi.org/10.3390/jmmp5020039.

48. Sariyer, G.; Mangla, S.K.; Kazancoglu, Y.; Ocal Tasar, C.; Luthra, S. Data analytics for quality management in Industry 4.0 from a MSME perspective. *Ann. Oper. Res.* **2021**. https://doi.org/10.1007/s10479-021-04215-9.

49. Ralph, B.J.; Woschank, M.; Miklautsch, P.; Kaiblinger, A.; Pacher, C.; Sorger, M.; Zsifkovits, H.; Stockinger, M. MUL 4.0: Systematic Digitalization of a Value Chain from Raw Material to Recycling. *Procedia Manuf.* **2021**, *55*, 335–342. https://doi.org/10.1016/j.promfg.2021.10.047.

50. Li, D.; Zhao, Y.; Zhang, L.; Chen, X.; Cao, C. Impact of quality management on green innovation. *J. Clean. Prod.* **2018**, *170*, 462–470. https://doi.org/10.1016/j.jclepro.2017.09.158.

51. Fonseca, L.; Amaral, A.; Oliveira, J. Quality 4.0: The EFQM 2020 Model and Industry 4.0 Relationships and Implications. *Sustainability* **2021**, *13*, 3107. https://doi.org/10.3390/su13063107.

52. Esterl, R.; Sonnleitner, M.; Weißensteiner, I.; Hartl, K.; Schnitzer, R. Influence of quenching conditions on texture and mechanical properties of ultra-high-strength steels. *J. Mater. Sci.* **2019**, *54*, 12875–12886. https://doi.org/10.1007/s10853-019-03787-z.

53. Lee, S.Y.; Tama, B.A.; Moon, S.J.; Lee, S. Steel Surface Defect Diagnostics Using Deep Convolutional Neural Network and Class Activation Map. *Appl. Sci.* **2019**, *9*, 5449. https://doi.org/10.3390/app9245449.

54. Wang, T.; Chen, Y.; Qiao, M.; Snoussi, H. A fast and robust convolutional neural network-based defect detection model in product quality control. *Int. J. Adv. Manuf. Technol.* **2018**, *94*, 3465–3471. https://doi.org/10.1007/s00170-017-0882-0.

55. Xing, S.; Ju, J.; Xing, J. Research on hot-rolling steel products quality control based on BP neural network inverse model. *Neural. Comput. Applic.* **2019**, *31*, 1577–1584. https://doi.org/10.1007/s00521-018-3547-5.

56. Jia, H.; Murphey, Y.L.; Shi, J.; Chang, T.-S. An intelligent real-time vision system for surface defect detection. In Proceedings of the 17th International Conference on Pattern Recognition, 2004, ICPR 2004, Cambridge, UK, 26 August 2004; Volume 3, pp. 239–242; ISBN 0-7695-2128-2.

57. Park, C.; Won, S. An automated web surface inspection for hot wire rod using undecimated wavelet transform and support vector machine. In Proceedings of the 2009 35th Annual Conference of IEEE Industrial Electronics, Porto, Portugal, 3–5 November 2009.

58. Shirvaikar, M. Trends in automated visual inspection. *J. Real-Time Image. Proc.* **2006**, *1*, 41–43. https://doi.org/10.1007/s11554-006-0009-6.

59. Kumar, A. Computer-Vision-Based Fabric Defect Detection: A Survey. *IEEE Trans. Ind. Electron.* **2008**, *55*, 348–363. https://doi.org/10.1109/TIE.1930.896476.

60. DuPont, F.; Odet, C.; Cartont, M. Optimization of the recognition of defects in flat steel products with the cost matrices theory. *NDTE Int.* **1997**, *30*, 3–10. https://doi.org/10.1016/S0963-8695(96)00045-X.

61. Chin, R.T.; Harlow, C.A. Automated visual inspection: A survey. *IEEE Trans. Pattern Anal. Mach. Intell.* **1982**, *4*, 557–573. https://doi.org/10.1109/TPAMI.1982.4767309.

62. Boudiaf, A.; Benlahmidi, S.; Harrar, K.; Zaghdoudi, R. Classification of Surface Defects on Steel Strip Images using Convolution Neural Network and Support Vector Machine. *J. Fail. Anal. Preven.* **2022**, *22*, 531–541. https://doi.org/10.1007/s11668-022-01344-6.

63. Sharifzadeh, M.; Alirezaee, S.; Amirfattahi, R.; Sadri, S. Detection of steel defect using the image processing algorithms. In Proceedings of the 2008 IEEE International Multitopic Conference, 27-29 May 2008, Cairo, Egypt.

64. Online measurements for quality in the metals industries: Does automated inspection meet the need? *Ironmak. Steelmak.* **2004**, *31*, 2–7. https://doi.org/10.1179/irs.2004.31.1.2.

65. Sheng, H.; Wang, P.; Tang, C. Predicting Mechanical Properties of Cold-Rolled Steel Strips Using Micro-Magnetic NDT Technologies. *Materials* **2022**, *15*, 2151. https://doi.org/10.3390/ma15062151.

66. Wolter, B.; Gabi, Y.; Conrad, C. Nondestructive Testing with 3MA—An Overview of Principles and Applications. *Appl. Sci.* **2019**, *9*, 1068. https://doi.org/10.3390/app9061068.

67. Cao, Q.; Liu, D.; He, Y.; Zhou, J.; Codrington, J. Nondestructive and quantitative evaluation of wire rope based on radial basis function neural network using eddy current inspection. *NDTE Int.* **2012**, *46*, 7–13. https://doi.org/10.1016/j.ndteint.2011.09.015.

68. Sreedhar, U.; Krishnamurthy, C.V.; Balasubramaniam, K.; v.d. Raghupathy; Ravisankar, S. Automatic defect identification using thermal image analysis for online weld quality monitoring. *J. Mater. Process. Technol.* **2012**, *212*, 1557–1566. https://doi.org/10.1016/j.jmatprotec.2012.03.002.

69. Connolly, C. The use of infrared imaging in industry. *Assem. Autom.* **2005**, *25*, 191–195. https://doi.org/10.1108/01445150510610908.

70. Hanke, R.; Fuchs, T.; Uhlmann, N. X-ray based methods for non-destructive testing and material characterization. *Nucl. Instrum. Methods Phys. Res. Sect. A: Accel. Spectrometers Detect. Assoc. Equip.* **2008**, *591*, 14–18. https://doi.org/10.1016/j.nima.2008.03.016.

71. Schryver, T. de; Dhaene, J.; Dierick, M.; Boone, M.N.; Janssens, E.; Sijbers, J.; van Dael, M.; Verboven, P.; Nicolai, B.; van Hoorebeke, L. In-line NDT with X-Ray CT combining sample rotation and translation. *NDTE Int.* **2016**, *84*, 89–98. https://doi.org/10.1016/j.ndteint.2016.09.001.

72. Ungár, T.; Gubicza, J.; Ribárik, G.; Borbély, A. Crystallite size distribution and dislocation structure determined by diffraction profile analysis: Principles and practical application to cubic and hexagonal crystals. *J. Appl. Cryst.* **2001**, *34*, 298–310. https://doi.org/10.1107/S0021889801003715.

73. Ungár, T.; Borbély, A. The effect of dislocation contrast on x-ray line broadening: A new approach to line profile analysis. *Appl. Phys. Lett.* **1996**, *69*, 3173–3175. https://doi.org/10.1063/1.117951.

74. Ungár, T.; Ott, S.; Sanders, P.; Borbély, A.; Weertman, J. Dislocations, grain size and planar faults in nanostructured copper determined by high resolution X-ray diffraction and a new procedure of peak profile analysis. *Acta Mater.* **1998**, *46*, 3693–3699. https://doi.org/10.1016/S1359-6454(98)00001-9.

75. Ungár, T.; Révész, Á.; Borbély, A. Dislocations and Grain Size in Electrodeposited Nanocrystalline Ni Determined by the Modified Williamson–Hall and Warren–Averbach Procedures. *J. Appl. Cryst.* **1998**, *31*, 554–558. https://doi.org/10.1107/S0021889897019559.

76. Wiessner, M.; Angerer, P.; Prevedel, P.; Skalnik, K.; Marsoner, S.; Ebner, R. Advanced X-ray Diffraction Techniques for Quantitative Phase Content and Lattice Defect Characterization during Heat Treatment of High Speed Steels. *Berg. Huettenmaenn Mon.* **2014**, *159*, 390–393. https://doi.org/10.1007/s00501-014-0292-7.

77. Zhong, F.; Zhang, C.; Li, W.; Jiao, J.; Zhong, L. Nonlinear ultrasonic characterization of intergranular corrosion damage in super 304H steel tube. *Anti-Corros. Methods Mater.* **2016**, *63*, 145–152. https://doi.org/10.1108/ACMM-05-2014-1390.

78. Heard, R.; Huber, J.E.; Siviour, C.; Edwards, G.; Williamson-Brown, E.; Dragnevski, K. An investigation into experimental in situ scanning electron microscope (SEM) imaging at high temperature. *Rev. Sci. Instrum.* **2020**, *91*, 63702. https://doi.org/10.1063/1.5144981.

79. Summers, W.D.; Alabort, E.; Kontis, P.; Hofmann, F.; Reed, R.C. In situ high-temperature tensile testing of a polycrystalline nickel-based superalloy. *Mater. High Temp.* **2016**, *33*, 338–345. https://doi.org/10.1080/09603409.2016.1180857.

80. Yuan, Z.Z.; Dai, Q.X.; Cheng, X.N.; Chen, K.M.; Pan, L.; Wang, A.D. In situ SEM tensile test of high-nitrogen austenitic stainless steels. *Mater. Charact.* **2006**, *56*, 79–83. https://doi.org/10.1016/j.matchar.2005.09.013.

81. Haddad, M.; Ivanisenko, Y.; Courtois-Manara, E.; Fecht, H.-J. In-situ tensile test of high strength nanocrystalline bainitic steel. *Mater. Sci. Eng. A* **2015**, *620*, 30–35. https://doi.org/10.1016/j.msea.2014.09.088.

82. Podor, R.; Ravaux, J.; Brau, H.-P. In Situ Experiments in the Scanning Electron Microscope Chamber. In *Characterization of Ceramic Materials Synthesized by Mechanosynthesis for Energy Applications*; Cortés-Escobedo, C.A., Ed.; IntechOpen: London, UK, 2012; ISBN 978-953-51-0092-8.

83. Lagattu, F.; Bridier, F.; Villechaise, P.; Brillaud, J. In-plane strain measurements on a microscopic scale by coupling digital image correlation and an in situ SEM technique. *Mater. Charact.* **2006**, *56*, 10–18. https://doi.org/10.1016/j.matchar.2005.08.004.

84. Wilkinson, A.J.; Meaden, G.; Dingley, D.J. High resolution mapping of strains and rotations using electron backscatter diffraction. *Mater. Sci. Technol.* **2006**, *22*, 1271–1278. https://doi.org/10.1179/174328406X130966.

85. Erdely, P.; Schmoelzer, T.; Schwaighofer, E.; Clemens, H.; Staron, P.; Stark, A.; Liss, K.-D.; Mayer, S. In Situ Characterization Techniques Based on Synchrotron Radiation and Neutrons Applied for the Development of an Engineering Intermetallic Titanium Aluminide Alloy. *Metals* **2016**, *6*, 10. https://doi.org/10.3390/met6010010.

86. Schmoelzer, T.; Liss, K.-D.; Staron, P.; Mayer, S.; Clemens, H. The Contribution of High-Energy X-Rays and Neutrons to Characterization and Development of Intermetallic Titanium Aluminides. *Adv. Eng. Mater.* **2011**, *13*, 685–699. https://doi.org/10.1002/adem.201000296.

87. Novoselova, T.; Malinov, S.; Sha, W.; Zhecheva, A. High-temperature synchrotron X-ray diffraction study of phases in a gamma TiAl alloy. *Mater. Sci. Eng. A* **2004**, *371*, 103–112. https://doi.org/10.1016/j.msea.2003.12.015.

88. Geuser, F. de; Styles, M.J.; Hutchinson, C.R.; Deschamps, A. High-throughput in-situ characterization and modeling of precipitation kinetics in compositionally graded alloys. *Acta Mater.* **2015**, *101*, 1–9. https://doi.org/10.1016/j.actamat.2015.08.061.

89. Fuchs, N.; Bernhard, C. In-situ-Untersuchung von Austenitkornwachstumsprozessen in Stählen mittels Hochtemperatur-Laser-Scanning-Konfokal-Mikroskop. *Berg Huettenmaenn Mon.* **2019**, *164*, 200–204. https://doi.org/10.1007/s00501-019-0850-0.

90. Klümper-Westkamp, H.; Vetterlein, J.; Lütjens, J.; Zoch, H.-W.; Reimche, W.; Bach, F.-W. Bainite Sensor—A new tool for process and quality control of the bainite transformation. *HTM J. Heat Treat. Mater.* **2008**, *63*, 174–180. https://doi.org/10.3139/105.100459.

91. Dong, J.; Skalecki, M.G.; Hatwig, R.A.; Bevilaqua, W.L.; Stark, A.; Epp, J.; Da Silva Rocha, A.; Zoch, H.-W. Study of Microstructural Development of Bainitic Steel using Eddy Current and Synchrotron XRD in-situ Measurement Techniques during Thermomechanical Treatment*. *HTM J. Heat Treat. Mater.* **2020**, *75*, 3–22. https://doi.org/10.3139/105.110402.

92. Klein, M., Sienicki, T., and Eichenbergeer, J. *Laser-Ultrasonic Detection of Subsurface Defects in Processed Metals*; Patent: US7278315, United States 2007.

93. Everton, S.K.; Hirsch, M.; Stravroulakis, P.; Leach, R.K.; Clare, A.T. Review of in-situ process monitoring and in-situ metrology for metal additive manufacturing. *Mater. Des.* **2016**, *95*, 431–445. https://doi.org/10.1016/j.matdes.2016.01.099.

94. Klein, M.; Sears, J. Laser ultrasonic inspection of laser cladded 316LSS and TI-6-4. *Int. Congr. Appl. Lasers Electro. -Opt.* **2018**, *2004*, 1006. https://doi.org/10.2351/1.5060183.

95. Edwards, R.S.; Dutton, B.; Clough, A.R.; Rosli, M.H. Scanning laser source and scanning laser detection techniques for different surface crack geometries. In Proceedings of the Review of Progress in Quantitative Nondestructive, Burlington, VT, USA, 17–22 July 2011; Volume 31, pp. 251–258.

96. Silva, M.Z.; Gouyon, R.; Lepoutre, F. Hidden corrosion detection in aircraft aluminum structures using laser ultrasonics and wavelet transform signal analysis. *Ultrasonics* **2003**, *41*, 301–305. https://doi.org/10.1016/S0041-624X(02)00455-9.

97. Maddumahewa, K.K.; Madusanka, N.; Piyathilake, S.; Sivahar, V. Ultrasonic nondestructive evaluation of corrosion damage in concrete reinforcement bars. In Proceedings of the 2017 Moratuwa Engineering Research Conference (MERCon), Moratuwa, Sri Lanka, 29–31 May 2017; pp 79–82; ISBN 978-1-5090-6491-5.

98. Falkenström, M.; Engman, M.; Lindh-Ulmgren, E.; Hutchinson, B. Laser ultrasonics for process control in the metal industry. *Nondestruct. Test. Eval.* **2011**, *26*, 237–252. https://doi.org/10.1080/10589759.2011.573553.

99. Hutchinson, B.; Moss, B.; Smith, A.; Astill, A.; Scruby, C.; Engberg, G.; Björklund, J. Online characterisation of steel structures in hot strip mill using laser ultrasonic measurements. *Ironmak. Steelmak.* **2002**, *29*, 77–80. https://doi.org/10.1179/030192302225001910.

100. Lévesque, D.; Kruger, S.E.; Lamouche, G.; Kolarik, R.; Jeskey, G.; Choquet, M.; Monchalin, J.-P. Thickness and grain size monitoring in seamless tube-making process using laser ultrasonics. *NDTE Int.* **2006**, *39*, 622–626. https://doi.org/10.1016/j.ndteint.2006.04.009.

101. Malmström, M.; Jansson, A.; Hutchinson, B.; Lönnqvist, J.; Gillgren, L.; Bäcke, L.; Sollander, H.; Bärwald, M.; Hochhard, S.; Lundin, P. Laser-Ultrasound-Based Grain Size Gauge for the Hot Strip Mill. *Appl. Sci.* **2022**, *12*, 10048. https://doi.org/10.3390/app121910048.

102. Astill, A. G., Tweed, J. H., Stacey, K., Moss, B. C. *Prospects for On-Line Structure Monitoring by Laser Ultrasonics for Process Control in Rolling Heat Treatment*. In Institute of Materials Conference, London, UK, 1999, pp. 27-28.

103. Stolzenberg, M.; Schmidt, R.; Casajus, A.; Kebe, T.; Falkenstrom, M.; Martinez de Guerenu, A.; Link, N.; Ploegaert, H.; van den Berg, F.; Peyton, A. Online Material Characterisation at Strip Production (OMC): Final Report; EUR EUR-25879-EN, Luxembourg, 2013. Available online: http://bookshop.europa.eu/en/online-material-characterisation-at-strip-production-omc--pbKINA25879/ (accessed on 23 September 2022).

104. Damoiselet, F.; Nogues, M.; Midroit, F. New Approaches to Non-Destructive Characterisation of Microstructure and Applications to Online Control of Steel Quality (NANDACS): Final Report; EUR. Technical steel research EUR-21977-EN, Luxembourg, 2006. Available online: http://bookshop.europa.eu/en/-pbKINA21977/ (accessed on 13 November 2022).

105. Djordjevic, B.B.; Dos Reis, H. *TONE, Topics on Nondestructive Evaluation*; American Society for Nondestructive Testing, Inc.: Columbus, OH, USA, 1998; ISBN 1571170677.

106. Scruby, C.B.; Drain, L.E. *Laser Ultrasonics*: *Techniques and Applications*; Taylor & Francis: New York, NY, USA, 1990; ISBN 0750300507.

107. Royer, D.; Dieulesaint, E. *Elastic Waves in Solids*; Springer: Berlin, Germany; London, UK, 2011; ISBN 9783642085215.

108. Dubois, M.; Moreau, A.; Bussière, J.F. Ultrasonic velocity measurements during phase transformations in steels using laser ultrasonics. *J. Appl. Phys.* **2001**, *89*, 6487–6495. https://doi.org/10.1063/1.1363681.

109. Lamouche, G.; Bolognini, S.; Kruger, S.E. Influence of steel heat treatment on ultrasonic absorption measured by laser ultrasonics. *Mater. Sci. Eng. A* **2004**, *370*, 401–406. https://doi.org/10.1016/j.msea.2003.07.019.

110. Smith, A.; Kruger, S.E.; Sietsma, J.; van der Zwaag, S. Laser-ultrasonic monitoring of ferrite recovery in ultra low carbon steel. *Mater. Sci. Eng. A* **2007**, *458*, 391–401. https://doi.org/10.1016/j.msea.2006.12.102.

111. Kerschbaummayr, C.; Ryzy, M.; Reitinger, B.; Hettich, M.; Džugan, J.; Wydra, T.; Scherleitner, E. In-Situ Laser Ultrasound Measurements of Austenitic Grain Growth in Plain Carbon Steel. In Proceedings of the 2021 48th Annual Review of Progress in Quantitative Nondestructive Evaluation, Virtual, Online, 28–30 July 2021; American Society of Mechanical Engineers: New York, NY, USA, 2021; p. 07282021, ISBN 978-0-7918-8552-9.

112. Hartl, K.; Kerschbaummayr, C.; Stockinger, M. In-situ investigation of grain size evolution of Alloy 718 using Laser-Ultrasonics. *XL. Colloquium on Metal Forming: Zauchensee, Austria 2022*. 31–38.

113. Militzer, M.; Garcin, T.; Poole, W.J. In Situ Measurements of Grain Growth and Recrystallization by Laser Ultrasonics. *MSF* **2013**, *753*, 25–30. https://doi.org/10.4028/www.scientific.net/MSF.753.25.

114. Garcin, T.; Schmitt, J.-H.; Militzer, M. Application of laser ultrasonics to monitor microstructure evolution in Inconel 718 superalloy. *MATEC Web Conf.* **2014**, *14*, 7001. https://doi.org/10.1051/matecconf/20141407001.

115. Maalekian, M.; Radis, R.; Militzer, M.; Moreau, A.; Poole, W.J. In situ measurement and modelling of austenite grain growth in a Ti/Nb microalloyed steel. *Acta Mater.* **2012**, *60*, 1015–1026. https://doi.org/10.1016/j.actamat.2011.11.016.

116. Militzer, M.; Maalekian, M.; Moreau, A. Laser-Ultrasonic Austenite Grain Size Measurements in Low-Carbon Steels. *MSF* **2012**, *715–716*, 407–414. https://doi.org/10.4028/www.scientific.net/MSF.715-716.407.

117. Yin, A.; Yang, Q.; He, F.; Xiao, H. Determination of Grain Size in Deep Drawing Steel Sheet by Laser Ultrasonics. *Mater. Trans.* **2014**, *55*, 994–997. https://doi.org/10.2320/matertrans.I-M2014808.

118. Dong, F.; Wang, X.; Yang, Q.; Yin, A.; Xu, X. Directional dependence of aluminum grain size measurement by laser-ultrasonic technique. *Mater. Charact.* **2017**, *129*, 114–120. https://doi.org/10.1016/j.matchar.2017.04.027.

119. He, F.; Anmin, Y.; Quan, Y. Grain Size Measurement in Steel by Laser Ultrasonics Based on Time Domain Energy. *Mater. Trans.* **2015**, *56*, 808–812. https://doi.org/10.2320/matertrans.M2014445.

120. Lindh-Ulmgren, E.; Ericsson, M.; Artymowicz, D.; Hutchinson, W.B. Laser-Ultrasonics as a Technique to Study Recrystallisation and Grain Growth. *MSF* **2004**, *467–470*, 1353–1362. https://doi.org/10.4028/www.scientific.net/MSF.467-470.1353.

121. Sarkar, S.; Moreau, A.; Militzer, M.; Poole, W.J. Evolution of Austenite Recrystallization and Grain Growth Using Laser Ultrasonics. *Met. Mat. Trans. A* **2008**, *39*, 897–907. https://doi.org/10.1007/s11661-007-9461-6.

122. Keyvani, M.; Garcin, T.; Militzer, M.; Fabregue, D. Laser ultrasonic measurement of recrystallization and grain growth in an L605 cobalt superalloy. *Mater. Charact.* **2020**, *167*, 110465. https://doi.org/10.1016/j.matchar.2020.110465.

123. Keyvani, M.; Garcin, T.; Fabrègue, D.; Militzer, M.; Yamanaka, K.; Chiba, A. Continuous Measurements of Recrystallization and Grain Growth in Cobalt Super Alloys. *Met. Mat. Trans. A* **2017**, *48*, 2363–2374. https://doi.org/10.1007/s11661-017-4027-8.

124. Smith, A.; Kruger, S.E.; Sietsma, J.; van der Zwaag, S. Laser-ultrasonic Monitoring of Austenite Recrystallization in C–Mn Steel. *ISIJ Int.* **2006**, *46*, 1223–1232. https://doi.org/10.2355/isijinternational.46.1223.

125. Keyvani, M. *Laser Ultrasonic Investigations of Recrystallization and Grain Growth in Cubic Metals* University of British Columbia, Vancouver, Canada, 2018.

126. Pandey, J.C. Study of Recrystallization in Interstitial Free (IF) Steel by Ultrasonic Techniques. *Mater. Manuf. Process.* **2011**, *26*, 147–153. https://doi.org/10.1080/10426910903202302.

127. Moreau, A. Laser-Ultrasonic Characterization of the Microstructure of Aluminium. *MSF* **2006**, *519–521*, 1373–1378. https://doi.org/10.4028/www.scientific.net/MSF.519-521.1373.

128. Kruger, S.E. Monitoring microstructure evolution of nickel at high temperature. In Proceedings of the AIP Conference Proceedings Quantitat Ive Nondestructive Evaluation, Brunswick, ME, USA, 29 July–3 August 2001; pp 1518–1525.

129. Malmström, M.; Jansson, A.; Hutchinson, B. Application of Laser-Ultrasonics for Evaluating Textures and Anisotropy. *Appl. Sci.* **2022**, *12*, 10547. https://doi.org/10.3390/app122010547.

130. Bate, P.; Lundin, P.; Lindh-Ulmgren, E.; Hutchinson, B. Application of laser-ultrasonics to texture measurements in metal processing. *Acta Mater.* **2017**, *123*, 329–336. https://doi.org/10.1016/j.actamat.2016.10.043.

131. Yin, A.; Wang, X.; Glorieux, C.; Yang, Q.; Dong, F.; He, F.; Wang, Y.; Sermeus, J.; van der Donck, T.; Shu, X. Texture in steel plates revealed by laser ultrasonic surface acoustic waves velocity dispersion analysis. *Ultrasonics* **2017**, *78*, 30–39. https://doi.org/10.1016/j.ultras.2017.02.016.

132. Dubois, M.; Moreau, A.; Militzer, M.; Bussière, J.F. Laser-ultrasonic monitoring of phase transformations in steels. *Scr. Mater.* **1998**, *39*, 735–741. https://doi.org/10.1016/S1359-6462(98)00179-1.

133. Shinbine, A.; Garcin, T.; Sinclair, C. In-situ laser ultrasonic measurement of the hcp to bcc transformation in commercially pure titanium. *Mater. Charact.* **2016**, *117*, 57–64. https://doi.org/10.1016/j.matchar.2016.04.018.

134. Rodrigues, M.C.; Garcin, T.; Militzer, M. In-situ measurement of α formation kinetics in a metastable β Ti-5553 alloy using laser ultrasonics. *J. Alloy. Compd.* **2021**, *866*, 158954. https://doi.org/10.1016/j.jallcom.2021.158954.

135. Chen, D.; Liu, Y.; Feng, W.; Wang, Y.; Hu, Q.; Lv, G.; Zhang, S.; Guo, S. In-situ prediction of α-phase volume fraction in titanium alloy using laser ultrasonic with support vector regression. *Appl. Acoust.* **2021**, *177*, 107928. https://doi.org/10.1016/j.apacoust.2021.107928.

136. Zhu, Z.; Peng, H.; Xu, Y.; Song, X.; Zuo, J.; Wang, Y.; Shu, X.; Yin, A. Characterization of Precipitation in 7055 Aluminum Alloy by Laser Ultrasonics. *Metals* **2021**, *11*, 275. https://doi.org/10.3390/met11020275.

137. Ralph, B.J.; Sorger, M.; Schödinger, B.; Schmölzer, H.-J.; Hartl, K.; Stockinger, M. Implementation of a Six-Layer Smart Factory Architecture with Special Focus on Transdisciplinary Engineering Education. *Sensors* **2021**, *21*, 2944. https://doi.org/10.3390/s21092944.